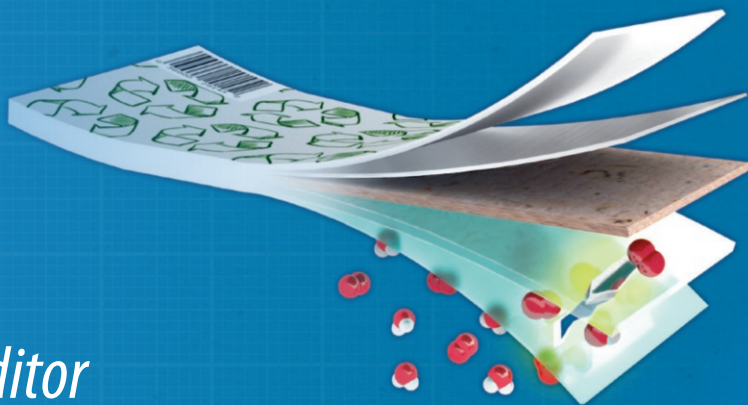


Methods and Protocols  
in Food Science

Springer Protocols



Caio Otoni *Editor*

# Food Packaging Materials

Current Protocols

 Humana Press

# METHODS AND PROTOCOLS IN FOOD SCIENCE

*Series Editor*  
**Anderson S. Sant'Ana**  
**University of Campinas**  
**Campinas, Brazil**

For further volumes:  
<http://www.springer.com/series/16556>

*Methods and Protocols in Food Science* series is devoted to the publication of research protocols and methodologies in all fields of food science.

Volumes and chapters will be organized by field and presented in such way that the readers will be able to reproduce the experiments in a step-by-step style. Each protocol will be characterized by a brief introductory section, followed by a short aims section, in which the precise purpose of the protocol will be clarified.

# **Food Packaging Materials**

## **Current Protocols**

Edited by

**Caio Otoni**

*Department of Materials Engineering, Federal University of São Carlos, São Carlos, Brazil*

*Editor*

Caio Otoni  
Department of Materials Engineering  
Federal University of São Carlos  
São Carlos, Brazil

ISSN 2662-950X                      ISSN 2662-9518 (electronic)  
Methods and Protocols in Food Science  
ISBN 978-1-0716-3612-1              ISBN 978-1-0716-3613-8 (eBook)  
<https://doi.org/10.1007/978-1-0716-3613-8>

© The Editor(s) (if applicable) and The Author(s), under exclusive license to Springer Science+Business Media, LLC, part of Springer Nature 2024

This work is subject to copyright. All rights are solely and exclusively licensed by the Publisher, whether the whole or part of the material is concerned, specifically the rights of translation, reprinting, reuse of illustrations, recitation, broadcasting, reproduction on microfilms or in any other physical way, and transmission or information storage and retrieval, electronic adaptation, computer software, or by similar or dissimilar methodology now known or hereafter developed.

The use of general descriptive names, registered names, trademarks, service marks, etc. in this publication does not imply, even in the absence of a specific statement, that such names are exempt from the relevant protective laws and regulations and therefore free for general use.

The publisher, the authors, and the editors are safe to assume that the advice and information in this book are believed to be true and accurate at the date of publication. Neither the publisher nor the authors or the editors give a warranty, expressed or implied, with respect to the material contained herein or for any errors or omissions that may have been made. The publisher remains neutral with regard to jurisdictional claims in published maps and institutional affiliations.

This Humana imprint is published by the registered company Springer Science+Business Media, LLC, part of Springer Nature.

The registered company address is: 1 New York Plaza, New York, NY 10004, U.S.A.

Printed on acid-free paper

---

## **Preface to the Series**

Methods and Protocols in Food Science series is devoted to the publication of research protocols and methodologies in all fields of food science. The series is unique as it includes protocols developed, validated, and used by food and related scientists as well as theoretical basis are provided for each protocol. Aspects related to improvements in the protocols, adaptations, and further developments in the protocols may also be approached.

Methods and Protocols in Food Science series aims to bring the most recent developments in research protocols in the field as well as very well-established methods. As such, the series targets undergraduate, graduate, and researchers in the field of food science and correlated areas. The protocols documented in the series will be highly useful for scientific inquiries in the field of food sciences, presented in such way that the readers will be able to reproduce the experiments in a step-by-step style.

Each protocol will be characterized by a brief introductory section, followed by a short aims section, in which the precise purpose of the protocol is clarified. Then, an in-depth list of materials and reagents required for employing the protocol is presented, followed by a comprehensive and step-by-step procedures on how to perform that experiment. The next section brings the dos and don'ts when carrying out the protocol, followed by the main pitfalls faced and how to troubleshoot them. Finally, template results will be presented and their meaning/conclusions addressed.

The Methods and Protocols in Food Science series will fill an important gap, addressing a common complain of food scientists, regarding the difficulties in repeating experiments detailed in scientific papers. With this, the series has a potential to become a reference material in food science laboratories of research centers and universities throughout the world.

*Campinas, Brazil*

*Anderson S. Sant'Ana*

---

## Preface

Once, I heard that the future of packaging is having “no packaging at all.” This is a groundbreaking approach that might solve some concerns related to the boundaries of the linear life cycle of materials: from the cradle, as far as the depletion of critical raw materials from nature; to the grave, in whatever concerns the environmental fate of such an often considered “useless piece of matter,” mainly when one deals with single-use packaging that is persistent and ends up being treated unsuitably once it has played its protective role.

Although revolutionary, this approach may be limited to short-range businesses, meaning that I consider it idealistic in our industrialized and globalized society, in which packaging actually plays vital roles as far as logistics, marketing, and quality assurance, to mention a few. The role of packaging gets even more pivotal when dealing with food systems, known to be prone to a range of spoilage mechanisms. Food Packaging is the core topic of this contribution, wherein I merge both disciplines in which I have been trained—namely, Food Engineering and Materials Engineering—to gather what I believe to be the most relevant nontraditional analytic techniques, detailed by a team of leading experts with the ultimate goal of supporting contemporary packagers in industry and academia during their journey toward consistency and innovations in the field.

This text is also devoted to encouraging sustainability, multifunctionality, safety, and performance through, respectively, linear-to-circular, passive-to-active, threatening-to-harmless, and disposable-to-durable paradigm shifts. In my opinion, these transitions will continue to be the main drivers of the packaging revolution that is already ongoing.

Herein, circularity is put forward when protocols are proposed to (i) track potentially hazardous compounds arising from mechanical recycling, (ii) monitor biodegradation from a biological recycling angle, and (iii) characterize the performance of packaging materials in terms of additives and defects, so these can be improved toward extended longevity within the economic cycle.

The different roles that packaging can play in an active fashion are addressed when methods are described to (i) predict microbial development in modified atmosphere packaging, evaluate the efficiency in actively preventing the growth of (ii) fungi and (iii) bacteria or the occurrence of (iv) oxidative reactions, (v) prospect the potential of edible packaging to carry and deliver probiotics and prebiotics, (vi) outlook the use of phase-change packaging for thermal control, and (vii) assess the interaction between packaging and consumers in terms of sensory perception and acceptance.

The safe use of packaging in food systems is well characterized by assays of (i) migration and release of potentially harmful molecules or particles, (ii) manifestations of toxicity in different biological contexts, and (iii) environmental and food contaminations with microplastics arising from the mismanagement of long-lasting packaging materials.

Finally, packaging performance is comprehensively pictured in terms of barrier against the permeation of (i) moisture, (ii) gases, and (iii) microorganisms, besides molecular-level (iv) microstructural investigation of defects and (v) spatio-spectral distribution of additives, both via nondestructive techniques.

While this text almost omits well-established protocols—e.g., those already commonplace in the literature—I do hope it catalyzes ongoing and future endeavors toward next-generation food packaging, soundly designed based on reliable, comparable, and reproducible characterizations. Enjoy the pack, wherein every layer unfolds a narrative of possibilities!

*Sao Carlos, Brazil*

*Caio Otoni*



---

# Contents

|                                    |     |
|------------------------------------|-----|
| <i>Preface to the Series</i> ..... | v   |
| <i>Preface</i> .....               | vii |
| <i>Contributors</i> .....          | xi  |

## PART I ENVIRONMENTAL AND TOXICOLOGICAL ASPECTS OF FOOD PACKAGING MATERIALS

|  |     |
|--|-----|
| 1 Biodegradability of Biodegradable Plastics in Compost, Marine, and Anaerobic Environments Assessed by Automated Respirometry.....  | 3   |
| <i>Joseph P. Greene, William Hart-Cooper, Lennard F. Torres, Julia Cunniffe, Artur Klamczynski, Gregory M. Glenn, and William J. Orts</i>  |     |
| 2 Biodegradability of Polymers by Relatively Low-Cost and Readily Available Nonautomated Respirometry.....   | 27  |
| <i>Alex S. Babetto, Laís T. Possari, Baltus C. Bonse, and Sílvia H. P. Bettini</i>   |     |
| 3 Detection and Identification of Microplastics in Food and the Environment ...  | 57  |
| <i>Walter R. Waldman, Cristiane Vidal, Mariana A. Dias, Victor Z. Resende, and Cassiana C. Montagner</i>   |     |
| 4 Identification of Intentionally and Non-intentionally Added Substances in Recycled Plastic Packaging Materials .....   | 75  |
| <i>Magdalena Wrona, Davinson Pezo, Robert Paiva, and Sandra A. Cruz</i>  |     |
| 5 Poly- and Perfluorinated Alkyl Substances in Food Packaging Materials.....   | 99  |
| <i>Rachel C. Scholes, William Hart-Cooper, Gregory M. Glenn, and William J. Orts</i>   |     |
| 6 Migration of Building Blocks, Additives, and Contaminants from Food Packaging Materials .....  | 115 |
| <i>Victor G. L. Souza, Regiane Ribeiro-Santos, Patricia F. Rodrigues, Carolina Rodrigues, João R. A. Pires, Ana T. Sanches-Silva, Isabel Coelho, Fátima Poças, and Ana L. Fernando</i> |     |
| 7 In Vitro Cytotoxicity Testing of Food Packaging .....  | 137 |
| <i>Arthur B. Ribeiro, Juliana G. F. Silva, Lucas N. F. Trevizan, Hernane S. Barud, Flávia A. Resende, and Denise C. Tavares</i>  |     |
| 8 In Vitro Genotoxicity/Mutagenicity Testing of Food Packaging.....  | 149 |
| <i>Flávia A. Resende, Juliana G. F. Silva, Arthur B. Ribeiro, Lucas N. F. Trevizan, Hernane S. Barud, and Denise C. Tavares</i>  |     |

## PART II MICROSTRUCTURAL AND BARRIER FEATURES OF FOOD PACKAGING MATERIALS

|   |     |
|---|-----|
| 9 Microstructural and Defect Analysis of Food Packaging Materials Through X-Ray Microtomography ..... | 167 |
| <i>Marcos V. Lovevica, Pedro I. C. Claro, Diego M. Nascimento, and Rubia F. Gouveia</i>               |     |

|  |  |     |
|--|--|-----|
| 10   | Mapping the Distribution of Additives Within Polymer Films Through Near-Infrared Spectroscopy and Hyperspectral Imaging.....               | 183 |
|  | <i>Jussara V. Roque, Cícero C. Pola, Larissa R. Terra, Taila V. Oliveira, Reinaldo F. Teófilo, Carmen L. Gomes, and Nilda F. F. Soares</i> |     |
| 11   | Water Vapor Permeability of Hydrophilic Films.....   | 205 |
|  | <i>Roberto J. Avena-Bustillos, Noah M. Klausner, and Tara H. McHugh</i>  |     |
| 12   | Permeation of Oxygen and Carbon Dioxide Through Food Packaging Materials.....  | 219 |
|  | <i>Victor G. L. Souza, Carolina Rodrigues, João R. A. Pires, Ana L. Fernando, Vitor Alves, and Isabel Coelho</i>                           |     |
| 13   | Microbial Permeation Through Food Packaging Materials.....   | 233 |
|  | <i>Julia V. Ernesto, Patricia Severino, Anna C. Venturini, Cristiana M. P. Yoshida, Classius F. da Silva, and Patricia S. Lopes</i>        |     |
| PART III NONTRADITIONAL ROLES PLAYED BY FOOD PACKAGING MATERIALS |  |     |
| 14   | Do Not “Pack and Pray”: Use Predictive Models to Assess the Microbial Safety and Shelf-Life of Modified Atmosphere Packaged Foods.....     | 245 |
|  | <i>Aricia Possas, Fernando Pérez-Rodríguez, and Antonio Valero</i>   |     |
| 15   | Antifungal Activity of Edible Films and Coatings for Packaging of Fresh Horticultural Produce.....   | 259 |
|  | <i>Lluís Palou and María B. Pérez-Gago</i>   |     |
| 16   | Antibacterial Activity of Active Food Packaging Materials.....   | 279 |
|  | <i>Paula J. P. Espitia and Rejane A. Batista</i>   |     |
| 17   | Antioxidant Activity Assays for Food Packaging Materials.....  | 293 |
|  | <i>Fabiana H. Santos, Danielle C. M. Ferreira, Julia R. V. Matheus, Ana E. C. Fai, and Franciele M. Pelissari</i>                          |     |
| 18   | Release of Active Agents from Food Packaging Materials.....  | 311 |
|  | <i>Murilo S. Pacheco, Mariana A. de Moraes, Mariana A. da Silva, and Andréa C. K. Bierhalz</i>   |     |
| 19   | Bioactive Properties of Probiotic and Prebiotic Edible Films.....  | 325 |
|  | <i>Jackson A. Medeiros, Carolina M. Niro, Mateus K. Salgaço, Kátia Sivieri, and Henriette M. C. Azeredo</i>                                |     |
| 20   | Sensory Acceptance Test of Edible Packaging Using Hedonic Scale.....   | 337 |
|  | <i>Suzana Maria Della Lucia and Tarcísio Lima Filho</i>  |     |
| 21   | Consumer Choice Probabilities for Food Packaging.....  | 349 |
|  | <i>Tarcísio Lima Filho, Suzana Maria Della Lucia, and Valéria Paula Rodrigues Minim</i>  |     |
| 22   | Thermal Performance of Food Packaging Containing Phase Change Materials.....   | 365 |
|  | <i>Bianca C. N. Fernandes and Ana S. Prata</i>   |     |
|  | <i>Index</i> .....   | 375 |

---

## Contributors

- VITOR ALVES • *Linking Landscape, Environment, Agriculture and Food (LEAF), Instituto Superior de Agronomia, Universidade de Lisboa, Lisbon, Portugal*
- ROBERTO J. AVENA-BUSTILLOS • *Western Regional Research Center, Agriculture Research Service (ARS), United States Department of Agriculture (USDA), Albany, CA, USA*
- HENRIETTE M. C. AZEREDO • *Embrapa Tropical Agroindustry, Fortaleza, CE, Brazil; Embrapa Instrumentation, São Carlos, SP, Brazil*
- ALEX S. BABETTO • *Graduate Program in Mechanical Engineering, Centro Universitário FEI, São Bernardo do Campo, SP, Brazil*
- HERNANE S. BARUD • *University of Araraquara (UNIARA), Araraquara, SP, Brazil*
- REJANE A. BATISTA • *Institute of Technology and Research of Sergipe, Aracaju, SE, Brazil*
- SÍLVIA H. P. BETTINI • *Graduate Program in Materials Science and Engineering (PPGCEM), Federal University of São Carlos (UFSCar), São Carlos, SP, Brazil*
- ANDRÉA C. K. BIERHALZ • *Center of Technology, Exact Sciences and Education, Federal University of Santa Catarina (UFSC), Blumenau, SC, Brazil*
- BALTUS C. BONSE • *Graduate Program in Mechanical Engineering, Centro Universitário FEI, São Bernardo do Campo, SP, Brazil*
- PEDRO I. C. CLARO • *Brazilian Nanotechnology National Laboratory (LNNano), Brazilian Center of Research in Energy and Materials (CNPEM), Campinas, SP, Brazil*
- ISABEL COELHO • *LAQV-REQUIMTE, Department of Chemistry, NOVA School of Science and Technology, Universidade NOVA de Lisboa, Lisbon, Portugal*
- SANDRA A. CRUZ • *Department of Chemistry, Federal University of São Carlos, São Carlos, São Paulo, Brazil*
- JULIA CUNNIFFE • *Western Regional Research Center, Agriculture Research Service (ARS), United States Department of Agriculture (USDA), Albany, CA, USA*
- CLASSIUS F. DA SILVA • *Institute for Environmental, Chemical, and Pharmaceutical Sciences (ICAQF), Federal University of São Paulo (UNIFESP), Diadema, SP, Brazil*
- MARIANA A. DA SILVA • *Center of Agricultural Sciences, Federal University of São Carlos (UFSCar), Araras, SP, Brazil*
- MARIANA A. DE MORAES • *Department of Chemical Engineering, Federal University of São Paulo (UNIFESP), Diadema, SP, Brazil; School of Chemical Engineering, Universidade Estadual de Campinas (UNICAMP), Campinas, SP, Brazil*
- SUZANA MARIA DELLA LUCIA • *Federal University of Espírito Santo (UFES), Alegre, ES, Brazil*
- MARIANA A. DIAS • *Institute of Chemistry, University of Campinas (UNICAMP), Campinas, SP, Brazil*
- JULIA V. ERNESTO • *Institute for Environmental, Chemical, and Pharmaceutical Sciences (ICAQF), Federal University of São Paulo (UNIFESP), Diadema, SP, Brazil*
- PAULA J. P. ESPITIA • *Nutrition and Dietetics School, Universidad del Atlántico, Puerto Colombia, Colombia*
- ANA E. C. FAI • *Food and Nutrition Graduate Program (PPGAN), Federal University of the State of Rio de Janeiro (UNIRIO), Rio de Janeiro, RJ, Brazil; Department of Basic and Experimental Nutrition, Institute of Nutrition, Rio de Janeiro State University (UERJ), Rio de Janeiro, RJ, Brazil*

- BIANCA C. N. FERNANDES • *Department of Food Engineering, School of Food Engineering, University of Campinas (UNICAMP), Campinas, SP, Brazil*
- ANA L. FERNANDO • *MEtRICs/CubicB, Departamen of Chemistry, NOVA School of Science and Technology, Universidade NOVA de Lisboa, Lisbon, Portugal*
- DANIELLE C. M. FERREIRA • *Institute of Science and Technology, Federal University of Jequitinbonha and Mucuri Valleys (UFVJM), Diamantina, MG, Brazil; Department of Food Technology, Federal University of Viçosa (UFV), Viçosa, MG, Brazil*
- GREGORY M. GLENN • *Western Regional Research Center, Agriculture Research Service (ARS), United States Department of Agriculture (USDA), Albany, CA, USA*
- CARMEN L. GOMES • *Nanoscale Biological Engineering Laboratory, Iowa State University, Ames, IA, USA*
- RUBIA F. GOUVEIA • *Brazilian Nanotechnology National Laboratory (LNNano), Brazilian Center of Research in Energy and Materials (CNPEM), Campinas, SP, Brazil; Center of Natural and Human Sciences, Federal University of ABC (UFABC), Santo Andre, SP, Brazil*
- JOSEPH P. GREENE • *Department of Mechanical Engineering, Mechatronic Engineering, and Manufacturing Technology, California State University, Chico, CA, USA*
- WILLIAM HART-COOPER • *Western Regional Research Center, Agriculture Research Service (ARS), United States Department of Agriculture (USDA), Albany, CA, USA*
- ARTUR KLAMCZYNSKI • *Western Regional Research Center, Agriculture Research Service (ARS), United States Department of Agriculture (USDA), Albany, CA, USA*
- NOAH M. KLAUSNER • *Environmental Engineering, College of Agriculture and Life Sciences, Cornell University, Ithaca, NY, USA*
- TARCÍSIO LIMA FILHO • *Federal University of Espírito Santo (UFES), Alegre, ES, Brazil*
- PATRICIA S. LOPES • *Institute for Environmental, Chemical, and Pharmaceutical Sciences (ICAQF), Federal University of São Paulo (UNIFESP), Diadema, SP, Brazil*
- MARCOS V. LOREVICE • *Brazilian Nanotechnology National Laboratory (LNNano), Brazilian Center of Research in Energy and Materials (CNPEM), Campinas, SP, Brazil*
- JULIA R. V. MATHEUS • *Food and Nutrition Graduate Program (PPGAN), Federal University of the State of Rio de Janeiro (UNIRIO), Rio de Janeiro, RJ, Brazil*
- TARA H. MCHUGH • *Western Regional Research Center, Agriculture Research Service (ARS), United States Department of Agriculture (USDA), Albany, CA, USA*
- JACKSON A. MEDEIROS • *Postgraduate Program in Food and Nutrition, School of Pharmaceutical Sciences, São Paulo State University (Unesp), Araraquara, SP, Brazil*
- VALÉRIA PAULA RODRIGUES MINIM • *Federal University of Viçosa (UFV), Viçosa, MG, Brazil*
- CASSIANA C. MONTAGNER • *Institute of Chemistry, University of Campinas (UNICAMP), Campinas, SP, Brazil*
- DIEGO M. NASCIMENTO • *Brazilian Nanotechnology National Laboratory (LNNano), Brazilian Center of Research in Energy and Materials (CNPEM), Campinas, SP, Brazil*
- CAROLINA M. NIRO • *Postgraduate Program in Biotechnology, Federal University of São Carlos (UFSCar), São Carlos, SP, Brazil*
- TAÍLA V. OLIVEIRA • *Food Packaging Laboratory, Universidade Federal de Viçosa (UFV), Vicoso, MG, Brazil*
- WILLIAM J. ORTS • *Western Regional Research Center, Agriculture Research Service (ARS), United States Department of Agriculture (USDA), Albany, CA, USA*
- MURILO S. PACHECO • *Department of Chemical Engineering, Federal University of São Paulo (UNIFESP), Diadema, SP, Brazil*

- ROBERT PAIVA • *Department of Chemistry, Federal University of São Carlos, São Carlos, São Paulo, Brazil*
- LLUÍS PALOU • *Centre de Tecnologia Postcollita (CTP), Institut Valencià d'Investigacions Agràries (IVIA), València, Spain*
- FRANCIELE M. PELISSARI • *Institute of Science and Technology, Federal University of Jequitinbonha and Mucuri Valleys (UFVJM), Diamantina, MG, Brazil*
- MARÍA B. PÉREZ-GAGO • *Centre de Tecnologia Postcollita (CTP), Institut Valencià d'Investigacions Agràries (IVIA), València, Spain*
- FERNANDO PÉREZ-RODRÍGUEZ • *Department of Food Science and Technology, UIC Zoonosis y Enfermedades Emergentes (ENZOEM), CeIA3, Universidad de Córdoba, Campus Rabanales, Cordoba, Spain*
- DAVINSON PEZO • *Faculty of Health Sciences, San Jorge University, Villanueva de Gállego, Spain*
- JOÃO R. A. PIRES • *MEtRICs, CubicB, Departamento de Química, NOVA School of Science and Technology, Universidade NOVA de Lisbon, Lisbon, Portugal; Bio4Plas – Biopolímeros, Lda, Cantanhede, Portugal*
- FÁTIMA POÇAS • *Centro de Biotecnologia e Química Fina (CBQF), Universidade Católica Portuguesa, Lisbon, Portugal*
- CÍCERO C. POLA • *Nanoscale Biological Engineering Laboratory, Iowa State University, Ames, IA, USA*
- LAÍS T. POSSARI • *Graduate Program in Materials Science and Engineering (PPGCEM), Federal University of São Carlos (UFSCar), São Carlos, SP, Brazil*
- ARÍCIA POSSAS • *Department of Food Science and Technology, UIC Zoonosis y Enfermedades Emergentes (ENZOEM), CeIA3, Universidad de Córdoba, Campus Rabanales, Cordoba, Spain*
- ANA S. PRATA • *Department of Food Engineering, School of Food Engineering, University of Campinas (UNICAMP), Campinas, SP, Brazil*
- FLÁVIA A. RESENDE • *University of Araraquara (UNIARA), Araraquara, SP, Brazil*
- VÍCTOR Z. RESENDE • *Institute of Chemistry, University of Campinas (UNICAMP), Campinas, SP, Brazil*
- ARTHUR B. RIBEIRO • *University of Franca, Franca, SP, Brazil*
- REGIANE RIBEIRO-SANTOS • *Instituto de Química, Laboratório de Bioquímica Nutricional e de Alimentos, Federal University of Rio de Janeiro, Rio de Janeiro, Brazil*
- CAROLINA RODRIGUES • *MEtRICs/CubicB, Department of Chemistry, NOVA School of Science and Technology, Universidade NOVA de Lisboa, Lisbon, Portugal*
- PATRICIA F. RODRIGUES • *Centre for Mechanical Engineering Materials and Process, CEMMPRE, Department of Mechanical Engineering, University of Coimbra, Coimbra, Portugal*
- JUSSARA V. ROQUE • *Multivariate Chemical Data Analysis Laboratory, Universidade Federal de Viçosa (UFV), Viçosa, MG, Brazil; Chemistry Institute, Universidade Federal de Goiás, Goiania, GO, Brazil*
- MATEUS K. SALGAÇO • *Postgraduate Program in Food and Nutrition, School of Pharmaceutical Sciences, São Paulo State University (Unesp), Araraquara, SP, Brazil*
- ANA T. SANCHES-SILVA • *National Institute for Agricultural and Veterinary Research, INLAV, Vila do Conde, Portugal; Faculty of Pharmacy, University of Coimbra, Polo III, Coimbra, Portugal; Center for Study in Animal Science (CECA), ICETA, University of Porto, Porto, Portugal; Associate Laboratory for Animal and Veterinary Sciences (AL4Animals), University of Lisbon, Lisbon, Portugal*

- FABIANA H. SANTOS • *Institute of Science and Technology, Federal University of Jequitinhonha and Mucuri Valleys (UFVJM), Diamantina, MG, Brazil; Department of Food Technology, School of Food Engineering, University of Campinas (UNICAMP), Campinas, SP, Brazil*
- RACHEL C. SHOLES • *Western Regional Research Center, Agriculture Research Service (ARS), United States Department of Agriculture (USDA), Albany, CA, USA; Department of Civil Engineering, University of British Columbia, Vancouver, Canada*
- PATRICIA SEVERINO • *Tiradentes University (UNIT), Aracaju, SE, Brazil*
- JULIANA G. F. SILVA • *University of Araraquara (UNIARA), Araraquara, SP, Brazil*
- KÁTIA SIVIERI • *Postgraduate Program in Food and Nutrition, School of Pharmaceutical Sciences, São Paulo State University (Unesp), Araraquara, SP, Brazil; Postgraduate Program in Biotechnology and Health Innovation, Anhanguera University (UNIAN), São Paulo, SP, Brazil*
- NILDA F. F. SOARES • *Food Packaging Laboratory, Universidade Federal de Viçosa (UFV), Vicoso, MG, Brazil*
- VICTOR G. L. SOUZA • *MEtRICs, CubicB, Departamento de Química, NOVA School of Science and Technology, Universidade NOVA de Lisbon, Lisbon, Portugal; International Iberian Nanotechnology Laboratory (INL), Braga, Portugal*
- DENISE C. TAVARES • *University of Franca, Franca, SP, Brazil*
- REINALDO F. TEÓFILO • *Multivariate Chemical Data Analysis Laboratory, Universidade Federal de Viçosa (UFV), Vicoso, MG, Brazil*
- LARISSA R. TERRA • *Laboratory for Theoretical and Applied Chemometrics, Institute of Chemistry, Universidade de Campinas (UNICAMP), Campinas, SP, Brazil*
- LENNARD F. TORRES • *Western Regional Research Center, Agriculture Research Service (ARS), United States Department of Agriculture (USDA), Albany, CA, USA*
- LUCAS N. F. TREVIZAN • *University of Araraquara (UNIARA), Araraquara, SP, Brazil*
- ANTONIO VALERO • *Department of Food Science and Technology, UIC Zoonosis y Enfermedades Emergentes (ENZOEM), CeIA3, Universidad de Córdoba, Campus Rabanales, Córdoba, Spain*
- ANNA C. VENTURINI • *Institute for Environmental, Chemical, and Pharmaceutical Sciences (ICAQF), Federal University of São Paulo (UNIFESP), Diadema, SP, Brazil*
- CRISTIANE VIDAL • *Institute of Chemistry, University of Campinas (UNICAMP), Campinas, SP, Brazil*
- WALTER R. WALDMAN • *Science and Technology Center for Sustainability, Federal University of São Carlos (UFSCar), Sorocaba, SP, Brazil*
- MAGDALENA WRONA • *Department of Analytical Chemistry, Aragon Institute of Engineering Research I3A, University of Zaragoza, Zaragoza, Spain*
- CRISTIANA M. P. YOSHIDA • *Institute for Environmental, Chemical, and Pharmaceutical Sciences (ICAQF), Federal University of São Paulo (UNIFESP), Diadema, SP, Brazil*

# **Part I**

## **Environmental and Toxicological Aspects of Food Packaging Materials**



# Chapter 1

## **Biodegradability of Biodegradable Plastics in Compost, Marine, and Anaerobic Environments Assessed by Automated Respirometry**

**Joseph P. Greene, William Hart-Cooper, Lennard F. Torres, Julia Cunniffe, Artur Klamczynski, Gregory M. Glenn, and William J. Orts**

### **Abstract**

Biodegradability is an increasingly beneficial property of sustainable materials, particularly for single-use packaging. Biodegradation rates can vary dramatically depending on the conditions, whether aerobic or anaerobic, aqueous or nonaqueous (e.g., compost). We describe protocols of several standard biodegradation test methods, spanning marine, compost, and anaerobic environments. Simple methods to analyze biodegradation rates are also described.

**Key words** Biodegradability, Biodegradation, Industrial composting, Marine environment, Standard test methods, ASTM D5338-15, ISO 14855-2, ASTM D6691, ISO 14851, ISO 14852

---

## **1 Introduction**

### **1.1 Background**

Biodegradable plastics are available throughout the world. These materials provide an opportunity to meet market needs for materials with increased biobased and biodegradable content, while mitigating environmental and human health concerns. Food packagers are adopting more of these materials into their supplies and utilizing them for everything from cups to coffee pods. One of the advantages of using biodegradable plastics, especially the ones made from sustainable resources, is the significant reduction in carbon emissions and energy requirements during the manufacturing process. The commercial appeal of biodegradable plastics hinges on their good processability and mechanical properties. For example, polylactic acid (PLA) is a biodegradable polymer derived from renewable resources, such as starch or sugar, through fermentation. It has good durability and can be processed using existing manufacturing equipment typically designed and originally



used for petroleum-based plastics. PLA has been widely used for food packaging and other single-use products, such as injection molded cups and cutlery. Of course, the most important feature of biodegradable plastics is the breakdown of these products by microorganisms, such as bacteria and fungi, in industrial composting facilities and marine environments. Crucially, biodegradable plastics can be made with reduced carbon emissions, waste, and toxic pollution compared to traditional plastics.

### **1.2 *Biobased and Biodegradable Definitions***

Biobased and biodegradable polymers have two different meanings. Biobased products are materials made from some amount of biomass, such as plants, trees, animals, and marine materials [1]. Biobased products have been defined in the 2002 Farm Bill as commercial or industrial products that are composed in whole, or in significant part, of biological products, renewable agricultural materials, or forestry materials. The definition has been expanded with the 2008 Farm Bill that incorporated biobased intermediate ingredients or feedstock [2]. The USDA has established minimum biobased content standards for many product categories. Products must meet or exceed the minimum biobased content in its category to be certified as biobased products.

Biodegradable polymers are converted to biomass, CO<sub>2</sub>, and water through a thermochemical process in a specified time frame and in a specified disposal environment. Biodegradable polymers meet ASTM or ISO standards for biodegradation in a specific surrounding, for example, industrial compost or marine environments. Many biobased polymers are biodegradable, but not all biodegradable polymers are biobased. While some biobased polymers do not biodegrade, some biodegradable or compostable polymers are petroleum-based synthetics. Compostable polymers are those that meet the ASTM requirements for biodegradation under industrial composting conditions. Replacing fossil carbon with renewable carbon can reduce the carbon footprint of the plastic material based on life cycle assessment (LCA) [3].

### **1.3 *Biodegradation Mechanism for Biodegradable and Compostable Plastics***

Biodegradation is an important feature of biodegradable plastics. Two essential components of the biodegradation process are that the material must be a food source for the bacteria in the disposal environment and that the biodegradation must take place within a six-month period of time. Therefore, biodegradation can occur in an industrial compost environment for biodegradable plastics if they are used as food source for the bacteria in the compost and that they are generally consumed within 4–12 weeks at 40–60 °C. Likewise, biodegradation can occur in the marine environment if the bacteria in the sea water generally consume a major portion of the plastic within 4–12 weeks at a minimum of 30 °C.

The biodegradation of plastics into carbon dioxide, methane, water, and biomass is achieved through interaction with

microorganisms and enzymes. The bacteria that degrade the polymers are widely distributed in various environments. The common biodegradation environments may be categorized as either hot or cool. The hot biodegradation environment includes industrial composting where the operating temperatures can range from 50 to 65 °C. The cool biodegradation environments include home composting, soil, anaerobic digestion, landfill, and marine waters. The mechanisms are similar in these environments, but the activity rates of the bacteria and enzymes are different. The processes involved in biodegrading a macromolecule to an oligomer and an oligomer to a monomer or small molecule can involve the following:

1. Wetting of the polymer
2. Abiotic hydrolysis
3. Chain scission
4. Transformation to simple chemicals
5. Conversion of carbon to humus and/or volatile carbon (e.g., carbon dioxide, methane)

The two key components of biodegradation are (i) the rate of biodegradation by microorganisms and (ii) the life span of the product in the disposal environment [4]. The rate of biodegradation is influenced by environmental factors, which can have a crucial effect on the microbial population and activity. Biodegradation typically occurs through a two-step process: (i) scission of the main and side chains of the macromolecules through hydrolysis induced by thermal activation, resulting in a decrease in molecular weight, followed by (ii) conversion of short polymer chains into a biogas through respiration by microorganisms. Environmental parameters such as humidity, temperature, pH, absence/presence of oxygen, and nutrients can dictate whether microorganisms consider the plastic as a viable food source. Aside from environmental factors, the biodegradation rate can also be dependent upon the chemical and physical characteristics of the plastic. Some of these characteristics include porosity, chemical reactivity, thermal property, and morphology. Finally, all these conditions must be considered when testing the biodegradability of plastics, which must occur within a relatively short time span.

#### **1.4 Biodegradation Certification**

Certification is needed for biodegradable plastics to ensure that they meet the performance specification requirements in the biodegradation standards. In the United States, Biodegradable Products Institute (BPI) and the US Composting Council (USCC) established the Compostable Plastics certification program in the United States that meet the American Standards for Testing Materials (ASTM) compostability standards as specified in ASTM D6400 or ASTM D6868 [5, 6].

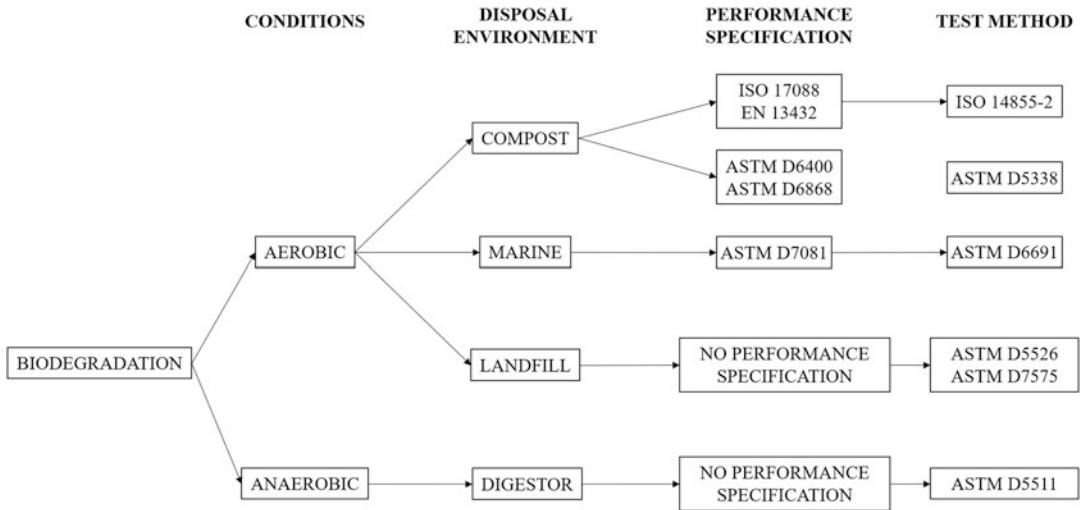


**Fig. 1** Overview of standard specifications and test methods for determining biodegradability in various disposal environments

### 1.5 Biodegradation Standards

Biodegradation can occur under a variety of conditions: anaerobic, aerobic, compost, landfills, and marine environments (Fig. 1). For example, biodegradable plastic products are degraded by microorganisms in landfill facilities in the absence of oxygen through anaerobic digestion. Alternatively, aerobic biodegradation refers to the conversion of plastic material into carbon dioxide and water with the consumption of oxygen. To place specific parameters on biodegradation, worldwide organizations developed acceptable standards for biodegradable products. These standards have an important role in the information infrastructure that guides design and manufacturing in the biodegradable plastics market.

Biodegradation standards for plastic materials are established in two necessary categories for biodegradation, one for biodegradation performance specifications and one for a biodegradation testing method (Fig. 1). Both types of standards are necessary and sufficient to adequately establish the biodegradation performance of plastic materials. The performance specification standard assigns a minimum value to establish biodegradation. Performance specification establishes the biodegradation requirement for a plastic product. ISO 17088 and EN13432 refer to the international and European specification standards, respectively, for plastics in industrial composting facilities. ASTM has developed specification standards for both industrial composting (ASTM D6400 and D6868) and marine (D7081) environments [7]. Currently, there are no international or European performance specification standards for plastics in a marine environment. Furthermore, neither one of the organizations has specification standards for plastic articles in landfills and anaerobic digestors, possibly due to extensive variabilities in those disposal environments.

**Table 1**  
**Summary of performance specification requirements**

| Disposal environment | Performance specification standard | Level of biodegradation <sup>a</sup>            | Rate of biodegradation <sup>a</sup>                     | Environmental effect <sup>b</sup> |
|----------------------|------------------------------------|---|---|-----------------------------------|
| Compost              | EN 13432                           | ≤10% original wt. after 84 d                    | ≥90% carbon converted to CO <sub>2</sub> after 6 months | None                              |
| Compost              | ISO 17088                          | ≤10% original wt. after 3 months                | ≥90% carbon converted to CO <sub>2</sub> after 6 months | None                              |
| Compost              | ASTM D6400                         | >90% original wt. disintegration after 12 weeks | ≥90% carbon converted to CO <sub>2</sub> after 180 d    | None                              |
| Compost              | ASTM D6868                         | ≤10% original wt. after 12 weeks                | ≥90% carbon converted to CO <sub>2</sub> after 180 d    | None                              |
| Marine               | ASTM D7081                         | ≤30% original wt. after 12 weeks                | ≥70% carbon converted to CO <sub>2</sub> after 180 d    | None                              |
| Landfill             | X                                  | X   | X   | X                                 |
| Digester             | X                                  | X   | X   | X                                 |

<sup>a</sup>At ≥58 °C, 50% humidity for industrial composting facilities. For marine environment, temperature requirement is 30 °C

<sup>b</sup>This effect refers to phytotoxicity and/or presence of heavy metals

Despite the different nomenclatures, all performance specification standards require the plastic products (e.g., packaging, coatings) and demonstrate three criteria [5–9]. Table 1 summarizes the specifications for each of the standards.

1. Sufficient disintegration of the plastic products.
2. Specified rate of biodegradation.
3. No adverse effects on the disposal environment.

The standards require the plastic products demonstrate ca. 90% loss of their original weight after 3–4 months. Furthermore, ca. 90% of the original carbon content must be converted to CO<sub>2</sub> by microorganisms after 6 months. Lastly, the end products must have low phytotoxicity and contain low levels of heavy metals or other toxic substances.

The biodegradation testing method accurately simulates the intended environment and specifies a method for measuring biodegradation. Table 2 summarizes the test methods associated with the specification standards.

The ISO 16929 and 20200 disintegration test methods involve gravimetric analysis of plastic products in industrial composting facilities or marine environment. The test duration is generally

**Table 2**  
**Summary of test methods for biodegradation of plastic materials**

| Disposal environment | Specification standard   | Disintegration test method | Respirometry test method | Biogas measured                   |
|----------------------|--------------------------|----------------------------|--------------------------|-----------------------------------|
| Compost              | EN 13432<br>ISO 17088    | ISO 16929<br>ISO 20200     | ISO 14855                | CO <sub>2</sub>                   |
| Compost              | ASTM D6400<br>ASTM D6868 | ISO 16929                  | ASTM D5338               | CO <sub>2</sub>                   |
| Marine               | X                        | X                          | ISO 14851<br>ISO 14852   | CO <sub>2</sub>                   |
| Marine               | ASTM D7081               | ISO 16929                  | ASTM D6691               | CO <sub>2</sub>                   |
| Landfill             | X                        | X                          | ASTM D5526<br>ASTM D7575 | CH <sub>4</sub> , CO <sub>2</sub> |
| Digester             | X                        | X                          | ISO 14853<br>ASTM D5511  | CH <sub>4</sub> , CO <sub>2</sub> |

12 weeks [10, 11]. The test method for determining the rate of biodegradation typically involves respirometric testing as specified by organizations such as ISO or ASTM. Respirometry techniques are an effective tool to measure the respiration of microorganisms and are associated with readily biodegradable plastics. Modern respirometers can automate data collection and are thus considered simple and effective instruments to measure carbon dioxide during respiration over a specified length of time. Because numerous readers may not have access to modern respirometers, they are invited to refer to Chapter 2 for nonautomated biodegradability assessments.

Currently, there are several testing methods used for evaluating biodegradable plastic products depending on the disposal environment (Table 2). ASTM D5338 and ISO 14855 are widely recognized by various municipalities and regulatory agencies as the test methods for biodegradability of products or materials in industrial composting facilities [12, 13]. These tests involve introducing a material to a mixed bacterial and fungal inoculum and use respirometry to measure biodegradation. ISO 14851, 14852, and ASTM D6691 are used for marine disposal environment, which typically involve similar procedures as their terrestrial counterparts but only in an aqueous medium and lower temperatures (ca. 30 °C).

While several test methods for measuring biodegradability have been developed, several issues can limit their applicability (and ultimately, their reliability) when attempting to predict rates of biodegradation. These issues originate from uncertainties pertaining to (i) inoculum, (ii) test sample morphology, and (iii) a suitable mathematical model used to predict product half-lives.

Recommendations for the type of inoculum used for the test methods are vague, and, given its rich diversity, it is difficult to obtain a standardized inoculum with constant characteristics for biodegradability tests. Moreover, the type of inoculum can significantly affect the rate of biodegradation [14–17]. Secondly, the available test methods recommend test samples to be ground and sieved through a specific mesh size to ensure a homogenous particle size and high surface area-to-volume ratio. Unfortunately, none of the published procedures provide guidelines for testing the biodegradability of samples with varying morphologies, such as semi-liquid resins or foamed plastic films, where grinding may not be applicable. Finally, the test methods do not provide simple mathematical models that would predict ultimate material half-life, a valuable parameter to end-users when designing and manufacturing their products.

This chapter describes the US biodegradation standards for biodegradable plastic food packaging, including starch-based packaging, in common disposal environments, including compost, marine, and anaerobic digestion. Compost environments include aerobic conditions within hot aerobic industrial compost environments and cool aerobic home composting environments. Marine environments include cold aerobic conditions. Landfill disposal environments include aerobic and anaerobic conditions. Anaerobic digestion environments include mesophilic anaerobic conditions.

---

## 2 Materials

### 2.1 *Biodegradation in a Composting Environment*

- Compost soil
- Plastic samples: films, powders, pellets, pieces, or fibers
- Positive control reference: biodegradable material (e.g., cellulose powder)
- Negative control reference: nonbiodegradable material (e.g., polyethylene film)
- Personal computer with software (e.g., Micro-Oxymax Respirometer proprietary software, Columbus Instruments)
- Respirometer (e.g., Micro-Oxymax Respirometer, Columbus Instruments):
  - Tank of compressed air (CO<sub>2</sub>-free and H<sub>2</sub>O-saturated)
  - Composting vessels (typically 125 mL to 1 L)
  - Humidified chamber
  - Flexible tubing nonpermeable to CO<sub>2</sub>
  - Stopper equipped with ports for the flexible tubing

## **2.2 Biodegradation in a Marine Environment**

- Aqueous medium (e.g., sea water or surface fresh water as indicated in the method; typically used within 3 days)
- Micronutrient supplementation (N, P, S) as indicated in the specified test method
- Plastic samples: films, powders, pellets, pieces, and fibers
- Positive control reference: biodegradable material (e.g., cellulose powder)
- Negative control reference: nonbiodegradable material (e.g., polyethylene film)
- Respirometer:
  - Tank of compressed air (CO<sub>2</sub>-free and H<sub>2</sub>O-saturated)
  - Composting vessels (typically 125 mL to 1 L)
  - Humidity controlled chamber
  - Flexible tubing nonpermeable to CO<sub>2</sub>
  - Stopper equipped with ports for the flexible tubing

## **2.3 Biodegradation in Anaerobic Digestion or Active Landfill**

- Blank anaerobic digester inoculum
- Plastic samples: films, powders, pellets, pieces, and fibers
- Positive control reference: biodegradable material (e.g., cellulose powder)
- Negative control reference: nonbiodegradable material (e.g., polyethylene film)
- Test vessels (typically 125 mL to 1 L)
- Low pH fluid bath or other temperature control device
- Flexible tubing nonpermeable to CH<sub>4</sub>, CO<sub>2</sub>, and O<sub>2</sub>
- Stoppers equipped with sampling ports
- Graduated cylinder or plastic tube
- Analytical balance ( $\pm 0.1$  mg)
- pH meter
- Gas chromatograph

---

## **3 Methods**

### **3.1 ASTM D6400-04. Standard Specification for Compostable Plastics**

#### *3.1.1 Summary*

This specification standard establishes the performance requirements for biodegradation of compostable plastic materials that are designed to biodegrade into CO<sub>2</sub>, water, and biomass in an industrial compost environment at a temperature maintained above 40 °C. It requires that the product must demonstrate each of the three characteristics as follows:

1. *Disintegration*: Sufficient disintegration during composting.
2. *Biodegradation rate*: Adequate level of inherent biodegradation.
3. *Nontoxic to plants*: No adverse impacts on the ability of compost to support plant growth.

### 3.1.2 Procedure

Three test procedures for the ASTM D6400-04 standard specify that three types of tests are performed on the plastic samples:

#### **Disintegration**

The first test measures the percentage of disintegration of the plastic samples while under hot and moist compost conditions.

1. The plastic samples are weighed prior to exposure to test conditions.
2. The samples are placed in compost soil (*see Note 1*) with the use of a sack, bag, or screened container. The composting conditions needs to be maintained at least 50 °C and 50% relative humidity.
3. The mass of the plastic sample (*see Note 2*) is measured after 12 weeks by passing the plastic sample and compost through a 2-mm sieve.

#### **Biodegradation Rate**

The second test procedure for D6400-04 standard specifies a biodegradation rate, which converts 90% of the carbon in the original plastic samples under composting conditions at least 50 °C and 50% moisture for 180 d into CO<sub>2</sub> as measured by a CO<sub>2</sub> respirometer. The details of the test procedure are listed in ASTM D53317-11 test method (*see* Subheading 3.2).

#### **Phytotoxicity**

The third test procedure for ASTM D6400-04 standard specifies the ability of the compost soil at the end of the biodegradation testing to support plant growth through phytotoxicity testing and very low regulated heavy metal concentrations.

1. Phytotoxicity testing is achieved through planting of tomato, cucumber, radish, rye, barley, or cress grass seeds in the tested compost soil.
2. Plant growth after 10 d indicates positive soil conditions. Plant biomass tests can reveal quality differences between composts and can indicate potential plant stress induced by the compost at the given level used in the test.



3. The level of regulated heavy metals (*see Note 3*) can be measured with flame atomic absorption spectrophotometer using an air-acetylene flame and equipped with a Pb hollow-cathode lamp.

**3.2 ASTM D5338-11. Standard Test Method for Determining Aerobic Biodegradation of Plastic Materials Under Controlled Composting Conditions**

3.2.1 Summary

3.2.2 Procedure

This test method standard measures the degree and rate of biodegradation of plastic materials under controlled composting conditions, simulating industrial composting conditions. The plastic test samples are exposed to an inoculum that is derived from industrial compost.

1. Sieve the compost through a 1.4-mm screen and analyze it for moisture content (*see Note 4*).
2. Place 40 g of compost in the vessel.
3. Cut the plastic samples into small pieces, ca. 0.5 g total weight, and then place in a vessel with warm and moist compost soil, making sure plastic sample is in good contact with the compost (*see Note 5*).
4. Adjust the moisture content to 58.5% (*see Note 6*).
5. Connect the composting vessels to the respirometer, equipped with the CO<sub>2</sub> sensor ranging from 0% to 3%.
6. Maintain the test containers at (58 ± 2) °C for 180 d, as indicated by the test method. The biogas from the container is measured for CO<sub>2</sub> and O<sub>2</sub> over the testing period. Analyze the headspace of the composting vessels for development of CO<sub>2</sub>. Sampling period can be 2 h (*see Note 7*).
7. Run samples in triplicates. Compost baseline controls lacking test sample are run in triplicate or quadruplicate.

**3.3 ASTM D-7081-05. Nonfloating Biodegradable Plastic in the Marine Environment**

3.3.1 Summary

This specification standard establishes the performance requirements for biodegradation of plastic materials and products, including packaging, films, and coatings in a marine environment, which includes conditions of aerobic marine waters or anaerobic marine sediments, or both. It establishes the requirements for biodegradation of plastic materials that have rates that are similar to known compostable materials. The standard requires the product must demonstrate each of the three characteristics as follows:

1. *Disintegration*: Sufficient disintegration during marine biodegradation.

2. *Biodegradation rate*: Adequate level of inherent biodegradation of the plastic material.
3. *Nontoxic to plants*: Minimal adverse effect on the marine environment.

### 3.3.2 Procedure

Three test procedures for the ASTM D-7081-05 standard specify that three types of tests are performed on the plastic samples.

#### **Disintegration**

The first test measures the percentage of disintegration of the plastic samples while under 30 °C marine conditions.

Biodegradation of biodegradable plastics in marine environment is based upon two sets of standards, the first for a test method standard and the second for a performance specification standard. The marine biodegradation standard covers nonfloating products made from plastics that are designed to biodegrade in the aerobic marine environment. It applies to deep sea water, shallow sea water, and brackish inland waters. Plastic materials must demonstrate disintegration and inherent biodegradation during marine water exposure and not exhibit adverse environmental impacts on the survival of marine organisms while in the marine environment.

#### **Biodegradation Rate**

The second test procedure for ASTM D-7081-05 standard specifies a biodegradation rate, which converts 90% of the carbon in the original plastic samples under marine conditions at least 30 °C and 50% moisture for 180 d into CO<sub>2</sub> as measured by a CO<sub>2</sub> respirometer. The details of the test procedure are listed in ASTM D53317-11 test method (*see* Subheading 3.4).

#### **Phytotoxicity**

The plastic sample also must pass several marine toxicity tests, including Polytox (microbial oxygen absorption), Microtox (microbial bioluminescence) test, Fish Acute Toxicity (static conditions) OPPTS 1750.1075, *Daphnia* Acute Toxicity (static conditions) OPPTS 1750.1010, or Static Algal Toxicity Test OPPTS 1750.5400. The plastic samples must also have less than 25% of maximum allowable concentrations of regulated heavy metals.

Marine biodegradation standards require that the plastic samples also pass the ASTM D-6400 standard for biodegradation under industrial aerobic compost conditions. The ASTM D-6400 standard requires plastic samples to convert 90% of the carbon in the plastic sample to CO<sub>2</sub> after 180 d while at 58 °C.

**3.4 ASTM D6691-09.  
Standard Test Method  
for Determining  
Aerobic  
Biodegradation of  
Plastic Materials in the  
Marine Environment by  
a Defined Microbial  
Consortium or Natural  
Sea Water Inoculum**

3.4.1 Summary

3.4.2 Procedure

This test method is used to determine the aerobic biodegradation rate of plastic materials exposed to sea water or synthesized sea water with pre-grown population of at least ten aerobic marine microorganisms of known genera. It consists of preparing a uniform inoculum of marine water, exposing the plastic samples to the marine water, measuring biodegradation with a carbon dioxide respirometer or equivalent measurement method, and assessing the percentage of carbon conversion in the plastic to carbon dioxide.

1. Filter water (*see Note 9*) through 0.5-mm screen to remove sand and other impurities.
2. Add  $\text{NH}_4\text{Cl}$  and  $\text{KH}_2(\text{PO}_4)$  salts as per ASTM 6691D.
3. Cut the plastic samples into small pieces, typically 20 mg to several grams, depending on the detection limits of the instrument in use.
4. Place the plastic sample with 75 mL of marine stock solution in 125-mL bottles.
5. Provide containers also for the following samples: blank (marine water only), positive control (e.g., cellulose or starch), and if needed, negative control (e.g., polyethylene).
6. Run experiments in triplicates. Use test water (e.g., ocean water) as a baseline in quadruplicates.
7. Connect the chambers to the respirometer and keep at  $(30 \pm 2)$  °C with continuous agitation for 180 d.
8. Analyze the headspace for development of  $\text{CO}_2$ . Take headspace samples in 2-h intervals and replace 50% of gas with atmospheric air to provide adequate oxygenation (*see Note 10*).

**3.5 ASTM D5511-02.  
Standard Test Method  
for Determining  
Anaerobic  
Biodegradation of  
Plastic Materials  
Under High-Solids  
Anaerobic-Digestion  
Conditions**

3.5.1 Summary

This test method measures the biodegradation rate of plastic materials under anaerobic thermophilic conditions in an aqueous environment. The plastic test samples are exposed to an inoculum that is derived from an aerobic digester or wastewater treatment operation. The plastic samples can be in the form of films, powders, pellets, or molded pieces and are placed in a vessel with warm inoculum with proper anaerobic bacteria.

### 3.5.2 Procedure

1. Place 1 kg of inoculum derived from properly operating anaerobic digester that is made from pretreated household waste. The inoculum should be derived from a digester operating under greater than 20% total solids conditions.
2. Add the plastic samples to each test container in quantities up to 100 g.
3. The test apparatus includes a graduated cylinder or plastic column [16]. The graduated cylinder or plastic column is inverted in a low-pH fluid to avoid CO<sub>2</sub> loss through the dissolution in the fluid. The biogas is calculated through a pressure measurement of the inverted tubes. Through ideal gas law, the pressure can be converted to grams of biogas. The concentration of biogas can be converted to concentrations of CO<sub>2</sub> and CH<sub>4</sub>. The conversion of carbon from the plastic sample to CO<sub>2</sub> and CH<sub>4</sub> can be determined. This will result in the carbon biodegradation percentage over 30 d in a high-solids anaerobic digester.
4. A minimum of 12 test vessels are required for the test.
5. Maintain the test containers at (50 ± 2) °C for 30 d.
6. Provide containers for the following samples: blank, positive control, and negative control, as described previously. The positive control must obtain greater than 70% biodegradation in 30 d.
7. Complete the testing in triplicate.
8. Test the inoculum for pH.
9. Measure the biogas from the container for CH<sub>4</sub>, CO<sub>2</sub>, and O<sub>2</sub> over the testing period.

### 3.6 Active Landfill (ASTM D5511-02)

Landfills in the United States are typically built with the EPA guidelines with the use of clay linings and a landfill cap (Criteria for Solid Waste Disposal Facilities 2013). The most common material for landfill caps is made from asphalt or concrete (Remediation Technologies Screening Matrix and Reference Guide 2013). Landfills can operate with the creation of biogas that is composed of methane, carbon dioxide, and other trace gases. Methane gas can be vented and burned or can be captured and stored for energy purposes. The carbon dioxide and other gases must be scrubbed to provide a clean methane gas without carbon dioxide or other gases. Some landfills are considered active and provide clean methane gas for energy consumption. Biodegradable plastics can hold the waste as trash bags for disposal and provide food source for the aerobic and anaerobic bacteria that are in the landfill. Standards are needed to evaluate the biodegradation of biodegradable plastics in landfills. Biodegradation of plastics in active landfill can use the ASTM standards in ASTM 5511 conditions to measure biodegradation under anaerobic conditions.

### 3.7 Analysis of Respirometry Results: Carbon Content and Mineralization Kinetics

The total amount of carbon in a plastic sample is generally determined by elemental analysis (*see* **Note 11**). In each round of experiments, a baseline must be established, which represents control media (e.g., compost, marine water, wastewater, etc.) lacking a test material (*see* **Note 12**). Subtracting the accumulated CO<sub>2</sub> of the baseline experiments from the test cases, which contain media and test material, gives the quantity of CO<sub>2</sub> that can be attributed to the mineralization of the test material. In both the baseline and test material conditions, mineralized gases measured through respirometry can be converted to moles carbon using the ideal gas law. The observed and theoretical moles carbon can be used to calculate percent mineralization and % theoretical carbon remaining in the test sample. Percent carbon mineralization can be converted to % theoretical carbon remaining and kinetic models can be applied to obtain rate constants.

The most practical interpretation of biodegradability rates can be obtained using linear fits which represent average biodegradation rates (Eq. 1), which represent the average percent degradation of a test material divided by the duration of the experiment. This approach is useful when measuring initial rates of degradation, which, like many other chemical processes, are often linear. However, biodegradation kinetics often deviate from linearity after the first ca. 30% of the starting material is consumed. This effect implies that, typically, linear approximations (Eq. 1) can accurately describe initial rate kinetics but are less accurate when describing kinetics curves where higher levels of degradation are observed. In Eq. 1, Δ% degradation represents the percent of material that was degraded over a given time span (Δtime). Linear fits can also be useful in determining induction periods, which describe kinetics where a period of slow degradation precedes a rapid increase in mineralization. Rates often vary by orders of magnitude, relative rates (relative rate constant =  $k_{\text{rel}}$ , Eq. 2) provide an intuitive ranking of biodegradation kinetics (Fig. 2). In Eq. 2,  $k_{\text{fast}}$  represents the most rapidly degraded rate constant, compared to  $k_{\text{slow}}$  that represents the slower rate constant:

$$\text{Average rate} = \frac{\Delta\% \text{degradation}}{\Delta \text{time}} \quad (1)$$

$$k_{\text{rel}} = \frac{k_{\text{fast}}}{k_{\text{slow}}} \quad (2)$$

Average biodegradation rates for various materials are listed in Table 3 [18–33].

These materials represent three groups: bioplastics, natural materials, and synthetic materials. In bioplastics, PLA degrades rapidly under industrial compost conditions, but degradation does not appreciably proceed in fresh water, marine water, soil, or

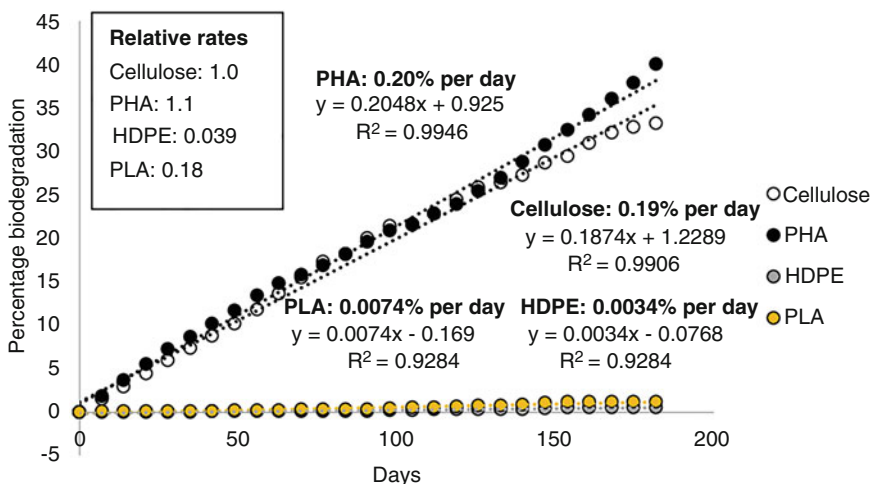


**Fig. 2** Linear fits and average rates of marine biodegradation data (ASTM D6691)

home compositing conditions. Polycaprolactone (PCL) and polyhydroxybutyrate (PHB) degrade much quicker than PLA in all conditions. Polyhydroxyoctanoate (PHO) underwent rapid degradation in fresh water, marine water, and industrial compost, whereas it barely degraded in soil. Poly(1,4-butylene succinate) (PBS) degraded similarly in both soil and compost conditions, presenting a large degradation range based on the condition temperature.

Of the literature data surveyed, most of the natural materials degraded in 2 months or less in soil or compost, except for beeswax which was 3–4 months in oil-contaminated soil. Of these natural materials, guar gum degraded the most rapidly. On the other hand, the synthetic materials had a larger range of degradation rates from months to years. Poly(vinyl alcohol) (PVA) degraded slowly under wastewater, soil, and compost environments. Carboxymethylcellulose (CMC) in wastewater showed that the higher the degree of substitution (DS), the longer the degradation rate. Low-density polyethylene (LDPE) showed similar results to PLA in soil with no significant degradation.

Pseudo first-order fits have been widely used to describe the nonlinear kinetics often observed in biodegradation tests. A pseudo first-order fit (Eq. 3) is applied to mineralization data (Fig. 3), affording rate constants that can be used to calculate half-lives (Eq. 4):

$$[A] = [A]_0 e^{-k_{\text{obs}} t} \quad (3)$$

$$t_{1/2} = \frac{\ln(2)}{k} \quad (4)$$

In Eq. 3,  $[A]$  represents the concentration of a material at a given time,  $[A]_0$  is the starting concentration of the same material,

**Table 3**  
**Biodegradation rates of bioplastics, natural, and synthetic materials from literature**

| Material                  | Condition                  | Temperature [°C] | Average biodegradation per day [%] | Residence time              | References |
|---------------------------|----------------------------|------------------|------------------------------------|-----------------------------|------------|
| <i>Bioplastics</i>        |                            |                  |                                    |                             |            |
| Poly(lactic acid) (PLA)   | Fresh water                | 21               | <0.01 <sup>a</sup>                 | >20 yr <sup>a</sup>         | [18]       |
|                           | Marine water               | 30               | <0.01 <sup>a</sup>                 | >20 yr <sup>a</sup>         |            |
|                           | Soil                       | 25               | 0.01                               | 20 yr                       | [19]       |
|                           | Industrial compost         | 58               | 1.33                               | 1–2 mo                      |            |
|                           | Soil                       | 25–37            | <0.01 <sup>a</sup>                 | >20 yr <sup>a</sup>         |            |
|                           | Compost                    | 25–50            | <0.01 <sup>a</sup> –0.37           | 8 mo to >20 yr <sup>a</sup> |            |
| Polycaprolactone (PCL)    | Fresh water                | 21               | 0.25                               | 1 yr                        | [18]       |
|                           | Marine water               | 30               | 0.30                               | 10 mo                       |            |
|                           | Soil                       | 25               | 0.55                               | 5–6 mo                      | [19]       |
|                           | Home compost               | 28               | 1.19                               | 2–3 mo                      |            |
|                           | Industrial compost         | 58               | 2.67                               | 1 mo                        |            |
|                           | Anaerobic digestion        | 52               | 0.71                               | 4–5 mo                      |            |
|                           | Soil                       | 25–37            | 0.19–0.21                          | 14–15 mo                    | [19]       |
|                           | Compost                    | 25–50            | 0.30–1.10                          | 2–10 mo                     |            |
|                           | Anaerobic methane sludge   | 37               | 0.38                               | 7–8 mo                      | [20]       |
|                           | Polyhydroxyoctanoate (PHO) | Fresh water      | 21                                 | 0.30                        | 10 mo      |
| Marine water              |                            | 30               | 0.86                               | 3–4 mo                      |            |
| Soil                      |                            | 25               | 0.01                               | 20 yr                       |            |
| Industrial compost        |                            | 58               | 0.85                               | 3–4 mo                      |            |
| Polyhydroxybutyrate (PHB) | Fresh water                | 21               | 1.50                               | 2 mo                        | [18]       |
|                           | Marine water               | 30               | 1.20                               | 2–3 mo                      |            |
|                           | Soil                       | 25               | 0.67                               | 4–5 mo                      | [19]       |
|                           | Industrial compost         | 58               | 2.56                               | 35 d                        |            |
|                           | Soil                       | 25–37            | 0.08–0.21                          | 1–3 yr                      |            |
|                           | Compost                    | 25–50            | 0.22–0.35                          | 8–14 mo                     |            |
|                           | Anaerobic methane sludge   | 37               | 2.38                               | 38 d                        | [20]       |

|  |                             |       |                            |                             |                    |
|--|-----------------------------|-------|----------------------------|-----------------------------|--------------------|
| Thermoplastic starch (TPS)                           | Fresh water                 | 21    | 2.00                       | 1–2 mo                      | [18]               |
|  | Marine water                | 30    | 3.00                       | 1 mo                        |                    |
|  | Soil                        | 25    | 0.55                       | 5–6 mo                      |                    |
|  | Home compost                | 28    | 1.22                       | 3–4 mo                      |                    |
|  | Anaerobic digestion         | 52    | 0.63                       | 1–2 mo                      |                    |
| Poly(butylene adipate-co-terephthalate) (PBAT)       | Compost                     | 28    | 0.03                       | 8–9 yr                      | [21]               |
| Poly-(β-hydroxybutyrate-co-β-hydroxyvalerate) (PHBV) | Anaerobic methane sludge    | 37    | 0.69                       | 4–5 mo                      | [20]               |
|  | Soil                        | 25–37 | 0.03–0.16                  | 1–10 yr                     | [19]               |
| Poly(1,4-butylene succinate) (PBS)                   | Compost                     | 25–50 | 0.01–0.21                  | 1–17 yr                     |                    |
|  | <i>Natural materials</i>    |       |                            |                             |                    |
| Beeswax  | Oil-contaminated soil       | 20    | 0.94                       | 3–4 mo                      | [22]               |
| Wheat gluten   | Soil                        | 20–22 | 1.90                       | 47 d                        | [22]               |
|  | Compost                     | 58    | 4.55                       | 20 d                        | [24]               |
| Cellulose  | Marine Water                | 30    | 0.19                       | 16 mo                       | This work (Fig. 2) |
|  | Compost                     | 58    | 1.06                       | 2–3 mo                      | [25]               |
| Sodium alginate edible film                          | Soil                        | 37    | 2.60                       | 35 d                        | [26]               |
| Guar gum   | Compost                     | 15–25 | 7.14                       | 13 d                        | [27]               |
| Zein film  | Soil (solid waste landfill) | 30    | 4.05                       | 22 d                        | [28]               |
|  | Soil (lagoon)               | 30    | 4.05                       | 22 d                        |                    |
| Alginate film  | Compost                     | 32    | 2.57                       | 35 d                        | [29]               |
| <i>Synthetic materials</i>                           |                             |       |                            |                             |                    |
| Poly(vinyl alcohol) (PVA)                            | Marine and Wastewater       | 25    | 0.62 to <0.01 <sup>a</sup> | 5 mo to >20 yr <sup>a</sup> | [30–33]            |
|  | Soil                        | 15–25 | 0.30–0.31                  | 9–10 mo                     | [34]               |
|  | Compost                     | 58    | 0.49                       | 6 mo                        | [25]               |

(continued)



**Table 3**  
(continued)

| Material   | Condition             | Temperature [°C] | Average biodegradation per day [%] | Residence time | References |
|--|-----------------------|------------------|------------------------------------|----------------|------------|
| Carboxymethyl cellulose (CMC) [DS 0.44]<br>CMC [DS 0.75] | Wastewater            | 25               | 1.34                               | 2–3 mo         | [30]       |
|  | Wastewater            | 25               | 0.54                               | 5–6 mo         |            |
| Cellulose acetate (CA) [2.85]                            | Soil                  | 15–25            | 0.25                               | 1 yr           | [35]       |
| Paraffin wax   | Oil contaminated soil | 20               | 1.01                               | 3 mo           | [22]       |
| Low-density polyethylene (LDPE)                          | Soil                  | 15–25            | 0.01                               | 20 yr          | [36]       |

<sup>a</sup>Material showed no biodegradation – set average % per day to “<0.01” and residence time to “>20 yr” as minimum and maximum cutoffs

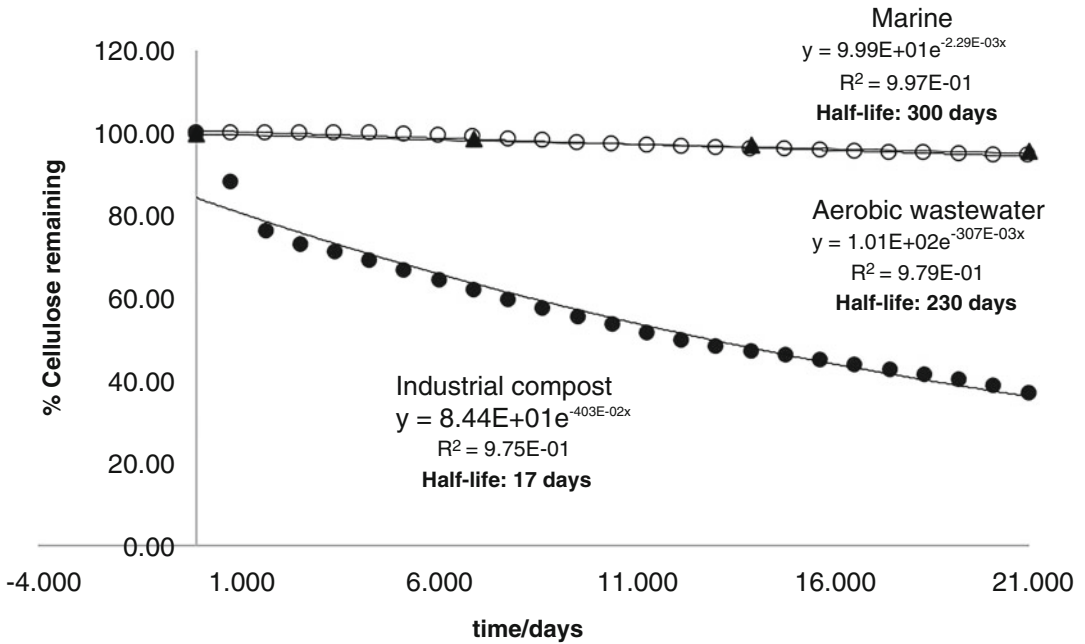


**Fig. 3** Pseudo first-order fits and half-lives of cellulose in marine, aerobic wastewater, and compost environments

$k_{\text{obs}}$  is the observed pseudo first-order rate constant, and  $t$  represents time. In Eq. 4,  $t_{1/2}$  signifies the material's half-life under the given test conditions and  $k$  is the first-order rate constant (e.g.,  $k_{\text{obs}}$  from Eq. 1). Residence times, defined as the time needed to obtain 90% biodegradation, can be estimated using linear fits of average rates, as shown in Table 3, or pseudo first-order kinetics. Due to the nonlinearity of typical kinetics, linear fits of initial rates tend to underestimate material residence times. In the absence of an induction period, which is typically modeled with additional parameters, a residence time is more accurately determined by ca. 3.3 half-lives obtained from a pseudo first-order fit.

### Conclusions

Biodegradation rates are a product of many factors, including test medium (e.g., compost, marine, active landfill), inoculum selection (e.g., organisms are acclimated or nonacclimated to the test material), and temperature. Standard conditions exist for many of these environments. Rates can be evaluated using kinetics to estimate material residence times under a given set of conditions. The rigorous evaluation of material biodegradability has the potential to mainstream the use of nonpersistent materials as part of a more circular economy that generates waste as a feedstock.

---

## 4 Notes

1. Compost needs to be either newly purchased or no more than 2 months old.
2. Sample selection process is of utmost importance for making proper comparisons. As the contact of compost with plastic within the respirometer chamber is critical, the plastic samples need to be uniformly selected for similar surface area. For this reason, grinding the samples can be performed. However, some would argue that the results obtained from ground plastic are unrealistic. On one hand, grinding of the plastic enlarges the specific surface area and provides better contact with the degradation media thus enhancing the overall degradation rate. While using films, the samples have to be selected for a uniform thickness and cut to the same size. This is especially difficult when plastic blends are analyzed. Foams and fiber mats that have smaller density than the media tend to float on the surface, thus only one surface is exposed for the degradation. This is a challenge that the experimenter must address individually.
3. The level of regulated heavy metals can be measured with flame atomic absorption spectrophotometer using an air-acetylene flame and equipped with a Pb hollow-cathode lamp. The compost samples must have regulated metals concentrations less than 50% of the acceptable levels of regulated heavy metals as prescribed in 40 CFR Part 503.13, that is, lead ( $75 \text{ mg}\cdot\text{kg}^{-1}$ ), cadmium ( $17.5 \text{ mg}\cdot\text{kg}^{-1}$ ), chromium (not specified), copper ( $375 \text{ mg}\cdot\text{kg}^{-1}$ ), nickel ( $105 \text{ mg}\cdot\text{kg}^{-1}$ ), zinc ( $700 \text{ mg}\cdot\text{kg}^{-1}$ ), and mercury ( $4.25 \text{ mg}\cdot\text{kg}^{-1}$ ).
4. The sieving process removes all large particles like stones, glass, metal, and pieces of wood. It is critical to minimizing experimental variations in the mineralization rate. After the screening, the compost is thoroughly mixed and is allowed to equilibrate for moisture.
5. To ensure there is good contact of the compost with the sample, first place half of the necessary amount of compost in the chamber. This is followed by the addition of the sample and finally by the rest of the compost.
6. The moisture of the compost, which usually falls within a 35–40% range, is determined in triplicates that have to agree within 0.25%. As the wet compost does not mix well with the sample, the final moisture is adjusted after the sample and appropriate amount of “dry” compost are placed in the respirometer chamber.

7. With every sampling time, 50% of the headspace gas is replaced with atmospheric air, providing adequate oxygenation of the compost.
8. It is important to have a positive control, either cellulose or starch, to observe total carbon released and the rate of the reaction. The positive control would show almost an instant response. Starch, either as film or as powder, degrades within the first week. Cellulose is used completely within 2–4 weeks.
9. The water is either collected from the open sea area or other surface water sources, and used within 3 days of collection.
10. The chambers were situated away from the sunlight to minimize the effect of ultraviolet degradation.
11. The amount of carbon can also be determined experimentally via calorimetry or found in the literature.
12. Biodegradation of bioplastic is calculated on the basis of carbon dioxide emitted from the samples with respect to CO<sub>2</sub> emitted from the positive control samples.

## References

1. Fornasiero P, Graziani M (2006) Renewable resources and renewable energy: a global challenge, 2nd edn. CRC Press
2. BioPreferred Program. <https://www.biopreferred.gov/BioPreferred/faces/pages/AboutBioPreferred.xhtml>. Accessed 5 Feb 2021
3. Choi B, Yoo S, Park S (2018) Carbon footprint of packaging films made from LDPE, PLA, and PLA/PBAT blends in South Korea. Sustainability 10:2369. <https://doi.org/10.3390/su10072369>
4. Greene JP (2014) Introduction to sustainability. In: Sustainable plastics. Wiley, Hoboken
5. ASTM D6400-19 (2019) Standard specification for labeling of plastics designed to be aerobically composted in municipal or industrial facilities. ASTM International, West Conshohocken. [www.astm.org](http://www.astm.org)
6. ASTM D6868-21 (2021) Standard specification for labeling of end items that incorporate plastics and polymers as coatings or additives with paper and other substrates designed to be aerobically composted in municipal or industrial facilities. ASTM International, West Conshohocken. [www.astm.org](http://www.astm.org)
7. ASTM D7081-05 (2005) Standard specification for non-floating biodegradable plastics in the marine environment (withdrawn 2014). ASTM International, West Conshohocken. [www.astm.org](http://www.astm.org)
8. International Organization for Standardization (2012) Specifications for compostable plastics (ISO 17088:2012) <https://www.iso.org>
9. European Standards (2000) Requirements for packaging recoverable through composting and biodegradation. (BS EN 13432:2000) <https://www.en-standard.eu>
10. International Organization for Standardization (2019) Determination of the degree of disintegration of plastic materials under defined composting conditions in a pilot-scale test. (ISO 16929:2019) <https://www.iso.org/>
11. International Organization for Standardization (2015) Determination of the degree of disintegration of plastic materials under simulated composting conditions in a laboratory-scale test. (ISO 20200:2015) <https://www.iso.org/>
12. ASTM D5338-15 (2021) Standard test method for determining aerobic biodegradation of plastic materials under controlled composting conditions, incorporating thermophilic temperatures. ASTM International, West Conshohocken. [www.astm.org](http://www.astm.org)
13. International Organization for Standardization (2018) Determination of the ultimate aerobic biodegradability of plastic materials under

- controlled composting conditions — Method by analysis of evolved carbon dioxide — Part 2: Gravimetric. (ISO 14855-2:2018) <https://www.iso.org/>
14. Ohtaki A, Akakura N, Nakasaki K (1998) Effects of temperature and inoculum on the degradability of poly-ε-caprolactone during composting. *Polym Degrad Stab* 62:279–284. [https://doi.org/10.1016/S0141-3910\(98\)00008-1](https://doi.org/10.1016/S0141-3910(98)00008-1)
  15. Mezzanotte V, Bertani R, Innocenti FD, Tosin M (2005) Influence of inocula on the results of biodegradation tests. *Polym Degrad Stab* 87: 51–56. <https://doi.org/10.1016/j.polymdegradstab.2004.06.009>
  16. Krzan A, Hemjinda S, Miertus S et al (2006) Standardization and certification in the area of environmentally degradable plastics. *Polym Degrad Stab* 91:2819–2833. <https://doi.org/10.1016/j.polymdegradstab.2006.04.034>
  17. Beegle JR, Borole AP (2017) An integrated microbial electrolysis-anaerobic digestion process combined with pretreatment of wastewater solids to improve hydrogen production. *Environ Sci Water Res Technol* 3:1073–1085. <https://doi.org/10.1039/C7EW00189D>
  18. Narancic T, Verstichel S, Reddy Chaganti S et al (2018) Biodegradable plastic blends create new possibilities for end-of-life management of plastics but they are not a Panacea for plastic pollution. *Environ Sci Technol* 52:10441–10452. <https://doi.org/10.1021/acs.est.8b02963>
  19. Al Hosni AS, Pittman JK, Robson GD (2019) Microbial degradation of four biodegradable polymers in soil and compost demonstrating polycaprolactone as an ideal compostable plastic. *Waste Manag* 97:105–114. <https://doi.org/10.1016/j.wasman.2019.07.042>
  20. Abou-Zeid D-M, Müller R-J, Deckwer W-D (2001) Degradation of natural and synthetic polyesters under anaerobic conditions. *J Biotechnol* 86:113–126. [https://doi.org/10.1016/S0168-1656\(00\)00406-5](https://doi.org/10.1016/S0168-1656(00)00406-5)
  21. Pinheiro IF, Ferreira FV, Souza DHS et al (2017) Mechanical, rheological and degradation properties of PBAT nanocomposites reinforced by functionalized cellulose nanocrystals. *Eur Polym J* 97:356–365. <https://doi.org/10.1016/j.eurpolymj.2017.10.026>
  22. Hanstveit AO (1992) Biodegradability of petroleum waxes and beeswax in an adapted CO<sub>2</sub> evolution test. *Chemosphere* 25:605–620. [https://doi.org/10.1016/0045-6535\(92\)90291-X](https://doi.org/10.1016/0045-6535(92)90291-X)
  23. Ye P, Reitz L, Horan C, Parnas R (2006) Manufacture and biodegradation of wheat gluten/basalt composite material. *J Polym Environ* 14: 1–7. <https://doi.org/10.1007/s10924-005-8701-3>
  24. Zhang X, Gozukara Y, Sangwan P et al (2010) Biodegradation of chemically modified wheat gluten-based natural polymer materials. *Polym Degrad Stab* 95:2309–2317. <https://doi.org/10.1016/j.polymdegradstab.2010.09.001>
  25. Lešinský D, Fritz J, Braun R (2005) Biological degradation of PVA/CH blends in terrestrial and aquatic conditions. *Bioresour Technol* 96: 197–201. <https://doi.org/10.1016/j.biortech.2004.05.008>
  26. Mahcene Z, Khelil A, Hasni S et al (2020) Development and characterization of sodium alginate based active edible films incorporated with essential oils of some medicinal plants. *Int J Biol Macromol* 145:124–132. <https://doi.org/10.1016/j.ijbiomac.2019.12.093>
  27. Kaith BS, Sharma R, Kalia S (2015) Guar gum based biodegradable, antibacterial and electrically conductive hydrogels. *Int J Biol Macromol* 75:266–275. <https://doi.org/10.1016/j.ijbiomac.2015.01.046>
  28. Romero-Bastida CA, Flores-Huicochea E, Martin-Polo MO et al (2004) Compositional and moisture content effects on the biodegradability of Zein/Ethylcellulose films. *J Agric Food Chem* 52:2230–2235. <https://doi.org/10.1021/jf0350414>
  29. Deepa B, Abraham E, Pothan LA et al (2016) Biodegradable nanocomposite films based on sodium alginate and cellulose Nanofibrils. *Materials* 9:50. <https://doi.org/10.3390/ma9010050>
  30. Wirick MG (1974) Aerobic biodegradation of Carboxymethylcellulose. *J Water Pollut Control Feder* 46:512–521
  31. Rolsky C, Kelkar V (2021) Degradation of Polyvinyl Alcohol in US Wastewater treatment plants and subsequent Nationwide emission estimate. *Int J Environ Res Public Health* 18(11):6027. <https://doi.org/10.3390/ijerph18116027>
  32. Chiellini E, Corti A, Solaro R (1999) Biodegradation of Poly(Vinyl Alcohol) based blown films under different environmental conditions 11 part of work herewith reported was presented at the 5th scientific workshop on biodegradable polymers and plastics, Stockholm (Se) June 1998. *Polym Degrad Stab*, 64(2): 305–312. [https://doi.org/10.1016/S0141-3910\(98\)00206-7](https://doi.org/10.1016/S0141-3910(98)00206-7)

33. Alonso-López O, López-Ibáñez S, Beiras R (2021) Assessment of toxicity and biodegradability of Poly(Vinyl Alcohol)-based materials in marine water. *Polymers* 13(21):3742. <https://doi.org/10.3390/polym13213742>
34. Abd El-Mohdy HL, Ghanem S (2008) Biodegradability, antimicrobial activity and properties of PVA/PVP hydrogels prepared by  $\gamma$ -irradiation. *J Polym Res* 16:1. <https://doi.org/10.1007/s10965-008-9196-0>
35. Fei Z, Huang S, Yin J et al (2015) Preparation and characterization of bio-based degradable plastic films composed of cellulose acetate and starch acetate. *J Polym Environ* 23:383–391. <https://doi.org/10.1007/s10924-015-0711-1>
36. Goheen SM, Wool RP (1991) Degradation of polyethylene–starch blends in soil. *J Appl Polym Sci* 42:2691–2701. <https://doi.org/10.1002/app.1991.070421007>



## Biodegradability of Polymers by Relatively Low-Cost and Readily Available Nonautomated Respirometry

Alex S. Babetto, Laís T. Possari, Baltus C. Bonse, and Sílvia H. P. Bettini

### Abstract

Humanity is currently consuming natural resources 1.75 times faster than the planet can regenerate in a year, so the regeneration of these natural resources has become an issue of pressing concern. New drivers have pointed to actions that minimize future impacts, which include reducing plastic waste in the environment, recycling, and the use of biodegradable polymers. The definition and determination of biodegradability of polymers has been a topic of discussion in the scientific community, mainly related to the criteria used to define biodegradability. Academic studies have shown excellent results on polymer biodegradation tests with automated respirometry methods; however, these tests are relatively expensive and may not be readily available. This protocol presents an alternative to automated respirometry (procedure and monitoring), detailing the procedure of a polymer biodegradation test with nonautomated respirometry and monitored by titrimetry. The protocol is based on the international standards ASTM D5338-15, ASTM D5988-18, ASTM D6400-19, ISO 14855-1:2012, and ISO 17556:2019. Proper execution of the protocol will guarantee the correct performance of respirometric polymer biodegradation tests, providing reproducible and accurate results.

**Key words** Biodegradation, Nonautomated respirometry, Titrimetry, Simplified Bartha, Standards

---

## 1 Introduction

Biodegradable polymers have shown to be a promising alternative to conventional nonbiodegradable polymers, which accumulate in landfills and ecosystems, contributing to serious environmental problems [1]. Briefly, biodegradable polymers can be described as those capable of undergoing degradation due to biotic action promoted by microorganisms, such as fungi, algae, and bacteria [2]. In this process, the polymer molecules are converted into an energy source for the microorganisms, as well as biomass and simple molecules, such as water (H<sub>2</sub>O), carbon dioxide (CO<sub>2</sub>), and methane (CH<sub>4</sub>) [3].

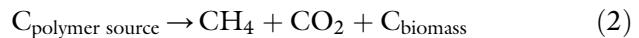
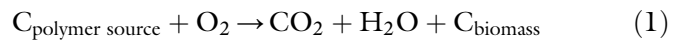
It should be mentioned that not all biodegradable polymers derive from renewable resources. Biodegradable polymers can be

obtained both from renewable (biobased) and fossil (fossil-based) resources [2]. The origin of the polymer is not directly related to its biodegradability [4].

The biotic degradation process is complex and can be divided into three important stages, namely: (i) biodeterioration (or bioerosion), (ii) biofragmentation, and (iii) assimilation. Biodeterioration occurs due to the adhesion and growth of microbial colonies onto the surface of the material. The biofilm formed penetrates the pores of the substrate changing their size and distribution, resulting in brittleness and cracks. The material starts disintegrating into smaller pieces and suffers significant loss in physical and mechanical properties. The growth of the biofilm may be either intensified or restricted by environmental conditions (such as pH, temperature, and moisture) as well as by the roughness and polarity of the material. In addition, microorganisms secrete enzymes that may catalyze the scission of specific bonds in the polymer chains, such as lipases and esterases that catalyze hydrolysis reactions, promoting surface erosion of the substrate [3, 5].

In the biofragmentation stage the biotic action causes polymer chain scission by degradation reactions catalyzed by the excretion of enzymes and byproducts (such as organic acids and peroxides), resulting in progressive reduction in molar mass and release of monomers and/or oligomers [3, 6]. For this to happen, the bond that will be attacked should be accessible to the active site of the enzyme. Therefore, amorphous regions and flexible linear chains are more susceptible to microbiological attack [7].

The final stage of biodegradation is assimilation, in which molecules of sufficiently low molar masses are diffused into cells and metabolized to produce adenosine triphosphate (ATP) and compose cellular structures (biomass). In this process, small molecules (e.g.,  $\text{H}_2\text{O}$ ,  $\text{CO}_2$ ,  $\text{CH}_4$ , and salts) are released, a phenomenon called mineralization [3]. Equations 1 and 2 represent, respectively, the chemical conversion involved in the aerobic and anaerobic biodegradation of any polymer composed only of carbon, hydrogen, and oxygen atoms [6]:



Biodegradation is a complex process, and its occurrence and rate are conditioned by several factors, from the chemical and physical characteristics of the material to the environmental conditions in which the material is used and disposed of. Therefore, assessing a polymer's biodegradability is not trivial, and several experimental methods can be used in the laboratory to monitor biodegradation at different stages [3, 8].

Some studies employ methods that use enzymes and cell culture; however, these tests provide situations that strongly deviate



from reality. Natural environments, into which plastic waste is often discarded, have a great diversity of microbiota and other carbon sources that may be preferable to microorganisms, in addition to the polymer. Therefore, for more reliable results, most of the methods standardized by the American Society for Testing and Materials (ASTM) and by the Organization for Economic Cooperation and Development (OECD) determine the use of simulated or real environments [8]. The incubation media for assessing biodegradation can be soil, compost, marine waters, activated sludge, or wastewater effluents [9].

Monitoring the level of disintegration and the percentage mass loss of the degraded material in different media are frequently used in scientific studies. These tests provide information on biodeterioration rather than on the biodegradation process as a whole [3]. Sample disintegration does not necessarily reflect mineralization and may result only from its fragmentation into microplastics—readers are invited to refer to Chap. 3 for more information on microplastics. This may even render the technique susceptible to high margins of error due to the difficulty of recovering the sample fragments as biodeterioration advances. Other methods are often used to complement this type of analysis, such as observing surface erosion with microscopic techniques and changes in physicochemical properties [10, 11].

Other techniques enable the identification of low-molar mass fragments, changes in the chemical structure of the polymer itself, and the presence of degradation products resulting from biofragmentation, such as size-exclusion chromatography (SEC), nuclear magnetic resonance (NMR), and Fourier-transform infrared spectrometry (FTIR). In this case, it is possible to access information about sample biofragmentation [3, 11].

The aforementioned analyses certainly provide important perspectives for understanding biodegradation; however, they are not sufficient to support claims on the biodegradability of a polymer [1]. The occurrence of mineralization and, therefore, of the biotic degradation process is only effectively assessed by monitoring O<sub>2</sub> consumption and/or CO<sub>2</sub> production under aerobic conditions and, in the case of anaerobic degradation, the release of CH<sub>4</sub>. These methods are called respirometric methods [3]. To avoid erroneous conclusions and guarantee some real progress in the field of biodegradable polymers, it is essential to carry out respirometry. Note that biodegradation is not an intrinsic characteristic of the material but depends on the conditions at which it occurs. Thus, rigorous discussion is needed [1]. In addition to the different possible media (soil, compost, seawater, etc.), the standards specify parameters such as presence or absence of oxygen (aerobic or anaerobic condition), pH range, relative humidity, and incubation temperature (thermophilic condition, typically 58 °C; or

mesophilic, up to 30 °C). Thermophilic temperatures are normally used in industrial composting plants or anaerobic digesters [12, 13].

Respirometric methods are specified by international (ISO, OECD) or regional (ASTM, CEN, etc.) regulatory agencies covering a wide range of time intervals, apparatuses, media, and conditions [14]. Some examples are shown in Table 1. More information on biodegradation standards can be found elsewhere [15, 16].

These standards also define the criteria (time and rate of mineralization) to certify a polymer as biodegradable in each culture medium and environmental conditions. ASTM 6400-19, ISO 17088:2012, and EN 13432:2012 standards, for example, state that for a polymer to be certified as biodegradable, at least 90% of its carbon must be converted into CO<sub>2</sub> within 6 months of biodegradation, compared to the positive reference polymer or in absolute terms, when in a simulated industrial composting medium. In addition, disintegration and ecotoxicity criteria are also established. In the case of biodegradation in soil, the European standard EN 17033:2018 for mulching films states that mineralization must reach 90% within 2 years.

In most of the published studies, respirometry is conducted under simulated industrial composting conditions [17]. Some polymers are considered biodegradable only under thermophilic conditions, as is the case with one of the most well-known polymers in this class—poly(lactic acid), PLA [13]. However, installing industrial composting plants is still not a reality in many locations, and the waste collection and separation systems are often ineffective. Annually, 400 Mt of plastic waste are produced worldwide and of this amount, 58% ends up in landfills and in the environment [11]. Therefore, the destination of most of the waste is common soil, where the temperature does not normally exceed 30 °C (mesophilic condition). In this context, respirometry systems in mesophilic and aerobic conditions (common soil or domestic compost) can be considered more realistic, although still scarce in the literature [17].

Quantification of mineralization over time is often performed by monitoring the evolution of CO<sub>2</sub>, using either continuous or discrete measurements. To this end, different methods can be used: (i) automated systems with direct analysis of evolved gases by means of gas chromatography or infrared spectroscopy (direct measurement respirometry, DMR)—readers can refer to Chapter 1 for details on automated respirometry; (ii) by capturing CO<sub>2</sub> in alkaline solutions (such as Ba(OH)<sub>2</sub>, KOH, or NaOH) and quantifying by titration (cumulative measurement respirometry, CMR); and (iii) CO<sub>2</sub> capture can also be carried out in absorption columns with NaOH pellets and is measured by gravimetric measurement respirometry (GMR), but the use of this technique is less frequent in the literature [12].

**Table 1**  
**Biodegradability standards and certifications of polymer materials in different types of environments**

| Simulated environment | Standard   | Certification organizations  |
|-----------------------|--|--|
| Industrial composting | EM 13432, ASTM D5338 and ISO 14855 for packaging; EN 14995 and ISO 17088 for polymer materials in general; ASTM 6868 materials containing polymer components | TÜV Austria (Austria), DIN CERTCO (Germany), Vinçotte (Belgium), Biodegradable Products Institute (BPI—USA), Japan BioPlastics Association (JBPA—Japan), Finnish Solid Waste Association (Finland) |
| Domestic composting   | prEN 17427, AS 5810 (Australia), NF T 51800 (France)   | TÜV Austria (Austria), DIN CERTCO (Germany), Vinçotte (Belgium)  |
| Soil                  | ASTM D5988, ISO 17556, EN 17033  | DIN CERTCO (Germany), Vinçotte (Belgium)   |
| Seawater              | OECD 306, ISO 16221, ASTM D6691  | Vinçotte (Belgium), TÜV Austria (Austria)  |
| Landfills             | ASTM D5526   |  |
| Anaerobic Digestion   | ISO 15985, ISO 14853, ASTM D5511   |  |
| Aqueous medium        | ISO 14851, ISO 14852, and ISO 14853  | Japan BioPlastics Association (JBPA—Japan)   |

Kale et al. [18] assessed the biodegradation of PLA bottles under composting conditions using CMR and GMR systems. In the former case, the experiment was developed by the researchers to comply with ASTM D5338-15 and ISO 14855-1:2012 standards. The GMR apparatus was purchased, and its construction was based on the ISO 14855-2:2012 standard. The results showed considerable differences between the biodegradation curves obtained with the different systems, which the authors attributed to the different compost/sample ratios and sample sizes. In addition, it should be mentioned that due to the configuration of the GMR device, the adequate number of samples required, according to the ISO 14855-2 standard, could not be met.

In the study of Cadar et al. [19], two methods were used to assess the biodegradation of PLA and its copolymers. In both cases, CO<sub>2</sub> was absorbed by alkaline solutions, one method with quantification by titrimetry and the other by elemental analysis of the solution, in a partially automated way. The same compost was used in both analyses, but the solutions were different: 0.125 M BaOH and 0.05 M NaOH, respectively. The curves obtained showed similar biodegradation behavior of the positive control and of the polymers; however, the total absolute values at the end of the period showed significant differences.

Comparing respirometry results of samples that do not belong to the same set of tests is hampered by the many variables affecting the biodegradation process [12]. Some of these cannot be strictly controlled, such as the characteristics of the culture medium and microorganisms present in this medium. As shown in the study by Castro-Aguirre et al. [12], even with the use of the same system (apparatus) and methodology, the activity of the pure compost (evolution of CO<sub>2</sub>) varied with its physicochemical properties and, consequently, from where and when it was taken.

This can be seen in Table 2, which presents the results of the biodegradation of microcrystalline cellulose (MCC) in the form of powder under the conditions set by ISO 14855-1:2012 and ASTM D5338-15, that is, compounded at a mass proportion of 6:1 in relation to the sample and temperature of (58 ± 2) °C. In the same way, procedures in accordance with the standards used in studies with PLA films are listed in Table 3. In this case, additional variables are included, such as characteristics of the PLA, film thickness, and the compost/sample ratio, which in most of the studies diverged from the value specified by the standards.

**Table 2**

**Biodegradation data of cellulose in an industrial composting environment reported in the literature, using different respirometry methods**

| Biodegradation [%] | Time [d] | Method                       | References | Standard    | Origin of the compost                       |
|--------------------|----------|------------------------------|------------|-------------|---|
| 72.4–82.5          | 45       | DMR                          | [14]       | ISO 14855-1 | 3-month-old industrial plant compost        |
| 78                 | 85       | DMR                          | [20]       | ISO 14855-1 | 2- to 3-month-old industrial plant compost  |
| 83                 | 110      | DMR                          | [21]       | ISO 14855-1 | 2-month-old municipal organic waste compost |
| 76                 | 110      | CMR                          | [19]       | ISO 14855-1 | 3-month-old organic domestic waste compost  |
| 83                 | 110      | CMR with automated measuring | [19]       | ISO 14855-1 | 3-month-old organic domestic waste compost  |
| 70                 | 46       | CMR                          | [22]       | ASTM D5338  | 3-month-old municipal organic waste compost |
| 90                 | 100      | CMR                          | [23]       | ASTM D5338  | Not mentioned                               |
| 74                 | 56       | CMR                          | [24]       | ISO 14855-1 | Industrial plant compost                    |
| 94.34              | 120      | CMR                          | [25]       | ASTM D5338  | Agriculture waste compost                   |

**Table 3**  
**Biodegradation data of poly(lactic acid) (PLA) in an industrial composting environment reported in the literature, using different respirometric methods**

| Biodegradation [%] | Time [d] | Method                       | References | Standard            | Origin of the compost                      | Compost/sample | Thickness [mm] | PLA                        |
|--------------------|----------|------------------------------|------------|---------------------|--|----------------|----------------|----------------------------|
| 45                 | 75       | DMR                          | [26]       | ISO 14855-1 adapted | Commercial compost                         | 15-1           | 0.2            | Ingeo 3001D                |
| 80                 | 90       | CMR                          | [27]       | ISO 14855-1         | Municipal solid waste compost              | 85-15          | 0.5            | 4032D                      |
| 69-72              | 110      | CMR                          | [19]       | ISO 14855-1         | 3-month-old organic domestic waste compost | 6-1            | Not mentioned  | Synthesized and commercial |
| 83-86              | 110      | CMR with automated measuring | [19]       | ISO 14855-1         | 3-month-old organic domestic waste compost | 6-1            | Not mentioned  | Synthesized and commercial |
| 94.2               | 136      | DMR                          | [28]       | ASTM D5338          | Prepared by authors                        | 7-5            | 0.45           | 2003D                      |
| 85.75              | 120      | CMR                          | [25]       | ASTM D5338          | Organic agriculture waste compost          | 6-1            | 0.3            | Commercial grade           |

Results from laboratory aerobic biodegradation tests using conventional (nonautomated) respirometry allow one to estimate the biodegradability of polymer materials using soil or compost as a culture medium and, thus, simulate the material's aerobic biodegradation behavior when discarded in a terrestrial environment or discarded and destined to a composting plant (municipal, industrial, or domestic). For soil biodegradation, the test temperature may vary between 20 and 28 °C, simulating a condition that can be easily found worldwide. On the other hand, biodegradation in compost must be carried out at  $(58 \pm 2)$  °C, which is the standard temperature in the composting plants, as the microorganisms in these environments are thermophilic. The validation of the tests will depend mainly on the microbial activity of the culture medium. Therefore, the choice of culture medium is important for the success of the test, primarily in relation to the choice of the soil if the option is biodegradation in soil. If the test is conducted in compost, this concern is less significant, as this substrate is normally supplied with significant microbial activity. Comparatively, the biodegradation tests in compost are significantly more intense than in soil, even if the selected soil is extremely active (fertile), due to the amount and thermophilic characteristics of the microorganisms that compose the compost [29–35].

The Materials and Methods addressed in this chapter are based on the international standards ASTM D5338-15, ASTM D5988-18, ASTM D6400-19, ISO 14855-1: 2012, and ISO 17556:2019.

---

## 2 Materials

### ***2.1 System for the Development of Biodegradation in Large Volumes***

Glass vessel with internal volume between 2 and 4 L, glass lid with sealing ring (elastomer), and lock that guarantees the system is airtight. Inside this vessel, a 250-mL Erlenmeyer flask, a 100-mL beaker, and a perforated plate (glass or porcelain) will be fitted. The dimension of the perforated plate must be such to fit in the container and to hold the Erlenmeyer flask and the beaker. The culture medium is deposited on the bottom of the vessel and the perforated plate must be held by supports (glass or porcelain) at a minimum free height (i.e., above the culture medium) of 1 cm. A representative image of this system is shown in Fig. 1. See the required amounts in Subheading 3.1 of this protocol.

### ***2.2 System for the Assessment of Biodegradation in Small Volumes***

Simplified Bartha Respirometer consisting of a 250-mL Erlenmeyer flask and a 125-mL test tube (40 mm in diameter and 100 mm in height) connected to one another by a tube soldered on the side of both constituents, forming, together with two rubber stoppers, an airtight system. An illustrative image of this system is shown in Fig. 1. See the required amounts in Subheading 3.2 of this protocol.

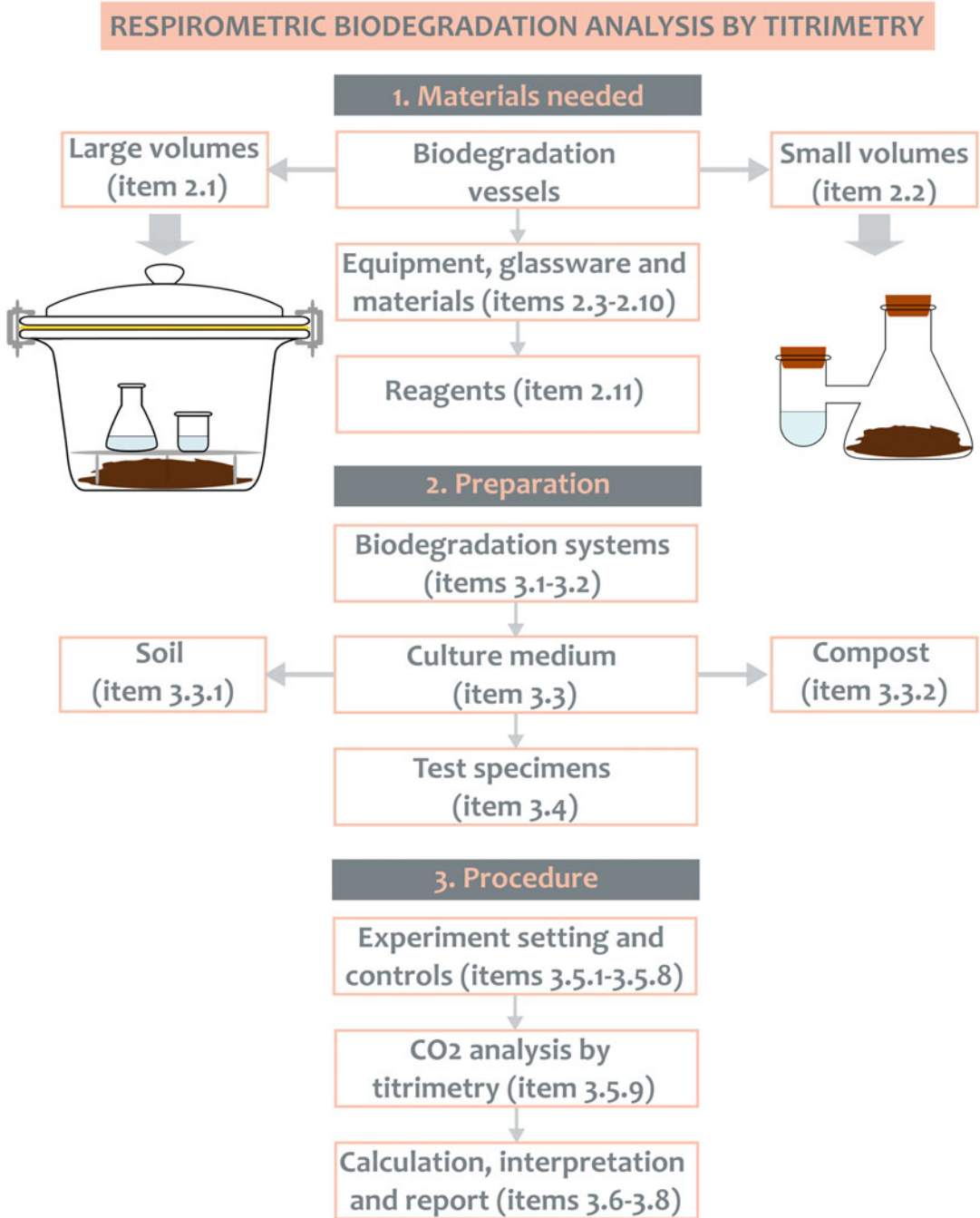


**Fig. 1** Flowchart for the assessment of polymer biodegradability via titrimetry in both large- and small-volume samples

**Note (1):** this system can be purchased ready-made. Compared to the previous system, it presents two drawbacks: low amount of culture medium (50 g) and sample for the test (between 0.4 and 2 mg per gram of culture medium) and increased possibility of errors in the analysis by titrimetry due to the need to transfer the analytical solution.

**2.3 Biodegradation Test Chamber**

Darkened temperature-controlled chamber (between 20 and 28 °C for soil and 58 °C for compost, maintaining the selected temperature at  $\pm 2$  °C).

**Note (2):** The volume of the chamber must be sufficient to hold all the systems (highlighted in Subheadings 2.1 or 2.2) of the same test, as it is not recommended to separate the systems of the same test in different chambers. Test temperature and darkness conditions should be equal.

**2.4 Apparatus for Analysis of the Sample and Culture Medium**

See ASTM D5988-18.

**2.5 Culture Medium**

See Subheadings 3.3.1 (soil) and 3.3.2 (compost) of this protocol.

**2.6 Positive Reference Polymer**

MCC with average particle size less than 20  $\mu\text{m}$  should be used as a positive reference for biodegradation. Thermoplastic starch can also be used as positive reference.

**2.7 Negative Reference Polymer**

Low-density polyethylene (LDPE) can be used as a negative reference. Other polyethylenes, such as high-density polyethylene (HDPE), can also be used as negative reference.

**2.8 Test Polymer**

Characteristics described in Subheading 3.4 of this protocol.

**2.9 Materials for Determining the Residual Moisture Content and the Field Capacity**

2.9.1 Conical polypropylene funnel (250 mL in volume, top diameter of 120 mm, stem diameter of 19 mm, stem length of 81 mm, and cone height of 89 mm): three units.

2.9.2 Ring stand: one unit.

2.9.3 Iron ring (diameter of 7 cm) with clamp: one unit.

2.9.4 Narrow-mouth Erlenmeyer flask (250 mL in volume): three units.

2.9.5 Pharmaceutical grade cotton ball: ca. 100 g.

2.9.6 Glass Petri dish 100/15 mm: three units.

2.9.7 Large rectangular stainless-steel tray (ca. 40 cm long, 30 cm wide, and 4 cm deep or greater): two units.



- 2.9.8 Plastic bucket (polyethylene or polypropylene) of at least 5 L, with lid: one unit.
- 2.9.9 Oven for drying at 105 °C: one unit.
- 2.9.10 Desiccator (minimum size of 5 L): one unit.
- 2.9.11 Semi-analytical balance (minimum accuracy: 0.01 g): one unit.
- 2.9.12 Beaker (500 mL in volume): one unit.
- 2.9.13 Beaker (150 mL in volume): one unit.
- 2.9.14 Common laboratory utensils (spatulas, glass rods, etc.).

### **2.10 Materials for Biodegradation Monitoring (Titrimetry)**

- 2.10.1 Glass Erlenmeyer flask (250 mL in volume): one unit per system under test.
- 2.10.2 Graduated glass burette (100 mL, for the system described in Subheading 2.1 of this protocol) or automatic titrator: two units.
- 2.10.3 Graduated glass burette (50 mL, for the system described in Subheading 2.2 of this protocol) or automatic titrator: two units.
- 2.10.4 Volumetric glass pipette (100 mL, for the system described in Subheading 2.1 of this protocol): one unit.
- 2.10.5 Volumetric glass pipette (10 mL, for the system described in Subheading 2.2 of this protocol): one unit.
- 2.10.6 Polypropylene syringe (10 mL): one unit.
- 2.10.7 Urinary catheter size 6 Fr (outer diameter of 2 mm): one unit.
- 2.10.8 Pipette filler bulb with a three-way valve system: two units.
- 2.10.9 Ring stand: two units.
- 2.10.10 Burette clamps: four units.
- 2.10.11 Glass beaker (1 L): one unit.
- 2.10.12 Stopwatch (analog or digital): one unit.

### **2.11 Reagents for Biodegradation Testing and Monitoring**

- 2.11.1 CO<sub>2</sub>-free distilled water.

**Note (3):** To remove CO<sub>2</sub> from distilled water, boil the water for 30 min and place the warm water in a glass vessel (Erlenmeyer flask, e.g.) equipped with an ascarite valve/filter (CO<sub>2</sub> absorber) to cool. After cooling, close the valve, keeping it closed when not in use. CO<sub>2</sub>-free water that is not used should be discarded at the end of the reagent preparation procedures. Whenever CO<sub>2</sub>-free water is needed, it should be prepared on the day of use.

2.11.2 Potassium hydroxide (KOH) or sodium hydroxide (NaOH) as 0.5 N solution in CO<sub>2</sub>-free distilled water. Prepare 1–2 L of solution at a time.

**Note (4):** Alternatively, a 0.25 N barium hydroxide [Ba(OH)<sub>2</sub>] solution may be used; however, this solution may promote formation of a barium carbonate (BaCO<sub>3</sub>) film, preventing diffusion of CO<sub>2</sub> in the alkaline solution. Therefore, KOH is more suitable. Yet, the use of KOH involves the preparation of a 1 N barium chloride (BaCl<sub>2</sub>) solution, which is used to precipitate the CO<sub>2</sub> from the test in the form of the stable BaCO<sub>3</sub> salt (*see* reactions in Subheading 3.6 of this protocol).

**Note (5):** Standardize the alkaline solution (KOH or NaOH or Ba(OH)<sub>2</sub>) against a 0.5 N solution of potassium acid phthalate (item 2.11.3 of this protocol) using methyl red (two drops) as an indicator; standardization should be carried out before each CO<sub>2</sub> determination. Note that 0.5 N is the nominal concentration of the alkaline solution, which must be confirmed or corrected by finding the correction factor ( $f_{cor}$ ), using a standard acid solution (in this protocol: potassium acid phthalate).

2.11.3 Standard solution of 0.5 N potassium acid phthalate in CO<sub>2</sub>-free distilled water. Prepare 1 L of solution at a time.

2.11.4 Methyl red indicator solution.

2.11.5 Hydrochloric acid (HCl) solution at 0.25 N in CO<sub>2</sub>-free distilled water. Standardize this solution against a 0.25 N sodium carbonate solution using methyl red (two drops) as indicator. Prepare 1–2 L at a time.

**Note (6):** 0.5 N is the nominal concentration of the acid solution, which must be confirmed or corrected by finding the correction factor ( $f_{cor}$ ), using a standard alkaline solution (in this protocol: sodium carbonate).

2.11.6 Sodium carbonate (Na<sub>2</sub>CO<sub>3</sub>) 0.25 N standard solution in CO<sub>2</sub>-free distilled water. Prepare 1 L at a time.

2.11.7 Barium chloride (BaCl<sub>2</sub>) solution in CO<sub>2</sub>-free distilled water at 1 N. Prepare 200–500 mL at a time.

2.11.8 Phenolphthalein indicator solution.

**Note (7):** All reagents used must meet purity standards in accordance with ASTM D5988-18 (item 7.1). The reagents must be kept in airtight packaging and stored away from light and under controlled temperature (between 20 and 25 °C).

---

## 3 Methods

### 3.1 System for the Assessment of Biodegradation in Large Volumes

3.1.1 The tests should be carried out in triplicate and, therefore, three systems will be required for the control (containing only culture medium, also called “blank”), three systems for the positive reference (culture medium and sample of a biodegradable polymer, such as MCC), three systems for each sample to be tested, and three systems for the negative reference.

**Note (8):** The ASTM D5988-18 standard does not describe the use of a system with a negative reference polymer; however, it is important to prepare a triplicate of this system to compare the biodegradation of the test polymer both with a positive reference polymer (e.g., MCC) and with a negative reference polymer (e.g., LDPE) and, thus, to determine the relative biodegradability, positive or negative, of the test polymer. The control has the function of discounting both the production of CO<sub>2</sub> from the organic matter present in the culture medium and the CO<sub>2</sub> introduced in the system during aeration after each titration.

**Note (9):** The ASTM D5988-18 standard calls for a triplicate set called “technical control,” which serves to check the airtightness of the system and to subtract the CO<sub>2</sub> introduced during aeration. However, from our point of view, this “technical control” is not necessary, as the CO<sub>2</sub> introduced during aeration has already been subtracted with the triplicate “control” and the airtightness of the vessels must be tested before the beginning of the experiments, as during the experiment this test is not possible. If any of the systems shows suspicious CO<sub>2</sub> determination, the experiment must be restarted, as there may have been a leak in the system.

**Note (10):** instead of the “technical control” system, prepare three systems (blank monitoring) equal to the blank for monitoring the loss of moisture in the biodegradation systems (by determining the mass of the systems at each titration). In the titration, these systems must be subjected to the same procedures of the other systems with two differences: first, these systems should not be titrated and, thus, the alkaline solution does not need to be changed and, second, the mass of the system must be determined at each titration step (monitoring) to check for moisture loss in the system. If moisture is not within the range determined by this protocol (Subheading 3.5.4 of this protocol), this should be corrected by adding CO<sub>2</sub>-free distilled water.

**Note (11):** this system may present relative difficulty in its construction, but it has two advantages: the system can be used in tests with relatively larger amount of culture medium (between 100 and

500 g) and test sample (between 0.4 and 2 mg per gram of culture medium) and eliminates possible errors due to analytical solution transfers in the titrimetric analysis.

**Note (12):** For the glass vessel (internal volume between 2 and 4 L) with glass lid and airtight sealing system, the parts that cannot be made of glass (sealing, e.g.) must be made of material that neither adsorbs nor absorbs and is impermeable to CO<sub>2</sub>. The container must have an opening that allows manipulation within. Note that desiccator containers are not recommended, as the biodegradation process, despite oxygen consumption, may generate positive pressure inside the system and the desiccator is not designed to operate with positive pressure. Desiccators may be used if changes are made (adaptation of an elastomeric sealing ring and fastening clips on the cover, e.g.) to guarantee airtightness under conditions of positive pressure.

**Note (13):** The ASTM D5988-18 standard indicates the use of a 150-mL beaker (to contain 100-mL of alkaline solution) and a 100-mL beaker (to contain 50 mL of distilled water) for each biodegradation system. However, we recommend replacing the 150-mL beaker with a 250-mL Erlenmeyer flask (Subheading 2.1 of this protocol), because 100 mL of alkaline solution is a relatively high volume to be contained in a 150-mL beaker that will afterward be used as the titration flask. Even with great care, spillage of solution may occur (due to agitation in the titration procedure), causing errors in the results.

### **3.2 System for the Assessment of Biodegradation in Small Volumes**

Alternatively, the use of a biodegradation system that involves reduced amounts of culture medium and sample may be used. The tests should also be carried out in triplicate and, therefore, the number of systems is the same as described in Subheading 3.1 of this protocol. In this system, the culture medium is deposited on the bottom of the Erlenmeyer flask and the reagent (alkaline solution) is deposited in the side tube. This system is described in Subheading 2.2 of this protocol.

### **3.3 Culture Medium**

#### **3.3.1 Soil**

The procedures for selecting, collecting, and determining soil properties for use as culture medium can be performed in accordance with ASTM D5988-18, item 9.

**Note (14):** Note that the definition and procedures for determining the moisture-holding capacity (MHC), also called field capacity (FC), may introduce errors in soil moisture during the biodegradation test and adversely affect the tests. If soil moisture content during the biodegradation test is lower than the amount

recommended by the standards, the microbial activity of the soil will be reduced, and biodegradation will be compromised. On the other hand, if the soil moisture during the biodegradation test is higher than the indicated amount, the microbial activity will also be reduced and, depending on the amount of excess water, aerobic biodegradation may change to anaerobic biodegradation (flooded soil), simulating a swamp. Therefore, the correct determination and interpretation of FC is important for the proper execution of the aerobic biodegradation tests.

**Note (15):** As an alternative to the FC determination methods presented in ASTM D5988-18, this protocol presents a more accessible and practical method for determining residual moisture (RM) and FC, as described next.

### 3.3.1.1 Preparation of the Soil for RM and FC Testing

After executing items 9.1 and 9.3 of the ASTM D5988-18 standard, separate approximately 1 kg of soil, divide into approximately equal parts, deposit in the stainless-steel trays, and allow to dry for 24 h in a temperature-controlled environment (between 20 and 25 °C) and without direct incidence of sunlight. After drying, perform intense tumble-mixing of the soil in a plastic bucket with lid. The resulting product is the test soil. If soil remains after the determinations, save it for use, together with additional soil obtained from ASTM D5988-18 (items 9.1 and 9.3), in the biodegradation tests.

### 3.3.1.2 Determination of RM

Add ca. 10 g of the test soil ( $m_t$ ) in a previously weighed and dried Petri dish and store in a drying oven at 105 °C for 24 h. Then, remove the Petri dish with dry soil from the oven and store in the desiccator to cool down to room temperature. After cooling, determine the mass of the set and determine (subtracting the mass from the Petri dish) the mass of dry soil ( $m_d$ ). RM is the original moisture of the soil (after drying for 24 h at room temperature) and is expressed in grams of water (which the soil originally has) per 100 g of dry soil, according to Eq. 3. It is important to know RM, as it is necessary to know how much water the test soil already has, to be able to adjust the biodegradation test moisture. This procedure should be performed in triplicate:

$$RM = [(m_t - m_d) \cdot 100] / m_d \quad (3)$$

### 3.3.1.3 Determination of FC

Start the procedure by blocking the exit of the conical part of the polypropylene funnel (250 mL) with cotton to prevent flow of soil (use minimum necessary cotton to avoid occupying too much free

space of the conical part of the funnel). Then, fill approximately 70% of the free height left in the conical part of the funnel with the test soil (Subheading 3.3.1.1), compacting it after every 2 cm of soil layer, using the “repeating impact” technique, which consists of releasing the funnel, containing the first layer of soil, in vertical position against the iron ring (fixed on the ring stand) from a height of approximately 10 cm between the iron ring and the exit of the cone (opening blocked by cotton). Repeat this procedure ten times for every 2 cm layer of added soil (CAUTION: perform the procedure with the funnel always in vertical position and centered with the iron ring to avoid accidental falls and loss of the procedure). After filling and packing the soil in the funnel, place the funnel with the soil in the Erlenmeyer flask and carefully add distilled water at will, to soak the soil. After soaking the soil, wait for the water to drain into the Erlenmeyer and, when draining stops (no dripping), extract a sample of ca. 10 g of the soaked soil ( $m_{ss}$ ) from the central part of the funnel and add in a previously weighed Petri dish. Place the Petri dish with the soaked soil in an oven for drying at 105 °C for 24 h and then place the Petri dish and the dry soil in a desiccator to cool down to room temperature. After cooling, determine the mass of the set (subtracting the mass of the Petri dish) to obtain the mass of dry soil ( $m_d$ ). This procedure should be performed in triplicate from the beginning, that is, a funnel for each determination. FC is defined as the amount of water that the soil can hold per 100 g dry soil, according to Eq. 4:

$$\text{FC (water/100 g dry soil)} = 100 \cdot (m_{ss} - m_d) / m_d \quad (4)$$

However, FC can also be expressed as the amount of water that the soil can hold per gram of dry soil (Eq. 5):

$$\text{FC (water/g dry soil)} = (m_{ss} - m_d) / m_d \quad (5)$$

### 3.3.2 Compost

If compost is chosen as culture medium, see ASTM D5338-15 (item 9) for selection, characterization, and care related to the culture medium.

**Note (16):** an adaptation related to the ASTM D5338-15 standard (item 9) must be performed. This adaptation is related to the average particle size of the compost, which must be less than 2 mm, requiring grinding of the compost in a rotary knife mill to reduce particle size.

### 3.4 Test Specimen

The characteristics that the test specimen (TS) must present are specified by ASTM D5988-18, item 10 (if the culture medium is soil) or by ASTM D5338-15, items 10 and 11.1, item 11.1.3 excluded (if the culture medium is compost).

**Note (17):** When the TS consists of pure polymer, or polymer with a known composition of additives, the amount of carbon can be determined depending on the chemical structure of the polymer. As an example, we demonstrate the calculation (Eq. 6) of the amount of carbon suitable for biodegradation for MCC (normally used as a positive reference in polymer biodegradation tests).

Cellulose:  $(C_{12}H_{20}O_{10})_n$ , molar mass of the repeating unit  $324 \text{ g}\cdot\text{mol}^{-1}$ .

Hence:  $X_c$  = fraction of carbon in the cellulose molecule

$X_{\text{Carb}}$

$$= \frac{(\text{molar mass of Carbon}) \times (\text{amount of Carbon in the molecule})}{(\text{molar mass of polymer repeating unit})}$$

$$X_{\text{Carb}} = \frac{12.12}{324} = 0.444 \text{ carbon in cellulose molecule} \quad (6)$$

Consequently, the amount of carbon in the MCC TS is the mass of the TS multiplied by the carbon fraction in the cellulose molecule ( $X_{\text{carb}}$ ). Use the same procedure to calculate the amount of carbon in the polymer molecule (or other organic material), either pure or having other constituents (known quantity), which will be subjected to the biodegradation test.

### 3.5 Biodegradation Procedure

Comply with ASTM D5988-18, item 11.1.

#### 3.5.1 Number of Systems per Sample

**Note (18):** It is important to guarantee the biodegradation systems are airtight (Subheadings 2.1 or 2.2 of this protocol) before the start of the test. One should not expect the technical control to perform this task, because if there is a “leak” during the test, the test must be discarded. It should also be mentioned that the  $\text{CO}_2$  present in the aeration air of the systems holding the samples (positive, negative, and test) is discounted (calculations) by the system containing only culture medium (blank soil or compost).

#### 3.5.2 Amount of Culture Medium

**Note (19)—soil:** For systems with a large internal volume (Subheading 2.1 of this protocol), comply with ASTM D5988-18, item 11.2. For systems with a small internal volume (Subheading 2.2 of this protocol), use  $(50.0 \pm 0.1) \text{ g}$ .

**Note (20)—compost:** For systems with a large internal volume (Subheading 2.1 of this protocol), comply with ASTM D5338-15,

item 11.1.3. For systems with a small internal volume (Subheading 2.2 of this protocol), use  $(50.0 \pm 0.1)$  g at the same mixing conditions described in item 11.1.3 of ASTM D5338-15. Adjust the carbon/nitrogen ratio according to item 11.1.3 of ASTM D5338-15 for the two system sizes (Subheadings 2.1 and 2.2 of this protocol).

**Note (21):** The samples (positive, negative, and test) that will be subjected to the biodegradation test must have similar mass (precision of 0.1 g), whether for large or small internal volume.

**Note (22):** The culture medium that will be used in the biodegradation tests of the samples (positive, negative, and test) must be extracted from the same batch of culture medium that has been subjected to the tests on determination of properties (Subheading 3.3 of this protocol, item 9 of ASTM D5988-18, and item 9 of ASTM D5338-15).

3.5.3 *Carbon/Nitrogen  
Ratio of the Culture  
Medium*

Perform in accordance with ASTM D5988-18, item 11.3.

**Note (23):** Alternatively, the use of the “as collected” culture medium is allowed (Subheadings 3.3.1 and 3.3.2 of this protocol) and, thus, the biodegradation test will provide results closer to the environmental reality.

**Note (24):** For compost, see ASTM D5338-15 (items 10.2 and 11.1.3).

3.5.4 *Adjusting Moisture  
Content of the Culture  
Medium*

3.5.4.1 If the culture medium is soil, perform in accordance with ASTM D5988-18, item 11.4.

**Note (25):** The procedures for determining RM and FC described in this protocol (Subheadings 3.3.1.2 and 3.3.1.3) are equivalent to those of the ASTM D2980-17 standard and, therefore, adjust the soil moisture content between 50% and 70% of the determined FC (or MHC).

3.5.4.2 If the culture medium is compost, adjust the moisture content of the system so that the total mass of the culture medium consists of 50 wt% dry solids (compost plus test sample) and 50 wt% distilled water.



3.5.5 *Recording the Mass of Each Biodegradation System*

Record the mass of each biodegradation system (Subheading 2.1 or 2.2 of this protocol) containing the culture medium with the adjusted moisture for monitoring soil moisture loss.

3.5.6 *Incubation*

3.5.6.1 If the culture medium is soil, perform in accordance with ASTM D5988-18, item 11.6.

**Note (26):** The ASTM D5988-18 standard recommends between 0.4 and 2.0 mg of sample per gram of culture medium. We suggest using the mean value of this interval, that is, 1.2 mg of sample per gram of culture medium.

3.5.6.2 If the culture medium is compost, prepare a homogeneous mixture of dry compost and dry sample using a compost:sample mass ratio of 6:1, considering the amount of culture medium for each biodegradation system size (Subheading 3.5.2 of this protocol).

3.5.7 *Selection of the Test Temperature*

3.5.7.1 If the culture medium is soil, select the chamber temperature between 20 and 28 °C, maintaining the selected temperature at  $\pm 2$  °C.

3.5.7.2 If the culture medium is compost, select the temperature of 58 °C, maintaining this temperature at  $\pm 2$  °C.

3.5.8 *Closing of the Systems and Initiating Biodegradation*

**3.5.8.1 Definitions**

At the beginning of the biodegradation (time zero), the alkaline solution is the last component added to each of the systems before closing. The systems must be closed one at a time, appreciating a time interval defined as the aeration time ( $t_{\text{acr}}$ ). The aeration time depends on the titration manipulation time ( $t_{\text{man}}$ ). It is, therefore, important to define each of the following times:

- $t_{\text{man}}$ : time interval related to titration manipulations (opening the system, removing the alkaline solution, titration, recording the result, and restoring the total volume in the titration burette). If the system is that addressed in Subheading 2.2 of this protocol, consider the time for the triple washing.
- $t_{\text{acr}}$ : time interval during which the systems must remain open and exposed to the environment for oxygen renewal within the systems. This time should range between 15 and 60 min (ASTM D5988-18).

**Note (27):** During the first  $t_{\text{acr}}$ , which takes place at time zero of the biodegradation (onset of biodegradation), no titration manipulation occurs, only aeration and closing sequence of the systems and the closing sequence at the start of biodegradation should be observed in each titration procedure throughout the biodegradation test.

### 3.5.8.2 Determination of $t_{\text{man}}$ and $t_{\text{aer}}$

To define all time intervals (i.e.,  $t_{\text{man}}$  and  $t_{\text{aer}}$ ), a titrimetric manipulation test is performed using a set with at least three systems containing only the alkaline solution. The test consists of simulating the titration procedure that occurs throughout the biodegradation process. The titrimetric manipulation test aims to determine the appropriate  $t_{\text{man}}$  for the titration operation and to allow the operator to become familiar with good laboratory practices, titration techniques, and manipulation of the titration instruments. Having determined  $t_{\text{man}}$ , then  $t_{\text{aer}}$  can be determined. It is recommended that  $t_{\text{aer}}$  be 5 min longer than  $t_{\text{man}}$  as long as the result of the sum of  $t_{\text{man}}$  plus 5 min lies within the interval between 15 and 60 min.

**3.5.8.3** To close and start biodegradation for a system with a large internal volume (Subheading 2.1 of this protocol), comply with ASTM D5988-18 item 11.7.

**Note (28):** It is recommended that the 150-mL beaker (for holding 100 mL of alkaline solution) be replaced by a 250-mL Erlenmeyer flask in the large volume system (Subheading 3.1 of this protocol), as 100 mL of solution is a relatively high volume for a 150-mL beaker that will afterward be used as titration flask. Even with great care, spillage of solution may occur, due to agitation in the titration procedure, introducing errors in the titration result.

**3.5.8.4** To close and start biodegradation for a small internal volume system (Subheading 2.2 of this protocol), add 10 mL of 0.5 N KOH solution (item 2.11.2 of this protocol) in the side test tube of the system (simplified Bartha). For this system, there is no need to add distilled water. After adding the alkaline solution, seal the system and store in a dark, temperature-controlled chamber.

**Note (29):** Regardless of system size (Subheading 2.1 or 2.2 of this protocol), the alkaline solution should be the last component incorporated into the system (one system at a time), following a procedure that consists of (i) identifying and organizing the systems; (ii) selecting the first system and starting the timer in countdown mode for a time interval equal to  $t_{\text{aer}}$ ; (iii) at the end of  $t_{\text{aer}}$ , add the alkaline solution and close the system; and (iv) repeat steps (ii) and (iii) for the next system, and so on up to the last system. Use the organizational sequence in the titrimetric procedure (Subheading 3.5.9.3).

3.5.9 *CO<sub>2</sub> Analysis***3.5.9.1 Caution with BaCO<sub>3</sub> Film Formation**

Comply with ASTM D5988-18, item 11.9.1.

**Note (30):** If the alkaline solution of choice is KOH 0.5 N, there are no concerns about the formation of a BaCO<sub>3</sub> film in the 150-mL beaker (system with large internal volume) or in the side test tube of the simplified Bartha (system with small internal volume). However, BaCl<sub>2</sub> should be used in the titration.

**3.5.9.2 Interval Between Titrations**

3.5.9.2.1 *Soil:* When the culture medium is soil, it is recommended to carry out the first titration approximately 12 h after the beginning of the biodegradation test, because at the beginning of the test the organic material present in the soil is activated (oxygenated and hydrated) due to its handling during the preparation procedures (sieving, homogenization, and moisture adjustment). When the period between titrations reaches 3 d, comply with ASTM D5988-18, item 11.9.2.

**Note (31):** It is important to know the maximum volume of HCl solution ( $V_{\max}$ ) required to neutralize the original alkaline solution (KOH, or other) (Subheading 3.2 of this protocol), that is, the alkaline solution that has not been subjected to the biodegradation test or any other form of contact with CO<sub>2</sub>. If, after a certain biodegradation interval (BI), the volume of HCl titrating solution equals  $V_{\max}$ , this means that no CO<sub>2</sub> was produced during this BI. On the other hand, if this volume equals zero (the turning point occurs when adding the indicator to the alkaline solution present in the biodegradation system), this means that during this BI the amount of CO<sub>2</sub> produced has saturated the alkaline solution. If this happens, the biodegradation test must be discarded and a new test must be prepared.

**Note (32):** In the titration procedures, carried out after each BI, it is recommended that the amount of HCl solution required to neutralize the alkaline solution that remained after the respective BI be in the range of 30–70% of  $V_{\max}$ . In the initial titration (first BI, i.e., 12 h), the volume of HCl solution may not comprise this range, but it should not equal zero. The titration of the first BI (12 h) will be the reference for the second BI and this, in turn, will be the reference for the third BI and so on, so that the volume of HCl solution required to neutralize the alkaline solution remains in the range between 30% and 70% of  $V_{\max}$ . If the volume of HCl titration solution is greater than 70% of  $V_{\max}$ , BI should be increased, and if less than 30%, BI should be reduced.

3.5.9.2.2 *Compost*: When the culture medium is compost, it is also recommended to perform the first titration after 12 h from the start of the biodegradation test due to the reasons mentioned in **step 3.5.9.2.1**. However, composts have a significantly higher microbial activity than soils and, therefore, the 12-h intervals between titrations may be repeated for a longer period when compared to soil. When the period between titrations reaches 3 d, comply with ASTM D5988-18, item 11.9.2.

**Note (33)**: Regardless of the biodegradation system (large or small internal volume), titration of the alkaline solution (after an incubation period) will be against the 0.25 N HCl solution using a burette.

### 3.5.9.3 Titrimetric Procedure

3.5.9.3.1 At the end of each incubation period, perform titrimetry of the alkaline solution that absorbed (pre-existing and generated) CO<sub>2</sub> in the systems (large or small internal volume).

3.5.9.3.2 For large internal volume systems (Subheading 2.1 of this protocol) and 0.5 N KOH solution, before titration add, via burette, 20 mL of 1 N BaCl<sub>2</sub> solution in the 250-mL Erlenmeyer flask containing the alkaline solution to cause precipitation, in the form of stable BaCO<sub>3</sub>, of all the CO<sub>2</sub> absorbed by the KOH solution, avoiding displacement of CO<sub>2</sub> during titration. Hence, only the KOH that did not absorb CO<sub>2</sub> will be titrated against the 0.25 N HCl solution.

3.5.9.3.3 For systems with a small internal volume (Subheading 2.2 of this protocol) and 0.5 N KOH solution, before titration add, via burette, 2 mL of 1 N BaCl<sub>2</sub> solution in the 250-mL Erlenmeyer flask that will receive the alkaline solution stored in the side test tube of the simplified Bartha. As previously mentioned, BaCl<sub>2</sub> will cause precipitation, in the form of stable BaCO<sub>3</sub>, of all the CO<sub>2</sub> absorbed by the KOH solution, avoiding displacement of CO<sub>2</sub> during titration and, hence, only the KOH that has not absorbed CO<sub>2</sub> will be titrated against the 0.25 N HCl solution.

3.5.9.3.4 Add phenolphthalein indicator to the titration flasks: four drops in the flask for the large internal volume system (Subheading 2.1 of this protocol) and two drops in the flask for the small internal volume system (Subheading 2.2 of this protocol).

3.5.9.3.5 For large internal volume systems (Subheading 2.1 of this protocol), perform the titration directly in the 250-mL Erlenmeyer flask containing the alkaline solution, to which 20 mL of the 1 N BaCl<sub>2</sub> solution and the phenolphthalein indicator have already been added.

3.5.9.3.6 For small internal volume systems (Subheading 2.2 of this protocol), transfer (using the urinary catheter attached to the 10-mL polypropylene syringe) the alkaline solution (which is in the simplified Bartha side test tube) to the titration flask (250-mL Erlenmeyer flask), which should already contain 2 mL of 1 N BaCl<sub>2</sub> solution and phenolphthalein.

**Note (34):** Regardless of the system used (Subheadings 2.1 or 2.2 of this protocol), titration must follow a standard procedure, which consists of (i) starting the timer in the countdown mode with the  $t_{\text{acr}}$ , opening the first system of the organizational sequence (*see Note 28*), and removing the alkaline solution to be titrated; (ii) during the aeration time countdown, perform titration, prepare the insertion of the new alkaline solution (250-mL Erlenmeyer flask containing 100 mL of alkaline solution for large volume system or 10-mL polypropylene syringe containing alkaline solution to be added to the side tube of the small volume system) and prepare the next system for titration; (iii) after the aeration time, insert the alkaline solution into the titrated system and close it; and (iv) repeat items (i) to (iii) for the next system in the organizational sequence (*see Note 28*).

**Note (35):** Regardless of the biodegradation system used (Subheadings 2.1 or 2.2 of this protocol), titration must be performed quickly to prevent CO<sub>2</sub> absorption by the alkaline solution from the environment wherein the procedure will be performed. To guarantee the success of the test, before starting the biodegradation, the operator should be knowledgeable about the titration procedures and precautions.

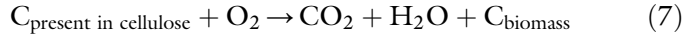
#### 3.5.9.4 Total Incubation Period

Comply with ASTM D5988-18, item 11.10.

### 3.6 Calculations

The calculations for determining the amount of CO<sub>2</sub> produced by the test polymer and the polymers used as positive and negative reference are based on the stoichiometry of the reactions involved in the process and on the titration outcome. Firstly, it is necessary to know the biodegradability potential of the polymer, which means the maximum amount of CO<sub>2</sub> the material can generate. This amount is defined as the theoretical amount of CO<sub>2</sub> (Th<sub>CO<sub>2</sub></sub>) produced [mg]. Th<sub>CO<sub>2</sub></sub> is calculated based on the amount of carbon

in the polymer. To simplify this protocol, we describe the calculations using cellulose as an example. In the biodegradation process:



Therefore, one mole of carbon produces one mole of  $CO_2$ , that is, 12 g of carbon produces 44 g of  $CO_2$ . If  $\gamma$  mg of carbon, from the polymer, is added to the biodegradation system, this amount  $\gamma$  can produce, at most, the following amount of  $CO_2$ :

$$Th_{CO_2} [\text{mg}] = \gamma \cdot (44/12) \quad (8)$$

As demonstrated in Subheading 3.4 of this protocol (Eq. 6), the molar fraction of carbon in the cellulose molecule ( $X_{\text{carb}}$ ) is 0.444.

If one adopts, as an example, system 2.2 of this protocol (simplified Bartha), the amount of culture medium is  $(50.0 \pm 0.1)$  g. Adopting the sample/culture medium ratio of 1.2 mg sample per gram culture medium, 60 mg MCC will be incubated and the amount of carbon ( $\gamma$ ) in 60 mg MCC is:

$$\gamma = X_{\text{carb}} \cdot \text{mass of sample} = 0.444 \cdot 60 = 26.64 \text{ mg} \quad (9)$$

Hence:

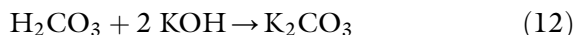
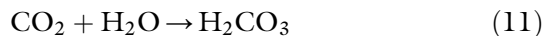
$$Th_{CO_2} = \gamma \cdot (44/12) = 26.64 \cdot (44/12) = 97.68 \text{ mg} \quad (10)$$

Therefore, 97.68 mg is the maximum amount of  $CO_2$  that 60 mg MCC (26.64 mg of carbon) can produce in the biodegradation system throughout the test. Therefore, 97.68 mg is the biodegradability reference of cellulose in the biodegradation test.

**Note (36):** If the 60 mg MCC produces 97.68 mg  $CO_2$ , the biodegradation of MCC will be 100% in relation to the production of  $CO_2$ ; however, this is a utopian result, because, in addition to  $CO_2$ , microorganisms also produce biomass (cell reproduction process) from carbon. The individual determination of  $CO_2$  and biomass in the same aerobic biodegradation system is complex due to biomass, which is intermixed with the culture medium, making quantification difficult. Therefore, this protocol considers the biodegradability of MCC (or another positive reference polymer, e.g., thermoplastic starch) as the biodegradation reference for the test polymers, considering only the data obtained with the quantification of  $CO_2$  in the biodegradability calculation of the test polymer and positive reference polymer. Hence, the biodegradability of the test polymer will be relative to the biodegradability of the positive reference polymer.

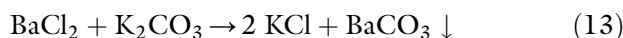
To proceed with the example of calculating biodegradation, it is important to know the reactions involved in the titration process,

which start with absorption, by the alkaline solution (we will adopt KOH), of the CO<sub>2</sub> generated in the biodegradation system:



Therefore, one mole of KOH is consumed by half a mole of CO<sub>2</sub>.

Because potassium carbonate, just like sodium carbonate, is not a stable salt, BaCl<sub>2</sub> is added before titration to shift the equilibrium toward the formation of barium carbonate:



So, the KOH that has not been consumed by CO<sub>2</sub> in each of the biodegradation systems (blank, positive reference polymer, negative reference polymer, and test polymer) is titrated using the HCl solution. It is at this moment that we highlight the importance of biodegradation systems containing only culture medium (blank), since the difference between the titration volume of the HCl solution of the blank system and the system containing the test sample (test polymer, positive reference polymer, and negative reference polymer) is exactly the volume of the HCl solution equivalent to the KOH that was consumed by the CO<sub>2</sub> produced by biodegradation of the test sample only.

**Note (37):** Note that in the blank system the culture medium produces CO<sub>2</sub> and the aeration air within the system also contains CO<sub>2</sub>, whereas in the test systems CO<sub>2</sub> is produced by the culture medium and by the test sample and is also present in the aeration medium, that is, the difference is the test sample (Eq. 14):

$$V_{\text{bio}} = V_{\text{blank}} - V_{\text{test sample}} \quad (14)$$

where:

$V_{\text{bio}}$  = volume of the HCl solution related to the amount of CO<sub>2</sub> produced by the test sample.

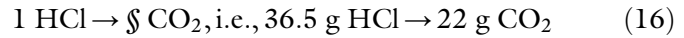
$V_{\text{blank}}$  = volume of HCl solution to titrate the blank system.

$V_{\text{test sample}}$  = volume of the HCl solution to titrate the system containing the test sample (test polymer, positive reference polymer, and negative reference polymer).

We already know that one mole of CO<sub>2</sub> consumes two moles of KOH. Regarding the neutralization reaction of KOH and HCl, one mole of HCl neutralizes one mole of KOH:



From Eqs. 12, 13, and 15, the stoichiometry involving KOH, HCl, and CO<sub>2</sub> is 1:1:1/2, respectively. As the titration data yield the volume of the HCl solution and we want to calculate the amount of CO<sub>2</sub> produced, from this point on we are only interested in the relationship between HCl and CO<sub>2</sub>. Hence:



We already have the correlation between mass HCl and our unknown (CO<sub>2</sub>) and hence we can calculate the mass of CO<sub>2</sub> using normality ( $N$ ):

$$N = (m.)/(\text{mol} \cdot V_{(L)}) \rightarrow m = (N \cdot \text{mol} \cdot V_{(L)})// \quad (17)$$

where:

\* = for acids, it is the number of ionizable hydrogens (for HCl, e.g., \* = 1).

mol = molar mass of the molecule (for HCl, mol = 36.5 amu).

$V_{(L)}$  = volume of solution [L] and, in our case,  $V_{[L]} = V_{\text{bio}} [L]$ .

Therefore:

$$m = N \cdot 36.5 \cdot V_{\text{bio}[L]} \quad (18)$$

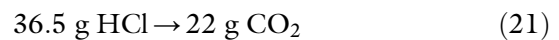
Note that the HCl solution used is 0.25 N, but 0.25 N is the nominal concentration ( $N_{\text{nom}}$ ). To know the final concentration of the HCl solution, this solution should be standardized against a standard Na<sub>2</sub>CO<sub>3</sub> solution (Subheading 2.11.5 of this protocol) and this standardization will generate a correction factor that may be different from one. Therefore, the final concentration of the solution of HCl will be:

$$N_f = N_{\text{nom}} \cdot f_{\text{cor}} \quad (19)$$

Hence:

$$m = 36.5 \cdot N_{\text{nom}} \cdot f_{\text{cor}} \cdot V_{\text{bio}} (L) \quad (20)$$

From stoichiometry:



$$36.5 \cdot N_{\text{nom}} \cdot f_{\text{cor}} \cdot V_{\text{bio}} (L) \rightarrow y \text{ g CO}_2 \quad (22)$$

Hence:

$$y [\text{g}] = 22 \cdot N_{\text{nom}} \cdot f_{\text{cor}} \cdot V_{\text{bio}} (L) \quad (23)$$

or:

$$y [\text{mg}] = 22 \cdot N_{\text{nom}} \cdot f_{\text{cor}} \cdot V_{\text{bio}}(\text{mL}) \quad (24)$$

Thus, from Eq. 24, one can calculate the mass of CO<sub>2</sub> [mg] produced by a sample in a biodegradation test, whether it is the test, the positive reference, or the negative reference polymer.



The titration is periodic, and each determination of CO<sub>2</sub> must be accumulated throughout the biodegradation test and the sum at the end of the six-month test will determine the amount of CO<sub>2</sub> ( $X$  [mg]) produced by the biodegradation of the different polymers tested (test,  $X_t$ ; positive reference,  $X_p$ ; and negative reference,  $X_n$ ). The data can be presented in the form of tables and/or figures according to Subheading 3.8 of this protocol. Note that the tests are performed in triplicate and, therefore, all statistical procedures of reliability (95%) must be performed using the results of the three tests of each test and blank sample.

### 3.7 Interpretation of the Results

The standards (ASTM D5338-15, ASTM D5988-18, ASTM D6400-19, ISO 14855-1:2012, and ISO 17556:2019) that supported this protocol do not consider which amount of carbon from the tested samples (test, positive, and negative) is used to produce biomass (Eq. 1) and, therefore, it is not possible to determine the absolute biodegradability without knowing the amount of biomass produced. This protocol, therefore, proposes the term “relative biodegradability” of the test sample ( $\text{Bio}_{rt}$ ), which consists of determining the biodegradability of the test sample relative to the biodegradability of the positive reference sample (e.g., MCC) over 6 months. The mathematical result of  $\text{Bio}_{rt}$  should be determined from the amount of CO<sub>2</sub> ( $X_t$  [mg]) accumulated during the test by the sample relative to the amount of CO<sub>2</sub> ( $X_r$  [mg]) accumulated during the test by the positive reference. Hence:

$$\text{Bio}_{rt} = X_t / X_r \quad (25)$$

$$\% \text{Bio}_{rt} = (X_t / X_r) \cdot 100 \quad (26)$$

In accordance with ASTM D6400-19, the polymer under test will be considered biodegradable if  $\text{Bio}_{rt}$  or  $\% \text{Bio}_{rt}$  is equal to or greater than 0.90 or 90%, respectively.

### 3.8 Report

Comply with ASTM D5988-18, item 14.

#### 3.8.1 Soil

#### 3.8.2 Compost

Comply with ASTM D5338-15, item 14.

---

## 4 Final Considerations

Respirometric polymer biodegradation tests are, in general, time-consuming and laborious procedures. The use of automatic systems significantly eases these obstacles (*see* Chapter 1 for details); however, access to automated biodegradation respirometric systems is restricted due to the relatively high cost of the system. On the other hand, correct execution of polymer biodegradation tests using

hand-operated respirometry reported in this protocol enables reproducible and accurate results at relatively low costs, using simple laboratory systems and routines. The accuracy and, mainly, the reproducibility of the results, associated with the low cost, are essential ingredients to globalize the biodegradation tests by means of nonautomated respirometry.

## References

- Zumstein MT, Narayan R, Kohler HPE et al (2019) Dos and do nots when assessing the biodegradation of plastics. *Environ Sci Technol* 53:9967–9969. <https://doi.org/10.1021/acs.est.9b04513>
- Emadian SM, Onay TT, Demirel B (2017) Biodegradation of bioplastics in natural environments. *Waste Manag* 59:526–536. <https://doi.org/10.1016/j.wasman.2016.10.006>
- Lucas N, Bienaime C, Belloy C et al (2008) Polymer biodegradation: mechanisms and estimation techniques - a review. *Chemosphere* 73:429–442. <https://doi.org/10.1016/j.chemosphere.2008.06.064>
- Vert M, Doi Y, Hellwich K-H et al (2012) Terminology for biorelated polymers and applications (IUPAC recommendations 2012). *Pure Appl Chem* 84:377–410. <https://doi.org/10.1351/pac-rec-10-12-04>
- Laycock B, Nikolić M, Colwell JM et al (2017) Lifetime prediction of biodegradable polymers. *Prog Polym Sci* 71:144–189. <https://doi.org/10.1016/j.progpolymsci.2017.02.004>
- Bastioli C (ed) (2005) Handbook of biodegradable polymers. Smithers Rapra Press, Shrewsbury
- Nikolic MS, Djonlagic J (2001) Synthesis and characterization of biodegradable poly(butylene succinate-co-butylene adipate)s. *Polym Degrad Stab* 74:263–270. [https://doi.org/10.1016/S0141-3910\(01\)00156-2](https://doi.org/10.1016/S0141-3910(01)00156-2)
- Haider TP, Völker C, Kramm J et al (2019) Plastics of the future? The impact of biodegradable polymers on the environment and on society. *Angew Chemie - Int Ed* 58:50–62. <https://doi.org/10.1002/anie.201805766>
- Bonilla J, Paiano RB, Lourenço RV et al (2020) Biodegradability in aquatic system of thin materials based on chitosan, PBAT and HDPE polymers: Respirometric and physical-chemical analysis. *Int J Biol Macromol* 164:1399–1412. <https://doi.org/10.1016/j.ijbiomac.2020.07.309>
- Banerjee A, Chatterjee K, Madras G (2014) Enzymatic degradation of polymers: a brief review. *Mater Sci Technol (United Kingdom)* 30:567–573. <https://doi.org/10.1179/1743284713Y.0000000503>
- Chamas A, Moon H, Zheng J et al (2020) Degradation rates of plastics in the environment. *ACS Sustain Chem Eng* 8:3494–3511. <https://doi.org/10.1021/acssuschemeng.9b06635>
- Castro-Aguirre E, Auras R, Selke S et al (2017) Insights on the aerobic biodegradation of polymers by analysis of evolved carbon dioxide in simulated composting conditions. *Polym Degrad Stab* 137:251–271. <https://doi.org/10.1016/j.polymdegradstab.2017.01.017>
- Kliem S, Kreutzbruck M, Bonten C (2020) Review on the biological degradation of polymers in various environments. *Materials (Basel)* 13:4586–4604
- Way C, Wu DY, Dean K, Palombo E (2010) Design considerations for high-temperature respirometric biodegradation of polymers in compost. *Polym Test* 29:147–157. <https://doi.org/10.1016/j.polymertesting.2009.10.004>
- Rudnik E (2008) Biodegradability testing of compostable polymer materials. In: Rudnik E (ed) *Compostable polymer materials*. Elsevier Science, Amsterdam
- Funabashi M, Ninomiya F, Kunioka M (2009) Biodegradability evaluation of polymers by ISO 14855-2. *Int J Mol Sci* 10:3635–3654. <https://doi.org/10.3390/ijms10083635>
- Rudnik E, Briassoulis D (2011) Degradation behaviour of poly(lactic acid) films and fibres in soil under Mediterranean field conditions and laboratory simulations testing. *Ind Crop Prod* 33:648–658. <https://doi.org/10.1016/j.indcrop.2010.12.031>
- Kale G, Auras R, Singh SP, Narayan R (2007) Biodegradability of polylactide bottles in real and simulated composting conditions. *Polym Test* 26:1049–1061. <https://doi.org/10.1016/j.polymertesting.2007.07.006>
- Cadar O, Paul M, Roman C et al (2012) Biodegradation behaviour of poly(lactic acid) and (lactic acid-ethylene glycol-malonic or succinic acid) copolymers under controlled composting

- conditions in a laboratory test system. *Polym Degrad Stab* 97:354–357. <https://doi.org/10.1016/j.polyimdegradstab.2011.12.006>
20. Petinakis E, Liu X, Yu L et al (2010) Biodegradation and thermal decomposition of poly(lactic acid)-based materials reinforced by hydrophilic fillers. *Polym Degrad Stab* 95: 1704–1707. <https://doi.org/10.1016/j.polyimdegradstab.2010.05.027>
  21. Weng YX, Wang XL, Wang YZ (2011) Biodegradation behavior of PHAs with different chemical structures under controlled composting conditions. *Polym Test* 30:372–380. <https://doi.org/10.1016/j.polymertesting.2011.02.001>
  22. Calil MR, Gaboardi F, Guedes CGF, Rosa DS (2006) Comparison of the biodegradation of poly( $\epsilon$ -caprolactone), cellulose acetate and their blends by the Sturm test and selected cultured fungi. *Polym Test* 25:597–604. <https://doi.org/10.1016/j.polymertesting.2006.01.019>
  23. Pradhan R, Reddy M, Diebel W et al (2010) Comparative compostability and biodegradation studies of various components of green composites and their blends in simulated aerobic composting bioreactor. *Polycaprolactone Int J Plast Technol* 45–50. <https://doi.org/10.1007/s12588-010-0009-z>
  24. Du YL, Cao Y, Lu F et al (2008) Biodegradation behaviors of thermoplastic starch (TPS) and thermoplastic dialdehyde starch (TPDAS) under controlled composting conditions. *Polym Test* 27:924–930. <https://doi.org/10.1016/j.polymertesting.2008.08.002>
  25. Leejarkpai T, Suwanmanee U, Rudeekit Y, Mungcharoen T (2011) Biodegradable kinetics of plastics under controlled composting conditions. *Waste Manag* 31:1153–1161. <https://doi.org/10.1016/j.wasman.2010.12.011>
  26. Brdlik P, Borůvka M, Borůvka B, et al (2021) Biodegradation of poly(lactic acid) biocomposites under controlled composting conditions and freshwater biotope. <https://doi.org/10.3390/polym13040594>
  27. Luo Y, Lin Z, Guo G Biodegradation assessment of poly (lactic acid) filled with functionalized titania nanoparticles (PLA/TiO<sub>2</sub>) under compost conditions. <https://doi.org/10.1186/s11671-019-2891-4>
  28. Kalita NK, Sarmah A, Bhasney SM et al (2021) Demonstrating an ideal compostable plastic using biodegradability kinetics of poly(lactic acid) (PLA) based green biocomposite films under aerobic composting conditions. *Environ Challng* 3:100030. <https://doi.org/10.1016/j.envc.2021.100030>
  29. Tate RL (2021) *Soil microbiology*, 3rd edn. Wiley, New Jersey
  30. Elsas JD, Trevors JT, Rosado AS, Nannipieri P (eds) (2019) *Modern soil microbiology*, 3rd edn. CRC Press, Boca Raton
  31. ASTM (2018) D5988-18: standard test method for determining aerobic biodegradation of plastic materials in soil. American Society for Testing and Materials, West Conshohocken
  32. ASTM (2015) D5338-15: standard test method for determining aerobic biodegradation of plastic materials under controlled composting conditions, incorporating thermophilic temperatures. American Society for Testing and Materials, West Conshohocken
  33. ASTM (2019) D6400-19: standard specification for labeling of plastics designed to be aerobically composted in municipal or industrial facilities. American Society for Testing and Materials, West Conshohocken
  34. ISO (2019) 17556:2019: plastics - determination of the ultimate aerobic biodegradability of plastic materials in soil by measuring the oxygen demand in a respirometer or the amount of carbon dioxide evolved. International Organization for Standardization, Geneva
  35. ISO (2012) 14855-1:2012: plastics - evaluation of the ultimate aerobic biodegradability and disintegration under controlled composting conditions—method by analysis of released carbon dioxide. International Organization for Standardization, Geneva



## Detection and Identification of Microplastics in Food and the Environment

Walter R. Waldman, Cristiane Vidal, Mariana A. Dias,  
Victor Z. Resende, and Cassiana C. Montagner

### Abstract

Microplastic contamination is a relevant topic in Food and Environmental Sciences. Microplastic analyses in matrices such as food, soil, sediment, water, and air require a specific method approach according to their respective aims and scope. This chapter presents a comprehensive discussion about standard practices currently applied to ensure representative sampling, adequate sample preparation, and unequivocal identification and characterization of microplastic particles.

**Key words** Microplastic contamination, Quality assurance, Quality control, Representative sampling, Density separation, Digestion, Chemical composition, Visual inspection, Microscopy, Spectroscopy.

---

### 1 Introduction

Plastic is an extensively used material in daily life and an obvious primary source of microplastics called by range size of 1  $\mu\text{m}$  to 5 mm. Almost a hundred years ago, the industry discovered the advantages of plastics, and the sector was heavily influenced by it ever since. Transportation and storage of food and beverages are safer and cheaper using plastics rather than glass or metal. Nowadays, research is primarily focused on environmentally friendly alternatives to replace or minimize plastic use, especially single-use plastics that have been demonstrated to negatively impact the environment because of inadequate waste disposal over the years. Biodegradable materials in composting conditions or in other environments—soil, sea water, among others (*see* Chapters 1 and 2 on biodegradability)—have been studied as compelling alternatives. However, conventional plastics are low-cost, and their physicochemical and mechanical properties, especially the low weight and easy processability, are exceptional for the packaging industry.

Over the last years, toxicologists have aimed to understand the human risk associated with plastic and microplastic exposure, such as inhalation and ingestion routes of exposure [1]. In general, polymers are nontoxic for humans, but the additives and plasticizers can be toxic depending on exposure level. Readers are invited to check Chapters 7 and 8 on toxicity assessment of food packaging materials. Chemicals migrating from polymer bulk to the surface and then to the food were the main concern for food contamination from the packaging so far [2, 3]—see Chapter 6 on migration of constituents of food contact materials. In addition, despite plastic resistance, mechanical stimuli such as shearing, folding, and fatigue can wear surfaces and produce fragments that might go into the food [4].

Scientific research has consistently shown the presence of microplastics in different types of food such as salt, honey, mineral water, etc. [5–10], their leaching from take-out containers [11], or microplastic generation by simple tasks such as opening food packaging (plastic containers, bags, tapes, caps) using scissors, tearing with hands, cutting with knives, or twisting manually [4]. Thus, primary, secondary, or tertiary packaging can be sources of microplastics depending on the contact with the food and the type of food (dry solid foods, pasty food, beverages, etc.). Finally, regarding in natural foods, contamination with microplastic is minimal and, if existent, it may be due to environmental contamination (air, soil, and water) during the cultivation [12–14].

Once disposed in the environment, the packaging can be a source of microplastics. Secondary microplastics are formed by the breakdown/degradation of macroplastics or primary microplastics in the environment (weathering exposure). Such small particles can be transported to long distances, carrying chemical contaminants or microorganisms. Today, microplastics are considered ubiquitous contaminants in the environment. Poor solid waste management causes soil and water contamination, both important compartments for food production [12, 13].

This chapter introduces an analytical protocol to extract, isolate, characterize, and chemically identify microplastics. Many procedure steps are common for both food and environmental matrices. However, food and environmental samples are intrinsically complex (*see Note 1*). The sample particularities (aqueous, viscous, solid, oleaginous, powder, etc.) will justify whether a step is necessary or not. There are no official methods yet, and accurate quantification is still challenging. Further details on the differences and similarities in analytical protocols for food and environmental samples are highlighted in the Notes section.

Figure 1 shows a didactic analytical workflow that synthesizes the topics discussed herein regarding contamination control, sampling, sample preparation, and characterization.

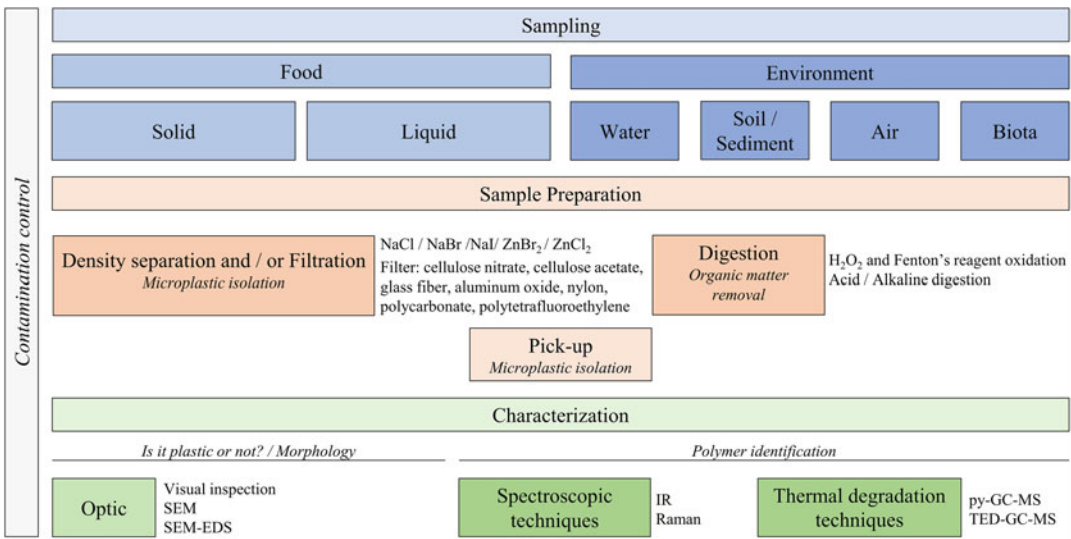


**Fig. 1** Analytical workflow presented in this chapter. SEM: scanning electron microscopy; EDS: energy-dispersive X-ray spectroscopy; IR: infrared; py-GC-MS: pyrolysis-gas chromatography mass spectrometry; TED-GC-MS: thermal extraction-desorption gas chromatography mass spectrometry

## 2 Materials

We consider as a minimal set of resources for assembling a general microplastic detection laboratory or setup:

- A laminar flow hood, to keep contamination out of the separation systems.
- A centrifugation system to separate better and faster by density.
- A separating funnel to separate the denser and lighter fractions.
- A vacuum filtration system to accelerate filtration when the filter might clog by the size of the dispersed phase.
- An analytical balance to weigh the samples accurately (precise to 0.1 mg [15]) and the filters to keep track of the mass balance.
- Specific chemicals and apparatuses depending on the method of choice, as detailed in the following sections.

## 3 Methods

### 3.1 Microplastic Background Contamination

First, this analytical protocol will address an important step to guarantee the quality of results that will be generated. To avoid microplastic contamination in sampling, sample preparation, and analysis, the analyst should pay attention to three main topics: air contamination (i.e., exposure to airborne microplastic contamination), cross-contamination (i.e., lab material contaminated during

sampling, sample preparation or analysis), and contamination control (i.e., measures to promote quality assurance and quality control) [16].

- Reducing air contamination:
  - Avoid personal protective equipment (PPE) manufactured of synthetic fibers (e.g., polyester); use preferably natural fibers (e.g., cotton). Cellulosic fibers can be digested if needed (*see Note 2*).
  - Always record the color and material of the clothes used during lab assays. This practice can facilitate the identification of possible contamination sources.
  - If possible, perform all lab activities in clean rooms with controlled air circulation and limited staff access.
  - Use laminar flow hood or similar during all lab work.
  - Maintain scheduled cleaning of the lab, at least once a week.
  - Whenever possible, cover all working solutions, samples, filters, and other related materials with precleaned aluminum foils. In the case of flasks, cap whenever not in use.
  - Provide proper storage to all lab materials.
- Reducing cross-contamination:
  - Use preferably lab materials made of glass and metals.
  - Wash lab materials with ultrapure or filtered distilled water before use.
  - Record sample information, sampling and sample preparation order, and adopted protocols to identify possible sources of cross-contamination.
  - All inner surfaces of the laminar flow hood or bench surfaces must be cleaned with residue-free detergent or ethanol followed by ultrapure or filtered distilled water before use.
  - Perform proper washing of lab materials between samples as stated above.
  - Filter all working solutions. Purity reagents p.a. must also be filtered (*see filter and conditions in Subheading 3.3.2*).
  - Filters composed of stainless steel or glass materials can undergo heat treatment (e.g., 450 °C for 3 h) to cleanse possible microplastic cross-contamination. On the other hand, materials such as natural or synthetic fibers (e.g., cellulose or polyamide) may not be thermally treated. In this case, compressed air can be used for decontamination, and the removal efficacy can be performed using optical microscopy.

- Performing contamination control:
  - Collect field controls during sampling.
  - Prepare blanks during sample preparation (e.g., filtration).
  - Collect open-air background to identify possible air contamination. Procedures for possible airborne microplastic contamination can be found at Zhang et al. [17] and Chen et al. [18] (*see Note 2*).

## 3.2 Sampling

The sampling protocol is dependent on the type of samples. Thus, several procedures may be found in the literature [19, 20]. However, the lack of standard procedures leads to relevant differences in sampling and sample processing steps. Therefore, microplastic abundance may be expressed in several different ways (e.g., fibers per cubic meter, microplastics per liter, microplastic mass per sample mass, pellets per square meter, etc.) (*see Note 3*). It is vital to keep the representative sampling in accordance with the analysis, methodology, and amount of collected material [19, 21]. This chapter addresses microplastic detection in food (solid or liquid) and environmental matrices (water and soil/sediment).

### 3.2.1 Food Matrices

Lower-viscous (e.g., bottled water, wine, beer, refreshments, and milk) and higher-viscous (e.g., honey, syrup, and ketchup) liquid samples can be collected from different batches, brands, or places. Viscous samples are usually diluted after sampling and before treatment. In general, a volume of 350–750 mL has been used for wine sampling [22]. About 500 mL to 2 L of the sample have been used for microplastics analysis for bottled water [5, 23, 24]. One liter of warm milk samples can be filtered in a dried precleaned glass vacuum system [25]. Liquid honey has been diluted in warm water and passed through a steel sieve [7, 26, 27].

For the sampling of solid matrices in food, defining the sample size is essential to obtain representative samples since they may not be homogeneous. Often, samples can be collected from different batches in several places to enhance representativeness.

Microplastics can contaminate animals destined for human consumption (e.g., fish, crustaceans, and mussels). Such particles may come from habitat surroundings (environment sample) or food processing (food sample). Samples can be stored until analysis under refrigeration in chemical preservatives (e.g., formaldehyde and ethanol). Generally, the digestive tract of these animals has been investigated for microplastics [28]. More information about biota sampling and sample preparation can be found in Hermsen et al. [29] and Lusher et al. [28].



### 3.2.2 *Environmental Matrices*

A wide range of equipment (trawl nets, pumps, Niskin bottles, etc.) has been used to collect microplastics in aquatic environmental samples (freshwater, seawater, drinking water, and groundwater from rivers, lakes, estuaries, and oceans). This sampling may be performed in the surface or depth water according to the aim of the study. The examples of equipment and sampling details can be found in the works of Prata et al. [19] and Silva et al. [30].

Similar to water, soil/sediment sampling requires specific equipment to collect microplastics in the environment. Surface sampling from marine sediment, river sediment, soil, and sandy beaches has been conducted using steel materials (spatula, tweezers, or spoon). Conversely, depth samples have been collected using grabs, augers, or corers. More detailed information can be found in Möller et al. [31] and in Yang et al. [32]. For detection of microplastics in atmospheric air (indoor and outdoor), we direct the reader to Zhang et al. [17] and Chen et al. [18].

### 3.3 *Sample Preparation*

Sample preparation is the process of extracting microplastics from their respective matrices. A single step, like a filtration, shall be enough for clear samples like drinking and bottled water. However, as the matrix complexity increases, it is necessary to combine different sample preparation steps, such as dissolving or digesting the matrix, using separation methods to isolate the microplastics from the matrix constituents. The protocol order is matrix-dependent. In cases where microplastic is trapped in samples (e.g., biota, processed food), digestion may be the first step to promote the release of the microplastic (for more comments on sample disassembling, *see Note 4*). Alternatively, in samples from water, salt, sugar, etc., this step usually occurs after density separation [28]. Commercial salt samples, for instance, can be directly dissolved in water and submitted to sample processing (density separation and digestion, if necessary). Warm water can be used to facilitate dissolution [8–10, 33–35]. Such a step has also been applied to commercial sugar and solid honey [7].

#### 3.3.1 *Digestion*

Several sample processing by digestion can be performed to eliminate or minimize the presence of organic matter. Among the options, the most used are acid/alkaline reagents (e.g., HNO<sub>3</sub>, HCl, NaOH, and KOH) and oxidizing agents (e.g., Fenton's reagent and hydrogen peroxide (H<sub>2</sub>O<sub>2</sub>) solution). Peroxide oxidizing digestion has been considered more effective to degrade natural organic matter than acidic or alkaline due to less damage being caused to the polymer. Enzymatic digestions are also adopted, leading to a reduction in polymer degradation compared to acid/alkaline processing. On the other hand, enzymes are costly and differences between biological matrices promote irregularly enzymatic activities [21].

Solid matrices composed of carbohydrates (e.g., honey and sugar), inorganic salts (e.g., sea salt), and proteins (e.g., fish,

mussel, shrimp, and bivalve) are usually pretreated using oxidizing agents as  $\text{H}_2\text{O}_2$  or Fenton's reagent and inorganic acids or bases [28]. The following procedure is based on the NOAA guidelines and literature specialized in microplastic extraction for these matrices [15, 28, 36, 37]. If necessary, literature shows that filtration steps combined with digestion steps would enable correct microplastic extraction [21].

Liquid matrices are mainly beverages, including soft drinks, beers, wines, and bottled and tap water. Beverage samples usually have low organic content and particulate matter. Thus, filtration as pretreatment can be adopted without digestion steps. However, some matrices with high organic content (e.g., milk or liquid honey) may require digestion steps to eliminate fats, carbohydrates, and larger proteins [21].

- *$\text{H}_2\text{O}_2$  and Fenton's Reagent Oxidizing Digestion/Acid or Alkaline Digestion*

CAUTION: Hydrogen peroxide solutions and respective mixtures are highly reactive. Safety precautions are necessary to avoid accidents in the laboratory. Please follow and review laboratory safety measures to comply with this reagent use.

- Use a dried precleaned glass flask to determine the mass of dried solids after the filtration steps. Always use an analytical balance to the nearest 0.1 mg. Liquid matrices or biological soft tissues, in some cases, cannot undergo dried solids determination. Whenever the case, proceed directly to digestion and use defined metrics in volume, mass, or size to identify the samples. The correct identification will allow microplastic counting by measure.
- Aqueous Fe(II) and  $\text{H}_2\text{O}_2$  solutions, used separately or jointly, acid or alkaline solutions can be added to remove organic matter in sequence. Strong acid or alkaline digestion might damage the microplastic structure. Thus, possible destruction of microplastics or incorrect results should be considered [28] (*see Notes 5 and 6*).
- Accurate reaction conditions will vary according to the matrix under analysis or microplastic intended to obtain:
- Usual concentrations:
  - Oxidizing digestion agents: 15–35 wt%  $\text{H}_2\text{O}_2$  solutions; 0.05 M Fe(II) aqueous solution.
  - Acidic or alkaline digestion agents: 10 wt% KOH solutions, 22.5 M or 65–100 wt%  $\text{HNO}_3$  solutions, 68 wt%  $\text{HClO}_4$  solution.
- Usual reaction time: 30 min up to 72 h. Longer reaction periods of 7 to 10 d may be used to eliminate all biological soft tissue [28].

- Magnetic agitation: 80–120 rpm. Orbital shakers may be used.
- Reaction temperatures:
  - Oxidizing digestion agents: 40–85 °C.
  - Acidic or alkaline digestion agents: 20–100 °C.
  - Room temperature and incubators may be used.
- After aqueous Fe (II) solution and/or H<sub>2</sub>O<sub>2</sub> solution, or acid/alkaline solutions addition, let the mixture stand on the lab bench at room temperature for some time before proceeding to the next step.
- Cover the flask with a watch glass or cap, add the magnetic stir bar, and heat up to the defined temperature.
- If the reaction exhibits excessive gas bubbles at the surface, remove the beaker from the hotplate and place it in the laminar flow hood until boiling decreases. In case of overflow, ultrapure or distilled filtered water can be added to slow down the reaction.
- Magnetic agitation or shaking is necessary during the reaction.
- If natural organic matter is still visible at the end of the reaction, add more digestion agent solution and repeat the procedure above.
- After oxidizing or acid/alkaline digestion, ultrapure or distilled filtered water and salts may be added for re-dissolution, filtration, and density separation steps (Subheading 3.3.2). In some cases, a manual pick-up can be used in glass Petri dish substrates.

### 3.3.2 Density Separation

Density separation is a simple step for isolating microplastics from other sample compounds, generally inorganic materials (e.g., sand) through salt solutions with known densities. Microplastics are separated by density from heavier fractions like minerals and undissolved impurities, organic matter, and even other microplastics (*see Note 7*). High-density salt solutions (1.2–1.8 g cm<sup>-3</sup>; e.g., NaBr, NaCl, NaI, ZnBr<sub>2</sub>, and ZnCl<sub>2</sub>) are added to the samples to separate the denser fraction of the media from the microplastics. The separation of the two fractions (low- and high-density fractions) can be performed by gravity or centrifugation systems.

NaCl is beneficial because it is inexpensive, nontoxic, and highly soluble in water. However, the density of NaCl solution is about 1.2 g cm<sup>-3</sup> (Table 1) which is lower than the densities of some polymers like poly(ethylene terephthalate) (PET), poly(vinyl chloride) (PVC), and poly(lactic acid) (PLA). Thus, such polymers cannot be separated using a NaCl solution, and other solutions must be used to solve this limitation. NaI, ZnCl<sub>2</sub>, and ZnBr<sub>2</sub>

**Table 1**  
**Densities and costs of salt solutions used in density separation for microplastics [19, 20, 38] (see Note 9)**

| High-density salt solution | Density [g cm <sup>-3</sup> ] | Cost per 100 g [US\$] <sup>a</sup> |
|----------------------------|-------------------------------|------------------------------------|
| NaBr                       | 1.37                          | 46.10                              |
| NaCl                       | 1.2                           | 6.79                               |
| NaI                        | 1.6–1.8                       | 88.70                              |
| ZnBr <sub>2</sub>          | 1.7                           | 51.40                              |
| ZnCl <sub>2</sub>          | 1.5–1.8                       | 27.40                              |

<sup>a</sup>Quotes for the United States dated from March 26, 2021 [39]

solutions have higher densities, expanding the range of polymers that can be separated. However, these salts have a higher cost, and they are environmentally unfriendly due to their toxicity [19, 20, 38] (see **Note 8**). It is worthy of highlighting that the densities on Table 1 are not all related to saturated solutions because there is a tradeoff between the density and the viscosity so, if needed, higher densities can be achieved but at the expenses of longer times for decantation and filtration.

Density separation presents some limitations, such as the interference of organic matter in samples, leading to overestimated or underestimated results in density separation. For instance, an organic film (biofilm) can adhere to a microplastic surface and change the particle density.

Microplastic particles have different degradation degrees, modifying some polymer physical properties as wettability and crystallization [40]. Additive concentrations and adsorbed substances can also change the processed polymer density [19].

- Add high-density salt solutions to the samples in a dried pre-cleaned glass separating funnel. Samples may be previously digested to reduce or eliminate the organic matter.

**CAUTION:** Use personal protective equipment when handling NaBr, NaI, ZnBr<sub>2</sub>, and ZnCl<sub>2</sub> salts.

- Water-soluble samples, such as commercial salt, can be directly dissolved in water.
- The sample may be manually shaken using a separating funnel. However, the separation step can take several hours (ca. 24 h).
- Alternatively, the sample may be centrifuged using dried pre-cleaned glass centrifuge tubes. In this case, the centrifugation step lasts for a few minutes according to the rotation speed (200–500 rpm).

- Particles with density higher than the salt solution will remain in the precipitate, whereas particles with lower density will remain in the supernatant (low-density fraction).
- After separation, the supernatant is filtered in a dried precleaned glass vacuum system covered with precleaned aluminum foil in a laminar flow hood (*see* **Notes 10** and **11**).
  - Filter diameter: 47 mm.
  - Filter porosity: 0.2–149  $\mu\text{m}$ .
  - Filter: cellulose nitrate, cellulose acetate, glass fiber, aluminum oxide, nylon, polycarbonate, or polytetrafluoroethylene.
- The filter is placed and sealed in dried precleaned Petri dishes and dried at room temperature or in an oven (40–50 °C) for 5–12 h. Afterward, it may be directly submitted to the next step of the sample preparation.
- The procedure of density separation may be repeated according to the matrix complexity.

### 3.4 Characterization

Microplastics are usually characterized by morphology (color, size, shape, and surface texture), origin (primary or secondary), and by chemical composition (polymer identification). Many techniques are presented below, and their choice will depend on the objective of the analysis, deeply influenced by the size of the microplastic. If the microplastics have been extracted and are isolated, the techniques can be chosen regardless of the original matrix they were extracted from.

#### 3.4.1 Objective: Sorting of Suspected Microplastics or Morphological/Origin Characterization

Visual inspection can be used to sort suspected microplastics [41, 42]. However, this is a subjective technique for environmental samples. The decision depends on the analyst skills to observe the particle features (texture, physical behavior, overall appearance) and recognize them as plastic (*see* **Note 12**). When not instrument-assisted, it is not suitable for small microplastics. For smaller particles, a visual inspection must be combined with optical microscopy. To enhance the detection, microplastics can be stained with dyes prior to visual inspection [43]. The dyeing process facilitates locating suspected microplastics via optical or fluorescence microscopy (*see* **Note 13**).

During sorting with visual inspection, assisted or not with a microscope, morphology is classified as size and shape. Shape classification includes pellets, sphere, hemisphere, grain, nurdle, fiber (singular fiber, fiber bundle), and fragment (foam, film, angular/sub-angular, rounded/sub-rounded).

Scanning electron microscopy (SEM) is used for surface analysis and to evaluate signs of degradation [44] (*see* **Note 14**).

### 3.4.2 Objective: Polymer Identification

To perform microplastic confirmation and polymer identification, use vibrational spectroscopy (infrared or Raman), or thermal analysis (pyrolysis, -py, or thermal desorption, TED) combined with gas chromatography coupled to mass spectrometry (py-GC-MS or TED-GC-MS) [43].

#### *Spectroscopic Techniques*

For spectroscopic techniques [45], microplastic identity confirmation is done by spectral signatures related to each polymer by using libraries or multivariate analysis (chemometric classification models). Quantification is performed by items (number of particles).

- Fourier-transform infrared (FTIR) spectroscopy

FTIR spectroscopy is the most used technique, and there is plenty of instrumentation described below [46].

- ATR-FTIR: More suitable for a size range of 0.5–5 mm, which is not likely to occur in food, but it is likely that food packaging breaks down to that size range in the environment. No substrate is required as the microplastic is individually pressed against the crystal for analysis.
- FTIR microscopy: Usually referred as  $\mu$ FTIR, which is a microscope coupled to the spectrometer. More suitable for microplastics smaller than 0.5 mm until ca. 20  $\mu$ m. Acquisition mode (transmittance, reflectance, or ATR) will depend on the particle size as well. Transmittance is the most used and compatible substrates are metallic filters (e.g., aluminum oxide) or  $\text{CaF}_2$  plates. For microplastics displayed on Petri dishes, analysis can be performed by reflectance or by the ATR objective (lens) as well, but not in transmittance.
- Imaging FTIR microscopy: The technique is usually reported as  $\mu$ -FPA-FTIR. The spatial dimension added to the spectroscopic analysis allows shape and size analyses, despite the chemical composition. Instruments with focal plane array detector (FPA) are faster than point scan FTIR microscopy made by single element detectors [47].
- Raman spectroscopy

Suitable for size ranges from 10  $\mu$ m to 5 mm, depending on instrumentation and particle characteristics [48–50].

Main optimization may include laser wavelength, laser power, and integration time to achieve proper signal-to-ratio spectra and to avoid fluorescence or other interference from polymer constituents. Raman microscopy is suitable for small microplastics down to ca. 3  $\mu$ m, covering a size range not possible with FTIR (<10–20  $\mu$ m). Raman imaging is also possible, but it is a slow

analysis. Compatible substrates are metallic filters, but not restricted to them, depending on the microplastic size.

#### *Thermal Degradation-Based Techniques*

The techniques py-GC-MS and TED-GC-MS are destructive, as the samples are thermally degraded. The identity of microplastics is confirmed through the evaluation of their degradation products. These techniques are suitable for the detection of additives or organic contaminants in the microplastics, as well as for the simultaneous analysis of different polymers, reaching detection and quantification levels in the nanogram range. Quantification is performed in mass-based concentration, upon construction of analytical curves of target microplastics [51–53].

- py-GC/MS

Suitable for microplastics down to 100  $\mu\text{m}$ , if the particle is previously isolated.

- TED-GC-MS

Suitable for bulk sample analysis and considered promising for the analysis of nanoplastics. However, for bulk analysis, it is not possible to directly assess microplastic size. Size can be known indirectly by analyzing previously size-fractionated samples (by sieving, e.g.) during sample preparation.

---

## 4 Notes

1. Plastic physical properties differ according to the two main contexts outlined in this chapter: (i) plastics collected in the environment exposed for a while to the weather will be more brittle, crystalline, with a lower molar mass or crosslinked, while (ii) plastics handled during the production process will be more inert, amorphous, and closer to the raw resin properties. It might influence the output of some assessments, for instance, the size of the microplastics after the separation process because more brittle materials are also more likely to fragment during the handling and the digestion step.
2. Cellulosic fibers are a common contamination for monitoring microfibers, and some environments may have more than 80% of the fibers as cellulosic ones [54]. In cases like that, an additional step of selective cellulosic digestion might be tried to reduce the burden of the characterization step if it is significantly time-consuming, like the spectroscopic identification [55].

3. When comparing your results with the literature, one topic is always present: the microplastics abundance. Because the need for quantification always answers a specific demand of knowledge, sometimes the determination of the microplastics concentration is made as a function of the area (relevant, for instance, for terrestrial epigeic species or the aquatic buoyant positive microplastics) or as a function of the volume (relevant, for instance, for terrestrial endogenic species or the aquatic buoyant neutral microplastics). The numerator of the concentration is a matter of dissent, with the number of particles and weight as the predominant units. The microplastics amount might be described by number, weight, or volume. Not so often, volume can also be found describing the quantity of microplastics. However, as there are no official or standardized methods yet, quantification accuracy is low as important figures of merit (recovery, repeatability, and reproducibility) are not yet established for microplastics. Concentration results are often estimative and not yet comparable.
4. The density separation step might change substantially according to the complexity of the system to be treated. Drinking products and samples from the aquatic bodies with a low amount of organic matter can be filtered and then passed through a digestion to clean the surface from, for instance, biofilms. More complex samples, such as soil or some multi-component solid food, might have microplastics heavily entangled inside microstructures, like soil aggregates or processed industrial food preparations. In that case, more aggressive treatments as continued stirring or ultrasound might help to disassemble organized soil structures to release the microplastics to be separated by density. In the case of complex food, where microplastics might come from the ingredients or the process and be heterogeneously spread through the sample, aggressive homogenization, like stirring, may be necessary. It comes, obviously, at the expense of information such as size, shape, and format since microplastic fragmentation can occur.
5. Nitric acid ( $\text{HNO}_3$ ) is the most effective digestion agent compared to the others in terms of removing organic content. However, high temperatures or concentrations could dissolve or degrade polymers sensible to acid hydrolysis—for example, polyamides, polyesters such as PET, and polycarbonates [28].
6. Potassium hydroxide (KOH) is proven to promote the dissolution of animal digestive tracts due to basic hydrolysis of chemical bonds presented in soft biological tissues, such as larger proteins and fat [56].
7. The separation of suspected collected microplastics is one of the main challenges for environmental researchers. Because the



origin and diversity of the plastics are unknown but likely to be broad regarding type and weathering time, the protocols must also follow broad criteria to separate the plastics from the media where they are. Concerning density, just for the most used plastics, there is a range from 0.9 to 1.4 g·cm<sup>-3</sup>, therefore the need for a general-purpose separation method. Regarding a controlled environment, like the development or optimization of new packaging, process, or even a quality control protocol, it is possible to develop a process to monitor a specific microplastic. A cost-effective way of doing that is fine-tuning the density separation, using solutions right below and above the range density of the chosen microplastic to perform the separation before the digestion and the identification of microplastics.

8. Regarding the separation by density, salts like ZnBr<sub>2</sub>, CaCl<sub>2</sub>, sodium polytungstate, lithium metatungstate, among others, one can optimize the process to have a faster or a better separation according to the system where the microplastic is [15, 57]. To choose the best salt for the separation step, one must consider several features, namely: (i) the microplastic density under analysis, usually unknown for environmental samples but likely to be known for packaging analysis. Examples of especially denser plastics are PTFE (ca. 2.2 g mL<sup>-1</sup>), polyvinylidene chloride (PVDC; ca. 1.6 g mL<sup>-1</sup>), or formulations with inorganic materials like TiO<sub>2</sub>, glass fibers, or colored pigments; (ii) the density of the media from which it is needed to separate the microplastic; (iii) the chemical affinity between the media where the microplastic is and the salt. One example worthy of highlighting is the ZnCl<sub>2</sub>, which forms a hydro soluble complex between the zinc and humid substances [58, 59], increasing the density of the liquid media, and darkening and contaminating the aqueous phase; (iv) salt hygroscopicity might lead to difficult handling if it is needed to fabricate several solutions at a time; (v) mixing heat might be intense, so the preparation must be a sensitive step regarding safety if the salt has an exothermic dissolution. It is recommended the analyst always test which salt offers the best benefit-to-cost ratio, checking the separation with positive controls of a known amount of the microplastic of interest in the media chosen to quantify the microplastics.
9. High-density salt solutions can be filtered and reused more than once. A dried precleaned pycnometer may be used to determine the density of these solutions.
10. Filtration might be a time-consuming step if the system contains small domains, like fine particles or unstable emulsions and colloids, which may clog the filter pores, demanding vacuum filtration or even several filtration repetitions. Some

strategies to prevent clogging are shifting the heterogeneous equilibrium of inorganic particulates using chelating agents [6], using oxidants to decompose globules of fatty acid in milk [60], or heat to decrease milk viscosity [60].

11. Chemical composition of the filter influences polymer characterization. Choose the filter according to its compatibility with the instrumental analysis performed in the next step (*see* Subheading 3.4).
12. When monitoring a well-controlled environment, the complexity of the unknown polymer types, which is the usual environmental monitoring condition, can be avoided. In a well-controlled environment with excellent contamination control, the identification step can be simplified considering that all microplastics come from specific process equipment or packaging. In that case, it might be considered that the optical microscopy or even visual inspection for larger microplastics could be enough identification if there is enough color contrast.
13. When the characterization step is optical microscopy, the risk of confusing plastic fragments with organic matter must be reduced using dyes with a remarkable interaction with nonpolar structures rather than polar ones. The most used dye is the Nile red [19, 61], which has a solvatochromic property, shifting the color as a function of the amount of hydrophobicity on the microplastics surface. Other dyes might also stain organic particles, misleading the identification.
14. Energy-dispersive X-ray spectroscopy (EDS) [44], usually coupled to microscopy SEM-EDS, is used for elementary analysis, and it is not a polymer identification method, but it is a technique that can eliminate if a suspected particle is not a plastic based on the elements ratio present. In other words, EDS may not confirm if the particle is a microplastic, but it can confirm if it is not, for example, if other elements are more abundant than carbon content.

## References

1. Campanale M, Savino L, Uricchio. (2020) A detailed review study on potential effects of microplastics and additives of concern on human health. *Int J Environ Res Public Health* 17(4):1212
2. Schmid P, Welle F (2020) Chemical migration from beverage packaging materials—a review. *Beverages* 6(2):37
3. Bang DY, Kyung M, Kim MJ, Jung BY, Cho MC, Choi SM et al (2012) Human risk assessment of endocrine-disrupting chemicals derived from plastic food containers. *Compr Rev Food Sci Food Safe* 11:453-470
4. Sobhani Z, Lei Y, Tang Y, Wu L, Zhang X, Naidu R et al (2020) Microplastics generated when opening plastic packaging. *Sci Rep* 10(1):4841
5. Zuccarello P, Ferrante M, Cristaldi A, Copat C, Grasso A, Sangregorio D et al (2019) Exposure to microplastics (<10 μm) associated to plastic bottles mineral water consumption: the first quantitative study. *Water Res* 157:365–371

6. Oßmann BE, Sarau G, Holtmannspötter H, Pischetsrieder M, Christiansen SH, Dicke W (2018) Small-sized microplastics and pigmented particles in bottled mineral water. *Water Res* 141:307–316
7. Liebezeit G, Liebezeit E (2013) Non-pollen particulates in honey and sugar. *Food Addit Contam Part A* 30(12):2136–2140
8. Yang D, Shi H, Li L, Li J, Jabeen K, Kolandhasamy P (2015) Microplastic pollution in table salts from China. *Environ Sci Technol* 49(22):13622–13627
9. Iñiguez ME, Conesa JA, Fullana A (2017) Microplastics in Spanish table salt. *Sci Rep* 7(1):8620
10. Karami A, Golieskardi A, Keong Choo C, Larat V, Galloway TS, Salamatinia B (2017) The presence of microplastics in commercial salts from different countries. *Sci Rep* 7(1):46173
11. Du F, Cai H, Zhang Q, Chen Q, Shi H (2020) Microplastics in take-out food containers. *J Hazard Mater* 399:122969
12. Crossman J, Hurley RR, Futter M, Nizzetto L (2020) Transfer and transport of microplastics from biosolids to agricultural soils and the wider environment. *Sci Total Environ* 724:138334
13. Huang Y (2020) Agricultural plastic mulching as a source of microplastics in the terrestrial environment. *Environ Pollut* 260:114096
14. Brahney J, Hallerud M, Heim E, Hahnenberger M, Sukumaran S (2020) Plastic rain in protected areas of the United States. *Science* 368(6496):1257–1260
15. Masura J, Baker J, Foster G, Arthur C (2015) Laboratory methods for the analysis of microplastics in the marine environment. NOAA
16. Prata JC, Reis V, da Costa JP, Mouneyrac C, Duarte AC, Rocha-Santos T (2021) Contamination issues as a challenge in quality control and quality assurance in microplastics analytics. *J Hazard Mater* 403:123660
17. Zhang Y, Kang S, Allen S, Allen D, Gao T, Sillanpää M (2020) Atmospheric microplastics: a review on current status and perspectives. *Earth-Sci Rev* 203:103118
18. Chen G, Fu Z, Yang H, Wang J (2020) An overview of analytical methods for detecting microplastics in the atmosphere. *TrAC Trends Anal Chem* 130:115981
19. Prata JC, da Costa JP, Duarte AC, Rocha-Santos T (2019 Jan) Methods for sampling and detection of microplastics in water and sediment: a critical review. *TrAC Trends Anal Chem* 110:150–159
20. Stock F, Kochleus C, Bansch-Baltruschat B, Brennholt N, Reifferscheid G (2019) Sampling techniques and preparation methods for microplastic analyses in the aquatic environment – a review. *TrAC Trends Anal Chem* 113:84–92
21. Shruti VC, Pérez-Guevara F, Elizalde-Martínez I, Kuttralam-Muniasamy G (2021) Toward a unified framework for investigating micro(nano)plastics in packaged beverages intended for human consumption. *Environ Pollut* 268:115811
22. Prata JC, Paço A, Reis V, da Costa JP, Fernandes AJS, da Costa FM et al (2020) Identification of microplastics in white wines capped with polyethylene stoppers using micro-Raman spectroscopy. *Food Chem* 331:127323
23. Makhdoumi P, Amin AA, Karimi H, Pirsahab M, Kim H, Hossini H (2021) Occurrence of microplastic particles in the most popular Iranian bottled mineral water brands and an assessment of human exposure. *J Water Proc Eng* 39:101708
24. Mason SA, Welch VG, Neratko J (2018) Synthetic polymer contamination in bottled water. *Front Chem* 6:407
25. Kuttralam-Muniasamy G, Pérez-Guevara F, Elizalde-Martínez I, Shruti VC (2020) Branded milks – are they immune from microplastics contamination? *Sci Total Environ* 714:136823
26. Liebezeit G, Liebezeit E (2015) Origin of synthetic particles in honeys. *Pol J Food Nutr Sci* 65(2):143–147
27. Mühlischlegel P, Hauk A, Walter U, Sieber R (2017) Lack of evidence for microplastic contamination in honey. *Food Addit Contam Part A* 34(11):1982–1989
28. Lusher AL, Welden NA, Sobral P, Cole M (2017) Sampling, isolating and identifying microplastics ingested by fish and invertebrates. *Anal Methods* 9(9):1346–1360
29. Hermesen E, Mintenig SM, Besseling E, Koelmans AA (2018) Quality criteria for the analysis of microplastic in biota samples: a critical review. *Environ Sci Technol* 52(18):10230–10240
30. Silva AB, Bastos AS, Justino CIL, da Costa JP, Duarte AC, Rocha-Santos TAP (2018) Microplastics in the environment: challenges in analytical chemistry - a review. *Anal Chim Acta* 1017:1–19
31. Möller JN, Löder MGJ, Laforsch C (2020) Finding microplastics in soils: a review of analytical methods. *Environ Sci Technol* 54(4):2078–2090
32. Yang L, Zhang Y, Kang S, Wang Z, Wu C (2021) Microplastics in soil: a review on

- methods, occurrence, sources, and potential risk. *Sci Total Environ* 780:146546
33. Fadare OO, Okoffo ED, Olasehinde EF (2021) Microparticles and microplastics contamination in African table salts. *Mar Pollut Bull* 164:112006
  34. Lee H-J, Song N-S, Kim J-S, Kim S-K (2021) Variation and uncertainty of microplastics in commercial table salts: critical review and validation. *J Hazard Mater* 402:123743
  35. Peixoto D, Pinheiro C, Amorim J, Oliva-Teles L, Guilhermino L, Vieira MN (2019) Microplastic pollution in commercial salt for human consumption: a review. *Estuar Coast Shelf Sci* 219:161–168
  36. Kim J-S, Lee H-J, Kim S-K, Kim H-J (2018) Global pattern of microplastics (MPs) in commercial food-grade salts: sea salt as an indicator of seawater MP pollution. *Environ Sci Technol* 52(21):12819–12828
  37. Conesa JA, Iñiguez ME (2020) Analysis of microplastics in food samples. In: Rocha-Santos T, Costa M, Mouneyrac C (eds) *Handbook of microplastics in the environment* [Internet]. Springer International Publishing [cited 2021 Mar 29], Cham, p 1–16. Available from: [http://link.springer.com/10.1007/978-3-030-10618-8\\_5-1](http://link.springer.com/10.1007/978-3-030-10618-8_5-1)
  38. Zarfl C (2019) Promising techniques and open challenges for microplastic identification and quantification in environmental matrices. *Anal Bioanal Chem* 411(17):3743–3756
  39. Merck (2021) Sigma-Aldrich [Internet]. Available from: <https://www.sigmaaldrich.com/>
  40. Waldman WR, Rillig MC (2020) Microplastic research should embrace the complexity of secondary particles. *Environ Sci Technol* 54(13):7751–7753
  41. Karlsson TM, Kärrman A, Rotander A, Hasselöv M (2020) Comparison between manta trawl and in situ pump filtration methods, and guidance for visual identification of microplastics in surface waters. *Environ Sci Pollut Res* 27(5):5559–5571
  42. Lusher AL, Bråte ILN, Munno K, Hurley RR, Welden NA (2020) Is it or isn't it: the importance of visual classification in microplastic characterization. *Appl Spectrosc* 74(9):1139–1153
  43. Renner G, Schmidt TC, Schram J (2018) Analytical methodologies for monitoring micro(nano)plastics: which are fit for purpose? *Curr Opin Environ Sci Health* 1:55–61
  44. Gniadek M, Dąbrowska A (2019) The marine nano- and microplastics characterisation by SEM-EDX: the potential of the method in comparison with various physical and chemical approaches. *Mar Pollut Bull* 148:210–216
  45. Käßler A, Fischer D, Oberbeckmann S, Schernewski G, Labrenz M, Eichhorn K-J et al (2016) Analysis of environmental microplastics by vibrational microspectroscopy: FTIR, Raman or both? *Anal Bioanal Chem* 408(29):8377–8391
  46. Renner G, Schmidt TC, Schram J (2017) Characterization and quantification of microplastics by infrared spectroscopy. In: *Comprehensive analytical chemistry* [Internet]. Elsevier; [cited 2021 Mar 29], pp 67–118. Available from: <https://linkinghub.elsevier.com/retrieve/pii/S0166526X16301556>
  47. Löder MGJ, Kuczera M, Mintenig S, Lorenz C, Gerdtts G (2015) Focal plane array detector-based micro-Fourier-transform infrared imaging for the analysis of microplastics in environmental samples. *Environ Chem* 12(5):563
  48. Araujo CF, Nolasco MM, Ribeiro AMP, Ribeiro-Claro PJA (2018) Identification of microplastics using Raman spectroscopy: latest developments and future prospects. *Water Res* 142:426–440
  49. von der Esch E, Kohles AJ, Anger PM, Hoppe R, Niessner R, Elsner M et al (2020) TUM-ParticleTyper: a detection and quantification tool for automated analysis of (microplastic) particles and fibers. George M, editor. *PLoS One* 15(6):e0234766
  50. Munno K, De Frond H, O'Donnell B, Rochman CM (2020) Increasing the accessibility for characterizing microplastics: introducing new application-based and spectral libraries of plastic particles (SLoPP and SLoPP-E). *Anal Chem* 92(3):2443–2451
  51. Picó Y, Barceló D (2020) Pyrolysis gas chromatography-mass spectrometry in environmental analysis: focus on organic matter and microplastics. *TrAC Trends Anal Chem* 130:115964
  52. Peñalver R, Arroyo-Manzanares N, López-García I, Hernández-Córdoba M (2020) An overview of microplastics characterization by thermal analysis. *Chemosphere* 242:125170
  53. Yakovenko N, Carvalho A, ter Halle A (2020) Emerging use thermo-analytical method coupled with mass spectrometry for the quantification of micro(nano)plastics in environmental samples. *TrAC Trends Anal Chem* 131:115979
  54. Suaria G, Achtypi A, Perold V, Lee JR, Pierucci A, Bornman TG et al (2020) Microfibers in oceanic surface waters: a global characterization. *Sci Adv* 6(23):eaay8493

55. Olsen LMB, Knutsen H, Mahat S, Wade EJ, Arp HPH (2020) Facilitating microplastic quantification through the introduction of a cellulose dissolution step prior to oxidation: proof-of-concept and demonstration using diverse samples from the Inner Oslofjord, Norway. *Mar Environ Res* 161:105080
56. Wu J, Lai M, Zhang Y, Li J, Zhou H, Jiang R et al (2020) Microplastics in the digestive tracts of commercial fish from the marine ranching in East China Sea, China. *Case Stud Chem Environ Eng* 2:100066
57. Quinn B, Murphy F, Ewins C (2017) Validation of density separation for the rapid recovery of microplastics from sediment. *Anal Methods* 9(9):1491–1498
58. Dinu MI (2010) Comparison of complexing ability of fulvic and humic acids in the aquatic environment with iron and zinc ions. *Water Resour* 37(1):65–69
59. Güngör EBÖ, Bekbölet M (2010) Zinc release by humic and fulvic acid as influenced by pH, complexation and DOC sorption. *Geoderma* 159(1–2):131–138
60. Diaz-Basantes MF, Conesa JA, Fullana A (2020) Microplastics in honey, beer, milk and refreshments in Ecuador as emerging contaminants. *Sustainability* 12(14):5514
61. Erni-Cassola G, Gibson MI, Thompson RC, Christie-Oleza JA (2017) Lost, but found with Nile Red: a novel method for detecting and quantifying small microplastics (1 mm to 20  $\mu\text{m}$ ) in environmental samples. *Environ Sci Technol* 51(23):13641–13648



## Identification of Intentionally and Non-intentionally Added Substances in Recycled Plastic Packaging Materials

Magdalena Wrona, Davinson Pezo, Robert Paiva, and Sandra A. Cruz

### Abstract

Intentionally added substances (IAS) and non-intentionally added substances (NIAS) play an important role in food contact materials. Even though food packaging is being used to ensure the quality and safety of food, chemicals may be transferred to food. This aspect is more critical for recycled polymers destined to contact with food. The presence of contaminants associated with the high shear rates and temperatures characteristics of the recycling process results in new molecules with low molar mass. These have a greater migration potential contaminating the food and constitute a risk to consumers. Despite the importance of NIAS and IAS, there are significant difficulties in their identification and quantification due to the confidential composition of the polymers, the complexity of the chemical structure, and unequivocal confirmation analytes. Therefore, this chapter addresses an overview of the challenge of NIAS and IAS determination, as well as the most modern analytical methods for determination and quantification in complex polymeric matrix. Moreover, the usage of analytical techniques has been shown in the context of direct analysis of recycled polymer surface, the importance of odorous research, and samples from migration assays (volatile and non-volatile IAS and NIAS). Therefore, techniques such as SERS, ASAP, HS-SPME-GC-O-MS, DI-GC-MS, SPME-GC-MS, GC-FID, APGC-Q-TOF-MS<sup>E</sup>, UPLC-Q-TOF-MS<sup>E</sup>, UPLC-QqQ-MS, LTQ-Orbitrap, and UPLC-IM-Q-TOF have been discussed, and examples of analysis of real IAS and NIAS in the complex matrix have been added. Finally, the application of European legislation and risk assessment have also been discussed.

**Key words** NIAS, IAS, Recycled packaging, Analytical methods, Migration, Food contamination, Legislation, Risk assessment, Food safety

---

## 1 Introduction

Food contact materials (FCMs) are defined as all materials that come into contact with food during processing, production, storage, packaging, transportation, preparation, and serving. Different types of materials, such as polymers, paper, glass, metal, as well as inks, adhesives, and/or even a combination of them, may be used as FCMs [1, 2]. In the last few years, studies and regulations on FCMs have increased significantly due to the presence of diverse chemicals

that may present potential adverse health effects to humans or the environment [1, 3, 4]. This is more critical for food contact articles based on polymers due to their greater diffusivity, and the potential migration of contaminants when compared to other materials such as metal or glass. The migration of a substance from a polymer to food depends on the mass transfer phenomenon, especially the diffusion process [5]. Readers can refer to Chap. 6 for further information on migration of constituents of FCMs. Additionally, the time, temperature, physicochemical properties of the substances, and characteristics of the molecular structure of the polymer impact these processes. Consequently, this is a complex system, and the migration depends on intrinsic and extrinsic factors and their relationship to the physicochemical properties of each polymer and substance [6, 7].

Although food contact articles, especially food packaging, are used to ensure the quality and safety of food, chemicals may still migrate and endanger the health of consumers [8]. The list of possible chemical migrants is very broad and includes substances that are named intentionally added substances (IAS). IAS can be defined as (i) residual compounds from the polymerization process, such as monomers, catalysts, initiators, and (ii) additives inserted deliberately to improve the properties or processability of polymers, for example, plasticizers, antioxidants, flow aids, and others [4, 9]. Recently, a new class of substances has been highlighted in the field of food safety: non-intentionally added substances (NIAS). NIAS may originate from degradation products, additives, and impurities, as well as the reactions between them. On the other hand, oligomers have recently been classified as NIAS once they form due to incomplete reactions during polymerization, according to the European Union Requirements [10]. IAS and NIAS can also be classified as volatile, semi-volatile, and non-volatile based on their molar masses. Therefore, highly sensitive analytical methods and digital libraries are required for their identification and quantification [11–13].

Most studies on chemicals present in plastics have focused on the identification of monomers [14, 15] and additives, especially antioxidants [16] and those used at higher concentrations as plasticizers [17, 18]. Ibarra and co-workers [17] studied the extraction of seven compounds, most of them phthalates, from real food matrices, such as snacks, cookies, and cakes. All compounds were previously identified in 34 packaged foodstuffs and the quantification was performed by gas chromatography coupled with mass spectrometry (GC-MS). The plasticizer acetyl tributyl citrate was detected in 94% of the samples, followed by different types of phthalates, and dibutyl phthalate at levels exceeding the specific migration limits established by Regulation 10/2011 [10].

Moreover, NIAS formation occurs most frequently due to degradative processes of polymers, additives, and/or impurities.

As a result, new molecules with low molar mass and high diffusion coefficients are formed, resulting in compounds with greater migration potential. Several studies have reported the formation of NIAS, mainly related to poly(ethylene terephthalate) (PET) [19–21], where the most relevant and well-known compounds are formaldehyde and acetaldehyde.

Subsequently, an additional aspect when using recycled materials in direct contact with food is the presence of contaminants and degradation products that can migrate into food. Despite its relevance, this is an issue that is rarely addressed in the literature [22, 23]. In this industry, the most used recycling process is mechanical due to its relative low-cost, large-scale, and solvent-free features, besides being applicable to most thermoplastics. However, the high shear rates and temperatures employed in the recycling result in an increase in the degradation process, which leads to chain scission, chain crosslinking, and branching formation, as well as the oxidation of polymer molecules. Additionally, the presence of contaminants, such as lids and labels, printing inks, pigments, foreign compounds due to misuse by consumers, and polymer cross-contamination may accelerate the degradation reactions during the recycling process. Moreover, the presence of contaminants from previously packaged foods associated with incorrect disposal has caused a more critical degradation [24, 25].

The packaging sector has always had the highest consumption in the global plastic market, with the largest amount destined for single-use applications. Around 36.5% of the world's plastic production in 2019 was attributed to this sector [26]. As a consequence, these products contribute significantly to environmental pollution and waste generation. The use of recycled plastic for the same application is one of the strategies to valorize it and close the loop for these materials. Notwithstanding this fact, the potentially hazardous compounds (e.g., NIAS, present in recycled packaging) may contaminate food and pose a risk to the consumers. Therefore, several works are being carried out to create a database, identify and develop methodologies for precise identification of NIAS using analytical techniques. Most studies on recycled polymers and NIAS are focused on PET [27], low-density polyethylene (LDPE) and high-density polyethylene (HDPE) [28, 29], expanded polystyrene (EPS) [30], and polypropylene [31].

As previously described, the greatest difficulty for the implementation of the use of recycled packaging for food contact is related to the migration of NIAS and IAS. Health authorities have clearly defined the criteria for the use of recycled FCM [32–35]. These recycled plastics must be submitted to a decontamination technology that is effective in reducing the level of contaminants to those allowed by regulatory agencies [36]. The regulations and directives follow the recommendations of the Codex Alimentarius Commission (CAC) and the Joint FAO/WHO Expert



Committee on Food Additives (JECFA) concerning the safety assessment of these substances [37, 38]. Although the use of IAS for the production of FCMs is allowed, these substances must meet the food safety profile established in the standards and directives of each country. In general, IAS must be registered and cataloged in a database, and they must not represent a health risk to the population. Another requirement is that the concentration of these substances in food must not exceed the specific migration limit established by the legislation [32, 39–42]. Regulatory agencies, however, encounter difficulties regarding registering NIAS. The European Commission and the US Food and Drug Administration recommend that these NIAS should not exceed the analytical migration tolerance of a maximum of  $0.01 \text{ mg kg}^{-1}$  in food [10, 43, 44]. In addition, if the substance has a potential mutagenicity (*see* Chap. 8 for the determination of genotoxicity and mutagenicity of food packaging materials), carcinogenicity, or toxicity (*see* Chap. 7 for the assessment of the cytotoxicity of food packaging) risk, it should not be used in FCMs.

### 1.1 Difficulties of NIAS and IAS Determination

Recycled materials have a complex chemical composition, especially when compared to their pristine counterparts. The degradative processes of a polymer, its additives, and impurities result in the formation of molecules denoted as NIAS. Due to the lack of information regarding the composition of plastic products by the manufacturer associated with new molecules formed due to the degradative process, the identification of NIAS via qualitative analysis is a very challenging task [12]. Establishing the structure of detected NIAS is also not easy to work on due to the lack of suitable references and low concentrations of those substances.

Figure 1 shows an example of isomers of nonylphenols (NPs) and nonylphenol ethoxylated (NPEO). NPs are formed as a result of hydrolysis of the antioxidant tris(nonylphenyl) phosphite (TNPP), which is used as a stabilizer for polymeric FCMs. NPs are endocrine disruptors and xenoestrogens, while NPEOs are

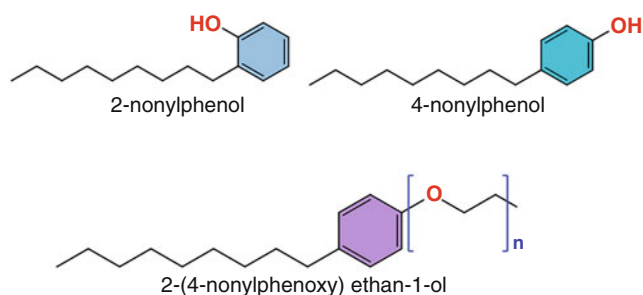


**Fig. 1** The structural formula of the example of nonylphenols and nonylphenol ethoxylated isomers considered as NIAS and are registered with different CAS numbers

nonionic surfactants that can be found as potential migrants from food packaging adhesives. NPEOs degrade into NPs in the environment and both families of compounds are considered NIAS [45–47]. NPs can be analyzed by direct injection GC-MS (DI-GC-MS), and NPEOs can be analyzed by ultra-high-performance liquid chromatography coupled to quadrupole time-of-flight with MS<sup>E</sup> technology (UPLC-Q-TOF-MS<sup>E</sup>) [48].

The non-target analysis is the most suitable analytical approach for the determination of NIAS. It is based on the screening of all chemical compounds detectable by the specific analytical method in one sample injection. By using non-target analysis, it is possible to determine new compounds that have not been yet studied, which is highly desirable in NIAS analysis [51, 52]. The reported findings of new NIAS [30, 51–53] prove that non-target analysis is an indispensable tool for the qualitative analysis of recycled polymers for food packaging applications.

On the other hand, the analysis of IAS is easier when compared to NIAS. For this reason, the target analysis can be used successfully. In this case, the target analysis is based on the detection and quantification of the list of known compounds. It would be convenient to use an internal standard containing a similar compound to IAS that is currently investigated. Furthermore, it would be perfect if the quantitative analysis of the detected IAS in recycled polymers for food packaging applications contained internal standards at similar concentrations to the analyte [33, 54, 55] (Fig. 2).

When analytical standards of chemical compounds are not available in the market, the quantitative analysis of IAS and NIAS is more complex [41, 56]. Another case is when the analyte is a complex mixture of different compounds giving a single signal, and its origin cannot be determined to match the best standards (e.g., mineral oils, as shown in Fig. 3) [43, 57]. Therefore, the concentrations of analytes are estimated by semi-quantification. Calibration is based on a standard that has a similar chemical structure to the analyzed NIAS, or on a standard of a known compound that is eluted in the center of the chromatogram [58]. In exceptional cases, small-scale synthesis of missing standards can be performed on a laboratory scale.

Finally, highly sensitive analytical techniques capable of separating and detecting IAS and NIAS need to be used. A wide range of analytical methods with well-established protocols of identification and quantification are required. Successful analysis of IAS and NIAS demonstrates the effectiveness of applying practical guidance on performance criteria and validation procedures for analytical methods used in the control of FCMs [59], the performance of migration assays [29], and the risk assessment [60].

Nowadays, new analytical methods are developed with lower limits of detection and quantification. Also, the future developments in the field of highly sensitive analytical methods will lead

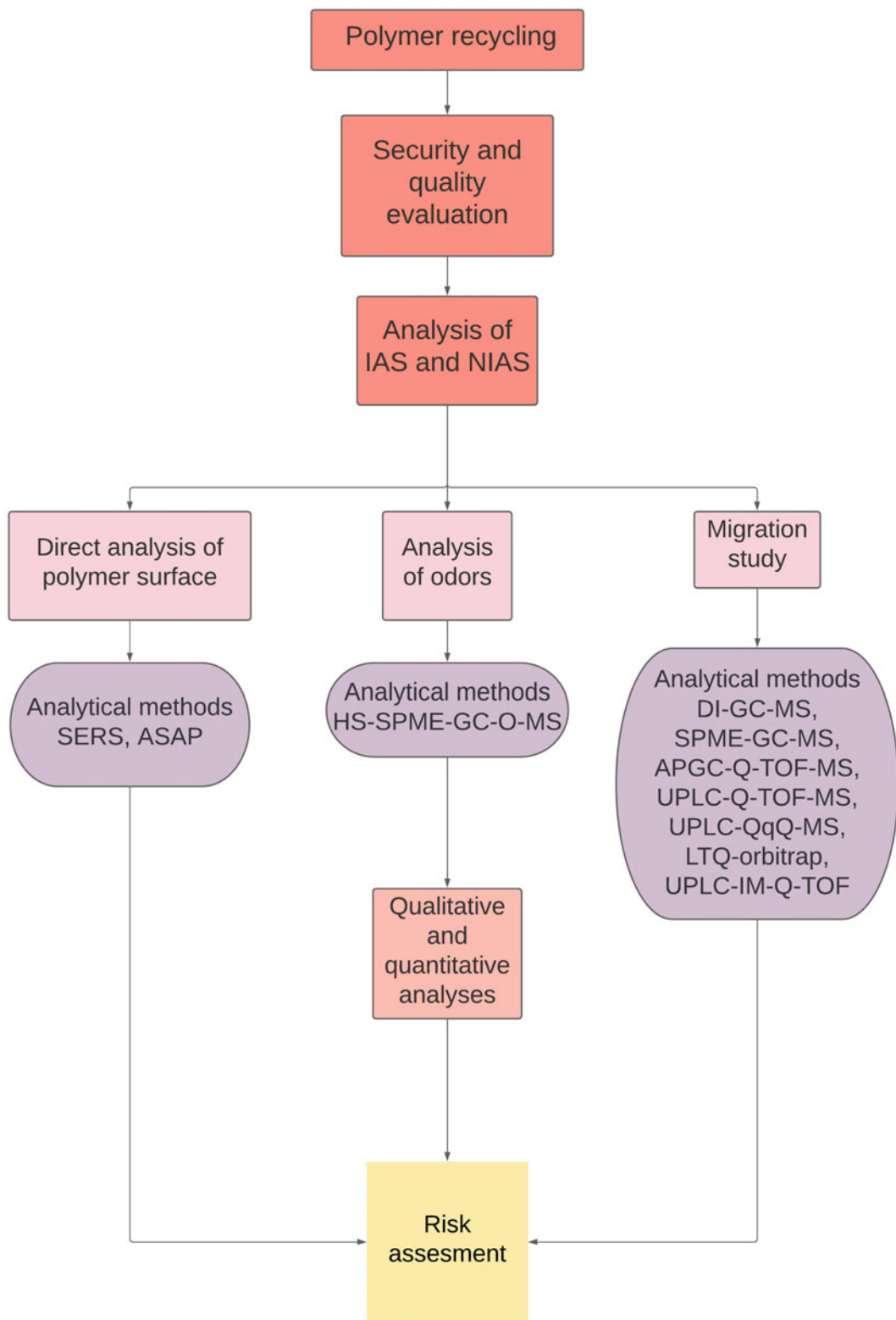


**Fig. 2** Dependency diagram of the safety and quality of recycled polymers in terms of analysis of IAS and NIAS and analytical methods

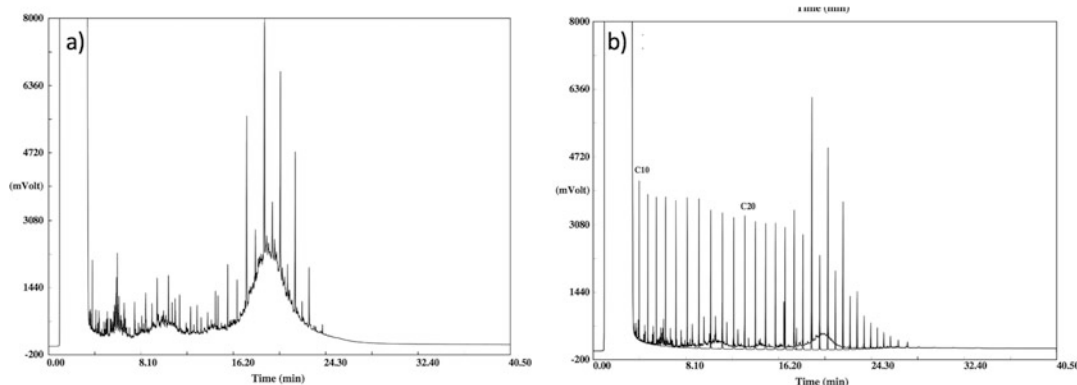


**Fig. 3** Chromatograms of (a) olive oil sample with a concentration of  $157.42 \mu\text{g g}^{-1}$  of mineral oil; (b) pure olive oil sample with a concentration of  $57.42 \mu\text{g g}^{-1}$  compared with the standard of alkanes C7–C40 with a concentration at  $10 \mu\text{g g}^{-1}$ . (Reproduced from Ref. [18] with permission from Elsevier, Copyright 2013)

to determining new IAS and NIAS that are present at the ultra-traces (ppb and sub-ppb) level. Those compounds will probably not cause health hazards due to a very low concentration. Although it should be highlighted that the toxicity of migrants depends not only on the dose but also on the exposure time.

Nevertheless, qualitative and quantitative analyses of migrating compounds from FCMs must comply with European legislation and all its amendments [61] in order to be available on the market. Therefore, proper characterization of recycled food packaging is critical.

Moreover, there is a strong tendency toward applying computation in the building of chemical libraries [62] that will allow the identification of chemical structures and named NIAS that are currently referred to as “unknown.” Modern libraries of screening compounds are already at the forefront of innovative chemical fingerprint matching design supporting the needs of scientists in their pursuit of novel molecules and NIAS identification.

---

## 2 Methods

### 2.1 Determination of IAS and NIAS

The assurance of quality and safety in the application of recycled polymers for food contact involves performing complex analyses utilizing a wide range of analytical methods. Only a broad spectrum of studies will give enough information on the plastic risk of containing toxic chemicals dangerous to human health. Both qualitative and quantitative research is crucial in the study of IAS and NIAS. The selection of the appropriate techniques depends on the type of sample being analyzed, whether it is a direct analysis of the polymer or a migration study to ensure polymer safety.

Moreover, target or non-target analysis can be performed depending on the information about the recycled polymer composition [33].

During the investigation of IAS and NIAS from recycled polymers, the application of modern analytical methods for determining and quantifying different analytes in the complex matrix is required. A dependency diagram describing the relationships between NIAS, IAS, risk assessment, recycled polymer development and safety, and analytical methods is shown in Fig. 2. The following analytical techniques are abbreviated: surface-enhanced Raman spectroscopy (SERS), atmospheric solids analysis probe (ASAP), headspace-solid phase microextraction gas chromatography-olfactometry-mass spectrometry (HS-SPME-GC-O-MS), direct injection gas chromatography-mass spectrometry (DI-GC-MS), solid-phase microextraction gas chromatography-mass spectrometry (SPME-GC-MS), atmospheric pressure gas chromatography coupled to quadrupole time-of-flight with high energy mass spectrometry (APGC-Q-TOF-MS<sup>E</sup>), ultra-high-performance liquid chromatography coupled to quadrupole time-of-flight with high energy mass spectrometry (UPLC-Q-TOF-MS<sup>E</sup>), ultra-high-performance liquid chromatography coupled to triple quadrupole with mass spectrometry (UPLC-QqQ-MS), hybrid linear ion trap–high-resolution mass spectrometry (LTQ-orbitrap), and ultra-high-performance liquid chromatography coupled to ion-mobility quadrupole time-of-flight mass spectrometry (UPLC-IM-Q-TOF-MS).

Analysis of IAS and NIAS can be performed by (i) direct analysis of the polymer surface, (2) odors analysis, and (3) migration study. As a result, volatile, semi-volatile, and/or non-volatile compounds can be detected depending on the analytical technique applied. In the sequence, the possibility of identifying NIAS and IAS will be discussed by (i) direct analysis of polymer surface, especially using ASAP and SERS, (ii) migration assays, and the analyses of (iii) volatile and (iv) non-volatile compounds.

## **2.2 Direct Analysis of Polymer Surface**

Regarding the ASAP, the sample is taken with a glass rod (immersed, rubbed) and then is entered into the ionization chamber, where it is evaporated and ionized under atmospheric pressure. The produced ions are analyzed by the MS detector. The advantage of ASAP analysis is that the analyte concentration in the sample analyzed directly is much higher than, for example, in samples after migration assays. This allows better identification of IAS and NIAS. It is a screening technique that directs the researcher to the appropriate choice for further analysis [63]. Still, ASAP has no necessity for treatment and manipulation of the sample and there is a lack of a precleaning step. Those additional tasks are very often time-consuming, expensive, and environmentally unfriendly due to the usage of a high number of solvents. It should be highlighted that there is no separation of the analytes on the chromatographic

column. This results in the simultaneous determination of all analyses from the recycled polymer matrix. Therefore, ASAP is commonly used for target analysis, because it is a rapid tool for screening purposes [12, 64].

A novel application of ASAP for the analysis of NIAS and IAS is the determination of characteristic markers of mineral oils hydrocarbons (MOH) [65]. MOH is a mixture of hydrocarbons containing thousands of chemical compounds of different structures and sizes derived from petroleum. Therefore, their presence in recycled packaging can come from polyolefins, paper, board, traces of adhesives, and industrial contamination [61, 66].

It was confirmed that the influence of mineral oils on human health is negative, and their migration to food should be avoided [67–69]. As qualitative and quantitative analysis is complicated, MOHs have been divided into two groups to facilitate the analysis, namely: mineral oil saturated hydrocarbons (MOSH) and mineral oil aromatic hydrocarbons (MOAH). The signal of both, commonly reported by gas chromatography with flame ionization detector (GC-FID), has the shape of a characteristic hump [18, 30], as can be seen in Fig. 3a. Injection of *n*-alkanes [70] under the same chromatographic conditions as samples of MOH can help the identification of individual fractions of mineral oils, as can be seen in Fig. 3b. Guidance on sampling, analysis, and data reporting for the monitoring of MOHs in food and FCMs can be helpful in MOH analysis [54]. Chemical markers are very useful tools to verify the origin of MOAH. They also avoid misinterpretation of the analysis by providing detailed and reliable chemical evidence of MOAH contamination. Samples of recycled PET, recycled paperboard, and packaging of couscous and semolina were analyzed in search for MOAH markers by ASAP coupled to Q-TOF-MS<sup>E</sup>, and APGC-Q-TOF-MS<sup>E</sup> [35].

Another technique that allows the direct analysis is surface-enhanced Raman spectroscopy or surface-enhanced Raman scattering (SERS). It is a surface-sensitive technique that results in the enhancement of Raman scattering by nanoparticles such as silver, gold, and copper or a mixture of them adsorbed on the rough support surface. Near a rough metal surface, the Raman cross-section can be dramatically enhanced by a factor of up to 10<sup>14</sup>. This allows very sensitive measurements of the analyte adsorbed on the surface [45, 71]. The enhancement mechanisms are broadly divided into chemical and electrochemical enhancement. The chemical theory claims that, when molecules are adsorbed on the surface, their electronic states can interact with the states in the metal and produce new transitions. The true nature of this theory is still not fully understood. The electrochemical theory is based on the enhancement of the local electromagnetic field on the surface of a metal. If the wavelength of the incident electromagnetic field is close to the plasma wavelength of the metal, electrons can be

excited into an extended surface electronic state (surface plasmon resonance). This leads to extensive local fields. On the other hand, there is the formation of charge-transfer complexes between the analyte and the surface (resonance enhancement) [58]. SERS measurement is carried out using a confocal microscope. The Raman microscope is by far one of the best instrumentation enhancements one can make. The new generation of Raman microscopes can offer a powerful nondestructive and noncontact method of sample analysis. One of the most incredible benefits is the use of the confocal Raman microscope design. This enables a very small sample area or volume to be analyzed down to the micron scale. Combine this micro Raman analysis with automatic focusing XYZ motion, and it becomes possible to produce “chemical” images of a sample [59]. It is worth mentioning that mapping of the sample can also be performed by applying NIR hyperspectral imaging (*see* Chap. 10).

An example of a rapid Raman approach for the detection of NIAS can be the determination of titanium dioxide, calcium carbonate, and calcium sulfate as contaminants in polymer pellets and food packaging [29]. This technique allows the verification of the distribution of analytes in the analyzed sample. In this case, it was found that calcium carbonate and calcium sulfate were environmental contaminants. At the same time, titanium dioxide was a contaminant from the origin of the production process since it was also found in the bulk material. Nevertheless, some of those additives (e.g., titanium dioxide) can also be IAS as they are commonly used as polymer additives (fillers and white pigments). Figure 4 shows the Raman spectrum of oxo-biodegradable polyethylene for food applications with marked shifts at 609 and 449  $\text{cm}^{-1}$  that are characteristic of titanium dioxide [72].

Additionally, the distribution of NIAS and its clustering can be better understood by Raman imaging. Moreover, image analysis can be used as a semi-quantitative analysis of NIAS on the sample surface [29]. Figure 5 shows a 2-D map and a 3-D representation of an oxo-biodegradable polyethylene sample for food packaging applications imaged with a shift of titanium dioxide (609  $\text{cm}^{-1}$ ). Different colors indicate different intensities of Raman shifts.

### 2.3 Migration Assays

Although food packaging is designed to contain food products and protect them from the environment during transport and storage, it can also be a very significant chemical contamination source [73]. Therefore, mass transfer between the packaging material and packaged food under certain conditions is called migration. This process is essential from an analytical point of view because migration assays based on different types of simulants determine the analytical methods applied in the analysis of migrants [15, 12, 46, 74].

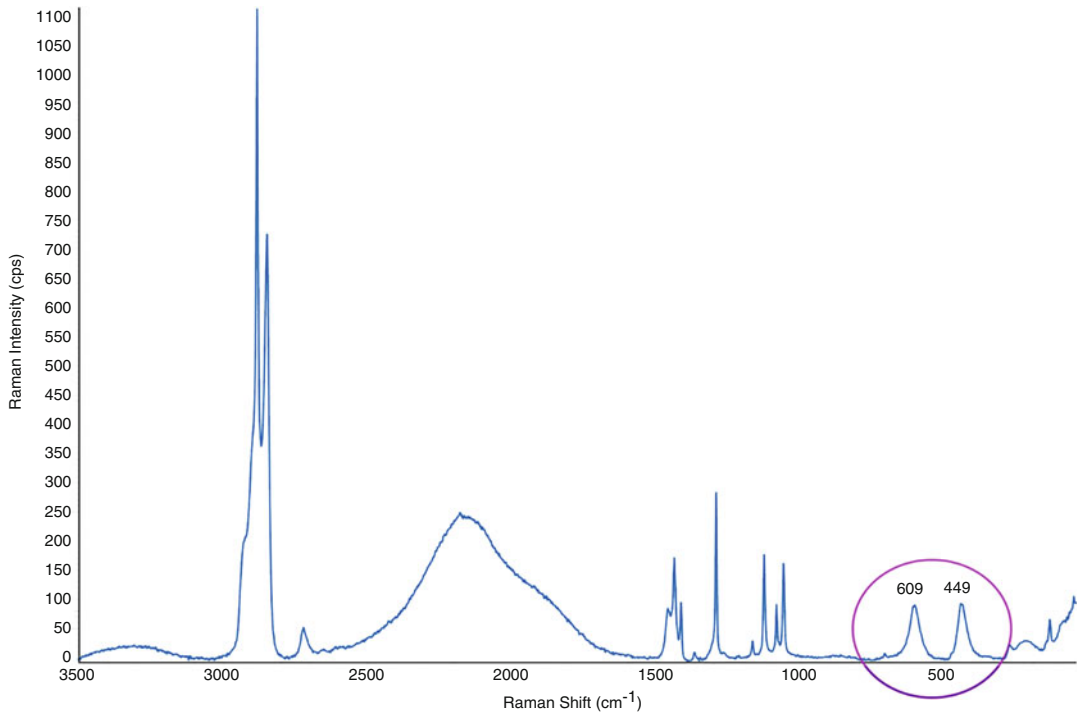


**Fig. 4** Raman spectrum of oxo-biodegradable polyethylene for food packaging applications with marked shifts corresponding to titanium dioxide

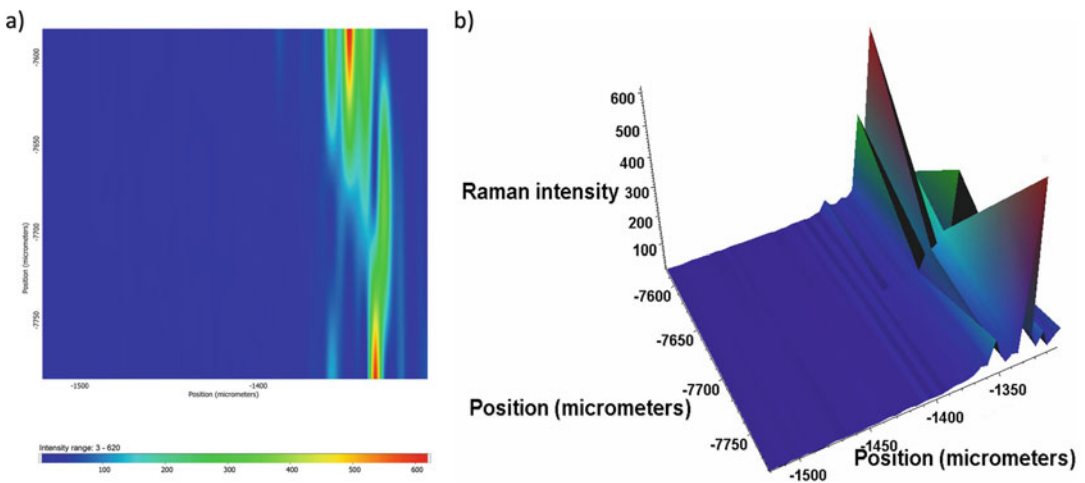


**Fig. 5** Raman (a) 2-D map and (b) 3-D representation (collected at  $609\text{ cm}^{-1}$ ) of an oxo-biodegradable polyethylene sample for food packaging applications

NIAS as migrants are compounds of low molar mass (considered to be less than 1000 Da) that are present in the recycled polymer. Food quality and safety can be compromised, and therefore, the health of consumers when these compounds reach a



specific limit. Consequently, research on the migration of chemical compounds from packaging to food is fundamental [47–50, 53, 75].

The European Union (EU) controls food-grade materials and articles distributed in the EU market. It is unacceptable that food packaging materials release substances in amounts hazardous to the consumers' health and change the composition of the food product. This is why strict formal requirements are imposed on plastics.

The European Commission Regulation EU 10/2011 [10] on plastic materials and articles intended to come into contact with food indicates in detail conditions for migration testing. There is no specific legislation for recycled polymers for food packaging applications. Standardized time-temperature conditions representing the particular food application and covering the maximum shelf-life of the packaged food are applied to the migration study. While it would be best to perform migration tests using real food, migration is usually tested using simulants. This is because food is a very complex matrix that is challenging to analyze. Simultaneously, food simulants imitate the behavior of food in contact with a sample of recycled plastic and are easier to analyze [12, 51, 66]. Table 1 shows types of food simulants, the proposition of analytical technique for analysis of migrants in each matrix, indication if its pretreatment is necessary, and what type of pretreatment may be successfully used.

The migration tests on NIAS delectation depend on whether the measurable material is mono or multilayer. Total immersion of the sample in food simulants is used for monolayer materials. Simultaneously, a special migration cell is needed for multilayer materials where only one side of the material is analyzed. Another option for multilayer packaging is migration assay performed by filling. In this case, a bag is made from the analyzed polymer and filled with food simulant. Only polymers with the property of thermosealing can be analyzed in this way.

## **2.4 Analysis of Volatile Compounds**

When migrants are determined in food simulants, both volatile and non-volatile compounds need to be analyzed. The group of volatile organic compounds (VOCs) includes organic compounds with boiling points less than or equal to 250 °C at a pressure of 101.3 kPa [86].

The method most frequently used to determine NIAS as VOCs in recycled polymer migration research is gas chromatography. It enables the separation of a mixture of compounds and, in combination with an appropriate detection system, gives information about the type and concentration of determined compounds after the calibration that precedes it. The essence of the chromatographic separation is the multiple division of the mixture components between two immiscible phases: the stationary phase and the mobile phase, the latter being a gas called a carrier gas. Together

**Table 1**  
**Summary of analytical techniques and sample pretreatment procedures for food simulants that are in EU 10/2011**

| Simulant | Food simulant  | Analytical technique   | Sample pretreatment  | Reference                               |
|----------|--|--|--|---|
| A        | Ethanol 10 vol%  | SPME-GC-MS, AQ-TOF-TOF-MS <sup>E</sup> , UPLC-Q-TOF-MS <sup>E</sup> , UPLC-QqQ-MS, LTQ-orbitrap, UPLC-IM-Q-TOF   | Not necessary; possible reconcentration of analytes may be done by HFLPME <sup>a</sup> or FPSE <sup>b</sup>                                      | [15, 30, 34, 50–52, 55, 60, 66, 76]     |
| B        | Acetic acid 3% (w/v)   | SPME-GC-MS, APGC-Q-TO-MS <sup>E</sup> , UPLC-QQ-TOFMS <sup>E</sup> , UPLC-QqQ-MS, LTQ-orbitrap, UPLC-IM-QQ-TOF   | Not necessary; possible reconcentration of analytes may be done by HFLPME <sup>a</sup> or FPSE <sup>b</sup>                                      | [15, 30, 34, 50–52, 55, 60, 66, 76]     |
| C        | Ethanol 20 vol%  | SPME-GC-MS, APGC-QQ-TOFMS <sup>E</sup> , UPLC-Q-Q-TOFS <sup>E</sup> , UPLC-QqQ-MS, LTQ-orbitrap, UPLC-IM-Q-TOF   | Not necessary; possible reconcentration of analytes may be done by HFLPME <sup>a</sup> or FPSE <sup>b</sup>                                      | [15, 50–52, 55, 62, 66, 77]             |
| D1       | Ethanol 50 vol%  | SPME-GC-MS, APGC-Q-TOF-MS <sup>E</sup> , UPLC-Q-TOF-MS <sup>E</sup> , UPLC-QqQ-MS, LTQ-orbitrap, UPLC-IM-Q-TOF   | Dilution in case of SPME-GC-MS analysis; possible reconcentration of analytes may be done by HFLPME <sup>a</sup> or FPSE <sup>b</sup>            | [15, 50–52, 55, 64–66, 77, 78]          |
| D2       | Vegetable oil or ethanol 95 vol%                               | Vegetable oil: Direct analysis with SERS and after extraction with methanol or ethanol the same techniques as for ethanol 95%<br>Ethanol 95%: DI-GC-MS, APGC-Q-TOF-MS <sup>E</sup> , UPLC-Q-TOF-MS <sup>E</sup> , UPLC-QqQ-MS, LTQ-orbitrap, UPLC-IM-Q-TOF | Extraction in case of vegetable oil<br>Ethanol 95%: Possible reconcentration of analytes may be done by HFLPME <sup>a</sup> or FPSE <sup>b</sup> | [15, 34, 50–52, 55, 60, 66, 75, 79, 80] |
| E        | Poly(2,6-diphenyl-p-phenylene oxide) called Tenax <sup>®</sup> | Direct analysis with ASAP<br>After extraction with ethanol or methanol: DI-GC-MS, APGC-Q-TOF-MS <sup>E</sup> , UPLC-Q-TOF-MS <sup>E</sup> , UPLC-QqQ-MS, LTQ-orbitrap, UPLC-IM-Q-TOF   | Extraction with ethanol or methanol; possible reconcentration of analytes may be done by HFLPME <sup>a</sup> or FPSE <sup>b</sup>                | [39, 50–53, 55, 61, 75, 81–85]          |

<sup>a</sup> HFLPME automatic multiple dynamic hollow fiber liquid-phase microextraction system

<sup>b</sup> FPSE fabric phase sorptive extraction

with the carrier gas, the analyzed substances move in the chromatographic column; those with higher affinity for the stationary phase move more slowly along the column and later reach the detector [87, 88].

Liquid simulants such as 95% ethanol is commonly analyzed by GC-MS. This method analyzes small molecules after electron-impact ionization (EI) to obtain mass spectra. Subsequent component identification is made by comparing the obtained spectrum, characteristic for each NIAS, with spectra in volatile compound libraries (e.g., NIST). The coefficient determining the agreement between the analyzed NIAS with recycled polymers for food applications and the standard is the match percentage. The greater the match percentage, the greater the agreement between the spectra. Confirmation (100%) of the qualitative analysis can be done by injecting pure standards of NIAS [66].

EI is a type of hard ionization using high energy and completely breaks down the molecules. Therefore, if the molecular ion characteristic of NIAS cannot be identified, it is recommended to try to analyze it with a complementary analytical method based on chemical ionization (CI) or atmospheric pressure ionization (APGC) using quadrupole and time-of-flight coupled to high-resolution MS. This technique allows direct analysis of all liquid simulants (Table 1). An example of such research can determine volatile NIAS from a starch-based polymer with a new formula for food packaging applications [89].

For the analysis of food simulants with high water content, SPME-GC-MS can be used. It is a high-speed technique that does not require the use of a solvent and therefore allows the analysis of volatile NIAS in aqueous solutions. Solid-phase microextraction (SPME) is based on adsorption of analytes in a hot fiber coated with different polymers or sorbents and their thermal desorption in

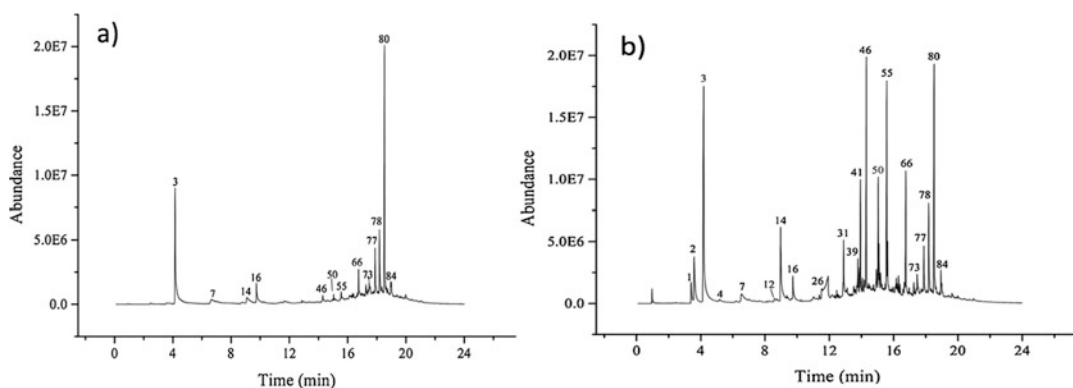


**Fig. 6** Representative total ion chromatograms (TIC) of (a) virgin and (b) recycled EPS containers with determined NIAS compounds. (Reproduced from Ref. [30] with permission from Elsevier, Copyright 2019)

the injection port of the chromatograph, where they are detected by MS. Figure 6 shows an example of the SPME-GC-MS spectra of volatile NIAS identified in recycled expanded polystyrene containers and their migration into food simulants such as 3% acetic acid and 10% ethanol. Chromatograms have market-detected NIAS with numbers with lists that can be seen in the literature [30].

Furthermore, a technique used to identify odor-active compounds that can result in NIAS [32] in a complex matrix such as recycled plastics is the headspace-solid phase microextraction-gas chromatography-olfactometry-mass spectrometry (HS-SPME-GC-O-MS). This technique contributed to the revolution in the analysis of the odors by the specific correlation with the chromatographic peaks of analytes and their aroma [40, 90]. Paiva et al. [31] analyzed the presence of volatiles and odoriferous compounds in samples of recycled polypropylene. Forty-five compounds were extracted by headspace solid-phase microextraction (HS-SPME) and detected by GC-MS and a sniffing port (GC-MS-O). Nine of these compounds interfere with the quality of food and had odoriferous characteristics, such as apple, vinegar, heavy-scented smell, hot oil, vinegar vapor, and burnt synthetics. Therefore, this work amplifies the importance of the detected odorous compounds for food applications and, concurrent with other literature [40, 78, 85], highlights the development of processes adequate to separate and decontaminate recycled polymers for food contact.

## **2.5 Analysis of Non-volatile Compounds**

Hyphenated techniques use the resolution capability of the analytical method and the capability of MS to identify the separated components. Liquid chromatography coupled to mass spectrometry (LC-MS) is such an analytical technique. The most important advantage of this technique is the ability to determine polar and macromolecular compounds; therefore, it is widely used in NIAS analysis. Unlike gas chromatography, liquid chromatography allows the analysis of non-volatile compounds.

As a result of the soft ionization of the analytes, a molecular ion is obtained. For liquid chromatography, there is no standard spectral library as the acquisition of samples can be performed using different experimental conditions (different energies of ionization).

UPLC-Q-TOF-MS<sup>E</sup> is the sensitive, fast, and effective technique used successfully for IAS and NIAS identification. Qualitative analysis is based on the simultaneous application of low and high collision energy for spectral acquisition. This mode provides accurate precursor and fragment ion mass information simultaneously. Therefore, this is a possible identification and pattern recognition of compounds such as aromatic amines [40], oligomers from starch-based polymer [89], and migrants from adhesives for food packaging applications [91]. Additionally, target analysis in single ion recording (SIR) mode, using even more sensitive equipment

UPLC-QqQ-MS, can be applied to make a quantitative analysis of the determined IAS and NIAS [15].

High-resolution ion trap hybrid linear mass spectrometry (LTQ-Orbitrap) compared to UPLC-Q-TOF-MS<sup>E</sup> can perform a multi-level NIAS fragmentation. This device is comprised of an MS linear ion trap and an Orbitrap mass analyzer. It has already been applied for the qualitative analysis of FCM non-volatile migrants [15].

Ion-mobility quadrupole time-of-flight mass spectrometry, coupled to the ultra-high-performance liquid chromatography (UPLC-IM-Q-TOF-MS), allows obtaining a very clean spectrum of the analyzed NIAS, because retention time together with the drift time is used to determine ions. Therefore, a novel collision cross-section (CCS) value connected directly with the shape and size of the analyzed NIAS is determined. Thus, the application of this analytical technique for analysis of migrants from recycled food packaging confirms much better-determined compounds. An example of its application can be the determination of polyamide 6 and polyamide 66 oligomers from kitchenware utensils to food. Oligomers are part of the polymer structure and are currently not legislated by the EU. They became NIAS in case of migration into food products from packaging [47].

---

### 3 Risk Assessment

Risk assessment of the negative impact of chemicals from recycled polymers on human health is based on the threshold of toxicological effects obtained from tests on animals. The threshold of toxicological concern (TTC) is defined as the level of the chemicals analyzed below which there would be no significant hazard to human health [92].

A positive list of migrants that can be detected in samples of migration assays has been presented in the European Regulation No 10/2011 on plastic materials and articles intended to contact foodstuffs. Therefore, these chemical substances can be used in recycled polymers for food packaging applications. Migration limits are a theoretical mathematical value that must not exceed the concentration of a given compound. Migration limits keep recycled plastics safe. Substances on the positive list of EU 10/2011 have assigned a specific migration limit (SML). These values were established based on the toxicity data of each chemical studied by the European Food and Safety Authority (EFSA). It should be emphasized that the term of global migration with the migration process is also connected. In this case, the total concentration of all substances migrating to the food (detected in the food simulant) must not exceed the overall migration limit (OML) of  $60 \text{ mg kg}^{-1}$  of food or  $10 \text{ mg dm}^{-2}$  of recycled material [66].

**Toxic Hazard** **by Cramer rules**

▶ Estimate









**Low (Class I)**

**Intermediate (Class II)**

**High (Class III)**

Verbose explanation

Cramer rules

-  Q1.Normal constituent of the body **No** Bisphenol A diglycidyl ether
-  Q2.Contains functional groups associated with enhanced toxicity **No** Bisphenol A diglycidyl ether
-  Q3.Contains elements other than C,H,O,N,divalent S **No** Bisphenol A diglycidyl ether
-  Q5.Simply branched aliphatic hydrocarbon or a common carbohydrate **No** Bisphenol A diglycidyl ether
-  Q6.Benzene derivative with certain substituents **No** Bisphenol A diglycidyl ether
-  Q7.Heterocyclic **Yes** Bisphenol A diglycidyl ether
-  Q8.Lactone or cyclic diester **No** Bisphenol A diglycidyl ether
-  Q10.3-membered heterocycle **Yes** Class **High (Class III)** Bisphenol A diglycidyl ether

**Fig. 7** Decision tree from Toxtree software for NIAS bisphenol A diglycidyl ether

Nevertheless, NIAS are very often new substances boasting toxicities with no prior study. The toxicity of chemicals not included in the positive list is estimated using Cramer's rules and the open-source application Toxtree in the TTC approach. Toxtree can assess toxic hazards by applying a decision tree approach. Cramer's classification assigns chemicals to one of three toxicity classes and proposes a maximum daily intake. Theoretical maximum migration amounts of 1.80, 0.54, and 0.09 mg kg<sup>-1</sup> are applied to classes I, II, and III, respectively [89]. Figure 7 presents a decision tree from Toxtree software for bisphenol A diglycidyl ether (BADGE). This toxic NIAS is an endocrine-disrupting substance and has been classified as class III [78, 89, 93].

Equation 1 is used to calculate the theoretical maximum migration amounts (mg kg<sup>-1</sup>) of NIAS coming from recycled polymer and not present in the positive list of EU 10/2011:

$$\text{EDI} = \text{migration} \cdot \text{food intake} \cdot \text{CF} \quad (1)$$

where EDI is the estimated daily intake (maximum daily intake for each substance per person, considered  $1 \text{ kg person}^{-1} \text{ d}^{-1}$  in Europe); CF = consumption factor [94].

In the case of BADGE, the endocrine-disrupting NIAS that has been assigned by Toxtree to Cramer class III EDI would be  $0.09 \text{ mg kg}^{-1}$ . This is because the maximum daily intake for each substance per person in Europe is considered  $1 \text{ kg person}^{-1} \text{ d}^{-1}$ , and the consumption factor is not applied in Europe. CF is fraction of the daily diet for a specific material that is part of the food contact materials. It is used for the analysis of recycled polymers in the USA. Therefore, obtained values of migrating BADGE concentration from recycled food packaging cannot exceed the calculated EDI value.

---

## 4 Final Considerations

Difficulties and challenges found in the analysis of IAS and NIAS in recycled food packaging have been present. The main challenges are summarized into the following: (i) the lack of information on the actual composition of the different ingredients and materials used for packaging production; (ii) extensive use of additives as stabilizers, antioxidants, plasticizers, among others, depending on the application; (iii) the need for high-sensitivity and precision analytical techniques; and (iv) the high shear rates and temperatures employed in recycling process that results in the formation of new molecules. Therefore, the identification and unequivocal confirmation of IAS and NIAS can be puzzling. In most cases, the non-target analysis is the most suitable analytical approach for the determination of NIAS, while the analysis of IAS is much easier, and the target analysis can be used favorably.

Successful analysis of IAS and NIAS is based on applying highly sensitive analytical techniques capable of their separation and detection. Migration assays, international legislation, and appropriate application of risk assessment are crucial for ensuring the quality and safety of recycled polymers to food contact. The use of analytical techniques has been shown for the direct analysis of surface. They are commonly used for target analysis and being a rapid tool for screening purpose. However, they present a lower limit of detection. Additionally, the importance of odorous research and samples from migration assays (volatile and non-volatile IAS and NIAS) are addressed in this chapter. Therefore, techniques such as SERS, ASAP, HS-SPME-GC-O-MS, DI-GC-MS, SPME-GC-MS, GC-FID, APGC-Q-TOF-MS<sup>E</sup>, UPLC-Q-TOF-MS<sup>E</sup>, UPLC-QqQ-MS, LTQ-orbitrap, and UPLC-IM-Q-TOF have been discussed, and examples of the analysis of real IAS and NIAS in the complex matrix have been added. Future developments in the field of super sensitive analytical techniques will probably lead to new

IAS and NIAS. Simultaneously, quick identification of those compounds will be possible due to the development of modern chemical libraries.

## Acknowledgments

The authors want to thank the PACMI group (Program for the Quality Assurance of Individualized Medications) of the Pharmacy area of the San Jorge University. Also, the authors wish to thank the Government of Aragon and the European Social Fund for financial support (T53-20R) to the GUIA group. Also, the authors would like to acknowledge FAPESP 2016/25703-2.

## References

- Groh KJ, Geueke B, Martin O, Maffini M, Muncke J (2020) Overview of intentionally used food contact chemicals and their hazards. *Environ Int* 106225:106225. <https://doi.org/10.1016/j.envint.2020.106225>
- Beneventi E, Tietz T, Merkel S (2020) Risk assessment of food contact materials. *EFSA J* 18:1–11. <https://doi.org/10.2903/j.efsa.2020.e181109>
- Frans FV, Jyrki V (2019) Circular economy: Commission welcomes Council final adoption of new rules on single-use plastics to reduce marine plastic litter. 30–31
- Groh KJ, Backhaus T, Carney-Almroth B, Geueke B, Inostroza PA, Lennquist A, Leslie HA, Maffini M, Slunge D, Trasande L, Warhurst AM, Muncke J (2019) Overview of known plastic packaging-associated chemicals and their hazards. *Sci Total Environ* 651: 3253–3268. <https://doi.org/10.1016/j.scitotenv.2018.10.015>
- Arvanitoyannis IS, Bosnea L (2004) Migration of substances from food packaging materials to foods. *Crit Rev Food Sci Nutr* 44:63–76. <https://doi.org/10.1080/10408690490424621>
- Hahladakis JN, Velis CA, Weber R, Iacovidou E, Purnell P (2018) An overview of chemical additives present in plastics: migration, release, fate and environmental impact during their use, disposal and recycling. *J Hazard Mater* 344:179–199. <https://doi.org/10.1016/j.jhazmat.2017.10.014>
- Dole P, Feigenbaum AE, De La Cruz C, Pastorelli S, Paseiro P, Hankemeier T, Voulzatis Y, Aucejo S, Saillard P, Papaspyrides C (2006) Typical diffusion behaviour in packaging polymers – application to functional barriers. *Food Addit Contam* 23:202–211. <https://doi.org/10.1080/02652030500373661>
- Vitrac O, Fractionnement UMR, Cedex R, Hayert M (2005) Risk assessment of migration from packaging materials into foodstuffs. 51. <https://doi.org/10.1002/aic.10462>
- Eaves D (2021) Consultant Regulatory I European Food Contact Compliance: Non-Intentionally Added Substances [NIAS]. [intertek.com/regulatory/food-contact/](https://intertek.com/regulatory/food-contact/). Accessed 22 Mar 2021
- Commission Regulation (EU) No 10/2011 (2011) Commission Regulation (EU) No 10/2011 of 14 January 2011 on plastic materials and articles intended to come into contact with food. *Off J Eur Union*:1–136
- NIST (National Institute of Standards and Technology) Libro del Web de Química del NIST, SRD 69. Retrieved March 26, 2020, from <https://webbook.nist.gov/>
- Nerin C, Alfaro P, Aznar M, Domeño C (2013) The challenge of identifying non-intentionally added substances from food packaging materials: a review. *Anal Chim Acta* 775:14–24. <https://doi.org/10.1016/j.aca.2013.02.028>
- Skjevraak I, Brede C, Steffensen IL, Mikalsen A, Alexander J, Fjeldal P, Herikstad H (2005) Non-targeted multi-component analytical surveillance of plastic food contact materials: identification of substances not included in EU positive lists and their risk assessment. *Food Addit Contam* 22:1012–1022. <https://doi.org/10.1080/02652030500090877>
- Tawakkal ISMA, Cran MJ, Miltz J, Bigger SW (2014) A review of poly(lactic acid)-based materials for antimicrobial packaging. *J Food*



- Sci 79:R1477. <https://doi.org/10.1111/1750-3841.12534>
15. Wrona M, Nerin C (2020) Analytical approaches for analysis of safety of modern food packaging: a review. *Molecules* 25. <https://doi.org/10.3390/molecules25030752>
  16. Bach C, Dauchy X, Severin I, Munoz JF, Etienne S, Chagnon MC (2013) Effect of temperature on the release of intentionally and non-intentionally added substances from polyethylene terephthalate (PET) bottles into water: chemical analysis and potential toxicity. *Food Chem* 139:672–680. <https://doi.org/10.1016/j.foodchem.2013.01.046>
  17. Ibarra VG, Rodríguez A, Quirós B, De Losada PP, Sendón R (2018) Identification of intentionally and non-intentionally added substances in plastic packaging materials and their migration into food products. 3789–3803
  18. Wrona M, Pezo D, Nerin C (2013) Rapid analytical procedure for determination of mineral oils in edible oil by GC-FID. *Food Chem* 141:3993–3999. <https://doi.org/10.1016/j.foodchem.2013.06.091>
  19. Dabrowska A, Borcz A, Nawrocki J (2003) Aldehyde contamination of mineral water stored in PET bottles. *Food Addit Contam* 20:1170–1177. <https://doi.org/10.1080/02652030310001620441>
  20. Bach C, Dauchy X, Chagnon MC, Etienne S (2012) Chemical compounds and toxicological assessments of drinking water stored in polyethylene terephthalate (PET) bottles: a source of controversy reviewed. *Water Res* 46:571–583. <https://doi.org/10.1016/j.watres.2011.11.062>
  21. Özlem KE (2008) Acetaldehyde migration from polyethylene terephthalate bottles into carbonated beverages in Türkiye. *Int J Food Sci Technol* 43:333–338. <https://doi.org/10.1111/j.1365-2621.2006.01443.x>
  22. Horodytska O, Cabanes A, Fullana A (2020) Non-intentionally added substances (NIAS) in recycled plastics. *Chemosphere* 251:126373. <https://doi.org/10.1016/j.chemosphere.2020.126373>
  23. Yusà V, López A, Dualde P, Pardo O, Fochi I, Pineda A, Coscolla C (2020) Analysis of unknowns in recycled LDPE plastic by LC-Orbitrap Tribrid HRMS using MS3 with an intelligent data acquisition mode. *Microchem J* 158:105256. <https://doi.org/10.1016/j.microc.2020.105256>
  24. Fitaroni LB, de Oliveira ÉC, Marcomini AL, Paranhos CM, Freitas FL, Cruz SA (2020) Reprocessing and solid state polymerization on contaminated post-consumer PET: thermal and crystallization behavior. *J Polym Environ* 28:91–99. <https://doi.org/10.1007/s10924-019-01579-9>
  25. Cruz SA, Scuracchio CH, Fitaroni LB, Oliveira C (2017) The use of melt rheology and solution viscometry for degradation study of post-consumer poly(ethylene terephthalate): the effects of the contaminants, reprocessing and solid state polymerization. *Polym Test* 60:236–241. <https://doi.org/10.1016/j.polymeresting.2017.03.026>
  26. Research GV (2020) Plastic market size, share & trends analysis report by product (PE, PP, PU, PVC, PET, polystyrene, ABS, PBT, PPO, epoxy polymers, LCP, PC, polyamide), by application, by region, and segment forecasts, 2020–2027
  27. Brouwer MT, Alvarado Chacon F, Thoden van Velzen EU (2020) Effect of recycled content and rPET quality on the properties of PET bottles. Part III: Modelling of repetitive recycling. *Packag Technol Sci* 33:373–383. <https://doi.org/10.1002/pts.2489>
  28. Geueke B (2018) Dossier – non-intentionally added substances (NIAS). *Food Packag Forum* 7. <https://doi.org/10.5281/zenodo.1265331>
  29. Portesi C, Visentin D, Durbiano F, Abete MC, Rizzi M, Maurino V, Rossi AM (2019) Development of a rapid micro-Raman spectroscopy approach for detection of NIAS in LDPE pellets and extruded films for food packaging applications. *Polym Test* 80:106098. <https://doi.org/10.1016/j.polymertesting.2019.106098>
  30. Song X-C, Wrona M, Nerin C, Lin Q-B, Zhong H-N (2019) Volatile non-intentionally added substances (NIAS) identified in recycled expanded polystyrene containers and their migration into food simulants. *Food Packag Shelf Life* 20:100318. <https://doi.org/10.1016/j.fpsl.2019.100318>
  31. Paiva R, Wrona M, Nerin C, Bertochi I, Gavrill L, Andrea S (2021) Importance of profile of volatile and off-odors compounds from different recycled polypropylene used for food applications. *Food Chem* 350:129250. <https://doi.org/10.1016/j.foodchem.2021.129250>
  32. Bauer A, Jesús F, Gómez Ramos MJ, Lozano A, Fernández-Alba AR (2019) Identification of unexpected chemical contaminants in baby food coming from plastic packaging migration by high resolution accurate mass spectrometry. *Food Chem* 295:274–288. <https://doi.org/10.1016/j.foodchem.2019.05.105>

33. Borzi F, Torrieri E, Wrona M, Nerín C (2019) Polyamide modified with green tea extract for fresh minced meat active packaging applications. *Food Chem* 300:125–242. <https://doi.org/10.1016/j.foodchem.2019.125242>
34. Gavril GL, Wrona M, Bertella A, Świeca M, Râpă M, Salafranca J, Nerín C (2019) Influence of medicinal and aromatic plants into risk assessment of a new bioactive packaging based on polylactic acid (PLA). *Food Chem Toxicol* 132:1–11. <https://doi.org/10.1016/j.fct.2019.110662>
35. Jaén J, Domeño C, Alfaro P, Nerín C (2021) Atmospheric Solids Analysis Probe (ASAP) and Atmospheric Pressure Gas Chromatography (APGC) coupled to Quadrupole Time of Flight Mass Spectrometry (QTOF-MS) as alternative techniques to trace aromatic markers of mineral oils in food packaging. *Talanta* 227:122079. <https://doi.org/10.1016/j.talanta.2020.122079>
36. Anvisa RDCN, Nacional A, Sanitária DV (2004) RDC N° 216\_ANVISA – Agência Nacional de Vigilância Sanitária
37. Food and Agriculture Organization of the United Nations (FAO), World Health Organization (WHO) (2015) CODEX ALIMENTARIUS COMMISSION. 2005. Procedural manual, 24th ed. Rome
38. Magnuson B, Munro I, Abbot P, Baldwin N, Lopez-Garcia R, Ly K, McGirr L, Roberts A, Socolovsky S (2013) Review of the regulation and safety assessment of food substances in various countries and jurisdictions. *Food Addit Contam Part A Chem Anal Control Expo Risk Assess* 30:1147–1220. <https://doi.org/10.1080/19440049.2013.795293>
39. Canellas E, Nerín C, Moore R, Silcock P (2010) New UPLC coupled to mass spectrometry approaches for screening of non-volatile compounds as potential migrants from adhesives used in food packaging materials. *Anal Chim Acta* 666:62–69. <https://doi.org/10.1016/j.aca.2010.03.032>
40. Wrona M, Vera P, Pezo D, Nerín C (2017) Identification and quantification of odours from oxobiodegradable polyethylene oxidised under a free radical flow by headspace solid-phase microextraction followed by gas chromatography-olfactometry-mass spectrometry. *Talanta* 172:37–44. <https://doi.org/10.1016/j.talanta.2017.05.022>
41. Bratinova S, Raffael B, Simoneau C (2009) Guidelines for performance criteria and validation procedures of analytical methods used in controls of food contact materials
42. Hoekstra E, Brandsch R, Dequatre C, Mercea P, Milana MR, Stoermer A, Trier X, Vitrac O, Schaefer A, Simoneau C (2015) Practical guidelines on the application of migration modelling for the estimation of specific migration. Publications Office of the European Union
43. PlasticsEurope (2011) Risk assessment of non-listed substances (NLS) and non-intentionally added substances (NIAS) under article 19. 32
44. Center for Food Safety and Applied Nutrition (2006) Guidance for industry: use of recycled plastics in food packaging (chemistry considerations). <https://www.fda.gov/regulatory-information/search-fda-guidance-documents/guidance-industry-use-recycled-plastics-food-packaging-chemistry-considerations>. Accessed 23 Mar 2020
45. Santos EDB, Sigoli FA, Mazali IO (2013) Metallic Cu nanoparticles dispersed into porous glass: a simple green chemistry approach to prepare SERS substrates. *Mater Lett* 108:172. <https://doi.org/10.1016/j.matlet.2013.06.110>
46. Koster S, Rennen M, Leeman W, Houben G, Muilwijk B, van Acker F, Krul L (2014) A novel safety assessment strategy for non-intentionally added substances (NIAS) in carton food contact materials. *Food Addit Contam Part A Chem Anal Control Expo Risk Assess* 31:422–443. <https://doi.org/10.1080/19440049.2013.866718>
47. Canellas E, Vera P, Song XC, Nerin C, Goshawk J, Dreolin N (2021) The use of ion mobility time-of-flight mass spectrometry to assess the migration of polyamide 6 and polyamide 66 oligomers from kitchenware utensils to food. *Food Chem* 350:129260. <https://doi.org/10.1016/j.foodchem.2021.129260>
48. Asensio E, Peiro T, Nerín C (2019) Determination the set-off migration of ink in cardboard-cups used in coffee vending machines. *Food Chem Toxicol* 130:61–67. <https://doi.org/10.1016/j.fct.2019.05.022>
49. Asensio E, Montañés L, Nerín C (2020) Migration of volatile compounds from natural biomaterials and their safety evaluation as food contact materials. *Food Chem Toxicol* 142:111457. <https://doi.org/10.1016/j.fct.2020.111457>
50. Otoukesh M, Nerín C, Aznar M, Kabir A, Furton KG, Es'haghi Z (2019) Determination of adhesive acrylates in recycled polyethylene terephthalate by fabric phase sorptive extraction coupled to ultra performance liquid chromatography – mass spectrometry. *J Chromatogr A* 1602:56–63. <https://doi.org/10.1016/j.chroma.2019.05.044>

51. Aznar M, Alfaro P, Nerin C, Kabir A, Furton KG (2016) Fabric phase sorptive extraction: an innovative sample preparation approach applied to the analysis of specific migration from food packaging. *Anal Chim Acta* 936: 97–107. <https://doi.org/10.1016/j.aca.2016.06.049>
52. Salafranca J, Pezo D, Nerin C (2009) Assessment of specific migration to aqueous simulants of a new active food packaging containing essential oils by means of an automatic multiple dynamic hollow fibre liquid phase microextraction system. *J Chromatogr A* 1216:3731–3739. <https://doi.org/10.1016/j.chroma.2009.03.001>
53. Otoukesh M, Vera P, Wrona M, Nerin C, Es'haghi Z (2020) Migration of dihydroxyalkylamines from polypropylene coffee capsules to Tenax® and coffee by salt-assisted liquid–liquid extraction and liquid chromatography–mass spectrometry. *Food Chem* 321:126720. <https://doi.org/10.1016/j.foodchem.2020.126720>
54. Bratinova S, Hoekstra E (2019) Guidance on sampling, analysis and data reporting for the monitoring of mineral oil hydrocarbons in food and food contact materials in the frame of Commission Recommendation (EU) 2017/84
55. Pezo D, Salafranca J, Nerin C (2007) Development of an automatic multiple dynamic hollow fibre liquid-phase microextraction procedure for specific migration analysis of new active food packagings containing essential oils. *J Chromatogr A* 1174:85–94. <https://doi.org/10.1016/j.chroma.2007.08.033>
56. Rycenga M, Camargo PHC, Li W, Moran CH, Xia Y (2010) Understanding the SERS effects of single silver nanoparticles and their dimers, one at a time. *J Phys Chem Lett* 1:696–703. <https://doi.org/10.1021/jz900286a>
57. Koster S, Bani-Estivals M-H, Bonuomo M, Bradley E, Chagnon M-C, Garcia ML, Godts F, Gude T, Helling R, Paseiro-Losada P, Pieper G, Rennen M, Simat T, Spack L. Guidance on best practices on the risk assessment of non-intentionally added substances (NIAS) in food contact materials and articles. Commissioned the ILSI Europe Packaging Materials Task Force
58. Sharma B, Frontiera RR, Henry A, Ringe E, Van Duyne RP (2012) SERS: materials, applications, and the future Surface enhanced Raman spectroscopy (SERS) is a powerful vibrational. *Mater Today* 15:16
59. Jahn IJ, Mühlhig A, Cialla-May D (2020) Application of molecular SERS nanosensors: where we stand and where we are headed towards? *Anal Bioanal Chem* 412:5999. <https://doi.org/10.1007/s00216-020-02779-2>
60. Su Q-Z, Vera P, Nerin C (2020) Direct immersion–solid-phase microextraction coupled to gas chromatography–mass spectrometry and response surface methodology for nontarget screening of (semi-) volatile migrants from food contact materials. *Anal Chem* 92:5577–5584. <https://doi.org/10.1021/acs.analchem.0c00532>
61. Vera P, Canellas E, Nerin C (2018) Identification of non volatile migrant compounds and NIAS in polypropylene films used as food packaging characterized by UPLC-MS/QTOF. *Talanta* 188:750–762. <https://doi.org/10.1016/j.talanta.2018.06.022>
62. Hoppe M, de Voogt P, Franz R (2018) Oligomers in polyethylene naphthalate and polybutylene terephthalate – identification and exploring migration. *Food Package Shelf Life* 17:171–178. <https://doi.org/10.1016/J.FPSL.2018.07.001>
63. Pietropaolo E, Albenga R, Gosetti F, Toson V, Koster S, Marin-Kuan M, Veyrand J, Patin A, Schilter B, Pistone A, Tei L (2018) Synthesis, identification and quantification of oligomers from polyester coatings for metal packaging. *J Chromatogr A* 1578:15–27. <https://doi.org/10.1016/J.CHROMA.2018.10.002>
64. Carrizo D, Domeño C, Nerin I, Alfaro P, Nerin C (2015) Atmospheric pressure solid analysis probe coupled to quadrupole-time of flight mass spectrometry as a tool for screening and semi-quantitative approach of polycyclic aromatic hydrocarbons, nitro-polycyclic aromatic hydrocarbons and oxo-polycyclic aromatic. *Talanta* 131:175. <https://doi.org/10.1016/j.talanta.2014.07.034>
65. García Ibarra V, Sendón R, García-Fonte XX, Paseiro Losada P, Bernaldo R, de Quirós A (2019) Migration studies of butylated hydroxytoluene, tributyl acetylcitrate and dibutyl phthalate into food simulants. *J Sci Food Agric* 99:1586. <https://doi.org/10.1002/jsfa.9337>
66. Nerin C, Wrona M (2018) *Polymers/food contact and packaging materials – analytical aspects*, 3rd edn. Elsevier
67. Morbeck DE, Fredrickson JR, Walker DL (2012) Factors that affect mineral oil toxicity: role of oxygen and protein supplement. *Fertil Steril* 98:S29. <https://doi.org/10.1016/j.fertnstert.2012.07.108>
68. Nygaard UC, Vege Å, Rognum T, Grob K, Cartier C, Cravedi JP, Alexander J (2019) Toxic effects of mineral oil saturated hydrocarbons (MOSH) and relation to accumulation in

- rat liver. *Food Chem Toxicol* 123:431. <https://doi.org/10.1016/j.fct.2018.11.022>
69. Otunga GN, Maiyoh GK, Macharia BN, Tui VC (2019) Transformer mineral oil ingestion induces systemic sub-acute toxicity in Wistar rats. *Heliyon* 5:e02998. <https://doi.org/10.1016/j.heliyon.2019.e02998>
70. Pezo D, Wrona M, Rodriguez-Lafuente A, Nerin C (2012) A sulphuric acid-impregnated silica gel clean-up procedure for the determination of n-alkanes migration from paraffin based paper packaging into cheddar cheese. *Food Chem* 134:405. <https://doi.org/10.1016/j.foodchem.2012.02.076>
71. Santos EDB, Sigoli FA, Mazali IO (2013) Surface-enhanced Raman scattering of 4-aminobenzenethiol on silver nanoparticles substrate. *Vib Spectrosc* 68:246. <https://doi.org/10.1016/j.vibspec.2013.08.003>
72. Wrona M, Salafraña J, Nerin C (2017) Fast assessment of oxo-biodegradable polyethylene film oxidation by surface-enhanced Raman scattering with in situ formation of a silver nanoparticle substrate. *J Mater Chem C* 5: 463. <https://doi.org/10.1039/c6tc04401h>
73. Trinetta V (2018) Obsolete: definition and function of food packaging. In: Reference Module in Food Science
74. Wrona M, Nerin C (2019) Chapter 7: Risk assessment of plastic packaging for food applications
75. Liu YQ, Wrona M, Su QZ, Vera P, Nerin C, Hu CY (2021) Influence of cooking conditions on the migration of silicone oligomers from silicone rubber baking molds to food simulants. *Food Chem* 347:128964. <https://doi.org/10.1016/j.foodchem.2020.128964>
76. Oliveira EC, Echegoyen Y, Cruz SA, Nerin C (2014) Comparison between solid phase microextraction (SPME) and hollow fiber liquid phase microextraction (HFLPME) for determination of extractables from post-consumer recycled PET into food simulants. *Talanta* 127:59–67. <https://doi.org/10.1016/j.talanta.2014.03.042>
77. Kim HS, Lee YJ, Koo YJ, Pack EC, Lim KM, Choi DW (2021) Migration of monomers, plastic additives, and non-intentionally added substances from food utensils made of melamine–formaldehyde resin following ultraviolet sterilization. *Food Control* 125:107981. <https://doi.org/10.1016/j.foodcont.2021.107981>
78. da Oliveira WS, Monsalve JO, Nerin C, Padula M, Godoy HT (2020) Characterization of odorants from baby bottles by headspace solid phase microextraction coupled to gas chromatography-olfactometry-mass spectrometry. *Talanta* 207:120301. <https://doi.org/10.1016/j.talanta.2019.120301>
79. Gelbke H-P, Banton M, Block C, Dawkins G, Eisert R, Leibold E, Pemberton M, Puijk IM, Sakoda A, Yasukawa A (2019) Risk assessment for migration of styrene oligomers into food from polystyrene food containers. *Food Chem Toxicol* 124:151–167. <https://doi.org/10.1016/J.FCT.2018.11.017>
80. Wrona M, Salafraña J, Rocchia M, Nerin C (2015) Application of SERS to the determination of butylated hydroxyanisole in edible and essential oils *Spectrosc (Santa Monica)* 30
81. Rubio L, Valverde-Som L, Sarabia LA, Ortiz MC (2019) The behaviour of Tenax as food simulant in the migration of polymer additives from food contact materials by means of gas chromatography/mass spectrometry and PAR-AFAC. *J Chromatogr A* 1589:18–29. <https://doi.org/10.1016/j.chroma.2018.12.054>
82. de Poças MF, Oliveira JC, Pereira JR, Brandsch R, Hogg T (2011) Modelling migration from paper into a food simulant. *Food Control* 22:303. <https://doi.org/10.1016/j.foodcont.2010.07.028>
83. Aznar M, Domeño C, Nerin C, Bosetti O (2015) Set-off of non volatile compounds from printing inks in food packaging materials and the role of lacquers to avoid migration. *Dyes Pigments* 114:85–92. <https://doi.org/10.1016/j.dyepig.2014.10.019>
84. García Ibarra V, Bernaldo R, de Quirós A, Paseiro Losada P, Sendón R (2019) Non-target analysis of intentionally and non intentionally added substances from plastic packaging materials and their migration into food simulants. *Food Packag Shelf Life* 21: 100325. <https://doi.org/10.1016/j.fpsl.2019.100325>
85. Vera P, Canellas E, Nerin C (2020) Compounds responsible for off-odors in several samples composed by polypropylene, polyethylene, paper and cardboard used as food packaging materials. *Food Chem* 309:125792. <https://doi.org/10.1016/j.foodchem.2019.125792>
86. European Parliament and the Council (2004) Directive 2004/42/EC on the limitation of emissions of volatile organic compounds due to the use of organic solvents in certain paints and varnishes and vehicle refinishing products
87. Kupiec T (2004) Quality-control analytical methods: gas chromatography. *Int J Pharm Compd* 8:305

88. Hopfer H (2020) Analytical methods: gas chromatography. Reference Module in Food Science
89. Osorio J, Dreolin N, Aznar M, Nerín C, Hancock P (2019) Determination of volatile non intentionally added substances coming from a starch-based biopolymer intended for food contact by different gas chromatography-mass spectrometry approaches. *J Chromatogr A* 1599:215–222. <https://doi.org/10.1016/j.chroma.2019.04.007>
90. Ubeda S, Aznar M, Nerín C (2019) Determination of volatile compounds and their sensory impact in a biopolymer based on polylactic acid (PLA) and polyester. *Food Chem* 294:171–178. <https://doi.org/10.1016/j.foodchem.2019.05.069>
91. Canellas E, Vera P, Nerín C (2015) Risk assessment derived from migrants identified in several adhesives commonly used in food contact materials. *Food Chem Toxicol* 75:79–87. <https://doi.org/10.1016/j.fct.2014.10.029>
92. Patlewicz G, Jeliaskova N, Safford RJ, Worth AP, Aleksiev B (2008) An evaluation of the implementation of the Cramer classification scheme in the Toxtree software. *SAR QSAR Environ Res* 19:495. <https://doi.org/10.1080/10629360802083871>
93. Dreolin N, Aznar M, Moret S, Nerin C (2019) Development and validation of a LC–MS/MS method for the analysis of bisphenol a in polyethylene terephthalate. *Food Chem* 274:246. <https://doi.org/10.1016/j.foodchem.2018.08.109>
94. Dewhurst I, Renwick AG (2013) Evaluation of the Threshold of Toxicological Concern (TTC) – challenges and approaches. *Regul Toxicol Pharmacol* 65:168. <https://doi.org/10.1016/j.yrtph.2012.03.007>



## Poly- and Perfluorinated Alkyl Substances in Food Packaging Materials

Rachel C. Scholes, William Hart-Cooper, Gregory M. Glenn,  
and William J. Orts

### Abstract

Poly- and perfluorinated alkyl substances (PFAS) are commonly used additives in food packaging materials that impart water and grease resistance. However, this class of compounds is coming under increased scrutiny due to human health and environmental concerns. As a result, regulatory agencies are developing limits on PFAS in food packaging. The development and enforcement of such limits highlights the need for robust PFAS detection methods. Unfortunately, targeted methods that detect specific PFAS compounds can measure only a small subset of PFAS. Thus, total fluorine methods are preferred for food packaging applications. Commercially available total fluorine methods include combustion followed by ion chromatography or fluoride ion-selective electrodes. Surface measurement techniques are also under development, which may be particularly useful for nondestructive, rapid screening of food packaging materials. This chapter provides a discussion of the various methods available, and under development, for quantifying PFAS in food packaging materials. Alternative strategies to impart water and grease resistance to food packaging are also discussed.

**Key words** PFAS, Perfluorinated compounds, Total fluorine, Detection methods, Food packaging, PFAS alternatives

---

## 1 Introduction

Food packaging materials rely on additives to improve gas and moisture barriers, oil resistance, and other properties. Among the most common, and recently scrutinized, classes of additives are poly- and perfluorinated alkyl substances (PFAS), which impart water- and oil-repellency to paper and molded fiber products [1]. PFAS contain multiple carbon-fluorine bonds, which are incorporated into alkyl chains to produce hydrophobic and oleophobic compounds [2]. In food packaging, the unique ability of these compounds to impart low surface tension has led to their widespread use in food contact materials that come in contact with oil and grease [3]. For instance, PFAS compounds are commonly

used in microwave popcorn bags [4] and fast-food packaging [1] including pizza boxes and French fry wraps.

However, PFAS have recently been linked to a wide range of toxic effects, raising questions about the safety of these additives [5, 6]. Studies conducted with one PFAS compound, perfluorooctanoic acid (PFOA), indicate likely links between exposure and several adverse outcomes, including high cholesterol, thyroid disease, reproductive and developmental toxicity, and cancer [6]. PFOA has been classified as a possible human carcinogen by the International Agency for Research on Cancer due to studies linking the compound to kidney and testicular cancers. Immunotoxicity has also been observed in children with elevated serum levels of three PFAS compounds. Most toxicity studies thus far focus on a handful of compounds, particularly PFOA and perfluorooctane sulfonic acid (PFOS), which were among the first PFAS to be widely detected in consumer products and the environment. The toxicity of other PFAS, including those used as replacements for PFOS and PFOA in industry applications, requires further study and the development of robust methodologies for read-across from structurally similar PFAS compounds [7]. In addition, although PFAS are often present as mixtures, the toxicity of PFAS mixtures is complex and poorly understood [8]. As a result of the growing evidence for PFAS toxicity, an increasing array of environmental experts recommend that PFAS should be treated as a hazardous chemical class and avoided wherever possible [9].

Food packaging can contribute to human exposure to PFAS through multiple routes. PFAS can leach from packaging into food during typical use of items such as microwave popcorn bags [10, 11]. PFAS have been detected in food items such as packaged meats [12], popcorn [13], and fast-food items [13, 14], which has raised concerns about dietary exposure to these compounds resulting from their use in food packaging. In addition, PFAS can contaminate the food supply through indirect pathways because the strong carbon-fluorine bonds in PFAS make these compounds recalcitrant to degradation, resulting in their introduction into the environment at the end-of-life of food packaging products [6]. For instance, PFAS can be introduced to food crops when food packaging-derived compost is applied to agricultural lands [15]. Indirect PFAS contamination also occurs due to the uptake of PFAS from contaminated irrigation water and from land-applied biosolids, which can result in exposures that exceed EPA health guidelines [16, 17]. The widespread use and recalcitrance of PFAS have resulted in these compounds becoming ubiquitous environmental contaminants that have now been detected on all continents [2, 18] including in arctic ice cores [19], in widespread aquatic environments [20], and in the atmosphere [21]. The full implications of PFAS contamination to our food chain is still unknown.

Regulatory agencies are now taking notice and beginning to restrict the use of PFAS in food packaging. For instance, in 2015, the Danish Ministry for Environment and Food issued a guideline level for organic fluorine in food contact materials in order to reduce consumer exposure. The limit was revised in 2018 to its current level,  $20 \mu\text{g g}^{-1}$ . In the USA, several states have passed or are considering legislation to ban PFAS-containing food packaging [22]. In 2018, San Francisco became the first USA city to ban the addition of fluorinated chemicals to all single-use compostable food packaging, effective in 2020 [23].

Regulatory action has also been taken to reduce the input of PFAS into compost. The EU Directive on Packaging and Packaging Waste, which provides a standard for compostable and biodegradable packaging, now includes a limit of  $100 \text{ mg kg}^{-1}$  fluorine [24]. The Biodegradable Products Institute, which provides compostability certification in the USA, has adopted this limit as of 2019 [25]. These actions effectively designate PFAS-containing packaging as non-compostable, further motivating the move away from PFAS in food packaging.

Enacting regulations that limit PFAS in food packaging is challenging, in part because PFAS can contaminate food contact materials (FCMs) even when not intentionally added. Regulations often limit the intentional addition of PFAS but allow for the possibility that PFAS may be present in the final product due to unintentional sources [26]. Readers are invited to refer to Chap. 4 for further details on intentionally and non-intentionally added substances. In addition to the use of PFAS in base materials or linings, PFAS are introduced to food packaging materials incidentally when used as release agents and lubricants during the manufacturing of FCMs [27]. PFAS can also be present in recycled fiber used in the manufacture of new food packaging products [26]. PFAS from these sources cannot be readily distinguished from “intentionally added” PFAS based on chemical structure and are instead determined based on the concentration of PFAS in the final product, following the assumption that high PFAS concentrations correspond to intentional use. However, the levels of PFAS imparted during manufacturing are not well characterized. For example, the US Food and Drug Administration allows for levels up to  $2000 \text{ mg kg}^{-1}$  of some PFAS compounds used as manufacturing aids for food packaging products [28], but the actual concentrations imparted during manufacturing are unknown and may vary widely. These challenges highlight the need for robust quantitative methods to measure PFAS in food packaging materials, in order to better constrain potential health effects and to inform and enforce future regulations.



---

## 2 Methods

### 2.1 Background

Reliably quantifying PFAS in food packaging requires particular attention to inclusivity, selectivity, and ease-of-use. The first challenge is inclusivity: while analytical methods for food contaminants typically quantify single compounds, PFAS comprises a broad class of thousands of individual chemicals, which cannot all be included in existing food safety workflows. Methods that measure total fluorine have been identified as a strategy to address this particular challenge. However, the possible presence of inorganic fluoride interferes with PFAS determination by total fluorine methods, resulting in a tradeoff between selectivity and inclusivity [29]. Furthermore, extensive sample preparation requirements, for instance, multi-step extractions from solid materials, limit the usefulness of some methods for regulatory, product screening purposes or online process monitoring. These considerations provide important context for considering the breadth of methods under development, and the promise of new innovations in solids analyses and rapid screening.

Initial methods for measuring PFAS in the environment used liquid chromatography and mass spectrometry to quantify specific PFAS compounds using targeted methods. Standard targeted methods exist for subsets of PFAS compounds found in water and soil (e.g., USEPA Method 537.v1; ISO Method 251010; ASTM D7979; ASTM D7968), but these methods detect only approximately 20 of the thousands of existing PFAS compounds, and do not target some of the compounds most commonly found in food packaging, such as the dialkyl and trialkyl phosphate esters (diPAPs and triPAPs, respectively). When compared side-by-side, targeted PFAS methods detect a small portion of total organofluorine compounds, indicating that existing targeted methods poorly represent total potential PFAS exposure [3, 30]. Importantly, compounds that are not detected in targeted analyses likely still pose health risks and, in some cases, are known precursors to contaminants with well-characterized toxicity. For instance, diPAPs found in food packaging materials act as endocrine disruptors [31] and are also metabolized to toxic perfluorinated carboxylic acids [13].

The total oxidizable precursor (TOP) assay was developed to address a broader suite of PFAS compounds compared to targeted methods. The TOP assay involves oxidizing a PFAS-containing sample to form PFAS oxidation end-products, specifically perfluorinated carboxylic acids (PFCAs), which are then analyzed with a targeted LC-MS/MS method. In this way, the TOP assay provides a total concentration of PFCAs and their precursors. This method was developed for aqueous samples where the source of PFAS was fire-fighting foams [32], and it has not been tested on polymers used in food packaging or newer ether-linked PFAS. The TOP assay

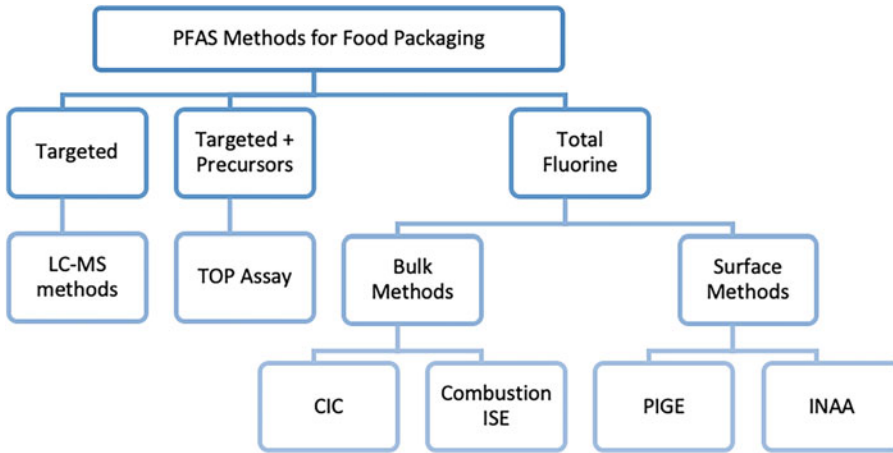


**Fig. 1** Classification of poly- and perfluorinated alkyl substances (PFAS) detection methods

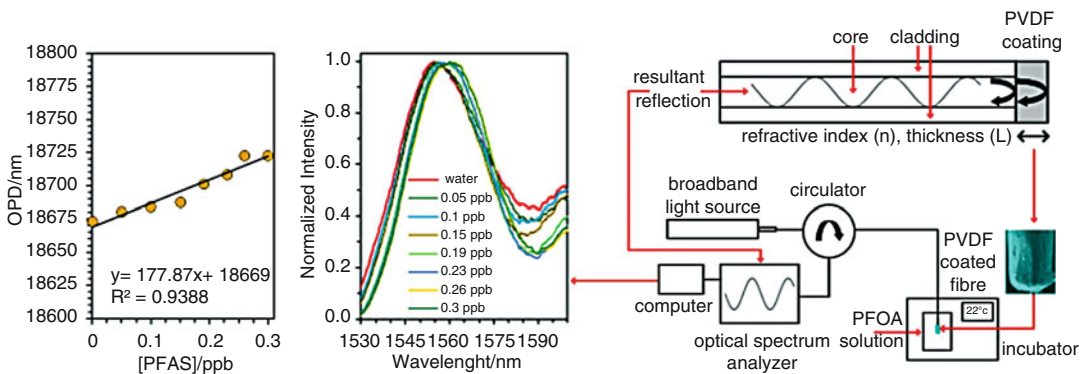


**Fig. 2** Portable poly- and perfluorinated alkyl substances (PFAS) sensor device. (Reproduced from Ref. [50] with permission from Elsevier)

also cannot detect short-chain compounds (e.g., C<sub>2</sub> and C<sub>3</sub> compounds) that are not retained by HPLC columns, although short-chain PFCAs could be quantified by pairing the TOP assay with ion chromatography [33]. The diPAPs commonly used in food contact materials were effectively converted to PFCAs detectable by the TOP assay in spiked soil samples [33], indicating that this technique could provide evidence for the presence of PFAS in food packaging [34]. However, further development of extraction methods for polymer-bound PFAS, along with verification that food packaging-relevant PFAS are effectively converted to PFCAs, would be required in order to implement the TOP assay for food packaging materials. With these uncertainties it is not clear that the TOP assay can be used to enforce regulations on PFAS in food packaging applications.

The accuracy, ease of use, and, thus, usefulness of mass spectrometry-based techniques depend on the pretreatment of

the samples, which necessarily includes an extraction protocol [35]. PFOA and PFAS from liquid matrices are typically extracted using solid-phase extraction [36], but other methods are also reported (Fig. 1). These methods include solid-phase [37] or liquid-phase microextraction [38] and ion-pair extraction [39]. Online solid phase extraction processes [40, 41] are appealing because they reduce sample preparation time, although extraction from solid products to liquid solutions would still be necessary in order to use this technique within the food packaging process chain.

In contrast to the above techniques, total F methods quantify the sum of all fluorine-containing compounds without identifying specific chemicals and can measure fluorine directly in a solid sample rather than relying on extraction. These techniques can be used for quantifying total PFAS if no inorganic fluoride is present or if inorganic fluoride can be separately measured and subtracted from total F. Combustion ion chromatography (CIC) is a relatively common, sensitive, and automated technique for total fluorine analysis. CIC is reportedly able to measure fluorine with detection limits as low as  $0.8 \mu\text{g g}^{-1}$  [3] or  $16 \text{ nmol cm}^{-2}$  [1]. Further analytical details of CIC detection methods are provided below. Extraction techniques—for example, extractable organofluorine (EOF) or adsorbable organofluorine (AOF)—have also been paired with CIC to determine the organic fraction of total F, in cases where inorganic F is significant. However, further development of these techniques for solid samples is needed, since the current methods have limited ability to extract fluoropolymers from solids, and therefore may underestimate PFAS concentrations. For instance, EOF extracted <5% of total F from food contact materials in a recent methods assessment where the contribution of inorganic F was unknown [3]. The EOF procedure also has low recovery for some nonpolymer compounds, such as fluorosulfonamides [42], and increases the total CIC method time from approximately 20 min to over 8 h. The regulatory agency for food packaging materials in Denmark is developing a method for CIC with inorganic F subtraction to be used for compliance testing of paper and board matrices [43], which may set a precedent for the use of a CIC method in regulatory screening processes. Combustion can alternatively be combined with detection using a fluoride ion-selective electrode (ISE). This method relies on readily available laboratory equipment [44, 45] and is currently conducted by commercial labs in the USA [46].

Surface characterization techniques provide an alternative to combustion-based methods for total fluorine. Multiple surface techniques have been used for food packaging, such as particle-induced  $\gamma$ -ray emission (PIGE) and instrumental neutron activation analysis (INAA) [3]. PIGE in particular has recently emerged as a promising analysis technique for total F on solid surfaces

[47]. However, to date, no adaptation exists to subtract inorganic F from the total F measured using PIGE, so this technique relies on the assumption that inorganic F is negligible. As a surface characterization technique, PIGE could be used to rapidly and nondestructively screen for PFAS-containing surface coatings. This technique may, however, overestimate bulk PFAS content because it measures F concentrations only within approximately 200  $\mu\text{m}$  of the surface, where PFAS concentrations may be higher [3]. Efforts are currently underway to miniaturize PIGE analysis so that it can be more easily conducted in the field. If these efforts are successful, PIGE may become a convenient technique for food packaging product screening.

Additional surface techniques that could be used for rapid testing are also under development but require significant further research. Spectroscopic techniques, including Fourier-transform infrared (FTIR) and Raman spectroscopies, are promising because they may require minimal sample preparation. However, most other spectroscopic techniques do not have the sensitivity to match mass spectrometry. Surface-enhanced Raman spectroscopy (SERS) has been proposed as a method with high sensitivity [48, 49] whereby Raman scattering is measured from molecules adsorbed onto nanostructured surfaces, such as gold or silver nanoparticles or activated carbon, thus enhancing the scattering through surface concentration of the target molecule. This surface-sensitive technique can theoretically provide increases in sensitivity of  $10^{10}$  to  $10^{14}$  compared to standard Raman spectroscopy, resulting in the ability to detect compounds at parts per billion (ppb) levels. For instance, Fang et al. detected PFAS via SERS using silver nanoparticles deposited onto a graphene surface, in conjunction with cationic Raman dyes (ethyl violet or methylene blue) that formed ion pairs with PFAS compounds. They detected PFOA, PFOS, and 1H,1H,2H,2H-perfluorooctanesulfonic acid (6:2FTS), with a detection limit of approximately 50 ppb for PFOA [49]. It should be noted that the Raman signal intensity was boosted by the dye, rather than the target PFOA molecule, making this an indirect method of detection. In addition, the applicability of this technique to solid samples has not been investigated.

Finally, there is a desire for robust, portable sensing systems that can be used for testing potentially contaminated materials in the field or to be used in industrial facilities for ensuring online compliance. Recently, Faiz et al. developed optical fiber sensors capped with poly(vinylidene fluoride) (PVDF) that rely on changes in optical interference to detect the presence of PFOA (Fig. 2) [50]. The PVDF interacts specifically with PFAS molecules via hydrophobic and dipole–dipole interactions, resulting in an offset interference pattern corresponding to the concentration of PFOA in an aqueous test solution. Work is underway to correlate

interference patterns that could differentiate other PFAS compounds, and further consideration of sensitivity is needed.

The advantage of sensors based on optical fibers is their compatibility with monitoring devices. Fiber optic monitoring devices can be coupled with standard smartphone apps, which could allow for real-time information from field tests or process monitoring [51].

A handful of other phone app-compatible sensors and kits for PFAS detection have been introduced [52]. These include optical test kits based on methylene blue active substances (MBAS) [53], surface-enhanced Raman scattering [49], and the use of molecular imprinted polymer-based ISE [54]. These systems usually require a color change in response to specific interactions between PFAS and indicator molecules.

Many PFAS surfactants are anionic and will interact with cationic dyes such as methylene blue or ethyl violet to form an ion-pair that results in color changes detectable by calibrated optical systems or even the naked eye. These surfactant-dye ion-pairs are often hydrophobic (since their hydrophilic ends have been blocked via their electrostatic interaction) which means they can be concentrated in a nonaqueous phase, which increases method sensitivity. However, color detection from these systems can vary with pH, temperature, and weather conditions, indicating a need for further development of these methods to ensure they are robust enough for field implementation. Additionally, ion-pair methods have primarily been developed to test for PFAS in water, not in solid matrices. Accordingly, assaying food packaging papers or plastic wraps with such methods would require standardizing extraction methods to achieve reproducible concentrations of fluorinated compounds over varying packaging samples.

## **2.2 Selection and Implementation**

Overall, each of the methods discussed above has unique advantages for different applications. Table 1 indicates the analytes detected, sensitivity, and sample preparation requirements of the relatively established methods. Targeted methods are useful for identifying the presence of specific PFAS compounds and quantifying concentrations at low levels. In contrast, total fluorine methods such as CIC, C-ISE, and PIGE can provide sensitive detection of fluorine with low sample preparation requirements, but do not provide information on the specific fluorinated compounds present.

In a regulatory context where PFAS are treated as a chemical class, the use of nontargeted methods is likely acceptable for food packaging products at the screening stage. For instance, total fluorine methods can be used for product screening, and can be followed by requests for material data sheets, additive lists, and information about manufacturing processing aids when fluorine is detected [46]. The use of total fluorine methods could also be

**Table 1**  
**Method characteristics**

| Method    | Analyte(s)  | Sensitivity                   | Sample preparation                            |
|-----------|---|-------------------------------|---|
| LC-MS/MS  | Specific PFAS compounds included in targeted method | ng L <sup>-1</sup> in extract | Solvent extraction                            |
| TOP assay | PFCAs and PFCA precursors                           | ng L <sup>-1</sup> in extract | Solvent extraction and oxidation              |
| CIC       | Total F, total organic F                            | μg g <sup>-1</sup>            | Total F: None<br>TOF: Extraction of organic F |
| C-ISE     | Total F   | μg g <sup>-1</sup>            | None—Uses solid material                      |
| PIGE      | Total F   | μg g <sup>-1</sup>            | None—Uses solid material                      |

**Table 2**  
**Commercial labs for PFAS in food packaging products**

| Lab       | Analytical technique | Location     |
|-----------|----------------------|--------------|
| Galbraith | C-ISE                | USA          |
| Eurofins  | LC-MS/MS, TOP, CIC   | USA          |
| SGS       | Total F              | Hong Kong    |
| ALS       | LC-MS                | USA          |
| Intertek  | CIC or C-ISE         | USA, Belgium |

supported by commercial laboratories that are beginning to offer total fluorine screening in food packaging products. A noncomprehensive list of commercial labs that advertise their services in offering PFAS measurements in food packaging products is provided in Table 2. These analyses are likely to become more widely available as demand for PFAS screening increases. As rapid detection methods and sensors are further developed, these techniques may also be incorporated into routine monitoring or screening processes.

### 3 Combustion Ion Chromatography (CIC)

#### 3.1 Materials

- Furnace with water supply (e.g., Auto Quick Furnace AQF-100, Dia Instruments Co. Ltd.)
- High purity Ar, O<sub>2</sub>.
- Ion chromatograph (e.g., ICS-3000, Dionex Co. Ltd. with conductivity detector).

- IonPac AS20 column (77.5  $\mu\text{g}/\text{column}$ ; 2 mm i.d.  $\times$  250 mm length, 7.5  $\mu\text{m}$ ).
- NaOH, KOH, NaF.
- Silica boats for solid samples.

### 3.2 Setup

The ion chromatography (IC) system must be set up specifically to run total fluorine samples because sources of fluorine contamination exist within typical IC systems. Sources of contamination must be removed or replaced, including substituting certain components in the flow path of the IC (i.e., polytetrafluoroethylene-containing tubing, gaskets, gas lines, valves, regulator) with non-fluorinated materials (e.g., stainless steel, polyetheretherketone, polyethylene tubing). A gas purifier with activated carbon should be used to remove trace fluorine from gases. After modification, background levels of fluorine  $<1$  ng-F can be achieved [42]. For additional details on minimizing background contamination, see [55].

### 3.3 Procedure

1. Prepare quantification standards using sodium fluoride.
2. Set food packaging sample on a silica boat and place into a furnace with water supply at 900–1000  $^{\circ}\text{C}$  for 5 min. Preferably, use a solids autosampler to automate analyses of multiple samples.
3. Online IC should be set to analyze liberated fluoride from the combustion chamber.
  - (a) IC software (e.g., Chromeleon if using Dionex IC) can be used to integrate peak areas and provide report of sample concentrations.
4. It is recommended to analyze samples in duplicate [56].

---

## 4 Alternatives to PFAS

The health and environmental hazards of PFAS, combined with their ability to migrate into food, have led to a surge in interest in developing alternatives for fiber and paper-based packaging. Alternative strategies include applying non-PFAS substances as sizing agents or replacing fiber products with compostable plastics or bamboo-based materials with inherent grease resistance. The application of non-PFAS substances can be achieved either as (1) external sizing agents (e.g., laminated films, coatings), which are added after molding, or (2) internal sizing agents, which, like small molecule PFAS additives, are added to the wet pulp before molding.

### 4.1 External Sizing Agents (Laminated Films, Coatings)

Laminated films have been widely used to provide paper and paper-board with oil and water barriers suitable for food packaging. A disadvantage of laminated films is that they increase material and

processing costs to production, do not homogeneously confer oil and water resistance to the entire paper/paperboard, and may crack or form pinholes, leading to leaks. Traditional petroleum-derived films include polymers and waxes, such as polyolefins, polystyrene, and hydrophobic acrylates [57, 58]. These films are inexpensive, widely available, provide good water, grease, and gas barriers, and remain stable at relatively high temperatures. A major disadvantage of most polymers is their end-of-life outcomes because paper-based multilayer materials containing recalcitrant plastic films are usually impossible to recycle economically, particularly when soiled with food residue. Furthermore, some polymer coatings contribute to human health concerns because they can leach endocrine disrupting compounds such as plasticizers and unpolymerized monomers [59].

Biodegradable thermoplastic materials, such as polylactide (PLA), polyhydroxyalkanoates (PHA; including polyhydroxybutyrate, PHB), polybutylenesuccinate (PBS), polycaprolactone (PCL), and thermoplastic starch (TPS) are less recalcitrant to environmental degradation than other polymers and can provide sufficient barrier properties for food. PBS and PLA degrade readily under industrial composting conditions, but effectively do not degrade under conditions representative of natural environments, such as ambient soil and aquatic conditions [60]. Despite its synthetic nature, PCL degrades under both industrial and home composting and soil conditions. PHB and TPS are biodegradable even when subjected to home composting, marine, fresh water, and soil environments [60]. PLA is widely used due to its low cost but requires additives in order to be stable in the presence of hot foods. PHAs are more expensive than PLA but tend to be more thermally stable and provide good moisture barriers, approaching those of polyolefins [61]. Although they are often sourced from sugar feedstocks, PLA and PHA can be prepared from food and agricultural waste streams [62, 63]. In addition to being used as sizing agents, both traditional and biodegradable plastics can be used as substitutes for the bulk packaging. However, polymer-based materials usually have lower biodegradability rates than comparable fiber-based products and may be more expensive. See Chaps. 1 and 2 for more on biodegradation.

Film coatings made of polysaccharides are another PFAS alternative that can be sourced from renewable feedstocks and can be readily biodegraded, although covalent modifications (e.g., the introduction of functional groups) can decrease their biodegradability. The barrier properties of chitosan films and paper coatings have been extensively investigated. Chitosan alone provided modest water repellency (contact angles: 55–85°), and excellent grease resistance when a heavy coating was applied [64]. Higher water contact angles, that is, greater hydrophobicity, were observed with chitosan that was functionalized with polydimethylsiloxane (PDMS) and zein (up to 110° for water and 40–70° for castor



oil) [65]. Moderate water absorbency was achieved in both examples, accompanied by a modest reduction in water vapor transmission rates. Optimized compositions of chitosan-PDMS-zein films achieved strong grease repellency. However, the addition of siloxanes to the polysaccharide-based films diminishes their environmental and health advantages. Although they exhibit excellent water repellency, siloxanes are persistent in the environment, potentially bioaccumulative, and may confer hazards such as endocrine disruption [66]. Another alternative combines high-molecular weight cationic and anionic starches, which slightly improved the water resistance of paper while retaining oil resistance comparable to polyethylene film [67]. Other high-molecular weight starch treatments increased water absorption but improved oil absorption. Commercial versions of alternatives with external sizing agents are already in use and include natural waxes, PLA, and clay coatings (e.g., tradenames: Practiv's Earthchoice, Ecotainer<sup>®</sup>, Eco-Products<sup>®</sup>, PrimeWare<sup>®</sup>, Bare<sup>®</sup>, Solo<sup>®</sup>, Eco-Forward<sup>®</sup>, Ecowax<sup>®</sup>, and World Centric<sup>®</sup>) [46].

#### **4.2 Internal Sizing Agents**

Internal sizing agents are advantageous in their ability to provide water and oil resistance throughout the packaging, as opposed to just the coated surface. These additives provide aesthetic advantages by enabling a more natural look to the paper. Internal sizing agents can also be directly substituted for PFAS in the manufacturing process and are therefore a simpler solution than laminated films or external sizing agents, which may introduce additional steps to production. Alkyl succinic anhydride, styrene acrylic emulsion, alkyl ketene dimer, and rosin function as liquid water barriers but may not impart similar enhancements to water vapor permeability [68]. The micro- and nanostructures of nanomaterials may also provide grease and water barriers, obviating the use of hazardous, persistent PFAS. Nanocellulose incorporated during the wet end of paper manufacture was shown to afford an excellent grease barrier [69].

---

## **5 Conclusions**

Several alternatives have been developed that can improve the grease and oil resistance of paper adequately to substitute for PFAS in food packaging. Laminated films and other external sizing agents span traditional petroleum-derived plastics, biodegradable bioplastics, and polysaccharides. Alternative internal sizing agents have also been identified, although fewer options have been reported in the literature to date. While the development of PFAS-free food packaging is an active area of research and more development is needed, adequate solutions exist that can achieve effective grease and water barriers without the significant human and environmental hazards of PFAS.

## References

- Schaider LA, Balan SA, Blum A, Andrews DQ, Strynar MJ, Dickinson ME, Lunderberg DM, Lang JR, Peaslee GF (2017) Fluorinated compounds in U.S. fast food packaging. *Environ Sci Technol Lett* 4(3):104–111
- Buck RC, Franklin J, Berger U, Conder JM, Cousins IT, de Voogt P, Jensen AA, Kannan K, Mabury SA, van Leeuwen SP (2011) Perfluoroalkyl and polyfluoroalkyl substances in the environment: terminology, classification, and origins. *Integr Environ Assess Manag* 7(4): 513–541
- Schultes L, Peaslee GF, Brockman JD, Majumdar A, McGuinness SR, Wilkinson JT, Sandlom O, Ngwenyama RA, Benskin JP (2019) Total fluorine measurements in food packaging: how do current methods perform? *Environ Sci Technol Lett* 6(2):73–78
- Zabaleta I, Negreira N, Bizkarguenaga E, Prieto A, Covaci A, Zuloaga O (2017) Screening and identification of per- and polyfluoroalkyl substances in microwave popcorn bags. *Food Chem* 230:497–506
- Knutsen HK, Alexander J, Barregård L, Bignami M, Brüschweiler B, Ceccatelli S, Cottrill B, Dinovi M, Edler L, Grasi-Kraupp B, Hogstrand C, Hoogenboom LR, Nebbia CS, Oswald IP, Petersen A, Rose M, Roudot AC, Vleminckx C, Vollmer G, Wallace H, Bodin L, Cravedi JP, Halldorsson TI, Haug LS, Johansson N, van Loveren H, Gergelova P, Mackay K, Levorato S, van Manen M, Schwerdtle T (2018) Risk to human health related to the presence of perfluorooctane sulfonic acid and perfluorooctanoic acid in food. *EFSA J* 16(12):5194
- Sunderland EM, Hu XC, Dassuncao C, Tokranov AK, Wagner CC, Allen JG (2019) A review of the pathways of human exposure to poly- and perfluoroalkyl substances (PFASs) and present understanding of health effects. *J Expo Sci Environ Epidemiol* 29:131–147
- Fenton SE, Ducatman A, Boobis A, DeWitt JC, Lau C, Ng C, Smith JS, Roberts SM (2020) Per- and polyfluoroalkyl substance toxicity and human health review: current state of knowledge and strategies for informing future research. *Environ Toxicol Chem* 40:606. <https://doi.org/10.1002/etc.4890>
- Goodrum PE, Anderson JK, Luz AL, Ansell GK (2020) Application of a framework for grouping and mixtures toxicity assessment of PFAS: a closer examination of dose-additivity approaches. *Toxicol Sci* 179:262. <https://doi.org/10.1093/toxsci/kfaa123>
- Kwiatkowski CF, Andrews DQ, Birnbaum LS, Bruton TA, DeWitt JC, Knappe DRU, Maffini MV, Miller MF, Pelch KE, Reade A, Soehl A, Trier X, Venier M, Wagner CC, Wang Z, Blum A (2020) Scientific basis for managing PFAS as a chemical class. *Environ Sci Technol Lett* 7(8): 532–543
- Begley TH, White K, Honigfort P, Twaroski ML, Neches R, Walker RA (2005) Perfluorochemicals: potential sources of and migration from food packaging. *Food Addit Contam* 22(10):1023–1031
- Begley TH, Hsu W, Noonan G, Diachenko G (2008) Migration of fluorochemical paper additives from food-contact paper into foods and food simulants. *Food Addit Contam* 25(3):384–390
- Jogsten IE, Perelló G, Llebaria X, Bigas E, Martí-Cid R, Kärrman A, Domingo JL (2009) Exposure to perfluorinated compounds in Catalonia, Spain, through consumption of various raw and cooked foodstuffs, including packaged food. *Food Chem Toxicol* 47(7): 1577–1583
- Gebbink WA, Shahid U, Oskar S, Berger U (2013) Polyfluoroalkyl phosphate esters and perfluoroalkyl carboxylic acids in target food samples and packaging-method development and screening. *Environ Sci Pollut Res* 20(11): 7949
- Tittlemier SA, Pepper K, Edwards L (2006) Concentrations of perfluorooctanesulfonamides in Canadian Total Diet Study composite food samples collected between 1992 and 2004. *J Agric Food Chem* 54(21):8385–8389
- Lazcano RK, Choi YJ, Mashtare ML, Lee LS (2020) Characterizing and comparing per- and polyfluoroalkyl substances in commercially available biosolid and organic non-biosolid-based products. *Environ Sci Technol* 54: 8640–8648
- Blaine AC, Rich CD, Hundal LS, Lau C, Mills MA, Harris KM, Higgins CP (2013) Uptake of perfluoroalkyl acids into edible crops via land applied biosolids: Field and greenhouse studies. *Environ Sci Technol* 47:14062–14069
- Blaine AC, Rich CD, Sedlacko EM, Hundal LS, Kumar K, Lau C, Mills MA, Harris KM, Higgins CP (2014) Perfluoroalkyl acid distribution in various plant compartments of edible crops grown in biosolids-amended soils. *Environ Sci Technol* 48:7858–7865
- Yamashita, N; Yeung, L.W.Y.; Taniyasu, S.; Kwok, K.Y.; Petrick, G.; Gamo, T.; Guruge, K.S.; Lam, P.K.S.; Loganathan, B.G. (2012)

- Global distribution of PFOS and related chemicals. B.G. Loganathan, P.K.S. Lam (Eds.), Global contamination trends of persistent organic chemicals, Taylor & Francis Group. pp. 593–628
19. Muir D, Bossi R, Carlsson P, Evans M, De Silva A, Halsall C, Rauert C, Herzke D, Hung H, Letcher R, Rigét F, Roos A (2019) Levels and trends of poly- and perfluoroalkyl substances in the Arctic environment – an update. *Emerg Contam* 5:240–271. ISSN 2405-6650
  20. Houde M, De Silva A, Letcher RJ, Muir DCG (2011) Monitoring of perfluorinated compounds in aquatic biota: an updated review. *Environ Sci Technol* 45(19):7962–7973
  21. Vierke L, Berger U, Cousins IT (2013) Estimation of the acid dissociation constant of perfluoroalkyl carboxylic acids through an experimental investigation of their water-to-air transport. *Environ Sci Technol* 47:11032–11039
  22. Safer States Bill Tracker. <https://www.saferstates.org/bill-tracker/FilterBills>. Accessed 8/3/2020
  23. Hogue C (2018) San Francisco moves to ban food containers made with fluorinated chemicals. *Chem Eng News* 96(32) <https://cen.acs.org/policy/legislation-/San-Francisco-moves-ban-food/96/i32>
  24. UNE 13432 (2001) Requirements for packaging recoverable through composting and biodegradation. Test scheme and evaluation criteria for the final acceptance of packaging
  25. Biodegradable Products Institute. Position on fluorinated chemicals. <https://bpiworld.org/page-1857568>. Accessed 6/20/2020
  26. Curtzwiler GW, Silva P, Hall A, Ivey A, Vorst K (2021) Significance of perfluoroalkyl substances (PFAS) in food packaging. *Integr Environ Assess Manag* 17(1):7–12
  27. Glüge J, Scheringer M, Cousins IT, DeWitt JC, Goldenman G, Herzke D, Lohmann R, Ng CA, Trier X, Wang Z (2020) An overview of the uses of per- and polyfluoroalkyl substances (PFAS). *enrXiv preprint*. <https://doi.org/10.31224/osf.io/2eqac>
  28. U.S. Food and Drug Administration. Inventory of Effective Food Contact Substances (FCS) Notifications. Accessed 7/15/2020
  29. McDonough CA, Guelfo JL, Higgins CP (2019) Measuring total PFASs in water: the tradeoff between selectivity and inclusivity. *Curr Opin Environ Sci Heal* 7:13–18
  30. Borg D, Ivarsson J (2017) Analysis of PFASs and TOF in products. Nordic Council of Ministers
  31. Chen P, Yang J, Chen G, Yi S, Liu M, Zhu L (2020) Thyroid-disrupting effects of 6:2 and 8:2 polyfluoroalkyl phosphate diester (diPAPs) at environmentally relevant concentrations from integrated *in silico* and *in vivo* studies. *Environ Sci Technol* 7(5):330–336
  32. Houtz EF, Sedlak DL (2012) Oxidative conversion as a means of detecting precursors to perfluoroalkyl acids in urban runoff. *Environ Sci Technol* 46(17):9342–9349
  33. Janda J, Nödler K, Scheruer M, Happel O, Nürenberg G, Zwiener C, Lange FT (2019) Closing the gap – inclusion of ultrashort-chain perfluoroalkyl carboxylic acids in the total oxidizable precursor (TOP) assay protocol. *Environ Sci: Processes Impacts* 21:1926–1935
  34. Yuan G, Peng H, Huang C, Hu J (2016) Ubiquitous occurrence of Fluorotelomer alcohols in eco-friendly paper-made food-contact materials and their implication for human exposure. *Environ Sci Technol* 50(2):942–950
  35. Rodriguez KL, Hwang J-H, Esfahani AR, Sadmani AHMA, Lee WH (2020) Recent developments of PFAS-detecting sensors and future direction: a review. *Micromachines* 11:667
  36. Shoemaker JA, Grimmert PE, Boutin BK (2009) Method 537, determination of selected perfluorinated alkyl acids in drinking water by solid phase extraction and liquid chromatography/tandem mass spectrometry (LC/MS/MS), Version 1.1, September 2009, National Exposure Research Laboratory, Office Of Research And Development, U. S. Environmental Protection Agency, Cincinnati, Ohio 45268: 600-R-08/092, Ver 1.1
  37. Huang Y, Li H, Bai M, Huang X (2018) Efficient extraction of perfluorocarboxylic acids in complex samples with a monolithic adsorbent combining fluorophilic and anion-exchange interactions. *Anal Chim Acta* 1011:50–58
  38. Wang J, Shi Y, Cai Y (2018) A highly selective dispersive liquid–liquid microextraction approach based on the unique fluorous affinity for the extraction and detection of per- and polyfluoroalkyl substances coupled with high performance liquid chromatography tandem–mass spectrometry. *J Chromatogr A* 1544:1–7
  39. Villaverde-de-Sáa E, Racamonde I, Quintana JB, Rodil R, Cela R (2012) Ion-pair sorptive extraction of perfluorinated compounds from water with low-cost polymeric materials: polyethersulfone vs polydimethylsiloxane. *Anal Chim Acta* 740:50–57
  40. Wilson SR, Malerød H, Holm A, Molander P, Lundanes E, Greibrokk T (2007) On-line SPE-Nano-LC-Nanospray-MS for rapid and sensitive determination of perfluorooctanoic

- acid and perfluorooctane sulfonate in river water. *J Chromatogr Sci* 45(3):146–152
41. Barreca S, Busetto M, Vitelli M, Colzani L, Clerici L, Dellavedova P (2018) Online solid-phase extraction LC-MS/MS: a rapid and valid method for the determination of perfluorinated compounds at sub ngL<sup>-1</sup> level in natural water. *J Chem* 2018:1
  42. Miyake Y, Yamashita N, So MK, Rostkowski P, Taniyasu S, Lam PKS, Kannan K (2007) Determination of trace levels of total fluorine in water using combustion ion chromatography for fluorine: a mass balance approach to determine individual perfluorinated chemicals in water. *J Chromatogr A* 1143(1–2):98–104
  43. Trier X, Taxvig C, Rosenmai AK, Pedersen GA (2017) PFAS in paper and board for food contact: options for risk management of poly- and perfluorinated substances. Nordic Council of Ministers
  44. Galbraith Laboratories. GLI method summary: determination of total fluorine by oxygen flask combustion and ion-selective electrode. Retrieved from: <http://galbraith.com/wp-content/uploads/2015/08/E9-3-Total-Fluorine-by-Oxygen-Flask-Combustion-ISE-GLI-Method-Summary.pdf>
  45. EPA Method 340.2. Fluoride (potentiometric, ion selective electrode). Revised 1974
  46. Safer Chemicals, Healthy Families (2020) A guide for quick-service restaurant chains: banning PFAS in food-contact materials. <https://saferchemicals.org>
  47. Ritter EE, Dickinson ME, Harron JP, Lunderberg DM, DeYoung PA, Robel AE, Field JA, Peaslee GF (2017) PIGE as a screening tool for per- and polyfluorinated substances in papers and textiles. *Nucl Instrum Methods Phys Res* 407:47–54
  48. Ong TTX, Blanch EW, Jones OAH (2020) Surface enhanced Raman spectroscopy in environmental analysis, monitoring and assessment. *Sci Total Environ* 720:137601
  49. Fang C, Megharaj M, Naidu R (2016) Surface-enhanced Raman scattering (SERS) detection of fluorosurfactants in firefighting foams. *RSC Adv* 6(14):11140–11145
  50. Faiza F, Baxter G, Collins S, Sidiroglou F, Crana M (2020) Polyvinylidene fluoride coated optical fibre for detecting perfluorinated chemicals. *Sens Actuators B Chem* 312:128006
  51. Wang F, Lu Y, Yang J, Chen Y, Jing W, He L, Liu Y (2017) A smartphone readable colorimetric sensing platform for rapid multiple protein detection. *Analyst* 142:3177–3182
  52. Fang C, Zhang X, Dong Z, Wang L, Megharaj M, Naidu R (2018) Smartphone appbased/portable sensor for the detection of fluoro-surfactant PFOA. *Chemosphere* 191:381–388
  53. Megharaj M, Ravendra N, Mercurio P (2011) Anionic surfactant detection. AG01N2162FI I. PCT, Australia. AG01N2162FI
  54. Fang C, Zuliang C, Megharaj M, Naidu R (2016) Potentiometric detection of AFFFs based on molecular imprinting polymer. *Environ Technol Innov* 5:52–59
  55. Wagner A, Raue B, Brauch HJ, Worch E, Lange FT (2013) Determination of adsorbable organic fluorine from aqueous environmental samples by adsorption to polystyrene-divinylbenzene based activated carbon and combustion ion chromatography. *J Chromatogr A* 1295:82–89
  56. Koch A, Aro R, Wang T, Yeung LWY (2020) Towards a comprehensive analytical workflow for the chemical characterization of organofluorine in consumer products and environmental samples. *TrAC Trends Anal Chem* 123:115423
  57. Vähä-Nissi M, Kervinen K, Savolainen A, Egolf S, Lau W (2006) Hydrophobic polymers as barrier dispersion coatings. *J Appl Polym Sci* 101:1958–1962
  58. Krook M, Gällstedt M, Hedenqvist MS (2005) A study on montmorillonite/polyethylene nanocomposite extrusion-coated paperboard. *Packag Technol Sci* 18:11–20
  59. Muncke J (2009) Exposure to endocrine disrupting compounds via the food chain: is packaging a relevant source? *Sci Total Environ* 407(16):4549–4559
  60. Narancic T, Verstichel S, Reddy Chaganti S, Morales-Gamez L, Kenny ST, De Wilde B, Babu Padamati R, O'Connor KE (2018) Biodegradable plastic blends create new possibilities for end-of-life management of plastics but they are not a panacea for plastic pollution. *Environ Sci Technol* 52:10441–10452
  61. Dilkes-Hoffman LS, Pratt S, Lant PA, Levett I, Laycock B (2018) Polyhydroxyalkanoate coatings restrict moisture uptake and associated loss of barrier properties of thermoplastic starch films. *J Appl Polym Sci* 135:46379
  62. Serafim LS, Lemos PC, Albuquerque MGE, Reis MAM (2008) Strategies for PHA production by mixed cultures and renewable waste materials. *Appl Microbiol Biotechnol* 81:615–628
  63. Fahim IS, Chbib H, Mahmoud HM (2019) The synthesis, production & economic feasibility of manufacturing PLA from agricultural waste. *Sustain Chem Pharm* 12:100142

64. Li Z, Rabnawaz M, Khan B (2020) Response surface methodology design for biobased and sustainable coatings for water- and oil-resistant paper. *ACS Appl Polym Mater* 2(3): 1378–1387
65. Hamdani SS, Li Z, Rabnawaz M, Kamdem DP, Khan BA (2020) Chitosan-*graft*-poly (dimethylsiloxane)/Zein coatings for the fabrication of environmentally friendly oil- and water-resistant paper. *ACS Sustain Chem Eng* 8(13):5147–5155
66. Surita SC, Tansel B (2014) A multiphase analysis of partitioning and hazard index characteristics of siloxanes in biosolids. *Ecotoxicol Environ Saf* 102:79–83
67. Chi K, Wang H, Catchmark JM (2020) Sustainable starch-based barrier coatings for packaging applications. *Food Hydrocoll* 103: 105696
68. Hubbe MA (2007) Paper's resistance to wetting – a review of internal sizing chemicals and their effects. *Bioresources* 2:106–145
69. Tayeb AH, Tajvidi M, Bousfield D (2020) Paper-based oil barrier packaging using lignin-containing cellulose nanofibrils. *Molecules* 25: 1344



# Chapter 6

## Migration of Building Blocks, Additives, and Contaminants from Food Packaging Materials

**Victor G. L. Souza, Regiane Ribeiro-Santos, Patricia F. Rodrigues, Carolina Rodrigues, João R. A. Pires, Ana T. Sanches-Silva, Isabel Coelho, Fátima Poças, and Ana L. Fernando**

### Abstract

Packaging plays an important role in the maintenance of the quality and safety of food products. It is also the link between the industry and the consumer, through which information is provided concerning nutritional composition, shelf-life, and storage conditions, in addition to playing the role of product advertising. Despite all these important functions of food packaging, it can pose a risk to consumers' health due to the possible migration of building blocks, additives, degradation products, and contaminants to the packaged food. In this regard, migration assays are designed to assess the safety of food packaging materials. This chapter provides a guideline of these assays, as well as some case studies on this topic and an insight on the safety of food contact materials and additives.

**Key words** Diffusion, Food simulants, Nanoparticles, Nanoforms, Analytical techniques, Migration, Food contact materials

---

## 1 Introduction

The main goal of food packaging is to protect the food from tampering or (re)contamination from chemical, physical, and/or biological sources [1]. Glass, metal, paper and paperboard, and plastics are the most important groups of materials used in the food packaging industry [2]. Traditionally, conventional packaging materials should be completely inert, that is, should not interact with the packaged food. Thus, it is important to assess if any additives, building blocks, or other contaminants migrate from the food contact materials (FCMs) to the food contained in it and at which levels. It is recognized that chemicals from packaging and other FCMs can migrate into the food itself and thus be ingested by the consumer. Monitoring this migration has become an integral part of ensuring food safety [3]. Some of the major recent chemical

hazards related to migrants from packaging are plasticizers, substances used in printing inks, hydrocarbons from mineral oils, and non-intentionally added substances—see Chap. 4 for details on the latter [4].

According to Regulation (EC) No 1935/2004 [5], a proper food packaging should be “the container that protects the food from dirt or dust, oxygen, light, pathogenic microorganisms, moisture and a variety of other destructive or harmful substances. Packaging must also be safe under its intended conditions of use, inert, cheap to be produced, lightweight, easy to dispose of or to reuse, able to withstand extreme conditions during processing or filling, impervious to a host of environmental storage and transport conditions and resistant to physical abuse.”

However, with the developments in this sector, novel functions have been attributed to the food packaging further than those traditional ones (i.e., to contain, inform, transport, sell, and protect). For instance, modified atmosphere packaging (MAP) and active/intelligent packaging are technologies recently created that beyond those basic functions are capable to increase the product quality and safety, by extending the food shelf-life [6]. Nanotechnology has also been increasingly used in the packaging field to improve physical properties and as a support to active and intelligent systems, nanosensors, and smart labels [7].

Concerning those new packaging technologies, as any FCM, they must also comply with the current FCM legal framework and guarantee that any substances migrating from the material into the food could endanger human health, change negatively the composition of food, or damage its organoleptic characteristics [8]. In the case of active packaging, where the active compound may be intended to migrate to the packaged food, such compounds must also be listed as generally recognized as safe (GRAS) by the United States Food and Drug Administration (FDA), being labelled as a food ingredient [9].

The partial replacement of oil-based and/or nonbiodegradable polymers by those from renewable resources and/or biodegradable—for some specific applications, for example, single-use plastics—represents a major trend in the packaging industry to address sustainability and circularity [10]. Thus, biopolymers emerge as alternative substitutes to petrochemical polymers; however, their use is often limited by their frequently poorer mechanical and barrier properties [6]. To overcome such hurdles, nanostructures are incorporated into these biopolymers for reinforcement purposes, which arouses another concern in terms of their safety to the consumers [11]. Yet, the implications of the use of engineered nanomaterials (ENMs) in FCM are not well established, and further research is demanded [12].

In this chapter, a guideline to evaluate the safety of food packaging materials is summarized, focusing on the migration of contaminants such as building blocks and additives. It presents a

description of the testing conditions, diffusion processes, and quantification techniques, followed by some recent studies in this field, and finishes with a short insight regarding the safety of nanomaterials intended for food contact (*see Note 1*).

## 2 Methods to Study the Migration of Contaminants from FCMs and Associated Analytical Techniques

Migration is defined as the mass transfer process (Fig. 1) from any constituent initially present in the packaging material to the packaged food product (food or beverages) [13]. The main mechanism ruling this phenomenon is the diffusion, which can be defined as the mass transfer resulting from the movement of molecules without the action of external forces (e.g., agitation), due to the differences in the chemical potential (i.e., from high concentration to the lower concentration) until the equilibrium is reached [14]. The migration is, therefore, often a diffusion process of undesirable compounds (in major cases, not intended) that may impact the food in two ways, namely (i) *safety*, due to the migration of harmful/toxic compounds, and (ii) *quality*, owing to the migration of substances that impart taint or flavor and odor.

There are also other phenomena related to the migration of substances from FCMS, such as set-off or leaching [15]; however, the most common is through diffusion, thus these two concepts are used interchangeably despite not being completely the same.

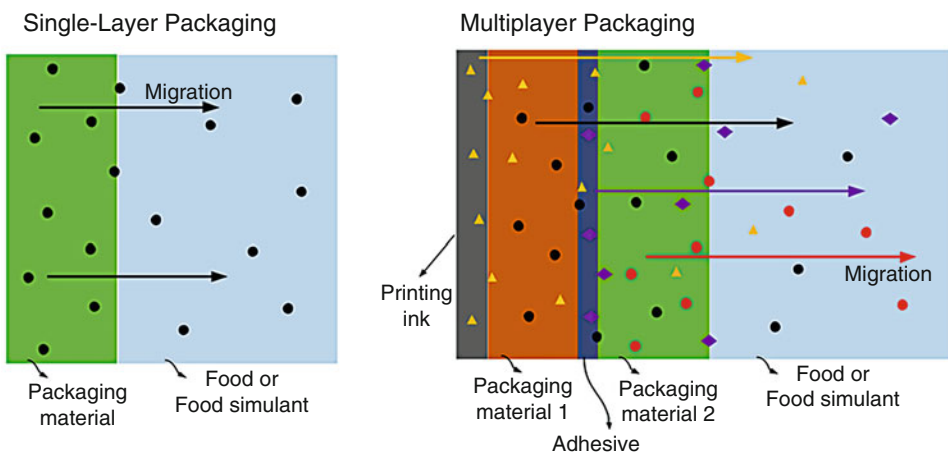


**Fig. 1** Migration process of contaminants, additives, nanostructures, and building blocks from food packaging material. Arrows indicate the direction of diffusion due to the concentration gradient. Color objects represent the migrants/contaminants, which can be additives, building blocks, or nanostructures. Food simulant to be assigned according to the regulation applied. Scheme can be used for both single- and multilayer packaging materials



In general, the diffusion process is governed by models based on Fick's second law, which can be simplified in Eq. 1 [6, 16–18]:

$$\frac{M_{F,t}}{M_{P,0}} = \frac{2}{L_P} \left( \frac{Dt}{\pi} \right)^{0,5} \quad (1)$$

where,  $M_{F,t}$  is the amount of migrant in the food (simulant) at time  $t$ ,  $M_{P,0}$  is the initial amount of migrant in the packaging,  $D$  [ $\text{cm}^2 \text{s}^{-1}$ ] is the diffusion coefficient of the migrant in the packaging, and  $L_P$  [cm] is the thickness of the packaging [18].

Overall, migration, specific migration, and diffusion and partition coefficients are important parameters to be determined, and are defined as follows:

- (a) Overall migration (also known as total migration): is the sum of all substances that can migrate from the FCM to the food (or food simulant) [19].
- (b) Specific migration: is the total of an individual and identified substance that can migrate from the FCM to the food (or food simulant); it is generally associated with toxicological studies [19].
- (c) Diffusion coefficient ( $D$ ): is the parameter that represents the speed of diffusion of substances/compounds from the packaging into the food or food simulant [20].
- (d) Partition coefficient ( $K$ ): describes the relation between the concentration in the packaging material and the food, at equilibrium, or the amount of migrant that is transferred to the food [21].

Each country or group of countries (e.g., European Union) defines their implemented legal procedures of the migration limits, in terms of overall migration limit (OML) and specific migration limit (SML) [22]—see **Note 2**.

The investigation of migration is important and should be carried out case by case, once the level of migration depends on several intrinsic and extrinsic factors, such as the physical-chemical nature of migrants (substances that tend to migrate) and foods, the type of packaged food, the exposure temperature and time of contact, the interfacial area between food and FCM packaging, and the characteristics of the packaging material itself [4, 18, 19].

Migration tests can be performed *in vitro* using food simulants or *in situ* (quantified in the food after its direct contact with the packaging material). The assay can be divided into two steps: (i) migration process; and (ii) identification/quantification of the migrant [22].

The identification/quantification of the diffused compounds is done using analytical techniques, chromatography and spectroscopy being the most widespread. Preferably, this quantification

should be done directly in the food (in situ assay), after contact with the packaging. However, this procedure can be difficult due to the complexity of food matrices that pose analytical difficulties [6, 22]. Different approaches ranging from estimation based on the assumption of total transfer to measurements in real food may be proposed [4]. In vitro methods have been standardized by regulatory agencies in rules/protocols such as the Regulation (EC) no. 10/2011 from European Union [19], which establishes the authorized food simulants and the assay conditions (time and temperature) to be followed—*see Note 3*.

The conditions of the migration tests are also defined in Regulation (EU) no. 10/2011 and its amendments [19] and take into consideration the contact time and temperature in the worst foreseeable use of the material (*see Note 4*).

In the case of paper and cardboard, one of the main concerns is regarding the possible migration of mineral oil hydrocarbons (MOH). MOH are mixtures of nonidentified substances that may have carcinogenic potential and can migrate from this class of packaging material [23]. For this purpose, Tenax<sup>®</sup> (commercial name for Simulant E), a porous polymer absorbent, is used as a food simulant for examining the migration of volatile and semi-volatile substances from paper and cardboard into dry, nonfatty foods [19, 23].

The safety of food products contained in metal packaging is generally assessed by in situ studies, which means that the quantification/identification of the migrants is done directly in the food after the contact time. Studies on long-term migration from metal packaging, corresponding to long storage times characteristic of the normal shelf-life of the packaged food have been reported, aiming at the search for bisphenol (present in the varnishes) and metal ions [24, 25].

When the test is done using food instead of food simulants, an extra step is required to extract/separate the migrant compounds from the food matrix, enabling its ideal characterization [25, 26]. The same is needed for some simulants, such as vegetable oil.

The path to a specific migration assay is summarized in the scheme illustrated in Fig. 2.

Once the goal of this test is the identification and quantification of the compounds diffused from the FCM toward the food, the application of analytical techniques with low detection limits is mandatory, and the choice of the technique and protocols to be followed will depend on the type of the compound searched, as summarized in Fig. 3 (*see Notes 5–7*).

Some studies based on the migration of contaminants are described in the following section.

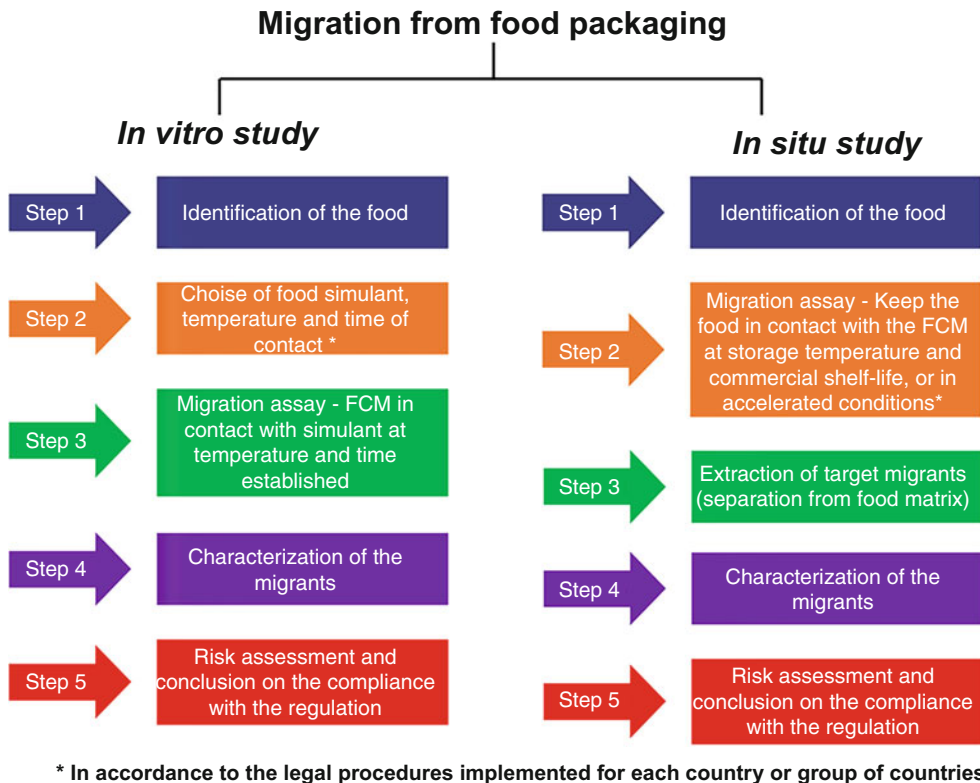


**Fig. 2** Scheme of the steps/protocols to be followed in a migration assay of contaminants, building blocks, nanostructures, and additives from food contact material

### **2.1 Migration of Contaminants, Building Blocks, and Additives**

Contaminants are substances that have not been intentionally added to the food, originating from different sources, which includes the packaging material. However, they can be intentionally added substances (IAS) to food packaging, such as building blocks and additives or non-intentionally added substances (NIAS), such as those obtained from degradation or collateral reactions or impurities. Readers can refer to Chap. 4 for further information on (N)IAS in food packaging. The transfer of these contaminants from the packaging into the food can occur at levels that can pose human health in danger, besides the negative impact on the quality of food [27]. Therefore, to minimize contaminants in foodstuffs and protect the population, European Union legislation establishes maximum limits for certain contaminants in food that are safe for consumption as well as a list of substances authorized to be used in the manufacture of FCM (positive list) [5, 19, 28].

With this regard, a variety of foods needs to be inspected and measured for the presence of contaminants to ensure that the food placed on the market is safe for the consumer. Examples of potentially migrating substances are: monomers, oligomers, alkanes, phthalates and other plasticizers, processing aids, photoinitiators

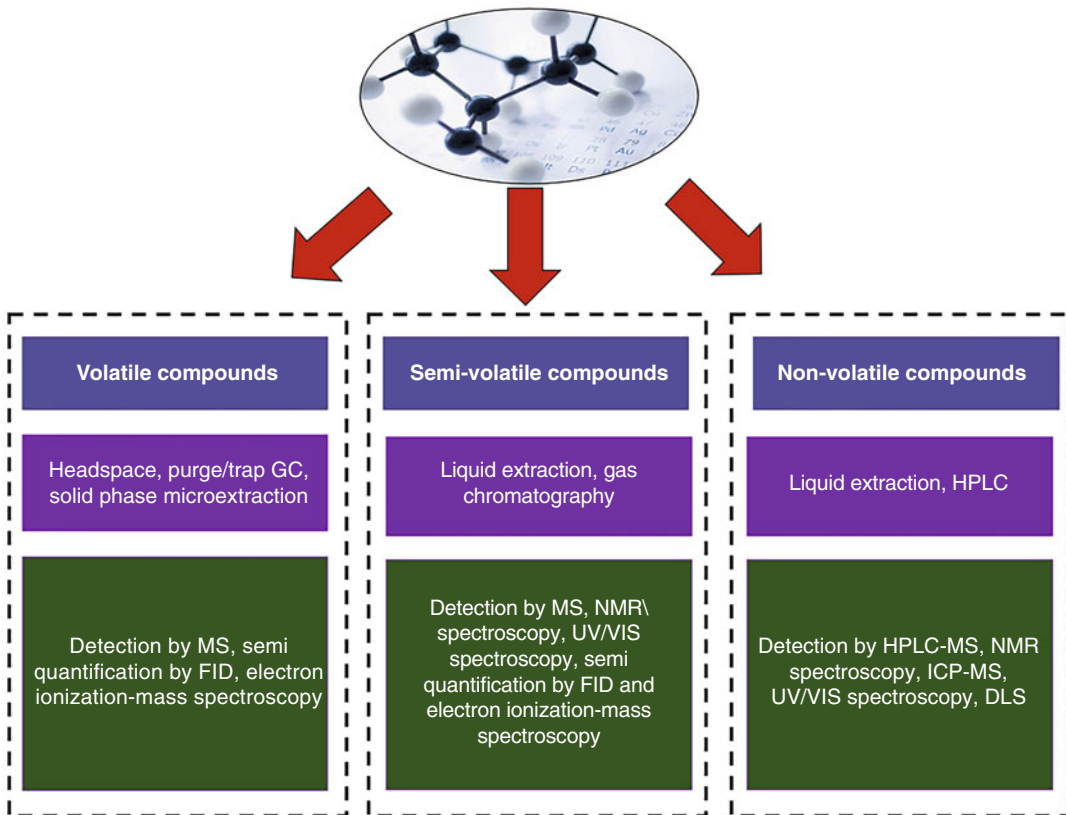


**Fig. 3** Analytical techniques used in the characterization of migrants: gas chromatography (GC), mass spectroscopy (MS), flame ionization detection (FID), nuclear magnetic resonance (NMR), inductively coupled plasma mass spectrometry (ICP-MS), high-performance liquid chromatography (HPLC), and dynamic light scattering (DLS)

(PIs), antioxidants, slipping agents, antimicrobial agents, flame-retardants, and others found in food depending on the type of food and FMC, such as PFAS (per- and polyfluoroalkyl substances)—see Chap. 5 for further details on PFAS [29–34]. These compounds may be originated from printing inks, adhesives, and materials used to manufacture glass, plastic, paper, cardboard, and metal-based food packaging. Several studies have indicated the potential of migration for certain substances from packaging materials, as depicted in Table 1. In this table, it is also possible to check which test conditions (protocols) were applied and also the analytical techniques used to identify the substances that migrated from food contact materials.

An overview done by He and Bayen [35] highlights the chemical contaminants in alcoholic beverages. Monomer, oligomer, phthalates, PIs such as isopropyl-thioxanthone (ITX) and benzophenone, bisphenol A, and other bisphenols have been detected in alcoholic beverages after their migration from the FCM—poly(ethylene terephthalate) (PET) and polyethylene (PE) [35]. Parabens

**Table 1**  
**Recent studies on contaminants migrated from food packaging materials into food or food simulants**

| Packaging/FMC  | Test condition   | Analytical technique   | Main findings  | Reference |
|--|--|--|--|-----------|
| Multilayer packaging (PET/Al/PE)                     | Baby food; food simulants: Acetic acid 3% and ethanol 20%. Migration experiments were performed at 40 °C/10 d  | UHPLC-ESI-QTOF MS. Zorbax Agilent eclipse plus C8 column (2.1 mm × 100 mm, 1.8 µm particle size). Mobile phase: Solvent A ultra pure water/methanol (98:2, v/v), solvent B methanol/ultrapure water (98:2, v/v), both mobile phases contained 5 mM ammonium formate and 0.1 vol% formic acid. Elution: Gradient. Column temperature: 35 °C. Injection volume: 5 µL. Flow: 300 µL min <sup>-1</sup> | In total 39 compounds were detected, whereby 35 of the compounds were polyester oligomers (29 cyclic and 6 linear oligomers) and 4 were detected as: Bis(2-hydroxyethyl) terephthalate, diethyl 5-(2-((2,4,5-trimethoxybenzoyloxy)acetamido)isophthalate, methoxyeugenol, and bis(2-methoxyethyl) sebacate. The detected chemicals were similar in both food simulants and baby food. Two oligomers were quantified at concentrations above 0.010 mg kg <sup>-1</sup> , exceeding the maximum residue levels for baby food.  | [30]      |
| Multilayer packaging (polyurethane used as adhesive) | Food simulants: Ultrapure water, ethanol 10%, and ethanol 95%. Tests were performed at 60 °C for 10 d; 40 °C for 3 d; 121 °C for 30 min (conditions for pasteurized materials); and 40 °C for 3 d (condition for biological samples) | UPLC-MS- QTOF. Chromatography with a waters UPLC BEH C18 column (199 2.1 mm × 100 mm and 1.7 µm). Column temperature: 40 °C. Column flow: 0.3 mL min <sup>-1</sup> . Injection volume: 10 µL (QTOF) and 5 µL (QqQ). Mobile phases: Water (phase A) and methanol (phase B) with 0.1% formic acid. Chromatography started at 98/10 phase A/phase B, changed to 0/100 in 7 min                        | Two cyclic esters, composed by AA, diethylene DEG, and IPA, present in the polyurethane adhesive were evaluated. AA-DEG migration values were higher than the AA-DEG-IPA-DEG values in all samples. For most multilayer materials, migration of the cyclic esters exceeded the migration limit (10 ng g <sup>-1</sup> ) established by EU/10/2011 [19] for not-listed substances. Both cyclic esters are classified as high toxicity according to the TTC. Thus, according to FDA and EFSA, 6 and 5, respectively, out of 20 multilayer packaging materials tested could be used | [40]      |

|  |  |  |   |
|--|--|--|---|
| <p>Plastic packaging (PE, PET, PP, EVA, polyamide)</p>                     | <p>Food simulant: Tenax<sup>®</sup> and isooctane. Migration experiments were performed at 60 °C/10 d and at 20 °C/2 d, respectively</p>   | <p>GC-MS; Phenomenex ZB-5MS column<br/>(30 m × 0.25 mm × 0.25 μm).<br/>Carrier gas: Helium. Flow: 1 mL min<sup>-1</sup>. Injector temperature: 300 °C. Injection mode: Split less. Injection volume: 1 μL.<br/>Oven ramp: 50 °C for 3 min ramped to 300 °C at 8 °C min<sup>-1</sup> and held for 3 min</p>                         | <p>In total 27 compounds were detected (such as: Slip agent, plasticizers, antioxidant, phthalate, alkanes, and others) in the migration experiments that occur to a larger extent in Tenax<sup>®</sup> than in isooctane. Moreover, most of detected compounds in plastic samples are not included in the positive list of monomers and additives that are allowed to be used in plastic [19]</p>  |
| <p>Paper-plastic from outside to inside: PE/PAP/PE and PE/PAP/PE/Al/PE</p> | <p>Food simulant: 10% ethanol, 3% acetic acid, 20% ethanol, 50% ethanol. Migration experiments were performed at: 20 °C e 40 °C for 1, 2, 4, 5, 7, 8, 10, and 11 d. at 60 °C for 3, 6, 9, 12, 18, 24, 48, and 60 h</p> | <p>Atomic fluorescence spectrometer (AFS -810). Wavelength: 196 nm. Atomic height: 10 mm. Negative high pressure: 210 V. Atomic temperature: 200 °C. Lamp current: 10 mA. Reading time: 10 s. delay time: 1 s. injection volume: 0.5 mL. Carrier gas flow: 500 mL min<sup>-1</sup>. Shielded air flow: 900 mL min<sup>-1</sup></p> | <p>Mobility and migration of mercury increase at certain temperatures when the contact time is extended. Migration rates are affected by solvent type, temperatures, and food stimulants. The rates of migration were highest to 3% acetic acid followed to 10% ethanol, 20% ethanol, and lowest migration to 50% ethanol. The results showed that the presence of aluminum film may hinder the migration of mercury and that amount of mercury in the printed sample is larger than that of the unprinted sample, it was suggesting that the mercury in the printed material is estimated to migrate</p> |
| <p>Paper and PET</p>   | <p>Migration experiments were performed at 40 °C for 10 d to food simulant: Ethanol 50%, ethanol 95%, and Tenax<sup>®</sup>; and at 20 °C for 2 d to isooctane food simulant</p>                                       | <p>GC-MS. Agilent J&amp;W column: 60 m × 0.25 mm id × 0.25 μm. Flow 1 mL min<sup>-1</sup>. Injection mode split (1:20). Injection volume: 1 μL. Oven ramp: Initial 35 °C held for 5 min, then rose at 10 °C min<sup>-1</sup> up to 300 °C held for 1.5 min. Acquisition was carried out in SCAN mode (40–400 m/z)</p>              | <p>A total of 149 volatile compounds were found in migration from on paper, and 156 from PET materials, some of them came from inks</p>   |

(continued)

**Table 1**  
(continued)

| Packaging/FMC       | Test condition   | Analytical technique  | Main findings   | Reference |
|---------------------|--|---|---|-----------|
| Paper and cardboard | <p>Food simulants: 50% and 95% ethanol, migration experiments were performed at 15, 30, or 60 min at room temperature or at 60 °C. Food simulants: Tenax, migration tests were performed at 150 °C and 250 °C during 15 min. Foodstuffs: Rice, cereals, and milk powder. Migration tests were performed after contact for 6 months at room temperature</p> | <p>UFPLC-qOrbitrap. Injection volume: 5 µL. SuperPhenylHexyl column (2.1 mm × 100 mm, 2.5 µm) with a prefilter (2.1 mm ID, 0.2 µm) from Thermo-fisher scientific. Mobile phase: Milli-Q water (solvent A) and ACN (solvent B) containing 0.1% HCOOH and 5 mM NH<sub>4</sub>OAc in the positive and negative modes, respectively. The LC gradient method was applied as follows: 0–4 min, 85–70% A; 4–8 min, 70–50% (hold 12 min); 20–30 min, 50–10% A. After 5 min at 5% A, the gradient returned to initial conditions for 5 min, with a flow rate set to 0.3 mL min<sup>-1</sup> at a column temperature of 35 °C</p> | <p>In general, migration of 10 photoinitiators, 4 phthalates, bis (2-ethylhexyl)adipate, acetyltributyl citrate, caprolactam, and BPA was observed to depend, main, on the material type and the physicochemical parameters of the migrants. Whereas the temperatures showed minor effects on migration, in the case of liquid simulants. However, compounds from a baking paper to Tenax, at 150 and 250 °C, evidenced an increment of migration when increasing temperature, except for the most volatile analytes. The photoinitiators Michler's ketone, 4,4'-bis (diethylamino)benzophenone and ethyl-4-dimethylaminobenzoate did not migrate to any of the food sample tested. Whereas the migrations of the photoinitiators: Benzophenone, 2,2'-dimethoxy-2-phenylacetophenone, 4-phenylbenzophenone, and 2,4-diethyl-9H-thioxanthin-9-one into milk powder were found over their specific migration limit values</p> | [56]      |

|                |  |   |   |      |
|----------------|--|---|---|------|
| Recycled paper | <p>Food simulant: Tenax and Sorb-Star. Migration experiments were performed: 20 °C, 40 °C, and 60 °C for 1–12 d. A longer migration time (14 days at 20 °C and 40 °C) and short-time (1 and 22 h at 20 °C) were also used</p>  | <p>HPLC-GC-FID. Phenomenex Normal phase column (250 mm × 2 mm ID). RESTEK pre-columns (10 m × 0.53 mm ID) and RESTEK separation columns (15 m × 0.25 mm ID × 0.25 μm). Two parallel FIDs. Injection volume: 50 μL</p>   | <p>As a replacement for the migration of mineral oil hydrocarbons from recycled food packaging into food products, 16 single substances (n-alkanes and 15 aromatic compounds) were used like model substances</p> <p>Migration was a function of temperature, time, contact type, molecular weight, and polarity of the substances. Alkylated aromatics represent mineral oil aromatic hydrocarbons more realistically.</p> <p>Migration values of the touching contact experiments were slightly higher than those of the gas-phase transfer for sorb-star simulant</p>  | [23] |
| Paperboard     | <p>Food simulant: Modified polyphenylene oxide</p> <p>Food: Pasta, ground pasta, egg pasta, biscuit, butter waffle, wheat semolina, rice semolina, dark chocolate, and milk chocolate. Migration experiments were performed at 22 °C, 60–70% RH, 2, 4, 10, and 16 weeks of storage</p> | <p>GC-FID. VF-1 MS column (30 m × 0.25 mm × 0.25 μm) with a 2 m deactivated fused silica precolumn. Carrier gas: Helium. Flow: 0.713 ml min<sup>-1</sup>. Injection mode: Split/split less inlet set at 250 °C and 1/40 split ratio. Oven ramp: 150 °C hold for 1 min, ramp to 200 °C at 10 °C min<sup>-1</sup> and hold for 1 min. Finally, ramp to 320 °C at 10 °C min<sup>-1</sup> and hold for 14 min</p> | <p>Eight representing classes of component chemicals are known to migrate from paperboard (1,3,5-Trit-butylbenzene, 2,6-diisopropyl naphthalene, t-butyl anthracene, n-hexadecane, n-heptadecane, n-octadecane, n-eicosane, Di-n-propyl phthalate). Volatility was identified as the most important characteristic of these migrants. Fat content and the conformation of starch had an influence on migration. The highest migration occurred in the case of paperboard in contact with fatty foods (biscuits and chocolate) followed by starchy and particulate foods (egg-based wheat pasta, wheat flour, and rice flour). Low migration was observed to wheat pasta</p> | [57] |

(continued)



**Table 1**  
(continued)

| Packaging/FMC   | Test condition  | Analytical technique  | Main findings  | Reference |
|---|---|---|--|-----------|
| Plastic, paper/board, and glass   | Food simulant: For plastic—3% acetic acid, for 10 d to 40 °C. For paper and cardboard—a cold aqueous extract was obtained (24 h at room temperature) which was stabilized with HNO <sub>3</sub> 65%; for glass: 24 h at room temperature, using as food simulant 4% acetic acid | GF-AAS and ICP-MS   | The values of heavy metals content found into paper and board are higher than for plastic. This occurs due the influence of printing inks and dyes which are a source of metals. On migration from food contact materials, the highest values were obtained for Fe and Zn, while the lowest values were obtained for Co. However, the results showed that the values migrated are lower than maximum allowed limits for all metals analyzed (Pb, Cd, Cr, Ba, Cu, Co, Fe, Mn, Ni, Zn)                       | [58]      |
| Metallic (in electrolytic chromium/chromium oxide coated steel packaging) | Canned sardines (oil and tomato sauce conserve) commercialized in Brazil  | ICP OES equipment equipped with a double-step nebulization camera and a sea spray nebulizer. Power of the radiofrequency generator (1200 W). Sample flow rate (0.50 L min <sup>-1</sup> ), argon flow from the nebulizer (0.60 L min <sup>-1</sup> ). Auxiliary argon flow rate (1.00 L min <sup>-1</sup> ). Main argon flow rate (12.0 L min <sup>-1</sup> ). Axial mode of vision | Metallic chromium internal coating from bottom and top (closure) and chromium oxide in inner steel sheets from packaging showed quality satisfactory. The body of these cans received two coating layers, guaranteeing the metallic material resistance to production process of this type of packaging and minimized the development of the corrosion in the cans. Levels above the maximum limits allowed by Brazilian and MERCOSUR regulations were observed for inorganic contaminants: As, Cd, and Cr | [25]      |

[24]

|                      |   |   |   |
|----------------------|---|---|---|
| Coated tinplate cans | Vegetable foods: Including canned fava beans, canned red beans, canned chickpeas, canned okra of different brands. Storage time: 0–730 d or purchase date +493 d. storage temperature: 5 °C, 22 °C, and 40 °C | For analysis of bisphenol: UHPLC equipped with a multi-wave fluorescence detector. Auto-sampler temperature: 10 °C; injected volume: 20 µL. C18-PFP column (150 × 2.1 mm ID, 2 µm particle size). Column temperature: 20 °C. Mobile phase: Milli-Q water (A) and HPLC plus gradient ACN (B). Flow rate: 0.3 mL min <sup>-1</sup> with the following binary gradient: 0 min—43% B, 1 min ramp to 50% B (maintained for 4 min), 2 min ramp to 60% B (maintained for 5 min), 1 min ramp to 100% B (maintained for 2 min), and back to 43% B in 1 min (total duration 16 min) | Among bisphenols, only BPA and BADGE•2H <sub>2</sub> O were found in canned food, the highest level was observed to BADGE•2H <sub>2</sub> O. Sn was undetected in samples. Heat treatment (main sterilization) favors more bisphenol migration than trace metals migration. However, metal release was influenced, main, by storage. Canned okra offers conditions that favor highest BADGE and Fe content in food during pasteurization due its low pH (3.7) and high water content (93.8%). Among trace metals, the highest levels were observed for Fe and Zn. BPA and Zn (and Pb to a lesser extent) showed similar migration trends, with dependence on food type (pH, water content), brand, and storage temperature. Cd, Ni, and Cu were similarly influenced by food type and can brand. Significant release of bisphenol and metals were observed main in acid food, probably due to corrosion result in can damage to the can as denting. The Fe release was enhanced by 86–90% |
|                      |   | For analysis of trace metals, AAS was used  |   |

high-performance liquid chromatography–gas chromatography with flame ionization detector (HPLC-GC-FID), gas chromatography coupled with quadrupole time of flight mass spectrometry (GC-qTOF-MS), high-performance liquid chromatography coupled to a quadrupole time-of-flight mass spectrometer (UHPLC-ESI-QTOF MS), sequential windowed acquisition of all theoretical mass spectrometry (SWATH), poly(ethylene terephthalate) (PET), aluminum (Al), polyethylene (PE), ethylene vinyl acetate (EVA), polypropylene (PP), polyamide (PA), ultrahigh-performance liquid chromatography (UHPLC) coupled to a Thermo Scientific™ Q Exactive™ Focus quadrupole-Orbitrap mass spectrometer (UHPLC-qOrbitrap), food contact material (FCM), inductively coupled plasma optical emission spectrometry (ICP OES), bisphenol A (BPA), bisphenol A diglycidyl ether (BADGE•2H<sub>2</sub>O), Threshold of Toxicological Concern (TTC), Food and Drug Administration (FDA), European Food Safety Authority (EFSA), adipic acid (AA), diethylene glycol (DEG), isophthalic acid (IPA), atomic absorption spectrometer with graphite furnace (GF-AAS), inductively coupled plasma mass spectrometer (ICP-MS), atomic absorption spectrometry (AAS)

(as ethylparaben and methylparaben), phenolic antioxidants (as butylated hydroxytoluene), and plasticizer (as N-butylbenzenesulfonamide) are also compounds that might be expected to be found in alcoholic beverages as a result of the migration from crown cap plastic seals in contact with the food [29].

In the study done by Wang et al. (2019) [36], the migration behavior of chlorinated paraffins (CPs) presented in plastic (foil-lined polypropylene) was related to their molecular weight and chlorine content. In general, CPs were able to migrate into food simulants (water, 3% acetic acid, 15% ethanol, and hexane) during the migration experiment (performed at 40 °C/10 d), with the highest migration concentration being found in hexane food simulants. However, the study revealed that migration of CPs does not pose immediate risks to human health. Another study with plastic packaging, carried out by García Ibarra et al. [31], showed that in a total of 100 compounds detected in plastic materials, 27 were NIAS migrating from FCM into food. The compounds found were: caprolactam (which was present in an external layer of polyamide of packaging material), 2,6-di-tert-butyl-1,4-benzoquinone, 2,4-di-tert-butylphenol, phthalates (as diethyl phthalate, diisobutyl phthalate and bis(2-ethylhexyl) phthalate), benzenesulfonamide, n-ethyl-2-methyl, benzenesulfonamide, N-ethyl-4-methyl, alkanes (tetradecane, hexadecane, heptadecane, octadecane, docosane), isopropyl myristate, octadecanal, 7,9 di-tert-butyl-1-oxaspiro (4,5)deca-6-9-diene-2,8-dione, tributyl acetyl citrate, slip agent (as oleamide, hexadecanamide erucamide and octadecanamide), plasticizers (as triphenyl phosphate and tributyl aconitate), squalene, butylated hydroxytoluene (BHT), 1-hexadecanol, and bis (2-ethylhexyl) adipate. However, some detected compounds are not included in Regulation EU no. 10/2011 [19] on plastic materials [31].

The migration of PIs from plastic baby bibs into Tenax<sup>®</sup> was measured in bibs collected in the European market. Results indicate that several no authorized PIs are in use to print bibs. The most commonly detected PIs were benzophenone, detected in nearly all samples, and isopropylthioxanthone, quantified in 12 out of 22 samples. Several non-evaluated PIs were detected: Triphenyl phosphate, 2-ethylanthraquinone, 2,2-dimethoxy-2-phenylacetophenone, 4-(4-methylphenylthio)benzophenone, 1-hydroxycyclohexyl phenyl ketone, and 4,4'-bis(diethylamino)-benzophenone [37].

Xue et al. [38] reported that the migration percentage of organic pollutants from Kraft paper-based packaging to packaged dry powdered foods increased at a higher temperature and longer contact time. Some organic substances introduced during the manufacture of paper packaging materials such as phenol, alkylbenzene, 2,6-dissopropyl naphthalene and phthalates (dibutyl phthalate and

Bis(2-ethylhexyl)phthalate (DEHP)) used as food packaging may migrate into dry food [38]. Migration of printing inks, which are printed on carton surface, may also occur. Compounds found in printing inks, as acrylate monomers and binders in UV offset inks, may migrate into carton food packaging [39].

Contaminants coming from the adhesive ingredients commonly used in multilayer films were detected by migration studies in baby food samples. Some concentration levels were found exceeding the maximum residue levels for baby food as revealed in the study of Bauer et al. [30], which raises the concern for potential adverse effects of these substances on health. Ubeda et al. [40] reported that polyurethane adhesives, commonly found in multilayer materials, may contain cyclic ester oligomers as potential migrants. The authors showed that the concentration of these compounds in migration to food simulants exceeded the maximum level for not-listed substances established by Regulation EU no. 10/2011 [19] for most samples.

Several metal traces, often used in metal containers, but also in pigments and catalyzers for polymerization, are prone to migrate into food, among them lead, iron, cadmium, nickel, chromium, tin, zinc, and copper are being considered as food contaminants. Thus, the use of metal cans or packaging with metals has to be carefully addressed since it occasionally develops integrity problems due to corrosion, which can lead to the migration of metal ions [24]. According to Rather et al. (2017) [27], metal ions from corrosion in metallic cans may migrate to food. By-products from the epoxy resins (varnish commonly used to coat the inner side of cans), such as bisphenol A (BPA), or bisphenol A diglycidyl ether (BADGE), as cyclo-di-BADGE can also migrate to food.

Fengler and Gruber [23] studied the migration of mineral oil hydrocarbons (mixtures of non-identified substances) from recycled food packaging into food products and concluded that migration was a function of contact type and polarity of the substances. Migration values of the direct contact experiments were slightly higher than those of the gas-phase transfer for Sorb-Star<sup>®</sup> simulant. Additionally, according to these authors, alkanes showed high migration to the lipophilic food simulants due to their low polarity.

Migration performance of contaminants from packaging materials into foods are affected by various factors, namely: the extended contact with final packaging materials during storage, the temperature (heating), contact type, characteristics of the migrating substances/migrants (molecular weight, volatility, and polarity) and food properties (composition—e.g., fat content—and properties), which could certainly play a significant role in the migration process [23, 38]. Therefore, it is important to evaluate how these factors interfere in the contaminant's migration in FCM, to minimize the risk of migration and ensure food safety [41, 42].

Other recent research studies on the detection of contaminants migrants from the food packaging material into food or food simulants are summarized in Table 1.

## **2.2 Migration of Nanoparticles**

The current experimental data shows that the research about the migration of ENMs is at young stages, especially for food packaging [43].

Once the food is a complex matrix, the characterization and detection of nanoparticles after their migration from the FCM are a complex task and require several procedures or combined detection methodologies, which limits the fundamental knowledge on how/if the ENM interacts with the food components, changing their properties. Thus the difficulty to predict whether the nanoparticles would pose a risk to the consumers when used in the reinforcement of FCM [6, 44].

These studies should consider the potential effect of nanoparticles' migration from FCM to the packaged food. Therefore, this can minimize the application of these nanocomposites as an alternative to conventional packaging materials without exploiting their possible harmful effects on the consumers [6, 43].

The studies are not conclusive, reporting different patterns, for example, Simon, Chaudhry, and Bakos [45] evaluated the migration of engineered nanoparticles from different polymer proposing to address polymers like highly viscous liquids and to derive diffusion coefficients by the Stokes–Einstein equation from viscosity and particle radius, and they concluded that the reduction in particle size and polymer dynamic viscosity leads to an increment in the migration rate [22, 45, 46]. On the other hand, the research group headed by Bott et al. [16] reported that when the nanoparticles are immobilized in the polymer chains the migration does not occur, as observed in low-density PE (LDPE) and polypropylene (PS) reinforced with carbon nanotubes, which did not diffuse toward the food simulant tested. They highlighted that the diffusion will always be smaller than the detection limit of any current sensitive method. This conclusion can be generalized to other FCM in which black carbon nanotubes are completely embedded [16].

In addition to the complexity of this topic, another factor that may also influence the migration of nanoparticles, for example, the diffusion process of silver nanoparticles (AgNPs), known for their antimicrobial properties [43, 47], is favorable in an acid environment (lower pH) [43, 47] and high temperature and time of storage results [47]. Ultimately, the diffusion process also depends on the type of polymer/nanoparticle and incorporation process used, for example, in commercial LDPE packaging incorporated with AgNPs in different formats presented distinct migration profiles [16, 43].

The research increasingly needs studies exclusively to understand the migration behavior of nanocomposites when in contact with foodstuffs. Moreover, it is also important to understand how

the migration process modifies and influences the structure of the material, in terms of size and morphology, considering the complexity of the mechanisms involved, due to the relevance of these factors to assess the risks to human health by exposure to increasingly common ENMs [6, 48].

What is expected is that under normal conditions of use, these packaging cannot transfer their constituents to food in quantities that could result in depletion of the food's organoleptic characteristics or changes in its composition, neither to pose dangerous consequences for human health [43].

More information about this topic is available in several reviews and technical papers such as in Störmer et al. [44], Bott et al. [16], Huang et al. [17], Souza et al. [49], and Souza et al. [22], to cite a few.

---

### 3 Notes

1. Migration of contaminants from contact materials to food can occur and may represent a risk to the consumers' health. To evaluate if it happens and how it happens is mandatory, thus the importance of migration assays. Ideally, the study of the migrants should be done directly in the food after its contact with the packaging. However, due to the complexity of food matrices, *in vitro* studies are done using simulants. It is important when planning this type of analysis to fully understand the type of food and packaging to decide the best method to use. Moreover, once the migration has occurred, the characterization of the migrants should be done using the most sensitive technique to obtain reliable results to make a proper risk assessment and conclude whether the packaging poses or not any danger to the consumer.
2. In the case of the European Union, the OML required for plastic material is 10 mg of substances per 1 dm<sup>2</sup> of the surface area of the FCM, or 60 mg kg<sup>-1</sup> of food [5], while SML [mg kg<sup>-1</sup>] depends on the risk assessment of each specific substance, and can also be found in the available regulation [5, 19, 22]. Some of the substances of the positive list (i.e., list of substances permitted in the manufacture of plastic materials intended for food contact) of Reg. no. 10/2011 and its amendments still do not have a defined SML.
3. Food simulants are the test media used to simulate/mimic the transfer of substances from the packaging material into food; thus, represent the major physical-chemical properties exhibited by food [19, 50]. According to Regulation (EC) no. 10/2011 and its amendments [19], there are six assigned food simulants, namely:

- (i) Ethanol 10 vol%—Simulant A: assigned for hydrophilic foods.
  - (ii) Acetic acid 3% (w/v)—Simulant B: assigned for hydrophilic and acidic (pH < 4.5) foods.
  - (iii) Ethanol 20 vol%—Simulant C: assigned for hydrophilic and mildly alcoholic (alcohol content  $\leq 20\%$ ) foods and food comprising a relevant amount of organic ingredients that render it a more lipophilic character.
  - (iv) Ethanol 50 vol%—Simulant D1: assigned to lipophilic and alcoholic (alcohol content  $> 20\%$ ) foods and for oil-in-water emulsions.
  - (v) Vegetable oil or ethanol 95 vol%—Simulant D2: assigned to lipophilic foods containing free fat at the surface.
  - (vi) Poly(2,6-diphenyl-p-phenylene oxide), particle size 60–80 mesh, pore size 200 nm—Simulant E: assigned for specific migration into dry food.
4. In general, migration assays are carried out for 10 d at 40 °C or at 60 °C (which are the conditions to simulate any long-term storage at room temperature or below, for products with shelf lives longer than 6 months). More detailed information on the choice of simulant and conditions of the assay can be found in this Regulation, which also classifies the type of food and the simulant(s) that are recommended for the migration tests.
  5. To study the migration of nanoparticles, the protocols can be even more demanding, once it is important to determine if after the diffusion process the migrant kept its nanometer scale [51]. Thus, even more robust techniques are generally required, such as microscopy techniques (scanning and transmission electron microscopies), dynamic light scattering, X-ray diffraction, and field-flow fractionation, to mention a few [22].
  6. It is important to highlight that the analytical methods used need to be in accordance with the legal requirements, for example, for the European countries/market with those set in Article 11 of Regulation (EC) no. 882/2004 [52], repealed by Regulation (EU) 2017/625 of the European Parliament and of the Council of March 15, 2017 [53], which defines the proper methods of analysis and sampling. Also, the technique quantification limit needs to be taken into consideration, as more robust characterization methods should be applied according to the level of migrants found.
  7. Depending on the migrant targeted, after the diffusion process, the samples may also need some preparation prior to the quantification. For example, to quantify the migration of inorganic compounds, such as minerals, all organic matter needs to be removed from the simulant or the food. This process can be accomplished by incinerating the sample followed by acid digestion with nitric acid solution (1:1).

## Acknowledgments

This research was funded by national funding by FCT, Foundation for Science and Technology, through the individual research grant (SFRH/BD/144346/2019) of J.P and the individual research grant (2020.04441.BD) of C.R. This work was supported by national funds from FCT/MCTES within the R&D Units Project Scope (UIDB/EMS/00285/2020, UIDB/00211/2020, and UIDB/50016/2020). This work has also been supported by MEtRICs—Mechanical Engineering and Resource Sustainability Center, which is financed by national funds from FCT/MCTES (UIDB/04077/2020 and UIDP/04077/2020). This work has also been supported by the Associate Laboratory for Green Chemistry—LAQV which is financed by national funds from FCT/MCTES (UIDB/50006/2020 and UIDP/50006/2020). This work has also been financially supported by PRR – Recovery and Resilience Plan and the Next Generation EU funds, INOV.AM project “Innovation in Additive Manufacturing” (C628518748-00464029 | 7999), and POCI-01-0145-FEDER-030446 funded by FEDER funds through COMPETE2020—Programa Operacional Competitividade e Internacionalização (POCI) and by national funds from FCT/MCTES (UIDB/00285/2020 – CEMMPRE ref, LA/P/0112/2020 ARISE ref).

## References

1. Prasad P, Kochhar A (2014) Active packaging in food industry: a review. *IOSR J Environ Sci Toxicol Food Technol* 8:01–07. <https://doi.org/10.9790/2402-08530107>
2. Tang XZ, Kumar P, Alavi S, Sandeep KP (2012) Recent advances in biopolymers and biopolymer-based nanocomposites for food packaging materials. *Crit Rev Food Sci Nutr* 52:426–442. <https://doi.org/10.1080/10408398.2010.500508>
3. Poças F, Hogg T (2007) Exposure assessment of chemicals from packaging materials in foods: a review. *Trends Food Sci Technol* 18:219–230. <https://doi.org/10.1016/j.tifs.2006.12.008>
4. Poças F (2018) Migration from packaging and food contact materials into foods. In: Reference module in food science. Elsevier, pp 1–18
5. European Commission (2004) Regulation (EU) No 1935/2004 of 27 October 2004 on plastic materials and articles intended to come into contact with food and repealing Directives 80/590/EEC and 89/109/EEC. *J da União Eur* L338:4–17
6. Souza VGL, Fernando AL (2016) Nanoparticles in food packaging: biodegradability and potential migration to food – a review. *Food Packag Shelf Life* 8:63–70. <https://doi.org/10.1016/j.fpsl.2016.04.001>
7. Poças F, Franz R (2018) Overview on European regulatory issues, legislation, and EFSA evaluations of nanomaterials. In: *Nanomaterials for food packaging*. Elsevier, pp 277–300
8. European Union (EU) (2016) Food contact materials – regulation (EC) 1935/2004 – European implementation assessment. *Off J Eur Union* 140. <https://doi.org/10.2861/162638>
9. Dainelli D, Gontard N, Spyropoulos D, Zondervan-van den Beuken E, Tobback P (2008) Active and intelligent food packaging: legal aspects and safety concerns. *Trends Food Sci Technol* 19:S103–S112. <https://doi.org/10.1016/j.tifs.2008.09.011>
10. Wani AA, Singh P, Langowski HC (2014) Food technologies: packaging. *Encycl Food Saf* 3:211–218. <https://doi.org/10.1016/B978-0-12-378612-8.00273-0>
11. Handford CE, Dean M, Henchion M, Spence M, Elliott CT, Campbell K (2014) Implications of nanotechnology for the agri-



- food industry: opportunities, benefits and risks. *Trends Food Sci Technol* 40:226–241. <https://doi.org/10.1016/j.tifs.2014.09.007>
12. Chaudhry Q, Scotter M, Blackburn J, Ross B, Boxall A, Castle L, Aitken R, Watkins R (2008) Applications and implications of nanotechnologies for the food sector. *Food Addit Contam Part A Chem Anal Control Expo Risk Assess* 25:241–258. <https://doi.org/10.1080/02652030701744538>
  13. Avella M, De Vlieger JJ, Errico ME, Fischer S, Vacca P, Volpe MG (2005) Biodegradable starch/clay nanocomposite films for food packaging applications. *Food Chem* 93:467–474. <https://doi.org/10.1016/j.foodchem.2004.10.024>
  14. Sarantópoulos CGL, Oliveira LM, Padula M, Coltro L, Aalves RMV, Garcia EC (2002) Embalagens plásticas flexíveis: principais polímeros e avaliação de propriedades, Campinas
  15. Schmid P, Welle F (2020) Chemical migration from beverage packaging materials – a review. *Beverages* 6:1–19. <https://doi.org/10.3390/beverages6020037>
  16. Bott J, Störmer A, Franz R (2014) Migration of nanoparticles from plastic packaging materials containing carbon black into foodstuffs. *Food Addit Contam Part A* 31:1769–1782. <https://doi.org/10.1080/19440049.2014.952786>
  17. Huang J-YY, Li X, Zhou W (2015) Safety assessment of nanocomposite for food packaging application. *Trends Food Sci Technol* 45:187–199. <https://doi.org/10.1016/j.tifs.2015.07.002>
  18. Chungy D, Papadakis SE, Yamy KL (2002) Simple models for assessing migration from food-packaging ® lms. *Food Addit Contam* 19:611–617. <https://doi.org/10.1080/0265203021012638>
  19. European Commission (2011) Commission Regulation (EU) No 10/2011. *Off J Eur Union*, pp 1–89
  20. Stoll L, Rech R, Flôres SH, Nachtigall SMB, de Oliveira RA (2019) Poly(acid lactic) films with carotenoids extracts: release study and effect on sunflower oil preservation. *Food Chem* 281:213–221. <https://doi.org/10.1016/j.foodchem.2018.12.100>
  21. Poças MF, Oliveira JC, Oliveira FAR, Hogg T (2008) A critical survey of predictive mathematical models for migration from packaging. *Crit Rev Food Sci Nutr* 48:913–928. <https://doi.org/10.1080/10408390701761944>
  22. Souza VGL, Ribeiro-Santos R, Rodrigues PF, Otoni CG, Duarte MP, Coelho IM, Fernando AL (2018) Nanomaterial migration from composites into food matrices. In: Cirillo G, Kozłowski MA, Spizzirri UG (eds) *Composite materials for food packaging*, 1st edn. Scrivener Publishing LLC, Beverly, pp 401–435
  23. Fengler R, Gruber L (2020) Mineral oil migration from paper-based packaging into food, investigated by means of food simulants and model substances. *Food Addit Contam Part A Chem Anal Control Expo Risk Assess* 37:845–857. <https://doi.org/10.1080/19440049.2020.1714750>
  24. Noureddine El Moussawi S, Ouaini R, Matta J, Chébib H, Cladière M, Camel V (2019) Simultaneous migration of bisphenol compounds and trace metals in canned vegetable food. *Food Chem* 288:228–238. <https://doi.org/10.1016/j.foodchem.2019.02.116>
  25. de Mello Lazarini TE, Milani RF, Yamashita DM, Saron ES, Morgano MA (2019) Canned sardines commercialized in Brazil: packaging and inorganic contaminants evaluation. *Food Packag Shelf Life* 21:100372. <https://doi.org/10.1016/j.fpsl.2019.100372>
  26. Luykx DMAM, Peters RJB, Van Ruth SM, Bouwmeester H (2008) A review of analytical methods for the identification and characterization of nano delivery systems in food. *J Agric Food Chem* 56:8231–8247. <https://doi.org/10.1021/jf8013926>
  27. Rather IA, Koh WY, Paek WK, Lim J (2017) The sources of chemical contaminants in food and their health implications. *Front Pharmacol* 8. <https://doi.org/10.3389/fphar.2017.00830>
  28. Commission of the European Communities (2006) Commission Regulation (EC) No 118/2006 of 19 December 2006 setting maximum levels for certain contaminants in foodstuffs. *Off J Eur Union*:5–24
  29. Žnideršič L, Mlakar A, Prosen H (2019) Development of a SPME-GC-MS/MS method for the determination of some contaminants from food contact material in beverages. *Food Chem Toxicol* 134:110829. <https://doi.org/10.1016/j.fct.2019.110829>
  30. Bauer A, Jesús F, Gómez Ramos MJ, Lozano A, Fernández-Alba AR (2019) Identification of unexpected chemical contaminants in baby food coming from plastic packaging migration by high resolution accurate mass spectrometry. *Food Chem* 295:274–288. <https://doi.org/10.1016/j.foodchem.2019.05.105>
  31. García Ibarra V, Bernaldo R, de Quirós A, Paseiro Losada P, Sendón R (2019) Non-target analysis of intentionally and non intentionally added substances from plastic

- packaging materials and their migration into food simulants. *Food Packag Shelf Life* 21: 100325. <https://doi.org/10.1016/j.fpsl.2019.100325>
32. Sanches Silva A, Cruz Freire JM, Sendón R, Franz R, Losada PP (2009) Migration and diffusion of diphenylbutadiene from packages into foods. *J Agric Food Chem* 57:10225–10230. <https://doi.org/10.1021/jf901666h>
  33. Sanches-Silva A, Pastorelli S, Cruz JM, Simoneau C, Paseiro-Losada P (2008) Development of a multimethod for the determination of photoinitiators in beverage packaging. *J Food Sci* 73:C92–C99. <https://doi.org/10.1111/j.1750-3841.2007.00642.x>
  34. Vilarinho F, Sendón R, van der Kellen A, Vaz MF, Silva AS (2019) Bisphenol A in food as a result of its migration from food packaging. *Trends Food Sci Technol* 91:33–65. <https://doi.org/10.1016/j.tifs.2019.06.012>
  35. He NX, Bayen S (2020) An overview of chemical contaminants and other undesirable chemicals in alcoholic beverages and strategies for analysis. *Compr Rev Food Sci Food Saf* 19: 3916–3950. <https://doi.org/10.1111/1541-4337.12649>
  36. Wang C, Gao W, Liang Y, Jiang Y, Wang Y, Zhang Q, Jiang G (2019) Migration of chlorinated paraffins from plastic food packaging into food simulants: concentrations and differences in congener profiles. *Chemosphere* 225:557–564. <https://doi.org/10.1016/j.chemosphere.2019.03.039>
  37. Galbiati E, Pereira J, Selbourne M, do Poças CF (2020) Photoinitiators use in printed baby bibs and their migration into Tenax® by gas chromatography–mass spectrometry. *Packag Technol Sci* pts.2546:203. <https://doi.org/10.1002/pts.2546>
  38. Xue M, Chai X-S, Li X, Chen R (2019) Migration of organic contaminants into dry powdered food in paper packaging materials and the influencing factors. *J Food Eng* 262:75–82. <https://doi.org/10.1016/j.jfoodeng.2019.05.018>
  39. Ateş Duru Ö, Özdemir L, Oktav M (2019) Occurrence and effects of migration in carton food packaging caused by printing inks. In: 3rd international printing technologies symposium, Istanbul, pp 139–144
  40. Ubeda S, Aznar M, Rosenmai AK, Vinggaard AM, Nerín C (2020) Migration studies and toxicity evaluation of cyclic polyesters oligomers from food packaging adhesives. *Food Chem* 311:125918. <https://doi.org/10.1016/j.foodchem.2019.125918>
  41. Silva AS, Freire JMC, García RS, Franz R, Losada PP (2007) Time–temperature study of the kinetics of migration of DPBD from plastics into chocolate, chocolate spread and margarine. *Food Res Int* 40:679–686. <https://doi.org/10.1016/j.foodres.2006.11.012>
  42. Silva AS, Freire JMC, Franz R, Losada PP (2008) Mass transport studies of model migrants within dry foodstuffs. *J Cereal Sci* 48:662–669. <https://doi.org/10.1016/j.jcs.2008.02.006>
  43. Metak AM, Nabhani F, Connolly SN (2015) Migration of engineered nanoparticles from packaging into food products. *LWT Food Sci Technol* 64:781–787. <https://doi.org/10.1016/j.lwt.2015.06.001>
  44. Störmer A, Bott J, Kemmer D, Franz R (2017) Critical review of the migration potential of nanoparticles in food contact plastics. *Trends Food Sci Technol* 63:39–50. <https://doi.org/10.1016/j.tifs.2017.01.011>
  45. Šimon P, Chaudhry Q, Bakoš D (2008) Migration of engineered nanoparticles from polymer packaging to food – a physicochemical view. *J Food Nutr Res* 47:105–113
  46. Souza VGL, Rodrigues C, Valente S, Pimenta C, Pires JRA, Alves MM, Santos CF, Coelho IM, Fernando ALL (2020) Eco-friendly ZnO/chitosan bionanocomposites films for packaging of fresh poultry meat. *Coatings* 10:110. <https://doi.org/10.3390/coatings10020110>
  47. Hetzer B, Burcza A, Gräf V, Walz E, Greiner R (2017) Online-coupling of AF4 and single particle-ICP-MS as an analytical approach for the selective detection of nanosilver release from model food packaging films into food simulants. *Food Control* 80:113–124. <https://doi.org/10.1016/j.foodcont.2017.04.040>
  48. Hannon JC, Kerry JP, Cruz-Romero M, Azlin-Hasim S, Morris M, Cummins E (2017) Kinetic desorption models for the release of nanosilver from an experimental nanosilver coating on polystyrene food packaging. *Innov Food Sci Emerg Technol* 44:149–158. <https://doi.org/10.1016/j.ifset.2017.07.001>
  49. Souza VGL, Rodrigues PF, Duarte MP, Fernando AL (2018) Antioxidant migration studies in chitosan films incorporated with plant extracts. *J Renew Mater* 6:548–558. <https://doi.org/10.7569/JRM.2018.634104>
  50. Souza VGL, Rodrigues C, Ferreira L, Pires JRA, Duarte MP, Coelho I, Fernando AL (2019) In vitro bioactivity of novel chitosan bionanocomposites incorporated with different essential oils. *Ind Crop Prod* 140:111563.

- <https://doi.org/10.1016/j.indcrop.2019.111563>
51. Blasco C, Picó Y (2011) Determining nanomaterials in food. *TrAC Trends Anal Chem* 30: 84–99. <https://doi.org/10.1016/j.trac.2010.08.010>
  52. European Commission (2004) Regulation (EC) No 882/2004 on official controls performed to ensure the verification of compliance with feed and food law, animal health and animal welfare rules. *Off J Eur Union* 2004:1–141
  53. European Commission (2017) Regulation (EU) 2017/625 on official controls and other official activities performed to ensure the application of food and feed law, rules on animal health and welfare, plant health and plant protection products. *Off J Eur Union* 95:1–142
  54. Peng X, Fu H, Hu J, Luo F (2020) Investigation on mercury migration discipline in different paper-plastic food packaging containers. *J Food Sci* 85:1186–1192. <https://doi.org/10.1111/1750-3841.15060>
  55. Clemente I, Aznar M, Nerín C, Bosetti O (2016) Migration from printing inks in multilayer food packaging materials by GC-MS analysis and pattern recognition with chemometrics. *Food Addit Contam Part A*:1–12. <https://doi.org/10.1080/19440049.2016.1155757>
  56. Blanco-Zubiaguirre L, Zabaleta I, Prieto A, Olivares M, Zuloaga O, Elizalde MPP (2020) Migration of photoinitiators, phthalates and plasticizers from paper and cardboard materials into different simulants and foodstuffs. *Food Chem* 344:128597. <https://doi.org/10.1016/j.foodchem.2020.128597>
  57. Baele M, Vermeulen A, Claes M, Ragaert P, De Meulenaer B (2020) Migration of surrogate contaminants from paperboard to foods: effect of food and surrogate properties. *Food Addit Contam Part A* 37:2165–2183. <https://doi.org/10.1080/19440049.2020.1778184>
  58. Ungureanu E, Mustăţea G, Popa ME (2020) Heavy metals contamination of food contact materials in Romania. *Sci Bull Ser F Biotechnol* XXIV:63–68



## In Vitro Cytotoxicity Testing of Food Packaging

Arthur B. Ribeiro, Juliana G. F. Silva, Lucas N. F. Trevizan,  
Hernane S. Barud, Flávia A. Resende, and Denise C. Tavares

### Abstract

Colorimetric assays with tetrazolium salts allow rapid evaluation of cytotoxicity endpoints. These assays are based on the ability of viable cells to convert tetrazolium salts into formazan products through the succinate dehydrogenase system in the mitochondrial respiratory chain. In the presence of NADH/NADPH, these salts are reduced to formazan products characterized by an intense and distinct color that depends on the original tetrazolium salt used as the substrate for the reaction. Only viable cells, which contain intact plasma and mitochondrial membranes, will have active dehydrogenase. Agents that break the membranes and interfere with the respiratory chain will deactivate the enzyme and consequently the formation of formazan products. Thus, the amount of formazan product can be correlated with the number of viable cells after exposure to the tested substance. In this chapter, the most common colorimetric cell viability assays with tetrazolium salts are present to assess the cytotoxicity of food packaging.

**Key words** Colorimetric assay, XTT, MTS, MTT, WST, Formazan, Respiratory chain, Dehydrogenase system

---

## 1 Introduction

In vitro cytotoxicity assays are becoming increasingly recognized as an extremely valuable tool to identify compounds that might pose certain health risks to humans [1, 2]. The need for sensitive, reliable, and easy methods has led to the development of several standard assays that allow rapid evaluation of chemically induced damages in physiologically normal cells that lead to death or cell proliferation disturbances [3–5]. Among the most basic types of in vitro bioassays, colorimetric assays using tetrazolium salts have been widely used to measure cellular metabolic activity as an indicator of cell viability, proliferation, and cytotoxicity [3, 6, 7].

The most commonly used tetrazolium salts can be classified into two basic categories: cationic and anionic salts. *Cationic salts* (Fig. 1a) are positively charged and easily penetrate viable eukaryotic cells through electrostatic interactions with the anionic plasma

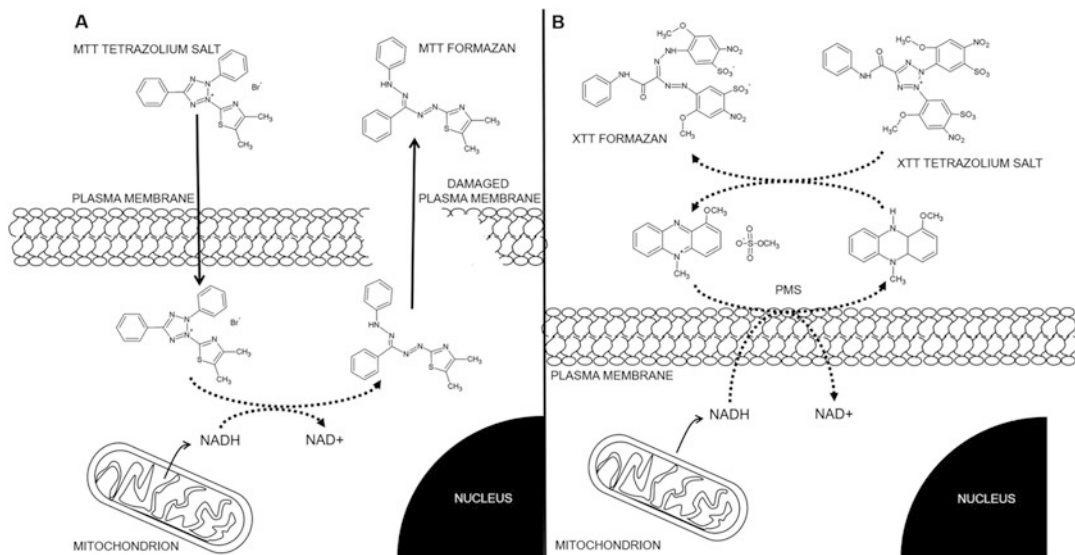


**Fig. 1** Schematic model of cellular reduction of (a) cationic salts (MTT) and (b) anionic salts (XTT) in viable cells

membrane, serving as substrates for active cellular dehydrogenases and reductase enzymes to be reduced to formazan products, as for example the MTT ((3-(4,5-dimethylthiazol-2-yl)-2,5-diphenyltetrazolium bromide)) tetrazolium salt, which gives name to the MTT colorimetric assay [2, 8].

The MTT colorimetric assay has been widely used to measure cytotoxicity or cytostatic activity of compounds. This methodology is based on the ability of viable cells to convert MTT into purple insoluble formazan crystals [8, 9]. Due to its lipophilic side groups and positive charge, the MTT salt can quickly penetrate viable cell membranes and be reduced by mitochondrial or cell plasma enzymes like oxidoreductases, dehydrogenases, oxidases, and peroxidases [2, 10]. The MTT formazan product then accumulates as insoluble needle-shaped crystals that precipitate inside cells and can also be deposited near the cell surface [2, 11]. The produced formazan is finally quantified by absorbance measurements using a spectrophotometer. For this, an organic solvent such as dimethyl sulfoxide (DMSO), acidified isopropanol, or sodium dodecyl sulfate (SDS) are required to solubilize the crystals [12–14]. Viable cells, with an active metabolism, convert MTT into a purple-colored formazan product with a maximum wavelength near 570 nm [7, 9, 15].

Tests using anionic tetrazolium salts were developed later. The *anionic salts* (Fig. 1b) are negatively charged and do not easily penetrate cell membranes. These require therefore an electron coupling reagent capable of penetrating viable cells and transferring electrons to the tetrazolium salt at the cell surface or at the plasma membrane level, converting the salt into a formazan product.

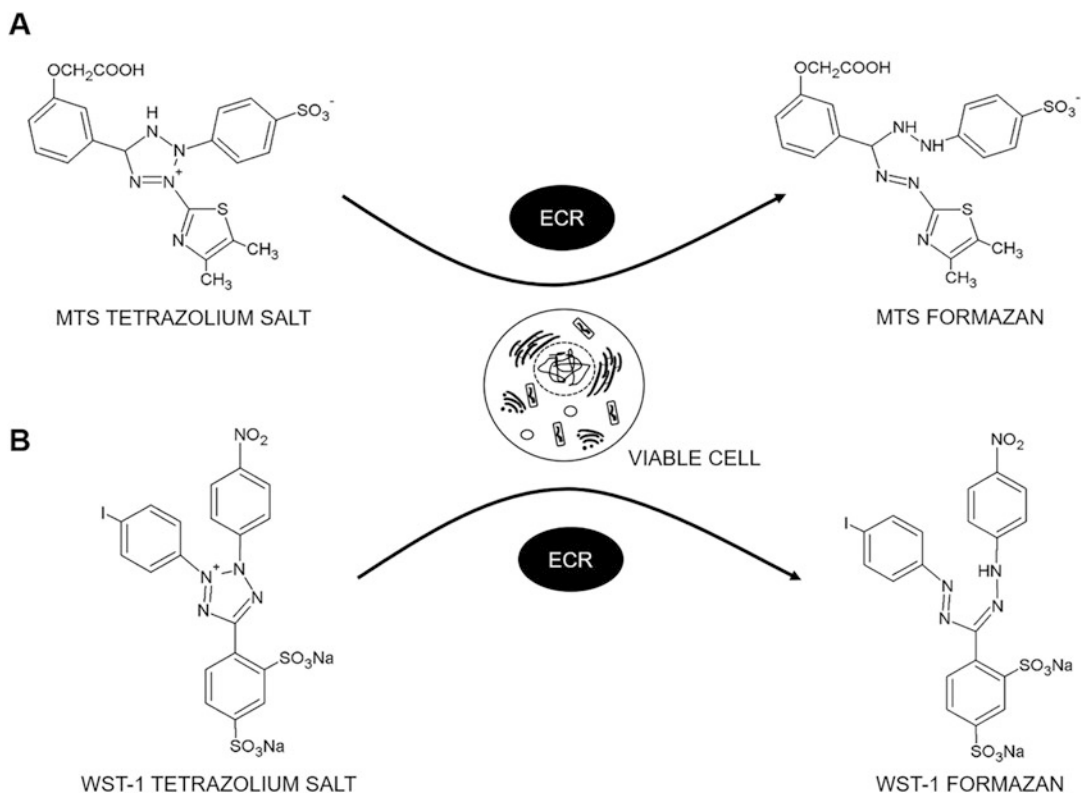


**Fig. 2** Schematic model of anionic tetrazolium salts cleavage: (a) MST and (b) WST-1—to formazan. (ECR electron coupling reagent)

Anionic salts include MTS (3-(4,5-dimethylthiazol-2-yl)-5-(3-carboxymethoxyphenyl)-2-(4-sulfohenyl)-2H-tetrazolium) (Fig. 2a), XTT (2,3-bis-(2-methoxy-4-nitro-5-sulfohenyl)-2H-tetrazolium-5-carboxanilide), and WST-1 4-[3-(4-iodophenyl)-2-(4-nitrophenyl)-2H-5-tetrazolio]-1,3-benzene disulfonate (Fig. 2b) [2, 8, 15].

MTS, XTT, or WST tetrazolium salts are widely used in cell viability and proliferation tests [2, 8, 15]. During the assays, the tetrazolium salt (MTS, XTT or WST) is reduced to a highly water-soluble formazan dye in cell culture medium through the succinate dehydrogenase system of the mitochondrial respiratory chain in metabolically active viable cells (Fig. 2) [10]. The reaction requires the presence of an electron coupling reagent, usually phenazine methosulfate (PMS) or phenazine ethyl sulfate (PES), capable of penetrating viable cells [7, 16]. The amount of water-soluble product generated from anionic salts reduction can be quantified measuring the absorbance at a wavelength of 420–570 nm using a spectrophotometer [7, 15]. The amount of formazan dye formed can be correlated with the number of viable cells after exposure to the tested substance.

In this chapter, the most common colorimetric cell viability assays with tetrazolium salts are presented. Methodologies are available to assess the cytotoxicity of food contact materials (of which potential cytotoxic components may be diffused into food) or even edible packaging.

---

## 2 Materials

### 2.1 General Equipment

- Laminar flow clean bench/cabinet
- 96-Well microtiter plate (flat-bottom)
- Water bath
- Inverse-phase contrast microscope
- 96-Well plate spectrophotometer (microplate reader) equipped with 420–650 nm filter
- Single channel pipette (10–100  $\mu\text{L}$ )
- Multi-channel pipette (20–200  $\mu\text{L}$ )
- Sterile pipette tips (10–200  $\mu\text{L}$ )
- Filters/filtration devices
- Hemocytometer or cell counter
- CO<sub>2</sub> incubator
- Vortex mixer

### 2.2 Chemicals

- Phosphate-buffered saline (PBS) without Ca<sup>2+</sup> and Mg<sup>2+</sup>
- Fetal bovine serum (FBS)
- Ham's F-10 Nutrient Mixture (HAM-F10) with l-glutamine (preferably) and without phenol red
- Hydrochloric acid (HCl)
- Sodium dodecyl sulfate (SDS)

### 2.3 Assay Kits

Commercial kits of tetrazolium salt colorimetric assays (MTT, XTT, MTS, and WST-1) are available from several companies (*see Notes 1 to 3*).

#### 2.3.1 MTT Assay

- Cell Proliferation Kit I (MTT)—Roche—Cat. No. 11 465 007 001
- MTT Assay Kit (Cell Proliferation)—AbCam—Cat. No. ab211091
- CyQUANT™ MTT Cell Viability Assay—Invitrogen—Cat. No. V13154

- 2.3.2 *XTT Assay*
- Cell Proliferation Kit II (XTT)—Roche—Cat. No. 11 465 015 001
  - XTT Assay Kit—AbCam—Cat. No. ab232856
  - CyQUANT™ XTT Cell Viability Assay—Invitrogen—Cat. No. X12223
- 2.3.3 *MTS Assay*
- MTS Assay Kit (Cell Proliferation)—AbCam—Cat. No. ab197010
  - CellTiter 96® AQueous One Solution Cell Proliferation Assay (MTS)—Promega—Cat. No. G3580
- 2.3.4 *WST-1 Assay*
- Cell Proliferation Reagent WST-1—Roche—Cat. No. 11 644 807 001
  - WST-1 Cell Proliferation Assay Kit—Abnova—Cat. No. KA1384
  - Ready-to-use Cell Proliferation Colorimetric Reagent (WST-1)—MyBioSource—Cat. No. MBS841449

---

### 3 Methods

#### 3.1 Extraction

According to the “International Standard ISO1 10993-1; 5 and 12 (2020)” [17–19], the conditions for the extraction of substances present in food packaging systems must simulate those found in clinical use, to determine the real toxicological potential of the material used. Therefore, the vehicles and extraction conditions used must be appropriate to the nature and use of the final product and the purpose of the test.

First, to ensure that the extraction containers do not adulterate the extract from the test sample, the extraction must be carried out in clean, chemically inert, closed containers using aseptic techniques. Then, the vehicle of choice should reflect the extraction purpose. The use of polar and non-polar vehicles should be considered to extract all substances present in the packaging. For assays with mammalian cells, the preferred extraction vehicle is the culture medium supplemented with 5–10% FBS due to its ability to support cell growth and extract substances of both polarities. In addition to the serum culture medium, using serum-free medium should be considered to specifically extract polar substances.

An extraction at  $37 \pm 1$  °C for  $24 \pm 2$  h in tissue culture is acceptable for the cytotoxicity test, since extraction temperatures higher than  $37 \pm 1$  °C can adversely impact the chemical characteristics and/or stability of serum and other constituents in the culture medium. Cultured primary human or rodent cell lines such as



CHO, V79, CHL/IU, and L5178Y cells or human cell lines such as TK6 can be used, according to the recommendations for in vitro toxicity tests [20]. For materials that are inherently cytotoxic, further testing using various dilutions of the tested solution may be necessary to determine the level at which cytotoxicity no longer occurs.

**3.2 Preparing the Working Solution of Commercial Kits of Tetrazolium Salt Colorimetric Assays (See Notes 4 and 5)**

- Cell Proliferation Kit I (MTT)—Roche—Cat. No. 11 465 007 001:

I. *MTT Labeling Reagent (Non-sterile, Ready-to-Use)*

- 5 × 5 mL MTT at 5 mg mL<sup>-1</sup> in PBS

II. *Solubilization Solution (1x—Ready-to-Use)*

- 3 × 90 mL 10% SDS in 0.01 M HCl

Filter the solution through a 0.20- $\mu$ m pore size membrane to sterilize the MTT solution and to remove all solid particles like nonspecifically formed formazan crystals. Store the solution in small aliquots protected from light at -20 °C.

- Cell Proliferation Kit II (XTT)—Roche—Cat. No. 11 465 015 001:

I. *XTT Labeling Reagent*

- 5 × 25 mL XTT at 1 mg mL<sup>-1</sup> in RPMI 1640 medium

II. *Electron-Coupling Reagent*

- 5 × 0.5 mL PMS (*N*-methyl dibenzopyrazine methyl sulfate)

Thaw the XTT labeling reagent and electron-coupling reagent in a water bath at 37 °C. Mix each vial thoroughly to obtain a clear solution. For one microplate (96 wells), mix 5 mL XTT labeling reagent with 0.1 mL electron coupling reagent. Store the solution in small aliquots protected from light at -20 °C.

- MTS Assay Kit (Cell Proliferation)—AbCam—Cat. No. ab197010

Thaw the solution and briefly centrifuge small vials at low speed prior to opening. All kit components are supplied as ready to be used. It is recommended to add 10  $\mu$ L/well of the MTS Assay Kit to the cells already cultured in 100  $\mu$ L/well (1:10 final dilution). Keep in ice while using. Store the solution in small aliquots protected from light at -20 °C (*see Note 5*).

- Cell Proliferation Reagent WST-1—Roche Cat. No. 11 644 807 001

Thaw the solution by heating at 37 °C for 2–10 min and vortex to dissolve the precipitates. The WST-1 reagent can be used

without any limitations after thawing. It is recommended to add 10  $\mu\text{L}$ /well of the Cell Proliferation Reagent WST-1 to the cells already cultured in 100  $\mu\text{L}$ /well (1:10 final dilution). Store at 2–8 °C, protected from light, for up to 4 weeks, or in aliquots at –20 °C for longer periods.

### 3.3 Cytotoxicity Assay

1. Seed cells at a density of  $1 \times 10^4$  cells/well in a 96-well flat-bottom microtiter plate and allow cells to adhere for 24 h at 37 °C in a CO<sub>2</sub> incubator (*see Note 6*).
2. The culture medium must be replaced with fresh medium after 24 h of incubation.
3. Add the food packaging extract to the cells and incubate for a desired period (24, 48, or 96 h) at 37 °C in a CO<sub>2</sub> incubator. The suggested total volume is 100  $\mu\text{L}$  for a 96-well plate (*see Note 7*).
4. Include, in each plate, (i) negative control wells (3–6 wells that contain the same number of cells as the experimental wells and that are not exposed to the tested substance), (ii) blank control wells (3–6 wells are needed to measure the blanks, which only contain the culture medium), and (iii) positive control wells (3–6 wells that contain the same number of cells as the experimental wells and that are exposed to known cytotoxic substances).
5. After the treatment period, discard the culture medium and wash cells with PBS, add 100  $\mu\text{L}$  of HAM-F10 culture medium (*see Note 8*).
6. Cell cytotoxicity measurements using the different test:
  - A. Using the *Cell Proliferation Kit I (MTT)—Roche—Cat. No. 11 465 007 001*:
    - 7A. Subsequently, add 10  $\mu\text{L}$  of the *MTT Labeling Reagent* (0.5 mg mL<sup>-1</sup>) per well and incubate for 4 h at 37 °C in a CO<sub>2</sub> incubator (*see Note 9*).
    - 8A. Following, add 100  $\mu\text{L}$  of the *solubilization solution* into each well. Allow the plate to stand overnight at 37 °C in a CO<sub>2</sub> incubator.
    - 9A. Check for complete solubilization of the purple formazan crystals (*see Note 10*).
    - 10A. Measure the spectrophotometric absorbance of the samples using a microplate reader. The wavelength to measure the absorbance of the formazan product is between 550 and 570 nm according to the filters available for the microplate reader used. The reference wavelength should be higher than 650 nm (*see Note 11*).

- B. Using the *Cell Proliferation Kit II (XTT)*—Roche—Cat. No. 11 465 015 001:
- 7B. Subsequently, add 50  $\mu\text{L}$  of the *XTT Labeling Mixture* ( $0.3 \text{ mg mL}^{-1}$ ) per well and incubate for 4–17 h at 37 °C in a  $\text{CO}_2$  incubator (*see Note 9*).
- 8B. Measure the spectrophotometric absorbance of the samples using a microplate () reader. The wavelength to measure the absorbance of the formazan product is between 450 and 500 nm according to the filters available for the microplate reader used. The reference wavelength should be higher than 650 nm (*see Notes 10 and 11*).
- C. Using the *MTS Assay Kit (Cell Proliferation)*—AbCam—Cat. No. ab197010:
- 7C. Subsequently, add 10  $\mu\text{L}$  of the *MTS Labeling Reagent* per well and incubate for 0.5–4 h at 37 °C in a  $\text{CO}_2$  incubator (*see Note 9*).
- 8C. Shake the plate briefly on a shaker.
- 9C. Measure the spectrophotometric absorbance of the samples using a microplate reader. The wavelength to measure the absorbance of the formazan product is between 490 and 500 nm according to the filters available for the microplate reader used (*see Note 10*).
- D. Using the *Cell Proliferation Reagent WST-1*—Roche Cat. No. 11 644 807 001:
- 7D. Subsequently, add 10  $\mu\text{L}$  of the *Cell Proliferation Reagent WST-1* per well and incubate for 4 h at 37 °C in a  $\text{CO}_2$  incubator (*see Note 11*).
- 8D. Shake thoroughly for 1 min on a shaker.
- 9D. Measure the spectrophotometric absorbance of the samples using a microplate reader. The wavelength to measure the absorbance of the formazan product is between 420 and 480 nm according to the filters available for the microplate reader. The reference wavelength should be higher than 600 nm (*see Notes 10 and 11*).

### 3.4 Cell Viability Calculation

- A. Subtract the culture medium background (blank group—*See Note 12*) from all samples reading, as described in the formula:

$$\text{Real Absorbance (R.Abs)} = \text{Absorbance Sample} - \text{Absorbance Blank Group}$$

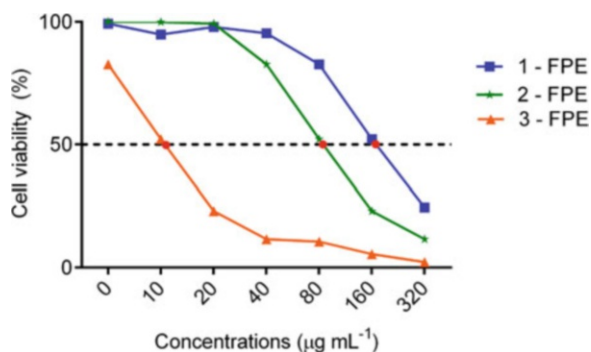


**Fig. 3** The fictitious graph represents the cell viability profile of X-cells treated with different concentrations of different food packaging extracts (FPE) (10–320 µg mL<sup>-1</sup>) in 24 h of incubation

B. The cell viability percentage is calculated using the following equation (*See Note 13*):

$$\text{Cell viability (\%)} = \left( \frac{\text{R.Abs Sample}}{\text{R.Abs Negative Control}} \right) \times 100$$

C. Plot the cell viability percentages against the tested food packaging extract (FPE) concentration. The 50% inhibiting concentration (IC<sub>50</sub>) can be determined graphically, as in the example below (Fig. 3):

## 4 Notes

1. All available tetrazolium salt kits are only for research; not for human or veterinary diagnostic or therapeutic use.
2. The reagents have good stability when stored at  $-15$  to  $-25$  °C, protected from light, until the expiration date printed on the label.
3. Before use, it is necessary to review the complete Safety Data Sheet, which is available directly on the website of the manufacturer or upon request.
4. To obtain reliable results, thaw the working solutions immediately before use.
5. The kits described in this topic were used to exemplify the procedures to be performed, however, without the intention of recommending.

6. Optimal sensitivity of a colorimetric assay is obtained with near-confluent cells at the time of the assay. In general, cells seeded at densities between  $5 \times 10^3$  and  $1 \times 10^4$  cells per well should reach optimal population densities. However, since there are cell types that have low metabolic activity, it is recommended to increase the concentration of cells to obtain formazan color development within the time suggested by the employed kit.
7. Colored compounds can have their own optical density (OD) that can influence the measurement when diluted. Thus, it is recommended to wash the cells with PBS before adding the tetrazolium salts to remove any trace of the tested substance that could give inaccurate results.
8. The culture conditions used to grow the cells can affect the results and must be taken into consideration when analyzing the data. The presence of serum or phenol red in the culture medium can generate background and seriously affect the sample absorption reading. It is recommended, if possible, to culture cells in phenol red or serum-free medium during the incubation period with the tetrazolium salt.
9. Incubation time with the tetrazolium salt varies according to the type and concentration of the cells. Incubation time can be optimized by an initial test reading the absorbance at various times (i.e., 4, 6, 8, and 12 h) after the addition of the tetrazolium detection solution, using the same plate.
10. The plate should be gently shaken (Shake mode: Slow/ Shake time: 2 s) to evenly distribute the dye in the wells prior to reading the absorbance with a spectrophotometer.
11. The tetrazolium-specific absorbance can be measured between 420 and 570 nm, depending on which kit is used. The reference wavelength absorbance reading is used to eliminate the background signal resulting from cell debris or other non-specific absorbance.
12. The use of the blank control (only the culture medium without cells and without treatment) is necessary to exclude the influence of color of the culture medium in the experiment, subtracting the blank readings from the sample readings.
13. Absorbance values that are lower than the control cells indicate a cell viability reduction. Conversely, a higher absorbance rate indicates a cell viability/proliferation increase, as in the example in Fig. 4.

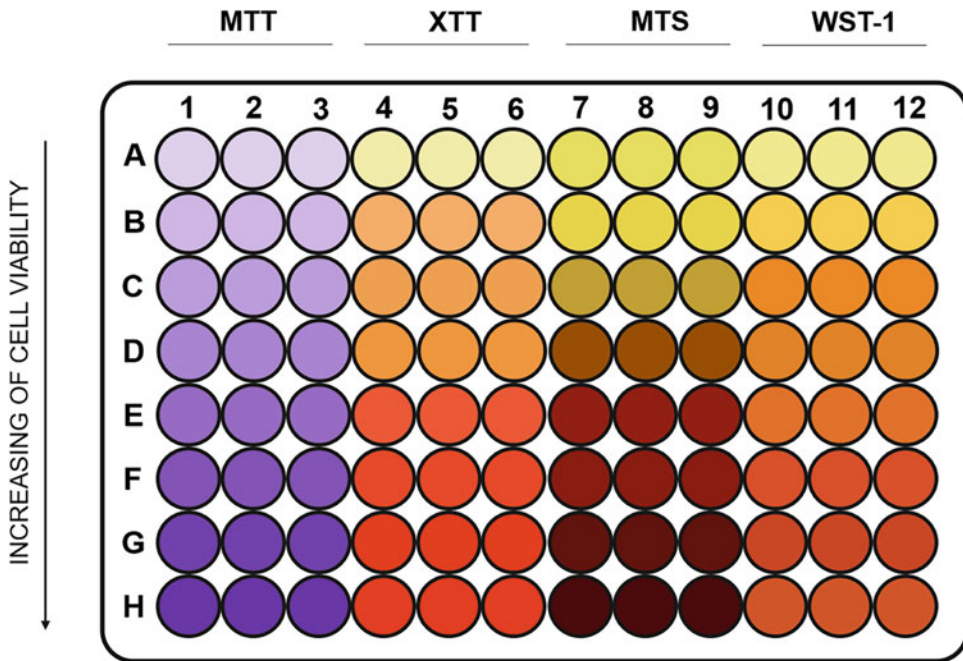


**Fig. 4** Schematic model of the 96-well plate representing the cell viability profile of X cells exposed to different tetrazolium salts

## Acknowledgments

A.B. Ribeiro was the recipient of a M.Sc. fellowship from the São Paulo Research Foundation (FAPESP, Brazil; grant # 2018/25770-7). D.C. Tavares is grateful to the National Council for Scientific and Technological Development (CNPq, Brazil) for the fellowship granted. H.S. Barud thanks CNPq (grant # 407822/2018-6; INCT-INFO), FAPESP (grants # 2018/25512-8 and 2013/07793-6), and TA Instruments Brazil.

## References

- Groh KJ, Muncke J (2017) In vitro toxicity testing of food contact materials: state-of-the-art and future challenges. *Compr Rev Food Sci F* 16:1123–1150. <https://doi.org/10.1111/1541-4337.12280>
- Stockert JC, Horobin RW, Colombo LL, Blázquez-Castro A (2018) Tetrazolium salts and formazan products in cell biology: viability assessment, fluorescence imaging, and labeling perspectives. *Acta Histochem* 120:159–167. <https://doi.org/10.1016/j.acthis.2018.02.005>
- Adan A, Kiraz Y, Baran Y (2016) Cell proliferation and cytotoxicity assays. *Curr Pharm Biotechnol* 17:1213–1221. <https://doi.org/10.2174/1389201017666160808160513>
- Shokrzadeh M, Modanloo M (2017) An overview of the most common methods for assessing cell viability. *J Res Med Dent Sci* 5:33–41. <https://doi.org/10.5455/jrmds.2017526>
- Liu X, Rodeheaver DP, White JC et al (2018) A comparison of in vitro cytotoxicity assays in medical device regulatory studies. *Regul Toxicol Pharmacol* 97:24–32. <https://doi.org/10.1016/j.yrtph.2018.06.003>
- Menyhárt O, Harami-Papp H, Sukumar S et al (2016) Guidelines for the selection of functional assays to evaluate the hallmarks of cancer.

- Biochim Biophys Acta 1866:300–319. <https://doi.org/10.1016/j.bbcan.2016.10.002>
7. Präbst K, Engelhardt H, Ringgeler S, Hübner H (2017) Basic colorimetric proliferation assays: MTT, WST, and Resazurin. *Methods Mol Biol* 1601:1–17. [https://doi.org/10.1007/978-1-4939-6960-9\\_1](https://doi.org/10.1007/978-1-4939-6960-9_1)
  8. Riss TL, Moravec RA, Niles AL et al (2016) Cell viability assays. In: Assay guidance manual [Internet]. Eli Lilly & Company and the National Center for Advancing Translational Sciences
  9. van Meerloo J, Kaspers GJ, Cloos J (2011) Cell sensitivity assays: the MTT assay. *Methods Mol Biol* 731:237–245. [https://doi.org/10.1007/978-1-61779-080-5\\_20](https://doi.org/10.1007/978-1-61779-080-5_20)
  10. Berridge MV, Herst PM, Tan AS (2005) Tetrazolium dyes as tools in cell biology: new insights into their cellular reduction. *Biotechnol Annu Rev* 11:127–152. [https://doi.org/10.1016/s1387-2656\(05\)11004-7](https://doi.org/10.1016/s1387-2656(05)11004-7)
  11. Lü L, Zhang L, Wai MS et al (2012) Exocytosis of MTT formazan could exacerbate cell injury. *Toxicol In Vitro* 26:636–644. <https://doi.org/10.1016/j.tiv.2012.02.006>
  12. Abbott A (2003) Biology's new dimension. *Nature* 424:870–872. <https://doi.org/10.1038/424870a>
  13. Hall MD, Martin C, Ferguson DJ et al (2004) Comparative efficacy of novel platinum (IV) compounds with established chemotherapeutic drugs in solid tumour models. *Biochem Pharmacol* 67:17–30. <https://doi.org/10.1016/j.bcp.2003.07.016>
  14. Wilson WR, Hay MP (2011) Targeting hypoxia in cancer therapy. *Nat Rev Cancer* 11:393–410. <https://doi.org/10.1038/nrc3064>
  15. Kamiloglu S, Sari G, Ozdal T, Capanoglu E (2020) Guidelines for cell viability assays. *Food Front* 1:332–349. <https://doi.org/10.1002/fft2.44>
  16. Dong G, Pan W, Zheng T et al (2006) Colorimetric assay to determine in vitro antibacterial activity against clinical isolates: enhanced activity in damaged Chinese masson pine needles. *J Integr Plant Biol* 48:1034–1046. <https://doi.org/10.1111/j.1744-7909.2006.00310.x>
  17. ISO 10993-1:2020 (2020) Part 1: evaluation and testing within a risk management process. In: Biological evaluation of medical devices. International Organization for Standardization ISO, Geneva
  18. ISO 10993-5:2020 (2020) Part 5: tests for in vitro cytotoxicity. In: Biological evaluation of medical devices. International Organization for Standardization ISO, Geneva
  19. ISO 10993-12:2020 (2020) Part 12: sample preparation and reference materials. In: Biological evaluation of medical devices. International Organization for Standardization ISO, Geneva
  20. OECD (2016) Test No. 487: in vitro mammalian cell micronucleus test, OECD guidelines for the testing of chemicals, section 4. OECD Publishing, Paris. <https://doi.org/10.1787/9789264264861-en>



## In Vitro Genotoxicity/Mutagenicity Testing of Food Packaging

Flávia A. Resende, Juliana G. F. Silva, Arthur B. Ribeiro,  
Lucas N. F. Trevizan, Hernane S. Barud, and Denise C. Tavares

### Abstract

To ensure the safe use of packaging materials and food contact materials, genotoxicity assessment is one of the requirements of regulatory agencies around the globe. Thus, it is essential to carry out preliminary tests to clarify this possible mechanism. The *Salmonella*/mammalian-microsome mutagenicity test, widely known as the Ames test, is a rapid, relatively simple procedure for testing chemicals for mutagenicity as well as for offering provision for the metabolism of otherwise nonmutagenic chemicals to their potentially DNA-reactive forms. However, a single test is not sufficient to detect all relevant genotoxic mechanisms in tumorigenesis. Thus, in order to complement the results in the Ames test and to contribute to the elucidation of the effects, ensuring their use or not, mutagenicity at the chromosomal level must also be evaluated. In the micronucleus (MN) assay, chromosomal damages induced by chemical products are evaluated. The MN is expressed in dividing cultured cells because fragments from damaged chromosomes or whole chromosomes that lag during anaphase become enveloped by nuclear membrane, independently from the main nucleus during telophase, prior to cell division. Together, these tests detect the most relevant events for the multistep process of malignancy, that is, gene mutations, clastogenicity, and aneugenicity. Detailed descriptions of the protocols used for detection of point mutations and chromosomal damage induced by food packaging in vitro are given in this chapter.

**Key words** Micronucleus test, Ames test, *Salmonella*/microsome assay, Genetic toxicology

---

## 1 Introduction

The genotoxic/mutagenic potential tests reveal, at the first level of evidence, the genotoxicological effect of edible and/or food contact packaging materials, having their safe use in mind. So, these tests are always required irrespective of the extent of migration (*see* Chapter 4 on IAS and NIAS, Chapter 5 on PFAS, and Chapter 6 on migration) and the resulting human exposure to these materials [1], because even though human exposure levels may be quantitatively low, these substances are considered to be of high toxicological concern if they act as DNA reactive mutagens [2].



Commonly, the toxicological tests of food contact materials are focused on single substances and their genotoxicity. However, most of the time, the material is not available as a pure chemical and the chemical identity is not known, causing people to be exposed to mixtures of chemicals [3], that can or cannot interact with genetic material. This interaction may result, under certain circumstances, not only in cancer, but also in degenerative conditions such as accelerated aging, immune dysfunction, cardiovascular and neurodegenerative diseases (in case of accumulation of DNA damage in somatic cells) and in spontaneous abortions, infertility, or heritable damage in the offspring and/or subsequent generations resulting in genetic diseases (in case of DNA damage in germ cells) [4]. Thus, sample preparation procedures need to be optimized and standardized and approaches on the concept of safe level of food packaging materials should be discussed. Regulatory agencies around the globe have conducted research and developed both guidance and regulations for safety assessments of materials intended to contact food. Although the food packaging safety assessment structures developed by these agencies have similar principles, they differ in the application of these principles [5], which is necessary for new approaches to meet this legal obligation for authorization applications of packaging materials.

DNA damage is a complex biological process involving several modes of actions, determining the cellular fate and the severity of the hazard. Currently, a wide variety of bioassays are available to assess the genotoxic potential of chemicals and materials. These assays have been evaluated for their ability to correctly predict the adverse effects of matter and are often used as screening tools [6].

The *Salmonella*/*Escherichia coli* microsome assay (Ames test) is required by regulatory authorities worldwide in order to identify substances that can produce genetic damage that leads to gene mutations (base substitution type mutations—*S. Typhimurium* strains TA1535, TA100, TA102, and TA104, and *E. coli* strains WP2 uvrA or WP2 uvrA (pKM101), frameshift mutations—*S. Typhimurium* strains TA1537, TA1538, TA97a, and TA98) [7]. The bacterial strains and mutagenicity test procedure, developed by Bruce Ames and published in 1973 [8, 9], still retain a primary role in the testing of chemicals and materials for commercial use [7].

The Ames test uses amino acid-dependent strains of *S. Typhimurium* and *E. coli*, each carrying different mutations in various genes of either histidine operon, in *S. Typhimurium* bacteria, or tryptophan operon in *E. coli* making them auxotrophic for the corresponding amino acids. These mutations act as hot spots for mutagens that cause DNA damage by different mechanisms. In addition, some strains may have (i) *rfa* mutations, which cause changes in the lipopolysaccharide barrier of the bacterial cell wall, thus facilitating the entry of large molecules (all *Salmonella* strains);

(ii) deficiency of the nucleotide excision repair system, preventing the bacterium from repairing the damage that has been done to its genetic material (uvrB detection in *Salmonella* strains, except TA102, or uvrA mutation in *E. coli* strains); and (iii) the plasmid R factor (plasmid pKM101) that confers resistance to ampicillin and induces an error-prone DNA repair pathway (strains TA97, TA97a, TA98, TA100, TA102, and WP2 uvrA (pKM 101)). Together, these mutations give the strains greater sensitivity in detecting several mutagens [10, 11].

Due to the inability to synthesize histidine, these strains cannot grow and form colonies in the absence of this essential amino acid [12]. However, when they are exposed to agents that induce new mutations in the gene, this function is restored and the auxotrophic character is reversed, allowing bacteria to grow and form colonies [11]. Thus, the assay detects the mutational reversion of his-dependent bacteria to his-independent colonies (*Salmonella*) or trp-dependent bacteria to trp-independent colonies (*E. coli*). The mutagenic potential of a compound can then be calculated from the number of colonies that are formed on the plate by the concentration of the compound used [12].

Another consideration about the test is the addition of the so-called S9 fraction, obtained from rat liver, which contains xenobiotic metabolizing enzymes for the identification of mutagenic agents of indirect action, which must be metabolized in order to become active [13]. Therefore, in the absence (–S9) or presence (+S9) of metabolic activation, the monitoring of the direct and indirect actions of a compound, respectively, is possible, guaranteeing the faithful identification of agents that cause gene mutations.

For the detection of chromosomal damage, the micronucleus (MN) test is a widely used method that detects chromosomal loss and breakage, being used as biomarker for the identification of clastogenic and aneugenic agents [14]. The chromosomal changes identified in the MN test are verified by counting circular structures surrounded by nuclear membrane, called MN, which are formed by chromosomal fragments or whole chromosomes that were delayed during anaphase and were not incorporated into the nuclei of daughter cells [15].

This test can be performed in vitro, using cultured primary human or other mammalian peripheral blood lymphocytes and several rodent cell lines such as CHO (Chinese hamster ovary cells), V79 (Chinese hamster lung fibroblasts, male), CHL/IU (*Cricetulus griseus*, Chinese hamster lung fibroblasts, female), and L5178Y (mouse lymphoma) cells, or human cells, such as TK6 (human spleen lymphoblasts). Other cell lines such as HT29 (human colorectal adenocarcinoma), Caco-2 (Caucasian colon adenocarcinoma), HepaRG (hepatic stem cell line), HepG2 cells (liver hepatocellular carcinoma), A549 (adenocarcinomic human alveolar basal epithelial cells), and primary Syrian Hamster Embryo cells

have been used for MN testing, but have not been extensively validated to date. Therefore, the choice of these cells should be justified [16]. The MN test can still be performed *in vivo* using hematopoietic rodent cells [17].

The OECD 487 Test Guideline [16] allows the use of protocols with and without cytochalasin B (cytoB). CytoB inhibits actin polymerization and blocks cytokinesis, and cells that have completed one cell cycle after treatment can be distinguished from undivided cells by their binucleate appearance. The advantage of using cytoB is that it allows the clear identification that treated and control cells have divided *in vitro*, and also provides a simple assessment of cell proliferation, allowing for the identification and analysis of MN only in cells that have completed one mitosis. The use of protocols without cytokinesis block can be accomplished, provided there is evidence that the cell population analyzed has undergone mitosis.

Thus, the bacterial reverse gene mutation test and the *in vitro* MN assay detect two main genetic endpoints, that is, gene and chromosome mutations, respectively. Therefore, these tests are currently considered equally appropriate in a standard genetic toxicology battery for predicting potential human risks [18].

---

## 2 Materials

1. General laboratory glassware (flasks, bottles, graduated cylinders, etc.).
2. Petri dishes (100 × 15 mm<sup>2</sup>).
3. Sterile glass tubes (50 × 16 mm<sup>2</sup>) with caps.
4. Test tube racks.
5. Pipets (1, 2, 5, and 10 mL).
6. Pipettors (adjustable volumes).
7. Sterile pipette tips.
8. Cryogenic tubes for freezing down permanent and working cultures.
9. Colony counter (manual or electronic).
10. 6-Well Microtiter Plate (flat-bottom).
11. Conical tubes (15 mL).
12. Microscope slides.
13. Cell culture flasks.

### General Apparatuses

1. Autoclave.
2. Shaking incubator set at 120 rpm and 37 °C.

3. Incubator for the GM agar plates.
4. Oven, heating, or water bath set at 43–48 °C to maintain temperature of top agar.
5. Boiling water bath or microwave oven for melting top agar.
6. Magnetic stirrers.
7. Analytical balances (up to 0.001 g).
8. Water purification system to generate distilled water.
9. Ultrafreezer or liquid nitrogen tank.
10. Refrigerator/freezer.
11. Biological safety cabinet.
12. Inverted light microscope.
13. Incubator with humidified atmosphere of 5% carbon dioxide (CO<sub>2</sub>) and temperature of 37 °C for cell growth.
14. Cytocentrifuge.
15. Microscope with excellent optics for bright-field and fluorescence examination of stained slides at ×1000 magnification.

### Chemicals

#### **2.1 Salmonella/ Microsome assay (Salmonella Test; Ames Test)**

1. Agar.
2. Glucose.
3. D-biotin.
4. L-Histidine·HCl.
5. Sodium chloride.
6. Oxoid nutrient broth No. 2.
7. Monobasic sodium phosphate.
8. Dibasic sodium phosphate.
9. Magnesium chloride.
10. Potassium chloride.
11. D-glucose-6-phosphate disodium.
12. Nicotinamide adenine dinucleotide phosphate sodium salt.
13. Mammalian tissue homogenate (S9 fraction).
14. Dimethyl sulfoxide (DMSO) or other solvents that maximize extraction of the substances present in the food packaging materials.
15. Glycerol.
16. Positive control chemicals (*see* **Note 1**).

## 2.2 *Micronucleus Test*

1. Cell growth media: Eagle's Minimal Essential Medium (EMEM), Dulbecco's Modified Eagle's medium (DMEM), RPMI, Ham's F10, Ham's F12 (check the most suitable one for each test cell).
2. Phosphate-buffered saline (PBS) without  $\text{Ca}^{2+}$  and  $\text{Mg}^{2+}$ .
3. Fetal bovine serum (FBS).
4. Cytochalasin B.
5. Dyes: Giemsa, acridine orange or panoptic (check the most suitable one for each test cell).
6. DMSO or other solvents that maximize extraction of the substances present in the food packaging materials.
7. Positive control chemicals (*see Note 1*).

---

## 3 Methods

### Extraction

Water and culture medium are the most commonly used solvents. In case of water, it is advised not to exceed a maximum concentration of 10 vol% because of molarity changes on the medium and dilution of nutrients.

If other than well-established solvents/vehicles are used, their inclusion should be supported by data indicating their compatibility with the test system and their ability to maximize extraction of the substances present in the food packaging materials. They must not interfere with cell proliferation, metabolic activation, and must not induce DNA changes.

The International Standard ISO 10993-12 [19] suggests that the extraction of substances from films (thickness <0.5 mm) should be carried out at  $37 \pm 1$  °C for  $72 \pm 2$  h. Other conditions for extraction also are described, but care should be taken that this does not alter the chemical characteristics of food packaging. The surface area of the films must be of 6 cm<sup>2</sup> to the volume of 1 mL of extraction vehicle. When surface area cannot be determined, a mass/volume of extracting fluid shall be used [19].

Fresh preparations should be employed unless stability data demonstrate the acceptability of storage.

Food packaging extract is added directly to the test systems and/or diluted prior to treatment if it interferes with bacterial or cellular growth and survival.

### 3.1 *Salmonella/Microsome Assay (Salmonella Test; Ames Test)*

According to the OECD Guidelines [20], at least five strains of bacteria should be used. The recommended combination of strains is TA1535; TA1537, TA97a or TA97; TA98; TA100; and TA102 of *S. Typhimurium*, *E. coli* WP2 uvrA, or *E. coli* WP2 uvrA (pKM101).

### Preparation of Permanent Cultures

Receive strains on a small sterile filter disk embedded in nutrient agar; first wipe the disk across the surface of a nutrient agar plate, and then transfer the disk to 5 mL of nutrient broth. For lyophilized culture, aseptically add 1 mL of nutrient broth to rehydrate the culture (a process which should take up to 2 min), then transfer the rehydrated culture to 4 mL of nutrient broth. Then, transfer a drop of the culture to a nutrient agar plate and streak the inoculum for individual colonies across the surface of the plate [11].

If single colonies are observed after overnight incubation at 37 °C, pick one healthy looking colony and restreak it for individual colonies on minimal agar medium (GM agar) plate supplemented with biotin and histidine for *S. Typhimurium* strains, and tryptophan for *E. coli* strains for purification and verification of genotypic characteristics [11, 20].

Other genotypic characteristics that should be similarly checked: ampicillin resistance in strains TA98, TA100 and TA97a or TA97, and WP2 *uvrA* (pKM101); ampicillin + tetracycline resistance in strain TA102 to assess the presence or absence of R-factor plasmids; *rfa* mutation in *S. Typhimurium* through sensitivity to crystal violet, and *uvrA* mutation in *E. coli* or *uvrB* mutation in *S. Typhimurium*, through sensitivity to ultraviolet light [20]. The strains should also yield spontaneous revertant colony plate counts within the frequency ranges expected from the laboratory's historical control data and preferably within the range reported in the literature [11, 13].

The strains grown in nutrient broth at a density of 1 to  $2 \times 10^9$  colony-forming unit (CFU)  $\text{mL}^{-1}$  (Optical Density<sub>540 nm</sub> between 0.1 and 0.2) are frozen with 0.5 mL of a sterile cryopreserver, such as glycerol or DMSO for the culture (final concentration, 10 vol%); mix well and dispense 1-mL aliquots in pre-marked sterile cryogenic tubes.

The tester strains should be kept frozen in ultrafreezer (−80 °C) or liquid nitrogen.

### Preparation of Solutions and Plates

1. *Minimal agar medium (GM agar) plates*: Add 15 g of agar to 900 mL distilled water. Autoclave it for 15 min at 121 °C (1.5 atm; relative pressure). Add 20 mL of sterile Vogel-Bonner E medium (VB salts), and mix thoroughly, then add 50 mL of a sterile glucose (40 or 8 vol%) solution; again, swirl thoroughly. Dispense the agar medium in  $100 \times 15 \text{ mm}^2$  Petri dishes (approximately 25 mL per plate). After the solidification, the plates must be stored in an oven at 37 °C for 48 h (*see Note 2*).
2. *Histidine/biotin solution (0.5 mM)*: Add 124 mg of D-biotin and 96 mg of L-Histidine·HCl to 1000 mL distilled water. Autoclave it for 30 min at 121 °C (1.5 atm; relative pressure).

3. *Top agar supplemented with histidine/biotin*: Add 6 g of agar and 6 g of sodium chloride to 900 mL of distilled water. Autoclave it for 30 min at 121 °C (1.5 atm; relative pressure). For the test, melt the top agar in a microwave oven or in boiling water, and then add 100 mL of limited histidine and biotin solution (0.5 mM). The top agar is used to deliver the bacteria, chemical, and buffer or S9 mix to the bottom agar and it is one of the most critical medium components in the Ames test because it contains the trace amount of histidine (0.05 mM) for limited growth and biotin at a concentration of 0.05 mM, which is in excess of what is needed for the growth of the *Salmonella* strains.
4. *Nutrient broth*: Add 0.75 g of nutrient broth (Oxoid nutrient broth No. 2) to 30 mL water. Autoclave it for 15 min at 121 °C (1.5 atm; relative pressure).
5. *Sodium phosphate buffer, 0.1 mM, pH 7.4*: After mixing 120 mL monobasic sodium phosphate (0.1 M) and 880 mL of dibasic sodium phosphate (0.1 M), adjust pH to 7.4 using 0.1 M dibasic sodium phosphate solution. Autoclave it for 30 min at 121 °C (1.5 atm; relative pressure). The buffer is used for testing chemicals in the absence of metabolic activation (*see Note 3*).
6. *Co-factors for S9 mix*: A number of commercial vendors provide S9 preparations, as Molecular Toxicology, in the United States. Once the S9 mix is prepared, it should be kept on ice for the duration of the experiment. The metabolic activation system consisted of 4% S9 fraction, 1% of magnesium chloride at 0.4 mol L<sup>-1</sup>, 1% of potassium chloride at 1.65 mol L<sup>-1</sup>, 0.5% of D-glucose-6-phosphate disodium at 1 mol L<sup>-1</sup>, 4% of nicotinamide adenine dinucleotide phosphate sodium salt (NADP) at 0.1 mol L<sup>-1</sup> in 50% of phosphate buffer at 0.2 mol L<sup>-1</sup>, and 39.5% of sterile distilled water.

### **Inoculum**

For each experiment, individual culture flasks are inoculated with each strain. Inoculate 0.1 mL of the tester strain cultures in 30 mL of Oxoid nutrient broth No. 2 and place on a shaker in the dark and gently shake (100 rpm) for 11–14 h (overnight) at 37 °C. On the next morning, remove the cultures from the incubator and keep at room temperature away from direct fluorescent light. It is essential that the cultures used in the experiment contain a high titer of viable bacteria. The titer may be demonstrated either from historical control data on growth curves, or in each assay through the determination of viable cell numbers by a plating experiment.

### Experimental Procedure

The procedure described here pertains to the preincubation method.

1. To the sterile glass tubes maintained at room temperature, add the following components in this order, with mild mixing after each addition:
  - 0.5 mL of metabolic activation (S9) mix or sodium phosphate buffer.
  - Different volumes of the food packaging extract. Include untreated, solvent/vehicle and strain-specific positive controls, both with and without metabolic activation, in each assay (*see* **Notes 1** and **4**).
  - 0.1 mL overnight culture of the bacterial strain.
2. Incubate the mixture at 37 °C for 20 min.
3. To each tube, add 2 mL of molten top agar supplemented with histidine/biotin maintained at 43–48 °C. The content of the test tubes is then mixed and poured onto the surface of GM agar plates (*see* **Note 5**).
4. When the top agar has solidified (2–3 min), the plates are inverted and incubated at 37 °C for 48 h.
5. The colonies are then counted, and the results are expressed as the number of revertant colonies per plate. If colonies cannot be counted immediately after the 48 h incubation, the plates can be stored in a refrigerator for up to 2 days. All plates must be removed from the incubator and counted at the same time (**Fig. 1**).

Preliminary experiments are useful to determine toxicity and insolubility of the food packaging samples. Cytotoxicity may be detected in the final population on the GM agar plate after the 48-h incubation by a thinning of the background lawn, which may be accompanied by a decrease in the number of revertant colonies,

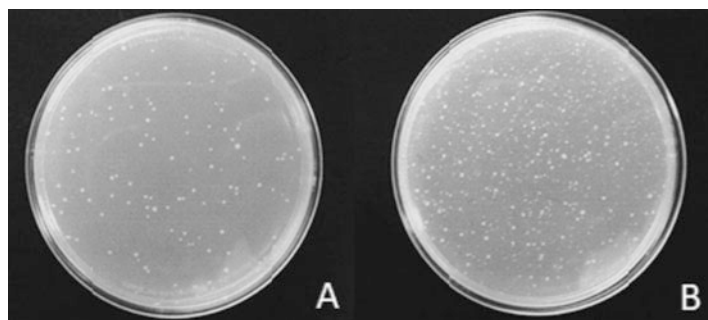


**Fig. 1** Petri dishes with revertant colonies of *Salmonella* Typhimurium (TA102 strain). (a) Untreated control; (b) Positive control (Mitomycin C)



absence of background lawn (i.e., complete absence of growth), or by presence of pinpoint non-revertant colonies (generally in conjunction with an absence of background lawn).

### Analysis of the Results

After the plates are removed from the incubator, the colonies are counted, and the results are expressed as mean revertant colonies per plate  $\pm$  standard deviation for each dose of the test sample and the controls. A sample is considered a mutagen (it induces point mutations by base substitutions or frameshifts in the genome of either *S. Typhimurium* and/or *E. coli*) if it produces a concentration-related increase over the range tested and/or a reproducible increase at one or more concentrations in the number of revertant colonies per plate in at least one strain with or without metabolic activation system. The determination of a positive vs. a negative result is made through evaluation procedures for comparing dosed plates with the concurrent solvent/vehicle control plates, including a requirement for a specific fold increase (2- or 3-fold, specific to the bacterial strain).

### 3.2 Micronucleus Test

#### Experimental Procedure

1. In 6-well plates, seed 100,000 cell per well in 2 mL of cell growth media (*see Note 6*) with 10% of fetal bovine serum (complete culture medium). Prepare an appropriate number of wells for the experiment from a single pool of cells. These cells should be in exponential growth phase at the time of treatment.
2. Incubate the plates at 37 °C in a 5% CO<sub>2</sub> atmosphere for 24 h. This time is necessary for the adhesion of cells to the plate, for the formation of a semiconfluent cell monolayer, and for the progression of cells to the exponential growth phase.
3. After incubation, the solutions for the treatment groups must first be prepared in a culture medium in an amount sufficient for the treatment of the test. For treatment, it is optional to change the culture medium or not.
4. Three non-cytotoxic concentrations of the food packaging extract should be evaluated. Include untreated, solvent/vehicle, and positive controls in each treatment series (*see Notes 1 and 7*). Prepare duplicate cultures/wells at each experimental test point.
5. Smoothly homogenize the cultures with cross movements, avoiding bubble formation.
6. For the treatment, cells should be exposed to the food packaging extract without metabolic activation for 3–6 h, and sampled at a time equivalent to about 1.5–2.0 normal cell cycle lengths after the beginning of treatment. To conclude a negative

outcome, cells should be continuously exposed without metabolic activation until sampling at a time equivalent to about 1.5–2.0 normal cell cycle lengths [19]. After treatment, all plates are placed in a CO<sub>2</sub> incubator at 37 °C and 5% CO<sub>2</sub>.

7. After the end of the exposure time, analyze the appearance of the cultures under an inverted microscope, mainly regarding the presence of precipitation, morphology, and cell death.
8. After the incubation period, remove the culture medium containing the test sample and wash the wells twice with 2 mL of PBS suitable for cell cultures.
9. Add fresh medium (2 mL per well).
10. Then add 20 µL per well of the 3 µg mL<sup>-1</sup> pre-prepared cytochalasin B solution.
11. The plates must be placed in the CO<sub>2</sub> incubator for 1.5–2 normal cell cycle lengths.

### Harvest

It is important to cast a water film on the slides, so that they can be ready and cold (2–8 °C) for use. To do this, wash the slides with neutral detergent, rinse them under running water, and then in distilled water. Then, the slides should be immersed, one by one, in distilled water and raised to check if a water film has formed on them. If the film does not form, wash again. The vial containing the slides must be kept and refrigerated until the moment of use. There is also another possibility of cleaning the slides, this being cleaning them in 70% ethanol and distilled water.

12. Collect the medium from each well into appropriately labelled 15-mL centrifuge tubes to avoid loss of detached mitotic cells.
13. The cells must be washed twice with PBS (2 mL), the first washing being reserved in the centrifuge tube and the second washing must be discarded. Remove excess PBS from each well with a pipette.
14. Add 0.3 mL of 0.1% trypsin to each well to bring cell monolayers into suspension. Time lapse (approximately 5 min) and temperature of incubation (37 °C) are indicative and should be standardized in each laboratory based on visual observations of cell detachment, as trypsin activity may vary among different lots.
15. When monolayer cells are completely detached, inactivate trypsin with 0.7 mL of complete culture medium (the medium reserved in the centrifuge tubes can be used) to block enzymatic digestion.

16. Add these cell suspensions to their respective centrifuge tubes and centrifuge them for 5 min at 1000 rpm.
17. Aspirate the supernatant carefully using a glass pipette, leaving approximately 0.5–1.0 mL as the pellet protection margin.
18. With the aid of the pipette, resuspend the cells, gently homogenizing the pellet (20×) and keep the solution inside the pipette so that all samples come into contact with the potassium chloride (KCl; 0.075 M) at the same time.
19. Add 3 mL of KCl previously cooled to 2–8 °C and incubate for approximately 7–10 min at room temperature. During this period, gently resuspend the cells, mixing 40× with the pipette.
20. After incubation with KCl, add 0.5 mL of the fixative (3:1 v/v methanol-glacial acetic acid), prepared at the time of use and kept at room temperature, and mix gently.
21. Centrifuge the cultures for 5 min at 1000 rpm. Remove the supernatant, leaving approximately 0.5–1.0 mL.
22. Homogenize the pellet (20×) and keep the solution inside the pipette.
23. Add 5 mL of fixative and mix immediately.
24. Centrifuge the cultures for 5 min. Remove the supernatant.
25. Add 5 mL fixative again and mix.
26. In this step, cultures should be kept in a refrigerator (2–8 °C) for at least 1 h and/or until the slides are prepared.
27. At the time of making the slides, centrifuge the tubes, remove the supernatant, and finally produce an appropriately concentrated cell suspension, maintaining approximately 0.5 mL of fixative.
28. Approximately five drops cellular solution should be dripped under the identified slide. Prepare at least three slides for each experimental point, labeled with the identity of the culture. Leave the slides to dry at room temperature prior to staining for at least 1 day. After this period, stain the slides or store in slide boxes.
29. The slides can be stained with 3 vol% Giemsa in tap water, 0.0125% (w/v) acridine orange in PBS, panoptic, among others, depending on the most suitable one for each test cell (Fig. 2).

#### **Analysis of the Results (See Note 8)**

The frequencies of cells with MN (with one, two, and more than two MN) are recorded. A total of 6000 binucleated cells are scored per treatment, corresponding to 2000 cells per treatment per repetition. Attention should be given to ensure that MN are scored only



**Fig. 2** Microphotograph (1000× magnification) of a micronucleated binucleated HepG2 cell. Staining with Giemsa (3%)

in binucleated cells and not in multinucleated cells, because multinucleated cells are not once-divided cells and tend to have greatly elevated MN frequencies relative to binucleated cells, which would result in inaccurate genome damage estimates [17].

A sample is considered a mutagen in this assay if statistically significant increases in the proportion of micronucleated cells over the negative/solvent controls (reference point for comparison in the statistical evaluation of the results) are observed at one or more concentrations.

Furthermore, the determination of the Cytokinesis-Block Proliferation Index (CBPI) may be used to calculate cell proliferation. CBPI indicates the average number of nuclei per cell. Cells with well-preserved cytoplasm containing 1–4 nuclei are scored. Analyze 1500 cells per treatment for a total of 500 cells per repetition. CBPI is calculated using the following formula [16]:

$$\text{CBPI} = \frac{((\text{No. mononucleate cells}) + (2 \times \text{No. binucleate cells}) + (3 \times \text{No. multinucleate cells}))}{(\text{Total number of cells})}$$

---

## 4 Notes

1. Examples of suitable positive controls for *Salmonella*/microsome assay (to confirm the reversion properties and specificity of each tester strain, and the efficacy of the metabolic activation system): 4-nitro-*o*-phenylenediamine (TA98 and TA97a, 10 µg per plate); sodium azide (TA100, 1.25 µg per plate); mitomycin C (TA102, 0.5 µg per plate), in the absence of S9 and 2-anthramine (TA98, TA100, TA 97a, 1.25 µg per plate), 2-aminofluorene (TA102, 10 µg per plate), in the presence of S9.

For MN test, the most commonly used positive control agents are: methyl methanesulfonate, mitomycin C, 4-nitroquinoline-N-oxide, cytosine arabinoside, benzo(a)pyrene,

**Table 1 Recipe for Vogel-Bonner medium E (50X)**

| Ingredients  | Quantity per liter |
|--|--------------------|
| 1. Warm distilled water (about 50 °C)  | 670 mL             |
| 2. Magnesium sulfate ( $\text{MgSO}_4 \cdot \text{H}_2\text{O}$ )                              | 10 g               |
| 3. Citric acid monohydrate   | 100 g              |
| 4. Potassium phosphate, dibasic, anhydrous ( $\text{K}_2\text{HPO}_4$ )                        | 500 g              |
| 5. Sodium ammonium phosphate ( $\text{Na}_2\text{NH}_2\text{PO}_4 \cdot 4\text{H}_2\text{O}$ ) | 175 g              |

cyclophosphamide, colchicine, or vinblastine. Concentrations should be defined in preliminary tests.

2. Vogel–Bonner (VB salts) medium E.

The ingredients must be added in the order indicated below. Make sure that each salt is dissolved thoroughly by stirring it on a magnetic stirrer before adding the next salt (Table 1).

- The agar should never be autoclaved together with the VB salts and glucose.
- The plates can be stored at 4 °C for several weeks when placed in sealed plastic bags to prevent dehydration. Before use, the plates should be warmed up to room temperature and examined for excess moisture.

3. Sodium phosphate, monobasic (0.1 M): To 1 L of water, add 13.8 g  $\text{NaH}_2\text{PO}_4 \cdot \text{H}_2\text{O}$ .

Sodium phosphate, dibasic (0.1 M): To 1 L of water, add 14.2 g  $\text{Na}_2\text{HPO}_4 \cdot \text{H}_2\text{O}$ .

4. At least five different concentrations of the food packaging extract should be selected for the test, and the interval between each concentration should be approximately half log ( $\sqrt{10}$ ). At least three plates for each dose level and for the controls is recommended.

Extracts obtained from aqueous solvents can be used at levels up to approximately 1 mL per plate before they interfere with the gelling of the top agar, while organic solvents are often used at a maximal dose of 0.1 mL per plate [21].

Untreated control: also called spontaneous control, as it aims to demonstrate the rate of spontaneous reversion of each strain and that no deleterious or mutagenic effects are induced by the chosen solvent.

Solvent/vehicle control: solvent or vehicle alone, without test substance, and treated in the used maximum volume in the

treatment group. In the Ames test, the solvent/vehicle control is also called negative control [20].

Positive control (*see Note 1*).

5. It is important to quickly swirl the plates after the addition of the top agar to the surface of the GM agar plates to ensure an even distribution of the top agar that contains the bacteria, test sample, and S9 mix or buffer.
6. The most common culture media for the cell lines mentioned in the Introduction section are Eagle's Minimal Essential Medium (EMEM), Dulbecco's Modified Eagle's medium (DMEM), RPMI, Ham's F10, Ham's F12.
7. When cytochalasin B is used, the most appropriate method to assess cytotoxicity is to calculate the cytokinesis-block proliferation index (CBPI). CBPI: the proportion of second-division cells in the treated population relative to the untreated control.

Untreated control: also called negative control, only 2 mL of complete culture medium.

Solvent/vehicle control: solvent or vehicle alone, without test substance, and treated in the used maximum volume in the treatment group.

Positive control (*see Note 1*).

8. MN are morphologically identical, but smaller than nuclei. The diameter of MN usually varies between 1/16th and 1/3rd of the mean diameter of the main nuclei, which correspond to 1/256th and 1/9th of the area of one of the main nuclei in a binucleated cell, respectively. MN are non-refractile and they are not linked or connected to the main nuclei. MN may touch but not overlap the main nuclei and the micronuclear boundary should be distinguishable from the nuclear boundary. Moreover, MN usually have the same staining intensity as the main nuclei, but occasionally staining may be more intense.

For analysis of CBPI, mono-, bi, and multinucleated cells are viable, with an intact cytoplasm and normal nucleus morphology containing one, two, and three or more nuclei, respectively.

---

## Acknowledgments

F. A. Resende thanks the São Paulo Research Foundation (FAPESP; grant # 2017/16278-9). H. S. Barud thanks the National Council for Scientific and Technological Development (CNPq; grant # 407822/2018-6; INCT-INFO), FAPESP (grants # 2018/25512-8 and 2013/07793-6), and TA Instruments Brazil. D. C. Tavares is grateful to CNPq for the fellowship granted.

## References

1. Bolognesi C, Castoldi AF, Crebelli R, Barthélémy E, Maurici D, Wölfle D, Volk K, Laurence Castle L (2017) Genotoxicity testing approaches for the safety assessment of substances used in food contact materials prior to their authorization in the European Union. *Environ Mol Mutagen* 58:361–374. <https://doi.org/10.1002/em.22094>
2. Rainer B, Mayrhofer E, Redl M, Dolak I, Mislivecek D, Czerny T, Kirchnawy C, Marin-Kuan M, Schilter B, Tacker M (2019) Mutagenicity assessment of food contact material migrates with the Ames MPF assay. *Food Addit Contam Part A Chem Anal Control Expo Risk Assess* 36:1419–1432. <https://doi.org/10.1080/19440049.2019.1634841>
3. Groh KJ, Muncke J (2017) In vitro toxicity testing of food contact materials: state-of-the-art and future challenges. *Compr Rev Food Sci Food Saf* 16:1123–1150. <https://doi.org/10.1111/1541-4337.12280>
4. Cartus A, Schrenk D (2017) Current methods in risk assessment of genotoxic chemicals. *Food Chem Toxicol* 106:574–582. <https://doi.org/10.1016/j.fct.2016.09.012>
5. Karmaus AL, Osborn R, Krishan M (2018) Scientific advances and challenges in safety evaluation of food packaging materials: workshop proceedings. *Regul Toxicol Pharmacol* 98:80–87. <https://doi.org/10.1016/j.yrtph.2018.07.017>
6. Pinter E, Rainer B, Czerny T, Riegel E, Schilter B, Marin-Kuan M, Tacker M (2020) Evaluation of the suitability of mammalian *in vitro* assays to assess the genotoxic potential of food contact materials. *Foods* 9:237. <https://doi.org/10.3390/foods9020237>
7. Zeiger E (2019) The test that changed the world: the Ames test and the regulation of chemicals. *Mutat Res* 841:43–48. <https://doi.org/10.1016/j.mrgentox.2019.05.007>
8. Ames BN, Lee FD, Durston WE (1973) An improved bacterial test system for the detection and classification of mutagens and carcinogens. *Proc Natl Acad Sci U S A* 70:782–786. <https://doi.org/10.1073/pnas.70.3.782>
9. Ames BN, Durston WE, Yamasaki E, Lee FD (1973) Carcinogens are mutagens: a simple test system combining liver homogenates for activation and bacteria for detection. *Proc Natl Acad Sci U S A* 70:2281–2285. <https://doi.org/10.1073/pnas.70.8.2281>
10. Tejs S (2008) The Ames test: a methodological short review. *Environ Biotechnol* 4:7–14
11. Mortelmans K, Zeiger E (2000) The Ames *Salmonella*/microsome mutagenicity assay. *Mutat Res* 455:29–60. [https://doi.org/10.1016/s0027-5107\(00\)00064-6](https://doi.org/10.1016/s0027-5107(00)00064-6)
12. Zeiger E (2001) Mutagens that are not carcinogens: faulty theory or fault tests? *Mutat Res* 492:29–38
13. Maron DM, Ames BN (1983) Revised methods for the *Salmonella* mutagenicity test. *Mutat Res* 113:173–215. [https://doi.org/10.1016/0165-1161\(83\)90010-9](https://doi.org/10.1016/0165-1161(83)90010-9)
14. Doherty AT (2012) The in vitro micronucleus assay. *Methods Mol Biol* 817:121–141. [https://doi.org/10.1007/978-1-61779-421-6\\_7](https://doi.org/10.1007/978-1-61779-421-6_7)
15. Fenech M (2006) Cytokinesis-block micronucleus assay evolves into a “cytome” assay of chromosomal instability, mitotic dysfunction and cell death. *Mutat Res* 600:58–66. <https://doi.org/10.1016/j.mrfmmm.2006.05.028>
16. OECD (2016) Test no. 487: in vitro mammalian cell micronucleus test, OECD guidelines for the testing of chemicals, section 4. OECD Publishing, Paris. <https://doi.org/10.1787/9789264264861-en>
17. Fenech M (2007) Cytokinesis-blocked micronucleus cytome assay. *Nat Protoc* 2:1084–1104. <https://doi.org/10.1038/nprot.2007.77>
18. EFSA Scientific Committee (2011) Scientific opinion on genotoxicity testing strategies applicable to food and feed safety assessment. *EFSA J* 9(9):2379. [69 pp.]. <https://doi.org/10.2903/j.efsa.2011.2379>
19. ISO 10993-12:2020, Biological evaluation of medical devices – Part 12: Sample preparation and reference materials
20. OECD (2020) Test no. 471: bacterial reverse mutation test, OECD guidelines for the testing of chemicals, section 4. OECD Publishing, Paris. <https://doi.org/10.1787/20745788>
21. Hamel A, Roy M, Proudlock R (2016) Chapter 4 – The bacterial reverse mutation test. In: *Genetic toxicology testing: a laboratory manual*. Elsevier, Amsterdam, pp 79–138. <https://doi.org/10.1016/B978-0-12-800764-8.00004-5>

# **Part II**

## **Microstructural and Barrier Features of Food Packaging Materials**





## Microstructural and Defect Analysis of Food Packaging Materials Through X-Ray Microtomography

Marcos V. Lorevice, Pedro I. C. Claro, Diego M. Nascimento, and Rubia F. Gouveia

### Abstract

Packaging is an important part of food products, preserving their main components and attracting consumer's interest. However, when damage or flaws are present, food stability can be compromised. Several factors related to the design (composition and function), processing, and production of food packaging materials may result in defects that, although unavoidable, must be traceable and monitored. Few protocols have been proposed to effectively identify defects, most of which destructively or invasively, preventing the in situ characterization of the internal microstructure. We herein propose a general, simple protocol to detect and quantify defects, and analyze engineered microstructures in food packaging by X-ray microtomography. The technique requirements, such as sample characteristics and preparation, equipment setup, data acquisition and processing, as well as image segmentation, are elucidated by showcasing two common food packaging materials: paper/plastic/metal multilayers (Tetra Pak<sup>®</sup>) and polyethylene. X-ray is comprehensively depicted as an easy, helpful, noninvasive, and nondestructive method to improve the quality control of food packaging materials.

**Key words** X-ray tomography, Microstructure, Failures, Defects

---

## 1 Introduction

Since the beginning of human civilization, packaging influences the way in which food is stored and consumed. The first record of packaging used to store and transport food dates of around 200 years before the common era BCE [1]. The main functions of food packaging are to protect and preserve the quality and safety of food during transportation, distribution, storage, commercialization, and consumption. Moreover, packaging should reduce food losses and contamination during storage and provide relevant information (e.g., nutrition facts and shelf-life). Even today, the food packaging sector plays a crucial role in the world economy [2, 3],

accounting for USD 228 billion in 2018 globally, value that is expected to reach USD 441 billion in 2025 [4].

Food products comprise a synergic sum of different harmonized features: food typology, packaging materials, subliminal messages, and sensory (e.g., color, taste, texture, flavor, etc.) impression [5]. From the materials science perspective, the right selection of raw materials for a particular food packaging requires the best mechanical, optical, thermal, and barrier properties in order to preserve and prolong food shelf-life. Food packaging materials are commonly based on metal, glass, paper and paper-board, plastics, and even combinations among these into complex and convenient containers, like Tetra Pak<sup>®</sup> [6]. Depending on the technical application, packaging materials can be classified as primary (direct contact with the food), secondary, and tertiary (the latter being external to the former and providing physical integrity) [7].

In spite of all technological efforts that have been made in the past decades to improve food packaging properties or to add new functions toward the so-called active and smart packaging [8–10], the occurrence of flaws or defects always overcomes the technological advances. The safety hazards or unhealthy appearance caused by damaged food products (food/packaging) generally leads to unattractive products to the consumers, and consequently, to an undesirable reduction of their selling [11].

Defect and flaws in food packaging are frequently caused during packaging and processing operations (structure/composition, inferior compatibility among the raw materials), product storage (temperature and relative humidity), or even by consumer handling and disposal. According to their effect in packaging integrity and effective applicability, flaws and/or damages have been categorized in critical (e.g., collapse, rupture, holes, seal cracks, tears, or cracks), major (e.g., poor mechanical resistance, misplaced lids or crimp seals), and minor defects (streaky pigmentation from inadequate pigment blending, scratches on the lamination, beads over surface of foil, mold, drawing lines, improper identification on label) [6].

The vast and well-known materials characterization, particularly of their morphological (optical and electron microscopies), mechanical (compression and tensile tests), thermal (thermogravimetry analysis, differential scanning calorimetry, and dynamic mechanical thermal analysis), barrier (oxygen, CO<sub>2</sub>, and water), or even active (antimicrobial and sensory) properties, have been applied to assess packaging performance and to identify possible failures with considerable accuracy, besides exhibiting sample-destructive or -invasive characteristics in most of the cases [12, 13].

Apart from defects easily identified by a rapid inspection (in some cases visual or by analyzing changes in packaging content, like off-flavor or color), the smaller ruptures or holes, internal and structural failures, imperfections, or poor phase compatibility in

packaging are usually visual-untraceable, and they can interfere substantially with the final packaging properties. Even for complex food packaging systems, like Tetra Pak<sup>®</sup>, which requires phase compatibility and can otherwise exhibit defects in one or more of the four layers, tracking imperfections is something difficult via some of the current materials analyses. In addition, the incorporation of micro and nanostructures to enhance packaging properties requires more accurate techniques in resolution, as well as in morphological statistics to identify and to infer the origin of these undesirable defects [14].

To overcome these drawbacks, nondestructive or noninvasive techniques, like ultrasound or X-ray tomography [15, 16, 17], have been widely applied as effective procedures to investigate internal characteristics of packaging samples, and in most of the cases, lacking any sample pretreatment or further preparation, allowing the analyses to be carried out *in situ* and helpful correlations with traditional materials characterizations to be established, as described above [18]. X-ray micro-computed tomography (Micro-CT) is a powerful, versatile, noninvasive, and nondestructive technique used for the three-dimensional (3D) structural characterization of varying types of systems [19–37]. This tool enables correlations between the microstructural and macroscopic characteristics of different types of materials as aforementioned, including food packaging [38–40], enabling quantifying and analyzing dispersions, second phases, and pores throughout the system [41]. To elucidate the Micro-CT procedure, Fig. 1 shows a schematic illustration of Tetra Pak<sup>®</sup> packaging projection acquisition, followed by pre-processing and processing of Tetra Pak<sup>®</sup> tomography images.

Concerning a brief overview of the X-ray microtomography procedure, Micro-CT is based on the attenuation of X-rays according to the Lambert–Beer law of exponential decay [42]. The X-rays pass through the sample (Fig. 1a) and they are attenuated according to the thickness, composition, and density of the analyzed material [43]. In addition, the attenuated X-rays produce a two-dimensional (2D) shadow of the material in the detector, producing several 2D X-ray projections of the object at each rotation step of the sample around its height *Z*-axis (Fig. 1b). The detector (Fig. 1a) and the X-ray source are strategically positioned in relation to the examined material. The source is located opposite to the detector, considering the *Z*-axis of the sample as reference [44]. The detector includes a charge-coupled device (CCD), a photodetector camera that transforms the attenuated X-ray photons into projections (Fig. 1a) [45, 46]. The projections (Fig. 1b) are aligned in the formation of sinograms (Fig. 1c), which are the origin of computational reconstruction signal of tomographic images (Fig. 1d) [47]. In terms of materials differentiation, from a high-quality reconstructed image, it is already possible to observe the layers that compose the Tetra Pak<sup>®</sup> packaging.

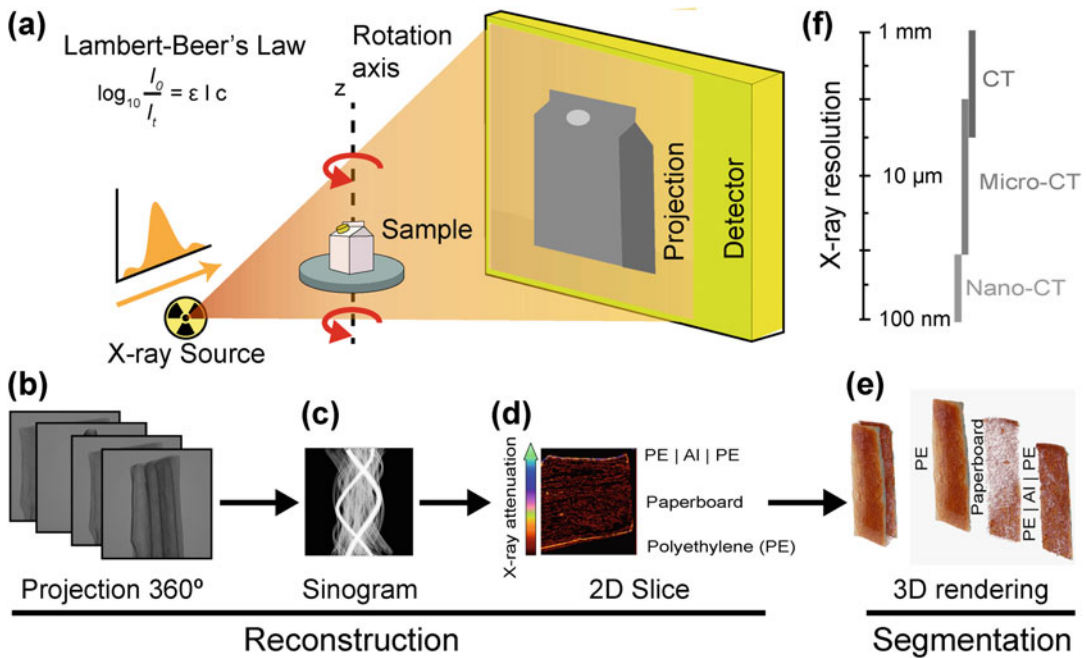


**Fig. 1** Schematic illustration of the basic principles of the Micro-CT technique and data processing: (a) Lambert-Beer's law, X-ray source and opposite detector to collect the signal; (b) Images projections from Z-axis 360° rotation; (c) Sinograms; (d) Two-dimensional slice; (e) High-quality reconstructed images of Tetra Pak® packaging and segmentation of packaging composition: paperboard, polyethylene (PE), and aluminum (Al) layers; and (f) Tomographic resolution

The lower attenuation for the paperboard and the polyethylene (PE) layers and the higher attenuation for the Al layer according to the colors of the X-ray attenuation scale can be noted (Fig. 1d, color-scale arrow). Considering the Tetra Pak® packaging 3D rendering (Fig. 1e), the compatibility of the interfaces among the layers and to analyze each 3D segmented layer can be noticed, assisting manufacturing engineers to minimize flaws/damage in the packaging of food products.

In the food industry, Micro-CT has risen as a valuable tool to correlate the common food characteristics (e.g., flavor, texture, ripening) with processing and storage conditions [48–52]. A 3D reconstruction of cream cheese from Micro-CT was applied to comprehend the influence of fat content on microstructures of cheese spreads [53]. Fat content was also correlated to the texture (hardness) of pork lean fermented sausages by Micro-CT, and geometric parameters obtained from this technique [54]. Cellular structure and porosity profile obtained from Micro-CT showed dependency of different baking conditions on bread [49], bread crumbs and crust [55]. Recently, in situ Micro-CT has been developed, setting new approaches and giving the possibility to observe the time-lapse collapse of micro-bubbles in the beer foams [18].

However, to date, the studies on Micro-CT as a nondestructive characterization tool for food packaging (macro and microstructures, defects, and failures) are scarce. Herein, we fully describe a useful step-by-step protocol of extruded PE composite characterization by using Micro-CT, containing tips and examples to identify interface regions, failures, defects, and imperfections in food packaging from tomography images.

---

## 2 Materials

The follow materials, equipment, and software were used for tomography images illustration on introduction and methods.

1. Commercial Tetra Pak<sup>®</sup> packaging and extruded low-density PE (LDPE) (Braskem, MFI = 8.3 g/10 min at 190 °C/2.160 kg) composite reinforced with cellulose fibers from sugarcane bagasse were used as materials models for Micro-CT characterization.
2. Tetra Pak<sup>®</sup> and extruded PE composite packaging were analyzed on a high-resolution Micro-CT equipment (Bruker 1272, Kontich, Belgium).
3. The acquisition was carried out using the SkyScan 1272 software provided by Bruker Micro-CT<sup>®</sup>.
4. The tomography images reconstruction was performed using Feldkamp algorithm by NRecon software (version 1.6.9.8, Bruker Micro-CT<sup>®</sup>).
5. The segmentation and extraction data from the reconstructed tomographic image were performed on CT analyzer (CTAn<sup>®</sup>) software (version 1.14.4.1, Bruker Micro-CT<sup>®</sup>).
6. The DataViewer software (version 1.5.1.2, Bruker Micro-CT<sup>®</sup>) was used to view the 2D images slice by slice, including the orthoslices of the reconstructed images and a linear X-ray attenuation.
7. 3D tomographic images were designed, rotated, and cropped on CTvox<sup>®</sup> software (version 2.7.0, Bruker Micro-CT<sup>®</sup>).

---

## 3 Methods

The Micro-CT protocol proposed here relies upon the real analysis of extruded PE composite, but one may extend it to other samples. The Micro-CT protocol was performed according to the following steps:

1. Place the sample symmetrically at the rotation stage, within the detector's field of view varying the sample rotation by  $360^\circ$  (*see Notes 1–5*).
2. Set up the Micro-CT according to the density of the material. For tomographic images in low-density materials (e.g., paper and polymers), low-energy and “unfiltered” or fine Al filters can be used (Table 1). To transmit X-ray radiation through denser materials (e.g., ceramics, metals, and glass), Al/Cu or Cu filters with associated higher X-ray source energies should be used.
3. Obtain images using a Micro-CT; we performed these analyses with a high-resolution Micro-CT equipment (*see Note 6*).
4. *Pre-processing*: Process the images using the NRecon software to apply the artifact's corrections, such as alignment, noise, ring, etc. (Fig. 2). In the case of PE composite packaging X-ray projections (Fig. 2a), it is recommended that the gray-scale range should be delimited on X-ray histogram to guarantee a faithful reconstruction image of the object. The example illustrated in Fig. 2b shows the following tomographic images problems:  $x/y$  drift and/or misalignment, noises, and ringing artifacts. Figure 2c illustrates the automatic alignment to correct the  $x/y$  drift and/or slight deviation due to misalignment of the X-ray projections. Following the tomographic image problem corrections, the noises are attenuated by the smoothing tool, as shown in Fig. 2d. Finally, ringing artifacts are corrected, extracting a reliable reconstruction image, as presented in Fig. 2e. The final image is generated by applying a color-scale (left side presents lower X-ray attenuation), as shown in Fig. 2f (*see Note 7*).
5. *Processing*: Open the reconstructed image and select several regions of interest (ROIs), previously preset, throughout the object using the CT analyzer (CTAn) software. For a specific ROI, establish the number of slices, thereby rendering a volume of interest (VOI), measuring in this case  $1.5 \times 1.5 \times 1.5 \text{ mm}^3$  (Fig. 3a, right). Using the binary selection command, a preset thresholding segmentation is applied on X-ray histogram, partitioning the analyzed object image by grayscale intensity [56], rendering different segmented images, containing pores/defects, the main matrix and microstructures agglomerations (Fig. 3b). It is important to delimit on the X-ray histogram for a specific grayscale range for all samples, as represented in Fig. 3c, where VOIs must present comparative X-ray attenuation and data extracted. Clearly, after this data processing defects (pores or matrix imperfections like filler agglomeration) can be identified in the analyzed packaging, as shown in Fig. 3b. After application of the previous

**Table 1**  
**Detailed information on the Micro-CT parameters for Tetra Pak® and extruded polyethylene (PE) composite analyses**

| Parameters                           | Tetra Pak®         | PE composite       |
|--------------------------------------|--------------------|--------------------|
| Source voltage (kV)                  | 20                 | 30                 |
| Source current ( $\mu\text{A}$ )     | 175                | 212                |
| Detector resolution (pixels)         | $2452 \times 1640$ | $2016 \times 1344$ |
| Nominal resolution ( $\mu\text{m}$ ) | 2                  | 1.4                |
| Exposure (ms)                        | 5340               | 2300               |
| Rotation step (deg)                  | 0.3                | 0.15               |
| Frame number                         | 4                  | 3                  |
| Random movement                      | 30                 | 10                 |
| Filter                               | No                 | No                 |

segmentation, quantitative segmentation data can be obtained as an outstanding and important morphometric analysis for a great number of images, which is very laborious to obtain via light-based microscopes. It can be done slice by slice (2D object) or for the entire VOI (3D object). In this case, the PE composite packaging presents a heterogeneous phase distribution along the slices, as illustrated in Fig. 3d (see Notes 8 and 9).

6. *Post-processing*: Use the DataViewer software to analyze the 2D images on the 3D perspective, as shown in Fig. 4. In this case, three different 2D-slice views are combined, such as 2D  $Z-X$  (coronal), 2D  $Z-Y$  (sagittal), and 2D  $X-Y$  (transversal) on the 3D object. From this perspective, it is possible to observe in detail the pores/defects (black phase), polymer matrix (red phase), dispersed microstructures/fibers (orange phase), and aggregates (white phase) contained in the PE composite for each 2D image of  $XYZ$  axis. Each 2D slice can be analyzed using a linear X-ray attenuation distribution, discriminating from lower to higher attenuation, according to pores/defects, matrix, dispersed microstructures/fibers, and aggregates increment, respectively (Fig. 4, bottom).
7. *Imaging and Analysis*: Regarding the representation of Micro-CT data in terms of 3D analysis of the reconstructed images and generated VOIs, different 3D geometries, colors and  $XYZ$  rotations can be performed using the CTvox® software. Some possible tomographic images are illustrated in Fig. 5. Considering a VOI of PE composite packaging reconstructed from X-ray projections, this volume can be cut, rotated, colored, and

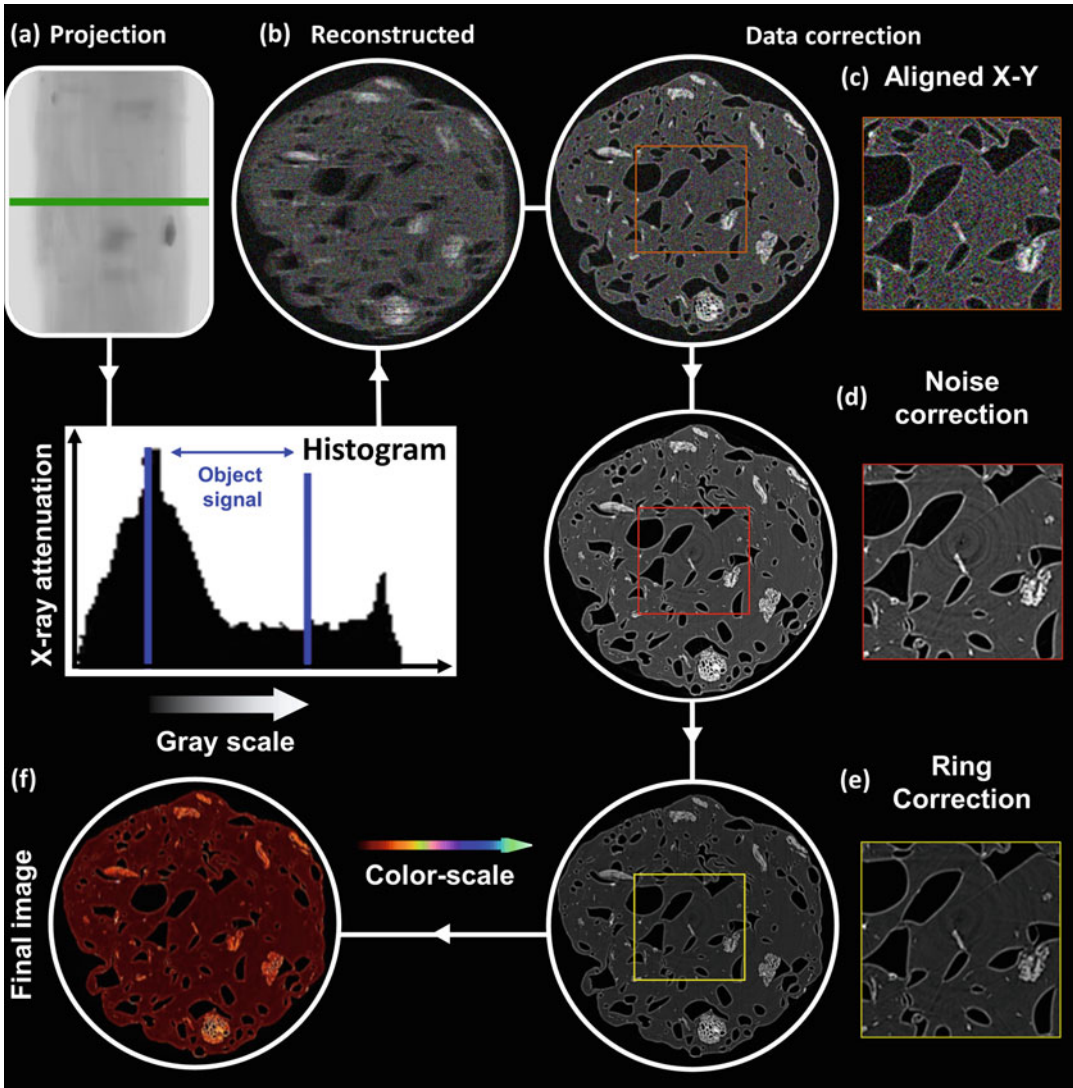


**Fig. 2** (a) X-ray projection and attenuation histogram; (b) Reconstruction tomographic imaging; workflow with the data correction: (c) alignment; (d) noise, and (e) ring. (f) Corrected image for the PE composite packaging

segmented using the simple CTvox<sup>®</sup> tools, as shown in Fig. 5. These tools allow viewing the interior and exterior of the VOI in different perspectives and color gradients. Furthermore, the color-scale segmentation (Fig. 5b) shows the 3D dispersion of the microstructures/fibers (green), of the agglomerates (light blue) along the PE matrix (brown), permitting to map the 3D microstructure. Note that those imperfections (agglomeration, in this case) within the PE matrix observed in orthoslices projection (Fig. 4) is trackable in most 3D maps (a white region in 3D-VOI, Fig. 5a, c) (*see Note 10*).



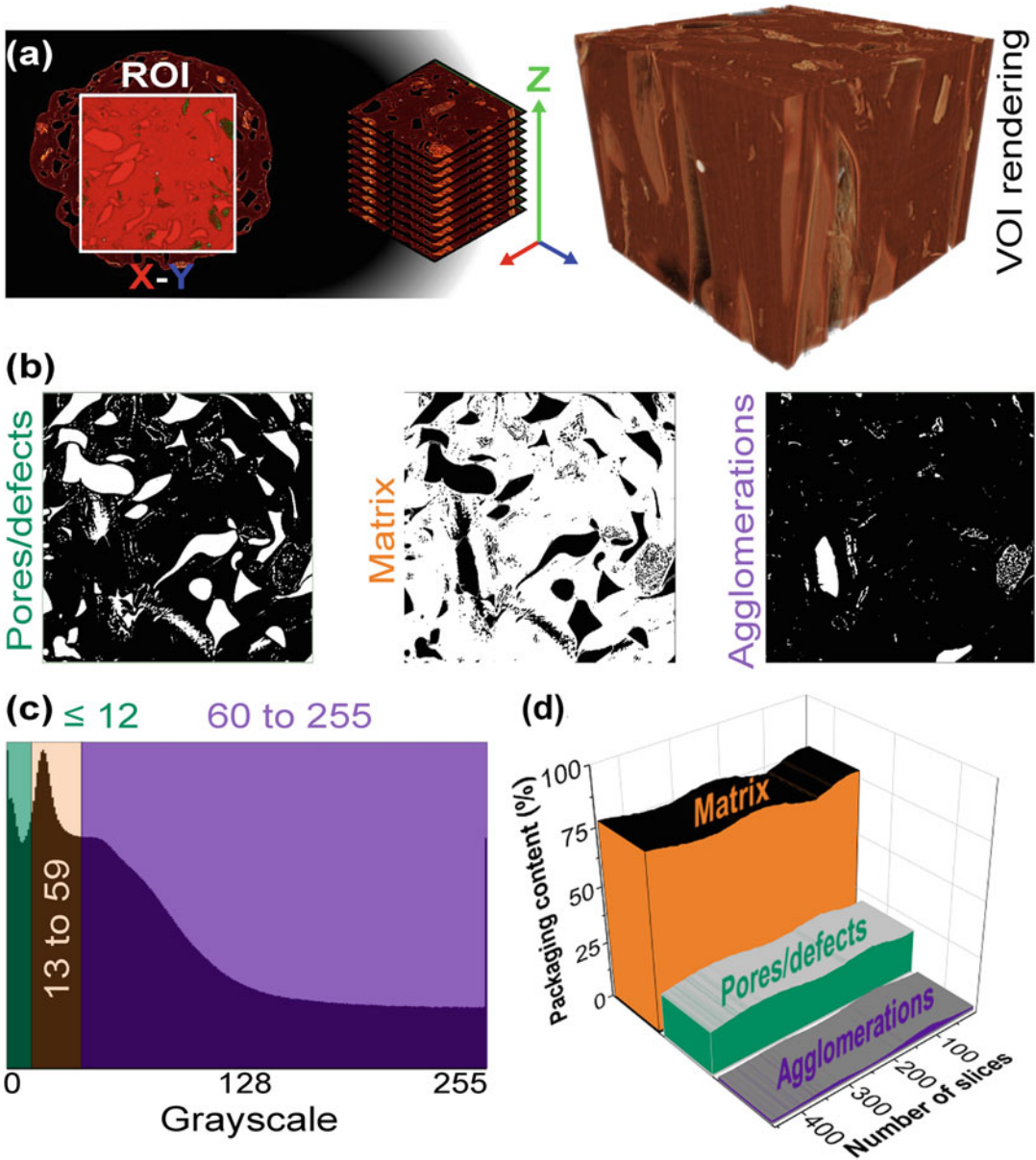


**Fig. 3** The Micro-CT analyzer software functional tools to segmentate a tomographic image. **(a)** Region of interest (ROI) selection (left) from the PE composite packaging reconstructed image to obtain a volume of interest (VOI) rendering (right). **(b)** Thresholding segmentation of PE composite in pores/defects (green), polymeric matrix (orange), and agglomerations (dark blue). **(c)** X-ray histogram partitioning the analyzed object image by grayscale intensity. **(d)** Quantitative morphometric data extracted from thresholding segmentation (from lower to higher attenuation) of a VOI: pores/defects, polymeric matrix and agglomerations content (%) variation in relation to the number of 2D slices

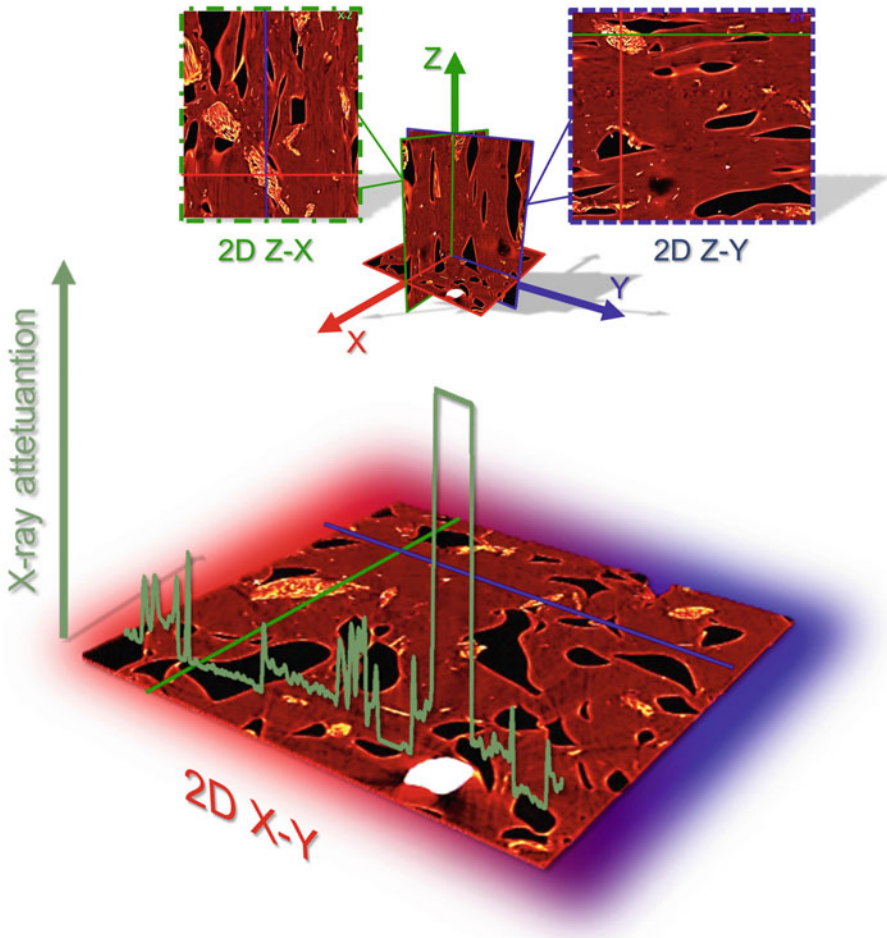


**Fig. 4** The orthoslices of polyethylene (PE) composite and the linear X-ray attenuation (green line) varying according to PE composite phases obtained and processed in the DataViewer<sup>®</sup> software

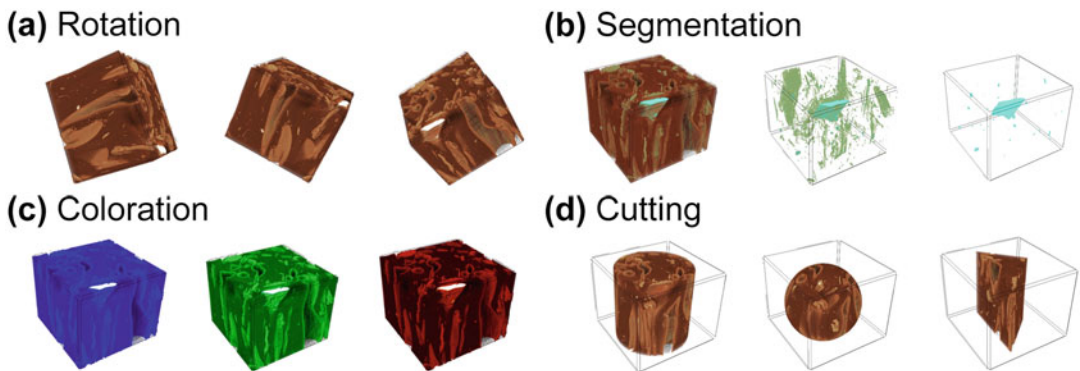


**Fig. 5** Polyethylene (PE) composite packaging VOI edited in the CTvox<sup>®</sup> software by different functional tools: (a) rotation, (b) segmentation, (c) coloration, and (d) cutting

---

## 4 Conclusion

The food packaging industry has shown technological advances in terms of renewable precursors, physical-mechanical performance, and innovative functions (check Part III for details on nontraditional functions of packaging materials). Nevertheless, this progress is limited by the occurrence of flaws/damage in the packaging material itself, decreasing or failing their purpose of ensuring food shelf-life. In this chapter, an innovative and useful noninvasive technique is proposed to investigate and point out 2D/3D damage maps in packaging, correlating morphometric data to possible causes (e.g., production, storage) and their influence on packaging properties. Two different packaging compositions were analyzed by Micro-CT, as showcases for the sake of didactics. Different types of data treatment (data acquisition, image processing) were considered in our protocol. This procedure provides as a helpful and nonconventional technique for predicting and manipulating end-use properties of food packaging.

---

## 5 Notes

The protocol described here was developed for the Bruker system available to users as an open facility at The Brazilian Nanotechnology National Laboratory (LNNano)/Brazilian Center of Research in Energy and Materials (CNPEM). It can be, however, extended to other manufacturers, considering the specificities of each apparatus. Should the reader have any query on calls for users, they are invited to contact the corresponding author or [edu@cnpem.br](mailto:edu@cnpem.br).

1. Samples usually do not require any preparation prior to Micro-CT analysis.
2. The best shape for samples is a cylinder (symmetrical rotation), improving the resolution due to the effective reduction in the diameter and alignment problems.
3. Sample holder with tape or glue can be used to ensure that the sample does not move during the data acquisition, keeping the effectiveness of 3D reconstructions procedure. The projections must be well aligned to ensure the high quality of the three-dimensional image of the object. It is worth mentioning that, in some cases, it is also necessary to minimize the noise and artifacts generated in the characterization process, using certain tools to not affect the quality of the reconstructed image [47, 57].
4. Small samples are preferred for enabling better resolution and less beam-hardening artifact.

5. The partial width option can be used for objects much smaller than the camera field, providing shorter scan times due to bigger rotation step and shorter reconstruction due to smaller datasets. This option is recommended for 4k binning mode (detector).
6. Other X-ray tomography approaches exist for other different scales and purposes, such as the computed tomography (CT) applied to the medical field for macroscale analysis [44] and the nano-computed tomography (Nano-CT) coupled to the synchrotron beamline to analyze sub-micrometer scale in higher resolution (*see* scale resolution on Fig. 1) [58].
7. The oversize scanning can be applied when the object is larger than a scan area, making a scout view and appropriated selection of the area of interest. The NRecon<sup>®</sup> software recognizes the object as a vertically connected dataset.
8. Some plug-ins can be applied in the CTAn<sup>®</sup> software to optimize the quantitative data and time acquisition, such as custom processing tool, enabling to create a task list for numerous parameters and samples.
9. Regarding an advanced characterization it is possible to select irregular surfaces in packaging (like the example of the Fig. 2) using the ROI shrink-wrap tool at the custom processing (CTAn<sup>®</sup> software), creating a VOI rendering.
10. The CTvox<sup>®</sup> software allows producing movies/animations using the flight recorder tools by adding different frames, shapes, rotation, and movements, some animations from CTvox<sup>®</sup> software are available on the Internet (<https://dentistry.llu.edu/micro-ct-imaging-gallery>).

---

## Acknowledgments

The authors thank The Brazilian National Council for Scientific and Technological Development (CNPq) for supporting this work DTI-A/SisNANO (grants 380312/2020-4 and 380173/2022-0), PCI-postdoctoral (grants 301362/2020-3, 301356/2020-3 and 302368/2021-3) and Productivity scholarship (grant 303621/2022-2), and the grant 2020/08651-4 provided by São Paulo Research Foundation (FAPESP).

## References

1. Risch SJ (2009) Food packaging history and innovations. *J Agric Food Chem* 57:8089–8092. <https://doi.org/10.1021/jf900040r>
2. Marsh K, Bugusu B (2007) Food packaging: roles, materials, and environmental issues. *J Food Sci* 72:R39–R55. <https://doi.org/10.1111/j.1750-3841.2007.00301.x>
3. Robertson GL (2016) Food packaging. CRC Press

4. Knorr D, Froehling A, Jaeger H et al (2011) Emerging technologies in food processing. *Annu Rev Food Sci Technol* 2:203–235. <https://doi.org/10.1146/annurev.food.102308.124129>
5. Parisi S (2012) Food packaging and food alterations: the user-oriented approach, 1st edn. Smithers Rapra Technology Ltd, Shawbury, Shrewsbury, Shropshire
6. Onwurah C, Mamah SC (2018) A method for damage detection in the packaging materials. *J Sci Eng Res* 5:235–249
7. Paine FA, Paine HY (1992) A handbook of food packaging. Springer US, Boston
8. Trajkovska Petkoska A, Daniloski D, D’Cunha NM et al (2021) Edible packaging: sustainable solutions and novel trends in food packaging. *Food Res Int* 140:109981. <https://doi.org/10.1016/j.foodres.2020.109981>
9. Sharma R, Jafari SM, Sharma S (2020) Antimicrobial bio-nanocomposites and their potential applications in food packaging. *Food Control* 112:107086. <https://doi.org/10.1016/j.foodcont.2020.107086>
10. Bagde P (2021) Biodegradable polymers for food packaging and active food packaging. In: *Advances in the domain of environmental biotechnology*. Springer, Singapore, pp 113–127
11. Parisi S (2013) Food industry and packaging materials: performance-oriented guidelines for users. Smithers Rapra Technology Ltd, Shawbury, Shrewsbury, Shropshire
12. Otoni CG, Avena-Bustillos RJ, Azeredo HMC et al (2017) Recent advances on edible films based on fruits and vegetables—a review. *Compr Rev Food Sci Food Saf* 16:1151. <https://doi.org/10.1111/1541-4337.12281>
13. Han J-W, Ruiz-Garcia L, Qian J-P, Yang X-T (2018) Food packaging: a comprehensive review and future trends. *Compr Rev Food Sci Food Saf* 17:860–877. <https://doi.org/10.1111/1541-4337.12343>
14. Sarfraz J, Gulin-Sarfraz T, Nilsen-Nygaard J, Pettersen MK (2020) Nanocomposites for food packaging applications: an overview. *Nanomaterials* 11:10. <https://doi.org/10.3390/nano11010010>
15. Ozguler A, Morris SA, O’Brien WD (1999) Evaluation of defects in the seal region of food packages using the ultrasonic contrast descriptor,  $\Delta BAI$ . *Packag Technol Sci* 12: 161–171. [https://doi.org/10.1002/\(SICI\)1099-1522\(199907/08\)12:4<161::AID-PTS464>3.0.CO;2-C](https://doi.org/10.1002/(SICI)1099-1522(199907/08)12:4<161::AID-PTS464>3.0.CO;2-C)
16. Landis EN, Keane DT (2010) X-ray microtomography. *Mater Charact* 61:1305–1316. <https://doi.org/10.1016/j.matchar.2010.09.012>
17. Claro PIC, Borges EPBS, Schleder GR et al (2023) From micro- to nano- and time-resolved x-ray computed tomography: Bio-based applications, synchrotron capabilities, and data-driven processing. *Appl Phys Rev* 10:021302. <https://doi.org/10.1063/5.0129324>
18. Dewanckele J, Boone MA, Coppens F et al (2020) Innovations in laboratory-based dynamic micro-CT to accelerate in situ research. *J Microsc* 277:197–209. <https://doi.org/10.1111/jmi.12879>
19. Stock SR (2008) Recent advances in X-ray microtomography applied to materials. *Int Mater Rev* 53:129–181. <https://doi.org/10.1179/174328008X277803>
20. Lorevice MV, Mendonça EO, Orra NM et al (2020) Porous cellulose nanofibril–natural rubber latex composite foams for oil and organic solvent absorption. *ACS Appl Nano Mater* 3(11):10954–10965. <https://doi.org/10.1021/acsanm.0c02203>
21. de Siqueira L, Gouveia RF, Grenho L et al (2018) Highly porous 45S5 bioglass-derived glass – ceramic scaffolds by gelcasting of foams. *J Mater Sci* 53:10718–10731. <https://doi.org/10.1007/s10853-018-2337-x>
22. Ferreira FV, Souza LP, Martins TM et al (2019) Nanocellulose/bioactive glass cryogels as scaffolds for bone regeneration. *Nanoscale* 11:19842–19849. <https://doi.org/10.1039/c9nr05383b>
23. Garcia PS, Gouveia RF, Maia JM et al (2018) 2D and 3D imaging of the deformation behavior of partially devulcanized rubber/polypropylene blends. *Express Polym Lett* 12:1047–1060. <https://doi.org/10.3144/expresspolymlett.2018.92>
24. Pandoli OG, Neto RJ, Oliveira NR et al (2020) Ultra-highly conductive hollow channels guided by a bamboo bio-template for electric and electrochemical devices. *J Mater Chem A* 8:4030–4039. <https://doi.org/10.1039/c9ta13069a>
25. Zhou G, Pei S, Li L et al (2014) A graphene – pure-sulfur sandwich structure for ultrafast, long-life lithium – sulfur batteries. *Adv Mater* 26:625–631. <https://doi.org/10.1002/adma.201302877>
26. Laperre K, Depypere M, van Gestel N et al (2011) Development of micro-CT protocols for in vivo follow-up of mouse bone architecture without major radiation side effects. *Bone* 49:613–622. <https://doi.org/10.1016/j.bone.2011.06.031>

27. Bultreys T, De Boever W, Cnudde V (2016) Imaging and image-based fluid transport modeling at the pore scale in geological materials: a practical introduction to the current state-of-the-art. *Earth Sci Rev* 155:93–128. <https://doi.org/10.1016/j.earscirev.2016.02.001>
28. Padilla-ortega E, Darder M, Aranda P et al (2016) Ultrasound assisted preparation of chitosan – vermiculite bionanocomposite foams for cadmium uptake. *Appl Clay Sci* 130:40–49. <https://doi.org/10.1016/j.clay.2015.11.024>
29. Moreira RLPO, Simão JA, Gouveia RF, Strauss M (2020) Exploring the hierarchical structure and alignment of wood cellulose fibers for bioinspired anisotropic polymeric composites. *ACS Appl Bio Mater* 3(4):2193–2200. <https://doi.org/10.1021/acsabm.0c00038>
30. Ferreira FV, Mariano M, Rabelo SC et al (2018) Isolation and surface modification of cellulose nanocrystals from sugarcane bagasse waste: from a micro- to a nano-scale view. *Appl Surf Sci* 436:1113–1122. <https://doi.org/10.1016/j.apsusc.2017.12.137>
31. Ferreira FV, Trindade GN, Lona LMF et al (2019) LDPE-based composites reinforced with surface modified cellulose fibres: 3D morphological and morphometrical analyses to understand the improved mechanical performance. *Eur Polym J* 117:105–113. <https://doi.org/10.1016/j.eurpolymj.2019.05.005>
32. Canencia F, Darder M, Aranda P et al (2017) Conducting macroporous carbon foams derived from microwave-generated caramel/silica gel intermediates. *J Mater Sci* 52:11269–11281. <https://doi.org/10.1007/s10853-017-1227-y>
33. Lopes JH, Magalhães JA, Gouveia RF et al (2016) Hierarchical structures of  $\beta$ -TCP/45S5 bioglass hybrid scaffolds prepared by gel-casting. *J Mech Behav Biomed Mater* 62:10–23. <https://doi.org/10.1016/j.jmbbm.2016.04.028>
34. Damasceno S, Corrêa CC, Gouveia RF et al (2020) Delayed capillary flow of elastomers: an efficient method for fabrication and nano-functionalization of flexible, foldable, twistable, and stretchable electrodes from pyrolyzed paper. *Adv Electron Mater* 6:1900826. <https://doi.org/10.1002/aelm.201900826>
35. Mariano M, Souza SF, Borges AC et al (2021) Tailoring strength of nanocellulose foams by electrostatic complexation. *Carbohydr Polym* 256:117547. <https://doi.org/10.1016/j.carbpol.2020.117547>
36. Lorevice MV, Claro PIC, Aleixo NA et al (2023) Designing 3D fractal morphology of eco-friendly nanocellulose-based composite aerogels for water remediation. *J Chem Eng* 462:142166. <https://doi.org/10.1016/j.cej.2023.142166>
37. Silva DB, Nascimento DM, Claro PIC et al Enhancing water resistance in cationic cellulose nanofibril adhesive with natural rubber latex. *ACS Appl Nano Mater*. <https://doi.org/10.1021/acsanm.3c04257>
38. Islam SF, Mancini L, Sundara RV et al (2017) Studying model suspensions using high resolution synchrotron X-ray microtomography. *Chem Eng Res Des* 117:756–772. <https://doi.org/10.1016/j.chemd.2016.11.034>
39. du Plessis A, le Roux SG, Tshibalanganda M (2019) Advancing X-ray micro computed tomography in Africa: going far, together. *Sci Afr* 3:e00061. <https://doi.org/10.1016/j.sciaf.2019.e00061>
40. Rouholamin D, Hopkinson N (2014) An investigation on the suitability of micro-computed tomography as a non-destructive technique to assess the morphology of laser sintered nylon 12 parts. *Proc Inst Mech Eng Part B J Eng Manuf* 228:1529–1542. <https://doi.org/10.1177/0954405414522209>
41. Stock SR (1999) X-ray microtomography of materials. *Int Mater Rev* 44:141–164. <https://doi.org/10.1179/095066099101528261>
42. Maire E, Buffière JY, Salvo L et al (2001) On the application of X-ray microtomography in the field of materials science. *Adv Eng Mater* 3:539–546. [https://doi.org/10.1002/1527-2648\(200108\)3:8<539::AID-ADEM539>3.0.CO;2-6](https://doi.org/10.1002/1527-2648(200108)3:8<539::AID-ADEM539>3.0.CO;2-6)
43. Vászrhelyi L, Kónya Z, Kukovecz A, Vajtai R (2020) Microcomputed tomography-based characterization of advanced materials: a review. *Mater Today Adv* 8:100084. <https://doi.org/10.1016/j.mtadv.2020.100084>
44. Eberhardt CN, Clarke AR (2002) Automated reconstruction of curvilinear fibres from 3D datasets acquired by X-ray microtomography. *J Microsc* 206:41–53. <https://doi.org/10.1046/j.1365-2818.2002.01009.x>
45. Ning R, Kruger RA (1998) Computer simulation of image intensifier based computed tomography detector: vascular application. *Med Phys* 188:188–192. <https://doi.org/10.1118/1.596250>
46. Karellas A, Harris LJ, Liu H et al (1992) Charge coupled device detector: performance considerations and potential for small field mammographic imaging applications. *Med Phys* 19:1015–1023. <https://doi.org/10.1118/1.596819>

47. Berg S, Saxena N, Shaik M, Pradhan C (2018) Generation of ground truth images to validate micro-CT image-processing pipelines. *Lead Edge* 37:412–420. <https://doi.org/10.1190/tle37060412.1>
48. Haff RP, Toyofuku N (2008) X-ray detection of defects and contaminants in the food industry. *Sens & Instrumen Food Qual* 2:262–273. <https://doi.org/10.1007/s11694-008-9059-8>
49. Cantre D, Herremans E, Verboven P et al (2014) Characterization of the 3-D microstructure of mango (*Mangifera indica* L. cv. Carabao) during ripening using X-ray computed microtomography. *Innov Food Sci Emerg Technol* 24:28–39. <https://doi.org/10.1016/j.ifset.2013.12.008>
50. Schoeman L, Williams P, du Plessis A, Manley M (2016) X-ray micro-computed tomography ( $\mu$ CT) for non-destructive characterisation of food microstructure. *Trends Food Sci Technol* 47:10–24. <https://doi.org/10.1016/j.tifs.2015.10.016>
51. Mulot V, Fatou-toutie N, Benkhelifa H et al (2019) Investigating the effect of freezing operating conditions on microstructure of frozen minced beef using an innovative X-ray micro-computed tomography method. *J Food Eng* 262:13–21. <https://doi.org/10.1016/j.jfoodeng.2019.05.014>
52. Mousavi R, Miri T, Cox PW, Fryer PJ (2007) Imaging food freezing using X-ray microtomography. *Int J Food Sci Technol* 42:714–727. <https://doi.org/10.1111/j.1365-2621.2007.01514.x>
53. Laverse J, Mastromatteo M, Frisullo P, Del Nobile MA (2011) X-ray microtomography to study the microstructure of cream cheese-type products. *J Dairy Sci* 94:43–50. <https://doi.org/10.3168/jds.2010-3524>
54. Santos-Garcés E, Laverse J, Gou P et al (2013) Feasibility of X-ray microcomputed tomography for microstructure analysis and its relationship with hardness in non-acid lean fermented sausages. *Meat Sci* 93:639–644. <https://doi.org/10.1016/j.meatsci.2012.11.027>
55. Besbes E, Jury V, Monteau J-Y, Le Bail A (2013) Characterizing the cellular structure of bread crumb and crust as affected by heating rate using X-ray microtomography. *J Food Eng* 115:415–423. <https://doi.org/10.1016/j.jfoodeng.2012.10.005>
56. Iassonov P, Gebrenegus T, Tuller M (2009) Segmentation of X-ray computed tomography images of porous materials: a crucial step for characterization and quantitative analysis of pore structures. *Water Resour Res* 45:1–12. <https://doi.org/10.1029/2009WR008087>
57. Zhang Y, Yu H (2018) Convolutional neural network based metal artifact reduction in X-ray computed tomography. *IEEE Trans Med Imaging* 37:1370–1381. <https://doi.org/10.1109/TMI.2018.2823083>
58. Withers PJ (2007) X-ray nanotomography. *Mater Today* 10:26–34. [https://doi.org/10.1016/S1369-7021\(07\)70305-X](https://doi.org/10.1016/S1369-7021(07)70305-X)



## Mapping the Distribution of Additives Within Polymer Films Through Near-Infrared Spectroscopy and Hyperspectral Imaging

Jussara V. Roque, Cícero C. Pola, Larissa R. Terra, Taíla V. Oliveira, Reinaldo F. Teófilo, Carmen L. Gomes, and Nilda F. F. Soares

### Abstract

Near-infrared (NIR) spectroscopy and hyperspectral imaging allow the study of spectral and spatial distribution of multiple chemical components in large sample areas. This technique is fast, non-destructive, contactless, and does not require sample preparation. The NIR spectrum of each sample pixel is acquired, resulting in a data cube that contains two spatial dimensions ( $x$  and  $y$ ) and one spectral dimension ( $z$ ), providing the spectral profiles of every part of the sample. This technique, for example, can provide significant information about the distribution of additives into polymer matrices with potential to be used as a tool for real-time quality control. Herein, the stepwise application of this method is demonstrated for determination of spatial and spectral distributions of film components, showcasing the plasticization of a biodegradable packaging.

**Key words** NIR-HSI, MCR-ALS, Chemical distribution, Chemical mapping, Macropixel, Homogeneity index, Polymer characterization

---

## 1 Introduction

Pristine polymers often show poor processability, physicochemical properties, and performance, limiting most of their applications in packaging. Such limitations are even more prominent when biopolymers are used. Additives, polymer blends, and composites are some of the most common strategies to overcome these technological hurdles [1–3]. The incorporation of additives, such as fillers, plasticizers, antistatics, stabilizers, and colorants into polymeric materials may improve their processability and tune their properties, making them suitable for packaging production [4–6].

Mechanical strength, gas barrier (check Part II for packaging as barrier materials), and thermal resistance are some of the properties that can be drastically affected by the incorporation of additives



[3]. Moreover, active properties can be acquired by the material with the incorporation of a specific class of additives, such as antimicrobial and antioxidant compounds [7] (check Part III for details on active roles played by food packaging). However, in all cases, the distribution and dispersion of the additive within the polymer matrix are critical for reaching the desired properties. Miscibility and aggregation problems can compromise the distribution of added compounds into the host polymer causing phase separation over time, which leads to undesirable changes and diffusion of the additive toward the material surface [8, 9]. Hence, knowing how the additive is distributed throughout the material becomes as important as its incorporation. Several high-sensitivity techniques have become available to study additives in polymeric matrices [9–13]. However, most of these techniques are costly, limited to small sampling areas, and require long sampling times and laborious sample preparations. Consequently, these are often unsuitable for real-time analysis [9, 10].

One way to simultaneously obtain spectral and spatial information is to use near-infrared spectroscopy (NIR) associated with hyperspectral imaging (HSI). NIR-HSI is a fast, contactless, non-destructive, and relatively low-cost technique (*see Note 1*) that does not require sample preparation and does not generate chemical waste [9, 14]. This technique provides chemical and spatial information on multiple chemical components in large sampling areas, even when in movement, making it suitable for real-time analysis [15–18].

NIR-HSI divides the entire sample area into individual pixels. For each pixel an NIR spectrum is acquired, which results in a data cube, containing multiple spatially co-registered spectra, with two spatial dimensions ( $x$  and  $y$ ) and one spectral dimension ( $z$ ), providing the spectral profiles of every part of the sample [9, 14, 16, 18, 19]. Hence, each pixel spectrum can be used to predict a map of the sample features (physical, chemical, or categorical) at the corresponding spatial location [20, 21]. Chemometric tools using multivariate data analysis play a fundamental role in extracting, treating, and displaying NIR-HSI information from the acquired data [16, 22]. Specifically, for NIR-HSI data, Multivariate Curve Resolution—Alternating Least Square (MCR-ALS) is one of the best choices for extracting chemical and spatial information. MCR is a bilinear model suitable for solving compound mixtures, in which the curve resolution method assumes that the observed spectra are linear combinations of the pure component spectra [22, 23]. The number of components in the mixture is determined or given by previous knowledge, then an estimation of the concentration and/or spectral profiles for each component is obtained. The ALS algorithm finds the optimum convergence among the components using different constraints (e.g., non-negativity,

unimodality, closure, and local rank) to obtain the optimum resolution and improve interpretation [22].

In this context, NIR-HSI techniques have been applied in several areas, such as agriculture [13, 24–26], pharmaceuticals [27–29], forensics [30–32], and food science [33–37]. However, studies involving NIR-HSI applications for packaging are still limited. Amigo et al. [10] demonstrated the potential of this technique and the steps required for the real-time detection of plastic materials containing flame-retardant additives. Recently, Terra et al. [9] determined the spatial distribution of four different plasticizers and sorbic acid within cellulose acetate-based biodegradable films. Herein, the stepwise application and suitability of this method are demonstrated for the determination of spatial and spectral distributions of additives into a polymeric matrix with the potential to be used for food packaging applications. A biodegradable cellulose acetate-based film incorporated with glycerol as a plasticizer is used to illustrate the application of this method.

---

## 2 Materials

### 2.1 Film Components

NIR-HSI method can be applied to all sorts of polymeric films used for food packaging applications [9]. Hence, the required materials are solely dependent on the type of film that will be evaluated. The use of high-quality grade chemicals is recommended. Each pristine component of the film is also indicated to be measured as a standard to provide the spectrum of the pure component required by the MCR-ALS. In this protocol, cellulose acetate, glycerol, and acetone are used for film production.

### 2.2 Instrumentation

Several camera systems are available for HSI acquisition. Our protocol is relied on the SisuCHEMA (Specim<sup>®</sup>, Oulu, Finland) chemical imaging system. SisuCHEMA is a complete chemical imaging workstation that combines NIR spectroscopy, optimized for short wave infrared (SWIR) (1000–2500 nm wavelength region), with high-resolution imaging, to provide detailed information on the chemical components, their quantities, and distributions within the sample [38] (*see Note 2*). The system consists of a line-scan imaging spectrometer equipped with a two-dimensional HgCdTe detector, which has 320 space channels and 256 spectral channels covering the 928–2524 nm wavelength range with a spectral resolution of approximately 6.3 nm [38].

### 2.3 Software

The chemical image workstation is controlled using ChemaDAQ<sup>™</sup> data acquisition software (Specim, Oulu, Finland), which allows the user to export the acquired NIR-HSI hypercubes directly as a MATLAB Data Cube file (.mat). NIR-HSI processing can be carried out in several ways, which depends on the operator

preferences. Any programming language can be used for this purpose and several algorithms and packages to perform this processing are available. Here, we propose the use of MATLAB (The MathWorks, Co., Natick, MA, USA) as the software to process the images and extract the chemical information. An algorithm package for MATLAB (*HSIAnalyzer*) was developed to perform NIR-HSI analysis. This package is available at <https://github.com/jussararoque/HSIAnalyzer> and from the authors upon request.

---

## 3 Methods

### 3.1 Film Production

A cellulose acetate film is used here as an example of the NIR-HIS application. This film is produced by mixing 2.5 g of cellulose acetate with 25 mL of acetone and 1.2 mL g<sup>-1</sup> of glycerol for 24 h in a closed container at room temperature [9]. Then, this film-forming formulation is poured and spread onto a glass plate using a paint applicator and allowed to dry for 2 h at room temperature (*see Note 3*). Finally, the films are peeled off the glass plates, inspected for defects, and stored in vacuum-sealed polyethylene/nylon bags until further use (*see Notes 4 and 5*). Before NIR spectra acquisition, films are placed onto a polytetrafluoroethylene (PTFE) plate and securely attached using an adhesive tape (*see Note 6*).

### 3.2 Image Acquisition

A HSI system is usually composed of a sample holder, a light unit, a light scattering device (spectrograph), a camera (detector), and a computer equipped with the image acquisition software. Optical radiation can interact with the sample through several mechanisms, depending on the light source arrangement, the sample, and the detector. The frequently observed mechanisms are transmittance, transreflectance, diffuse reflectance, interactance, and diffuse transmittance [39–41], which are illustrated in Fig. 1.

Transmittance (Fig. 1) is usually possible in transparent samples, where the incident light is partially absorbed by the sample, and the remaining light is detected without any scattering. In transreflectance (Fig. 1), the incident light goes through the sample, reaches a reflective apparatus, and goes back through the sample, increasing the optical path. For solid samples, the most common mechanism is diffuse reflectance (Fig. 1). In this mechanism, the radiation interacts with solid components of the sample, being dispersed and absorbed by them, which changes the intensity of the signal analyzed. In the interactance mechanism (Fig. 1), the incident light presents a higher probability of strong interaction with the sample, which leads to an emerging beam containing more information about the actual sample composition. The diffuse transmittance (Fig. 1) is the transmittance measurement applied to the dense solid samples, in which the light is internally scattered due to the sample's long optical path [40].

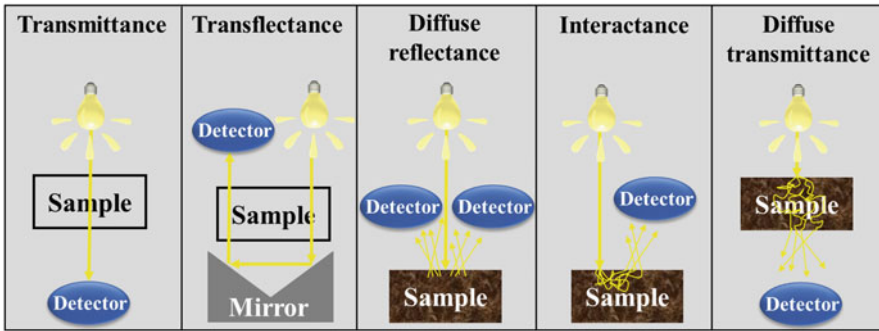


**Fig. 1** Examples of the interaction mechanisms between optical radiation and sample: transmittance; transreflectance; diffuse reflectance; interactance, and diffuse transmittance

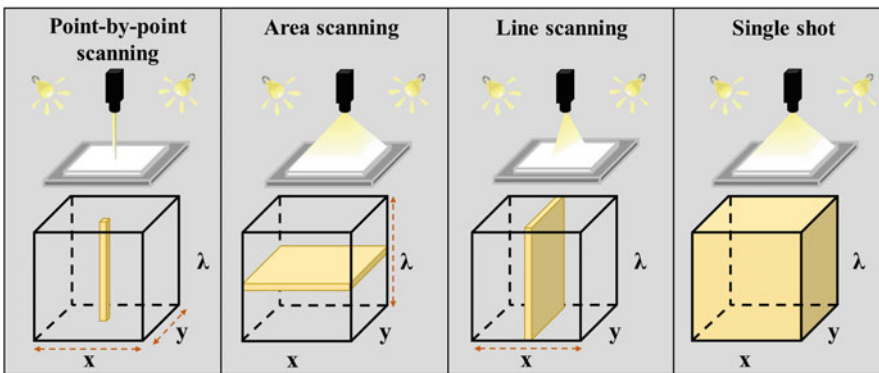


**Fig. 2** Acquisition modes of an HSI: point-by-point scanning, area scanning, line scanning, and single shot. The scanning directions are shown by arrows, and the yellow areas show data acquired each time. Sample film is shown on top of PTFE platform. Adapted from Wu and Sun [17] with permission from Elsevier

In film analysis, reflectance is the primary mechanism involved; however, transreflectance can also occur since the films are usually thin and have a certain level of transparency [9]. Depending on the mechanism applied, the attenuation of light when interacting with the sample can be reflectance ( $R$ ) or transmittance ( $T$ ), which are easily transformed into absorbance ( $\log 1/R$  or  $\log 1/T$ ) for chemometrics analysis. In NIR-HSI, a NIR spectrum is obtained for each pixel in which the object is divided to obtain the hypercube ( $x, y, z$ ). There are four convenient methods to obtain an HSI, based on the relative movement between the sample and the detection unit: point-to-point scanning, line scanning, area scanning, and single shot [17]. Figure 2 illustrates these acquisition modes.

The line scanning (Fig. 2) is the most used in the literature. In this case, spectra are obtained simultaneously from an entire line of pixels in the sample, and a complete hypercube can be obtained by moving the sample or the detector along the  $x$ -axis, similar to being placed in conveyor belt systems, which is ideal for industrial applications.

In the next section, the focus will be on the step-by-step analysis of film components' spatial distribution using the NIR-HSI obtained by using a SisuCHEMA (Specim<sup>®</sup>) chemical imaging system. The system employs an OLE15 lens with a 200 mm field of view resulting in a pixel size of 625  $\mu\text{m}$  (200 mm/320 spatial channels) in the  $x$ -direction (horizontal direction) (*see Note 7*). Hence, if 100 frames per second are used, the acquisition time of each frame is 0.01 s. Thus, to maintain the pixel proportionality in the  $y$ -direction (vertical direction), the distance of 625  $\mu\text{m}$  must be traversed in 0.01 s. Therefore, the scanning speed of 62.5  $\text{mm s}^{-1}$  must be chosen. Always ensure that the edges of the pixels are proportional by choosing the correct scanning velocity. Then, the hypercubes obtained by this system are 256 images (one image per wavelength) composed of 625  $\mu\text{m} \times 625 \mu\text{m}$  pixels. The total number of pixels per image changes according to the image size. The instrument itself performs the calibration of incident light, obtained using white and dark references.

For the study of spatial distribution of films with known composition, wherein a standard sample of each component is available, a NIR-HSI of each pure component standard must be acquired separately for further analysis by curve resolution methods (*see Note 8*).

### 3.3 Data Pretreatment

Once the NIR-HSI images are acquired, the hypercubes may be imported to MATLAB software. The raw NIR-HSI is a hypercube ( $x, y, z$ ) composed of millions of data points (e.g., a film NIR-HSI of 350  $\times$  200 pixels operating at 256 wavelengths contains more than 17 million data points). The  $xy$  plane is divided into regular squares, called pixels, containing chemical information represented by NIR spectra in the  $z$  dimension (Fig. 3). Such an amount of

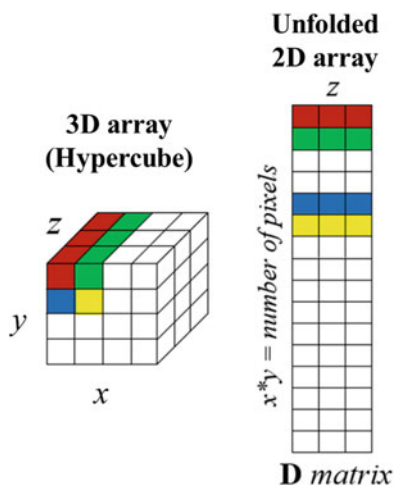


**Fig. 3** NIR-HSI data as a three-dimensional array (hypercube), and an unfolded two-dimensional array

information requires significant storage space and may make the data analysis more time-consuming. Thus, methods of data compression are frequently applied to reduce the data amount. This data reduction can be done both in the spectral or spatial dimension [42].

The application of pretreatment techniques is important to eliminate unwanted variations present in the raw data without compromising the analytical information. Initially, a dark and white correction is recommended and can be performed using a dark reference image, obtained with the light source turned off, and a white reference image obtained from a surface with maximum reflectance. The SisuCHEMA system performs the light calibration automatically, acquiring both white and dark references (*see Note 9*). After image collection, the image is usually reduced in the spatial dimension ( $x, y$ ) to require less storage space and reduce data analysis time. In most cases, the use of the entire image is not required, so regions of interest (ROIs) can be selected from the raw image to be used in the data analysis. After acquiring the *HSIAnalyzer* toolbox, the following steps can be performed.

- Add the *HSIAnalyzer* to MATLAB set path.
- Load the *SampExample.mat* (NIR-HSI of cellulose acetate film incorporated with glycerol):

```
» load ('SampExample.mat')
```

- Use *plotsi* and *selroi* functions to perform the ROIs selection. First, the image must be visualized (Fig. 4a):

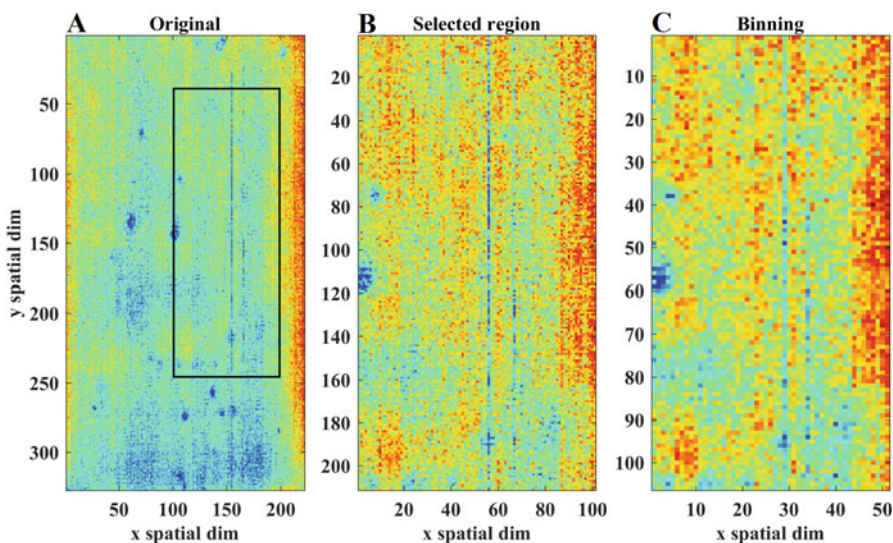


**Fig. 4** NIR-HSI image processing. (a) Original NIR-HSI image with selected ROI; (b) Selected region of NIR-HSI image; and (c) Binned NIR-HSI image

```
>> plothsi (HSI)
```

where *HSI* is a NIR-HSI image ( $x, y, z$ ).

- In figure plot, the zoom tool can be used to select the ROI. Then, the following command can be used:

```
>> HSIsel = selroi (HSI);
```

where *HSIsel* is a NIR-HSI image ( $x, y, z$ ) with the ROI selected (Fig. 4b).

Next, the removal of dead pixels, which are missing values in some pixels caused, for instance, by a dysfunction of one of the diodes in the detector array, is recommended since this is a common issue in NIR-HSI images [42]. Dead pixels can be removed by simple interpolation using the mean or median of the neighboring pixels. The *rmvdeadpx* function can be used to perform the removal of dead pixels.

- In the MATLAB environment

```
>> HSIcorr = rmvdeadpx (HSIsel, type);
```

where *HSIcorr* is a NIR-HSI image ( $x, y, z$ ) with dead pixels removed and *type* can be the removal of dead pixels by “mean” or “median” of the neighboring pixels.

Data binning is another technique frequently applied for spatial dimension reduction. In this technique the original values or pixels from a specific interval are replaced with a representative value of the same interval. The original pixels are replaced by an average value in our algorithm.

- In the MATLAB environment:

```
>> HSIbin = binning (HSIcorr, bin);
```

where *HSIbin* is a NIR-HSI image ( $x, y, z$ ) binned by bin size defined by bin input (Fig. 4c).

Because NIR spectra usually present overlapping bands, chemometric methods are required to extract the chemical information in NIR-HSI, which is contained in the spectral dimension. However, before applying these chemometric methods, it is important to consider the use of spectral pretreatments to remove data

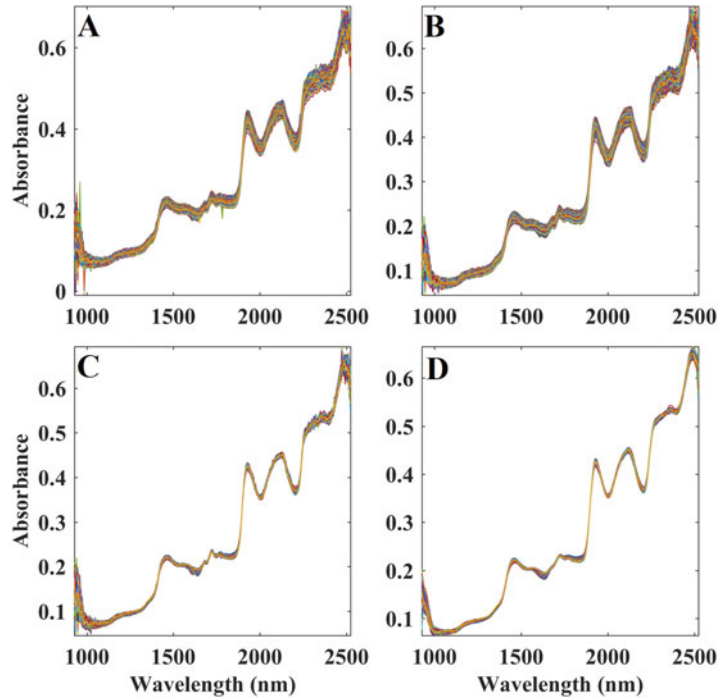


**Fig. 5** Spectral pretreatments examples. (a) Spectra of all pixels without any spectral pretreatment; (b) Spectra with spikes removed; (c) Spectra with MSC smoothing; and (d) Spectra Savitzky-Golay smoothing ( $win = 11$ )

anomalies, correct baseline and scattering to enhance the spectral characteristics.

Spikes are one of the most common anomalies that can mask real information and could lead to misleading interpretation. Spikes can be defined as a sudden and abrupt rise followed by a sharp decline in the spectrum. Spikes removal can be done by pixel comparison in the hypercube arrangement, as follows:

- In the MATLAB environment:

```
» HSIspi = rmvspike(HSIbin,win);
```

where *HSIspi* is a NIR-HSI image ( $x, y, z$ ) without spikes (Fig. 5b) and *win* (5) is the pixel window to do spike search.

Because the chemical information is present in a spectral dimension, bilinear chemometric methods are usually applied. Thus, the three-dimensional array must be unfolded to a bilinear matrix  $\mathbf{D}$  ( $x^*y, z$ ), according to Fig. 3. In this new arrangement, the spectra from pixels are the rows and the wavelengths ( $z$  dimension) are the columns. The unfolding can be performed by the following command:



- In the MATLAB environment:

```
➤ D = unfoldhsi(HSIspi, samp);
```

where *D* is a matrix containing all pixels ( $x^*y, z$ ), and *samp* is the number of samples vertically concatenated.

Several spectral correction methods can be applied to enhance spectral characteristics [43]. Standard normal variate (SNV) and multiplicative scatter correction (MSC) are frequently used to correct NIR light scattering. Smoothing methods are commonly used to reduce instrumental noise. Baseline and slope offset are usually corrected by using Savitzky-Golay derivatives, baseline corrections, and detrend approaches. However, this process must be applied carefully, without losing important chemical information. All the spectral pretreatments must be applied in the two-dimensional array. In the example presented here, MSC and Savitzky-Golay smoothing are used on the **D** matrix through the commands presented below:

- In the MATLAB environment:

```
➤ Dmsc = msc(D, type);
```

where *Dmsc* is the matrix corrected (Fig. 5c) and *type* can be the correction by “mean” or “median” of spectra. Here the median spectrum is used as reference:

```
➤ Dsmoo = svtgl(Dmsc, win);
```

where *Dsmoo* is the corrected matrix (Fig. 5d) and *win* (11) is the variables window to be smoothed. Once pretreatment methods are performed, we can proceed to the image treatment.

After all the required pretreatment, the multivariate methods must be applied to the **D** matrix to extract the main information about the image components.

### 3.4 Image Treatment

Multivariate calibration and curve resolution are the most common methods used to quantify all the pixels' constituents in hyperspectral images. Partial least squares (PLS) are the most used method from multivariate calibration. Initially, the calibration samples are used to build a model, which is required to quantify the constituents of all pixels. MCR-ALS is a curve resolution method that can directly quantify the constituents of all pixels in hyperspectral images without calibration samples. These two methods are discussed in the next sections.

### 3.4.1 Partial Least Squares (PLS)

Initially, a calibration set needs to be created. At least ten calibration samples with known bulk concentrations of all components of interest must be prepared. Then, each mean spectra of pretreated and unfolded image ( $\mathbf{D}$  matrix) must be calculated. Next, the mean spectra of the entire calibration set and the respective bulk concentration of each component are used to build the PLS model. The PLS model is based on equation  $\mathbf{y} = \mathbf{X}\mathbf{b}$ , where  $\mathbf{y}$  can be either a vector with the concentration of a component or a  $\mathbf{Y}$  response matrix with the concentration of several components simultaneously [44]. The  $\mathbf{X}$  matrix is composed of the mean spectra of each calibration sample. The  $\mathbf{X}$  and  $y$  variables can be mean-centered to build a PLS model using leave-one-out cross-validation to choose the number of latent variables. From the developed models, a regression vector  $\mathbf{b}$  is obtained and by multiplying an unfold  $\mathbf{D}$  matrix with spectra of all pixels by  $\mathbf{b}$  ( $\mathbf{D}^*\mathbf{b}$ ), components' concentration of all pixels can be predicted in new samples. The concentration is a vector or matrix  $\mathbf{C}$  ( $x^*y, n$ ), depending on the number of components ( $n$ ), which can be used to generate distribution maps. This step will be further explained in Subsection 3.4.2.

Additionally, a small validation set (e.g., five samples) can be prepared for external validation of the PLS model. Moreover, variable selection methods can be used to enhance the PLS model and to reduce the spectral dimension ( $z$ ). Genetic algorithm (GA) [45], ordered predictors selection (OPS) [46, 47], interval partial least squares (*i*PLS) [48], and successive projection algorithm (SPA) [49] are variable selection methods described in the literature to improve PLS model predictions.

Notably, for the current example illustrating the use of NIR-HSI it is not possible to perform PLS, since there is only one sample. However, an algorithm package for MATLAB to build PLS (*PLSpack*) is also available upon request, as mentioned previously.

### 3.4.2 Multivariate Curve Resolution with Alternating Least Squares (MCR-ALS)

The MCR-ALS method is based on the bilinear equation  $\mathbf{D} = \mathbf{C}\mathbf{S}^T + \mathbf{E}$ , where  $\mathbf{D}$  is the unfolded matrix ( $x^*y, z$ ),  $\mathbf{C}$  is the concentrations' matrix,  $\mathbf{S}$  is the pure components' matrix, and  $\mathbf{E}$  is the error matrix. In order to find the  $\mathbf{C}$  matrix and build distribution maps, MCR-ALS requires an initial estimation of  $\mathbf{S}$  to iteratively solve the equations  $\mathbf{C} = \mathbf{D}\mathbf{S}(\mathbf{S}^T\mathbf{S})^{-1}$  and  $\mathbf{S}^T = (\mathbf{C}^T\mathbf{C})^{-1}\mathbf{C}^T\mathbf{D}$ . This process is performed until a convergence criterion is achieved, which can be defined by the maximum number of iterations or when the difference between results of consecutive iterations is lower than a predefined value [50].

During the optimization of the MCR-ALS method, the application of constraints is highly recommended due to its rotational ambiguity, that is, more than one response can be found in a resolution of the bilinear equation. The commonly applied

constraints are non-negativity, unimodality, closure, and local rank information [50].

MCR-ALS can be applied directly to the samples of interest, without requiring a previous calibration. However, it is necessary to know the pure spectra of each component of interest present in the sample. Such information is critical to find the **C** matrix and to build the distribution maps. The MCR-ALS 2.0 toolbox is available at <https://mcrals.wordpress.com/download/mcr-als-2-0-toolbox/> [50].

The sample used as an example here is a thin film placed over a PTFE support for NIR spectrum acquisition. The NIR radiation crossed through the sample capturing information of the thin film and the PTFE support. Therefore, PTFE spectra were also obtained to be used as pure spectra in MCR-ALS resolution as it is considered a component of the film NIR image.

The pure spectra are used for initial estimation in MCR-ALS (**S** matrix) and are also incorporated into the **D** matrix (vertically concatenated).

In the MATLAB environment:

- Add the *MCR-ALS 2.0* toolbox in MATLAB set path.
- Load the *StandExample.mat* (containing NIR-HSI images of all known individual components, called standards):

```
>> load('StandExample.mat')
```

Sometimes, it is not possible to obtain the standard NIR-HSI images. In this case, the pretreated **D** matrix can be used directly in MCR-ALS and the initial estimation can be done using the MCR-ALS 2.0 toolbox. Furthermore, the use of column-wise augmented matrix—that is, multiple matrices obtained from films with the same components in different proportions—helps to obtain more accurate results since greater variability is included in the data set.

When the standards are available, the following steps are recommended in MATLAB:

- Unfold NIR-HSI images of each standard component.

```
>> Dace = unfoldhsi(HSIace,1);
```

```
>> Dgli = unfoldhsi(HSIgli,1);
```

```
>> Dtef = unfoldhsi(HSItef,1);
```

It is important to highlight the application of spectral pretreatments on the standard spectra. The application of the same spectral pretreatment in each standard spectra of  $\mathbf{D}$  matrix is mandatory only when the spectral profile is modified, for instance, when the first or second derivative is applied. In this example, the application of the same pretreatments on  $\mathbf{D}$  matrix was evaluated. Better results were obtained without pretreatments. Then, the application of the spectral pretreatments must be evaluated for each dataset. Here, better results were obtained without pretreatments. Hence, the application of the spectral pretreatments must be evaluated for each dataset:

- Calculate the average spectra to be used as initial estimation:

```
>> pure_spectra = [mean(Dace); mean(Dgli); mean(Dtef)];
```

- Concatenate the film pretreated  $\mathbf{D}$  matrix with the  $\mathbf{D}$  matrices of all standards:

```
>> Dmcr = [Dsmoo; Dace; Dgli; Dtef];
```

Then, the *mcr\_main* command can be used to initiate the MCR-ALS 2.0 toolbox. The *Dmcr* is the data matrix to be selected. The number of components can be informed manually (three in this example). The *pure\_spectra* are used as the initial estimation. The non-negativity concentration must be selected by implementation of *fnls* with all components presenting non-negativity profile. The normalization with the spectra divided by Euclidean norm must be used. The number of interactions must be set as 100 and convergence criterion as 0.01. The outputs of MCR-ALS analysis are the recovered spectra (*sopt* output or  $\mathbf{S}$  matrix) and concentration (*copt* output or  $\mathbf{C}$  matrix) of all components. More information about the MCR-ALS 2.0 toolbox can be found in Jaumot et al. [50].

The MCR-ALS results of the example presented here are available at *ResultExample.mat*.

- On MATLAB environment:

```
>> load('ResultExample.mat')
```

The recovered NIR spectra by MCR-ALS for all components are presented in Fig. 6 (blue dashed line) in comparison with pure NIR spectra of all constituents (red solid lines).

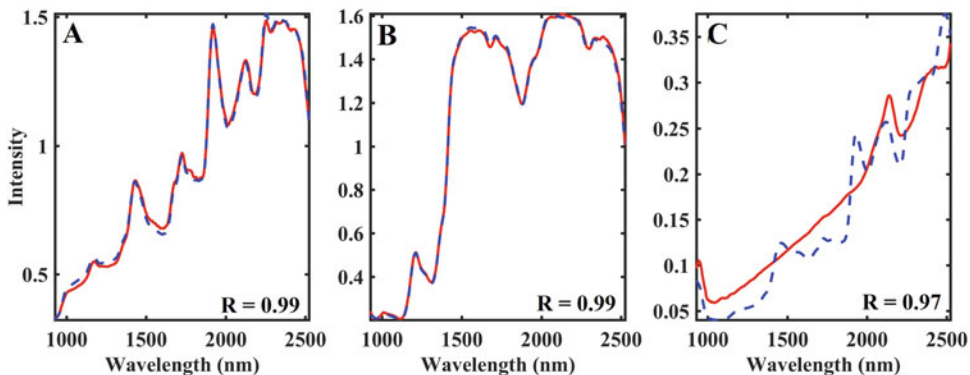


**Fig. 6** MCR-ALS recovered NIR spectra profile (blue dashed lines) compared to the standards' profile of each component (red solid lines) and the correspondent correlation coefficient (R) for cellulose acetate (a), glycerol (b), and PTFE (c)

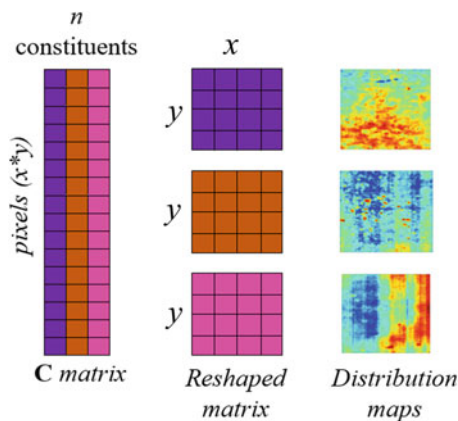


**Fig. 7** Reshape of **C** matrix and building of distribution maps

This comparison can be obtained by *compspec* function using the following command in MATLAB:

```
>> spec = compspec (sopt,pure_spectra, w);
```

where *spec* is the normalized spectra, and *w* is the wavelength range.

3.4.3 Distribution Maps and Homogeneity Analysis

Regardless of the method used to obtain the concentrations of the components of interest, distribution maps can be obtained by reshaping the relative intensity of the **C** matrix for each component (Fig. 7).

The reshaping of **C** matrix into distribution maps can be obtained by *distmaps* function using the following command in MATLAB:

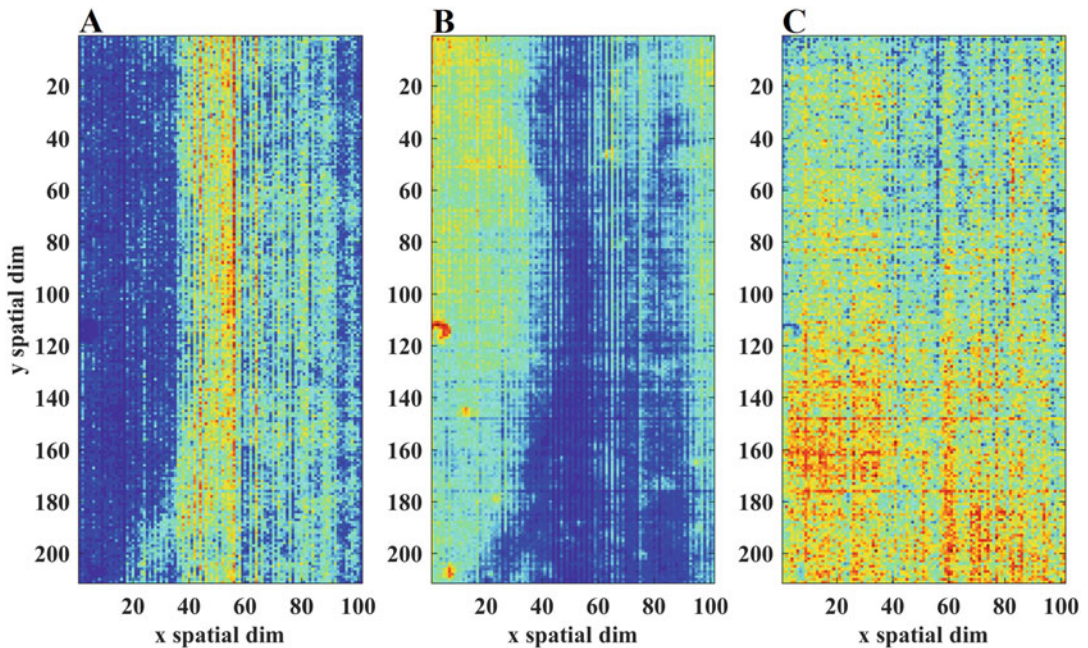


**Fig. 8** Distribution maps of cellulose acetate (a), glycerol (b), and PTFE (c)

- Reshaping the **C** matrix unfold NIR-HSI images of each standard:

```
» Ximg = distmaps (copt,m,n);
```

where *Ximg* is the cell output containing the distribution maps of all components, *m* (rows) and *n* (columns) are the spatial dimension of NIR-HSI image before unfolding (*HSIspi*). Figure 8 shows the distribution maps of each component.

Next, the homogeneity of the image can be evaluated through macropixel analysis. The homogeneity concept is related to the random distribution of the components in the image. First, an image must be split into non-overlapping square pixels. Then, the macropixel is calculated by the intensity of the average of all pixels and the homogeneity parameters can be calculated. These homogeneity parameters are obtained by comparing a real image with a random version obtained from the same pixels, which allows the calculation of a homogeneity index [9].

In the present example, the *Ximg* of each component was divided into  $10 \times 10$  pixels, which was then used to calculate the macropixel:

```
» Macro1 = macroindex (Ximg{1,1}, mpsize);
```

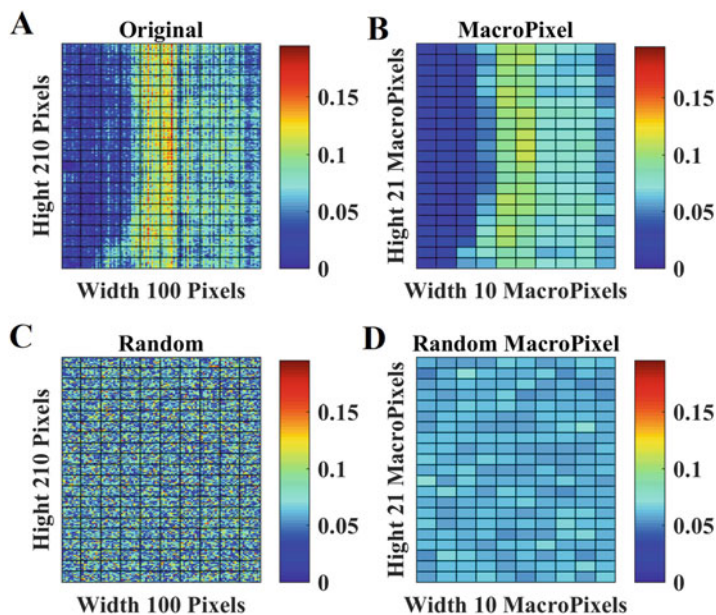


**Fig. 9** Macropixel analysis of cellulose acetate. (a) Distribution map of cellulose acetate concentration; (b) Macropixel of distribution map of cellulose acetate; (c) Random distribution map of cellulose acetate; and (d) Macropixel of random distribution map of cellulose acetate

```
» Macro2 = macroindex (Ximg{2,1}, mpsize);
```

```
» Macro3 = macroindex (Ximg{3,1}, mpsize);
```

where *Macro1*, *Macro2*, and *Macro3* are struct outputs with the macropixel image and homogeneity indexes of each component. Macropixel size is defined by *mpsize* input. Figure 9 shows an example of the results generated by the *macroindex* function.

The obtained homogeneity index is the homogeneity ratio of Poole (*H%Poole*). As this index gets closer to 100, the distribution of the components in the image, or in this case in the film, becomes more random (*see Note 10*). For the cellulose acetate, glycerol, and PTFE example, the indexes obtained were 62%, 52%, and 82%, respectively, emphasizing heterogeneous distribution of cellulose acetate and glycerol, that is, in the film composition, since PTFE is only the support.

## 4 Notes

1. The most significant cost associated with NIR-HIS analysis is obviously related to the instrument acquisition, such as

NIR-HIS chemical imaging system. High processing capabilities computers might be required for large datasets.

2. One of the main limitations of NIR-HSI is associated with its sensitivity, which can make difficult to differentiate spectra of highly homogeneous samples [14]. Hence, some degree of heterogeneity is required, since the difference in each pixel spectrum is used to identify and locate the chemical species present in the polymeric matrix. The limit of detection associated with this method depends mainly on the NIR capabilities, and it is generally around 0.1 wt% [40].
3. Film thickness plays an important role in the data acquisition since it can affect the signal intensity. Polymeric films with thickness ranging from 45 to 150  $\mu\text{m}$  have been successfully analyzed using NIR-HSI by our group.
4. Conditioning of the films is recommended before the NIR-HSI acquisition. Conditioning procedures are carried out to bring the material to an equilibrium state with reproducible conditions. The American Society for Testing and Materials (ASTM) D618-13 standard [51] describes the practice for conditioning plastics for testing and it is recommended before NIR-HSI data collection. Basically, the samples should be kept at  $23 \pm 2$  °C and  $50 \pm 2\%$  of relative humidity for at least 24 h before analysis.
5. Image treatment requires a uniform film sample. The presence of holes, bubbles, wrinkles, or other defects in the film sample limits NIR-HSI analysis. For instance, the stacking sequence and thickness of the structure can affect the detection and representability of the method. Combinations of vibrational modes are important information of NIR spectroscopy, which are dependent on the compounds distribution and are directly affected by the presence of defects, which might lead to band overlapping, displacement, or disappearance [40]. Flat samples still result in some light loss due to reflections at interfaces, such as the air-sample interface; however, the magnitude of this is usually rendered negligible compared to the absorbance of light by the sample. When scattering occurs, the light that does not reach the detector is still interpreted as absorbance even though it was not absorbed by the sample [52]. This scattering effect can be increased when the infrared light strikes the defects.
6. Before analysis, film samples can be accommodated in a support to avoid possible movement and to guarantee that the sample is lying flat and to avoid any wrinkles or fold marks. PTFE can be successfully used as support and an adhesive tape can be used to securely attach the sample onto the support.



Concomitantly, it is important to preserve the film integrity and avoid excessive stretching tension to the sample.

7. SisuCHEMA system can analyze samples up to  $200 \times 300 \text{ mm}^2$ , which allows the evaluation samples with variables sizes. This system can image samples from 10 mm at 30 microns pixel resolution up to 100 mm at 300 microns resolution [38].
8. The collection of the pure component spectra is crucial to perform the NIR-HSI analysis. Film components are available in the liquid, powder, or pellet form. In this case, blank film sample (without any additive) could be used. When blank film samples cannot be produced, the spectra of each component could be acquired separately. If possible, the pure component spectra should be collected following the same method as for the film samples. For that, it is important to prepare this pure component sample using a similar support on which the individual component samples are uniformly placed.
9. Some instruments might require manual acquisition of the dark and white references. According to Amigo and Grassi [53], this calibration could be performed by taking an image of a dark and a white reference. The dark reference can be obtained by turning off the light sources or covering the camera with a non-reflective opaque black cap. The white reference can be acquired by measuring a uniform, high-reflectance standard or white ceramic. Then, the relative reflectance image can be obtained by subtracting the raw spectral image from the dark and dividing the result by the difference between the white and dark references. Refer to Amigo and Grassi [53] for more detail.
10. Despite being herein showcased with a biodegradable polymer, the presented method can be applied to analyze any polymeric film.

---

## Acknowledgments

The authors are grateful for the financial support of Conselho Nacional de Desenvolvimento Científico e Tecnológico (CNPq), Fundação de Amparo à Pesquisa do Estado de Minas Gerais (FAPEMIG), and Coordenação de Aperfeiçoamento de Pessoal de Nível Superior—Brasil (CAPES)—Finance Code 001. We also thank Cristiane Vidal for the experimental support in the HSI acquisition and Prof. Celio Pasquini for promptly receiving us in the laboratory that he coordinates (Grupo de Instrumentação e Automação em Química Analítica, Instituto de Química, Universidade Estadual de Campinas, Campinas-SP, Brazil) to obtain

the images. C. L. G. and C. C. P. gratefully acknowledge funding support from National Science Foundation under award numbers CBET-1756999. C. L. G. and C. C. P. also acknowledge the National Institute of Food Agriculture, US Department of Agriculture, award numbers 2021-67017-33344, 2020-67021-31375, and 2018-672 67016-27578 awarded as a Center of Excellence for financial support.

## References

- Pfaendner R (2006) How will additives shape the future of plastics? *Polym Degrad Stab* 91(9):2249–2256. <https://doi.org/10.1016/j.polymdegradstab.2005.10.017>
- Rabello M (2000) Aditivaco de polmeros. Artliber
- Rabello M, De Paoli M (2013) Aditivaco De Termoplasticos. Artliber
- Ambrogi V, Carfagna C, Cerruti P, Marturano V (2017) Chapter 4 – Additives in polymers. In: Jasso-Gastinel CF, Kenny JM (eds) *Modification of polymer properties*. William Andrew Publishing, pp 87–108. <https://doi.org/10.1016/B978-0-323-44353-1.00004-X>
- Groh KJ, Backhaus T, Carney-Almroth B, Geueke B, Inostroza PA, Lennquist A, Leslie HA, Maffini M, Slunge D, Trasande L, Warhurst AM, Muncke J (2019) Overview of known plastic packaging-associated chemicals and their hazards. *Sci Total Environ* 651: 3253–3268. <https://doi.org/10.1016/j.scitotenv.2018.10.015>
- Harper CA, Harper C (2006) *Handbook of plastics technologies: the complete guide to properties and performance*. McGraw-Hill Education
- Han J-W, Ruiz-Garcia L, Qian J-P, Yang X-T (2018) Food packaging: a comprehensive review and future trends. *Compr Rev Food Sci Food Saf* 17(4):860–877. <https://doi.org/10.1111/1541-4337.12343>
- Avolio R, Castaldo R, Avella M, Cocca M, Gentile G, Fiori S, Errico ME (2018) PLA-based plasticized nanocomposites: effect of polymer/plasticizer/filler interactions on the time evolution of properties. *Compos Part B* 152:267–274. <https://doi.org/10.1016/j.compositesb.2018.07.011>
- Terra LR, Roque JV, Pola CC, Gonalves IM, Soares NFF, Tefilo RF (2020) Study of chemical compound spatial distribution in biodegradable active films using NIR hyperspectral imaging and multivariate curve resolution. *J Chemom* 34(1):e3193. <https://doi.org/10.1002/cem.3193>
- Amigo JM, Babamoradi H, Elcoroaristizabal S (2015) Hyperspectral image analysis. A tutorial. *Anal Chim Acta* 896:34–51. <https://doi.org/10.1016/j.aca.2015.09.030>
- Fraser DG, Jordan RB, Knnemeyer R, McGlone VA (2003) Light distribution inside mandarin fruit during internal quality assessment by NIR spectroscopy. *Postharvest Biol Technol* 27(2):185–196. [https://doi.org/10.1016/S0925-5214\(02\)00058-3](https://doi.org/10.1016/S0925-5214(02)00058-3)
- Li Q, Tang Y, Yan Z, Zhang P (2017) Identification of trace additives in polymer materials by attenuated total reflection Fourier transform infrared mapping coupled with multivariate curve resolution. *Spectrochim Acta A Mol Biomol Spectrosc* 180:154–160. <https://doi.org/10.1016/j.saa.2017.03.019>
- Li N, Taylor LS (2016) Nanoscale infrared, thermal, and mechanical characterization of telaprevir–polymer miscibility in amorphous solid dispersions prepared by solvent evaporation. *Mol Pharm* 13(3):1123–1136. <https://doi.org/10.1021/acs.molpharmaceut.5b00925>
- Manley M (2014) Near-infrared spectroscopy and hyperspectral imaging: non-destructive analysis of biological materials. *Chem Soc Rev* 43(24):8200–8214. <https://doi.org/10.1039/C4CS00062E>
- Calvini R, Ulrici A, Amigo JM (2020) Growing applications of hyperspectral and multispectral imaging. In: *Data handling in science and technology*, vol 32. Elsevier, pp 605–629
- De Juan A, Piqueras S, Maeder M, Hancewicz T, Duponchel L, Tauler R (2014) Chemometric tools for image analysis. In: *Infrared and Raman spectroscopic imaging*. Wiley-VCH, Weinheim, pp 57–110. <https://doi.org/10.1002/9783527678136.ch2>
- Wu D, Sun D-W (2013) Advanced applications of hyperspectral imaging technology for food quality and safety analysis and assessment: a review—Part I: fundamentals. *Innovative*

- Food Sci Emerg Technol 19:1–14. <https://doi.org/10.1016/j.ifset.2013.04.014>
18. Zhang C, Jiang H, Liu F, He Y (2017) Application of near-infrared hyperspectral imaging with variable selection methods to determine and visualize caffeine content of coffee beans. *Food Bioprocess Technol* 10(1):213–221. <https://doi.org/10.1007/s11947-016-1809-8>
  19. Prats-Montalbán JM, de Juan A, Ferrer A (2011) Multivariate image analysis: a review with applications. *Chemom Intell Lab Syst* 107(1):1–23. <https://doi.org/10.1016/j.chemolab.2011.03.002>
  20. ElMasry G, Sun D-W, Allen P (2012) Near-infrared hyperspectral imaging for predicting colour, pH and tenderness of fresh beef. *J Food Eng* 110(1):127–140. <https://doi.org/10.1016/j.jfoodeng.2011.11.028>
  21. Kamruzzaman M, Barbin D, ElMasry G, Sun D-W, Allen P (2012) Potential of hyperspectral imaging and pattern recognition for categorization and authentication of red meat. *Innovative Food Sci Emerg Technol* 16:316–325. <https://doi.org/10.1016/j.ifset.2012.07.007>
  22. Rodrigues e Brito L, Braz A, Saldanha Honorato R, Pimentel MF, Pasquini C (2019) Evaluating the potential of near infrared hyperspectral imaging associated with multivariate data analysis for examining crossing ink lines. *Forensic Sci Int* 298:169–176. <https://doi.org/10.1016/j.forsciint.2019.02.043>
  23. Piqueras S, Duponchel L, Tauler R, de Juan A (2011) Resolution and segmentation of hyperspectral biomedical images by multivariate curve resolution-alternating least squares. *Anal Chim Acta* 705(1):182–192. <https://doi.org/10.1016/j.aca.2011.05.020>
  24. Adam E, Mutanga O, Rugege D (2010) Multispectral and hyperspectral remote sensing for identification and mapping of wetland vegetation: a review. *Wetl Ecol Manag* 18(3):281–296. <https://doi.org/10.1007/s11273-009-9169-z>
  25. Lee H, Kim MS, Song Y-R, Oh C-S, Lim H-S, Lee W-H, Kang J-S, Cho B-K (2017) Non-destructive evaluation of bacteria-infected watermelon seeds using visible/near-infrared hyperspectral imaging. *J Sci Food Agric* 97(4):1084–1092. <https://doi.org/10.1002/jsfa.7832>
  26. Sun H, Zhang S, Chen C, Li C, Xing S, Liu J, Xue J (2019) Detection of the soluble solid contents from fresh jujubes during different maturation periods using NIR hyperspectral imaging and an artificial bee colony. *J Anal Methods Chem* 2019:5032950. <https://doi.org/10.1155/2019/5032950>
  27. Alexandrino GL, Poppi RJ (2013) NIR imaging spectroscopy for quantification of constituents in polymers thin films loaded with paracetamol. *Anal Chim Acta* 765:37–44. <https://doi.org/10.1016/j.aca.2012.12.017>
  28. Amigo JM, Cruz J, Bautista M, Maspoch S, Coello J, Blanco M (2008) Study of pharmaceutical samples by NIR chemical-image and multivariate analysis. *TrAC Trends Anal Chem* 27(8):696–713. <https://doi.org/10.1016/j.trac.2008.05.010>
  29. Carneiro RL, Poppi RJ (2014) Infrared imaging spectroscopy and chemometric tools for in situ analysis of an imiquimod pharmaceutical preparation presented as cream. *Spectrochim Acta A Mol Biomol Spectrosc* 118:215–220. <https://doi.org/10.1016/j.saa.2013.08.104>
  30. de la Ossa MAF, Amigo JM, García-Ruiz C (2014) Detection of residues from explosive manipulation by near infrared hyperspectral imaging: a promising forensic tool. *Forensic Sci Int* 242:228–235. <https://doi.org/10.1016/j.forsciint.2014.06.023>
  31. de la Ossa MAF, García-Ruiz C, Amigo JM (2014) Near infrared spectral imaging for the analysis of dynamite residues on human handprints. *Talanta* 130:315–321. <https://doi.org/10.1016/j.talanta.2014.07.026>
  32. Silva CS, Pimentel MF, Honorato RS, Pasquini C, Prats-Montalbán JM, Ferrer A (2014) Near infrared hyperspectral imaging for forensic analysis of document forgery. *Analyst* 139(20):5176–5184. <https://doi.org/10.1039/C4AN00961D>
  33. Weinstock BA, Janni J, Hagen L, Wright S (2006) Prediction of oil and oleic acid concentrations in individual corn (*Zea mays* L.) kernels using near-infrared reflectance hyperspectral imaging and multivariate analysis. *Appl Spectrosc* 60(1):9–16. <https://doi.org/10.1366/000370206775382631>
  34. ElMasry G, Wang N, ElSayed A, Ngadi M (2007) Hyperspectral imaging for nondestructive determination of some quality attributes for strawberry. *J Food Eng* 81(1):98–107. <https://doi.org/10.1016/j.jfoodeng.2006.10.016>
  35. Forchetti DAP, Poppi RJ (2017) Use of NIR hyperspectral imaging and multivariate curve resolution (MCR) for detection and quantification of adulterants in milk powder. *LWT Food Sci Technol* 76:337–343. <https://doi.org/10.1016/j.lwt.2016.06.046>
  36. Zhao J, Vittayapadung S, Chen Q, Chaitep S, Chuaviroj R (2009) Nondestructive measurement of sugar content of apple using hyperspectral imaging technique. *Maejo Int J Sci Technol* 3(1):130–142

37. Taghizadeh M, Gowen A, Ward P, O'Donnell CP (2010) Use of hyperspectral imaging for evaluation of the shelf-life of fresh white button mushrooms (*Agaricus bisporus*) stored in different packaging films. *Innovative Food Sci Emerg Technol* 11(3):423–431. <https://doi.org/10.1016/j.ifset.2010.01.016>
38. Specim (2015) SisuChema chemical imaging analyzer. [https://www.specim.fi/wp-content/uploads/2020/03/SisuCHEMA\\_2\\_2015.pdf](https://www.specim.fi/wp-content/uploads/2020/03/SisuCHEMA_2_2015.pdf). Accessed 12 Sept 2020
39. Cortés V, Blasco J, Aleixos N, Cubero S, Talens P (2019) Monitoring strategies for quality control of agricultural products using visible and near-infrared spectroscopy: a review. *Trends Food Sci Technol* 85:138–148. <https://doi.org/10.1016/j.tifs.2019.01.015>
40. Pasquini C (2003) Near infrared spectroscopy: fundamentals, practical aspects and analytical applications. *J Braz Chem Soc* 14:198–219
41. Pasquini C (2018) Near infrared spectroscopy: a mature analytical technique with new perspectives – a review. *Anal Chim Acta* 1026: 8–36. <https://doi.org/10.1016/j.aca.2018.04.004>
42. Vidal M, Amigo JM (2012) Pre-processing of hyperspectral images. Essential steps before image analysis. *Chemom Intell Lab Syst* 117: 138–148. <https://doi.org/10.1016/j.chemolab.2012.05.009>
43. Amigo JM, Santos C (2020) Chapter 2.1 – Preprocessing of hyperspectral and multispectral images. In: Amigo JM (ed) *Data handling in science and technology*, vol 32. Elsevier, pp 37–53. <https://doi.org/10.1016/B978-0-444-63977-6.00003-1>
44. Wold S, Sjöström M, Eriksson L (2001) PLS-regression: a basic tool of chemometrics. *Chemom Intell Lab Syst* 58(2):109–130. [https://doi.org/10.1016/S0169-7439\(01\)00155-1](https://doi.org/10.1016/S0169-7439(01)00155-1)
45. Leardi R, Lupiáñez González A (1998) Genetic algorithms applied to feature selection in PLS regression: how and when to use them. *Chemom Intell Lab Syst* 41(2):195–207. [https://doi.org/10.1016/S0169-7439\(98\)00051-3](https://doi.org/10.1016/S0169-7439(98)00051-3)
46. Roque JV, Cardoso W, Peternelli LA, Teófilo RF (2019) Comprehensive new approaches for variable selection using ordered predictors selection. *Anal Chim Acta* 1075:57–70. <https://doi.org/10.1016/j.aca.2019.05.039>
47. Teófilo RF, Martins JPA, Ferreira MMC (2009) Sorting variables by using informative vectors as a strategy for feature selection in multivariate regression. *J Chemom* 23(1): 32–48. <https://doi.org/10.1002/cem.1192>
48. Leardi R, Nørgaard L (2004) Sequential application of backward interval partial least squares and genetic algorithms for the selection of relevant spectral regions. *J Chemom* 18(11): 486–497. <https://doi.org/10.1002/cem.893>
49. de Araújo Gomes A, Galvão RKH, de Araújo MCU, Vêras G, da Silva EC (2013) The successive projections algorithm for interval selection in PLS. *Microchem J* 110:202–208. <https://doi.org/10.1016/j.microc.2013.03.015>
50. Jaumot J, de Juan A, Tauler R (2015) MCR-ALS GUI 2.0: new features and applications. *Chemom Intell Lab Syst* 140:1–12. <https://doi.org/10.1016/j.chemolab.2014.10.003>
51. ASTM (2013) ASTM D618-21: Standard practice for conditioning plastics for testing
52. Bassan P (2011) *Light scattering during infrared spectroscopic measurements of biomedical samples*. The University of Manchester
53. Amigo JM, Grassi S (2020) Chapter 1.2 – Configuration of hyperspectral and multispectral imaging systems. In: Amigo JM (ed) *Data handling in science and technology*, vol 32. Elsevier, pp 17–34. <https://doi.org/10.1016/B978-0-444-63977-6.00002-X>



# Chapter 11

## Water Vapor Permeability of Hydrophilic Films

Roberto J. Avena-Bustillos, Noah M. Klausner, and Tara H. McHugh

### Abstract

The modified procedure for water vapor permeability (WVP) is a modification to the established ASTM E96 method for measuring the WVP of films. The E96 method works by putting water in cups and measuring the mass transfer rate of water vapor through films that are secured as lids to the cups. The WVP is calculated from a formula including this mass transfer rate as well as estimated partial water vapor pressure under the film lid at the testing constant temperature. Using the E96 method, the partial water vapor pressure under the film lid is assumed to be the same as the saturated water vapor pressure at the surface of the water. This assumption is only true for hydrophobic films, which is why the partial water vapor pressure under the film lid must be calculated in this modified procedure when measuring the WVP of hydrophilic films. Here, we provide a detailed account of the foundation for this correction and the procedure to reliably use it to measure the permeability of water vapor through hydrophilic films.

**Key words** Water vapor permeability, Partial water vapor pressure, Hydrophilic, Hydrophobic, Water vapor transmission rate, Permeance, Diffusion, Solubility, Barrier

---

## 1 Introduction

The water vapor permeability (WVP) of hydrophilic edible films is used in determining the shelf-life of food products as well as designing edible films to match specific food applications. The accuracy of WVP determinations can influence food stability; therefore, it is important to use an accurate method to determine WVP. The established method for determining the WVP of polymeric films is the ASTM E96 method [1]. This method entails filling a cup partially with deionized water and sealing the top of the cup with the film being tested as a lid (Fig. 1).

### 1.1 Water Vapor Permeability Formula

In order to calculate WVP, the transport of water vapor through the film is modeled under the following assumptions:

- Water vapor transports one-dimensionally in the positive  $z$  direction.

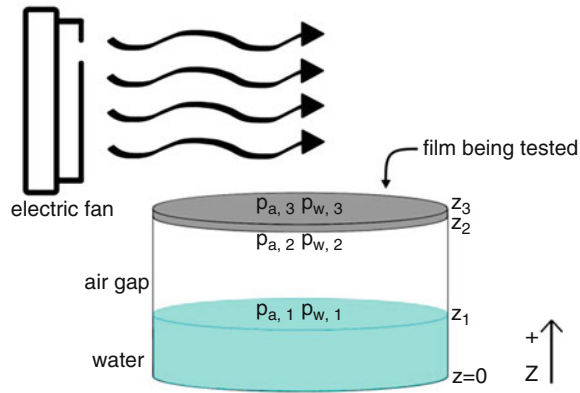


**Fig. 1** The cup and film are modeled as an ideal cylindrical system. The partial vapor pressures of air and water vapor at position  $z_i$  are  $p_{a,i}$  and  $p_{w,i}$  respectively. If the fan is circulating air fast enough to maintain 0% relative humidity at  $z_3$ ,  $p_{w,3}$  will be negligible. The temperature is kept constant and homogenous throughout the system

- The mode of transport is diffusion, which can be modeled by Fick's laws.
- Water vapor transport reaches steady-state conditions throughout the film.
- The solubility of water vapor on the film matrix can be modeled with Henry's law.

**List of Symbols**

- $C(z,t)$  = mass concentration of water vapor at position  $z$ , time  $t$  [ $\text{g m}^{-2}$ ]
- $J(z,t)$  = mass flux of water vapor at position  $z$ , time  $t$  [ $\text{g m}^{-2} \text{s}^{-1}$ ]
- $A$  = area of the mouth of the cup [ $\text{m}^2$ ]
- $V$  = volume [ $\text{m}^3$ ]
- $D$  = diffusion coefficient of water vapor [ $\text{m}^2 \text{s}^{-1}$ ]
- $S$  = solubility of water vapor in the film [ $\text{s}^2 \text{m}^{-2}$ ]
- $p$  = partial pressure of water vapor [kPa]
- $Q$  = mass of water vapor transferred [g]

The WVP derivation begins with a mass balance on a horizontal differential slice of the film [3]:

$$\frac{\delta C}{\delta t} = \frac{(J_{\text{in}} - J_{\text{out}}) * A}{\delta V} = \frac{-\delta J * A}{\delta z * A} = \frac{-\delta J}{\delta z} \tag{1}$$

Invoking Fick's first law:

$$J = -D \frac{dC}{dz} \rightarrow \frac{-\delta J}{\delta z} = D \frac{\delta^2 C}{\delta z^2} \tag{2}$$

Substituting Eq. 2 into Eq. 1 gives the following partial differential equation:

$$\frac{\delta C}{\delta t} = D \frac{\delta^2 C}{\delta z^2} \quad (3)$$

Because the water vapor concentration at any point will have reached a steady state,  $\frac{\delta C}{\delta t} = 0$  and Eq. 3 can be reduced to the following boundary value problem:

$$\frac{d^2 C}{dz^2} = 0 : C(z_2) = C_2, C(z_3) = C_3 \quad (4)$$

Solving Eq. 4 yields the following formula for water vapor concentration at position  $z$ :

$$C(z) = C_2 + \frac{C_3 - C_2}{z_3 - z_2} (z - z_2) \quad (5)$$

Taking the  $z$  derivative of Eq. 5 and substituting it back into Fick's Law provides the following expression for mass flux of water vapor:

$$\left. \begin{aligned} \frac{dC}{dz} &= \frac{C_3 - C_2}{z_3 - z_2} \\ J &= D \frac{C_2 - C_3}{z_3 - z_2} \\ J &= -D \frac{dC}{dz} \end{aligned} \right\} \quad (6)$$

Henry's Law states that  $C = Sp$ , and  $J$ , the mass flux of water vapor, is defined as  $\frac{Q}{At}$  where  $t$  is the time duration of mass transfer. Substituting these two expressions into Eq. 6 gives the following equation:

$$\frac{Q}{At} = SD \frac{p_{w,2} - p_{w,3}}{z_3 - z_2} \quad (7)$$

Since the WVP of a film is the solubility of water vapor on the matrix of the film multiplied by the diffusivity of water through the film, the expression  $WVP = SD$  can be substituted, and Eq. 7 can be rearranged to solve for WVP:

$$WVP = \frac{Q(z_3 - z_2)}{At(p_{w,2} - p_{w,3})} \quad (8)$$

Because  $p_{w,3}$  is controlled at 0 (Fig. 1) the following equation, Eq. 9, is the final WVP formula [2]:

$$WVP = \frac{Q(z_3 - z_2)}{At p_{w,2}} \quad (9)$$

The basis of the ASTM E96 method for WVP is measuring the mass loss from the cup over time ( $Q/t$ ) while controlling the other parameters of the equation. To do so, the cup is placed in a cabinet kept at 0% relative humidity (RH) by fans moving air at a speed of

152 m min<sup>-1</sup> to assure constant and complete wipeout of water vapor coming out of the film top surface [2], while the cabinet is inside a controlled-temperature incubator, chamber, or room. The loss of mass of the cup is monitored over time, and the data gathered is analyzed through linear regression to determine the rate at which water molecules transport through the film in units of mass per time. This mass loss rate is divided by the area of the film to obtain the water vapor transmission rate (WVTR). The permeance of the film is obtained by dividing the WVTR by the partial vapor pressure of water on the underside of the film. Finally, the WVP is determined by multiplying the permeance by the thickness of the film, as suggested by the derived equation.

Under the ASTM E96-80 method, the assumption is made that water molecules will diffuse through the air gap between the water surface and the film underside and being largely trapped by the film until eventually reaching a homogeneous equilibrium value throughout the air gap, similar to the saturated partial water vapor pressure at the constant testing temperature. This assumption is only correct for hydrophobic films because they have more efficient moisture barrier properties than hydrophilic films [4]. In the case of hydrophilic films, water molecules move faster through the film, and the transport of water molecules causes a gradient of partial water vapor pressure values through the air gap when equilibrium is reached [2]. As a result of the partial water vapor pressure gradient, the partial water vapor pressure at the underside of a hydrophilic film is lower than the saturated partial water vapor pressure at the surface of the water at the bottom of the cup.

## **1.2 Partial Water Vapor Pressure Formula**

The WVP correction method [2] to the ASTM E96 method is a correction for the water vapor pressure value used in the WVP calculation. To determine the correct WVP for a hydrophilic film, the partial vapor pressure of water at the underside of the lid must be calculated by modeling the gradient of water vapor pressure across the air gap. To do so, the transport of water vapor across the air gap must be modeled under the following assumptions [5]:

- Transport occurs within a binary molecular system of air and water vapor. Subscripts of  $a$  and  $w$  will be used to denote the properties of air and water vapor, respectively.
- Transport of a species occurs via a combination of diffusive flux and bulk motion.
- Diffusive flux can be modeled with Fick's Law.
- Transport of air is negligible ( $N_a = 0$ ).
- The ideal gas law holds true.



### List of Symbols

- $N_i$  = total molecular transport of species  $i$  [mol m<sup>-2</sup> s<sup>-1</sup>]  
 $C_i$  = molar concentration of species  $i$  [mol m<sup>-3</sup>]  
 $C$  = molar concentration of the mixture =  $\sum_{i=1}^n C_i$  for  $n$  number of species in the mixture [mol m<sup>-3</sup>]  
 $v_i$  = velocity of species  $i$  [m s<sup>-1</sup>]  
 $v$  = molar average velocity of the mixture =  $\frac{\sum_{i=1}^n C_i v_i}{C}$  [m s<sup>-1</sup>]  
 $y_i$  = molar fraction of species  $i$  =  $\frac{C_i}{C} * 100$  [%]  
 $J_i$  = diffusive molar flux of species  $i$  [mol m<sup>-2</sup> s<sup>-1</sup>]  
 $D_{aw}$  = diffusion coefficient between air and water vapor [m<sup>2</sup> s<sup>-1</sup>]  
 $p$  = pressure of the mixture [atm]  
 $p_{j,i}$  = partial pressure of species  $j$  at position  $z_i$  [kPa]  
 $V$  = volume [m<sup>3</sup>]  
 $T$  = temperature (constant) [K]  
 $R$  = the gas constant [m<sup>3</sup> atm K<sup>-1</sup> mol<sup>-1</sup>]

We start by defining the total molecular transport of water vapor ( $N_w$ ) as the product of the molar water vapor concentration ( $C_w$ ) and the velocity of water vapor in the mixture ( $v_w$ ):

$$N_w = C_w v_w \quad (10)$$

The right-hand expression can be manipulated to include the diffusive velocity of water vapor ( $v_w - v$ ) where  $v$  is the molar-average velocity of the mixture:

$$N_w = C_w(v_w - v) + C_w v : v = \frac{C_w v_w + C_a v_a}{C_w + C_a} \quad (11)$$

$$N_w = C_w(v_w - v) + \frac{C_w}{C_w + C_a} (C_w v_w + C_a v_a) \quad (12)$$

Given that  $C_w + C_a$  is the mixture concentration  $C$ , the mole fraction of substance  $i$  ( $y_i$ ) is defined as  $\frac{C_i}{C}$ . Also, air transport is defined as  $N_a = C_a v_a$  in the same fashion as water vapor.

Plugging in these definitions to Eq. 12 yields the following equation:

$$N_w = C_w(v_w - v) + y_w(N_w + N_a) \quad (13)$$

The first term on the right side of Eq. 13 accounts for the diffusive molar flux of water ( $J_w$ ) and the second term accounts for the flux of water due to bulk motion. Since the transport of air is negligible ( $N_a = 0$ ), Eq. 13 can be simplified as follows:

$$N_w = J_w + y_w N_w \rightarrow N_w = \frac{J_w}{1 - y_w} \quad (14)$$

Invoking Fick's first law:

$$J_w = -D_{aw} \frac{dC_w}{dz} \rightarrow N_w = \frac{-D_{aw}}{1-y_w} * \frac{dC_w}{dz} \quad (15)$$

$$C_w = Cy_w \rightarrow N_w = \frac{-CD_{aw}}{1-y_w} * \frac{dy_w}{dz} \quad (16)$$

Integrating both sides of Eq. 16 across the  $z$ -axis of the water gap progresses as follows:

$$N_w \int_{z_1}^{z_2} dz = -CD_{aw} \int_{y_{w,1}}^{y_{w,2}} \frac{dy_w}{1-y_w} \quad (17)$$

where  $y_{w,i}$  = mole fraction of water vapor at position  $z_i$

$$N_w(z_2 - z_1) = CD_{aw} \ln\left(\frac{1-y_{w,2}}{1-y_{w,1}}\right) \quad (18)$$

By definition,  $y_{w,i} + y_{a,i} = 1 \rightarrow 1 - y_{w,i} = y_{a,i}$ .

The expression inside the natural logarithm of Eq. 18 can be manipulated as follows to obtain an equation that depends on partial pressures of water at  $z$  positions 1 and 2:

$$\frac{1-y_{w,2}}{1-y_{w,1}} = \frac{y_{a,2}}{y_{a,1}} = \frac{\frac{C_{a,2}}{C}}{\frac{C_{a,1}}{C}} = \frac{C_{a,2}}{C_{a,1}} \quad (19)$$

By the ideal gas law,  $pV = nRT \rightarrow C_{a,i} = \frac{n_{a,i}}{V_{a,i}} = \frac{p_{a,i}}{RT}$  and  $C = \frac{n}{V} = \frac{p}{RT}$

$$\frac{C_{a,2}}{C_{a,1}} = \frac{\frac{p_{a,2}}{RT}}{\frac{p_{a,1}}{RT}} = \frac{p_{a,2}}{p_{a,1}} = \frac{1-p_{w,2}}{1-p_{w,1}} \quad (20)$$

Substituting the expression from Eq. 20 into Eq. 18 gives the following:

$$N_w(z_2 - z_1) = \frac{pD_{aw}}{RT} \ln\left(\frac{1-p_{w,2}}{1-p_{w,1}}\right) \quad (21)$$

Rearranging ends the derivation for partial pressure of water vapor directly under the film ( $p_{w,2}$ ):

$$p_{w,2} = 1 + (p_{w,1} - 1) \exp\left(\frac{RTN_w(z_2 - z_1)}{pD_{aw}}\right) \quad (22)$$

Eq. 22 is used to approximate the partial pressure of water vapor on the film underside, which is a key parameter in Eq. 9, the WVP formula.

This correction is advantageous firstly because more accurate WVP values can be obtained, and secondly because the effect of film thickness on WVP in hydrophilic films can be explained. Previous studies have indicated similar relationships between film thickness

and permeability properties in hydrophilic film systems; however, those studies could not adequately define the relationships in their explanations for the thickness effect. WVP was found to increase when the thickness of a given hydrophilic film was increased, which is counterintuitive. Examining the conditions on the film's underside was necessary to explain this relationship.

Using the correction method [2], an exponential relationship between WVP and the RH at the underside of the film (proportional to the water vapor pressure there) can be established by varying the air gap distance over WVP tests. This exponential relationship is remarkably similar to the relationship between film thickness and WVP, so it can be logically deduced that there is a relationship between film thickness and RH at the film's underside. Supporting this logic is the idea that a thicker hydrophilic film will resist mass transfer more than a thinner one, causing a higher RH (and consequently a higher water vapor pressure) at the film underside. This higher water vapor pressure value causes a higher WVP value, based on the relationship previously established.

A limitation to the WVP correction method is that it relies on experimental saturated water pressure and heat of vaporization values. To calculate the partial water vapor pressure under the film, the partial water vapor pressure at the surface of the water (saturated vapor pressure) must be known. This value can be obtained from a steam table at a given constant temperature—or calculated using the Clausius–Clapeyron equation [6]. If the saturated vapor pressure is calculated, other experimentally derived values must be used. Using experimentally derived values introduces some amount of error between the actual conditions of the WVP test and the conditions under which those values were obtained. That said, accurate steam tables such as the 1967 ASME Steam Tables [7] are readily accessible, making the reliance on tabulated values a minor limitation.

---

## 2 Materials

1. Controlled-temperature room or incubator to keep temperature constant and large enough to house one or more cabinets kept at 0% RH.
2. Desiccating cabinet—such as catalog no. 08-647-28 from Fisher Scientific, Inc. (Fair Lawn, NJ, USA) or other models and manufacturers—to hold at least eight cups.
3. Motor—such as the Bodine motor model no. 574—with variable speed controller—such as the Motor Master Series 20,000, both from Minarik Electric Co. (Fresno, CA, USA) or other models and manufacturers—as well as a fan—such as

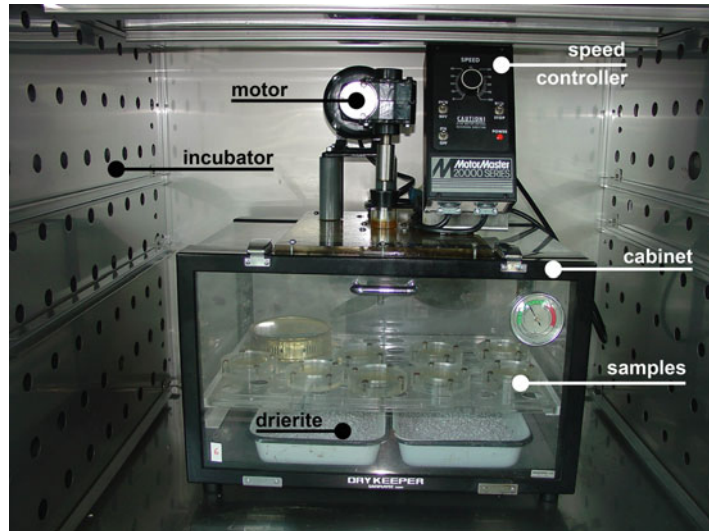


**Fig. 2** Water vapor permeability cabinet with motor and fan rotation speed controller, Drierite in bottom shallow pans and sample cups on top tray, with cabinet inside a temperature-controller incubator

model no. 607601-01 from Refrigeration Supply House (Sacramento, CA, USA) or other models and manufacturers—installed in each hermetically sealed cabinet to control RH at 0% (*see Note 1*). The motor is attached to the desiccating cabinet such that the rotating shaft goes through the roof of the cabinet, and the gap between the shaft and the hole in the cabinet is sealed by a chamber with oil. The fan is attached to the shaft of the motor, so that it spins horizontally near the ceiling of the cabinet (Fig. 2).

4. Calcium sulfate desiccant—for example, 6-mesh Drierite from Fisher Scientific, Inc. (Fair Lawn, NJ, USA) or other suppliers—is recommended to equilibrate cabinets to 0% RH prior to each experiment (*see Note 2*).
5. Mid-sized plastic trays to hold the desiccant are placed underneath the test cups.
6. Cups made of poly(methyl methacrylate) (PMMA), aluminum, or stainless steel—in a uniform cylindrical fashion. For a typical cup-shaped configuration, the cup could be 1.25-cm tall and have a diameter of 8.2 cm, externally. The cup opening could have a diameter of 5 cm for an area of  $19.6 \text{ cm}^2$  for the cup mouth where water will permeate through the testing film, and the cup interior depth could be 1.05 cm.
7. To seal in the film, an 8.2 cm outside diameter, 5-cm-diameter ring opening, and 0.60-cm-tall PMMA or other cup material containing a  $19.6\text{-cm}^2$  lid opening are placed on top of the film through a face previously greased for tight sealing (*see Note 3*).

8. Silicon sealant—e.g., in the form of high vacuum grease from Dow Corning (Midland, MI)—is used to create a barrier under and over the film (*see Note 4*).
9. Deionized water (6 mL for previously described cup dimensions) was added to the bottom of the cup to provide a source of water vapor for the film to be exposed to (*see Note 5*).
10. A volumetric pipette was used to measure water for the test cups.
11. Screws symmetrically located around the ring circumference are used to tighten the seal.
12. Electric screwdriver—such as Checkline TSD-400 from Electromatic Equipment Co. (Cedarhurst, NY, USA) or other models and manufacturers—to tighten four screws in each cup. Seal ring tightening can also be done manually with a regular screwdriver.
13. Anemometer—such as model no. 127MS from Solomat (Stamford, CT, USA) or other models and manufacturers—is to measure air velocity in the cabinet.
14. Hygrometer—such as model no. 605 from Airguide (Chicago, IL, USA) or other models and manufacturers—to measure RH inside the cabinet.
15. Analytic balance of at least 0.001 g sensitivity—such as Excellence XPE Analytical Balance from Mettler Toledo (Columbus, OH, USA) or other models and manufacturers—to weigh cups at different time intervals during testing.
16. Micrometer—such as model no. 515 from Lufkin Rule Co. (Saginaw, MI, USA) or other models and manufacturers—used to measure film thickness (*see Note 6*).
17. Linear regression and subsequent calculations can be done in an Excel spreadsheet such as in Fig. 3.

---

### 3 Methods

1. Place the cabinet in a temperature-controlled room or incubator with the temperature set at a known value near, usually 20–25 °C (*see Fig. 2*).
2. Spread out the Drierite in an inch-thick layer on shallow trays at the bottom of the desiccating cabinet (*see Note 2*). Place the hygrometer on the bottom of the cabinet next to the Drierite (*see Fig. 2*).

**\*Steps 3–15 apply to each film individually**

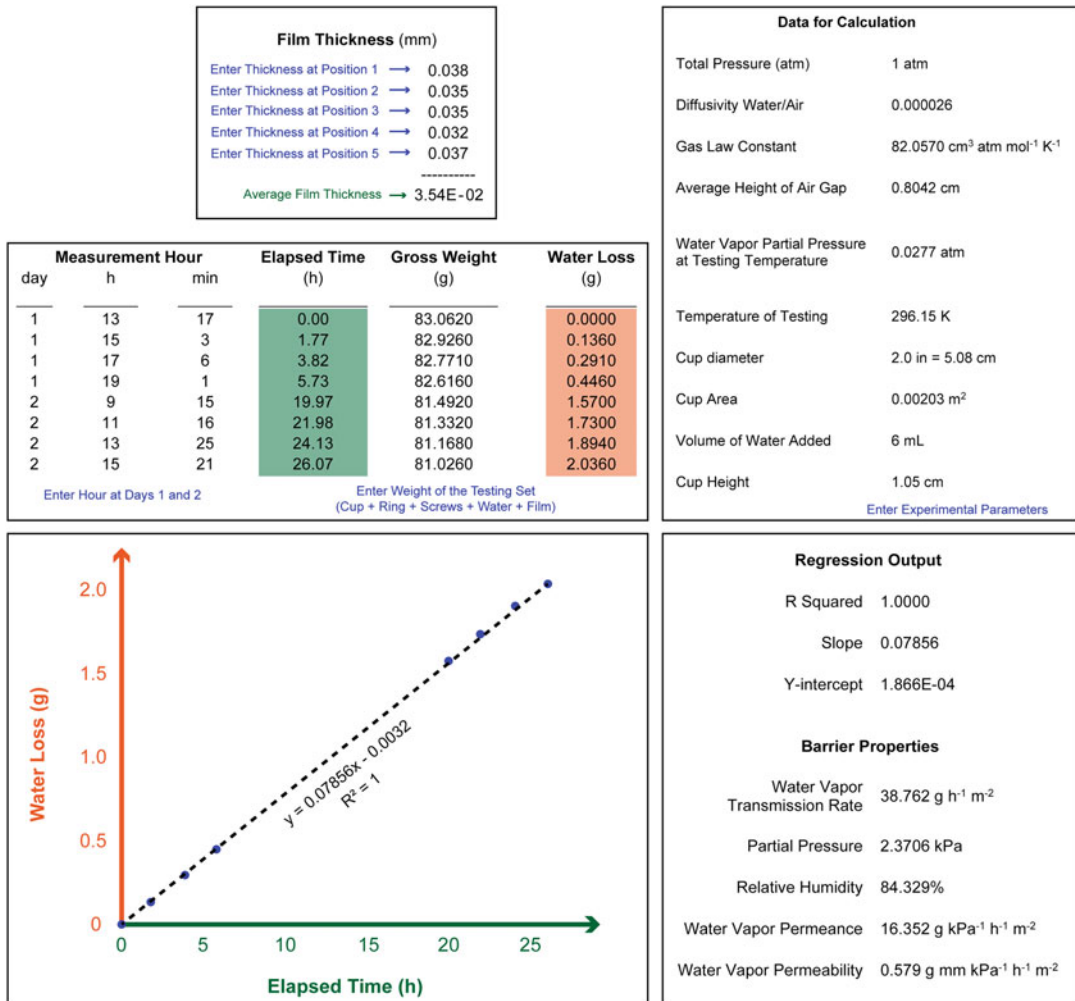


**Fig. 3** Example of a spreadsheet for calculations of the water barrier properties of a gelatin film. Each sample and replicate will have its own spreadsheet

3. Inspect eight films of the material to be tested, making sure they appear identical and uniform in composition and without pinholes.
4. Label each testing cup so they can be easily identified.
5. Apply a thin line of high-vacuum grease around the rim of each cup and ring (*see Note 7*).
6. Using a pipette, transfer 6 mL of deionized water or saturated salt solution to the bottom of the testing cup.
7. Measure the thickness of films to the nearest 0.001 mm at five random positions using the micrometer. Average the five values to obtain the thickness value to be used in the WVP calculation for the film (*see Note 6*).

8. Place the film on the rim of the cup, centered.
9. Place the ring on top of the film, centered.
10. Using the screwdriver, tighten four screws symmetrically along the circumference of the cup (*see Note 8*).
11. Place all eight testing cups on a tray inside the cabinet near the walls for the greatest airflow. Take note of each cup's position, as they need to be rotated regularly to ensure each cup undergoes the same air velocity conditions.
12. If the suggested components are used in the fan apparatus, the motor controller can simply be set to maximum speed to ensure proper airflow. If other components are used, implement the anemometer to measure airflow inside the cabinet and calibrate the motor such that air velocity in the cabinet is at least  $152 \text{ m min}^{-1}$  (*see Note 9*).
13. Wait an hour for steady-state water vapor conditions to be achieved.
14. Using the balance, weigh each cup at least once every 2 h, for a period of 24–28 h (*see Note 10*). Keep track of the time elapsed in relation to the start of the experiment.
15. Each time the cups are weighed, rotate the positions of the cups in the cabinets (*see Note 11*).
16. The average water gap is estimated using the initial and final volumes of water added and the dimensions of the cup (*see Note 5*).
17. For each cup, the data obtained can be interpreted as a set of points on a graph consisting of time on the  $x$ -axis and cup mass on the  $y$ -axis. Analyze the data with a linear regression, producing a formula for cup mass as a linear function of time.
18. Divide the slope of the linear mass function by the area of the mouth of the testing cup to obtain the WVTR, the mass flux of water vapor through the film.
19. Convert the WVTR into  $N_w$ , the molar flux of water vapor, by dividing the WVTR by the molar mass of water.
20. Calculate the saturated water vapor pressure at the water's surface based on the air temperature (*see Note 12*).
21. Input the parameters into Eq. 22 to calculate the partial water vapor pressure on the underside of the film  $p_{w,2}$  (*see Subheading 1.2*).
22. Divide the WVTR by the partial water vapor pressure under the film surface to obtain the permeance of the film.
23. Multiply the permeance of the film by its average thickness to obtain its WVP.

---

## 4 Notes

1. The fan systems use airflow to maintain 0% RH in each cabinet in order to keep the water vapor pressure outside of the film controlled at 0 for the WVP measurement.
2. To make sure Drierite is fully activated, take a half-pound of 6-mesh, non-indicating Drierite and spread it into a one-granule-thick layer on a tray and heat the layer at 210 °C for 1 h [8]. Contact with Drierite may cause various bodily irritations, and prolonged and repeated exposure can result in lung disease and/or cancer, so it is recommended to use appropriate PPE (nitrile gloves, respiratory mask, and goggles) [9].
3. The sealant is important because, without it, water vapor can escape through the gap underneath the film and become a source of error in the measure of mass transfer through the film. Sealant should not be applied excessively in a way that will protrude from the junctures of the film and cup mouth and lid as it may result in errors during weighing as sealant could smear fingers after touching cups.
4. Avoid direct eye contact with high vacuum grease, as it may cause temporary redness and discomfort [10].
5. Initial height from the surface of the water in the cup to the film underside is calculated from a 6-mL volume right cylinder subtracted from the cup depth:  $1.05 - 6 / 2\pi (2.5)^2 = 1.05 - 0.153 = 0.897$  cm. The final height is calculated from the final volume of water remaining at the end of the test, and an average height is used for the calculation of the stagnant air gap inside the testing cup.
6. For a given film, the thickness may vary at different points. For this reason, the thicknesses at different points must be averaged to best describe the overall thickness.
7. Avoid using too much grease, or it will seep across the edges of the rim once under pressure. Grease on the technician's fingers after repeating WVP cup weighing will affect WVTR.
8. Make sure the screws apply even downward pressure on all points of the ring by tightening each screw in small amounts at a time and alternating between screws that are across from each other in an "X" pattern.
9. Air speeds inside the cabinet may not be lower than  $152 \text{ m min}^{-1}$ . This speed is the minimum airspeed necessary to maintain 0% RH on the top surface of films.
10. Do not let the experiment run over 30 h long because the cups can dry out and change the modeling parameters.



11. Rotating the cups after each mass measurement ensures that all cups experience the same air velocity conditions over the course of the procedure.
12. The following formula can be used to calculate the saturated water vapor pressure at the water's surface [6]:

$$p_{w,1} = \frac{\exp\left(34.494 - \frac{4924.99}{T+237.1}\right)}{(T + 105)^{1.57}} \quad (23)$$

---

## Acknowledgments

Our gratitude to Dr. John M. Krochta, *Emeritus* Professor at the Department of Food Science and Technology and the Biological and Agricultural Engineering Department at the University of California, Davis, for guiding authors Avena and McHugh to develop the water vapor permeability method for hydrophilic films during their PhD thesis work.

## References

1. ASTM (1980) Standard test methods for water vapor transmission of materials. Standards Designation: E96-80. In: Annual book of ASTM. ASTM, Philadelphia, pp 771–778
2. McHugh TH, Avena-Bustillos R, Krochta JM (1993) Hydrophilic edible films: modified procedure for water vapor permeability and explanation of thickness effects. *J Food Sci* 58:899–903
3. Zang L (2016) Lecture 4: diffusion: Fick's second law. <https://my.eng.utah.edu/~lzang/images/lecture-4.pdf>. Accessed 16 July 2020
4. Morillon V, Debeaufort F, Capelle M et al (2000) Influence of the physical state of water on the barrier properties of hydrophilic and hydrophobic films. *J Agric Food Chem* 48: 11–16. <https://doi.org/10.1021/jf990809z>
5. King Abdulaziz University (n.d.) Molecular mass transport. <https://www.kau.edu.sa/Files/0001424/Subjects/notes/20333.pdf>. Accessed 16 July 2020
6. Huang J (2018) A simple accurate formula for calculating saturation vapor pressure of water and ice. *J Appl Meteorol Climatol* 57(6): 1265–1272. <https://doi.org/10.1175/JAMC-D-17-0334.1>
7. ASME (1968) The 1967 ASME steam tables. *Nav Eng J*. <https://doi.org/10.1111/j.1559-3584.1968.tb04564.x>
8. WA Hammond Drierite (n.d.) Technical data-regeneration of drierite desiccants. <https://secure.drierite.com/catalog3/page19b.cfm#:~:text=Exhausted%20Commercial%20DRIERITE%20or%20Du,container%20and%20sealed%20while%20hot.> Accessed 16 July 2020
9. W A Hammond Drierite (2019) Drierite [Material Safety Data Sheet]. <https://secure.drierite.com/RegularDrieriteSDS.pdf>. Accessed 16 July 2020
10. Dow Corning (2002) High vacuum grease [Material Safety Data Sheet]. [https://www.conncoll.edu/media/website-media/offices/ehs/envhealthdocs/High\\_Vacuum\\_Grease.pdf](https://www.conncoll.edu/media/website-media/offices/ehs/envhealthdocs/High_Vacuum_Grease.pdf). Accessed 16 July 2020



## Permeation of Oxygen and Carbon Dioxide Through Food Packaging Materials

Victor G. L. Souza, Carolina Rodrigues, João R. A. Pires, Ana L. Fernando, Vitor Alves, and Isabel Coelho

### Abstract

Barrier properties of packaging materials are important requirements when selecting and developing optimal packaging systems. The determination of the barrier properties of a polymer film is crucial to estimating and predicting the product-packaging shelf-life. The specific barrier requirements of the package are related to the product characteristics and the intended end-use application. Much of the design of barrier packaging involves controlling the exchange of gaseous components (e.g., O<sub>2</sub>, CO<sub>2</sub>) between the external and internal package environments. Thus, this chapter intends to give an overview of the methods and equipment used for the evaluation of the permeation of oxygen and carbon dioxide through polymer-based packaging films.

**Key words** Permeation of gases, Oxygen, Carbon dioxide, Permeability, Transmission rate, Barrier properties

---

### 1 Introduction

Packaging materials may prevent the transport of oxygen (O<sub>2</sub>) and keep the desired balance of oxygen and carbon dioxide (CO<sub>2</sub>) within the headspace for extended food shelf-life [1]. Thus, when a polymer film has low oxygen permeability, the oxygen pressure inside the container drops, retarding oxidation reactions and respiration rate (in the case of fruits and vegetables), extending the shelf-life of the product. Carbon dioxide transport is also important for packaging with modified active atmosphere (MAP) technology and for products that release carbon dioxide over time, as is also the case with fruits and vegetables [2].

Food can be packaged using different materials, such as plastic, paper and cardboard, metal, and glass. Polymers show important advantages over traditional packaging materials (glass, paper, and metal) namely flexibility, lightweight, toughness, versatility, and

cost. However, unlike glass and metals, polymers do not offer an infinite gas barrier [1]. Combinations of different polymers, in the form of multilayer structures or blends, can provide sufficient barrier properties for the intended shelf-life of most products [3]. Polymers with inorganic/organic materials in nanoscale dimensions, such as clays, metal oxides, and cellulose, can boast significantly enhanced barrier properties [4–7].

Gas transport through polymers is described by the solution-diffusion model. According to this model, permeation through a flat sheet or film occurs in three steps: permeant (i) dissolves into the upstream side of the film (where there is a high permeant partial pressure or high thermodynamic activity), then (ii) diffuses through the film, and (iii) desorbs from the downstream side of the film (where there is a low permeant partial pressure or low thermodynamic activity). In one dimension, gas diffusion through a polymer follows the first Fick's law:

$$J = -D \frac{dC}{dx} \quad (1)$$

where  $J$  is the gas flux ( $\text{mol m}^{-2} \text{s}^{-1}$ ),  $D$  is the effective diffusion coefficient for the gas in the polymer ( $\text{m}^2 \text{s}^{-1}$ ), and  $dC/dx$  is the local concentration gradient of the gas ( $\text{mol m}^{-4}$ ).

Permeability ( $P$ ) can be expressed as the product of the effective diffusion coefficient,  $D$ , and the solubility coefficient,  $S$  ( $\text{mol m}^{-3} \text{Pa}$ ), the latter being the ratio of the equilibrium gas concentration in the polymer at the upstream side of the film  $C$  ( $\text{mol m}^{-3}$ ) divided by the permeant partial pressure  $p$  (Pa), resulting in the following equation:

$$C = S p \quad (2)$$

Substituting Eq. 2 in Eq. 1 and integrating through the film thickness ( $l$ ) results:

$$J = \frac{P}{l} (p_1 - p_2) \quad (3)$$

The permeability characterizes the steady-state rate of mass transport of gas molecules through polymers. In a dense polymer film, the permeability,  $P$ , is defined as the molar flux of gas through the polymer relative to a fixed coordinate system,  $J$ , normalized by the film thickness,  $l$  (m), and by the difference between the gas partial pressures in the upstream ( $p_1$ ) and downstream compartments ( $p_2$ ).

Accordingly, permeability has dimensions of quantity of gas (either mass or moles or volume) times thickness divided by area, time, and pressure. Several units have been used to report the permeability of gases in the literature (*see Note 1*). Though SI units are  $\text{mol m m}^{-2} \text{s}^{-1} \text{Pa}^{-1}$ , barrer [8] is a commonly used non-SI unit for the permeability of gases, which was originally

defined for convenience because many polymer membranes had permeabilities around 1 barrer. It is defined as  $10^{-10} \text{ cm}^3 \text{ (STP) cm/cm}^{-2} \text{ s}^{-1} \text{ cm Hg}^{-1}$ , where STP refers to standard temperature and pressure (273.15 K and  $10^5 \text{ Pa}$ ) and 1 barrer is equal to  $3.35 \times 10^{-16} \text{ mol m m}^{-2} \text{ s}^{-1} \text{ Pa}^{-1}$  [9].

Oxygen and carbon dioxide are two of the main permeants studied in food packaging applications. The oxygen and carbon dioxide barriers are quantified by their permeabilities (OP and  $\text{CO}_2\text{P}$ , respectively), which indicate the amount of gas that permeates per unit of area, time, and pressure multiplied by the film thickness. Together with the permeability, the oxygen and carbon dioxide *transmission rates* (OTR and  $\text{CO}_2\text{TR}$ , respectively) express the quantity of gas passing through a unit area of a film per unit time under the conditions of the test. The SI units of transmission rate are  $\text{mol m}^{-2} \text{ s}^{-1}$ . The permeability ( $P$ ) is correlated to the *transmission rate* ( $TR$ ) by the following equation:

$$P = l \frac{TR}{\Delta P} \quad (4)$$

where  $l$  is the thickness of the film (m),  $\Delta P = p_1 - p_2$  is the difference between gas partial pressure across the film (Pa), where  $p_1$  is the gas partial pressure at the temperature test on the feed side and  $p_2$  is the gas partial pressure at the temperature test on the permeate side.

The permeability through plastic materials depends on several factors, namely, (i) the permeant properties (molecule size and chemical nature); (ii) material/polymer characteristics (molecular orientation, degree of crystallinity, free volume, and chain stiffness); and (iii) external conditions (such as temperature and relative humidity) [10]. The temperature and humidity conditions to which the food product will be exposed in the supply chain are vital for calculating the required barrier, so that it applies to the conditions expected. Furthermore, the specific barrier requirement of a packaging system depends upon the food characteristics and the intended end-use applications [11, 12].

The temperature dependence of permeability and diffusivity are usually modeled using the Arrhenius equations of the following forms:

$$P = P_0 \exp(-E_p/RT) \quad (5)$$

$$D = D_0 \exp(-E_D/RT) \quad (6)$$

where  $E_p$  and  $E_D$  are activation energies for permeation and diffusion, and  $P_0$  and  $D_0$  are pre-exponential factors.

The effect of temperature on solubility is usually expressed by the van't Hoff relationship:

$$S = S_0 \exp(-\Delta H_s/RT) \quad (7)$$

where  $S_0$  is a pre-exponential factor, and  $\Delta H_s$  is the heat of sorption of permeant in the polymer.

The presence of polar groups in the polymer chains often increases chain rigidity, which can increase glass transition temperature and improve gas barrier properties. Increasing crystallinity in a polymer generally decreases gas permeability. Crystallinity influences both solubility and diffusion coefficients. The absorption of water vapor can increase, decrease, or have no effect on the gas permeability of barrier polymers. Hydrophilic barrier polymers, except for certain amorphous polyamides, lose their barrier properties with increasing relative humidity (RH) [9]. Thus, this chapter intends to give an overview of the methods and equipment used for the evaluation of the permeation of oxygen and carbon dioxide through polymer-based packaging films.

---

## 2 Materials

1. Polymer film with a 6.5-cm diameter for each replicate.
2. Stainless steel cell composed of two cylindrical chambers (e.g., 7 cm in diameter and 5 cm in length each chamber), with sealing O rings (e.g., Viton™ rubber) and a porous stainless-steel support, equipped with high-pressure stainless-steel fittings, valves, and tubing.
3. Two pressure transducers.
4. Thermostatic bath with a 2-L volume, a temperature range of 20–100 °C with a precision of  $\pm 0.03$  °C.
5. Micrometer (precision of  $\pm 0.001$  mm).
6. High-purity grade carbon dioxide (99.998%), oxygen (99.999%), and nitrogen (99.999%).
7. A computer for data acquisition and the *LabView* software from National Instruments.

---

## 3 Methods

There are two basic methods for measuring permeability: isostatic and *quasi*-isostatic. Isostatic methods use a continuous flow on both sides of the polymer film to provide constant permeant concentrations (Fig. 1a). *Quasi*-isostatic methods, in turn, use a continuous flow to maintain constant penetrant concentration only on the upstream side and allow penetrant accumulation on the downstream side of the film (Fig. 1b).

The time-lag method is one of the most employed for measuring the permeability of gases through films and membranes [13]. It allows the determination of both the permeability and diffusion

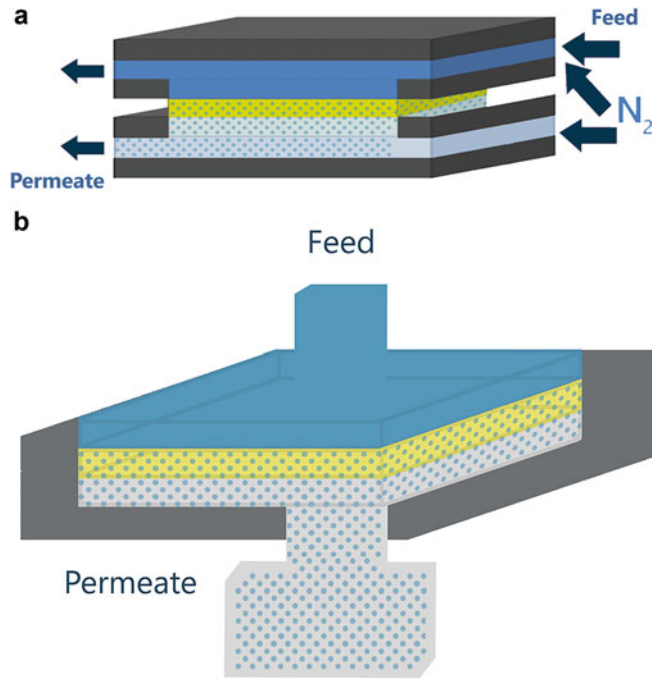


**Fig. 1** Schematic representations of cells for measuring the permeability in isotstatic **(a)** and *quasi-isostatic* **(b)** modes

coefficient of pure gases in a polymer matrix and, indirectly, the solubility coefficient.

Before the system reaches a steady state, the flux across the film and the pressure in the permeate compartment vary with time using a *quasi-isostatic* method (Fig. 1b).

Representing the pressure of the gas as a function of time, when  $t$  tends toward very long times, a steady state is reached and a straight line is observed (Eq. 8).

$$p_t = \frac{RTA p_f SD}{V_p V_m l} \left( t - \frac{l^2}{6D} \right) \quad (8)$$

where  $R$  is the universal gas constant ( $\text{J mol}^{-1} \text{K}^{-1}$ ),  $T$  is the absolute temperature (K),  $A$  is the membrane area ( $\text{m}^2$ ),  $p_f$  is pressure in the feed compartment (Pa),  $V_p$  is the volume of the permeate compartment ( $\text{m}^3$ ),  $V_m$  is the molar volume of the gas at STP conditions (273.15 K and  $10^5$  Pa) ( $\text{m}^3 \text{mol}^{-1}$ ),  $l$  is the film thickness (m), and  $D$  ( $\text{m}^2 \text{s}^{-1}$ ) is the diffusion coefficient.

From the interception of the time axis with the extrapolated linear steady state, it is possible to obtain the time lag:

$$\theta = \frac{l^2}{6D} \quad (9)$$

where  $\delta$  is the time lag (s), which allows the determination of the diffusion coefficient. From the slope of the straight line is obtained the permeability, and since  $P = SD$ , the solubility coefficient can be determined.

Another *quasi*-isostatic method for measuring gas permeability is based on the diaphragm cell method for obtaining diffusion coefficients. It is also known as a pressure decay method [14]. The experimental apparatus (Fig. 2) is composed of a stainless-steel cell with two identical chambers separated by the testing film. During the measurement, two porous plates support the polymer film on both sides to prevent sagging. However, the plates allow the gas to freely contact the film.

The permeability is evaluated by pressurizing one of the chambers (feed) up to constant pressure (e.g., 0.7 bar), with pure carbon dioxide or oxygen followed by the measurement of the pressure change in both chambers over time, using two pressure transducers. The measurements are made at a constant temperature, usually 30 °C, using a thermostatic bath. High-purity grade carbon dioxide (99.998%) and oxygen (99.999%) are used. The permeability is calculated with the pressure data obtained from both compartments according to the following equation [14]:

$$\frac{1}{\beta} \ln \left( \frac{\Delta p_0}{\Delta p} \right) = P \frac{t}{\delta} \tag{10}$$

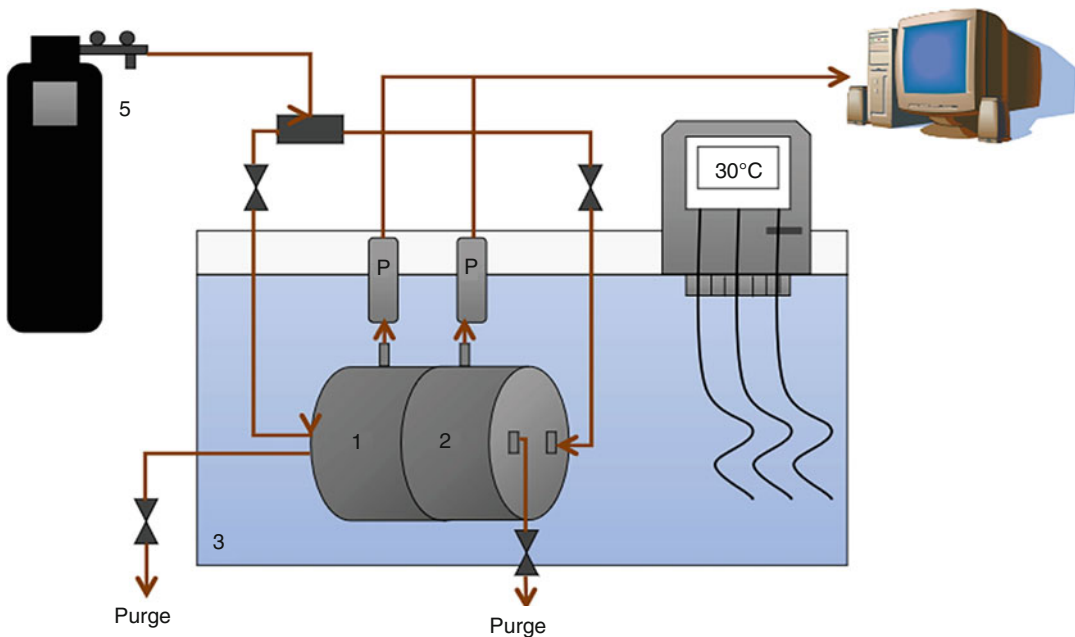


**Fig. 2** Experimental setup for measuring the permeability using the pressure decay method ((1) feed compartment, (2) permeate compartment, (3) water bath, (4) thermostatic head, (5) feed gas)

where  $\Delta p_0$  and  $\Delta p$  (bar) are the pressure differences between feed and permeate compartments at the beginning of the experiment and at any time, respectively,  $P$  ( $\text{m}^2 \text{s}^{-1}$ ) is the gas permeability,  $t$  (s) is the time,  $\delta$  (m) is the film thickness, and  $\beta$  is the geometric parameter:

$$\beta = A \left( \frac{1}{V_f} + \frac{1}{V_p} \right) \tag{11}$$

where  $A$  is the film’s area ( $\text{m}^2$ ) and  $V_f$  and  $V_p$  are the volumes ( $\text{m}^3$ ) of the feed and permeate compartments, respectively.

The data are plotted as  $\frac{1}{\beta} \ln \left( \frac{\Delta p_0}{\Delta p} \right)$  versus  $\frac{t}{\delta}$ , and the permeability is determined from the slope.

The geometric factor of the cell can be obtained by calibration of the equipment using a film with known permeability to an inert gas (i.e.,  $\text{N}_2$ ). It is normally used as a polydimethylsiloxane (PDMS) film because of its low barrier to gases (e.g.,  $\text{N}_2$ ), thus a low time needed for permeation. Figure 3 shows the pressure of  $\text{N}_2$  in the permeate and feed compartments during a calibration experiment.

Using the  $\text{N}_2$  permeability value ( $P$ ) and plotting  $\frac{1}{\beta} \ln \left( \frac{\Delta p_0}{\Delta p} \right)$  versus  $\frac{t}{\delta}$ , the geometric parameter  $\beta$  is obtained from the slope (Fig. 4).

The detailed protocol for measuring the  $\text{O}_2$  or  $\text{CO}_2$  permeability at 30 °C is the following:

**3.1 Calibration of the Permeation Cell**

1. Measure the PDMS film thickness.
2. Place the film inside the permeation cell and close it.
3. Introduce the permeation cell in the water bath regulated for 30 °C.

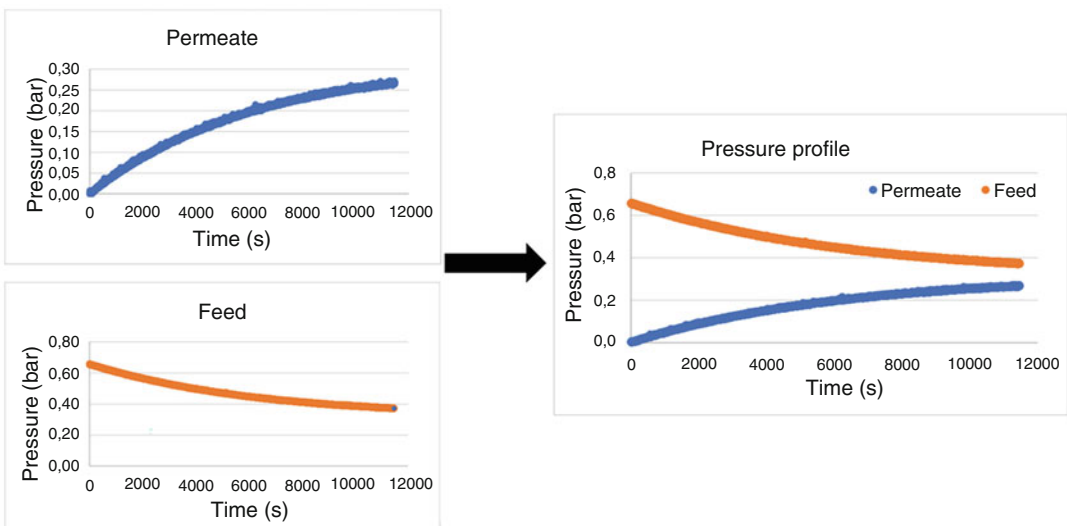


**Fig. 3**  $\text{N}_2$  pressure in the feed and permeate compartments of the cell during a calibration experiment



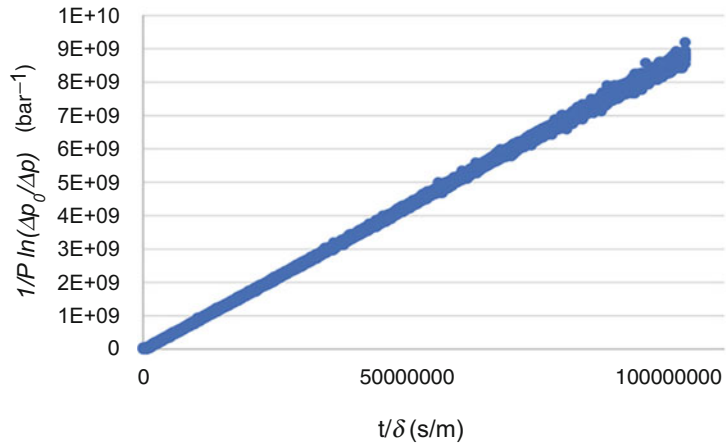


**Fig. 4** Representation of  $\frac{1}{P} \ln\left(\frac{\Delta p_0}{\Delta p}\right)$  versus  $\frac{t}{\delta}$  for obtaining the geometric parameter  $\beta$  from the slope

4. Open all the valves and the N<sub>2</sub> gas bottle.
5. Turn on the computer and start the acquisition program, *LabView*.
6. With all the valves opened, open the N<sub>2</sub> gas regulator up to 0.1 bar.
7. After 1 min, close the exit valves and increase the N<sub>2</sub> pressure up to 0.7 bar.
8. Close the entrance valves and wait 5 min to see if the pressure is constant in both compartments.
9. Open and close the exit valve connected to the permeate compartment.
10. Follow the evolution of pressure in both compartments (feed and permeate) with time.
11. Using the N<sub>2</sub> permeability value for that PDMS film given by the manufacturer and plotting  $\frac{1}{P} \ln\left(\frac{\Delta p_0}{\Delta p}\right)$  versus  $\frac{t}{\delta}$ , the geometric parameter  $\beta$  is obtained from the slope.

**3.2 O<sub>2</sub> or CO<sub>2</sub> Permeability of the Film**

1. Measure the film thickness.
2. Place the film inside the permeation cell and close it.
3. Introduce the permeation cell in the water bath regulated for 30 °C.
4. Open all the valves and the O<sub>2</sub> or CO<sub>2</sub> gas bottle.
5. Start the acquisition program.
6. With all the valves opened, open the O<sub>2</sub> or CO<sub>2</sub> gas regulator up to 0.1 bar.
7. After 1 min, close the exit valves and increase the O<sub>2</sub> or CO<sub>2</sub> pressure up to 0.7 bar.

**Table 1**  
**Water activity of saturated saline solutions at 25 °C**

| Saturated salt solution                         | Water activity |
|---|----------------|
| LiCl  | 0.115          |
| CH <sub>3</sub> COOK                            | 0.225          |
| MgCl <sub>2</sub> ·6H <sub>2</sub> O            | 0.324          |
| K <sub>2</sub> CO <sub>3</sub>                  | 0.447          |
| Mg (NO <sub>3</sub> ) <sub>2</sub>              | 0.520          |
| NaNO <sub>2</sub>                               | 0.649          |
| NaCl  | 0.769          |
| (NH <sub>4</sub> ) <sub>2</sub> SO <sub>4</sub> | 0.806          |
| BaCl <sub>2</sub>                               | 0.920          |
| K <sub>2</sub> SO <sub>4</sub>                  | 0.977          |

8. Close the entrance valves and wait 5 min to see if the pressure is constant in both compartments.
9. Open and close the exit valve connected to the permeate compartment.
10. Follow the evolution of pressure in both compartments (feed and permeate) with time.
11. Plot the data as  $\frac{1}{\beta} \ln\left(\frac{\Delta p_0}{\Delta p}\right)$  versus  $\frac{t}{\delta}$ , and the permeability is determined from the slope.

### 3.3 Conditioning of Hydrophilic Films at Constant Relative Humidity

Film equilibration is usually carried out by placing samples in desiccators containing at the bottom a saturated salt solution with a known water activity ( $a_w$ ) value (*see Note 2*). Different relative humidity values may be achieved by using different saturated salt solutions. The  $a_w$  of the saturated salt solutions at 25 °C is shown in Table 1 [15]. The relative humidity,  $RH = a_w \times 100$ . The equilibration process is complete when the film mass remains unchanged over time.

### 3.4 Standard Methods for Oxygen and Carbon Dioxide Permeation

The most used standard methods for measuring OTR are ASTM D3985, ASTM F1927, and ASTM F2622 [16–18]. They use an isostatic permeation measurement with a flow-through technique as represented in Fig. 5.

The differences between standards are related to:

- (a) Test gas.
- (b) Type of samples.
- (c) Method and type of sensor.
- (d) Measurement conditions.

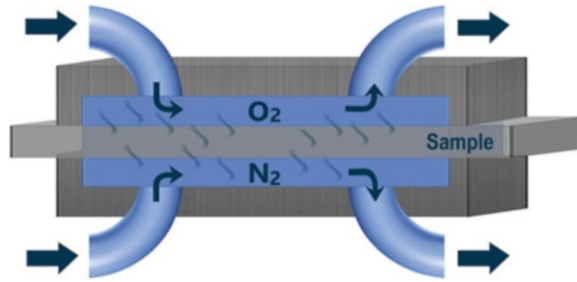


**Fig. 5** Isostatic permeation measurement of O<sub>2</sub> using a flow-through technique

#### **ASTM D3985**

This test method covers a procedure for the determination of the steady-state rate of transmission of oxygen gas through plastics in the form of film, sheeting, laminates, coextrusions, or plastic-coated papers or fabrics. It provides the determination of (i) OTR, (ii) the permeance of the film to oxygen gas (PO<sub>2</sub>), and (iii) OP in the case of homogeneous materials. It relies on a coulometric sensor and uses nitrogen as a carrier gas. It applies to dry conditions at a constant temperature.

#### **ASTM F1927**

This test method covers a procedure for the determination of the rate of transmission of oxygen gas, at a steady state, at a given temperature, and at %RH level, through film, sheeting, laminates, coextrusions, or plastic-coated papers or fabrics. This test method extends the common practice of dealing with zero humidity to a controlled relative humidity. Humidity plays an important role in the OTR of many materials, in particular hydrophilic polymers.

#### **ASTM F2622**

This test method covers a procedure for the determination of the steady-state rate of transmission of oxygen gas through plastics in the form of film, sheeting, laminates, coextrusions, or plastic-coated papers or fabrics. It uses various sensors, including coulometric, electrochemical, and zirconium oxide. The standard methods most used for measuring CO<sub>2</sub>TR are ASTM F2476 and DIN 53380-4 [19, 20].

#### **ASTM F2476**

This method covers a procedure for the determination of the steady-state rate of transmission of carbon dioxide gas through plastics in the form of film, sheeting, laminates, coextrusions, or plastic-coated papers or fabrics. It provides for the determination of (i) CO<sub>2</sub>TR, (ii) the permeance of the film to carbon dioxide gas (PCO<sub>2</sub>), and (iii) CO<sub>2</sub>P in the case of homogeneous materials. It

uses an infrared sensor and nitrogen as a carrier gas. It applies to dry conditions at a constant temperature.

#### DIN 53380-4

This method covers a procedure for the determination of the steady-state rate of transmission of carbon dioxide gas through plastics in the form of film, sheeting, laminates, coextrusions, or plastic-coated papers or fabrics.

#### Instruments for Measuring O<sub>2</sub> and CO<sub>2</sub> Permeation

MOCON [21] has commercial instruments for measuring oxygen transmission rates of flat films and packages being the Ox-Tran<sup>®</sup> analyzers the most popular. Measurements are made following ASTM method D3985. In this isostatic coulometric method, flat film samples are clamped into a diffusion cell, which is then purged of residual oxygen using an oxygen-free carrier gas such as N<sub>2</sub>. The carrier gas is routed to the instrument sensor until a stable zero has been established. Pure oxygen is then introduced into the outside chamber of the diffusion cell. Oxygen molecules diffusing through the film to the inside chamber are conveyed to the sensor by the carrier gas. The Ox-Tran system uses a patented coulometric sensor (CoulOX<sup>®</sup>) to detect oxygen transmission through both flat films and packages.

Modern Controls, Inc. (MOCON) also makes instruments for measuring carbon dioxide permeation. Their Permatran-C<sup>®</sup> line of instrument analyzer can test the CO<sub>2</sub>TR on both films and packages from low to high barriers. MOCON's patented modulated infrared sensor is the only modulated sensor system on the market meeting ASTM F2476 and capable of measuring low CO<sub>2</sub>TR detection levels down to 0.5 cm<sup>3</sup> m<sup>-2</sup> d<sup>-1</sup>.

Labthink [22] also has gas permeability instruments for O<sub>2</sub> and CO<sub>2</sub>, which are described in Table 2.

**Table 2**  
**Gas permeability instruments for O<sub>2</sub> and CO<sub>2</sub>**

| Testing instrument | Testing method                             | Test gas  | Type of packaging            |
|--------------------|--|---|------------------------------|
| C230, OX2/231      | Coulometric sensor method (equal pressure) | O <sub>2</sub>  | Films and sheeting, packages |
| VAC Series         | Differential pressure                      | O <sub>2</sub> , N <sub>2</sub> , and CO <sub>2</sub> , special gases | Films and sheeting           |
| G2/131, G2/132     | Differential pressure                      | O <sub>2</sub> , N <sub>2</sub> , and CO <sub>2</sub>                 | Films and sheeting, packages |
| G2/130             | Differential pressure                      | O <sub>2</sub> , N <sub>2</sub> , and CO <sub>2</sub>                 | Packages                     |

## 4 Notes

### 1. *Permeability units*

A wide variety of units are used for gas permeability due to the variation in industries measuring permeability. Other common units of gas permeability include:

- $\text{cm}^3$  (STP)  $\text{mil in}^{-2} (100 \text{ d})^{-1} \text{ atm}^{-1}$ , where 1 mil is equal to 0.00254 cm and 1 d is 24 h.
- $\text{ft}^3$  (STP)  $\text{mil ft}^{-2} \text{ d}^{-1} \text{ atm}^{-1}$ , where 1 ft is equal to 0.3048 cm.
- $\text{m}^3$  (STP)  $\text{m m}^{-2} \text{ s}^{-1} \text{ Pa}^{-1}$ .

The permeability in Eq. 8 is given in  $\text{m}^2 \text{ s}^{-1}$  because the solubility coefficient is dimensionless. In order to convert 1 barrer to  $\text{m}^2 \text{ s}^{-1}$ , it is necessary to use the molar volume at STP conditions and multiply by RT resulting in 1 barrer equal to  $8.4 \times 10^{-5} \text{ m}^2 \text{ s}^{-1}$  at 30 °C where 1 barrer is equal to  $3.35 \times 10^{-16} \text{ mol m m}^{-2} \text{ s}^{-1} \text{ Pa}^{-1}$ .

### 2. *Permeation in hydrophilic films*

As the oxygen and carbon dioxide permeabilities of hydrophilic films are highly dependent on their adsorbed moisture content, they should be previously equilibrated at constant relative humidity in desiccators with saturated saline solutions: LiCl,  $\text{CH}_3\text{COOK}$ ,  $\text{MgCl}_2 \cdot 6\text{H}_2\text{O}$ ,  $\text{K}_2\text{CO}_3$ ,  $\text{Mg}(\text{NO}_3)_2$ ,  $\text{NaNO}_2$ , NaCl,  $(\text{NH}_4)_2\text{SO}_4$ ,  $\text{BaCl}_2$ , and  $\text{K}_2\text{SO}_4$  (Table 1).

The barrier properties of different hydrophilic materials should be compared under the same relative humidity and temperature conditions. The  $\text{CO}_2$  and  $\text{O}_2$  permeability of hydrophilic films, namely, from polysaccharides and proteins, are extremely dependent on their water content, as observed by several authors. Gontard et al. [23] reported for wheat gluten films an increase of the oxygen permeability of about 950 times for a change of the film water content from 7.5% to 42% (dry basis) and an increase of nearly 36,550 times on the  $\text{CO}_2$  permeability for a variation of the relative humidity of the atmosphere in contact with the film from 60% to 95%. It is difficult to compare the results presented by different authors unless the exact film water content or testing %RH for each study is specified.

## Acknowledgments

This research was funded by national funding from FCT, Foundation for Science and Technology, through the individual research grant (SFRH/BD/144346/2019) of J.P. and the individual research grant (2020.04441.BD) of C.R. It was supported by

national funds from FCT/MCTES (UID/AGR/04129/2020) and by MEtrICs—Mechanical Engineering and Resource Sustainability Center, which is financed by national funds from FCT/MCTES (UIDB/04077/2020 and UIDP/04077/2020). Finally, this work has been supported by the Associate Laboratory for Green Chemistry—LAQV, which is financed by national funds from FCT/MCTES (UIDB/50006/2020 and UIDP/50006/2020).

## References

1. Robertson GL (2006) Food packaging: principles and practice, 2nd edn. CRC Press, Boca Raton
2. Vaclavik VA, Christian EW (2014) Essentials of food science, 4th edn. Springer Science+Business Media, New York
3. Mohamed SAA, El-Sakhawy M, El-Sakhawy MAM (2020) Polysaccharides, protein and lipid-based natural edible films in food packaging: a review. *Carbohydr Polym* 238:116178. <https://doi.org/10.1016/j.carbpol.2020.116178>
4. Souza VGL, Pires JRA, Rodrigues C et al (2019) Physical and morphological characterization of chitosan/montmorillonite films incorporated with ginger essential oil. *Coatings* 9(11):700. <https://doi.org/10.3390/coatings9110700>
5. Souza VGL, Rodrigues C, Valente S et al (2020) Eco-friendly ZnO/chitosan bionanocomposites films for packaging of fresh poultry meat. *Coatings* 10(2):110. <https://doi.org/10.3390/coatings10020110>
6. Pires JRA, Souza VL, Fernando AL (2019) Valorization of energy crops as a source for nanocellulose production—current knowledge and future prospects. *Ind Crop Prod* 140:111642. <https://doi.org/10.1016/j.indcrop.2019.111642>
7. Tian F, Chen W, Wu CE et al (2019) Preservation of Ginkgo biloba seeds by coating with chitosan/nano-TiO<sub>2</sub> and chitosan/nano-SiO<sub>2</sub> films. *Int J Biol Macromol* 126:917–925. <https://doi.org/10.1016/j.ijbiomac.2018.12.177>
8. Barrer RM (1941) Diffusion in and through solids. Macmillan, New York
9. Mulder M (2003) Basic principles of membrane technology. Kluwer Academic Publishers, Springer Netherlands
10. Alves VD, Costa N, Coelho IM (2010) Barrier properties of biodegradable composite films based on kappa-carrageenan/pectin blends and mica flakes. *Carbohydr Polym* 79:269–276. <https://doi.org/10.1016/j.carbpol.2009.08.002>
11. Siracusa V (2012) Food packaging permeability behaviour: a report. *Int J Polym Sci* 2012:1–11. <https://doi.org/10.1155/2012/302029>
12. Souza V, Pires JJRA, Torrico É et al (2019) Activity of chitosan-montmorillonite bionanocomposites incorporated with rosemary essential oil: from in vitro assays to application in fresh poultry meat. *Food Hydrocoll* 89:241–252. <https://doi.org/10.1016/j.foodhyd.2018.10.049>
13. Crank J (1975) The mathematics of diffusion, 2nd edn. Clarendon Press, Oxford
14. Cussler EL (2009) Diffusion: mass transfer in fluid systems, 3rd edn. Cambridge University Press
15. Hong TD, Edgington S, Ellis RH et al (2005) Saturated salt solutions for humidity control and the survival of dry powder and oil formulations of *Beauveria bassiana* conidia. *J Invertebr Pathol* 89:136–143. <https://doi.org/10.1016/j.jip.2005.03.007>
16. ASTM D3985-17 (2017) Standard test method for oxygen gas transmission rate through plastic film and sheeting using a coulometric sensor. ASTM International, West Conshohocken
17. ASTM F1927-20 (2020) Standard test method for determination of oxygen gas transmission rate, permeability and permeance at controlled relative humidity through barrier materials using a coulometric detector. ASTM International, West Conshohocken
18. ASTM F2622-20 (2020) Standard test method for oxygen gas transmission rate through plastic film and sheeting using various sensors. ASTM International, West Conshohocken
19. ASTM F2476-20 (2020) Standard test method for the determination of carbon dioxide gas transmission rate (CO<sub>2</sub>TR) through barrier materials using an infrared detector. ASTM International, West Conshohocken

20. DIN 53380-4:2006-11 (2006) Testing of plastics – determination of gas transmission rate – Part 4: Carbon dioxide specific infrared absorption method for testing of plastic films and plastic mouldings. German Institute for Standardization, Berlin
21. Gas Measurement Instruments & Testing Services | AMETEK MOCON. <https://www.ametekmocon.com/>
22. Packaging Testing Instruments & Testing Services – Labthink International. <https://www.labthinkinternational.com/>
23. Gontard N, Thibault R, Cuq B, Guilbert S (1996) Influence of relative humidity and film composition on oxygen and carbon dioxide permeabilities of edible films. *J Agric Food Chem* 44:1064–1069. <https://doi.org/10.1021/jf9504327>



# Chapter 13

## Microbial Permeation Through Food Packaging Materials

Julia V. Ernesto, Patricia Severino, Anna C. Venturini,  
Cristiana M. P. Yoshida, Classius F. da Silva, and Patricia S. Lopes

### Abstract

Microbial permeation is an essential property in developing food packaging materials. Here we describe a simple method to determine it by placing the film on open vials containing nutrient broth. Negative and positive vials are also provided in this method. The tested vials are placed in an open environment for about ten days. The turbidity of the nutrient broth in any vial is recorded as microbial contamination, meaning the microorganism could permeate through the packaging material. This straightforward protocol can be invoked by material developers targeting microbial-tight packaging.

**Key words** Permeation of microorganisms, Turbidity, Flexible packaging, Food innocuity, Food safety, Microorganism-proof packaging

---

### 1 Introduction

The microbial permeation assay allows analyzing whether a given packaging system constitutes a barrier to microorganisms' passage, preventing contamination. The primary roles of food packaging materials are to provide physical protection, prevent post-processing contamination, extend shelf-life, and communicate information to consumers [1]. The properties of packaging materials play a significant role in food quality and safety. It is essential to control the microbial barrier protection to prevent spoilage and pathogenicity of food products.

Among the aforementioned functions of food packaging, protecting food from microbiological contamination after processing stands out. Disrupting the hermeticity of the packaging system may allow microbial contamination. An example is when sealing or closing such systems, which could be solved by adjusting machinery or revising standard protocols. Classic materials such as glass, rigid plastics, and metals are used in food packaging and usually do not pose risks of microbial permeation when used according to



pre-established processing standards. Although these traditional materials have excellent barrier properties against microbial permeation, in addition to suitable mechanical properties, most of these materials have very slow biodegradation, lasting in nature for centuries. Thus, such materials might represent an environmental problem for the planet if discarded incorrectly. New biodegradable materials based on biopolymers have been tested in food packaging to circumvent these low biodegradation rates.

However, flexible packaging, particularly those from biopolymers, still faces challenges concerning mechanical and barrier properties (against, e.g., water vapor and microorganisms). The barrier properties of a packaging system are closely related to the chemical, physical, sensory, and microbiological stability of the product. Specifically, in the case of food packaging, the methodologies for the quantitative determination of gas (e.g., oxygen and carbon dioxide; *see* Chap. 12) and moisture (*see* Chap. 11) permeabilities are well standardized, even with specific commercial equipment for measuring these properties. On the other hand, there is no standardized methodology for the quantitative determination of microbial permeation through food packaging. Blocking the passage of small molecules such as gases and water vapor is intuitively harder for packaging than it is for larger objects such as microbial cells. However, porous or defective films could allow microorganisms to pass through packaging, therefore leading to the problems pointed out above.

As far as biopolymer-based packaging, it is to be considered that biopolymers are usually hydrophilic. According to Mondal and Hu [2], membranes (or films) of hydrophilic polymers can absorb water very quickly and create a “wicking” action that attracts water molecules and then enables the transmission of steam through an active diffusion mechanism. In addition, the thickness and chemical structure are determinants in the permeability of a nonporous membrane (or film).

Also, biopolymers can present amorphous and crystalline domains (i.e., semicrystalline) in different proportions. Polymer chains do not pack perfectly, and there is some unoccupied space between them. The amount of many small spaces between the polymer chains in amorphous, noncrystalline materials is the free volume. Even if this volume accounts for only a small portion of the overall volume, it is sufficient to allow some rotation of polymer backbone segments. Therefore, a dense polymer may be thought of as a “porous medium,” with the local free volume serving as the “pores.” Fluid transport through porous media is identical to penetrant transport through a dense polymer membrane (or film). The distinction between these two scenarios is that the size and location of “pores” inside the dense polymer membrane change with time, implying that a penetrant will pass through a “pore” with a certain probability. As a result, it is fair to consider a dense

polymer membrane to be a porous material, with pores identified as gaps in the polymer matrix [3].

The barrier against microbial permeation is a topic of great importance in applying plastic films for food, and the methodologies used to evaluate microbial permeation are scarce. However, methods for determining microbial permeation are described in the development of films and membranes used as wound dressings because microbial contamination represents a major problem in wound healing. Such methods may be extended to flexible packaging. Several articles report methods for determining microbial permeation in dressings [4–11], most of these relying on the methodology described by Wittaya-Areekul and Prahsarn [12], which has also been used to assess microbial permeation in food packaging [13, 14].

The method described by Wittaya-Areekul and Prahsarn [12] consists of fixing the packaging material on the top of a vial containing a nutrient broth. This vial is exposed to the environment and analyzed after a few days. As the vial and broth are previously sterilized, any turbidity of the broth indicates that microorganisms could permeate through the material. On the other hand, if there is no broth turbidity, the material is considered impermeable to microorganisms. These techniques can be applied to (bio)-polymeric films and even flexible composites or any materials that can be fixed on the top of the vial. Several advantages can be mentioned for this technique, such as low cost, unsophisticated equipment, and the possibility of evaluating the permeation of specific microorganisms by using different broths, from the simplest to the most sophisticated. Yet, like most microbiological analyses, this method is not rapid; instead, it takes a few days to thoroughly assess the microbial permeation through the material.

---

## 2 Materials

### 2.1 Experimental Devices and Sample Preparation (See Note 1)

1. Ultrapure or deionized water (*see Note 2*).
2. Glass flasks (vials) with a 100-mL capacity, sanitized and dried (calculate enough for the number of replicates that will be carried out per sample). Penicillin flasks (Fig. 1a) are recommended.
3. Graduated cylinders or glass beakers.
4. Nutrient broth—approximate formula (per liter): beef extract, 3 g; enzymatic digest of gelatin, 5 g; final pH, 6.8 ( $\pm 0.2$  at 25 °C).
5. Autoclave (*see Note 3*).
6. Poly(vinyl chloride) (PVC) weldable unions (Fig. 1b) with 25-mm-diameter opening (in sufficient quantity for the



**Fig. 1** Materials for the determination of microbial permeation

number of replicates that will be carried out per sample, one set per flask).

7. Gamma radiation source (25 kGy) or 70 vol% ethanol solution plus sterilized phosphate buffer saline.
8. Laboratory auto-sealing, flexible, and moldable film, as Parafilm<sup>®</sup>.
9. Tweezers and scissors sterilized by autoclaving.

## 2.2 Result Evaluation

1. Digital camera.
2. Absorbance reader using 96-well plates, from Biotek Synergy HT or another manufacturer.
3. 3,5-Triphenyl tetrazolium (TTC) at 0.1% (w/v) diluted in a sterile 0.9% (w/v) NaCl solution (*see Note 4*).

---

## 3 Methods

It is suggested that at least one triplicate be tested for each type of packaging sample.

1. Prepare the liquid medium (nutrient broth) for microbial growth (*see Notes 5–8*).
2. Perform steam sterilization by autoclaving glass flasks containing culture medium, usually for 15 min at 121 °C. A typical standard for steam sterilization is achieved after 15 min under a pressure of 106 kPa (1 atm) once all surfaces have reached a temperature of 121 °C.
3. Cut the film samples into 5-cm-diameter disks (in the number of replicates that will be carried out per sample).
4. Sterilize the sample disks, e.g., by exposure to ultraviolet radiation, in laminar flow for 15 min on each side, or another suitable sterilization method, such as ionizing radiation or

even ethylene oxide. Please be aware that you must perform previous tests to ensure that the samples do not undergo modifications after the sterilization process.

5. Hatch the sample disks between the PVC devices (as shown in Fig. 2). Ensure that the sample does not present a tear or hole from the manipulation.
6. Fit the PVC apparatus containing the sample attached to the mouths of the flasks containing the culture medium (as shown in Fig. 2).
7. Seal the apparatus and the upper part of the flasks laterally with Parafilm<sup>®</sup> so that the packaging samples are the only communication between the culture medium in the flasks and the external environment.
8. As controls, set six vial systems (triplicates for positive and negative controls) comprising the PVC union and the flasks filled with the culture medium. For the positive control, seal these only laterally using Parafilm<sup>®</sup>; that is, these flasks will not have barriers between the culture medium and the external environment. For the negative control, seal the flask and union entirely using Parafilm<sup>®</sup>; that is, there should be no communication between the culture medium and the external environment.
9. Expose the systems to environmental conditions, e.g., in the lab (for specific microorganisms, *see* **Notes 5–9**) for 10 days, depending on the study design. On days 1, 5, and 10, for example, macroscopically assess the turbidity of the culture medium, which indicates microbial growth (*see* **Notes 10–12**).
10. Take pictures of all systems throughout the evaluation period (Fig. 3).
11. At the end of the test period, transfer aliquots from each flask to 96-well culture plates (Fig. 4) and perform an absorbance reading at 600 nm. To confirm the result, insert 100  $\mu$ L of TTC dye solution in each well. Incubate the plates for 1 h and evaluate again using the plate reader at 540 nm (*see* **Note 13**).

---

## 4 Notes

1. Perform all the procedures in a laminar flow cabinet, preferably a class II A1. The operator must be appropriately dressed, wearing a cap, mask, gloves, and lab coat. Manipulate the samples using sterilized tweezers.
2. Prepare all solutions using ultrapure water or deionized water, according to the reagents and analytical grade.

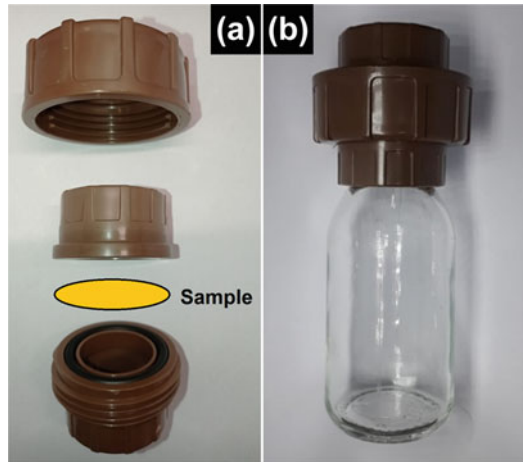


**Fig. 2** Schematic representation of the microbial permeation-measuring device: poly(vinyl chloride) union (a) before (note the position of the sample specimen) and (b) after assembling and attachment into the penicillin flask

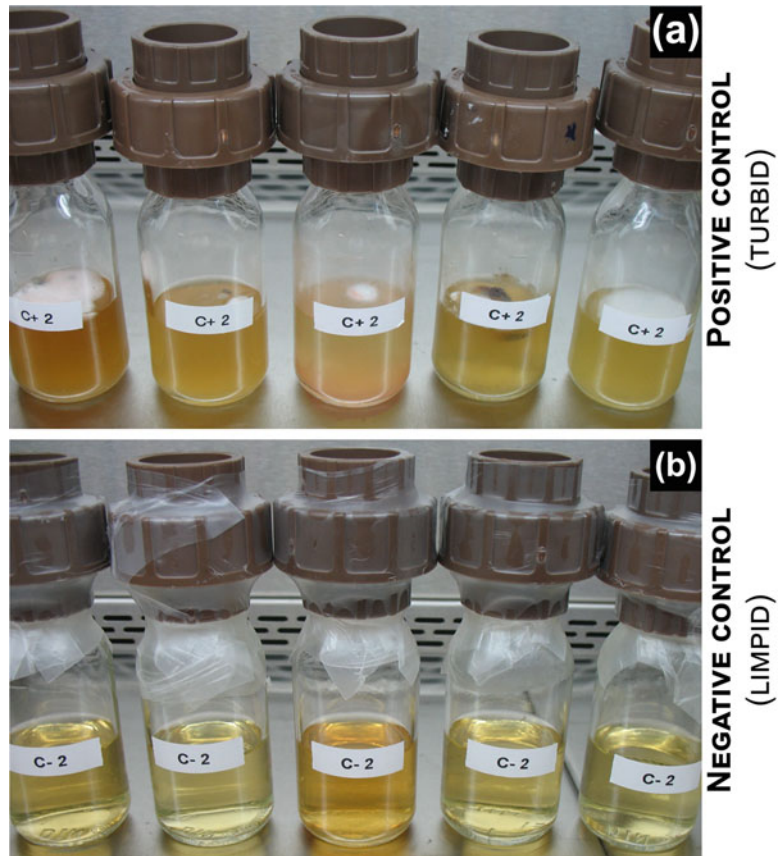


**Fig. 3** Visual aspect of the (a) positive- and (b) negative-control vials after exposure to the laboratory environment

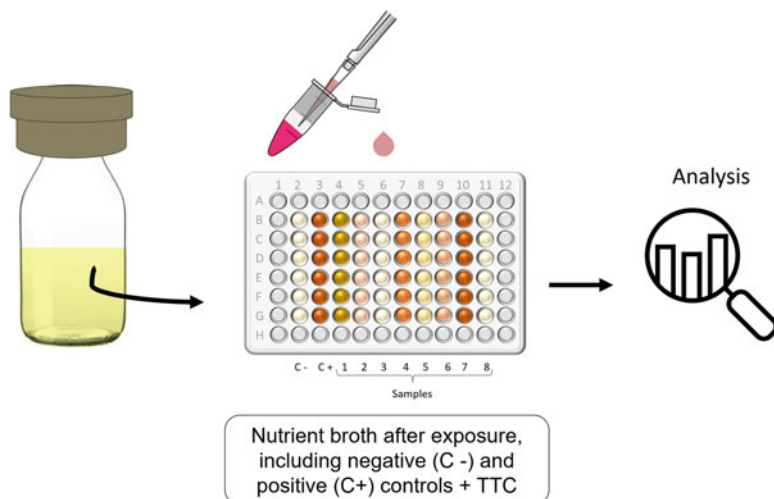


**Fig. 4** Schematic representation of microbial penetration analysis

3. Perform the correct disposal or sanitization of all materials that come into contact with the biological culture medium. Ensure that all sterilized material for the experiment (when indicated) has gone through the correct sterilization procedure, using autoclaving sterilization tapes, for example.
4. The TTC dye solution must be prepared and immediately used. The laminar flow cabinet lights must be off, and the plates must be covered with aluminum foil until the reading process. This solution is extemporary and must not be stored.
5. Add 50 mL of water to a 100-mL graduated cylinder or a glass beaker. Weigh 0.4 g of nutrient broth and transfer it to a glass flask of item 1. Add the water to the glass flask. Perform the same procedure for each flask used in the test.
6. Should the purpose be the evaluation of a specific class of microorganisms, like anaerobic as the *Clostridium* sp. [15], the culture medium can be switched to, e.g., Fluid Thioglycolate Medium or even Reinforced Clostridial Medium. After the exposure period, the flasks must be incubated in anaerobiosis at 30–35 °C for 48 h. It is important to remember that the *Clostridium* species can sporulate; that is, the spores, which are forms of resistance of the microorganism that are released to the environment when the conditions are not conducive to its growth, can be spread around the environment and can reach the product if this packaging is not adequate. Anaerobiosis conditions could be assessed using an anaerobiosis chamber or even a CO<sub>2</sub> incubator.
7. The culture medium can be modified according to the type of microorganisms to be evaluated in the test: if the intention is to evaluate the permeation of fungi only, one can use the

Sabouraud Dextrose Broth. This medium is poor in nutrients and limits the growth of bacteria, which are more nutritionally demanding. For more demanding microorganisms, the brain and heart infusion broth or even the tryptic soy broth can be used instead.

8. It is important to note that, if the intention is to evaluate a specific microorganism that is not usually found in the lab environment, the target microorganism can be inoculated directly onto the packaging material at the top of the system (induced test). When this method is used, it is essential that, once the microorganism is inoculated, the upper PVC union is capped with aluminum foil and that the systems are incubated at an appropriate temperature. This allows the evaluation of a specific packaging behavior.
9. To evaluate specific microorganisms, the usual concentration is  $10^3$ – $10^6$  CFU  $\text{cm}^{-2}$  depending on the microorganism type [16]. The use of microorganisms obtained from a culture collection, like ATCC (American Type Culture Collection) or NIH (National Institute of Health), is preferable to the use of wild microorganisms or even those isolated from humans or animals. To obtain standard cultures, use methods like dilution followed by counting or turbidity assays using an absorbance reader or even MacFarland scale.
10. The exposure times may vary, depending, for example, on the shelf-life or transportation conditions of the target products, so that the real situation of the product is simulated. In this context, other parameters such as temperature and humidity can be adjusted to mimic the targeted environmental conditions.
11. The herein described test was modified from Wittaya-Areekul and Prahsarn (2006), similar to Augustine et al. [17]. The macroscopic evaluation of the positive control flasks ensures that the nutrient broth was suitable for microbial growth and could represent a free-condition system. In contrast, the negative control flasks are tested to illustrate the efficiency of the sterilization process and to ensure that all the microorganisms observed in the culture medium of the devices containing the samples arose from the external environment and must have passed through the packaging material.
12. The packaging is microorganism-proof when microbial growth is evidenced in the positive control, but all the tested membranes prevent any visible microbial contamination.
13. Other methods can be used to evaluate the results, for example, the preparation of slides with the contaminated medium for identifying the microorganism followed by the Gram staining process and then by molecular assays (polymerase chain reaction) or even mass spectroscopy.

## References

- Singh P, Wani AA, Langowski H-C (2017) Food packaging materials: testing & quality assurance, 1st edn. CRC Press
- Mondal S, Hu JL (2006) Segmented shape memory polyurethane and its water vapor transport properties. *Des Monomers Polym* 9(6):527–550. <https://doi.org/10.1163/156855506778944028>
- Chen C, Han B, Li J, Shang T, Zou J, Jiang W (2001) A new model on the diffusion of small molecule penetrants in dense polymer membranes. *J Membr Sci* 187(1–2):109–118. [https://doi.org/10.1016/S0376-7388\(00\)00689-X](https://doi.org/10.1016/S0376-7388(00)00689-X)
- Singh B, Sharma S, Dhiman A (2013) Design of antibiotic containing hydrogel wound dressings: biomedical properties and histological study of wound healing. *Int J Pharm* 457:82–91. <https://doi.org/10.1016/j.ijpharm.2013.09.028>
- Singh B, Kumar A (2016) Radiation formation of functionalized polysaccharide-protein based skin mimicking semi-inter penetrating network for biomedical application. *Int J Biol Macromol* 92:1136–1150. <https://doi.org/10.1016/j.ijbiomac.2016.08.011>
- El-Hosary R, El-Mancy SMS, El-Deeb KS et al (2020) Efficient wound healing composite hydrogel using Egyptian *Avena sativa* L. polysaccharide containing  $\beta$ -glucan. *Int J Biol Macromol* 149:1331–1338. <https://doi.org/10.1016/j.ijbiomac.2019.11.046>
- Genevro GM, Gomes Neto RJ, Beppu MM et al (2019) Glucomannan asymmetric membranes for wound dressing. *J Mater Res* 34:481–489. <https://doi.org/10.1557/jmr.2018.463>
- Salehi M, Niyakan M, Ehterami A et al (2020) Porous electrospun poly( $\epsilon$ -caprolactone)/gelatin nanofibrous mat containing cinnamon for wound healing application: in vitro and in vivo study. *Biomed Eng Lett* 10:149–161. <https://doi.org/10.1007/s13534-019-00138-4>
- Prabu D, Majdalawieh A, Abu-Yousef I et al (2016) Preparation and characterization of gatifloxacin-loaded sodium alginate hydrogel membranes supplemented with hydroxypropyl methylcellulose and hydroxypropyl cellulose polymers for wound dressing. *Int J Pharm Investig* 6:86. <https://doi.org/10.4103/2230-973x.177810>
- Tomoda BT, Corazza FG, Beppu MM et al (2020) Silk fibroin membranes with self-assembled globular structures for controlled drug release. *J Appl Polym Sci* 137:48763. <https://doi.org/10.1002/app.48763>
- Oliveira RN, McGuinness GB, Rouze R et al (2015) PVA hydrogels loaded with a Brazilian propolis for burn wound healing applications. *J Appl Polym Sci* 132. <https://doi.org/10.1002/app.42129>
- Wittaya-Areekul S, Prahsarn C (2006) Development and in vitro evaluation of chitosan-polysaccharides composite wound dressings. *Int J Pharm* 313:123–128. <https://doi.org/10.1016/j.ijpharm.2006.01.027>
- de Silva FM, Lopes PS, da Silva CF et al (2016) Active packaging material based on buriti oil – *Mauritia flexuosa* L.f. (Arecaceae) incorporated into chitosan films. *J Appl Polym Sci* 133. <https://doi.org/10.1002/app.43210>
- Rodrigues MÁV, Bertolo MRV, Marangon CA et al (2020) Chitosan and gelatin materials incorporated with phenolic extracts of grape seed and jabuticaba peel: rheological, physicochemical, antioxidant, antimicrobial and barrier properties. *Int J Biol Macromol* 160:769–779. <https://doi.org/10.1016/j.ijbiomac.2020.05.240>
- Taclindo C, Nygaard GS, Bodily HL (1967) Examination of prepared foods in plastic packages for *Clostridium botulinum*. *Appl Microbiol* 15:426–430. <https://doi.org/10.1128/aem.15.2.426-430.1967>
- Spanu C, Scarano C, Ibba M et al (2014) Microbiological challenge testing for *Listeria monocytogenes* in ready-to-eat food: a practical approach. *Ital J Food Saf* 3:231–237. <https://doi.org/10.4081/ijfs.2014.4518>
- Augustine R, Kalarikkal N, Thomas S (2014) Advancement of wound care from grafts to bioengineered smart skin substitutes. *Prog Biomater* 3:103–113. <https://doi.org/10.1007/s40204-014-0030-y>



# **Part III**

## **Nontraditional Roles Played by Food Packaging Materials**



## Do Not “Pack and Pray”: Use Predictive Models to Assess the Microbial Safety and Shelf-Life of Modified Atmosphere Packaged Foods

Arícia Possas, Fernando Pérez-Rodríguez, and Antonio Valero

### Abstract

Besides protecting food from contact with the external environment and from airborne contamination, packaging can also contribute to prolong food shelf-life and increase food safety. The gaseous environment within a package can delay or inhibit microbial growth or modify the microbial ecology of the product. Evaluating the microbiological safety and the shelf-life of foods through predictive microbiology tools implies developing or selecting appropriate models that consider the impacts of different static and/or dynamic concentrations of O<sub>2</sub>, CO<sub>2</sub>, and N<sub>2</sub> on the behavior of spoilage and pathogenic microbiota. There is an increasing demand for predictive models that would allow one to identify in advance the headspace gas composition and the packaging material suitable for increasing food safety and shelf-life. The development of such numerical tools would decrease the number of time-consuming challenge-testing experiments necessary for experimentally quantifying and assessing the microbial fate in terms of changes in headspace composition. The objective of the present chapter is to provide information on the adequate development, validation, and interpretation of predictive microbiology models, including the effect of packaging atmosphere to achieve more reliable estimates of microbial behavior in packaged foods. A case study on a validated predictive model in cooked meat products is presented using the MicroHibro software tool.

**Key words** Predictive microbiology, Food packaging, Headspace composition, Shelf-life, Food safety, Modeling, Gas transfer, Carbon dioxide, Predictive modeling

---

### 1 Introduction

Besides protecting foodstuffs from contact with external environments and airborne contamination, food packaging can also help prolong food shelf-life and increase food safety [1]. The gaseous mixture present in a modified atmosphere packaging (MAP) can inhibit or slow down microbial growth in foods and even modify their ecology [1]. To avoid the transfer of gases through packaging, high-barrier films with multilayers are usually used in MAP

[2]. Such materials in many cases are oversized in terms of barrier properties, as most of the time there is no knowledge a priori of the specific requirements of the product regarding the gaseous mixture necessary to avoid microbial spoilage or proliferation of foodborne pathogens. Since high-barrier materials are usually expensive, MAP represents direct costs for the food industry [1].

In this context, identifying the headspace gas composition and the appropriate packaging material to assure a prolonged shelf-life and the control of microbial pathogens in MAP is of great interest. Predictive microbiology is the field of food microbiology aimed at describing microbial processes in foods—i.e., growth, inactivation/survival, and transfer—through the application of mathematical models [3]. These models enable estimating microbial populations in foods as functions of intrinsic, extrinsic, and implicit factors, such as pH,  $a_w$ , temperature, and microbial interactions, denoting relevant tools for shelf-life estimation, product development, microbial risk assessment, and aid in the compliance with microbiological criteria established for foods [3–5]. The development of predictive microbiology models, therefore, represents a breakthrough in the understanding of the effects of different factors on microbial behavior, including gaseous compounds present in MAP.

Traditionally, predictive models are classified as primary or secondary models according to their response variable [6]. Primary models are those describing the microbial kinetics, i.e., the evolution of microbial levels in foods over time at constant conditions. These models are used to estimate microbial growth and survival/inactivation parameters in foods (e.g., growth or survival rates, lag times, and maximum population density). On the other hand, secondary models relate changes in the primary model parameters with intrinsic or extrinsic factors (e.g., temperature,  $a_w$ , pH). Primary and secondary models as well as other modeling structures are usually implemented in user-friendly predictive microbiology software tools, the so-called tertiary models, to be applied in simulations for decision making in the food industry. Existing software for predictive microbiology have been reviewed by Tenenhaus-Aziza and Ellouze [7] and more recently by Possas et al. [8]. Usually, software users specify the values of the model factors such as storage temperature, and the software provides the results of model simulations as growth or survival/inactivation estimates.

Attention has been given to the impacts of the gaseous atmosphere of food packaging on microbial behavior [5, 9–12]. Carbon dioxide (CO<sub>2</sub>) is the most important component in the choice of a gaseous mixture to be applied in MAP [1]. The inhibiting effect of a constant CO<sub>2</sub> concentration distributed homogeneously in the headspace, together with the effects of food intrinsic and extrinsic factors, has been explored in predictive microbiology studies [4, 13,

14]. The choice of using a point-estimate approach when dealing with MAP gases can be associated with difficulties in quantifying their dynamics, which may be associated with their solubilization and diffusion into the food and mass transfer through the packaging materials [4, 11, 15]. Therefore, although the integration of the impact of gas dynamics in predictive models developed in MAP foods would result in more realistic predictions of microbial behavior, the development of such models remains a challenge [4, 11]. Examples of models integrating the impact of gas dynamics are the ones developed for *Pseudomonas* spp. and lactic acid bacteria (LAB) in chicken fillets [11] and the one developed for *Listeria monocytogenes* in processed cheese [16].

Comparison of results derived from different investigations with MAP products is very difficult due to the use of packaging materials with different permeabilities to O<sub>2</sub> and CO<sub>2</sub> (see Chapter 12 for protocols to determine the gas barrier of food packaging materials) and/or due to the lack of information provided in studies regarding the gas/product (G/P) ratio used in MAP [5]. To overcome the latter problem, instead of considering the concentration of CO<sub>2</sub> in the headspace, some authors considered more reasonable the evaluation of dissolved CO<sub>2</sub> in the water phase of the product in modeling studies [5, 10]. In addition, the simultaneous effect of both O<sub>2</sub> and CO<sub>2</sub> on the behavior of microorganisms in MAP foods has not been frequently investigated in modeling studies [17–20], due to difficulties in measuring O<sub>2</sub> concentrations [4]. These variability sources imply that predictive models, including the effect of MAP, should be built based on extensive challenge testing studies to assure a proper model validation.

For more information regarding predictive models built with growth data obtained from MAP foods, see the review by Chaix et al. [4]. The schematic flow for the development of predictive microbiology models in foods is shown in Fig. 1. In Subheading 2 of this chapter, methods traditionally performed for data generation for model development, fitting, and validation are briefly described based on information compiled from various studies. In addition, we present an example of how predictive models can be applied for shelf-life estimation, using our user-friendly predictive microbiology software MicroHibro ([www.microhibro.com](http://www.microhibro.com)) [21].

---

## 2 Methods

### 2.1 Data Generation to Evaluate Microbial Growth Kinetics in MAP Foods

Assuming that the objective of a study is to evaluate and model the effects of MAP on the growth kinetics of a microorganism in a foodstuff, growth curves expressed as microbial concentrations over time are developed at different conditions (e.g., temperature,  $a_w$ , pH) and various MAP configurations to cover a large range of

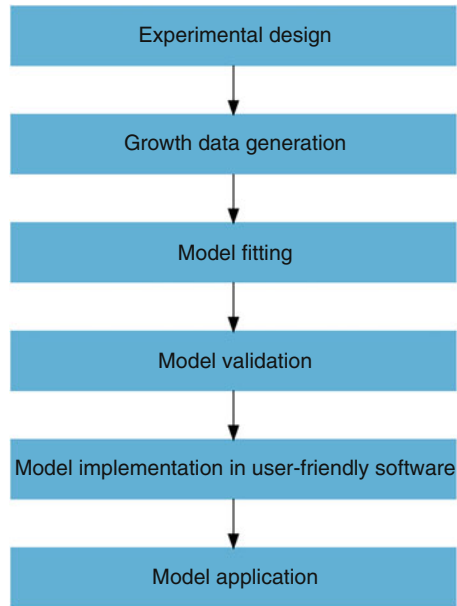


**Fig. 1** Schematic flowchart of the development of predictive microbiology models in MAP foods

possibilities, following a previously defined experimental design (*see Note 1*). For more information regarding guidelines for the performance of challenge tests for model development, *see* ISO 20976-1 [22]. For data generation, representative samples of the food product under evaluation are usually inoculated with the target spoilage or pathogenic microorganisms.

The atmosphere of the packaging containing the inoculated samples can be modified by means of gas packaging units, which remove the air and insert the desired food-grade gas mixtures of CO<sub>2</sub>, O<sub>2</sub>, and N<sub>2</sub> in selected packaging materials. The proportions of CO<sub>2</sub>, O<sub>2</sub>, and N<sub>2</sub> in MAP depend on the product nature and the ratio between the volume of the package and that of food [23]. For instance, low levels of O<sub>2</sub> are typically applied to reduce respiration and the related quality loss of vegetables, while high levels of this gas are used to stabilize the red color of fresh meat [18]. After sealing, the packages are stored under the environmental conditions set at the experimental design. Storage times are defined based on the shelf-life of the evaluated product.

Inoculated packaged samples are analyzed immediately after inoculation (time 0) and withdrawn and microbiologically analyzed at proper time intervals by applying traditional methods for microbial detection and enumeration, e.g., plate count method [22]. The physicochemical characteristics of samples that will be included as explanatory variables in the predictive model and other relevant parameters are also monitored in samples at different time points during shelf-life, e.g.,  $a_w$ , pH, and lactic acid content.

The headspace composition is measured immediately after packing and at each sampling time using gas analyzers. Aliquots of the headspace gas are collected with syringes after piercing packaging materials with the aid of a septum, e.g., film cover. In high-barrier packages, it is reasonable to assume that, once the gaseous mixture in the package has reached equilibrium, the CO<sub>2</sub> concentration in the headspace is proportional to the amount of CO<sub>2</sub> adsorbed by the product [24].

Different methodologies have been applied to estimate the concentration of CO<sub>2</sub> dissolved in the product as functions of the initial CO<sub>2</sub> concentration in the headspace (*see* **Notes 2** and **3**) [9, 12]. For instance, the concentrations of the CO<sub>2</sub> adsorbed by the product samples have been estimated by assessing the volume changes in the package headspace using a buoyancy technique and performing calculations based on volumetric measures and Henry's constant [12, 24]. A quadratic polynomial model has been developed to estimate the CO<sub>2</sub> dissolved in the water phase of cooked meat products as a function of the initial CO<sub>2</sub> concentration in the headspace, the storage temperature, and the relation G/P volume ratio [10].

The microbial data obtained in samples at different time points under different conditions are then subjected to model fitting.

## **2.2 Model Selection and Fitting**

Predictive models that consider the impact of a gas mixture on microbial growth are needed to predict the growth of microorganisms in a MAP system. These models should be able to describe the microbial patterns as influenced by the gaseous composition of the product. An exponential-type law is usually used to describe microbial kinetics in foods. Examples of predictive models used are shown in Fig. 2. Different primary models have been proposed to translate microbial growth kinetics in foods, including parameters with biological meaning, being the Baranyi and Roberts model [25], the modified Gompertz model [26], and the logistic model [27], the most commonly applied ones. Four microbial kinetic parameters can be estimated by fitting these models to growth kinetic data: the initial and maximum population densities ( $N_0$  and  $N_{\max}$ , respectively), the lag time (lag), and the maximum growth rate ( $\mu_{\max}$ ).

The growth parameters estimated through fitting primary models to growth data are dependent on the environmental and intrinsic factors evaluated (temperature, pH,  $a_w$ , CO<sub>2</sub>, etc.). The relationship between the estimated kinetic parameters and the evaluated factors can be described using secondary models. To this end, the most applied mathematical equations are the Ratkowsky-type or square-root models [28], cardinal models [29], polynomial models [30], and artificial neural network (ANN) models [31]. While polynomial and ANN models are purely empirical, square root models and the models belonging to the “cardinal”

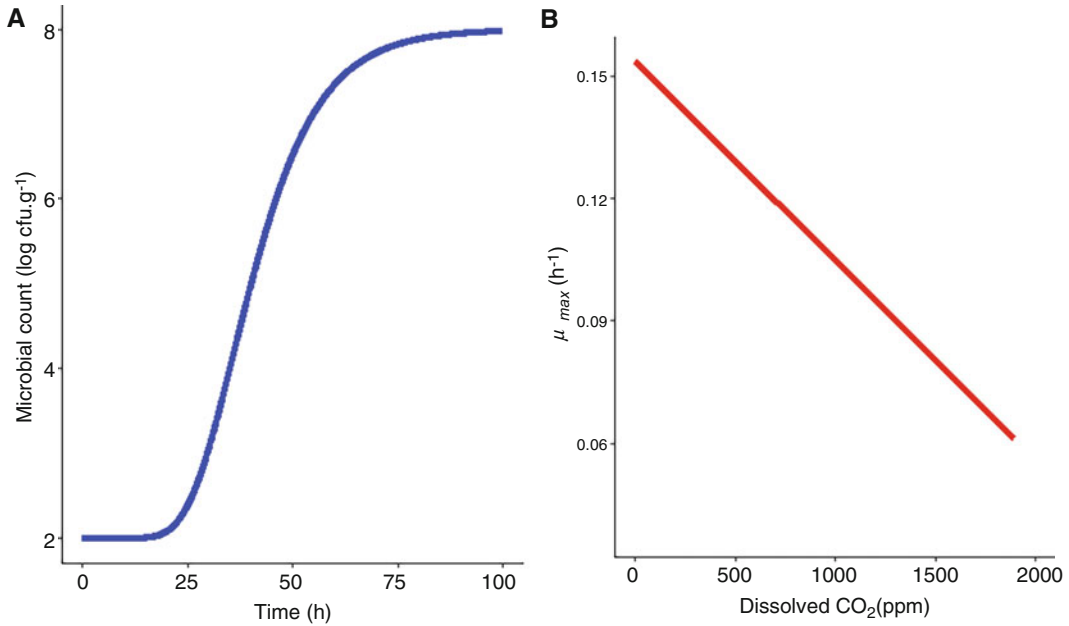


**Fig. 2** Examples of mathematical models fitted to growth data. **(a)** Gompertz primary model; **(b)** Square root secondary model

family have biological meaning, including parameters with biological significance such as the minimum temperature required for the growth of the target microorganism ( $T_{\min}$ ). Besides their mechanistic nature, Ratkowsky type and cardinal models can be extended to account for the influence of multiple relevant factors that affect microbial growth using the gamma concept approach (*see Note 4*) [32]. More information regarding modeling structures and approaches and their advantages and drawbacks can be found in Pérez-Rodríguez and Valero [3].

Regression methods are applied to estimate the parameters of the selected models that result in a better description of the observed data [3]. The most widely used regression method is the least square method [3]. In addition, the one-step and two-step regression analysis methods have been applied to fit models to microbial data. In the first approach, primary models describing the microbial kinetics as a function of time can be combined with secondary functions describing the effect of environmental conditions on microbial fate, and the combined model is fitted to the observed data. In this way, the parameter estimation can be done using a single-step procedure [18]. In the standard two-step modeling regression analysis, first the primary models are fitted to the microbial kinetic data, and then the secondary model is fitted to the primary model parameters estimates. Both approaches can result in accurate and precise models depending on the growth data used for model development (*see Note 5*). Such parameter estimation

techniques can be applied when a set of static experiments is available [33]. However, when evaluating dynamic conditions, the two-step parameter estimation method can no longer be used.

Model fitting can be performed by using different statistical and programming software, such as the SSP, Excel, MATLAB, and R. In addition, model fitting tools have been developed to fit different growth models to microbial data, such as the DMFit (available online at [www.combase.cc](http://www.combase.cc)) and the *biogrowth* (available online at <https://foodlab-upct.shinyapps.io/biogrowth4/>) [34]. Different statistical goodness-of-fit indexes can be applied to assess the goodness-of-fit indexes of predictive models, mainly the simple Root Mean Square Error (*RMSE*) (Eq. 1). The lower the *RMSE*, the better the fitting of the model to the data.

$$RMSE = \sqrt{\frac{\sum_{i=1}^n (\mathcal{Y}_i - \widehat{\mathcal{Y}}_i)^2}{n}} \quad (1)$$

where  $\mathcal{Y}_i$  corresponds to the observed value;  $\widehat{\mathcal{Y}}_i$  is the predicted value; and  $n$  is the number of data points or observations.

Finally, when comparing two models, the *F*-ratio and the so-called corrected Akaike's information criterion (AIC) [35] are two indexes frequently used [3]. For more details on how to perform calculations and the interpretation of these indexes, *see* refs. [3, 26].

### 2.3 Model Validation

Predictive models might be validated in foods prior to use, to evaluate the reliability of their predictions with real data [3]. To validate a predictive model, additional experiments with a MAP food artificially contaminated with the microorganism of interest are usually designed [18]. The experimental conditions set for these challenge tests (temperature,  $a_w$ , pH, CO<sub>2</sub> concentration, etc.) may be within the domain used for model development. Although validation should be performed with data derived from experiments with a given food, microbial data from the literature are usually used for validation to avoid the costs of additional challenge tests. Data on microbial responses in foods for model validation can be also found in databases, mainly the ComBase database ([www.combase.cc](http://www.combase.cc)) [36].

Modelers classify the models as fail-safe or fail-dangerous if the prediction overestimates or underestimates the observed growth, respectively. From the public health point of view, a fail-safe model is preferred compared to a fail-dangerous one, as the former yields more conservative predictions. Graphical representations of model predictions versus model observations are useful in evaluating whether a model is fail-safe or fail-dangerous. To determine in which degree model predictions coincide with the observed data derived from validation studies, traditional goodness-of-fit indexes



can be calculated, such as the abovementioned RMSE [3]. Moreover, specific validation indexes—namely, the accuracy ( $A_f$ ) and bias ( $B_f$ ) factors—can be determined to evaluate the capacity of the models to predict microbial behavior [37]. The  $A_f$  indicates how well the growth model predictions coincide with the observed data and a value equal to 1 indicates a perfect coincidence. On the other hand, the  $B_f = 1$  indicates that observations are equally distributed below and above model predictions, while  $B_f < 1$  and  $B_f > 1$  evidence a fails-dangerous and a fail-safe model, respectively [37].

Once validated, models are implemented in software tools to be available for prediction purposes.

---

### 3 Application of Predictive Models to Evaluate the Shelf-Life of Foods Using the Software Micro Hibro

The objective of this section is to demonstrate how validated predictive microbiology models available in the literature can be applied to assess the shelf-life of a MAP product with respect to the presence of a foodborne pathogen. The freely available software MicroHibro ([www.microhibro.com](http://www.microhibro.com)), which is a software for predictive microbiology and risk assessment in foods developed by our group [21], was used to implement and simulate the predictive models selected for this case study.

#### 3.1 Case Study

A food manufacturer is interested in evaluating if the MAP configurations of a processed cooked ham, together with storage temperature and physicochemical characteristics, assure that the product is safe during its shelf-life with regards to the presence of *L. monocytogenes*. Otherwise, another gaseous mixture may be used.

According to the European Regulation 2073/2005, for those ready-to-eat (RTE) foods supporting the growth of *L. monocytogenes*, food manufacturers might demonstrate that the levels will not exceed 100 cfu g<sup>-1</sup> during their shelf-life [38]. According to the mentioned regulation, durability studies, challenge tests, or predictive microbiology models can be applied by manufacturers to demonstrate to the competent authority that their RTE foods comply with the criteria established with regard to the presence of the pathogen [38].

#### 3.2 Model Selection and Implementation

After an extensive bibliographic search with the aid of predictive microbiology experts, a predictive model was identified as a candidate to be applied for the evaluation of *L. monocytogenes* behavior during the shelf-life of MAP cooked ham using the following criteria: (i) the characteristics of the MAP cooked ham under evaluation (pH,  $a_w$ , Na-lactate (NaL) concentration, and storage temperature) are within the domain used for model development; (ii) additional experiments for model validation in MAP cooked

ham were performed and a good agreement between observations and model predictions were noted.

The selected secondary model was constructed with microbial data obtained in modified Brain Heart Infusion agar and validated with microbial data obtained in MAP-cooked meat products [9]. The model describes the dependence of the specific maximum growth rate ( $\mu_{\max}$ ,  $\text{h}^{-1}$ ) of *L. monocytogenes* in MAP cooked ham to temperature,  $a_w$ , NaL, and  $\text{CO}_2$  dissolved in the water phase, and it was derived from an extended Ratkowsky model (Eq. 2). For model application, Eq. 2 was implemented in MicroHibro combined with the Gompertz primary model [32].

$$\sqrt{\mu_{\max}} = 0.000713(T + 3.5419) \times \sqrt{(a_w - 0.9295)(3140 - \text{CO}_2)(5.9547 - \text{NaL})} \quad (2)$$

where  $T$  is the storage temperature ( $^{\circ}\text{C}$ );  $a_w$  is the water activity of the product; NaL is the concentration of NaL (wt%) in the product and  $\text{CO}_2$  is the concentration of  $\text{CO}_2$  dissolved in the water phase of the product ( $\text{mg L}^{-1}$ ).

Once implemented, the combined predictive model is available in MicroHibro to be applied by users in a friendly interface. The software has a database gathering model parameter values. Likewise, if readers are interested in performing simulations using predictive models that are not currently available in the software database, feel free to contact the authors.

### 3.3 Conditions for Model Predictions

According to the manufacturer's information, the mean characteristics of the product under evaluation are  $a_w = 0.96$ ,  $\text{NaL} = 2.3\%$ ,  $\text{pH} = 6.18$ , storage temperature =  $4^{\circ}\text{C}$ , MAP gaseous mixture =  $20\% \text{CO}_2/80\% \text{N}_2$ , and constant G/P volume ratio of 4/1. The concentration of dissolved  $\text{CO}_2$  ( $\text{mg L}^{-1}$ ) in the water phase can be deduced from the empirical equation developed by Devlieghere et al. [10], based on the initial  $\text{CO}_2$  (%) in the headspace, the storage temperature, and the G/P volume ratio. Under the mentioned conditions, the concentration of  $\text{CO}_2$  dissolved in the water phase is  $590 \text{mg L}^{-1}$ . The product is packaged in high-barrier polyethylene packaging, and its shelf-life is 28 days.

Assuming an initial level of contamination of *L. monocytogenes* in the product ( $y_0$ ) equal to  $1 \text{cfu g}^{-1}$  ( $0 \log \text{cfu g}^{-1}$ ), and that the pathogen does not require an adaptation time before it starts to grow in the product, i.e., lag time = 0 h, the safe shelf-life of the product can be estimated by simulations using the implemented predictive model. The safe shelf-life is defined as the time required by *L. monocytogenes* to achieve the limit established ( $N_t$ ) by the current European Regulation for RTE foods, i.e.,  $100 \text{cfu g}^{-1}$  ( $2 \log \text{cfu g}^{-1}$ ). If this level is reached within 28 days, which according to the manufacturer is the shelf-life of the product, another MAP configuration may be selected as a control measure

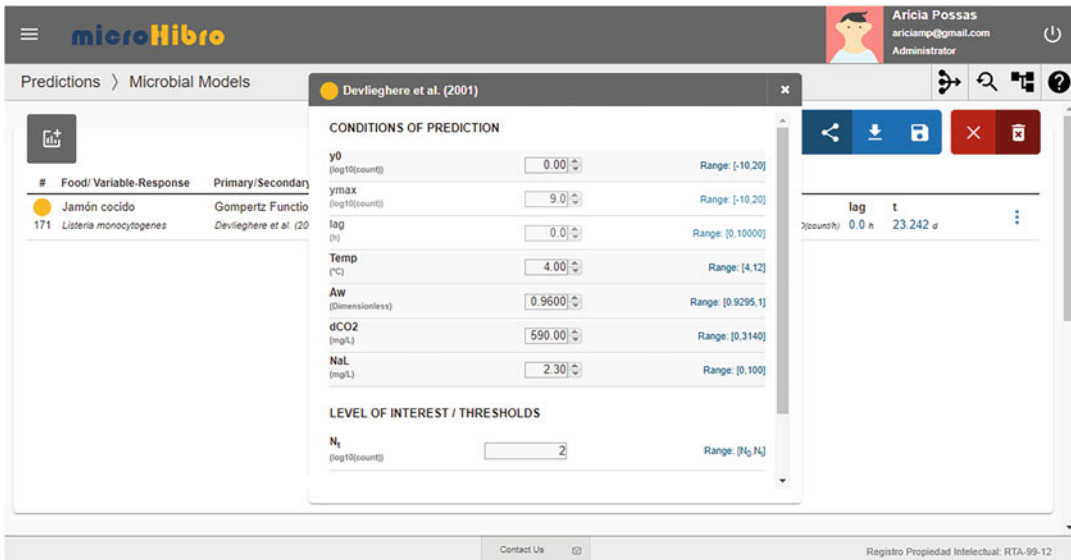


Fig. 3 Prediction module of the MicroHibro software: definition of the conditions for model simulations

to reduce the exposure of cooked ham consumers to *L. monocytogenes*.

After selection of the implemented model in the prediction module of MicroHibro, the conditions for model simulations may be defined (Fig. 3), i.e.,  $y_0$ , temperature, product  $a_w$ , concentration of  $CO_2$  dissolved in water phase, NaL concentration, and  $N_t$ .

### 3.4 Results of Simulations Using Predictive Models

The kinetic parameters and the time required by a microorganism to reach a given concentration in a food product are estimated by using the predictive models implemented in MicroHibro. Under the evaluated conditions, the estimated  $\mu_{max}$  of *L. monocytogenes* is  $0.009 \text{ h}^{-1}$ . The time required for *L. monocytogenes* to reach  $2 \log \text{ cfu g}^{-1}$  is 23 days. The kinetic growth curve of the evaluated pathogen under the evaluated conditions can be seen in Fig. 4. Based on these results, it can be concluded that the current MAP configuration, together with storage temperature and product characteristics, does not assure that the product is safe during its shelf-life under the evaluated conditions.

According to the manufacturer, two new different gaseous mixtures could be evaluated to increase the safe shelf-life of MAP-cooked ham with respect to the presence of *L. monocytogenes*: 30%  $CO_2$ /70%  $N_2$  and 40%  $CO_2$ /60%  $N_2$ . Under these two MAP conditions, the *L. monocytogenes* growth kinetic parameters estimated using the predictive models implemented in MicroHibro are shown in Table 1. Estimated growth curves are shown in Fig. 4. Based on these results, it can be concluded that the MAP gaseous mixture that would assure a safe shelf-life of cooked ham would be 40%  $CO_2$ /60%  $N_2$ , since under the

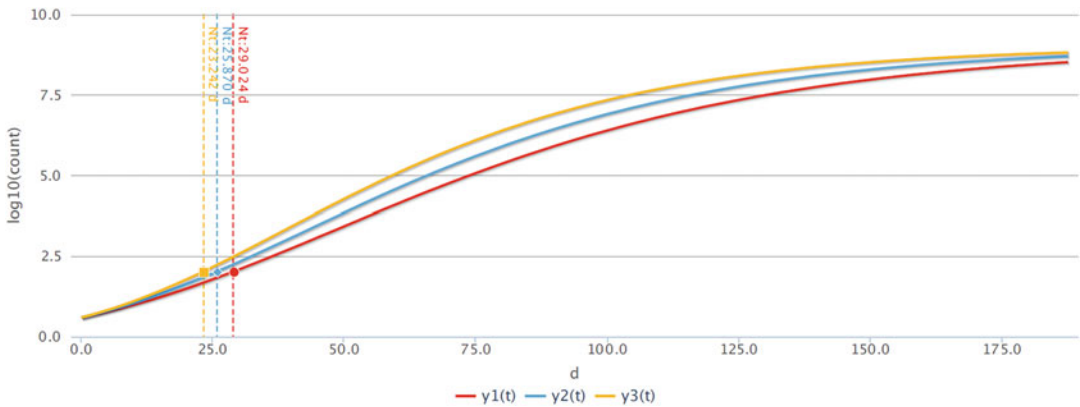


**Fig. 4** *Listeria monocytogenes* growth curves in cooked ham under the evaluated conditions:  $T = 4\text{ }^{\circ}\text{C}$ ,  $a_w = 0.979$  and  $\text{NaL} = 1.5\text{ wt\%}$ , and MAP configurations: 20%  $\text{CO}_2/80\%\text{ N}_2$  (red curve), 30%  $\text{CO}_2/70\%\text{ N}_2$  (blue curve), 40%  $\text{CO}_2/60\%\text{ N}_2$  (yellow curve) (simulations using the predictive models developed by Devlieghere et al. [9])

**Table 1**

Results of simulations using the predictive models developed by Devlieghere et al. [9]

| MAP                               | $\text{CO}_2$ dissolved ( $\text{mg L}^{-1}$ ) | $\mu_{\max}$ ( $\text{h}^{-1}$ ) | Time to reach 2-log (d) |
|-----------------------------------|--|----------------------------------|-------------------------|
| 20% $\text{CO}_2/80\%\text{ N}_2$ | 590  | 0.009                            | 23                      |
| 30% $\text{CO}_2/70\%\text{ N}_2$ | 849  | 0.008                            | 26                      |
| 40% $\text{CO}_2/60\%\text{ N}_2$ | 1098   | 0.007                            | 29                      |

evaluated conditions the time required by *L. monocytogenes* to reach the microbiological limit would be 29 days (Table 1), thus complying with the established shelf-life of the manufacturer. Therefore, it is demonstrated through this case study that validated predictive models available in the literature can be used for decision making in the food industry. Further, the applied model can be used as a scientific tool to demonstrate product compliance with the EU legislation regarding *L. monocytogenes* levels in RTE foods.

## 4 Notes

1. It is important to highlight that, before setting up experiments for data generation and subsequent model development, it is convenient to perform a bibliographic review of the scientific literature and research on predictive microbiology software to check for the availability of published models that, once validated, could be useful for a given application. This would avoid the performance of unnecessary, time-consuming challenge tests.

2. In most of the predictive models developed so far, it is considered that only the gases present in the packaging headspace are relevant for food safety, as if microbial contamination were present only on the surface of the product. Microorganisms are generally located in the aqueous phase of foods, or spatially distributed [3], which implies that the concentration of gases that diffuse through the product would be relevant for food safety.
3. Although there is a great interest in using predictive microbiology models as tools to support the selection of appropriate packaging materials based on their barrier properties, the transfer of gases through packaging materials has been quantified in just a few predictive modeling approaches.
4. In modular modeling approaches, factors affecting microbial behavior in foods are considered independent from each other. However, pH changes in the products are induced by the dissolution or desorption of CO<sub>2</sub> present in MAP, which highlights that, to obtain more reliable predictive models, the impacts of CO<sub>2</sub> dynamics on the pH must also be considered [4].
5. Some controversies have arisen between the comparison of fitting procedures, as the two-step method minimizes the error of the predicted growth/survival parameters, while the one-step procedure minimizes the error of the predicted growth. However, in the last few years, the model fitting has been carried out using a single-step fitting because it normally provides more accurate model estimations when validated in food matrices.

---

## 5 Conclusions

In this chapter, an overview of methods used for data generation, model fitting, and validation was presented in the context of MAP products. Validated models implemented in user-friendly software such as MicroHibro can be useful for a series of applications, including product development, microbial risk assessment, and food safety management.

Models considering the dynamics of gases present in MAP associated with their solubilization, diffusion through the food-stuffs, and transfer through packaging materials are lacking mainly due to limitations in methods for gas quantification in foods. Despite that, some currently available models provide valuable information regarding the impacts of dissolved CO<sub>2</sub> in the water phase against spoilage microbiota or contaminating pathogens in foods.

Finally, the case study presented in this chapter demonstrates that validated predictive models can be applied for decision making

and to evaluate whether the MAP configuration of a food product, its storage temperature, and physicochemical characteristics would allow the growth of a foodborne pathogen to undesirable levels according to current regulations, limiting its shelf-life. Likewise, predictive models could be applied to evaluate the growth potential of spoilage microorganisms in foods and its consequences on their shelf-life.

---

## Acknowledgements

The authors are greatly acknowledged by the Council of Economy, Knowledge, Business and University of Junta de Andalucía (Project AT 2017-5686) and FEDER European funds. The authors are grateful to the EU PRIMA program and the International Joint Programming (Project Reference PCI2019-103453) R&D Projects 2019 from the Spanish Ministry of Science and Innovation (Plan Estatal de Investigación Científica y Técnica y de Innovación 2017–2020: State R&D Program Oriented to the Challenges of the Society) for funding the ArtiSaneFood project (PRIMA/0001/2018). The authors wish to thank the Spanish Government (Ministry of Science and Innovation, research project PID2019-108420RB-C31-ASEQURA) for its financial support.

## References

- Guillard V, Couvert O, Stahl V et al (2016) Validation of a predictive model coupling gas transfer and microbial growth in fresh food packed under modified atmosphere. *Food Microbiol* 58:43–55
- Hutchings N, Smyth B, Cunningham E et al (2021) Development of a mathematical model to predict the growth of *Pseudomonas* spp. in, and film permeability requirements of, high oxygen modified atmosphere packaging for red meat. *J Food Eng* 289:110251
- Perez-Rodríguez F, Valero A (2013) Predictive microbiology in foods. In: *Predictive microbiology in foods*. Springer, New York, p 128
- Chaix E, Couvert O, Guillaume C et al (2015) Predictive microbiology coupled with gas (O<sub>2</sub>/CO<sub>2</sub>) transfer in food/packaging systems: how to develop an efficient decision support tool for food packaging dimensioning. *Compr Rev Food Sci Food Saf* 14:1–21
- Devlieghere F, Van Belle B, Debevere J (1999) Shelf life of modified atmosphere packed cooked meat products: a predictive model. *Int J Food Microbiol* 46:57–70
- Buchanan RL (1993) Predictive food microbiology. *Trends Food Sci Technol* 4:6–11
- Tenenhaus-Aziza F, Ellouze M (2015) Software for predictive microbiology and risk assessment: a description and comparison of tools presented at the ICPMF8 Software Fair. *Food Microbiol* 45:290–299
- Possas A, Valero A, Pérez-Rodríguez F (2022) New software solutions for microbiological food safety assessment and management. *Curr Opin Food Sci* 44:100814
- Devlieghere F, Geeraerd AH, Versyck KJ et al (2001) Growth of *Listeria monocytogenes* in modified atmosphere packed cooked meat products: a predictive model. *Food Microbiol* 18: 53–66
- Devlieghere F, Debevere J, Van Impe J (1998) Concentration of carbon dioxide in the water-phase as a parameter to model the effect of a modified atmosphere on microorganisms. *Int J Food Microbiol* 43:105–113
- Dolan KD, Meredith H, Bolton DJ et al (2019) Coupling the dynamics of diffused gases and microbial growth in modified atmosphere packaging. *Int J Food Microbiol* 292: 31–38
- Meredith H, Valdramidis V, Rotabakk BT et al (2014) Effect of different modified atmospheric packaging (MAP) gaseous combinations on *Campylobacter* and the shelf life of chilled poultry fillets. *Food Microbiol* 44: 196–203

13. Geeraerd AH, Valdramidis VP, Devlieghere F et al (2004) Development of a novel approach for secondary modeling in predictive microbiology: incorporation of microbiological knowledge in black box polynomial modeling. *Int J Food Microbiol* 91:229–244
14. Mejlholm O, Dalgaard P (2009) Development and validation of an extensive growth and growth boundary model for *Listeria monocytogenes* in lightly preserved and ready-to-eat shrimp. *J Food Prot* 72:2132–2143
15. Simpson R, Almonacid S, Acevedo C (2001) Development of a mathematical model for MAP systems applied to nonrespiring foods. *J Food Sci* 66:561–567
16. Chaix E, Broyart B, Couvert O et al (2015) Mechanistic model coupling gas exchange dynamics and *Listeria monocytogenes* growth in modified atmosphere packaging of non respiring food. *Food Microbiol* 51:192–205
17. Alfaro B, Hernández I, Le Marc Y et al (2013) Modelling the effect of the temperature and carbon dioxide on the growth of spoilage bacteria in packed fish products. *Food Control* 29:429–437
18. Geysen S, Verlinden BE, Geeraerd AH et al (2005) Predictive modelling and validation of *Listeria innocua* growth at superatmospheric oxygen and carbon dioxide concentrations. *Int J Food Microbiol* 105:333–345
19. Pin C, Baranyi J, De Fernando GG (2000) Predictive model for the growth of *Yersinia enterocolitica* under modified atmospheres. *J Appl Microbiol* 88:521–530
20. Geysen S, Escalona VH, Verlinden BE et al (2006) Validation of predictive growth models describing superatmospheric oxygen effects on *Pseudomonas fluorescens* and *Listeria innocua* on fresh-cut lettuce. *Int J Food Microbiol* 111:48–58
21. González SC, Possas A, Carrasco E et al (2019) “MicroHibro”: a software tool for predictive microbiology and microbial risk assessment in foods. *Int J Food Microbiol* 290:226–236
22. ISO/FDIS (2018) ISO/FDIS 20976-1: microbiology of the food chain—requirements and guidelines for conducting challenge tests of food and feed products—Part 1: Challenge tests to study growth potential, lag time and maximum growth rate. ISO, p 36
23. McMillin KW (2008) Where is MAP going? A review and future potential of modified atmosphere packaging for meat. *Meat Sci* 80:43–65
24. Rotabakk BT, Lekang OI, Sivertsvik M (2007) Volumetric method to determine carbon dioxide solubility and absorption rate in foods packaged in flexible or semi rigid package. *J Food Eng* 82:43–50
25. Baranyi J, Roberts TA (1994) A dynamic approach to predicting bacterial growth in food. *Int J Food Microbiol* 23:277–294
26. Zwietering MH, Jongenburger I, Rombouts FM et al (1990) Modeling of the bacterial growth curve. *Appl Environ Microbiol* 56:1875–1881
27. Ratkowsky DA (1983) Nonlinear regression modeling: a unified practical approach. In: Marcel Decker I (ed) *Nonlinear regression modeling: a unified practical approach*. Marcel Dekker, New York
28. Ratkowsky DA, Olley J, McMeekin TA et al (1982) Relationship between temperature and growth rate of bacterial cultures. *J Bacteriol* 149:1–5
29. Rosso L, Lobry JR, Bajard S et al (1995) Convenient model to describe the combined effects of temperature and pH on microbial growth. *Appl Environ Microbiol* 61:610–616
30. Gibson AM, Bratchell N, Roberts TA (1988) Predicting microbial growth: growth responses of salmonellae in a laboratory medium as affected by pH, sodium chloride and storage temperature. *Int J Food Microbiol* 6:155–178
31. Hajmeer MN, Basheer IA, Najjar YM (1997) Computational neural networks for predictive microbiology II. Application to microbial growth. *Int J Food Microbiol* 34:51–66
32. Zwietering MH, Wijnztes T, De Wit JC et al (1992) A decision support system for prediction of the microbial spoilage in foods. *J Food Prot* 55:973–979
33. Possas A, Valero A, García-Gimeno RM et al (2021) Combining UV-C technology and caffeine application to inactivate *Escherichia coli* on chicken breast fillets. *Food Control* 129:108206
34. Garre A, Koomen J, den Besten HMW, Zwietering MH (2023) Modeling population growth in R with the biogrowth Package. *J Stat Soft* 107:1–51
35. Akaike H (1974) A new look at the statistical model identification. *IEEE Trans Autom Control* 19:716–723
36. Baranyi J, Tamplin ML (2004) ComBase: a common database on microbial responses to food environments. *J Food Prot* 67:1967–1971
37. Ross T (1996) Indices for performance evaluation of predictive models in food microbiology. *J Appl Bacteriol* 81:501–508
38. European Commission (2005) COMMISSION REGULATION (EC) No 2073/2005 of 15 November 2005 on microbiological criteria for foodstuffs



## Antifungal Activity of Edible Films and Coatings for Packaging of Fresh Horticultural Produce

Lluís Palou and María B. Pérez-Gago

### Abstract

Protocols for in vitro and in vivo evaluation of the antifungal activity of edible films and coatings (ECs) used for postharvest treatment of fresh fruits and vegetables are described in this chapter. Antifungal ECs are typically prepared by incorporating particular antimicrobial ingredients into EC matrix formulations. Different methods and numerous variations can be adopted for both in vitro and in vivo evaluation, mostly depending on the specific purpose of the assay, the components and properties of the EC matrix and the antifungal agent(s), the nature of the target fungal pathogen, and the characteristics and usual postharvest handling of each horticultural product. In any case, however, the inoculum of the target fungi will be used in the experiments, and its preparation is also detailed in this chapter. In general, while EC solid dry films are used for in vitro tests, EC liquid emulsions are used for in vivo assays. We describe three of the most common and, in our opinion, useful antimicrobial in vitro tests specifically intended for use with fungal strains, i.e., agar diffusion or disk diameter tests, film surface inoculation tests, and plate counting germination tests. Coating of fresh produce artificially inoculated with the pathogen is commonly used in laboratory-scale in vivo experiments to assess the ability of ECs to control disease. Further larger-scale semicommercial or commercial trials conducted in pilot plants or packinghouse facilities with naturally infected, cold-stored produce can also be considered.

**Key words** Edible films and coatings, Fresh fruits and vegetables, Postharvest fungal decay, Fungal inoculum preparation, In vitro antifungal activity, In vivo disease control

---

### 1 Introduction

Harvested fresh horticultural products are highly susceptible to dehydration, physiological changes, mechanical injuries, and pathological decay that affect quality attributes, reduce produce storability, and cause major product losses throughout the supply chain. Typically, fungi are the most prevalent causal agents of postharvest diseases, particularly in the case of fresh fruits. Some of them have a wide range of hosts and attack many different fresh products, while others are much more specific and only attack particular commodities. Thus, for example, pathogenic species in



the genera *Botrytis*, causing gray mold, *Alternaria*, causing black spot or black rot, *Colletotrichum*, causing anthracnose, *Fusarium*, causing Fusarium rot, *Lasiodiplodia*, causing stem-end rot, *Penicillium*, causing blue or green molds, or *Rhizopus* and *Mucor*, causing soft rot, are important postharvest pathogens of a large variety of fruits and vegetables, including citrus, pome fruits, stone fruits, tropical fruits, berries, grapes, persimmons, pomegranates, tomatoes, peppers, cucumbers, squash, eggplants, and melons, among others. In contrast, fungal species that only attack particular fruit families include *Penicillium digitatum* (Pers.:Fr.) Sacc., *Penicillium italicum* Wehmer, and *Geotrichum citri-aurantii* (Ferraris) Butler, which cause green and blue molds and sour rot, respectively, of citrus fruit; and *Monilinia* ssp., which are especially virulent on stone fruits, causing postharvest brown rot [1–3].

Traditionally, postharvest disease control of fresh fruits and vegetables involves the use of synthetic chemical fungicides, alone or incorporated into commercial waxes. However, human health risks, environmental issues associated with fungicide residues, and the proliferation of resistant strains of the pathogens have raised important concerns worldwide, increasing the need to look for safer alternatives [4].

In the last years, a considerable amount of research work has focused on the development of edible coatings (ECs) with antifungal activity for fruits and vegetables as a sustainable alternative to conventional fungicides to control postharvest diseases and maintain the quality of fresh horticultural produce. Edible films and coatings are thin layers of material composed mainly of natural biopolymers (i.e., proteins or polysaccharides), lipids, or a mixture of them. ECs for fresh horticultural produce provide important functions, including a semipermeable barrier to water vapor, oxygen, and carbon dioxide between the coated fruit and the surrounding atmosphere, enhancement of fruit appearance, and carriers of active ingredients such as antimicrobials, antioxidants, nutraceuticals, etc. Therefore, ECs can preserve the postharvest quality of fruits and vegetables by reducing weight loss, respiration rate, senescence, and also fungal decay if they exert appropriate antifungal activity [5].

In the particular case of ECs with antifungal activity, two different general types can be considered: (i) film-forming capacity biopolymers with inherent antifungal activity, such as chitosan coatings and *Aloe vera* gels, which have received a lot of attention for postharvest treatment of fruits and vegetables [6–8], and (ii) ECs designed with the incorporation as additional ingredients to the coating formulation matrix of food-grade antifungal compounds able to reduce the growth of spoilage microorganisms and control postharvest diseases. Thus, antifungal agents of potential use in edible films and coatings comprise a wide variety of compounds from natural or synthetic sources, such as mineral salts, organic

acids and their salts, parabens, enzymes, bacteriocins, polypeptides, natural extracts, essential oils, and metal-based nanoparticles or nanocomposites. In addition, antifungal ingredients can also be antagonistic microorganisms that perform as biocontrol agents [6, 9].

In general, the development of antifungal ECs requires an initial optimization of coating formulations based on the chemical compatibility of the ingredients to achieve stable emulsions capable of forming films with good structural properties when applied to the fruit surface [10]. Although films and coatings are the same in nature and sometimes are used as synonymous, they refer to different concepts according to their different purposes and utilization. Films are defined as stand-alone, solid, thin layers of materials and are usually prepared from coating emulsions by casting, molding, or extrusion procedures. Among these, casting is the most commonly used method for film formation at laboratory and pilot scales, whereas extrusion is one of the major polymer processing techniques currently in use at commercial scales [11]. Edible films can be used as covers, wraps, or separation layers in foods, although they are primarily used as testing structures for the determination of barrier, mechanical, solubility, structural, and other properties of interest, such as antimicrobial or antioxidant activity provided by certain film-forming materials or ingredients. On the other hand, coatings are applied to fruits and vegetables by dipping or spraying and involve the formation of films directly on the surface of the commodity they are intended to protect or enhance, forming part of the final fresh product [12, 13]. Therefore, from the research point of view, antifungal EC formulations can be used to form stand-alone films intended for *in vitro* studies or can be directly applied to the commodity for *in vivo* studies.

Protocols for both *in vitro* and *in vivo* evaluation of the antifungal activity of ECs for fresh fruits and vegetables are described in this chapter. Moreover, methods for fungal inoculum preparation are also detailed, as this is an essential step to conduct both types of experiments. In both cases, different methods and numerous variations can be adopted depending on the specific purpose of the assay, the components and properties of the EC matrix and the antifungal agent, the nature of the target fungus, and the characteristics and usual postharvest handling of the horticultural product [14]. *In vitro* studies with films are generally a good approach for the preliminary evaluation and screening of specific EC formulations against particular target microorganisms. Although considerable variations of *in vitro* assays can be found in the literature, many refer to general antimicrobial activity, and in practice often explain methods suitable to test bacterial strains [15, 16]. After describing the procedure for film formation, we describe here three of the most common and, in our opinion, useful procedures specifically intended for use with fungal strains, i.e., agar diffusion or disk

diameter tests, film surface inoculation tests, and plate counting germination tests.

In any case, the performance of films on agar medium will often fail to appropriately predict the performance of ECs once applied to fruits or vegetables because of obvious differences between *in vitro* and *in vivo* conditions. Therefore, the disease control ability of EC formulations cannot be anticipated by the antifungal activity *in vitro* and, in all cases, ECs effective *in vitro* against the target pathogen must be tested *in vivo* with infected fruit, taking into account all the factors involved in disease development and trying to simulate as much as possible the actual disease conditions in the packinghouse.

Although more laborious, time consuming, and expensive than *in vitro* tests, *in vivo* tests are required to determine the effectiveness of antifungal ECs for each specific pathosystem. Since natural infection rates on harvested produce can be low or highly variable, it is common in laboratory assays to artificially inoculate the fruit host with the pathogen to get high and uniform levels of infection. Posterior semicommercial or commercial evaluation of selected EC treatments is usually conducted in pilot plants or packinghouse facilities using a large sample size of naturally infected fruit. In general, two different kinds of antifungal activity can be assessed on inoculated commodities: (i) curative activity, intended to assess the ability to control fungal infections already established in the fruit, and for which the antifungal EC is applied after the inoculation of the fruit, and (ii) preventive activity, intended to evaluate the capacity of the EC to protect the fruit from posterior infections. In this case, the fruit is coated and artificially inoculated with the pathogen afterwards [17]. Inoculated and coated fruit can be incubated at 20–25 °C to favor fast fungal development or long-term stored at low temperatures to resemble commercial fruit handling. Disease incidence and severity and pathogen sporulation are periodically determined on each fruit during storage and disease control ability of ECs is usually given as a percentage of disease reduction with respect to the control treatment. General protocols for these *in vivo* assays are also described in this chapter.

---

## 2 Materials

### 2.1 Preparation of Fungal Inoculum

- Laboratory laminar flow hood. Bunsen burner. Inoculating loops.
- Vortex mixer. Sterile test tubes, Erlenmeyer flasks, glass funnel, gloves, cheesecloth, Pasteur pipettes, and micropipettes.
- Potato dextrose agar (PDA) (*see Note 1*): typically prepared from the commercial medium: 4.0 g L<sup>-1</sup> potato extract or

potato peptone (equivalent to 200 g infusion from potatoes) + 20.0 g L<sup>-1</sup> glucose + 15.0 g L<sup>-1</sup> agar.

- Petri dishes: typically, 90-mm diameter x 15-mm height plastic plates are used. These are conveniently autoclavable and disposable.
- Emulsifier aqueous solution: Polysorbate 80 (Tween<sup>®</sup> 80) or Triton<sup>™</sup> X-100, at 0.05% (w/v).
- Hemacytometer: Thoma chamber or Fuchs–Rosenthal chamber is usually used.
- Optical microscope. Laboratory incubator.

## **2.2 In Vitro Antifungal Activity**

- Antifungal EC emulsions to be evaluated.
- Spore suspensions of the target fungal pathogen (inoculum).
- Laboratory laminar flow hood. Bunsen burner. Inoculating loops. Sterile Petri dishes, test tubes, tweezers, scalpels, cork borers, Erlenmeyer flasks, glass rods, gloves, stirring rods, and micropipettes.
- Casting plates for film formation.
- PDA (*see Note 1*). Potato dextrose broth (PDB): liquid culture medium prepared as PDA without the agar.
- Ruler, caliper, or digital caliper.
- Laboratory incubator. Refrigerator.

## **2.3 In Vivo Assessment of Disease Control**

- Antifungal EC emulsions to be evaluated.
- Spore suspensions of the target fungal pathogen (inoculum).
- Target commodity: Samples of fresh fruits or vegetables.
- Sterile inoculating stainless-steel rod (with probe tip), pricker, scalpel, cork borer, gloves, test tubes, Erlenmeyer flasks, and micropipettes.
- Surface disinfection solutions, e.g., 0.5% sodium hypochlorite, 70% ethanol.
- Immersion containers, stirring rods, mesh screen, plastic or metal grid, plastic cavity sockets, corrugated cartons, and plastic trays.
- Chronometer, ruler, caliper, digital caliper.
- Incubation cabinets or walk-in rooms. Cold storage rooms.
- Pilot plant-scale or commercial-scale fresh produce packingline.

### 3 Methods

#### 3.1 Preparation of Fungal Inoculum

Suspend 39 g of commercial PDA powder in 1 L of distilled water. If necessary, bring pH to a final value of  $5.6 \pm 0.2$ . Autoclave at 121 °C for 15 min. Leave to cool to 40–45 °C and pour into plates within the laminar flow hood (about 20 mL in each 90-mm-diameter dish). Put the plate lids on and allow to dry within the hood.

##### 3.1.1 Preparation of PDA Petri Dishes

##### 3.1.2 Culture of Fungal Strains

Strains are generally obtained from known culture collections or isolated from infected produce, purified, identified, and cultured and maintained (replated) in artificial media. For replating, work within the laminar flow hood. Take spores or mycelium with a sterile inoculating loop (heated to red hot in the burner flame and allowed to cool) from a grown colony on a PDA dish and transfer them to a fresh PDA plate by gently touching the agar surface. Depending on the fungal species, inoculation of the fresh plate can be more convenient in one central point or three equidistant points on the agar surface. Incubate inoculated plates at 20–25 °C inside a laboratory incubator, generally in the dark for 7–21 d (*see Note 2*).

##### 3.1.3 Obtaining Spore Suspensions

Within the laminar hood, take abundant spores from a 7- to 21-d-old fungal culture and transfer them to a sterile test tube containing a known volume of aqueous emulsifier solution (0.05% Tween<sup>®</sup> 80 or Triton<sup>™</sup> X-100) to obtain a very high concentrated suspension. Mix roughly in a vortex mixer for 2 min and filter the content to another sterile test tube through a glass funnel containing two layers of sterile cheesecloth. This will allow the separation of spores from mycelial fragments. Mix the suspension again and use a Pasteur pipette to transfer drops to a hemacytometer (*see Note 3*). Count the spores in an optical microscope ( $\times 10$  or  $\times 40$ ) to determine the spore concentration and calculate the suspension volume needed to add using a micropipette to a known volume of fresh emulsifier solution to obtain the final suspension at the desired inoculum concentration (*see Note 4*). Mix again this final suspension before use in the experiments. *See Note 5* for an alternative method to prepare large volumes of certain spore suspensions. When fruit are going to be inoculated in *in vivo* tests with weak fungal pathogens, some additional ingredients can be added to the spore suspension to favor actual infection rates (*see Note 6*).

#### 3.2 In Vitro Antifungal Activity

The purpose of these tests is to evaluate the antifungal activity of ECs against the target fungal pathogen in a rapid, easy, cheap, and simple manner that does not involve the use of fresh produce. For this, the most practical approach is to work with films instead of coating liquid emulsions. As a solid thin layer produced by drying the emulsion, the film will appropriately simulate the characteristics of the emulsion once applied onto the surface of fresh produce (*see Note 7*).

### 3.2.1 Film Casting

For film production from liquid coating formulations, pipette and evenly spread an appropriate volume of the degassed emulsion on rimmed, smooth plates (e.g., Petri dishes, Teflon plates, high-density polyethylene (HDPE) casting plates, etc.; *see Note 8*) resting on a leveled slab and allow to dry at ambient conditions, normally at approximately 21–25 °C and 50% RH until drying is complete (*see Note 9*). While whole films dried in Petri dishes can be directly used in some tests (e.g., plate counting germination tests), in other cases the dry film is peeled intact from the casting surface using a sterile scalpel and tweezers and aseptically cut into smaller disks of the desired diameter using a sterile cork borer. Use the films immediately or aseptically store them at 4 °C in the refrigerator until use in the experiments.

### 3.2.2 Agar Diffusion or Film Disk Diameter Tests

These tests are intended to determine the ability of coating films to inhibit the spore germination and the mycelial growth of a particular fungal pathogen in an artificial agar culture medium.

Working within the laminar hood, place 100 µL of spore suspension of the target pathogen on the center of a PDA, DRBCA, or other agar medium plate and spread uniformly over the entire agar surface by gently rubbing with a sterile glass rod. A series with different concentrations of inoculum can be used, usually from  $10^3$  to  $10^6$  spores  $\text{mL}^{-1}$ , depending on the fungus. Aseptically transfer the film disk (16-mm diameter) to the center of the agar surface and lid the plate. In some cases, smaller film disks (5-mm diameter) can be produced and three of them can equidistantly be plated in the same Petri dish. Depending on the objective of the test and the nature of the EC, control disks can be simply of sterile filter paper or disks of film formulated without the antifungal ingredient (s). For each pathogen, type of coating film, and inoculum level, three to five replicated plates are generally prepared. Depending on the type of film and antifungal ingredient, put the plates in a standard refrigerator at 4 °C for 3 h to allow, if that is the case, the diffusion of film ingredients from the disk to the agar medium [18]. Then transfer them to an incubator set at 20 °C, 25 °C, or the most adequate temperature (Table 1) and incubate for a variable period of 4–14 d, depending on the fungal species. Periodically (every 1, 2, or 3 d, depending on the growth rate of the fungus) measure, in two or four directions, the length of the inhibition zone around the film disk (from the perimeter of the film disk until the edge of the inhibited area; Fig. 1). These quantitative zone measurements are giving in fact qualitative results, and results from different studies are difficult to compare because of the many specific conditions of the experiments including film size and properties, antifungal agent, temperature, incubation time, target fungus, inoculum concentration, etc. [19].

This method is particularly suitable for fungal pathogens of easy sporulation in vitro that produce large amounts of small-size

**Table 1**  
**Appropriate incubation temperature for optimal growth of common fungal pathogens causing postharvest disease on fresh horticultural produce**

| Pathogen                   | Disease                | Temperature (°C) |
|----------------------------|------------------------|------------------|
| <i>Penicillium</i> spp.    | Blue/green molds       | 25               |
| <i>Botrytis</i> spp.       | Gray mold              | 20               |
| <i>Alternaria</i> spp.     | Black spot, black rot  | 25               |
| <i>Monilinia</i> spp.      | Brown rot              | 25               |
| <i>Colletotrichum</i> spp. | Anthraco nose          | 25               |
| <i>Geotrichum</i> spp.     | Sour rot               | 28               |
| <i>Aspergillus</i> spp.    | Black rot              | 30               |
| <i>Rhizopus</i> spp.       | Soft rot, Rhizopus rot | 25               |
| <i>Mucor</i> spp.          | Mucor rot              | 25               |
| <i>Lasiodiplodia</i> spp.  | Stem-end rot           | 28               |
| <i>Fusarium</i> spp.       | Fusarium rot           | 25               |

Variations among different species in the same genus may occur. For example, while 25 °C is the most appropriate temperature for *Monilinia fructicola*, it is 20 °C for *Monilinia laxa*

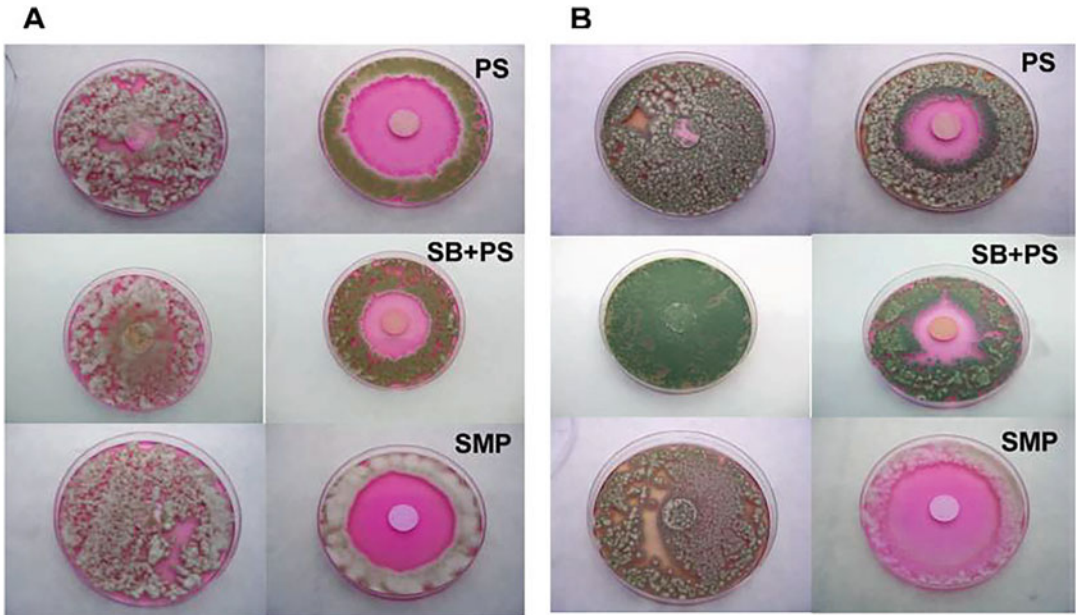


**Fig. 1** Disk diameter tests on DRBC agar plates for evaluation of the in vitro inhibition of *Penicillium digitatum* (a) and *Penicillium italicum* (b) by control HPMC-lipid films (left-hand side images) and HPMC-lipid films containing potassium sorbate (PS), a mixture of sodium benzoate and potassium sorbate (SB + PS) and sodium salt of methyl paraben (SMP) (right-hand side images). (Reproduced from Ref. [10] with permission from ACS Publications)

spores (e.g., *Penicillium* spp., *Aspergillus*, spp., etc.), which allow the uniform distribution of the fungal inoculum on the agar surface in the test culture plates. A variation employing mycelial plugs can be considered with target fungi of difficult sporulation or with spores of large size (e.g., *Lasiodiplodia* spp., *Alternaria*, spp., *Rhizopus* spp., etc.; see **Note 10**).

### 3.2.3 Film Surface Inoculation Tests

These assays are intended to assess the ability of the target pathogen to either grow on the coating material itself or penetrate and pass through it. The purpose is to simulate coating surface contamination and determine if, once applied to the fruit, the coating will provide a barrier functionality and will be able to prevent new infections caused by external contaminating inoculum, usually airborne spores or spores and mycelia from rotten adjacent fruit (i.e., fungi causing nests of decay on stored produce). Although different variations of this type of test have been proposed, we describe here two of the simplest versions.

Working within the laminar hood, place equidistantly film disk pieces inside an empty sterile Petri dish and drop 10–20  $\mu\text{L}$  of spore suspension of the target pathogen on the surface of each disc. Four 16-mm-diameter disks can be used in a four-section compartmentalized 100-mm-diameter plastic Petri dishes [18], but less disks of higher diameter can also be used. A series with different concentrations of inoculum can be used, usually from  $10^3$  to  $10^6$  spores  $\text{mL}^{-1}$ , depending on the fungus. Transfer the plates to an incubator set at 20 °C, 25 °C, or the most adequate temperature (Table 1) and visually assess fungal growth periodically during incubation (every 1, 2, or 3 d) for a variable period of 4–14 d, depending on the observed rate of fungal growth. No control disks are needed for this test, although in some cases could be of interest to use disks of film matrix without the antifungal agent(s). Typically, for each pathogen, film treatment, and inoculum level, three to five replicated plates are prepared. Results are qualitative and usually given just as positive (+) or negative (–) growth.

A variation of this test consists in using PDA Petri dishes instead of empty dishes and carefully inoculate the surface of film disks placed on the PDA surface. It is important that the inoculum drop does not move from the disk surface to the surrounding agar medium. In this case, the artificial media resembles the fruit surface and, if evaluations during incubation give positive fungal growth on the agar medium, it will mean that the coating disc is not acting as an effective barrier for contaminating fungal inoculum since the spores have been able to pass through the film disk and germinate and growth on the media. More sophisticated versions of this test involving plate counting of fungal populations have been described [14].



### 3.2.4 Plate Counting Germination Test

As an adaptation from tests designed to work with bacterial cells [20, 21], the purpose of these tests is to indirectly assess the effect of the antifungal film on the spore germination of the target fungal pathogen, avoiding the large amount of time and labor typically needed for observation of germination in the microscope. Plate counting methods are time, space, and labor consuming, but, in contrast to the aforementioned *in vitro* tests, they give quantitative results that can be used to measure log reductions due to the antifungal film [16, 19].

Prepare a spore suspension of the target pathogen in a PDB solution at a final concentration of  $10^2$ – $10^4$  spores  $\text{mL}^{-1}$ , depending on the fungus, by adding aseptically with a micropipette the correspondent volume of aqueous spore suspension of known concentration into sterilized and cooled PDB flasks. Working within the laminar hood, pour 15 mL of PDB spore suspension into a 90-mm-diameter Petri dish containing the dry film to be tested, put the lid on, and hold the inoculated plates on an orbit shaker at 50 rpm at room temperature. At various time intervals, from 4 to 24 h, depending on the experiment, take 100  $\mu\text{L}$  of PDB spore suspension on the film surface and plate them homogeneously in fresh PDA dishes by gently rubbing over the entire agar surface with a sterile glass rod. Control disks are usually sterile paper disks or disks of coating matrix formulated without the antifungal agent. When the objective of the test is to find out the influence of the concentration of the antifungal ingredient on spore mortality, a series of increasing antifungal agent concentrations in the film are prepared. Incubate the plates at 25 °C for 3–5 d and count the number of fungal colonies growing on each plate. For each pathogen, film treatment, and time interval, two replicated plates are usually prepared, and, if needed, serial dilutions with duplicate plating can be performed. Depending on the number of grown colonies, results are given directly as spores  $\text{mL}^{-1}$  or as log spores  $\text{mL}^{-1}$  (*see Note 11*). Results can also be given as a percentage of inhibition of germination with respect to control disks (*see Note 12*).

### 3.3 *In Vivo* Assessment of Disease Control

Due to the large variety of postharvest fungal diseases that affect fresh horticultural produce, many variations of the general procedures described here can be found in the literature. In general, the objective of these *in vivo* trials is to evaluate the disease control ability of antifungal EC formulations after their application to fruits and vegetables actually infected by the target pathogen. Common laboratory assays with fruit artificially inoculated with the pathogen are described. Figure 2 represents a schematic diagram for this type of experiment, particularly for the evaluation of ECs containing “generally recognized as safe” (GRAS) salts as antifungal ingredients for the control of *Alternaria* black spot on cherry tomato [22]. Notes in this section will refer to procedural variations,

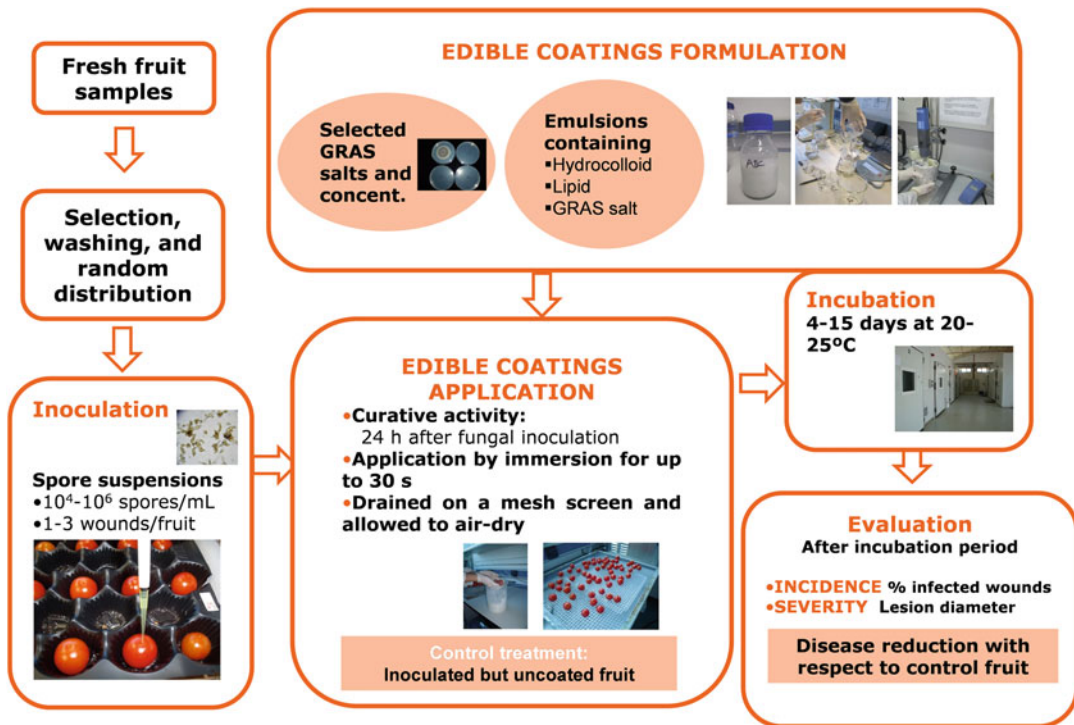


**Fig. 2** Methodological procedure for formulation and in vivo evaluation of the ability of edible coatings containing GRAS salts to control black spots of tomato caused by the fungus *Alternaria alternata*. (Reproduced from Ref. [22]; Open Access)

particularly those to be considered in larger-scale semicommercial or commercial trials conducted in pilot plants or packinghouse facilities.

### 3.3.1 Fresh Produce Sample Preparation

Select by hand and use in the experiments healthy fresh fruits or vegetables of uniform size and good condition. If possible, use produce from local organic or commercial orchards located in the area surrounding the laboratory or research facility. If the fruit are from a packinghouse or store, always acquire them before any postharvest treatments are applied. Use the fruit the same day or one day after harvest or, if not possible, store them at the most adequate commercial cold storage temperature for each commodity (Table 2) and high relative humidity (RH > 90%) only for several days. If cold-stored, allow the fruit to warm and dry at room temperature for several hours before use in the experiments. Before each experiment, randomize and wash the fruit with fresh water, a biodegradable detergent solution or, if needed, dip them for 1–2 min in a surface disinfection solution at room temperature, usually a diluted bleach solution (sodium hypochlorite at 0.5 vol%). In the case of small sample sizes, spraying with 70% ethanol

**Table 2**  
**Recommended conditions for long-term storage of major fresh fruits and vegetables**

| Commodity                                     | Storage temperature (°C) | Approximate storage life |
|---|--------------------------|--------------------------|
| Avocado                                       | 3–7                      | 2–4 weeks                |
| Banana  | 13–15                    | 1–4 weeks                |
| Berries                                       |                          |                          |
| Blackberry, blueberry, raspberry              | –0.5–0                   | 3–10 days                |
| Strawberry                                    | 0                        | 7–10 days                |
| Cherry, sweet                                 | –1–0                     | 2–3 weeks                |
| Citrus  |                          |                          |
| Orange  | 3–5                      | 3–12 weeks               |
| Mandarin                                      | 4–7                      | 2–4 weeks                |
| Lemon   | 10–13                    | 1–6 months               |
| Lime  | 9–10                     | 6–8 weeks                |
| Grapefruit                                    | 10–15                    | 6–8 weeks                |
| Eggplant                                      | 10–12                    | 1–2 weeks                |
| Grape   | –0.5–0                   | 1–6 months               |
| Guava   | 5–10                     | 2–3 weeks                |
| Kiwifruit                                     | 0                        | 3–5 months               |
| Mango   | 13                       | 2–3 weeks                |
| Melons  |                          |                          |
| Cantaloupes and other melons                  | 2–5                      | 2–3 weeks                |
| Honeydew and Orange-flesh                     | 5–10                     | 3–4 weeks                |
| Papaya  | 7–13                     | 1–3 weeks                |
| Persimmon                                     | 0                        | 1–3 months               |
| Pineapple                                     | 7–13                     | 2–4 weeks                |
| Pome fruit                                    |                          |                          |
| Apple   | –1.1–1                   | 3–6 months               |
| Pear (European)                               | –1.5–(–0.5)              | 2–7 months               |
| Pomegranate                                   | 5–7                      | 2–3 months               |
| Squash  |                          |                          |
| Summer squash                                 | 7–10                     | 1–2 weeks                |
| Winter squash                                 | 12–15                    | 2–3 months               |
| Tomato  | 8–13                     | 1–5 weeks                |
| Stone fruit (apricot, nectarine, peach, plum) | –0.5–0                   | 1–4 weeks                |
| Watermelon                                    | 10–15                    | 2–3 weeks                |

Adapted from: [http://postharvest.ucdavis.edu/Commodity\\_Resources/Storage\\_Recommendations/](http://postharvest.ucdavis.edu/Commodity_Resources/Storage_Recommendations/)

solution can also be considered. Rinse the surface-disinfected fruit with abundant tap water and allow to air-dry at room temperature.

### 3.3.2 *Experimental Design, Fungal Inoculation, and Coating Application*

In order to determine curative activity, wound the surface of selected and randomized fruit with a sterile stainless steel pricker, scalpel, or rod and place with a micropipette a known volume (10–30  $\mu\text{L}$ ) of spore suspension of the target pathogen in the wound (*see Note 13*). When the inoculum drop is dried or after a certain period of time, typically 24 h at room temperature to resemble incipient field infections, coat the fruit by immersion (10–30 s) with the corresponding EC emulsion, and leave the coated fruit to drain on a mesh screen or an adequate plastic or metal grid and air-dry at room temperature (*see Note 14*). To test preventive activity, coat the fruit with the corresponding EC treatment, allow to drain and air-dry, and, once dried or after a particular period of time (e.g., 24 h), wound inoculate them with the pathogens as previously described [17]. In any case, inoculated but uncoated fruit (immersed in water for the same 10- to 30-s period) are used as a negative control. Depending on the purpose of the experiment, in some cases, negative control fruit can be coated with EC formulated without the antifungal ingredient(s). In other cases, a positive control treatment can be added, normally fruit treated with a commercial postharvest chemical fungicide of known and high efficacy on that pathosystem.

Use a completely randomized design in which each treatment is applied to a variable number of replicates and fruit per replicate, depending on fruit size. For instance, common sample sizes for laboratory experiments are three to five replicates of 10–25 fruits per treatment (*see Note 15*).

### 3.3.3 *Storage Conditions and Assessment of Disease Control*

After draining and air-drying at room temperature, place coated fruit on plastic cavity sockets on corrugated cartons or plastic trays and incubate them in a climatic walk-in storage room for 7–21 days at 20 °C or the most convenient growth temperature for each target pathogen (Table 1). This procedure will allow to obtain quick results on the disease control ability of each EC treatment. Assess periodically (every 1–7 days) disease incidence by counting the number of infected wounds or fruit in each replicate (Fig. 3, bottom left) and, for each evaluation date, express mean values as percentage; disease severity by measuring the lesion diameter of each infected wound (Fig. 3, bottom right) and express mean values in mm; and pathogen sporulation by counting the number of sporulated wounds or fruit in each replicate (Fig. 3, bottom left) and express mean values as percentage (*see Note 16*). For each evaluation date, all these results can also be expressed as a percentage of reduction with respect to the control treatment (*see Note 17*). Disease severity over time can also be directly expressed as the area under the disease progress curve (AUDPC) or, more accurately, the area under the disease progress stairs (AUDPS [23]).



**Fig. 3** Concurrent rind wound and inoculation of a spore suspension of *Penicillium* sp. on orange fruit (top). Determination of disease incidence (number of infected fruit) and pathogen sporulation (number of sporulated fruit) (bottom left), and disease severity (lesion diameter; bottom right) on citrus fruit wound inoculated with *Penicillium* sp. and incubated at 20 °C for 7 days

If among the objectives of the experiment there is the assessment of the ability of antifungal ECs to control disease on fresh produce stored at low temperatures for prolonged periods, after draining and air-drying at room temperature, place coated samples on plastic cavity sockets on plastic trays and store them in a cold storage room at the recommended commercial conditions for each commodity (Table 2). Assess periodically (typically every 1–2 weeks) disease incidence and severity and pathogen sporulation in each replicate as described above. For each evaluation date, give the results as described above.

#### 4 Notes

1. PDA is a universal medium for in vitro fungal growth. In particular cases, other media can be used that favor the growth of certain fungi. In other cases, media can be amended with antibiotics (streptomycin and chlortetracycline are among the most common) or specific fungicides to avoid the growth of certain potential contaminating microorganisms. For example,

Dichloran Rose Bengal Chloramphenicol Agar (DRBCA) is often used to inhibit the growth of bacteria and contaminate Mucorales fungi (e.g., *Rhizopus* spp., *Mucor* spp.).

2. Although optimal incubation conditions of PDA cultures can vary depending on the fungal species (Table 1) [1–3], the large majority of postharvest pathogens attacking fresh horticultural produce will grow well in the range of 20–25 °C and complete their life cycle (full colony growth) after 7–21 days of incubation at these temperatures.
3. Common hemacytometers used to count spores of postharvest pathogens include the Thoma counting chamber, mostly used for fungal species with a small spore size (e.g., *Penicillium* spp., *Aspergillus*, spp., *Geotrichum* spp., *Botrytis* spp., etc.), and the Fuchs-Rosenthal chamber, typically used for species with a larger spore size (e.g., *Alternaria* spp., *Monilinia* spp., *Rhizopus* spp., *Mucor* spp., etc.). Counting instructions and calculations to determine the spore concentration are particular for each type of chamber.
4. The following equation is used to obtain the spore suspension at the desired final concentration ( $C_f$ ):  $C_i \times V_i = C_f \times V_f$ , where  $C_i$  is the known high spore concentration determined by counting in the hemocytometer (initial concentration),  $V_f$  is the final volume of suspension at the desired inoculum concentration that we wish to prepare, and  $V_i$  is the unknown volume of initial suspension that we need to transfer to the volume of fresh emulsifier solution ( $V_e$ ). Obviously,  $V_f = V_i + V_e$ .
5. If large volumes of spore suspension of fungal species with a small spore size (e.g., *Penicillium* spp., *Aspergillus*, spp., *Geotrichum* spp.) are needed for semicommercial trials, they can be prepared by rubbing with a sterile glass rod all the spores on the agar surface of a 90-mm-diameter culture plate after adding 5 mL of 0.05% emulsifier solution. This can be repeated with additional culture plates, if needed. Then, pass the spore suspension through two layers of cheesecloth and dilute with sterile water to an absorbance of 0.1 at 420 nm determined with a spectrophotometer. This density is approximately equivalent to  $10^6$  spores  $\text{mL}^{-1}$  [24].
6. Additional substances that can be added to the fungal inoculum suspension include fruit juice to enhance the nutrition of the fungus, hence boosting spore germination and mycelium development, fungicides and/or antibiotics to kill other contaminating microorganisms potentially present in the inoculation site, and cycloheximide or other analog protein inhibitors to retard the possible healing of the rind wound inflicted for inoculation [24].

7. The results of *in vitro* tests will not predict the effectiveness to control disease on specific fruits and vegetables due to the complex interactions among host, pathogen, and environment that occur during *in vivo* disease development and/or to differences on the release capability of antifungal active ingredients from films located on agar medium and from coatings located on the surface of the fruit peel [4]. In general, factors such as temperature, water activity, nutrient availability, components and properties of the coating matrix and the antifungal agent, and potential interactions of the agent or other coating ingredients with fruit tissue components will greatly influence the antifungal activity. Furthermore, surface properties of the cuticle and the whole peel of fruits and vegetables can especially influence the diffusion rate of antifungal agents in the host peel. Thus, the release capability of antifungal agents from films located on agar medium can differ from that of coatings located on the fresh product peel surface, and the overall performance of coating formulations is typically highly dependent on the commodity species and even cultivar [25]. Nevertheless, *in vitro* tests can be very useful in sequential research to properly identify and select the most promising ECs among a variety of candidates (screening of ECs with different antifungal agents and/or concentrations) or to investigate the activity of particular ECs against a variety of fungal pathogens.
8. Material and size of the casting plate will vary depending on the final purpose of the film. Examples of common use are 9-cm-diameter whole film disks produced in standard Petri dishes and 14.1-cm-diameter film disks dried on HDPE plates. In the latter case, the purpose is to cut the original disk into numerous smaller disks and the material should ensure the release of the films after drying. Films that are difficult to peel from the plates can be cast onto plates covered with sterile wax paper (0.2-mm thickness). Typically, the thickness of the obtained dry films is 0.1–0.5 mm and it is very important to minimize the thickness variation among film treatments.
9. Drying rates can also be improved with hot air ovens, microwaves, and vacuum driers. However, controlling the drying conditions is critical since different evaporative levels and temperatures can affect the physical and structural properties of the resulting film [11]. This is especially relevant in the case of some antifungal agents such as essential oils and natural extracts where exposure to high temperatures might be a limitation. If needed, film drying can be performed under aseptic conditions by placing the emulsion plates inside a previously sterilized laminar flow hood.
10. Aseptically produce agar plugs (5-mm diameter) with a sterile cork borer from grown PDA cultures of the target pathogen

and plate three of them equidistantly on the surface of the test dish containing fresh PDA medium. Afterwards, place the film disk (16-mm diameter or smaller) on the center of the agar surface and lid the plate. The rest of the indications are those described in Subheading 3.2.2. Periodically during incubation, measure the length of the inhibition zone in the direction from the disk to each of the fungal plugs. In other cases, the agar plate surface can be divided mentally into two equal areas, and while the fungal plug is placed in the center of one of them, the disk is placed in the center of the other.

11. Spores are often also referred to as colony-forming units (CFU).
12. The following formula is used to obtain the percentage of inhibition of spore germination ( $I$ ):  $I (\%) = [(CFU_c - CFU_f) / CFU_c] \times 100$ , where  $CFU_c$  is the number of germinated spores (grown colonies) on PDA dishes plated with PDB spore suspension from the plates containing the control film disks, and  $CFU_f$  is the number of germinated spores on PDA dishes plated with PDB spore suspension from the plates with film disks correspondent to each different treatment.
13. Artificial fungal inoculation of fresh produce can be performed in different ways depending on the target pathogen and the commodity. When the pathogen is a fungal species with a small spore size (e.g., *Penicillium* spp., *Aspergillus*, spp., *Geotrichum* spp., *Botrytis* spp., etc.), wounding and inoculation can be performed simultaneously by immersing a stainless-steel rod with a 1-mm-wide, 2-mm-long probe tip into the spore suspension and wounding the fruit peel (Fig. 3, top). Small- and medium-size fruit are usually wounded once in the equator while several equidistant wounds can be inflicted in large-size fruit. In some experiments with large fruit, it can be convenient to inoculate the same fruit with two or even more different target pathogens in order to save fruit and labor. Fruit inoculation with fungal mycelial plugs can be considered with target fungi of difficult sporulation (e.g., *Lasiodiplodia* spp. etc. [26]).
14. Although brief fruit immersion is the most uniform and effective way to coat the fruit with the EC emulsion, in some cases, it could be interesting to mimic coating application in industrial packingline roller conveyors by pipetting a small amount of the emulsion (0.1–0.5 mL, depending on the commodity) onto each fruit and rubbing manually with gloved hands [27]. This type of EC application will consume much lower amounts of emulsion, so it can also be useful when the preparation for research purposes of a large quantity of the emulsion is a limitation. In semicommercial or commercial trials, EC



treatments are habitually performed as spray application in packingline machinery. Research pilot plants intended to conduct semicommercial trials are generally equipped with small-scale versions of fruit packinglines used in commercial packinghouses, whereas commercial trials are directly conducted in packinghouse facilities. When packingline machinery is used, it is mandatory to thoroughly clean nozzles and roller conveyors between treatments.

15. Semicommercial or commercial trials are typically conducted with larger sample sizes. While samples of three to five replicates of 100–300 fruit per treatment, depending on the type of fruit commodity, are frequently used in semicommercial assays, several replications per treatment of various entire fruit field boxes, bins, or packages are used in commercial trials [22].
16. Semicommercial or commercial trials are typically conducted with naturally infected fruit; i.e., intact fruit from the field not artificially inoculated with the target pathogen. In this case, it is important to determine the etiology of the lesions, i.e., the pathogen(s) causing disease. Results are often reported only as disease incidence (number of decayed fruit or visible lesions) and pathogen sporulation, but the severity of natural decay can also be assessed as disease indexes based on the quantification of disease severity according to particular quantitative or qualitative scales. For instance, common scales give scores as a function of the relative surface of the fruit covered by the disease lesion. The following example was developed for pomegranate postharvest crown decay caused by *B. cinerea* [28]: 0 = no lesion (visible infected area) or fungal mycelium present, 1 = mycelium present in the crown, 2 = lesion  $\leq 25\%$  of skin surface, 3 = lesion on 26–50% of skin surface, 4 = lesion  $> 50\%$  of skin surface. In other cases, even more simple qualitative scales are used: 0 = no visible decay, 1 = slight decay symptoms, 2 = moderate decay symptoms, and 3 = severe decay symptoms.
17. All three parameters determined for in vivo assessment of disease control (disease incidence and severity and pathogen sporulation) can be expressed as reduction percentage with respect to the control treatment. For example, in the case of disease incidence:  $DIR (\%) = [(DIc - DI_t) / DIc] \times 100$ , where *DIR* is the disease incidence reduction, *DIc* is the disease incidence (number of infected wounds or fruit) in the control treatment (uncoated or coated with EC without antifungal ingredient(s)), and *DI<sub>t</sub>* is the disease incidence (number of infected wounds or fruit) in the corresponding antifungal EC treatment.

## Acknowledgements

Spanish IVIA, INIA, AEI, and the European Union through the project StopMedWaste (PRIMA Programme) and the European Regional Development Fund (ERDF) of the Generalitat Valenciana 2021–2027 are gratefully acknowledged for providing financial support to conduct research on this topic. In memory of Dr. Miguel Ángel del Río, for his unconditional friendship, guidance, and support.

## References

1. Barkai-Golan R (2001) Postharvest diseases of fruits and vegetables: development and control. Elsevier, Amsterdam
2. Bautista-Baños S (ed) (2014) Postharvest decay: control strategies. Academic Press/Elsevier, London
3. Palou L, Smilanick JL (eds) (2020) Postharvest pathology of fresh horticultural produce. CRC Press/Taylor and Francis Group, Boca Raton
4. Palou L, Pérez-Gago MB (2021) GRAS salts as alternative low-toxicity chemicals for postharvest preservation of fresh horticultural products. In: Spadaro D, Droby S, Gullino ML (eds) Postharvest pathology. Next generation solutions to reducing losses and enhancing safety, plant pathology in the 21st century, vol 11. Springer, Cham, pp 163–179
5. Valencia-Chamorro SA, Palou L, del Río MA et al (2011) Antimicrobial edible films and coatings for fresh and minimally processed fruits and vegetables: a review. Crit Rev Food Sci Nutr 51:872–900. <https://doi.org/10.1080/10408398.2010.485705>
6. de Souza EL, Ramos Berger LR, Marín A et al (2020) Chitosan and other edible coatings for the control of postharvest diseases of fresh fruit. In: Palou L, Smilanick JL (eds) Postharvest pathology of fresh horticultural produce. CRC Press/Taylor and Francis Group, Boca Raton, pp 403–452
7. Martínez-Romero D, Guillén F, Castillo S et al (2020) *Aloe* spp. gels to reduce fruit disease and maintain quality properties. In: Palou L, Smilanick JL (eds) Postharvest pathology of fresh horticultural produce. CRC Press/Taylor and Francis Group, Boca Raton, pp 713–756
8. Rajestary R, Landi L, Romanazzi G (2020) Chitosan and postharvest decay of fresh fruit: meta-analysis of disease control and antimicrobial and eliciting activities. Compr Rev Food Sci Food Saf 20:563–582. <https://doi.org/10.1111/1541-4337.12672>
9. Palou L, Ali A, Fallik E et al (2016) GRAS plant- and animal-derived compounds as alternatives to conventional fungicides for the control of postharvest diseases of fresh horticultural produce. Postharvest Biol Technol 122:41–52. <https://doi.org/10.1016/j.postharvbio.2016.04.017>
10. Valencia-Chamorro SA, Palou L, del Río MA et al (2008) Inhibition of *Penicillium digitatum* and *Penicillium italicum* by hydroxypropyl methylcellulose-lipid edible composite films containing food additives with antifungal properties. J Agric Food Chem 56:11270–11278. <https://doi.org/10.1021/jf802384m>
11. Suhag R, Kumar N, Petkoska AT et al (2020) Film formation and deposition methods of edible coating on food products: a review. Food Res Int 136:109582. <https://doi.org/10.1016/j.foodres.2020.109582>
12. Andrade RD, Skurtys O, Osorio FA (2012) Atomizing spray systems for application of edible coatings. Compr Rev Food Sci Food Saf 11:323–337. <https://doi.org/10.1111/j.1541-4337.2012.00186.x>
13. Palou L, Valencia-Chamorro SA, Pérez-Gago MB (2015) Antifungal edible coatings for fresh citrus fruit: a review. Coatings 5:962–986. <https://doi.org/10.3390/coatings5040962>
14. Campos CA, Gerschenson LN, Flores SK (2011) Development of edible films and coatings with antimicrobial activity. Food Bioprocess Technol 4:849–875. <https://doi.org/10.1007/s11947-010-0434-1>
15. Balouiri M, Sadiki M, Koraichi Ibsouda S (2016) Methods for in vitro evaluating antimicrobial activity: a review. J Pharm Anal 6:71–79. <https://doi.org/10.1016/j.jpha.2015.11.005>
16. Aloui H, Khwaldia K (2016) Natural antimicrobial edible coatings for microbial safety and food quality enhancement. Compr Rev Food

- Sci Food Saf 15:1080–1130. <https://doi.org/10.1111/1541-4337.12226>
17. Valencia-Chamorro SA, Pérez-Gago MB, del Río MA et al (2009) Curative and preventive activity of hydroxypropyl methylcellulose lipid edible composite coatings containing antifungal food additives to control citrus postharvest green and blue molds. *J Agric Food Chem* 57: 2770–2777. <https://doi.org/10.1021/jf803534a>
  18. Min S, Krochta JM (2005) Inhibition of *Penicillium commune* by edible whey protein films incorporating lactoferrin, lactoferrin hydrolysate, and lactoperoxidase system. *J Food Sci* 70:87–94. <https://doi.org/10.1111/j.1365-2621.2005.tb07108.x>
  19. Franssen LR, Krochta JM (2000) Edible coating containing natural antimicrobials for processed foods. In: Roller S (ed) *Natural antimicrobial for minimal processing of foods*. CRC Press, Boca Raton, pp 250–262
  20. Padgett T, Han IY, Dawson PL (2000) Effect of lauric acid addition on the antimicrobial efficacy and water permeability of corn zein films containing nisin. *J Food Process Preserv* 24:423–432. <https://doi.org/10.1111/j.1745-4549.2000.tb00429.x>
  21. Kristo E, Koutsoumanis KP, Biliaderis CG (2008) Thermal, mechanical and water vapor barrier properties of sodium caseinate films containing antimicrobials and their inhibitory action on *Listeria monocytogenes*. *Food Hydrocoll* 22:373–386. <https://doi.org/10.1016/j.foodhyd.2006.12.003>
  22. Palou L (2018) Postharvest treatments with GRAS salts to control fresh fruit decay. *Horticulturae* 4:46. <https://doi.org/10.3390/horticulturae4040046>
  23. Simko I, Piepho HP (2012) The area under the disease progress stairs: calculation, advantage, and application. *Phytopathology* 102:381–389. <https://doi.org/10.1094/PHYTO-07-11-0216>
  24. Eckert JW, Brown GE (1986) Evaluation of postharvest fungicide treatments for citrus fruits. In: Hickey KD (ed) *Methods for evaluating pesticides for control of plant pathogens*. APS Press, St Paul, pp 92–97
  25. Pérez-Gago MB, Palou L (2016) Antimicrobial packaging for fresh and fresh-cut fruits and vegetables. In: Pareek S (ed) *Fresh-cut fruits and vegetables: technology, physiology, and safety*. CRC Press/Taylor and Francis Group, Boca Raton, pp 403–452
  26. Guimarães JER, de la Fuente B, Pérez-Gago MB et al (2019) Antifungal activity of GRAS salts against *Lasiodiplodia theobromae* in vitro and as ingredients of hydroxypropyl methylcellulose-lipid composite edible coatings to control *Diplodia* stem-end rot and maintain postharvest quality of citrus fruit. *Int J Food Microbiol* 301:9–18. <https://doi.org/10.1016/j.ijfoodmicro.2019.04.008>
  27. Gunaydin S, Karaca H, Palou L et al (2017) Effect of hydroxypropyl methylcellulose-beeswax composite edible coatings formulated with or without antifungal agents on physicochemical properties of plums during cold storage. *J Food Qual* 2017:8573549. <https://doi.org/10.1155/2017/8573549>
  28. Palou L, Crisosto CH, Garner D (2007) Combination of postharvest antifungal chemical treatments and controlled atmosphere storage to control gray mold and improve storability of ‘Wonderful’ pomegranates. *Postharvest Biol Technol* 43:133–142. <https://doi.org/10.1016/j.postharvbio.2006.08.013>



## Antibacterial Activity of Active Food Packaging Materials

Paula J. P. Espitia and Rejane A. Batista

### Abstract

Active food packaging materials with antimicrobial properties have stood out from other technological products for food preservation due to its practical application and cost-benefit. This analytical protocol was based on the “Antimicrobial Disk Susceptibility Tests” and adapted to its application for antibacterial food packaging. It points out in a simplified, careful, and objective way the entire step-by-step methodology to evaluate antimicrobial activity applied to food packaging incorporated with active compounds against different microorganisms of interest to the food industry. Therefore, it is an interesting tool for students, researchers, laboratories, and companies interested in the science of food packaging technology.

**Key words** Antimicrobial activity, Active food packaging, Disk diffusion method

---

### 1 Introduction

Spoilage microorganisms are one of the main reasons for food loss and waste according to the Food and Agriculture Organization of the United Nations (FAO), resulting in an estimated yearly loss of 40–50% fruits and vegetables, 35% fish, 30% cereals, and 20% dairy and meat products [1]. On the other hand, foodborne pathogens are affecting the lives of consumers, resulting in deaths, hospitalizations, and illnesses worldwide [2]. In this regard, the World Health Organization has indicated that around 600 million people get sick after consuming food that has been contaminated after its production [3].

Safe production and commercialization of food require the use of proper packaging materials, which allows for protecting it from external threats, such as spoilage and pathogenic microorganisms, oxygen, moisture, light, and heat, among others, as well as increasing its shelf-life, decreasing postcontamination, and preserving its quality until it reaches the final consumer [2, 4]. Moreover, food packaging plays the role of unitizing food products and attracting consumers with a marketing appeal, features that are essential in different links of the food supply chain [5]. The worldwide market

of food packaging has been estimated at over USD 300 billion in 2019, with a predicted increase rate of 5.2% yearly [1]. Thus, this is a domain of high relevance not only from the food preservation point of view and the economical perspective but also from the innovation standpoint. In this regard, consumers' demand for healthier and safer food, together with the necessity of convenience, has led to the development of innovative food packaging technologies, including active food packaging [6].

Active food packaging interacts with the contained food product in order to provide it with one or more beneficial function(s), including scavenging of oxygen, moisture, or ethylene; emission of flavor; and antioxidant or antimicrobial activities, among others [7]. Antimicrobial food packaging stands out as a particular type of active food packaging having in its structure an antimicrobial agent that might be released into foodstuff, reducing or even inhibiting the growth of spoilage microorganisms or foodborne pathogens therein [8]. This results in food safety and quality assurance, as well as increased shelf-life [1, 6].

Polymer-based antimicrobial food packaging can be developed by direct incorporation of the antimicrobial agent into the polymer matrix, followed by its progressive diffusion from the packaging to the food surface. Readers can refer to Chap. 18 for detailed protocols to determine the release kinetics of several active compounds, including antimicrobials. Alternatives include intrinsically antimicrobial polymers or sachets that are previously incorporated with volatile antimicrobial agents and placed within the packaging headspace [1, 8]. In the latter strategy, although the antimicrobial agent is inside the packaging, it does not touch the food surface, but instead creates a modified atmosphere as a result of its progressive vapor release.

Most of the tests applied to determine the antimicrobial activity of food packaging materials include the use of foodborne pathogens (e.g., *Escherichia coli*, *Staphylococcus aureus*, and *Salmonella enterica*) as well as different fungal strains, such as yeasts and postharvest molds [1]. While antibacterial assays are detailed herein, protocols for determining the antifungal efficiency of edible packaging are depicted in Chap. 15. Yet, the recent pandemic of Sars-CoV-2 served as a wake-up call for the scientific community to also track the antiviral activity of active packaging materials.

Studying the antimicrobial activity allows researchers to have an estimated performance of the biological activity of developed films against selected microorganisms. However, it is highly important to assess the antimicrobial activity in real food systems, considering that variations in results might be observed due to the interaction of the antimicrobial agent with some food components once it has been released into the food matrix [9].

The antimicrobial activity packaging materials can be determined in vitro relying on optical density after applying the

antimicrobial packaging material on a simulated solid food model system, by colony counting, minimum inhibitory concentration (MIC), or by the disc diffusion method [9]. The latter has been reported with several names in the literature, including agar diffusion method [9], antibacterial activity Kirby–Bauer test—disc diffusion method [10], disc diffusion assay [11], disc diffusion method [12], disk—or disc—diffusion method [12–15], Kirby–Bauer disk diffusion assay [16], and overlay diffusion test [17, 18]. Although difference in designations, all the reported tests are based on the “Antimicrobial Disk Susceptibility Tests” organized and presented by the Clinical and Laboratory Standards Institute (CLSI)<sup>1</sup> in its document “M02-A11—Performance Standards for Antimicrobial Disk Susceptibility Tests; Approved Standard” [19]. This protocol presents the methodology necessary to apply the disk diffusion test in a standardized manner. This protocol is reviewed and analyzed periodically, and its performance, applications, and limitations are presented as well. This standardized method is based on the “Antibiotic susceptibility testing by a standardized single disk method” originally described by Bauer and collaborators in 1966 [20], and currently known as the “Kirby-Bauer Disk Diffusion Susceptibility Test”. This is the most detailed disk diffusion method, and it is based on the correlation of the inhibition zone diameter with the MIC of different antimicrobial agents against microbial strains in order to determine if they are susceptible or resistant [19].

Considering that the disk diffusion test is one the most widely used techniques for determining the biological activity of antimicrobial food packaging, this protocol presents its main materials, methods, and remarks for its successful application and performance.

### **1.1 Brief History of the Method**

The discovery of penicillin and its effects against bacterial infection caused by *Staphylococci* and *Streptococci* by Alexander Fleming was one of the greatest findings of modern medicine. This led to the development and application of microbiological analyses to determine susceptibility or resistance to antimicrobials of antibiotic compounds, to further being used in treating human pathologies. Although the original method for determining susceptibility to antimicrobials was based on broth dilution techniques, the disk diffusion method was a widely accepted and adopted methodology among most US clinical microbiology laboratories by the decade of 1950s. However, this methodology was not standardized, and each

---

<sup>1</sup> “The Clinical and Laboratory Standards Institute (CLSI) is an international, voluntary, nonprofit, interdisciplinary, standards-developing, and educational organization accredited by the American National Standards Institute, which develops and promotes the use of consensus-developed standards and guidelines within the health care community. These consensus standards and guidelines are developed to address critical areas of diagnostic testing and patient health care, and are developed in an open and consensus-seeking forum” [19].

laboratory had an internal modification concerning methodological variables (culture media, incubation time, incubation temperature, among others). Thus, researcher Kirby and colleagues at the University of Washington School of Medicine and the King County Hospital, after an extensive research regarding this methodology, presented a single disk diffusion methodology intended to assess the antimicrobial susceptibility in 1956. However, during the 1960s, the lack of standardization of this methodology was still a problem. Kirby and collaborators continued to work on organizing systematically and updating all information related to the disk diffusion method and finally published their findings. This resulted in the organization of a committee in 1961 by the World Health Organization, with the goal of developing a standardized technique for testing the antimicrobial susceptibility. The result was the worldwide known Kirby–Bauer disk diffusion test [21]. In this regard, the standardized method was widely adopted in microbiology clinical laboratories by 1972. The advantages of this technique include its relative simplicity of application from the technological point of view and its reproducibility [22]. At present, the organization in charge of updating and modifying the original procedure of the Kirby–Bauer disk diffusion test is the CLSI, in order to allow uniformity and reproducibility of results.

On the other hand, the first studies regarding antimicrobial food packaging are dated from 1985, with the development of waxes and other edible coatings incorporated with antimycotic agents to protect food products [23]. In 1989, the term “active packaging” was defined by Labuza and Breene as packaging that “fosters desirable interactions” [24]. In 1990, the first reports regarding the use of food-grade antimycotic agents incorporated in cellulose edible films and their effectivity for food preservation were published. In 1995, Rooney presented a complete literature review on active and antimicrobial food packaging [25], which was a compilation of published research in these areas. However, published literature indicating the use or the adoption of the Kirby–Bauer disk diffusion test in the field of antimicrobial food packaging was scarce in the 1990s. The first studies related to the adaptation of this technique to study the antimicrobial activity of active food packaging date from 2000 and 2001, in which researchers referred usually as “inhibition zone assay.”

Currently, the Kirby–Bauer disk diffusion test with modifications is extensively used to study the antimicrobial activity of active food packaging incorporated with organic and inorganic antimicrobial agents, which can also be found in the polymer matrix even at the nanoscale.

---

## 2 Materials

The following materials are needed for carrying out the disk diffusion test:

- Sterile saline in 2-mL tubes.
- 0.5 McFarland standard.
- Wickerham card.
- Mueller–Hinton agar plates (100 or 150 mm).
- Caliper or ruler.
- Antibiotic disks.
- Forceps.
- Vortex.
- Sterile swabs.
- Alcohol 70%.
- Incubator.
- Disk of the developed packaging material intended to be tested.
- Laminar hood.
- Autoclave.
- UV light source.
- Bunsen burner.
- Microorganism to the antimicrobial activity of the developed food packaging (foodborne or spoilage microorganism is recommended).

---

## 3 Methods

### **3.1 Preparation of the Mueller–Hinton Agar Plates**

1. Prepare the Mueller–Hinton agar from dehydrated media according to the manufacturer’s instructions.
2. Pour the Mueller–Hinton agar medium into Petri dishes. The depth of the prepared agar should be 4 mm. This corresponds to 25 mL of liquid culture medium in 100-mm Petri dishes or 60 mL of liquid culture medium poured in 150-mm Petri dishes (*see Note 4.1*).
3. Once the Mueller–Hinton agar medium is poured into the Petri dishes, allow the agar to equilibrate at room temperature.
4. If there is liquid on the surface of the poured agar, place the Petri dishes ajar on their lids, to allow removal of the liquid and its evaporation. It is important to do this procedure in a pre-sterilized laminar flux hood for 10–30 min.





**Fig. 1** McFarland standards representing different microbial concentrations (left to right: 0.5, 1.0, 2.0, 3.0, and 4.0 McFarland unit), positioned in front of a Wickerham card. (Adapted from Bioanalytic GmbH [[www.bioanalytic.de](http://www.bioanalytic.de)] with permission)

5. Once dried and ready to use, label each Petri dish regarding tested microorganisms and antimicrobial agents incorporated in the food packaging.

### **3.2 McFarland Standard**

- The 0.5 McFarland Standard corresponds to  $1.5 \times 10^8$  colony-forming unit (CFU)  $\text{mL}^{-1}$ . The standard should be used together with the Wickerham card, which is a card with black and white lines in parallel that allows visual comparison of the 0.5 McFarland Standard with the prepared bacterial suspension (*see Note 4.2*) that will be used in the disk diffusion test as inoculum (Fig. 1).
- Prior to its use, agitate the 0.5 McFarland Standard vigorously to achieve a homogeneous turbidity.
- In order to determine the adequacy of the prepared bacterial suspension (inoculum), hold side by side the 0.5 McFarland Standard and the inoculum in front of the Wickerham card.
- Compare the turbidity of the inoculum and the 0.5 McFarland Standard with proper light. The comparison should be done by observing the parallel lines through both suspensions.
- If the prepared inoculum is less turbid than the 0.5 McFarland Standard, add more microorganisms.
- Add more saline solution to the prepared inoculum if it is denser (more turbid) than the 0.5 McFarland Standard. However, if the difference in turbidity is too big, then it is recommended to start over, instead of continuing to dilute the prepared bacterial dilution.

### **3.3 Streaking Technique**

This technique consists of placing an aliquot of the microbiological material on a point on the surface of the culture medium and then spreading it out in order to obtain progressively smaller amounts of the targeted microbiological material on the agar surface. The main aim of the streaking technique is to obtain sufficient rarefaction of the microbiological material, to the point of obtaining isolated colonies, of bacteria or yeasts, in the solid culture medium.

To ensure successful application of this technique, pay attention to the following recommendations:

- Use a nickel–chrome inoculation loop to seed the material through streaks on the surface of the culture medium contained in a Petri dish.
- Always pass the bacteriological loop through a flame or use a disposable loop.
- Do not return the bacteriological loop over the streaked section of the culture medium.
- Avoid a large number of streaked sections on the culture medium.
- Do not pierce the medium with the bacteriological loop.
- Take a small amount of the initial microbiological material to be isolated.
- Always work with all material close to the flame (Bunsen burner) to avoid external contamination in your experiment.
- Follow a single direction when streaking the sample, for example, from the edge to the center of the plate.
- Passing the bacteriological loop through the flame between each streak sequence increases the likelihood of obtaining isolated colonies.

A step-by-step is suggested below and illustrated in Fig. 2:

1. Unload the swab or the inoculating loop in an isolated corner of the culture medium.
2. Make the first streaking. Following this, make streak sequences in order to obtain the depletion of the inoculum from the loop and consequently allow the microorganisms to develop forming isolated colonies.
3. The beginning of the next streaking sequence should overlap with the end of the previous one and may occupy the rest of the plate.



**Fig. 2** Steps involved in streaking a plate for discrete colonies (right-hand side): Parallel line quadrant streak followed by undulating line quadrant streak. After each streak, the inoculating loop or needle should be flamed to red hot and allowed to cool before proceeding to the next step. (Reproduced from Microbe Notes [[www.microbenotes.com/streak-plate-method-principle-methods-significance-limitations](http://www.microbenotes.com/streak-plate-method-principle-methods-significance-limitations)] with permission from the author and owner)

### 3.3.1 Incubation

After applying the streaking methodology, the Petri dishes should be incubated inverted in a bacteriological incubator at  $36 \pm 2^\circ\text{C}$  for 24–48 h (conditions favorable to most microorganisms of interest. This should be checked according to each study). After 24 h, it is possible to evaluate the morphological characteristics of isolated growing colonies.

### 3.3.2 Interpretation of the Isolation Results from the Exhaustion Methods

1. Observe the appearance of isolated colonies on agar plates and differentiate according to the distinctive characteristics of the target microorganism.
2. To obtain pure cultures, remove, with a sterile inoculation needle, a portion of a chosen colony and transfer it aseptically to an inclined simple agar tube, making a streak on its surface. Incubate at  $36 \pm 2^\circ\text{C}$  for 24 h.
3. After the incubation period, observe the culture grown in the tube and check the purity considering its homogeneous aspect and through Gram stain.

### 3.4 Inoculum Elaboration

1. Take 4–5 isolated colonies from the Petri dish with the cultured microorganism to be tested, using an inoculating loop (*see Note 4.3*).
2. Suspend the colonies in sterile saline (2 mL).
3. Homogenize the tube with the suspended colonies.
4. Verify the desired turbidity according to the 0.5 McFarland Standard and adjust it if necessary according to item 3.2.
5. Use the inoculum within 15 min after it is prepared.

### 3.5 Inoculation of the Petri Dishes Containing Mueller–Hinton Agar

1. Immerse a sterile swab in the prepared inoculum.
2. Rotate the swab against the internal side of the tube containing the inoculum. This should be done with pressure enough to remove the excess liquid contained in the swab, which should not be dripping wet.

3. Proceed to inoculate the Petri dish containing the Mueller–Hinton agar by streaking three times the agar surface with the swab containing the bacterial suspension. Then rotate the plate ( $60^\circ$  approximately) and repeat the procedure. Ensure an equal distribution of the inoculum on the entire agar surface.
4. Verify that there is no excess inoculum liquid on the agar surface. To avoid this, rim the Petri dish with the swab.
5. Prepare the used swab for disposal by autoclaving beforehand and discard in the appropriate container.
6. Allow the surface of the agar to dry by placing the lid of the Petri dish ajar. This procedure should be done at room temperature for a maximum of 15 min.

### 3.6 Placement of Antimicrobial Packaging Disks in the Inoculated Petri Dishes

1. To place the antimicrobial food packaging disks, slightly remove the lid from the Petri dish and with the help of a previously sterilized forceps, place the antimicrobial food packaging disks (6 mm in diameter) on the surface of Mueller–Hinton agar (Fig. 3).
2. Apply gentle pressure with the forceps on top of the disks to ensure its contact with the agar surface.
3. Place the lid on the Petri dish to minimize the exposure of the agar to the external environment and repeat the process according to the numbers of antimicrobial food packaging desired to be tested. For each antimicrobial food packaging tested, a control treatment—food packaging without any antimicrobial—should be prepared and tested simultaneously (*see Note 4.4*).

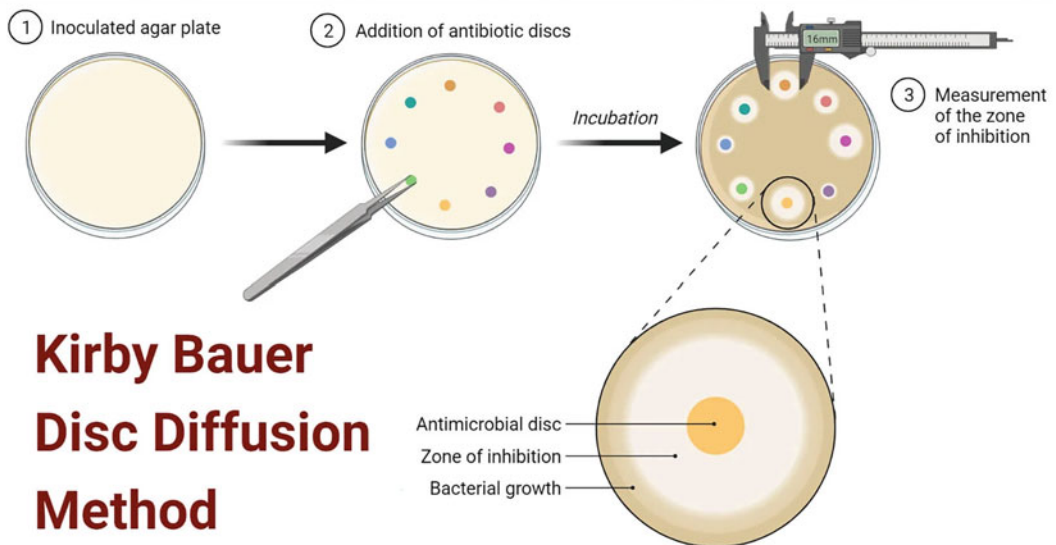


**Fig. 3** Placement of disk on the surface of inoculated Petri dishes. Reproduced from Microbe Notes with permission from the author and owner [[www.microbenotes.com/kirby-bauer-disc-diffusion/](http://www.microbenotes.com/kirby-bauer-disc-diffusion/)]

4. Once all disks are placed on the agar surface, invert the Petri dishes and incubate. Ideal incubation conditions for foodborne pathogens and spoilage microorganisms should be checked in each specific case.

### 3.7 Measurement of the Inhibition Zone

- After the incubation period, measure the inhibition zone on the back of each Petri dish with a caliper or a ruler (*see Note 4.5*). The diameter of the disk should be considered in this measurement (Fig. 3).
- The results should be determined without any visual aid. The Petri dish should be held on a black surface, and enough light should be provided to see the back of the Petri dishes. The results should be observed using a vertical sight line.
- Microbial growth starting at the edge of the disk should be reported as 0 mm.

### 3.8 Results Report and Presentation

The obtained results are presented as a measurement of the diameter of the inhibition zone [mm].

Although the original “Kirby-Bauer Disk Diffusion Susceptibility Test” establishes a guideline published by the CLSI to determine the level of susceptibility of the selected microorganism to the tested antimicrobial—susceptible (S), intermediate (I), or resistant (R)—based on an interpretation chart, in the field of antimicrobial food packaging there is so far no standardization regarding the microbial susceptibility level. This is in part due to the lack of a specific institution in charge of that task in this field, as well as due to the increasing number of antimicrobial agents that are incorporated in polymeric matrices to later be studied with the potential application for food preservation.

---

## 4 Notes

All procedures described in this protocol should be done in a sterile environment. Agar and Petri dishes should be sterilized, e.g., in an autoclave while packaging disks (samples to be tested) should be sterilized with UV, autoclave, or any other suitable method. Researchers should be provided with laboratory coats or appropriate clothes, as well as gloves for personal protection.

Besides this general warning, notes on specific steps are listed below:

### 4.1 Preparation of the Mueller–Hinton Agar Plates

1. Erroneous results might be produced if the Mueller–Hinton agar medium poured in Petri dishes has a different depth. If the agar medium is too shallow in the Petri dishes, the antimicrobial agent released from the developed packaging material will diffuse further than it should, and the resulted inhibition zone

will be bigger than expected. If the depth of the agar medium in the Petri dishes is higher, it will result in an inaccurate resistant result.

#### **4.2 McFarland Standard**

1. This Standard can be commercially purchased or prepared in house [26].
2. The 0.5 McFarland Standard should be replaced when large particle aggregates are observed instead of a homogeneously turbid suspension.

#### **4.3 Inoculum Elaboration**

1. The selected microorganism for testing the antimicrobial activity of the food packaging should be in the log phase. Thus, the microorganism should be activated to its log phase the previous day to performing this technique. This procedure should be adjusted according to the selected microorganism.
2. Different microorganisms have been reported to be used to test the antimicrobial activity of active food packaging. Table 1 presents the reported microorganisms used, as well as polymer matrices and antimicrobial agents tested using the disk diffusion method.

#### **4.4 Placement of Antimicrobial Packaging Disks in the Inoculated Petri Dishes**

1. It is recommended to place the disks not closer than 24 mm on the Mueller–Hinton agar. For Petri dishes of 150 mm in diameter, a maximum of 12 disks (6 mm in diameter each) should be placed, and for Petri dishes of 100 mm in diameter, a maximum of five disks should be placed on the surface of the Mueller–Hinton agar. When the diameter of the disk is larger, less disks should be used.
2. A template of the positions at which the disks will be placed on the Mueller–Hinton agar surface should be used, considering the spacing among disks and the maximum number of disks according to each type of Petri dish.
3. Prevent the placement of disks close to the border of the Petri dish, since after incubation, the results are likely not to be possible to read with accuracy.
4. Avoid altering the physical integrity of the Mueller–Hinton agar surface (any disruption) due to excessive pressure when inoculating or placing the disks, or by dipping the disk inside the agar. In these cases, the procedure should be repeated since the obtained results will not be possible to read due to the lack of accuracy.

#### **4.5 Measurement of the Inhibition Zone**

1. It is expected that the inhibition zone exhibited should be circular, with a convergent microbial growth around it, if the agar was inoculated and the disks were placed properly.

**Table 1**  
**Microorganisms used to test the antimicrobial activity of active food packaging using the disk diffusion method**

| Microorganism   | Antimicrobial agent   | Food packaging material  | Reference |
|---|---|--|-----------|
| <i>Listeria monocytogenes</i>   | Olive leaf extract  | Fish gelatin   | [17]      |
| <i>Staphylococcus aureus</i> and <i>Salmonella</i>  | Pomegranate peel extract  | Hydroxypropyl high-amylose starch                              | [12]      |
| <i>Salmonella enterica</i> , <i>L. monocytogenes</i> , <i>Yersinia enterocolitica</i> , <i>Pseudomonas aeruginosa</i> , <i>Escherichia coli</i> , <i>S. aureus</i> , and <i>Enterococcus faecalis</i> | ZnO nanoparticles and ascorbic acid   | Nanocomposites comprising tragacanth gum and polyvinyl alcohol | [10]      |
| <i>E. coli</i>  | Carvacrol and thymol  | Low-density polyethylene filled with halloysite nanotubes      | [16]      |
| <i>E. coli</i> O157:H7 and <i>S. aureus</i>   | Rosin-grafted cellulose nanocrystals  | Bovine gelatin   | [27]      |
| <i>E. coli</i> and <i>Bacillus subtilis</i>   | Rosin used to modify the surface of cellulose nanocrystals to obtain rosin-modified CNF (R-CNF) | Halloysite nanotubes coated with chitosan                      | [28]      |
| <i>S. aureus</i> (MRSA) and <i>E. coli</i> (DH5- $\alpha$ )   | Silver  | Gelatin  | [14]      |
| <i>Bacillus cereus</i> , <i>S. aureus</i> , <i>E. coli</i> , and <i>Salmonella</i> Typhi  | Chitosan nanoparticles  | Tapioca starch   | [11]      |
| <i>E. coli</i> O157:H7 and <i>S. aureus</i>   | Chitosan  | Chitosan/ $\epsilon$ -PL bionanocomposites films               | [29]      |
| <i>B. subtilis</i> and <i>E. coli</i>   | Lauric acid   | Bacterial cellulose  | [15]      |

2. If it is not possible to read the complete diameter of the inhibition zone, it is recommended to measure the radius to another edge of the circumference of the inhibition zone and multiply this result by two to determine the diameter.
3. The test must be rerun when the microbial growth is not consistent on the agar's surface, but instead individual colonies are observed across the surface.
4. When measuring the inhibition zone, this should be determined bearing in mind that this corresponds to a zone without any evident microbial growth.

## Acknowledgments

The authors thank the support provided by the Foundation for Research and Technological Innovation Support of the State of Sergipe (FAPITEC/SE).

## References

- Motelica L, Ficaí D, Ficaí A, Oprea OC, Kaya DA, Andronescu E (2020) Biodegradable antimicrobial food packaging: trends and perspectives. *Foods* 9:1438
- Al-Tayyar NA, Youssef AM, Al-hindi R (2020) Antimicrobial food packaging based on sustainable bio-based materials for reducing food-borne pathogens: a review. *Food Chem* 310: 125915. <https://doi.org/10.1016/j.foodchem.2019.125915>
- Kim I, Viswanathan K, Kasi G, Thanakkasaranee S, Sadeghi K, Seo J (2020) ZnO nanostructures in active antibacterial food packaging: preparation methods, antimicrobial mechanisms, safety issues, future prospects, and challenges. *Food Rev Int*:1–29. <https://doi.org/10.1080/87559129.2020.1737709>
- Kim I, Viswanathan K, Kasi G, Sadeghi K, Thanakkasaranee S, Seo J (2019) Poly(lactic acid)/ZnO bionanocomposite films with positively charged ZnO as potential antimicrobial food packaging materials. *Polymers* 11:1427
- Espitia PJP, Otoni CG (2018) Nanotechnology and edible films for food packaging applications in bio-based materials for food packaging. In: Ahmed S (ed) *Bio-based materials for food packaging*. Springer, Singapore
- Kumar S, Mukherjee A, Dutta J (2020) Chitosan based nanocomposite films and coatings: emerging antimicrobial food packaging alternatives. *Trends Food Sci Technol* 97:196–209. <https://doi.org/10.1016/j.tifs.2020.01.002>
- Huang T, Qian Y, Wei J, Zhou C (2019) Polymeric antimicrobial food packaging and its applications. *Polymers* 11:560
- Santos JCP, Sousa RCS, Otoni CG, Moraes ARF, Souza VGL, Medeiros EAA, Espitia PJP, Pires ACS, Coimbra JSR, Soares NFF (2018) Nisin and other antimicrobial peptides: production, mechanisms of action, and application in active food packaging. *Innov Food Sci Emerg Technol* 48:179–194. <https://doi.org/10.1016/j.ifset.2018.06.008>
- Espitia PJP, Batista RA (2015) Non-thermal food preservation: control of food-borne pathogens through active food packaging and nanotechnology in advances in food biotechnology. In: Ravishankar RV (ed) *Advances in food biotechnology*. Wiley, New York
- Janani N, Zare EN, Salimi F, Makvandi P (2020) Antibacterial tragacanth gum-based nanocomposite films carrying ascorbic acid antioxidant for bioactive food packaging. *Carbohydr Polym* 247:116678. <https://doi.org/10.1016/j.carbpol.2020.116678>
- Shapi'i RA, Othman SH, Nordin N, Kadir Basha R, Nazli Naim M (2020) Antimicrobial properties of starch films incorporated with chitosan nanoparticles: in vitro and in vivo evaluation. *Carbohydr Polym* 230:115602. <https://doi.org/10.1016/j.carbpol.2019.115602>
- Ali A, Chen Y, Liu H, Yu L, Baloch Z, Khalid S, Zhu J, Chen L (2019) Starch-based antimicrobial films functionalized by pomegranate peel. *Int J Biol Macromol* 129:1120–1126. <https://doi.org/10.1016/j.ijbiomac.2018.09.068>
- Fuenmayor CA, Espitia PJP (2018) Electrospun nanofibers: development and potential in food packaging applications in nanotechnology applications in the food industry. In: Rai V, Bai J (eds) *Nanotechnology applications in the food industry*. CRC Press, Boca Raton
- Sarwar MS, Niazi MBK, Jahan Z, Ahmad T, Hussain A (2018) Preparation and characterization of PVA/nanocellulose/Ag nanocomposite films for antimicrobial food packaging. *Carbohydr Polym* 184:453–464. <https://doi.org/10.1016/j.carbpol.2017.12.068>
- Zahan KA, Azizul NM, Mustapha M, Tong WY, Abdul Rahman MS, Sahuri IS (2020) Application of bacterial cellulose film as a biodegradable and antimicrobial packaging material. *Mater Today Proc* 31:83–88. <https://doi.org/10.1016/j.matpr.2020.01.201>
- Krepker M, Shemesh R, Danin Poleg Y, Kashi Y, Vaxman A, Segal E (2017) Active food packaging films with synergistic antimicrobial activity. *Food Control* 76:117–126. <https://doi.org/10.1016/j.foodcont.2017.01.014>
- Albertos I, Avena-Bustillos RJ, Martín-Diana AB, Du W-X, Rico D, McHugh TH (2017) Antimicrobial olive leaf gelatin films for enhancing the quality of cold-smoked Salmon.



- Food Packag Shelf Life 13:49–55. <https://doi.org/10.1016/j.fpsl.2017.07.004>
18. Espitia PJP, Avena-Bustillos RJ, Du W-X, Chiou B-S, Williams TG, Wood D, McHugh TH, Soares NFF (2014) Physical and antibacterial properties of Açai edible films formulated with thyme essential oil and apple skin polyphenols. *J Food Sci* 79:M903–M910. <https://doi.org/10.1111/1750-3841.12432>
  19. CLSI (2012) Performance standards for antimicrobial disk susceptibility tests; approved standard-eleventh edition. CLSI document M02-A11. 76p
  20. Bauer AW, Kirby WM, Sherris JC, Turck M (1966) Antibiotic susceptibility testing by a standardized single disk method. *Am J Clin Pathol* 45:493–496
  21. Hudzicki J (2009) Kirby-Bauer disk diffusion susceptibility test protocol. 23p
  22. Biemer JJ (1973) Antimicrobial susceptibility testing by the Kirby-Bauer disc diffusion method. *Ann Clin Lab Sci* 3:135–140
  23. Hotchkiss JH (1995) Safety considerations in active packaging in active food packaging. In: Rooney ML (ed) *Active food packaging*. Springer, New York
  24. Hotchkiss JH (1997) Food-packaging interactions influencing quality and safety. *Food Addit Contam* 14:601–607. <https://doi.org/10.1080/02652039709374572>
  25. Rooney ML (1995) Overview of active food packaging in active food packaging. In: Rooney ML (ed) *Active food packaging*. Springer, New York
  26. Garcia L (2010) Preparation of routine media and reagents used in antimicrobial susceptibility testing in clinical microbiology procedures handbook. In: Garcia LS (ed) *Clinical microbiology procedures handbook*. Washington, DC, ASM Press
  27. Leite LSF, Bilatto S, Paschoalin RT, Soares AC, Moreira FKV, Oliveira ON, Mattoso LHC, Bras J (2020) Eco-friendly gelatin films with rosin-grafted cellulose nanocrystals for antimicrobial packaging. *Int J Biol Macromol* 165: 2974–2983. <https://doi.org/10.1016/j.ijbiomac.2020.10.189>
  28. Niu X, Liu Y, Song Y, Han J, Pan H (2018) Rosin modified cellulose nanofiber as a reinforcing and co-antimicrobial agents in polylactic acid/chitosan composite film for food packaging. *Carbohydr Polym* 183:102–109. <https://doi.org/10.1016/j.carbpol.2017.11.079>
  29. Wu C, Sun J, Lu Y, Wu T, Pang J, Hu Y (2019) In situ self-assembly chitosan/ $\epsilon$ -polylysine bio-nanocomposite film with enhanced antimicrobial properties for food packaging. *Int J Biol Macromol* 132:385–392. <https://doi.org/10.1016/j.ijbiomac.2019.03.133>



## Antioxidant Activity Assays for Food Packaging Materials

Fabiana H. Santos, Danielle C. M. Ferreira, Julia R. V. Matheus,  
Ana E. C. Fai, and Franciele M. Pelissari

### Abstract

Antioxidant packaging is an emerging technology that limits deteriorative reactions in oxidation-sensitive food products. The direct interaction of the antioxidant material with the packaged product may inhibit oxidation reactions by scavenging free radicals, consequently improving the food stability and extending its shelf-life. Although these packages represent a promising alternative for preserving food, until now, standardized procedures to accurately quantify their efficacy have been lacking. The methodologies employed to assess the antioxidant activity of food packaging are the same as those already used for natural extracts. These methods measure the ability of the analyzed material to scavenge free radicals. Herein, we describe in detail the principal methodologies that have been used to evaluate the antioxidant activity of food packaging materials.

**Key words** Antioxidant packaging, Methodologies, Free radicals, DPPH, ABTS, FRAP, ORAC, Spectrophotometry

---

## 1 Introduction

Packaging plays a fundamental role in food quality and preservation. However, in the last years, traditional packaging has failed to prevent or even delay food degradation reactions, such as lipid oxidation, enzymatic browning, and microbial growth. Thus, considerable efforts have been made to reduce degradation effects and meet the growing consumer demand for safe and high-quality products [1].

Antioxidant packaging is an innovative strategy that limits deteriorative reactions in oxidation-sensitive food products, consequently improving their stability and extending their shelf-life [1, 2]. The direct interaction of the antioxidant material with the packaged product may inhibit oxidation reactions by scavenging free radicals [2]. Commonly, the deactivation of radicals occurs by

two main mechanisms, namely, single-electron transfer (SET) and hydrogen atom transfer (HAT) [3]. SET is related to the antioxidant ability to transfer one electron to reduce free radicals, including metals and carbonyls [4]. HAT is associated with the antioxidant ability to quench free radicals by hydrogen donation [3].

Given that, several *in vitro* methods have been used to assess the antioxidant activity of a wide variety of matrices, including food packaging materials [5]. One of the most important methods is the oxygen radical absorbance capacity (ORAC), which is based on the HAT reaction mechanism [3]. ORAC evaluates the antioxidant capacity to inhibit the dissolution of a fluorescent probe, usually fluorescein [6]. In this assay, a peroxy radical reacts with fluorescein, forming a nonfluorescent product. However, the presence of antioxidants inhibits or protects the fluorescein from this reaction. The protective effect (antioxidant activity) is measured by comparing the area under the fluorescence decay curve of the antioxidant sample with the area of the control sample [7].

One of the most useful SET-based methods is the ferric reducing antioxidant power (FRAP) [3]. This assay measures the antioxidant capacity of the material based on the reduction of the FRAP ferric ion ( $\text{Fe}^{3+}$ ) to ferrous iron ( $\text{Fe}^{2+}$ ). The reduction leads to a color change in the solution from light blue to dark blue [8]. ABTS (2,2'-azino-bis(3-ethylbenzothiazoline-6-sulphonic acid)) and DPPH (2,2-diphenyl-1-picryl-hydrazyl-hydrate) methods are often related to SET reaction mechanisms. However, their radicals may be neutralized either by a direct reduction via electron transfer or by a radical quenching via H atom transfer [3]. Therefore, they can be classified as SET- or HAT-based methods.

The ABTS assay, also known as TEAC (Trolox equivalent antioxidant capacity), evaluates the antioxidant capacity to scavenge the ABTS radical. The presence of antioxidants can change the color of the solution containing the ABTS radical from dark green to light green. On the other hand, the DPPH method measures the capacity of the antioxidant to reduce the DPPH radical [3]. DPPH is a stable hydrophobic radical with a deep purple color. Reactions with other radicals, electrons, or hydrogen atoms lead to color loss. The antioxidant activity is determined according to the color change [9].

These assays are often low-cost, easy to perform, and do not require ultra-sensitive equipment [4]. However, most of them are global and nonspecific, which requires more than one test to assess the antioxidant activity of a product [10]. This chapter will present a description of the main methods to evaluate the antioxidant activity of food packaging materials.

---

## 2 Materials

### 2.1 DPPH Assay

1. Packaging sample.
2. 2,2-Diphenyl-1-picrylhydrazyl (DPPH•).
3. Methanol or another organic solvent (*see Note 1*).
4. Grade-1 qualitative filter paper.
5. 6-Hydroxy-2,5,7,8-tetramethylchroman-2-carboxylic acid (Trolox).
6. Glass beaker.
7. Scissors.
8. Falcon tube.
9. Analytical balance.
10. Vortex homogenizer.
11. Ultrasound bath.
12. Aluminum foil.
13. Amber bottle.
14. UV-visible spectrophotometer.

### 2.2 ABTS Assay

1. Packaging sample.
2. 2,2'-Azino-bis(3-ethylbenzothiazoline-6-sulfonic) acid (ABTS) (PubChem CID: 6871216).
3. Potassium persulfate ( $K_2S_2O_8$ ) (PubChem CID: 54602120).
4. Distilled water.
5. Absolute ethanol ( $C_2H_6O$ ) (PubChem CID: 702).
6. Standard Trolox (PubChem CID: 40634).
7. Glass beaker.
8. Volumetric flask.
9. Amber bottle.
10. Analytical balance.
11. UV-visible spectrophotometer.

### 2.3 FRAP Assay

1. Packaging sample.
2. Hydrochloric acid P.A. (HCl).
3. 2,4,6-Tris(2-pyridyl)-1,3,5-triazine (TPTZ) (PubChem CID: 77258).
4. Ferric chloride ( $FeCl_3$ ).
5. Acetate buffer pH 3.6: sodium acetate ( $C_2H_3NaO_2$ ) and acetic acid ( $CH_3COOH$ ).
6. Distilled water.

7. Volumetric flask.
8. Amber bottle.
9. UV-visible spectrophotometer.

#### 2.4 ORAC Assay

1. 75 mmol L<sup>-1</sup> phosphate buffer pH 7.0: monosodium phosphate monohydrate, disodium phosphate heptahydrate, and 1 M hydrochloric acid (HCl).
2. Packaging sample.
3. Distilled water.
4. Fluorescein disodium salt.
5. 2,2'-Azobis(2-amidinopropane) dihydrochloride (AAPH).
6. 6-Hydroxy-2,5,7,8-tetramethylchroman-2-carboxylic acid (Trolox).
7. Micropipette.
8. Fluorescence spectrophotometer.

---

### 3 Methods

#### 3.1 DPPH Assay

##### 3.1.1 Packaging Sample Extracts (See Note 2)

1. Cut the packaging sample into small pieces.
2. Weigh 100 mg of the sample using an analytical balance.
3. Place the sample in a Falcon tube and add 5 mL of methanol.
4. Shake the solution for 3 min using a vortex homogenizer.
5. Keep the solution at room temperature for 3 h and shake it again for 3 min before use.
6. To calculate the inhibitory concentration (IC<sub>50</sub>), at least three more concentrations of packaging extracts must be prepared.

##### 3.1.2 0.06 mmol L<sup>-1</sup> DPPH Solution (See Note 3)

1. Weigh 4 mg of DPPH in a glass beaker wrapped with aluminum foil.
2. Add 100 mL of methanol (*see Note 4*).
3. Place the solution in an ultrasound bath for 5 min at room temperature.
4. Filter the solution using a grade I qualitative filter paper.
5. Store in an amber bottle at 4 °C in the dark (*see Note 5*).

##### 3.1.3 Performing the DPPH Assay (Fig. 1) (See Note 6)

1. Add 0.1 mL of the package extract to 3.9 mL of a DPPH methanol solution (0.06 mmol L<sup>-1</sup>).
2. Prepare a control sample only with methanol and a DPPH solution using the proportions previously described (0.1 mL of methanol and 3.9 mL of a DPPH solution).

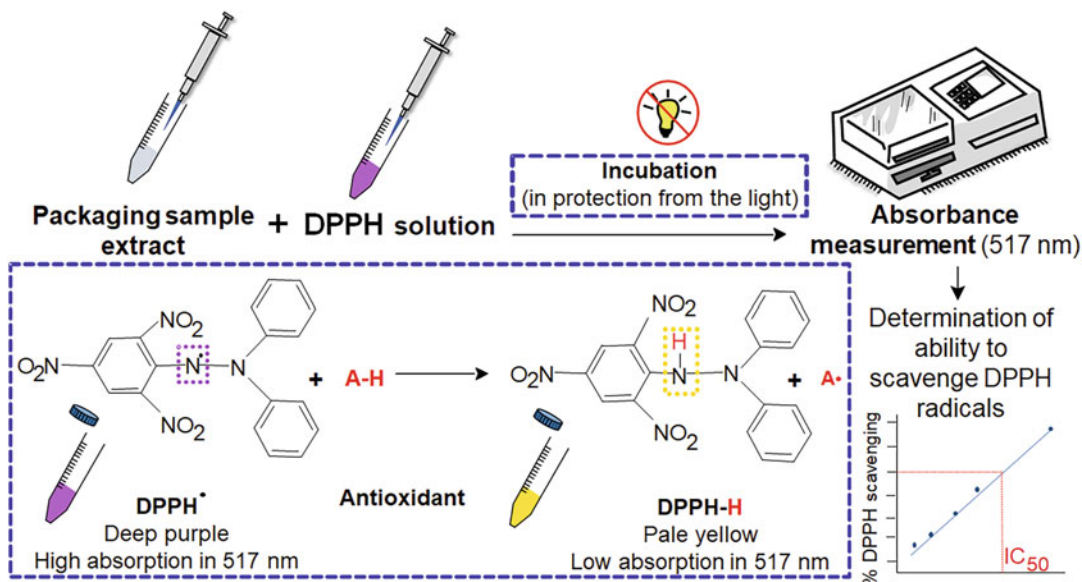


**Fig. 1** Simplified flowchart for the DPPH analysis with principle of DPPH radical scavenging by the HAT reaction mechanism

3. Keep the solutions at room temperature for 30 min in the dark (*see Note 7*).
4. While the solutions are incubated, turn on the spectrophotometer and reset the equipment with methanol.
5. Transfer the solution to an optical glass cuvette and measure its UV absorbance at 517 nm (*see Notes 8 and 9*).
6. Assays should be performed at least in triplicate for each sample (*see Note 10*).
7. The antioxidant capacity of each sample can be calculated using Eq. 1:

$$\text{DPPH inhibition (\%)} = [(A_c - A_s) / (A_c)] \times 100 \quad (1)$$

where  $A_c$  is the absorbance value at 517 nm of the control solution and  $A_s$  is the absorbance value at 517 nm of the sample solution.

8. To compare the results obtained with the antioxidant activity of a known antioxidant sample, build a Trolox standard curve (*see Notes 11 and 12*) using the procedure described for the packaging sample at different concentrations (*see Note 13*). The standard curve is obtained by plotting the Trolox absorbance as a function of the Trolox concentration ( $\text{mmol L}^{-1}$ ). The results are expressed as  $\mu\text{mol Trolox equivalents (TE)}/\text{g dry sample}$ .

- The antioxidant capacity of the packaging can also be expressed as  $IC_{50}$  (inhibitory concentration), which represents the required concentration of the packaging to reduce the initial concentration of DPPH by 50% (*see Note 14*). The results are expressed as mg of packaging sample/mL of extract.

### 3.2 ABTS Assay

#### 3.2.1 Packaging Sample Extracts [11]

1. Weigh 1 g of the food packaging material (*see Note 15*).
2. Cut the sample into small pieces and immerse them in 5 mL of a hydroalcoholic mixture (*see Note 16*).
3. Keep the mixture under stirring overnight (*see Note 17*).
4. Prepare at least three different dilutions of the sample extract [12, 13] (*see Note 18*).
5. Store under refrigeration in a dark amber bottle until assay.

#### 3.2.2 7 mmol L<sup>-1</sup> ABTS Stock Solution

1. Weigh 192 mg of ABTS and dissolve in distilled water until the volume is 50 mL in a volumetric flask.
2. Homogenize and transfer the solution to an amber glass bottle.
3. Store under refrigeration for up to a month.

#### 3.2.3 140 mmol L<sup>-1</sup> Potassium Persulfate Solution

1. Weigh 378.4 mg of potassium persulfate and dissolve in distilled water until the volume is 10 mL in a volumetric flask.
2. Homogenize and transfer the solution to an amber glass bottle.
3. Store at room temperature for up to a month.

#### 3.2.4 1 mmol L<sup>-1</sup> Trolox Standard Solution

1. Weigh 12.5 mg of Trolox and dissolve in ethyl alcohol until the volume is 50 mL in a volumetric flask.
2. Homogenize and transfer the solution to an amber glass bottle. Prepare and use only on the day of analysis.
3. Prepare the standard curve using the standard 1 mmol L<sup>-1</sup> Trolox solution, as shown in Table 1.

**Table 1**  
Preparation of the calibration curve

| Trolox 1 mmol L <sup>-1</sup> solution concentration (mL) | Ethanol (mL) | Final concentration (μmol L <sup>-1</sup> ) |
|---|--------------|---|
| 0   | 10.0         | 0   |
| 0.5   | 9.5          | 50  |
| 2.0   | 8.0          | 200   |
| 3.0   | 7.0          | 300   |
| 4.0   | 6.0          | 400   |
| 5.0   | 5.0          | 500   |
| 6.0   | 4.0          | 600   |

### 3.2.5 Performing the ABTS Assay

1. Mix an ABTS solution ( $7 \text{ mmol L}^{-1}$ ) with a potassium persulfate solution ( $2.45 \text{ mmol L}^{-1}$ ) (1:0.5 v/v).
2. Keep the mixture at room temperature for 16 h in the dark [15] (*see Note 19*).
3. Dilute an aliquot of the  $\text{ABTS}^{\bullet+}$  solution with ethanol to obtain an absorbance value of 0.70 at 734 nm using a UV-Vis spectrophotometer [15] (*see Note 20*).
4. Solubilize each sample extract dilution or pure solvent (control) ( $60 \mu\text{L}$ ) with the  $\text{ABTS}^{\bullet+}$  diluted solution ( $2940 \mu\text{L}$ ) and incubate at  $37^\circ\text{C}$  for 10 min in the dark [15–18].
5. Measure the absorbance at 734 nm in a UV-Vis spectrophotometer [15–18] (*see Note 21*).
6. Use Trolox as a standard to obtain the calibration curve (concentration ranging from 0 to  $600 \mu\text{mol L}^{-1}$ ) (*see Note 22*) and express the results as  $\mu\text{mol L}^{-1}$  Trolox equivalent/g of dry sample (*see Note 23*).
7. Perform all measurements in triplicate.

## 3.3 FRAP Assay

### 3.3.1 Packaging Sample Extracts

1. The food packaging extract in the FRAP assay should be prepared as described in Subheading 3.2.1.

### 3.3.2 $40 \text{ mmol L}^{-1}$ HCl Solution

1. Add 3.34 mL of concentrated HCl in a volumetric flask and add distilled water until the volume is 1 L.
2. Homogenize and transfer the mixture to a glass bottle. Store at room temperature.

### 3.3.3 $10 \text{ mmol L}^{-1}$ TPTZ Solution

1. Weight 3.12 g of TPTZ and dissolve in 5 mL of an HCl  $40 \text{ mmol L}^{-1}$  solution.
2. Add HCl  $40 \text{ mmol L}^{-1}$  until the volume is 1 L in a volumetric flask.
3. Homogenize and transfer the solution to an amber glass bottle.
4. Store under refrigeration for up to a month.

### 3.3.4 $20 \text{ mmol L}^{-1}$ Ferric Chloride Solution ( $\text{FeCl}_3 \cdot 6\text{H}_2\text{O}$ )

1. Weight 5.4 g of ferric chloride and dissolve in distilled water until the volume is 1 L in a volumetric flask.
2. Homogenize and transfer the mixture to an amber glass bottle.
3. Store under refrigeration for up to a month.

### 3.3.5 $30 \text{ mmol L}^{-1}$ Acetate Buffer Solution (pH 3.6)

1. Weight 0.31 g of sodium acetate ( $\text{C}_2\text{H}_3\text{NaO}_2$ ) and dissolve in 1.6 mL of acetic acid ( $\text{CH}_3\text{COOH}$ ).
2. Add distilled water until the volume is 1 L in a volumetric flask.



3. Homogenize and transfer the mixture to an amber glass bottle.
4. Store at room temperature.

### 3.3.6 1 mmol L<sup>-1</sup> Trolox Standard Solution

1. Use the procedure described in Subheading 3.2.4 to prepare the Trolox standard solution.

### 3.3.7 Performing the FRAP Assay

1. Mix 25 mL of acetate buffer 30 mmol L<sup>-1</sup> (pH 3.6), 2.5 mL of TPTZ solution (10 mmol L<sup>-1</sup>), and 2.5 mL of a FeCl<sub>3</sub>·6H<sub>2</sub>O solution (20 mmol L<sup>-1</sup>) and incubate at 37 °C for 30 min in a water bath [19] (*see Note 24*).
2. Solubilize each sample extract dilution (150 µL) with a FRAP solution (2850 µL) and keep at room temperature for 30 min in the dark [19–22].
3. Measure the absorbance at 593 nm using a spectrophotometer [19, 20] (*see Note 25*).
4. Use Trolox as a standard to obtain the calibration curve (concentration ranging from 0 to 600 µmol L<sup>-1</sup>) as described in the ABTS assay (*see Note 26*).
5. Calculate the antioxidant activity of the sample by subtracting the blank sample (*see Note 27*) and express the results as µmol L<sup>-1</sup> Trolox equivalent/g of dry sample.
6. Perform all measurements in triplicate.

## 3.4 ORAC Assay (See Note 28)

### 3.4.1 Phosphate Buffer (pH 7.0)

1. 75 mmol L<sup>-1</sup> aqueous phosphate buffer can be prepared in a 2-L solution with monosodium phosphate monohydrate and disodium phosphate heptahydrate at pH 7.0 using 1 mol L<sup>-1</sup> hydrochloric acid (HCl).

### 3.4.2 Final Reaction Mixture Based on the 2 mL Volume (See Notes 29 and 30)

1. The samples (packages) must be initially solubilized in distilled water (0.0500 g/10 mL of water, 50 °C, 1 h), and, subsequently, each initial solution must be adequately diluted in sodium phosphate buffer (75 mmol L<sup>-1</sup>, pH 7.0) [14].

### 3.4.3 Performing the ORAC Assay

1. Add 1650 µL of fluorescein sodium salt (0.05 µL) to sodium phosphate buffer 0.075 mol L<sup>-1</sup> at pH 7.0 (*see Note 31*).
2. Mix 200 mL of the diluted sample or 50 mmol L<sup>-1</sup> of Trolox (Trolox at five calibration solutions (0–50 µmol L<sup>-1</sup>) is used as a standard) with the previous solution.
3. Incubate the mixture at a constant temperature of 37 °C for 15 min (*see Note 32*).
4. Check the fluorescence intensity (485 nm<sub>excitation</sub>/525 nm<sub>emission</sub>) every 5 min for 80 min in a quartz cuvette (*see Note 33*).

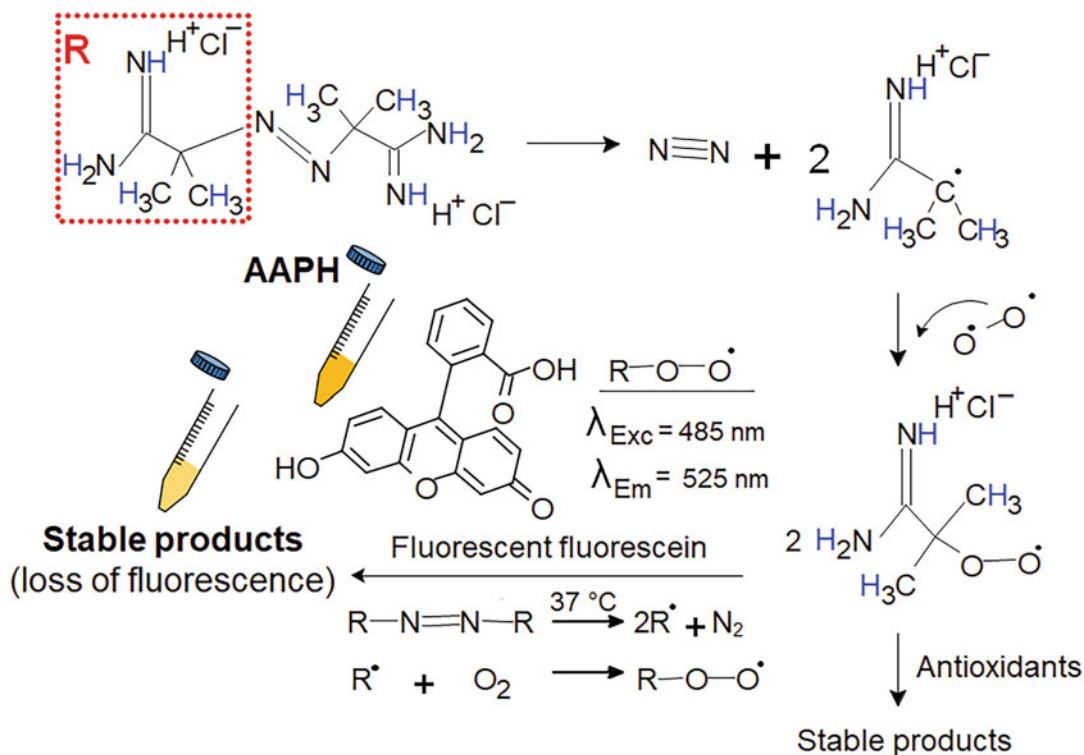


**Fig. 2** Reaction of 2,2'-Azobis (2-amidinopropane) dihydrochloride (AAPH) during the ORAC assay using fluorescein as the fluorescent probe. (Adapted from Zulueta et al. [23] with permission from Elsevier, see Note 35)

- When the stability is achieved, quickly add (*see Note 34*) 150  $\mu\text{L}$  of 2,2'-azobis(2-amidinopropane) dihydrochloride (AAPH) at 5.55  $\text{mmol L}^{-1}$  concentration (Fig. 2) using a multichannel pipette.
- Read the fluorescence until it reaches a value of zero.
- The control is the 75  $\text{mmol L}^{-1}$  Na phosphate buffer at pH 7.0, which must be used to reset the equipment (*see Note 36*).
- After the analysis, a graph of fluorescence intensity vs. time is obtained. The area under the fluorescence decay curve (AUC) can be calculated using Eq. 2:

$$AUC = 1 + f_1/f_0 + \dots + f_i/f_0 + f_{80}/f_0 \quad (2)$$

where  $f_0$  is the fluorescence obtained at time 0 and  $f_i$  is the fluorescence obtained at times between 0 and 80 min (*see Note 37*).

9. The ORAC value is calculated by Eq. 3:

$$\text{ORAC} \left( \frac{\mu\text{mol Trolox equivalents}}{g} \right) = [(A_s - A_b)/(A_t - A_b)] kab \quad (3)$$

where  $A_s$  is the AUC of the fluorescein in the sample, which was calculated by an integrating program,  $A_t$  is the AUC of the Trolox,  $A_b$  is the AUC of the control,  $k$  is the dilution factor,  $a$  is the concentration of the Trolox expressed as  $\text{mmol L}^{-1}$ , and  $b$  is the ratio between the liters of extract and the grams of packaging used for the extraction.

10. To establish the reproducibility of the analytical method, the sample preparation must be repeated four times and the values expressed as  $\mu\text{mol Trolox equivalent per g}$  of dry sample. At least three independent tests must be performed for each sample.

---

## 4 Notes

### 4.1 DPPH Assay

1. Because DPPH is a hydrophobic radical, the reactions must be carried out in organic solvents [9], such as methanol, ethanol, and acetone. The solvent depends on the material.
2. The preparation of the packaging extract was based on the method described by Noronha et al. (2014) [24] and Kam et al. (2018) [22].
3. A  $0.06 \text{ mmol L}^{-1}$  DPPH solution is equivalent to a 0.0024% (w/v) DPPH solution.
4. Add the solvent used in the preparation of the packaging sample extract.
5. The DPPH solution must be prepared daily and stored at  $4 \text{ }^\circ\text{C}$  in amber bottles until the assay. It is recommended to cover the bottles with aluminum foil.
6. Based on the method described by Brand-Williams, Cuvelier, and Berset (1995) [25], Piñeros-Hernandez et al. (2017) [26], and Rodríguez et al. (2020) [27].
7. The tubes must also be wrapped with aluminum foil to avoid any exposure to light. DPPH reactions are highly sensitive to the reaction environment, i.e., water and solvent, pH, oxygen, and light exposure.
8. The reduction degree of the DPPH radical during its reaction with antioxidants is measured at 515–517 nm [28].

9. In the DPPH assay, the antioxidants react with the stable DPPH free radical, leading to a discoloration of the molecule from deep violet to light yellow. The degree of discoloration indicates the antioxidant activity of the analyzed sample.
10. Before measuring each sample, clean the cuvette with distilled water to avoid interference and inaccurate results.
11. The standard curve is used to quantitatively determine the antioxidant activity of an unknown sample from a sample with a known property.
12. A standard curve can also be built with gallic acid and ascorbic acid.
13. It is recommended to plot the Trolox standard curve with at least five points. To prepare the Trolox solutions, use the procedure described in Subheading 3.2.4 with methanol as a solvent instead of ethanol. The solvent must be the same as in the preparation of the packaging extract.
14. Lower IC<sub>50</sub> values indicate a product with higher antioxidant activity.

#### 4.2 ABTS Assay

15. Choosing the adequate extraction techniques (maceration, infusion, vortex, supercritical fluid extraction, ultrasound-assisted extraction, and others), the solvent type (hydrophilic or lipophilic), and its proportion to the solids (solid/solvent ratio) depends on the antioxidant compound present in the active food packaging material [29, 30].
16. Several solvents can be used in the extraction of antioxidant compounds. Polar solvents (hydrophilic), such as methanol, ethanol, and water, are used for extracting phenolic acids, flavonoids, and ascorbic acid, while nonpolar solvents (lipophilic), such as ether, or low-polarity solvents, namely chloroform and acetone, are used for extracting carotenes, xanthophylls, alkaloids, terpenoids, and tocopherols [30, 31]. The material of the active packaging will indicate which disintegration procedure is the most appropriate. Simpler procedures can be used for water-soluble packaging, such as chitosan. In contrast, materials with more complex structures, such as alginate, require more elaborate procedures to be dissolved (freezing, grinding, and methanol extraction) [32].
17. In some cases, it is necessary to perform a more complex extraction than soaking or immersing [11, 20]. Other techniques may be included in order to enhance the extraction of antioxidant compounds, such as stirring [33], heating [15], shaking [19], centrifuging, and filtering with supernatant removal [16, 19, 34].

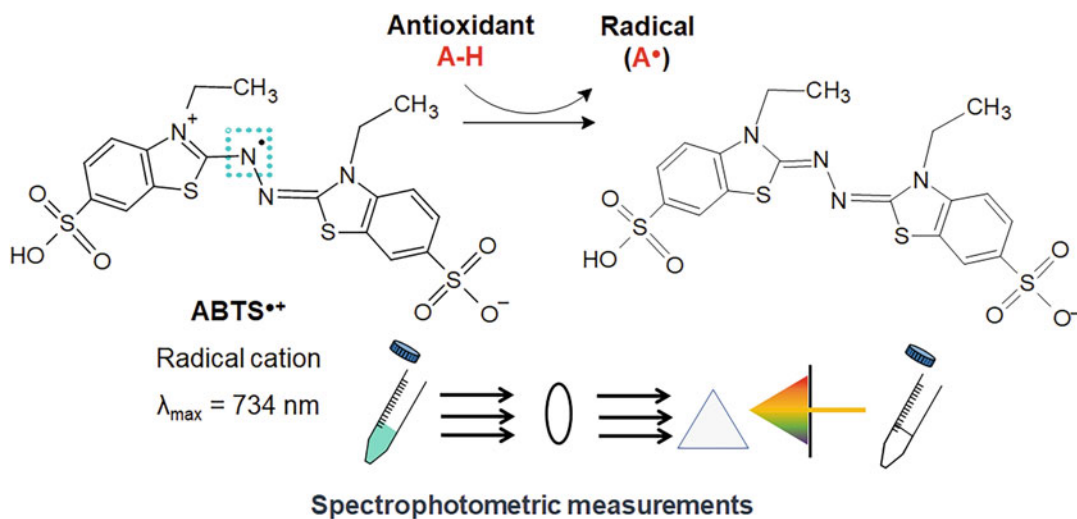


**Fig. 3** Reaction scheme of ABTS (2,2'-azinobis(3-ethylbenzothiazoline-6-sulphonic acid) and ABTS radical cation (ABTS<sup>•+</sup>)

18. Depending on the antioxidant activity of the sample, more dilutions of the sample extract may be required. The higher the antioxidant potential of the sample is, the more efficient the dilution must be. The absorbance of the samples must be within the limits of the standard curve.
19. This step is fundamental to produce an ABTS radical cation (ABTS<sup>•+</sup>), which is visually perceived due to the blue color of the mixture. The principle of the ABTS method is based on the antioxidant reaction with ABTS<sup>•+</sup> generated by potassium persulfate, followed by the absorbance diminution of the blue solution at 734 nm [30]. In other words, the antioxidant compounds present in the active food packaging act by eliminating this cationic radical ABTS<sup>•+</sup> and converting it into its colorless neutral form, which is measured by spectrophotometry (Fig. 3) [35].
20. The ABTS solution must be prepared right before each assay. Instead of ethanol [13, 15, 20, 21, 36], other solvents must be used, such as water [11, 16] and methanol [19].
21. Before reading the samples and the standard, use the solvent as a blank to reset the spectrophotometer.
22. The analytical response of this method is obtained by comparing the standard antioxidant with the ability of the sample to scavenge the ABTS<sup>•+</sup> radical in a dose-response curve. The most common standard antioxidants are Trolox (water-soluble vitamin E analog), gallic acid (3,4,5-trihydroxybenzoic acid), and ascorbic acid [30, 35]. To determine the standard curve, follow the same procedures

performed with the samples using different concentrations of the standard (in triplicate). It is important to highlight that, depending on the antioxidant capacity of the sample, different Trolox concentrations can be used to keep the sample absorbance within the limits of the standard curve. First, mix an aliquot (60  $\mu\text{L}$ ) of each Trolox solution (0, 50, 200, 300, 400, 500, and 600  $\mu\text{mol L}^{-1}$ ) with the  $\text{ABTS}^{\bullet+}$  radical solution (2940  $\mu\text{L}$ ) for 10 min. Then, read the absorbance at 734 nm. Plot the Trolox concentrations ( $\mu\text{mol L}^{-1}$ ) on the X axis and the respective absorbance on the Y axis and calculate the line equation. From the line equation, calculate the Trolox absorbance by Eq. 4:

$$y = ax + b \quad (4)$$

where  $x$  is the concentration of Trolox and  $y$  is the corresponding absorbance.

Once the standard curve is defined, it is possible to use the absorbance of the analyzed samples to determine the antioxidant capacity as  $\mu\text{mol L}^{-1}$  Trolox equivalent. Divide the result by the mass of film in the sample to obtain the antioxidant capacity per gram of the film sample. By using 1 g of film in the sample preparation, it is possible to determine the mass by the dilution in the assay.

23. The results of the antioxidant capacity may also be expressed as percentages of inhibition using Eq. 5:

$$\text{ABTS}^{\bullet+} \text{ scavenging effect (\%)} = \frac{A_{\text{ABTS}} - A_{\text{sample}}}{A_{\text{ABTS}}} \times 100 \quad (5)$$

where  $A_{\text{ABTS}}$  is the absorbance of the  $\text{ABTS}^{\bullet+}$  solution and  $A_{\text{sample}}$  is the absorbance of the sample.

### 4.3 FRAP Assay

24. At this stage, the working solution (FRAP solution) is produced. When preparing this solution, you should initially mix the acetate buffer with the TPTZ solution and then add the  $\text{FeCl}_3$  solution. It is important to emphasize that this solution must be prepared on the day of analysis and stored in an amber bottle. The principle of the FRAP method is based on the ability of antioxidants to reduce the ferric ion ( $\text{Fe}^{\text{III}}$ ) complexed with TPTZ (ferric tripyridyl triazine complex) to the ferrous ion ( $\text{Fe}^{\text{II}}$ ) complex (ferrous tripyridyl triazine complex) at low pH, in which it is possible to perceive the blue color of the mixture and spectrophotometrically measure at 593 nm (Fig. 4). Thus, the change in absorbance is directly associated with the total reducing capacity of electron-donating antioxidants present in the sample [37, 38].

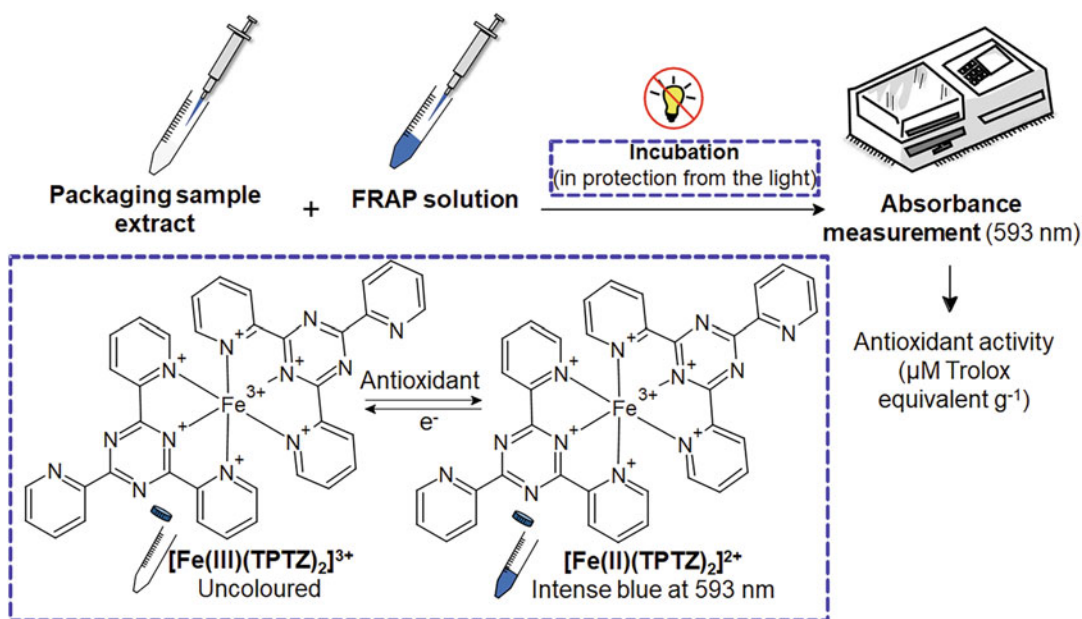


**Fig. 4** Reduction of the  $\text{Fe}^{\text{III}}$  (ferric ion) complexed with TPTZ (2,4,6-tris(2-pyridyl)-1,3,5-triazine) to  $\text{Fe}^{\text{II}}$  (ferrous ion) complexed with TPTZ. Adapted from Rufino et al. [39] with permission from Embrapa

25. First, use the FRAP solution to calibrate the spectrophotometer and then measure the  $\text{Fe}^{\text{II}}$ -TPTZ complex (colored product) in the samples.
  26. Several standard antioxidants can be used, such as gallic acid (3,4,5-trihydroxybenzoic acid) [20], ferrous sulfate solutions ( $\text{FeSO}_4 \cdot 7\text{H}_2\text{O}$ ) [21, 40], and Trolox (water-soluble vitamin E analog), which is the most common [12, 19, 22, 33].
  27. Prepare the blank sample using distilled water in the FRAP solution instead of the  $\text{FeCl}_3 \cdot 6\text{H}_2\text{O}$  solution.
- #### 4.4 ORAC Assay
28. Based on the method described by Cao et al. (1993) [41], Ninfali et al. (2005) [42], and Madhujith and Shahidi (2007) [43].
  29. All the solutions must be prepared right before analysis and all working standard solutions must rigorously dilute the respective stock solutions in the phosphate buffer (75  $\text{mmol L}^{-1}$ , pH 7.0).
  30. In most techniques, phosphate buffer is used to dilute all extracts since fluorescein is more stable at pH 7.0 [43].
  31. Prepare the solution on the day of analysis. In the case of contact with eyes or skin, fluorescein sodium salt causes severe eye injuries and skin sensitization. Therefore, wear suitable gloves and safety glasses with side shields.

32. 37 °C is the ideal temperature to produce peroxy radicals that are responsible for oxidizing fluorescein during the test to produce decay curves [44].
33. The fluorescence determination must be performed using a fluorescence spectrophotometer.
34. Due to the thermal sensitivity of AAPH, the working solution must be prepared right before analysis.
35. In this assay, the peroxy radical reacts with a fluorescent compound (fluorescein, oxidizable substrate) to form a non-fluorescent product. The antioxidant when donating hydrogen atoms inhibits the loss of fluorescence intensity, in which the inhibition is proportional to the antioxidant activity.
36. The standard stock solution of the Trolox antioxidant can be prepared weekly and serial dilutions with stock buffer must be performed daily to reach the range indicated in the preparation of the calibration graphs. The standard curve is generated with five Trolox concentrations, and the Trolox equivalent of the sample is calculated by the linear ( $Y = a + bX$ ) or quadratic ( $Y = a + bX + cX^2$ ) relationships between the Trolox ( $Y$ ) concentration ( $\mu\text{M}$ ) and the liquid area under the fluorescein  $X$  decay curve ( $\text{AUC}_{\text{sample}} - \text{AUC}_{\text{white}}$ ) [45].
37. The antioxidant protective effect is determined by calculating the area formed under the fluorescence decay curve of the sample vs. time when compared to the blank, where no antioxidants are presented. The area under the curve is calculated for both the standard and the sample. The AUC is also calculated for the blank. The control is obtained only from fluorescein to check the maintenance of its fluorescence over time.

---

## Acknowledgments

The authors would like to thank the Brazilian research funding agencies CAPES (Coordination for the Improvement of Higher Education Personnel) and CNPq (National Council for Scientific and Technological Development) for providing financial support for this study.

## References

1. Han JW, Ruiz-Garcia L, Qian JP, Yang XT (2018) Food packaging: a comprehensive review and future trends. *Compr Rev Food Sci Food Saf* 17:860–877
2. Pelissari FM, Sartori T, Santos F, Molina G, Menegalli FC (2016) Active bio-packaging. In: Inamuddin (ed) *Green polymer composites technology: properties and applications*. CRC Press
3. Gómez-Estaca J, López-de-Dicastillo C, Hernández-Muñoz P, Catalá R, Gavara R (2014) Advances in antioxidant active food packaging. *Trends Food Sci Technol* 35:42–51
4. Granato D, Shahidi F, Wrolstad R, Kilmartin P, Melton LD, Hidalgo FJ, Miyashita K, van Camp J, Alasalvar C, Ismail AB, Elmore S, Birch GG, Charalampopoulos D, Astley SB, Pegg R, Zhou P, Finglas P (2018) Antioxidant



- activity, total phenolics and flavonoids contents: should we ban in vitro screening methods? *Food Chem* 264:471–475
5. Licciardello F, Wittenauer J, Saengerlaub S, Reinelt M, Stramm C (2015) Rapid assessment of the effectiveness of antioxidant active packaging-study with grape pomace and olive leaf extracts. *Food Packag Shelf Life* 6:1–6
  6. Nerin C (2010) Antioxidant active food packaging and antioxidant edible films. In: *Oxidation in foods and beverages and antioxidant applications*. Woodhead, pp 496–515
  7. Bentayeb K, Vera P, Rubio C, Nerin C (2009) Adaptation of the ORAC assay to the common laboratory equipment and subsequent application to antioxidant plastic films. *Anal Bioanal Chem* 394:903–910
  8. Eça KS, Sartori T, Menegalli FC (2014) Films and edible coatings containing antioxidants – a review. *Braz J Food Technol* 17:98–112
  9. Schaich KM, Tian X, Xie J (2015) Reprint of “Hurdles and pitfalls in measuring antioxidant efficacy: a critical evaluation of ABTS, DPPH, and ORAC assays”. *J Funct Foods* 18:782–796
  10. Sanches-Silva A, Costa D, Albuquerque TG, Buonocore GG, Ramos F, Castilho MC, Machado AV, Costa HS (2014) Trends in the use of natural antioxidants in active food packaging: a review. *Food Addit Contam Part A Chem Anal Control Expo Risk Assess* 31:374–395
  11. Bonilla J, Sobral PJA (2016) Investigation of the physicochemical, antimicrobial and antioxidant properties of gelatin-chitosan edible film mixed with plant ethanolic extracts. *Food Biosci* 16:17–25
  12. Ruiz-Navajas Y, Viuda-Martos M, Sendra E, Perez-Alvarez JA, Fernández-López J (2013) In vitro antibacterial and antioxidant properties of chitosan edible films incorporated with *Thymus moroderi* or *Thymus piperella* essential oils. *Food Control* 30:386–392
  13. Re R, Pellegrini N, Proteggente A, Pannala A, Yang M, Rice-Evans C (1999) Antioxidant activity applying an improved ABTS radical cation decolorization assay. *Free Radic Biol Med* 26(9–10):1231–1237
  14. Bondini RB, Pugine SMP, Melo MP, Carvalho RA (2020) Antioxidant and anti-inflammatory properties of orally disintegrating films based on starch and hydroxypropyl methylcellulose incorporated with *Cordia verbenacea* (Erva baleeira) extract. *Int J Biol Macromol* 159:714–724
  15. Bitencourt CM, Fávoro-Trindade CS, Sobral PJA, Carvalho RA (2014) Gelatin-based films additivated with curcuma ethanol extract: antioxidant activity and physical properties of films. *Food Hydrocoll* 40:145–152
  16. Go EJ, Song KB (2020) Development and characterization of Citrus junos pomace pectin films incorporated with rambutan (*Nephelium lappaceum*) peel extract. *Coatings* 10(8):714
  17. Yang HJ, Lee JH, Won M, Song KB (2016) Antioxidant activities of distiller dried grains with solubles as protein films containing tea extracts and their application in the packaging of pork meat. *Food Chem* 196:174–179
  18. Eça KS, Machado MTC, Hubinger MD, Menegalli FC (2015) Development of active films from pectin and fruit extracts: light protection, antioxidant capacity, and compounds stability. *J Food Sci* 80(11):C2389–C2396
  19. Tongnuanchan P, Benjakul S, Prodpran T (2012) Properties and antioxidant activity of fish skin gelatin film incorporated with citrus essential oils. *Food Chem* 134:1571–1579
  20. Rambabu K, Bharath G, Banat F, Show PL, Cocolletzi HH (2019) Mango leaf extract incorporated chitosan antioxidant film for active food packaging. *Int J Biol Macromol* 126:1234–1243
  21. Oliveira Filho JG, Rodrigues JM, Valadares ACF, Almeida AB, Lima TM, Takeuchi KP, Alves CCF, Sousa HAF, Silva ER, Dyszy FH, Egea MB (2019) Active food packaging: alginate films with cottonseed protein hydrolysates. *Food Hydrocoll* 92:267–275
  22. Kam WYJ, Mirhosseini H, Abas F, Hussain N, Hedayatnia S, Chong HLF (2018) Antioxidant activity enhancement of biodegradable film as active packaging utilizing crude extract from durian leaf waste. *Food Control* 90:66–72
  23. Zulueta A, Esteve MJ, Frígola A (2009) ORAC and TEAC assays comparison to measure the antioxidant capacity of food products. *Food Chem* 14:310–316
  24. Noronha CM, De Carvalho SM, Lino RC, Barreto PLM (2014) Characterization of antioxidant methylcellulose film incorporated with  $\alpha$ -tocopherol nanocapsules. *Food Chem* 159:529–535
  25. Brand-Williams W, Cuvelier ME, Berset C (1995) Use of a free-radical method to evaluate antioxidant activity. *LWT Food Sci Technol* 28:25–30
  26. Piñeros-Hernandez D, Medina-Jaramillo C, López-Córdoba A, Goyanes S (2017) Edible cassava starch films carrying rosemary antioxidant extracts for potential use as active food packaging. *Food Hydrocoll* 63:488–495
  27. Rodríguez GM, Sibaja JC, Espitia PJP, Otoni CG (2020) Antioxidant active packaging based on papaya edible films incorporated with

- Moringa oleifera and ascorbic acid for food preservation. *Food Hydrocoll* 103:105630
28. Olszowy M, Dawidowicz AL (2018) Is it possible to use the DPPH and ABTS methods for reliable estimation of antioxidant power of colored compounds? *Chem Pap* 72:393–400
  29. Khan MK, Paniwnyk L, Hassan S (2019) Polyphenols as natural antioxidants: sources, extraction and applications in food, cosmetics and drugs. In: *Plant based “Green chemistry 2.0”*, pp 197–235
  30. Pisoschi AM, Pop A, Cimpeanu C, Predoi G (2016) Antioxidant capacity determination in plants and plant-derived products: a review. *Oxidative Med Cell Longev* 2016:1–36
  31. Silva BV, Barreira JCM, Oliveira MBPP (2016) Natural phytochemicals and probiotics as bioactive ingredients for functional foods: extraction, biochemistry and protected-delivery technologies. *Trends Food Sci Technol* 50:144–158
  32. Bonilla J, Atarés L, Vargas M, Chiralt A (2012) Edible films and coatings to prevent the detrimental effect of oxygen on food quality: possibilities and limitations. *J Food Eng* 110(2):208–213
  33. Sganzerla WG, Rosa GB, Ferreira ALA, Rosa CG, Beling PC, Xavier LO, Hansen CM, Ferrareze JP, Nunes MR, Barreto PLM, Lima Veeck AP (2020) Bioactive food packaging based on starch, citric pectin and functionalized with *Acca sellowiana* waste by-product: characterization and application in the postharvest conservation of apple. *Int J Biol Macromol* 147:295–303
  34. Franco GT, Otoni CG, Lodi BD, Lorevice MV, de Moura MR, Mattoso LHC (2020) Escalating the technical bounds for the production of cellulose-aided peach leathers: from the benchtop to the pilot plant. *Carbohydr Polym*:116437
  35. Arnao MB, Cano A, Acosta M (2001) The hydrophilic and lipophilic contribution to total antioxidant activity. *Food Chem* 73:239–244
  36. Urbina L, Eceiza A, Gabilondo N, Corcuera MÁ, Retegi A (2019) Valorization of apple waste for active packaging: multicomponent polyhydroxyalkanoate coated nanopapers with improved hydrophobicity and antioxidant capacity. *Food Packag Shelf Life* 21:100356
  37. Frankel EN, Meyer AS (2000) The problems of using one-dimensional methods to evaluate multifunctional food and biological antioxidants. *J Sci Food Agric* 80:1925–1941
  38. Benzie I, Strain J (1996) The ferric reducing ability of plasma (FRAP) as a measure of “antioxidant power”: the FRAP assay. *Anal Biochem* 239(1):70–76
  39. Rufino MSM, Alves RE, Brito ES, Morais SM, Sampaio CG, Pérez-Jiménez J, Saura-Calixto FG (2006) Metodologia científica: Determinação da atividade antioxidante total em frutas pelo método de redução do ferro (FRAP) Comunicado técnico online EMBRAPA Agroindústria Tropical 125
  40. Crizel TM, Rios AO, Alves VD, Bandarra N, Moldão-Martins M, Flôres SH (2018) Biodegradable films based on gelatin and papaya peel microparticles with antioxidant properties. *Food Bioprocess Technol* 11:536–550
  41. Cao G, Alessio HM, Cutler RG (1993) Oxygen-radical absorbance capacity assay for antioxidants. *Free Radic Biol Med* 14:303–311
  42. Ninfali P, Gloria M, Giorgini S, Rocchi M, Bacchiocca M (2005) Antioxidant capacity of vegetables, spices and dressings relevant to nutrition. *Br J Nutr* 93:257–266
  43. Madhujith T, Shahidi F (2007) Antioxidative and antiproliferative properties of selected barley (*Hordeum vulgare* L.) cultivars and their potential for inhibition of low-density lipoprotein (LDL) cholesterol oxidation. *J Agric Food Chem* 55:5018–5024
  44. Stockham K, Paimin R, Orbell JD, Adorno P, Buddhadasa S (2011) Modes of handling Oxygen Radical Absorbance Capacity (ORAC) data and reporting values in product labelling. *J Food Compos Anal* 24:686–691
  45. Prior RL, Wu X, Schaich K (2005) Standardized methods for the determination of antioxidant capacity and phenolics in foods and dietary supplements. *J Agric Food Chem* 53:4290–4302



## Release of Active Agents from Food Packaging Materials

Murilo S. Pacheco, Mariana A. de Moraes, Mariana A. da Silva,  
and Andréa C. K. Bierhalz

### Abstract

Active packaging (AP) is an innovative type of food packaging from which active compounds, such as antimicrobials or antioxidants, may be released in order to enhance food quality and safety and extend its shelf-life. The efficiency of the AP system depends on the release rate, since too high rates may lead to a premature loss of the AP activity, while too low rates may not be sufficient to prevent food deterioration. In this context, the study of the active agent release mechanisms and kinetics is pivotal to determining the performance of AP systems. Here we describe a general method to evaluate the release of an active compound from a (bio)polymeric film, including the protocol for the release test, the quantification methods, and the mathematical models used to estimate diffusivity and elucidate the release mechanism. As a showcase, we focus on the release of the antimicrobial natamycin entrapped in a biopolymeric matrix to a food simulant liquid medium (ethanol solution), and we provide suggestions and protocols that can be extended to other biopolymers and analytes.

**Key words** Polymeric film, Active compound, Mathematical modeling, Fickian diffusion, Swelling, Release mechanism

---

## 1 Introduction

Active packaging (AP) has been defined, according to the European FAIR-Project CT 98–4170, as “a type of packaging that changes the condition of the packaging to extend shelf-life or improve safety or sensory properties while maintaining the quality of the food” [1]. AP can act either as absorbing or releasing systems, depending on their mechanism of action. The former absorbs substances from the food or the packaging headspace, such as ethylene and oxygen scavengers. The latter, on the other hand, allow active compounds to diffuse from the AP to the food surface and includes the release of antimicrobials, antioxidants, CO<sub>2</sub> emitters, flavors, aromas, enzymes, probiotic bacteria, nutraceuticals, and plant growth hormones [2].

The active agent can be applied by several methods to polymer-based AP systems, namely, (i) physical adsorption onto the surface of the polymeric material; (ii) immobilization onto polymers by ionic or covalent bonds; (iii) addition into sachets, pouches, or pads, which are placed inside the packaging; and (iv) incorporation within the bulk of the polymer matrix [2]. The latter can be achieved either by directly adding or encapsulating the active agent during polymer processing [3], by its adsorption (e.g., by immersion), or by supercritical impregnation through the use of solutions or suspensions containing the active agent [4, 5].

The diffusion of the active agent may be achieved by direct contact between food and packaging material or through gas phase diffusion (volatile systems) from packaging to the food surface, which depends on the AP design and the nature of the active compound [6, 7].

Antimicrobial packaging is a promising and advantageous form of AP because microbial contamination problems are known to occur mostly on food surfaces. Thus, the AP system would allow the incorporated antimicrobial to be continuously delivered to the food surface, maintaining an effective concentration of the active agent where it is most needed [7]. Besides, multifunctional AP materials have also been investigated, combining more than one active agent or even actives that act both as antioxidant and antimicrobial, which is the case of some essential oils [8, 9].

The main mechanisms that describe the release of an active agent from an AP system are diffusion, swelling, and/or disintegration. In exclusively diffusive-driven systems, mainly synthetic and water-resistant polymers, the active agent diffuses through the polymeric matrix and from the film surface into the food. The swelling takes place when the polymer matrix is put in contact with compatible solvents, usually hydrophilic matrices in water or hydrophobic matrices in organic media. In the swollen state, the relaxation of the polymer chains increases the diffusion coefficient and enables the transport of the active molecules to the food. The disintegration mechanism occurs when there is hydrolysis, cleavage, or erosion of the matrix according to the medium conditions, which is typically induced by the absorption of fluids [2].

Matching the release rate with the kinetics of food deterioration is crucial for food-targeted AP systems. If the migration is too fast, the active agent will be depleted before the expected storage period, and the AP system will lose its functionality earlier than needed. On the other hand, if the release rate is too low, the released amount of active compound can be insufficient to prevent food deterioration [9, 10]. The release rate will be dependent on the permeability, which in turn depends on the characteristics of the polymer (type, concentration, glass transition temperature, and molecular weight), fabrication parameters, and chemical interactions among the polymer, active agent, and food. Several strategies

can tune the film properties and develop ideal controlled release systems, including crosslinking, UV irradiation, encapsulation, complexation, multilayer systems, and nanocomposite films, among others [2].

### 1.1 Methods to Evaluate the Release of Active Agents from Polymeric Films

Considering the release of an active compound from a polymeric film to the food, there are three steps involved in the process: (i) molecular diffusion through the film, (ii) mass transfer across the film/food interface, and (iii) dispersion into food or desorption into packaging headspace. Typically, the diffusion of the active compound through the matrix is assumed as the slowest and rate-controlling step, in which the concentration difference is the driving force of the mass transfer phenomenon [9].

The diffusion of the active agent and its solubility in the matrix are the two main parameters that govern the release rate in the specific matrix. Diffusivity, which indicates how fast the active compound moves within the film, and partition coefficient, which indicates the affinity of the active agent for the two phases (film and food)—and therefore suggests how much active agent is released to the food at equilibrium—are the two model parameters used to describe the release behavior [9].

Empirical and semiempirical mathematical models can be fitted to kinetic data in order to elucidate the active agent release mechanisms. The most commonly applied model is the so-called Power Law Model (Eq. 1) [11].

$$\frac{M_t}{M_\infty} = kt^n \quad (1)$$

where  $t$  is time,  $k$  is a constant related to the structural and geometric characteristics of the matrix, and  $n$  is the release exponent.

From the coefficient  $n$  in Eq. 1, it is possible to determine the release mechanism. For thin films,  $n = 0.5$  indicates that the mass release is proportional to the square root of time and controlled by diffusion. This mechanism is known as Fickian transport. On the other hand, when  $n = 1.0$ , the release is controlled by the swelling or erosion of the polymeric matrix, which is known as case-II transport. When  $0.5 < n < 1.0$ , the diffusion and swelling mechanisms overlap, and the transport is considered anomalous [12].

When the mechanism is predominantly diffusive, the transient mass transfer process of the active compound through the film can be described by Fick's second law (Eq. 2), assuming one-dimensional diffusion from an infinite flat plate [13, 14]. The solutions of the diffusional equation can be fitted to the experimental kinetic release data, enabling the prediction of the diffusivity of the active compound through the polymeric film.

$$\frac{\partial C}{\partial t} = D \frac{\partial^2 C}{\partial x^2} \quad (2)$$

Several models based on solutions of the Fickian differential equation with appropriate initial and boundary conditions are used to predict the release behavior, obtain the concentration profile, and estimate the diffusivity. However, many assumptions are required, as follows: (i) the diffusion of the active through the film is the rate-controlling step; (ii) no structural change occurs in the film during the release; (iii) the active compound can be readily desorbed from the film; (iv) the active compound is initially homogeneously distributed in the film; (v) the initial concentration of the active in the food is zero; (vi) no concentration gradient of the active exists in the food; (vii) the partition coefficient and diffusivity are constant at a given temperature; (viii) interactions between food simulant and film are negligible; and (ix) no degradation of the active compound occurs [9]. Based on these assumptions, the integrated solution of Eq. 2 in terms of released mass is given by Eq. 3.

$$\frac{M_t}{M_\infty} = 1 - \sum_{n=1}^{\infty} \frac{2\alpha(1+a)}{1+\alpha+\alpha^2q_n^2} \exp\left(\frac{-Dq_n^2t}{\delta^2}\right) \quad (3)$$

where  $M_t$  is the mass of active compound that migrated to the food simulant at time  $t$ ,  $M_\infty$  is the mass of active compound in the food simulant at equilibrium,  $D$  is the diffusivity of the active compound in the film,  $\delta$  is the film thickness,  $q_n$  is the nonzero positive roots of Eq. 4, and  $\alpha$  is given by Eq. 5 [13, 14].

$$\tan q_n = -\alpha q_n \quad (4)$$

$$\alpha = \frac{V_F}{K_P V_P} \quad (5)$$

where  $V_F$  is the volume of food simulant,  $V_P$  is the volume of the film (AP), and  $K_P$  is the partition coefficient given by Eq. 6.

$$K_P = \frac{C_{P,\infty}}{C_{F,\infty}} \quad (6)$$

where  $C_{P,\infty}$  and  $C_{F,\infty}$  are the concentrations of the active compound, respectively, in the film (AP) and the food simulant, both at equilibrium.

Typically, the volume of the food simulant is larger than the volume of the AP ( $V_F \gg V_P$ ), which makes  $\alpha \gg 1$ . In this case, a simplified solution is obtained (Eq. 7) [13].

$$\frac{M_t}{M_\infty} = 1 - \frac{8}{\pi^2} \sum_{n=0}^{\infty} \frac{1}{(2n+1)^2} \exp\left(-Dt \frac{(2n+1)^2 \pi^2}{\delta^2}\right) \quad (7)$$

For short times, when  $M_t/M_\infty \leq 0.6$ , Eq. 7 assumes boundary conditions of a semi-infinite solid model, being simplified to Eq. 8 for a flat plate [15].

$$\frac{M_t}{M_\infty} = 4\sqrt{\frac{Dt}{\pi\delta^2}} \quad (8)$$

Liquid or food simulant may cause swelling of the (bio)-polymeric matrix, and in this case, the release kinetics may not follow the Fickian diffusion model [9]. When case-II or anomalous transport governs the release, models that include the influence of matrix swelling are more appropriate. Equation 9 allows the prediction of diffusivity considering both the Fickian and swelling contributions, as well as the relaxation time associated with polymer relaxation ( $\tau$ ) and the deviation from the ideal Fickian behavior ( $X_F$ ) [16].  $X_F$  ranges from 0 to 1; for  $X_F$  equal to 1, Eq. 9 is the solution of the Fick's second law (Eq. 7), whereas for  $X_F$  equal to 0, anomalous diffusion is obtained.

$$\begin{aligned} \frac{M_t}{M_\infty} = X_F \cdot & \left[ 1 - \frac{8}{\pi^2} \sum_{n=0}^{\infty} \frac{1}{(2n+1)^2} \exp\left(-Dt \frac{(2n+1)^2 \pi^2}{\delta^2}\right) \right] \\ & + (1 - X_F) \cdot \left[ 1 - \exp\left(-\frac{t}{\tau}\right) \right] \end{aligned} \quad (9)$$

Usually, the methods used to study the release of an active compound from a polymeric film involve the immersion of the film in a release (sink) medium, and periodic monitoring of the cumulative concentration of the compound in the liquid medium. The fractional mass released is calculated, and the mathematical models are fitted to the kinetic data. Several food simulants with different pH and water activity are used as sink media for release studies allowing standardization, reproducibility, and ease of analysis. These media can predict the active agent diffusion from the AP to the real food. The Food and Drug Administration (FDA) recommends the use of 10 vol% ethanol solution in water as a simulant of aqueous and acidic foods; 10 and 50 vol% ethanol solution in water as simulants of low- and high-alcohol content foods, respectively; and food oil (e.g., corn or olive oil), HB307 (mixture of synthetic triglycerides), Miglyol 812 (derived from coconut oil), and others (such as ethanol solutions—used for specific polymeric matrices) as simulants of fatty foods [17]. On the other hand, the European legislation recommends the use of water for aqueous foods with a pH above 4.5; 3 vol% acetic acid solution in water for acidic aqueous foods with a pH below 4.5; 10 vol% ethanol solution in water for alcoholic products; and olive oil for fatty foods [18]. Other food simulants are reported in the literature, such as heptane, isooctane, ether, isopropanol [19], cyclohexane, ethyl acetate, glyceryl tripelargonate, terpenes, tributyrin [13], and sunflower oil [20].

When the release test is designed for a solid medium, mathematical modeling becomes much more complex, as the resistance to mass convection plays an important role in the release and a finite

food volume must be considered. Many studies involving migration in a food packaging system are related to contaminants and synthetic packaging components. In this approach, it is also necessary to use solid food simulants, such as agar or gelatin gels, cheeses, or Tenax<sup>®</sup>—a dry food simulant recommended by the European Regulation 10/2011 [21–23].

Thus, based on the authors' expertise [5, 24–26], the protocols to evaluate the release of an active compound (natamycin) from an AP (crosslinked biopolymeric film) to a liquid medium (ethanol solution as a food simulant) are described in this chapter. This approach may be extrapolated to other cases, involving different analytes and release media, according to the proposed application, and following the required assumptions for suitably fitting the mathematical models.

---

## 2 Materials

### 2.1 Reagents and Film Sample

- Absolute ethanol.
- Ultrapure water.
- Analyte (natamycin) solution to prepare a standard curve.
- Active loaded crosslinked polymeric film sample (4 cm × 4 cm).

### 2.2 Equipment

- Digital micrometer (0–25 mm, 0.001 mm).
- Analytical balance (0.0001 g).
- Glassware to prepare solutions.
- Orbital shaker water bath.
- UV-Vis spectrophotometer.
- Quartz 1-mL cuvettes.
- Covered or screw-capped containers.
- Tweezers.

---

## 3 Methods

The method described herein is based on the release into a liquid medium, with complete renewal of the release medium. The samples are transferred through recipients, ensuring no resistance to mass transfer at the film surface (i.e., the active agent concentration at the film surface is zero). Other methods can be used, such as collecting aliquots from the release medium during the test, with partial renewal of the medium or return of the aliquot after quantification (*see Note 1*).



- 3.1 Food Simulant** Prepare an ethanol solution at a predetermined concentration, e.g., 10 vol% (*see* **Notes 2** and **3**), adding 100 mL of absolute ethanol in 900 mL of water. Cover the solution until use. The total amount of solution needed for the test depends on the time intervals selected to collect the experimental points (*see* **Note 4**).
- 3.2 Sample Preparation** Prepare the sample of the actively loaded biopolymeric crosslinked film with a determined dimension, e.g., 4 cm × 4 cm, and with a known average thickness (*see* **Note 5**). The mass of the active compound (natamycin) loaded in the film sample must be known (*see* **Note 6**).
- 3.3 Equipment Setup** Prepare a shaker bath with distilled water at a determined temperature for the experiment, e.g., 25 °C (*see* **Note 7**). Prepare a spectrophotometer UV-Vis to measure the absorbance of the samples collected during the release test.
- 3.4 Quantification Method** Prepare the standard curve of the analyte used. Prepare a solution of the natamycin (analytical standard) at a determined concentration, e.g., 40 mg L<sup>-1</sup>, using the food simulant 10 vol% ethanol as solvent, and prepare several dilutions to obtain a range of different concentrations. Using a UV-Vis spectrophotometer at 317 nm (*see* **Note 8**), a quartz bucket, and the ethanolic solution as a baseline, measure the absorbance of the different concentrations of natamycin. If necessary, dilute the natamycin solutions so that the absorbance values are between 0 and 1. Plot the absorbance values versus concentrations and perform a linear regression,  $R^2 > 0.99$ , to obtain the analytical standard curve equation.
- 3.5 Release Test**
1. Place 25 mL of the ethanolic solution in covered or screw-capped containers.
  2. Place the containers with the solutions in the shaker bath and set the appropriate rotation speed to the shaker, e.g., 150 rpm (*see* **Notes 9** and **10**).
  3. At time zero, immerse the film sample in the first container and start time counting.
  4. After a predetermined time interval, quickly transfer, using tweezers, the film sample from the first to the second container (*Fig. 1*).
  5. Remove the first container from the shaker bath and store it for later quantification of the released active compound (*see* **Note 11**).
  6. Repeat steps 4 and 5 at predetermined time intervals, quickly transferring the sample to the next container, and storing the solution from the previous one; prepare all solutions using ultrapure water and analytical grade reagents. Store all reagents

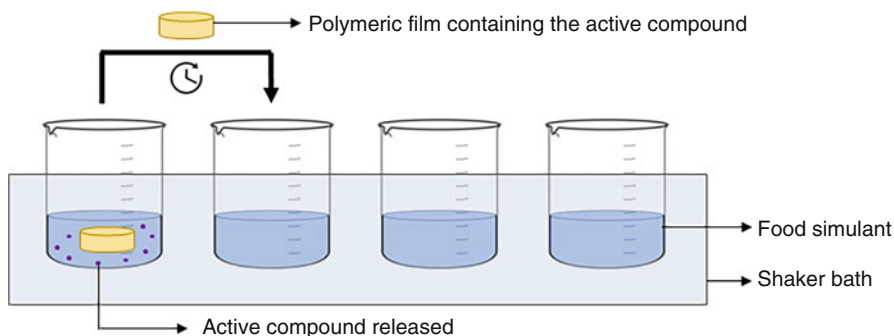


**Fig. 1** Schematic representation of the release test: The polymeric active film is placed in the first container with the food simulant and at determined time intervals it is quickly transferred to the next container. The food simulant containing the active compound released is stored to further quantification

at room temperature unless indicated otherwise. Diligently follow all waste disposal regulations when disposing waste materials.

7. After removing the previous containers, replace the spaces of the shaker bath with new containers with blank solutions to ensure temperature preconditioning.
8. The time intervals can be determined according to the total duration of the test until no further release can be detected, considering a fast-release behavior in the beginning of the test and a slow-release behavior at the end of the test. The sample can be transferred at predetermined test times, e.g., 5 min, 10 min, 15 min, 20 min, 30 min, 45 min, 1 h, 2 h, 3 h, 4 h, 5 h, 10 h, 24 h, 48 h, 72 h, 96 h, 120 h, 200 h, 300 h, 400 h, 500 h, 600 h, 700 h, 800 h, 900 h, and 1000 h (*see Note 12*).
9. After the last time interval, collect the film sample and store in an appropriate place.
10. Turn off the shaker bath and remove all distilled water, according to the manufacturer's recommendations.

### 3.6 Quantification

Considering natamycin as the active compound, UV-Vis spectrophotometry would be indicated for quantification. Other quantification methods can be used for other analytes (*see Note 13*).

1. Read the absorbance at 317 nm of the 10 vol% ethanol solution used as a food simulant on the UV-Vis spectrophotometer and set as blank.
2. Measure the absorbances of all solutions stored during the release test, rinsing the bucket after each reading, and measuring from the lowest to the highest concentration.

3. Using the equation obtained by the standard curve, convert all the absorbance data to natamycin concentrations.
4. Use the volume of each container (25 mL) to convert all the concentrations to mass values of natamycin released at each step.

### 3.7 Mathematical Modeling

1. Sum all the mass values of natamycin released during the test, obtaining the total mass of natamycin released from the film to the food simulant at equilibrium ( $M_\infty$ ).
2. Sum the mass released at each previous point from the beginning of the test to the time interval being calculated into the cumulative mass release ( $M_t$ ) at each time.
3. Divide each cumulative mass ( $M_t$ ) by the total mass released ( $M_\infty$ ) to calculate the cumulative mass fraction released for each time ( $M_t/M_\infty$ ).
4. Plot the  $M_t/M_\infty$  values as a function of time  $t$  to obtain the natamycin release profile (exemplified in Fig. 2).
5. Fit the Power Law Model (Eq. 1) to the release kinetic data when  $M_t/M_\infty \leq 0.6$  to elucidate the rate-controlling mechanism of release. Plot  $\ln(M_t/M_\infty)$  as a function of  $\ln(t)$ , considering the linearization form of the equation, and obtain a linear regression (Fig. 3). The diffusional exponent  $n$  is obtained from the angular coefficient (slope), while the constant  $k$  is calculated from the linear coefficient (intercept).

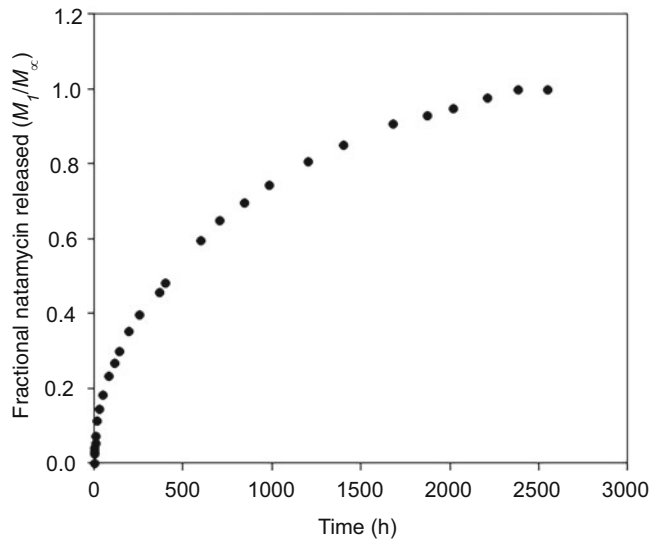


**Fig. 2** Example of a release profile of natamycin from crosslinked alginate films to an ethanol solution

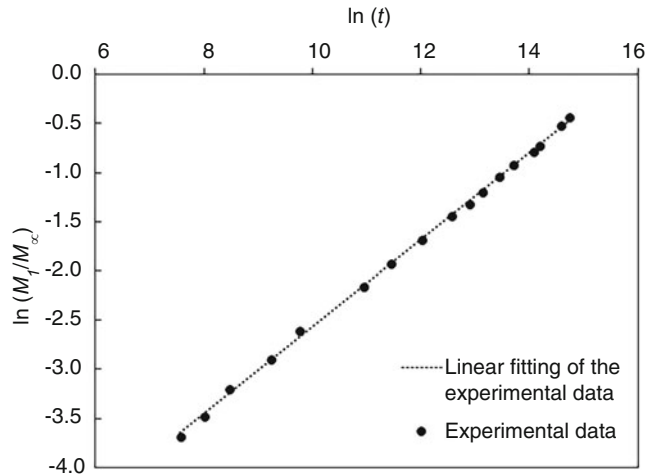


**Fig. 3** Example of the fitting of linearized Power Law Model to the kinetic data of natamycin released from crosslinked alginate films to ethanol solution

6. If the diffusional exponent  $n$  is close to 0.5, Fickian diffusion is the rate-controlling mechanism of release. If  $n$  is close to 1.0, swelling or erosion of the matrix is the rate-controlling mechanism. If  $n$  falls between 0.5 and 1.0, there is an anomalous transport, in which both Fickian diffusion and swelling are important mechanisms that drive the active release from the film.
7. Fit the series solution of the Fick's second law (Eq. 7) to the release of kinetic data (Fig. 4) and use nonlinear regression to obtain the model parameters, including diffusivity ( $D$ ) (see **Notes 14** and **15**).
8. Fit the semi-infinite solid or short times model (Eq. 8) to the release kinetic data when  $M_t/M_\infty \leq 0.6$  to determine the diffusivity ( $D$ ) at the beginning of the release test. Plot  $M_t/M_\infty$  data as a function of  $t^{0.5}$  [ $s^{0.5}$ ] and obtain a linear fit. From the angular coefficient, according to the equation, calculate diffusivity (Fig. 5).
9. Compare the diffusivity found by the two models. The good fitting of the short times model and the proximity of the diffusivity value found by the short times model with that found by the series solution model may indicate that swelling has a low influence on diffusivity.
10. If the release models show a great influence on swelling, fit the model described in Eq. 9 to determine diffusivity and evaluate the deviation from the ideal Fickian behavior ( $X_F$ ).
11. Evaluate the fitted models using fitting coefficients, e.g.,  $R^2$  (see **Note 16**).

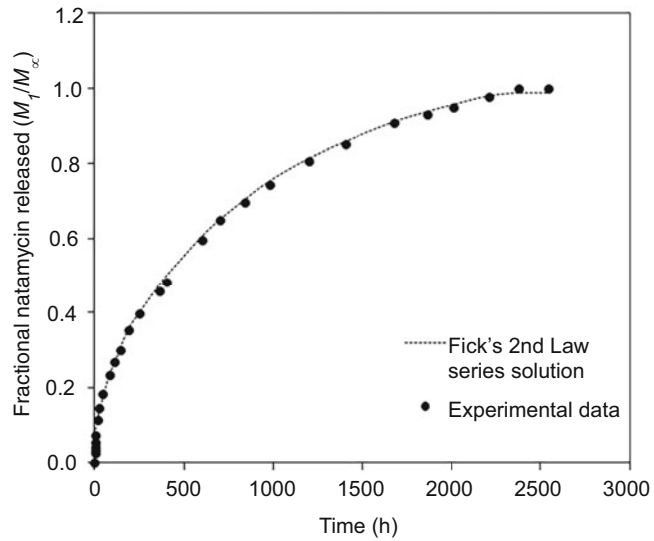


**Fig. 4** Example of a release profile of natamycin from crosslinked alginate films to ethanol solution with fitting of Fick's second Law series solution

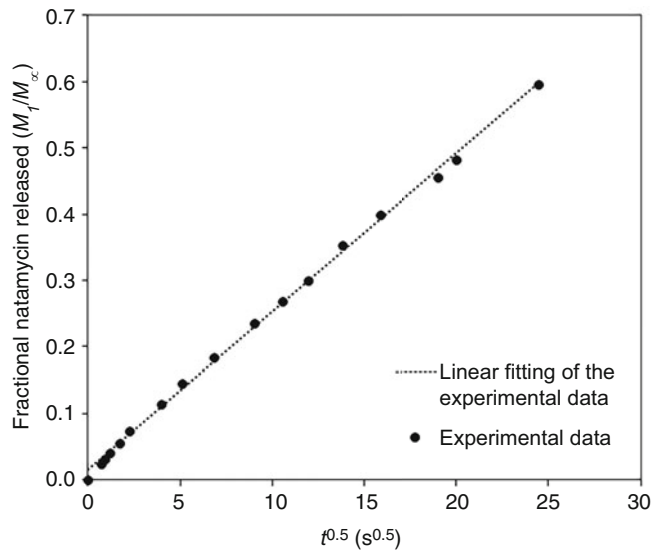


**Fig. 5** Example of the fitting of linearized short times model to the kinetic data of natamycin released from crosslinked alginate films to ethanol solution

## 4 Notes

1. Several methods can be used to carry out the release test to liquid medium. The complete renewal of the release medium ensures no resistance to mass transfer at the film surface and maintains a low concentration of the active in the medium, avoiding the need for the partition coefficient determination, which is sometimes difficult to obtain. When using the method

of collecting aliquots during the test with partial renewal of the medium, the concentration gradient is still favored, but the partition coefficient will be of greater importance, as well as the miscibility of the analyte in the release medium. In this case, it is necessary to consider the changes in the concentration at each point by the added volume to measure the released mass at each time interval. On the other hand, when the aliquot is returned after quantification, the test gets more proximity with the reality, although it may be necessary to obtain the partition coefficient due to the increase of the active compound concentration, once it could play an important role in the release behavior.

2. Prepare all solutions using ultrapure water and analytical-grade reagents. Store all reagents at room temperature unless indicated otherwise. Diligently follow all waste disposal regulations when disposing waste materials.
3. Prepare the solution of food simulant according to the concentration recommended by the FDA or other regulatory agencies, as well as to the type of food that is being simulated, e.g., acidic, alcoholic, fatty.
4. Prepare a sufficient volume of food simulant for the complete release test, e.g., if 30 experimental points are expected to be collected to construct the release profile, with complete renewal of the release medium, prepare at least  $30 \times 25 \text{ mL}$  of solution = 750 mL.
5. The thickness of the film sample will be necessary to fit the data to the mathematical models. Measure the film thickness at least at five points along the film sample using a micrometer and use the mean value. Measure it before and after the release test to evaluate whether the swelling behavior plays an important role in the release kinetics.
6. It is important to quantify the initial amount of the active compound incorporated into the film sample used in the release test in order to determine the % of active released.
7. FDA recommends that the release test must be carried out under the most severe conditions of temperature and time for the proposed use. It is recommended a test temperature of 40 °C for 10 days for room-temperature applications and 20 °C for refrigerated applications [17].
8. Use the absorption peak related to the quantification of the specific analyte used in the food simulant. It is recommended to perform a wavelength scan to determine the correct peak of the analyte dissolved in the food simulant solution.
9. The continuous stirring during all the release tests decreases mass convection resistance, which is necessary for the application of the mathematical models.

10. Partition coefficient can be obtained using Eq. 6 with  $M_{\infty}$  and the amount of active compound remaining in the film at equilibrium.
11. During storage, all containers must be kept closed to avoid sink medium evaporation and consequent changes in solute concentration.
12. Frequently, there is a faster release in the first instants of the test, being necessary to collect experimental points at shorter time intervals, in order to allow proper release profiles and a good fitting of the mathematical models.
13. Besides UV-Vis spectrophotometry, several methods can be used to quantify natamycin or other active compounds, such as high-performance liquid (HPLC) and gas chromatography. For example, nisin can be quantified through reverse-phase HPLC [27], spectrofluorimetry [28], and colorimetry [22] when released from films.
14. Typically, the diffusivity is given in  $\text{cm}^2 \text{s}^{-1}$ . Use time in [s] and thickness in [cm] for model fitting to obtain diffusivity.
15. In the case of performing the release test using the release from only one side of the polymeric film, it is important to correctly consider the boundary conditions to obtain the correct form of solution of the diffusional equation.
16. Other fitting coefficients can be used to analyze the fitting accuracy and compare the models used properly, such as root mean square error [29].

---

## Acknowledgments

The authors thank the São Paulo Research Foundation (FAPESP, grants #2017/20274-9 and #2018/25656-0) and the National Council for Scientific and Technological Development (CNPq, grants #473972/2011-5 and #140303/2012-0). The authors are grateful to Professor Theo Guenter Kieckbusch for his long-term dedication, collaboration, and numerous discussions on the mathematics of diffusion for active food packaging. Thank you for always being a source of inspiration to our career and life.

## References

1. Vermeiren L, Devlieghere F, VanBeen M et al (2000) Development in the active packaging of foods. *J Food Technol Africa* 5:6–13
2. Almasi H, Jahanbakhsh Oskouie M, Saleh A (2020) A review on techniques utilized for design of controlled release food active packaging. *Crit Rev Food Sci Nutr* 0:1–21
3. Dos Pires ACS, De Soares NFF, De Andrade NJ et al (2008) Development and evaluation of active packaging for sliced mozzarella preservation. *Packag Technol Sci* 21:375–383
4. De Souza AC, Dias AMA, Sousa HC et al (2014) Impregnation of cinnamaldehyde into cassava starch biocomposite films using

- supercritical fluid technology for the development of food active packaging. *Carbohydr Polym* 102:830–837
5. Bierhalz ACK, Da Silva MA, De Sousa HC et al (2013) Influence of natamycin loading methods on the physical characteristics of alginate active films. *J Supercrit Fluids* 76:74–82
  6. Mastromatteo M, Mastromatteo M, Conte A et al (2010) Advances in controlled release devices for food packaging applications. *Trends Food Sci Technol* 21:591–598
  7. Yam KL, Zhu X (2012) *Controlled release food and beverage packaging*. Woodhead Publishing Limited
  8. Appendini P, Hotchkiss JH (2002) Review of antimicrobial food packaging. *Innov Food Sci Emerg Technol* 3:113–126
  9. Chen X, Chen M, Xu C et al (2019) Critical review of controlled release packaging to improve food safety and quality. *Crit Rev Food Sci Nutr* 59:2386–2399
  10. Han JH (2000) *Antimicrobial food packaging*. Woodhead Publishing Limited
  11. Siepmann J, Peppas NA (2001) Modeling of drug release from delivery systems based on hydroxypropyl methylcellulose (HPMC). *Adv Drug Deliv Rev* 48:139–157
  12. Serra L, Doménech J, Peppas NA (2006) Drug transport mechanisms and release kinetics from molecularly designed poly(acrylic acid-g-ethylene glycol) hydrogels. *Biomaterials* 27:5440–5451
  13. Poças MF, Oliveira JC, Oliveira FAR et al (2008) A critical survey of predictive mathematical models for migration from packaging. *Crit Rev Food Sci Nutr* 48:913–928
  14. Crank J (1975) *The mathematics of diffusion*. Oxford University, Bristol
  15. Siepmann J, Siepmann F (2008) Mathematical modeling of drug delivery. *Int J Pharm* 364:328–343
  16. Flores S, Conte A, Campos C et al (2007) Mass transport properties of tapioca-based active edible films. *J Food Eng* 81:580–586
  17. FDA (2007) *Guidance for industry: preparation of premarket submissions for food contact substances (Chemistry Recommendations)*, U.S.
  18. Grob K (2008) The future of simulants in compliance testing regarding the migration from food contact materials into food. *Food Control* 19:263–268
  19. Feigenbaum AE, Riquet AM, Scholler D (2000) Fatty food simulants: solvents to mimic the behavior of fats in contact with packaging plastics. *ACS Symp Ser* 753:71–81
  20. Silva AS, García RS, Cooper I et al (2006) Compilation of analytical methods and guidelines for the determination of selected model migrants from plastic packaging. *Trends Food Sci Technol* 17:535–546
  21. Cruz JM, Sanches Silva A, Sendón García R et al (2008) Studies of mass transport of model chemicals from packaging into and within cheeses. *J Food Eng* 87:107–115
  22. Ripoche AC, Chollet E, Peyrol E et al (2006) Evaluation of nisin diffusion in a polysaccharide gel: influence of agarose and fatty content. *Innov Food Sci Emerg Technol* 7:107–111
  23. Van Den Houwe K, Van LJ, Lynen F et al (2017) The use of Tenax® as a simulant for the migration of contaminants in dry foodstuffs: a review. *Packag Technol Sci* 31:781–790
  24. da Silva MA, Bierhalz ACK, Kieckbusch TG (2012) Modelling natamycin release from alginate/chitosan active films. *Int J Food Sci Technol* 47:740–746
  25. Bierhalz ACK, da Silva MA, Kieckbusch TG (2012) Natamycin release from alginate/pectin films for food packaging applications. *J Food Eng* 110:18–25
  26. Bierhalz ACK, da Silva MA, Braga MEM et al (2014) Effect of calcium and/or barium cross-linking on the physical and antimicrobial properties of natamycin-loaded alginate films. *LWT Food Sci Technol* 57:494–501
  27. Rivera-Hernández L, Chavarría-Hernández N, del López Cuellar MR et al (2020) Pectin-gellan films intended for active food packaging: release kinetics of nisin and physico-mechanical characterization. *J Food Sci Technol*
  28. Imran M, Klouj A, Revol-Junelles AM et al (2014) Controlled release of nisin from HPMC, sodium caseinate, poly-lactic acid and chitosan for active packaging applications. *J Food Eng* 143:178–185
  29. Lavoine N, Guillard V, Desloges I et al (2016) Active bio-based food-packaging: diffusion and release of active substances through and from cellulose nanofiber coating toward food-packaging design. *Carbohydr Polym* 149:40–50





## Bioactive Properties of Probiotic and Prebiotic Edible Films

Jackson A. Medeiros, Carolina M. Niro, Mateus K. Salgaço, Kátia Sivieri, and Henriette M. C. Azeredo

### Abstract

Edible films have been increasingly studied as carriers for bioactive components, including probiotic microorganisms and/or prebiotic compounds. Whereas the incorporation of prebiotic compounds does not usually require wide modifications to the usual processing protocols to produce edible films, the addition of live microorganisms requires special attention when it comes to processing conditions, in order to assure that their viability is preserved as much as possible. In this chapter, we describe the basic procedures for obtaining probiotic and/or prebiotic edible films as well as the specific determinations that are required to properly characterize them in terms of their bioactive properties and stability.

**Key words** Probiotic bacteria, Film casting, Gastrointestinal tract, In vitro digestion, *Lactobacillus*

---

### 1 Introduction

The global probiotic market has been evaluated at USD 49.4 billion in 2020 and estimated to grow to USD 69.3 billion by 2025. Although probiotics may also be consumed as dietary supplements, the market for probiotic foods outweighs that of supplements [1].

Edible films and coatings containing probiotics may be used as primary packaging materials, but also function as part of the food itself, since they are designed to be consumed with the food product. Since those edible films are usually based on biopolymer matrices capable of including probiotic cultures, providing some degree of protection against external factors (including the low pH during the passage through the stomach), they have been suggested as interesting carriers of probiotic microorganisms, acting thus as bioactive edible films by contributing to consumers' health, eventually also contributing to food stability due to the competitive effects of probiotics against deteriorating microorganisms [2]. Prebiotic compounds (such as inulin and several oligosaccharides) are

nondigestible components capable of selectively stimulating the growth and/or activity of probiotics. They have also been suggested as bioactive components of edible films containing probiotics [3, 4] or not [5, 6].

The ability of an edible film to keep a good probiotic stability upon processing and storage depends on the ability of its components to protect the bacteria and also on the ability of the bacteria themselves to survive processing and storage conditions.

---

## 2 Materials

### 2.1 *Film Preparation*

1. Autoclave.
2. Incubation chamber.
3. Centrifuge.
4. Hot plate and magnetic stirrer (when the film dispersion requires heating).
5. 50-mL sterile tubes.
6. Petri dishes (or a flat glass plate with a drawdown bar).
7. Ethanol 70 vol%.
8. NaCl.
9. Probiotic culture.
10. Prebiotic compound (if it is to be included).
11. Culture medium for the probiotic culture of choice (e.g., DeMan–Rogosa–Sharpe [MRS] broth).
12. Film matrix (polysaccharide or protein).
13. Plasticizer (e.g., polyols such as glycerol or sorbitol).

### 2.2 *Estimating Probiotic Viability on Film-Forming Dispersions and Films*

1. Lab scale with an accuracy of 0.1 mg.
2. Incubation chamber.
3. Air oven.
4. Vortex.
5. Hot plate and magnetic stirrer.
6. Aluminum pans.
7. Petri dishes.
8. 10- $\mu$ L and 1000- $\mu$ L micropipettes and sterile tips.
9. Solidified culture medium suitable for the bacteria of choice.
10. 15-mL sterile tubes.
11. NaCl.

### 2.3 Evaluating the Prebiotic Activity of Films

1. Incubation chamber.
2. UV-vis spectrometer.
3. Standard bacterial strain.
4. Culture medium (e.g., MRS broth), with and without glucose.
5. Prebiotic compound.
6. 0.5 McFarland standard (*see Note 1*).
7. 15-mL sterile tubes.

### 2.4 In Vitro Digestion Method

1. Lab scale with an accuracy of 0.1 mg.
2. Stomacher.
3. Metabolic bath.
4. Shaking water bath.
5. 500-mL threaded vials.
6. Volumetric flasks.
7. Sterile or ultrapure water.
8. KCl.
9.  $\text{KH}_2\text{PO}_4$ .
10.  $\text{NaHCO}_3$ .
11. NaCl.
12.  $\text{MgCl}_2(\text{H}_2\text{O})_6$ .
13.  $(\text{NH}_4)_2\text{CO}_3$ .
14.  $\text{CaCl}_2(\text{H}_2\text{O})_2$ .
15.  $\text{CaCl}_2$ .
16. NaOH.
17. Pepsin (e.g., Sigma-Aldrich P7000 or similar).
18. Bile (e.g., Sigma-Aldrich B8631 or similar).
19. Pancreatin (e.g., Sigma-Aldrich P1750 or similar).

---

## 3 Methods

### 3.1 Film Preparation

*See Note 2* for precautions to avoid the growth of any contaminant microorganisms.

1. Activate the probiotic culture, according to the specific growth requirements of the strain of choice. When it comes to bacteria from the *Bifidobacterium* genus and those from the Lactobacillaceae family, proceed as follows [7]: Inoculate the culture into MRS broth and incubate it at 37 °C for 48 h. Aseptically transfer the cell suspensions into 50-mL sterile tubes and centrifuge them at 4000 *g* for 10 min. Discard the supernatant,

wash the bacteria pellet with 35-mL sterile saline solution (0.85% w/v NaCl), and centrifuge it again. Repeat the discarding–washing–centrifuging steps one more time and add the resulting bacteria pellet directly to the film formulation.

2. Prepare the film-forming dispersion by adding the matrix to the solvent (usually distilled water), as well as the plasticizer and the prebiotic component (if the formulation includes a prebiotic). Homogenize the dispersion as required for the chosen formulation. When using a matrix that requires heating (e.g., starch, which is typically heated at 80–90 °C for gelatinization), the film-forming dispersion should be cooled down to no more than 40 °C before adding the probiotic (*see Note 3*).
3. Add the probiotic pellet in such an amount (calculated from a previous viable cell count on the pellet) to provide the film-forming dispersion with the desired probiotic counting (*see Note 4*). Stir the probiotic-containing dispersion (*see Note 5*).
4. Set aside at least 3 g of the dispersion (for plating and counting) and spread the remaining dispersion onto the casting surface (e.g., Petri dish or a flat glass plate) for a uniform wet thickness (defined by using a drawdown bar when on a flat surface).
5. Dry the film-forming dispersion (*see Note 6*).

### **3.2 Estimating the Viability Loss of the Probiotics on Film Drying**

#### *3.2.1 Total Solid Contents*

The viable probiotic counts should always be taken on a dry basis, and that is why the total solid content of the sample to be analyzed should be previously determined. The reference method to determine the solid content is AOAC 968.11 [8], for which we suggest some adaptations:

1. Weigh a sample of the film-forming dispersion (about 5 g) or the dried film (about 0.5 g), with an accuracy of 0.1 mg, in a previously dried aluminum pan (in triplicate).
2. Dry the aluminum pan + sample in an air oven at 105 °C for as long as it takes to obtain three consecutive weighings (with no less than 1 h between them) with differences of no more than 2 mg.
3. Determine the total solid content (g/g) as the weight of the sample that was kept during drying.

#### *3.2.2 Viable Cell Count on the Film-Forming Dispersion*

1. Transfer 1 g of the film-forming dispersion into 9 mL of a sterile saline solution (0.85% NaCl), obtaining thus a  $10^{-1}$  dilution.
2. Homogenize the  $10^{-1}$  dilution and make serial dilutions by transferring 1 mL of the original dilution into 9 mL of the sterile saline solution for the next dilution (Fig. 1).

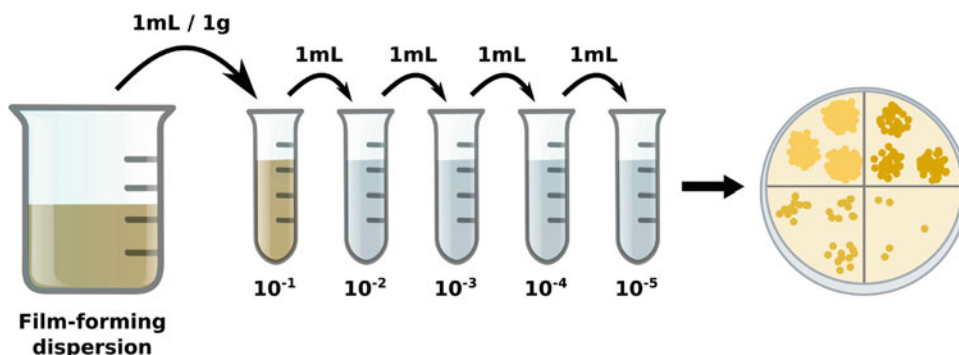


**Fig. 1** Scheme of the serial dilutions from a film-forming dispersion, followed by drop plating in a petri dish divided into quadrants

3. Plate the different dilutions by the drop plate method [9] (see **Note 7**). Use Petri dishes containing the solidified culture medium, e.g., MRS agar for bacteria from the Lactobacillaceae family [7], or Tryptone Glucose Yeast (TGY) agar for *Bacillus coagulans* [3], and divide each agar plate into four quadrants, each quadrant for a dilution. Pipette out 10  $\mu$ L (“drop”) from each dilution on the proper quadrant (at least in triplicate) (Fig. 1). Leave the plates open until the drops are absorbed by the culture medium.
4. Incubate the plates under the prescribed conditions for bacterial growth (e.g., 37  $^{\circ}$ C for 72 h in anaerobic conditions for *Lactobacillus acidophilus*).
5. Search for a dilution (quadrant) in which the number of colonies per drop is in the 3–30 range, and count the colonies [10].
6. Calculate the viable cell count (on a dry basis), using Eq. 1 (see **Note 8**).

$$\begin{aligned} \text{Cell count}(\text{cfu g}^{-1}, \text{d.b.}) \\ = \frac{\text{number of colonies} \times \text{dilution factor}}{\text{sample volume (mL)} \times \text{solid content}(\text{g/g})} \end{aligned} \quad (1)$$

### 3.2.3 Viable Cell Count on the Dried Film

1. Transfer a 0.1 g sample of the film into 9.9 mL of a sterile saline solution (0.85% NaCl). Vortex it for 1 min, then stir it at 80 rpm for 1 h at the temperature of incubation (which depends on the microorganism), obtaining a  $10^{-2}$  dilution.
2. Proceed as in Subheading 3.2.2 from **step 2**. With those results (from Subheadings 3.2.2 and 3.2.3), you will be able to check the viability loss derived from drying.

### 3.3 Estimating the Viability Loss of the Probiotics on Films During Storage

1. Store the film samples aseptically under previously defined temperatures (e.g., storage at 4 and 25 °C, as proposed by Kanmani and Lim [11]).
2. Proceed to periodic viable counts (e.g., at 10-days intervals), as described in Subheading 3.2.3.

### 3.4 Assessing the Antimicrobial Capacity of Probiotic Films

The presence of probiotic microorganisms may provide the films with some antimicrobial activity due to the competitive advantages of the probiotics over other microorganisms. A recent review has addressed the antimicrobial testing methods to be applied to films [12], including disk diffusion method, viable cell count method, and optical density-based methods. Antifungal and antibacterial assessments of food packaging materials are also addressed in Chaps. 15 and 16 of this volume, respectively.

### 3.5 Evaluating the Prebiotic Activity of Films

The prebiotic activity of a prebiotic-containing film may be assessed by measuring the effect of the presence of the film on the growth of probiotic bacteria. The following example is based on assessing the growth of bacteria that use MRS broth as a culture medium (e.g., *Bifidobacterium* genus and Lactobacillaceae family).

1. Transfer a sample of a previously plated standard bacterial strain into 10 mL of MRS broth, leave it to grow at 37 °C for 24 h, and read its optical density (OD) in a UV-vis spectrometer at 425 nm. Read also the OD of a 0.5 McFarland standard at the same wavelength, which corresponds to  $1 \times 10^8$  cfu mL<sup>-1</sup>, and assess the bacterial concentration in the culture by using Eq. 2.

$$\text{Bacterial concentration (cfu mL}^{-1}\text{)} = \frac{OD_{\text{sample}} \times 10^8}{OD_{\text{McFarland}}} \quad (2)$$

2. Transfer 2 mL of the cultured broth into each of the following: (A) 10 mL of MRS broth (positive control), (B) 10 mL of MRS broth without glucose containing 20 g L<sup>-1</sup> of the prebiotic film, (C) 10 mL of MRS broth without glucose containing 20 g L<sup>-1</sup> of a control film without the prebiotic (negative control), and (D) 10 mL of MRS broth without glucose containing only the prebiotic agent (at the same amount as in the film sample in B). Leave them to grow at 37 °C for 48 h under anaerobic conditions.
3. Read the OD from all the treatments at 425 nm, as well as the OD of the 0.5 McFarland standard, to assess the bacterial concentration in each treatment by using Eq. 2, in order to evaluate the prebiotic effect of the prebiotic film (B) when compared to the control film (C) and the free prebiotic (D).

### 3.6 Evaluating the Prebiotic Effect on Probiotic Viability on Film Processing and Storage

When a prebiotic agent is added to the formulation of a film containing a probiotic microorganism, the prebiotic may have a positive effect on the probiotic viability during processing and/or storage. This effect (when it occurs) may be assessed by using Eq. 3.

$$\text{Prebiotic effect} = (P_0 - P_f)_{\text{nonpreb}} - (P_0 - P_f)_{\text{preb}} \quad (3)$$

$P_0$ : initial (i.e., before processing or storage) probiotic cell count ( $\log \text{ cfu g}^{-1}$ , on a dry basis);  $P_f$ : final (i.e., after processing or storage) probiotic cell count ( $\log \text{ cfu g}^{-1}$ , on a dry basis); nonpreb: film containing the probiotic but not the prebiotic; preb: film containing both probiotic and prebiotic.

### 3.7 In Vitro Digestion Method

In vitro digestion models have been widely used to overcome the constrictions associated with in vivo methodologies. COST Action INFOGEST has developed a harmonized international protocol for static simulation of digestion in the upper gastrointestinal tract of adults [13]. This protocol is easily accessible, relatively inexpensive, and widely used for digestion assessments. However, it has some restrictions, especially in the gastric phase. Therefore, recently, COST Action INFOGEST proposed a semi-dynamic model including kinetic aspects, gradual acidification, secretion, and emptying of fluid and enzyme [14]. These adaptations were made to provide kinetic data on digestion and absorption of nutrients. Since our objective here is to propose methods for the simulated digestion of probiotic films, not involving digestion and absorption of nutrients, we detail below the protocol of Minekus et al. [13], with some adaptations.

#### 3.7.1 Preparation of Solutions for In Vitro Digestion Protocol

1. Perform all weightings described in Table 1 for solution preparation. All dilution processes should be in sterile and/or ultrapure water (see Notes 9 and 10).
2. Prepare three digestive fluids: (A) *salivary simulated fluid*—SSF, (B) *gastric simulated fluid*—SGF, and (C) *intestinal simulated fluid*—SIF (Table 2), in 500-mL threaded vials.

#### 3.7.2 In Vitro Digestion Process

1. *Oral simulated phase*: Transfer 200–300 mg of probiotic film into 4 mL of a simulated salivary solution—SSF (25  $\mu\text{L}$  of 0.3  $\text{mmol L}^{-1}$   $\text{CaCl}_2$  and 975  $\mu\text{L}$  of ultrapure water) and homogenize it in a Stomacher for 1 min at 150 rpm. Incubate the mixture for 2 min at 37 °C in a metabolic bath (Fig. 2). Prepare three vials, one of which to be used to assess this phase itself, and the others to be conducted to the subsequent phases.
2. *Gastric simulated phase*: Add 7.5 mL of simulated gastric solution—SGF [1.6 mL of pepsin solution 25,000  $\text{U mL}^{-1}$ , 5  $\mu\text{L}$  of 0.3  $\text{mmol L}^{-1}$   $\text{CaCl}_2$ ; 0.2 mL of 1  $\text{mmol L}^{-1}$  HCl and 0.695 mL of ultrapure water] into each of the vials coming from the simulated oral phase. Adjust the pH to 3 and incubate

**Table 1**  
**Stock solutions for simulated digestion fluids**

| Constituent                                       | g L <sup>-1</sup> | mol L <sup>-1</sup> |
|---|-------------------|---------------------|
| KCl   | 37.3              | 0.5                 |
| KH <sub>2</sub> PO <sub>4</sub>                   | 68.0              | 0.5                 |
| NaHCO <sub>3</sub>                                | 84.0              | 1.0                 |
| NaCl  | 117.0             | 2.0                 |
| MgCl <sub>2</sub> (H <sub>2</sub> O) <sub>6</sub> | 30.5              | 0.15                |
| (NH <sub>4</sub> ) <sub>2</sub> CO <sub>3</sub>   | 48.0              | 0.5                 |
| CaCl <sub>2</sub> (H <sub>2</sub> O) <sub>2</sub> | 44.1              | 0.3                 |

**Table 2**  
**Recommended concentrations of electrolytes for Simulated Salivary Fluid (SSF), Simulated Gastric Fluid (SGF), and Simulated Intestinal Fluid (SIF)**

| Constituent                                       | SSF (pH 7)<br>Volume of stock solution (mL) | SGF (pH 3)<br>Volume of stock solution (mL) | SIF (pH 7)<br>Volume of stock solution (mL) |
|---|---|---|---|
| KCl   | 15.10                                       | 6.90  | 6.80  |
| KH <sub>2</sub> PO <sub>4</sub>                   | 3.70  | 0.90  | 0.80  |
| NaHCO <sub>3</sub>                                | 6.80  | 12.50                                       | 42.50                                       |
| NaCl  | –   | 11.80                                       | 9.60  |
| MgCl <sub>2</sub> (H <sub>2</sub> O) <sub>6</sub> | 0.50  | 0.40  | 1.10  |
| (NH <sub>4</sub> ) <sub>2</sub> CO <sub>3</sub>   | 0.06  | 0.50  | –   |
| HCl   | 0.09  | 1.30  | 0.70  |
| H <sub>2</sub> O (Milli-Q)                        | 373.75                                      | 365.70                                      | 338.50                                      |
| Total (mL)  | 400   | 400   | 400   |

the mixture at 37 °C for 2 h to simulate gastric digestion (*see Note 11*) (Fig. 2).

3. *Intestinal Simulated phase*: Add 11 mL of simulated intestinal solution—SIF (6.8 mmol L<sup>-1</sup> KCl; 0.8 mmol L<sup>-1</sup> KH<sub>2</sub>PO<sub>4</sub>; 85 mmol L<sup>-1</sup> NaHCO<sub>3</sub>; 38.4 mmol L<sup>-1</sup> NaCl; 0.33 mmol L<sup>-1</sup> MgCl<sub>2</sub>), 5 mL of pancreatin 800 U mL<sup>-1</sup> solution, 2.5 mL of 160 mmol L<sup>-1</sup> bile solution, 40 µL of 0.3 mmol L<sup>-1</sup> CaCl<sub>2</sub>, 0.15 mL of NaOH 1 mmol L<sup>-1</sup>, and 1.31 mL of ultrapure water) to the gastric chyme (*see Note 12*) (Fig. 2).
4. A complete experiment should be conducted in parallel with three incubation vials (white/control).



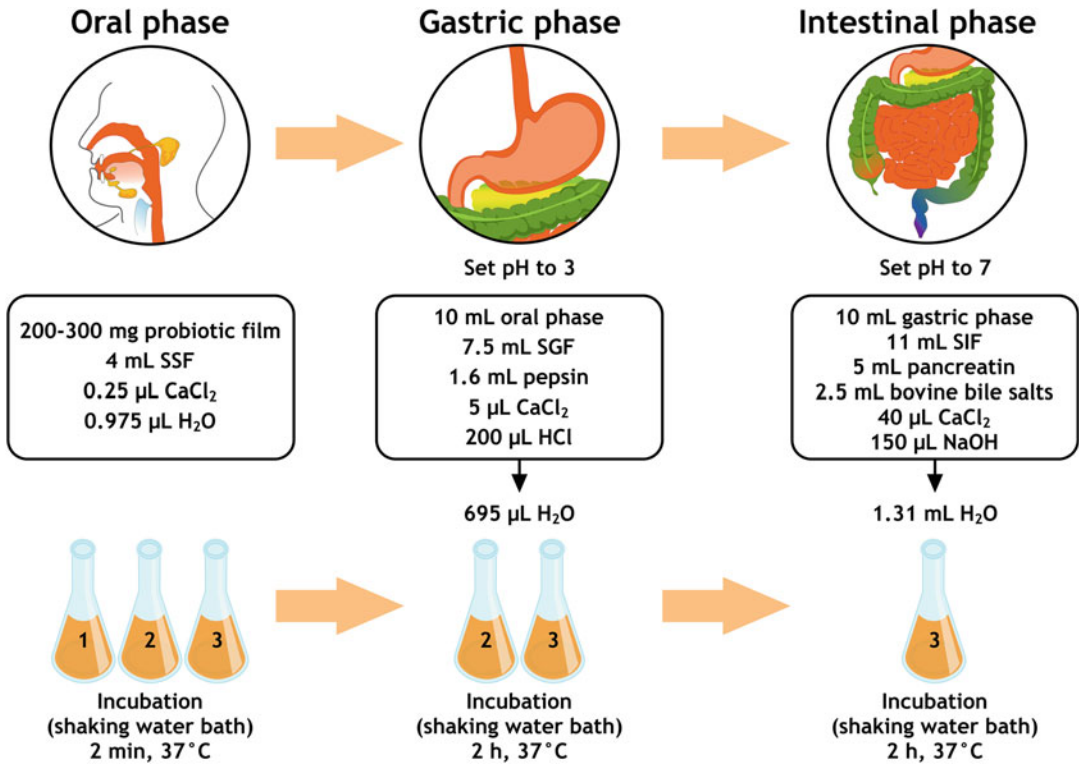


Fig. 2 Illustration of the in vitro digestion process

#### 4 Notes

1. The 0.5 McFarland standard is a mixture of 0.5 mL of  $\text{BaCl}_2$  at 1% and 99.5 mL of  $\text{H}_2\text{SO}_4$  at 1%.
2. Edible films should be free from pathogenic and deteriorating microorganisms for safety reasons. Moreover, it is important to avoid the growth of any contaminant microorganisms, which may impair the probiotic viable cell counting along the process. All surfaces that will come into contact with film components, film-forming dispersions, or the dried films should be thus previously sanitized. Steam-sterilizable glassware and equipment components should be autoclaved at 121 °C for 15 min, whereas non-sterilizable surfaces should be sanitized with ethanol 70 vol%.
3. Because each strain has its own susceptibilities, an ideal temperature for adding the probiotic should be determined on a case-by-case basis.
4. Although there is not a standard recommendation for probiotic viable counts in edible films, we propose here a final count (for the dried film) of about 9 log cfu  $\text{g}^{-1}$ . Considering that

non-spore-forming and spore-forming strains have been reported as presenting viability losses of about 2 and 1 log cfu g<sup>-1</sup> (respectively) on processing [3, 15], it may be established as a general rule that the film-forming dispersions should contain about 11 log cfu g<sup>-1</sup> (for formulations with nonspore-forming strains) or 10 log cfu g<sup>-1</sup> (for formulations with spore-forming strains), on a dry basis. Ideally, however, we recommend that the actual losses in each case are assessed by preliminary tests, since the losses depend not only on the used strain but also on interactions of the bacteria with the formulation components, as well as the processing conditions.

5. Spore-forming bacteria may be subjected to a stirring speed of about 10,000 rpm for no longer than 20 min. For nonspore-forming bacteria, the stirring speed should be no more than 2000 rpm for no longer than 20 min.
6. The drying (time and temperature) conditions depend not only on the drying equipment used (e.g., air circulation speed), but also on the solid content and thickness of the dispersion. The definition of the drying conditions of probiotic-containing films should also take the thermal stability of the probiotic strain into consideration. Nonspore-forming bacteria should ideally be dried at no more than 30 °C, whereas spore-forming ones may be subjected to about 50 °C (although films containing *Bacillus coagulans* have been reported to be dried at 80 °C for 150 min) [3]. We recommend preliminary tests in order to establish the drying conditions; eventual adjustments in dispersion formulation (solid content) and/or wet thickness may be necessary in order to enhance probiotic viability.
7. The plating may be carried out by traditional methods such as pour plate or spread plate [9]. We recommend the drop plate method because it is time-saving and cheaper (requiring less petri dishes and culture medium). On the other hand, the micropipette should be very well calibrated, since the sample volume is too small.
8. The counts are usually expressed as log cfu g<sup>-1</sup>, since changing the values to their logarithms makes it easier to compare values.
9. In order to obtain better volumetric accuracy, it is suggested that each reagent should be prepared in volumetric flasks.
10. All materials are of standard analytical grade. Sodium bicarbonate (0.5 M) should be filtered through a 0.22- $\mu$ m membrane under vacuum.
11. Add 1 g of pepsin into 10 mL of ultrapure water.
12. Add 0.8 g of pancreatin into 10 mL of ultrapure water. Add 0.7 g of bile into 10 mL of ultrapure water.

## References

1. Market Data Forecast Probiotics Market (2020). <https://www.marketdataforecast.com/market-reports/probiotics-market>. Accessed 8 Apr 2021
2. Espitia PJP, Batista RA, Azeredo HMC et al (2016) Probiotics and their potential applications in active edible films and coatings. *Food Res Int* 90:42. <https://doi.org/10.1016/j.foodres.2016.10.026>
3. Oliveira-Alcântara AV, Soares Abreu AA, Gonçalves C et al (2020) Bacterial cellulose/cashew gum films as probiotic carriers. <https://doi.org/10.1016/j.lwt.2020.109699>
4. Pruksarojanakul P, Prakitchaiwattana C, Settachaimongkon S et al (2020) Synbiotic edible film from konjac glucomannan composed of *Lactobacillus casei*-01® and Orafti®GR, and its application as coating on bread buns. *J Sci Food Agric* 100:2610–2617. <https://doi.org/10.1002/jsfa.10287>
5. Fernandes LM, Guimarães JT, Silva R et al (2020) Whey protein films added with galactooligosaccharide and xylooligosaccharide. *Food Hydrocoll* 104:105755. <https://doi.org/10.1016/j.foodhyd.2020.105755>
6. Bersaneti GT, Garcia S, Mali S et al (2019) Evaluation of the prebiotic activities of edible starch films with the addition of nystose from *Bacillus subtilis* natto. 116:108502. <https://doi.org/10.1016/j.lwt.2019.108502>
7. Ebrahimi B, Mohammadi R, Rouhi M et al (2018) Survival of probiotic bacteria in carboxymethyl cellulose-based edible film and assessment of quality parameters. *LWT Food Sci Technol* 87:54–60. <https://doi.org/10.1016/j.lwt.2017.08.066>
8. Association of Official Analytical Chemists (AOAC) (2000) Official methods of analysis. AOAC International, Arlington
9. da Silva N, Taniwaki MH, Junqueira VCA et al (2018) Microbiological examination methods of food and water: a laboratory manual. CRC Press
10. Herigstad B, Hamilton M, Heersink J (2001) How to optimize the drop plate method for enumerating bacteria. *J Microbiol Methods* 44:121–129. <https://doi.org/10.1016/S0167-7012>
11. Kanmani P, Lim ST (2013) Development and characterization of novel probiotic-residing pullulan/starch edible films. *Food Chem* 141:1041–1049. <https://doi.org/10.1016/j.foodchem>
12. Abdollahzadeh E, Nematollahi A, Hosseini H (2021) Composition of antimicrobial edible films and methods for assessing their antimicrobial activity: a review. *Trends Food Sci Technol* 110:291–303. <https://doi.org/10.1016/j.tifs.2021.01.084>
13. Minekus M, Alming M, Alvito P et al (2014) A standardised static in vitro digestion method suitable for food—an international consensus. *Food Funct* 5:1113–1124. <https://doi.org/10.1039/c3fo60702j>
14. Mulet-Cabero A-I, Egger L, Portmann R et al (2020) A standardised semi-dynamic in vitro digestion method suitable for food – an international consensus. *Food Funct* 11:1702–1720. <https://doi.org/10.1039/C9FO01293A>
15. Soukoulis C, Singh P, Macnaughtan W et al (2016) Compositional and physicochemical factors governing the viability of *Lactobacillus rhamnosus* GG embedded in starch-protein based edible films. *Food Hydrocoll* 52:876–887. <https://doi.org/10.1016/j.foodchem.2014.03.008>



## Sensory Acceptance Test of Edible Packaging Using Hedonic Scale

Suzana Maria Della Lucia and Tarcísio Lima Filho

### Abstract

Food packaging has various functions, including protecting food and food products from potential damage and degradation and providing information to consumers. Conventional packaging is commonly a one-time-use item that is then discarded. Therefore, there is a demand to achieve more sustainable, higher-quality, and healthier food production systems. In this context, edible packaging can be a good alternative because they can be manufactured from biobased, biodegradable, and/or edible materials. Studies aiming at developing edible packaging must be based on tests involving packaging formulations, physical-mechanical properties, microbiological safety, and others. However, one must have in mind that, because edible packaging can be eaten, it is essential to study their sensory characteristics and the influence of such on consumers' acceptance. In this chapter, a protocol for evaluating the sensory acceptance test of edible packaging using a nine-point hedonic scale is presented. We expect to assist researchers and professionals that are involved in the development and production of edible packaging, which is a permanent tendency in the food industry.

**Key words** Affective methods, ANOVA, Food packaging, Principal component analysis

---

### 1 Introduction

Food packaging has various functions. Its primary role is to provide protection to food, extending food shelf-life by reducing exposure to spoilage agents (such as microorganisms, oxygen, water vapor, and off-flavors) and avoiding losses of food compounds, such as flavor volatiles [1, 2]. Therefore, food packaging plays an important role in society, protecting food products from potential damage and degradation while ensuring safety and hygiene, and reducing food waste. Other important functions include providing information on nutritional content, storage, handling of packaging material after use, and marketing [1–3].

Conventional packaging is commonly a one-time-use item that is discarded soon after the use of the product by the consumer. As such, conventional, single-use packaging poses a terrible environmental problem when it is not biodegradable [3].

In this context, recently, there has been a demand for more sustainable, higher-quality, and healthier food production systems. This includes food packaging that does not increase pollution, that is, packaging that is environmentally friendly, manufactured from renewable natural resources and of biodegradable character. Thus, the search for sustainable packaging that is biodegradable and/or edible has led to the development of various edible packaging systems [2, 3].

The materials of the edible packaging are derived from edible ingredients, such as natural polymers that can be directly consumed by humans without any potential health risk. Most proteins and polysaccharides are edible and can be used as matrices for edible films and coatings.

Polysaccharides (such as starches, cellulose and its derivatives, chitosan/chitin, and gums), polypeptides (animal or plant-based proteins), and lipids can be used to manufacture edible packaging. The utility and the value of edible packaging are seen in its capacity to maintain food quality, extend shelf-life, reduce waste, and contribute to the economic efficiency of packaging materials [1, 3].

In recent years, a strong research effort has been driven toward edible food packaging for different foods and beverages. Each packaging has its peculiar characteristics in order to be as suitable as possible for each product. Many edible packaging systems are still in the stages of laboratory tests, but numerous are already being commercialized. Examples are as follows: coffee cups made of white chocolate coated wafer; seaweed-based cups made with natural sweeteners, gluten, and gelatin; cookie-based cups; starch-based films for sandwiches printed with vegetable-based inks; seaweed-based sachets used to pack pasta seasoning that can be dissolved and consumed along with the pasta; trays, pots, and cups made from starch, natural fibers, sugarcane, bamboo, and rice; seaweed-based films used to pack hamburgers that can be eaten along with the meat; edible films made from food industry tailings, tomato, spinach, papaya, and guava, ensuring sustainability and the reduction of food waste; seaweed-based film with seasonings that can be dissolved in warm water to prepare a soup; and many other examples of edible packaging [4–7].

It is important to emphasize that the studies aiming at developing edible packaging must be based on tests involving packaging formulations, physical-mechanical performance, barrier and thermal properties, microbiological safety, nutritional characteristics, among others. However, one must have in mind that, because edible packaging is expected to be eaten, it is essential to study

their sensory characteristics and the influence of such on consumers' acceptance. It is useless for an edible packaging to have the desirable physical-chemical, microbiological, and other qualities, if it does not have support from the consumers in terms of its appearance, aroma, flavor, and texture. Edible packaging can be sensorially inert, acting just as a protection layer, without any sensory alteration, or have sensory appeal, which is desirable in many products, since they can complement the sensory characteristics of the food and increase the sensory acceptance of the product by the consumer. From this point of view, sensory acceptance tests are essential tools for providing the optimal answers about the acceptance of edible packaging by the market.

Sensory acceptance tests are part of one of the groups of classical sensory evaluation methods: the Affective Methods, which express consumers' subjective reactions to food, beverages, and other materials, such as degree of liking or disliking, accepting or rejecting, and preferring order. They are divided into qualitative and quantitative tests. Qualitative tests aim to obtain subjective information in an exploratory way, studying the thoughts, attitudes, perceptions, and behaviors of the consumers in relation to the product. Quantitative Affective Methods aim to obtain direct information from consumers in relation to their preferences and/or acceptance of sensory attributes or the product as a whole [8, 9].

Acceptance tests are among the quantitative Affective Methods. These tests aim to assess the degree to which consumers like or dislike the product. Among the most widely used acceptance tests is the Hedonic Scale test. In this test, the consumer expresses the degree of liking or disliking a given product, globally or in relation to a specific attribute. The most used scales are those of seven and nine points, which contain the defined terms located, for example, between "like extremely" and "dislike extremely" [8–10].

In this chapter, a protocol for evaluating the sensory acceptance test using a nine-point Hedonic Scale of edible packaging is presented. We expect to assist researchers and professionals that are involved in the development and production of edible packaging, which is a permanent tendency in the food industry.

---

## 2 Materials

- Edible packaging samples.
- Laboratory with individual booths for Sensory Analysis.
- White light.
- Answer sheet.

### 3 Methods

The acceptance test described in this protocol can be performed to evaluate only the edible packaging, to evaluate the acceptance of food consumption together with the edible packaging, or to evaluate the acceptance of only the food. In cases where the packaging is designed to be consumed together with the food, without making sense to evaluate only the packaging, the protocol can be applied in two assays: (i) to analyze the sensory acceptance of the food consumed together with the edible packaging and (ii) to analyze the sensory acceptance of the food. Thus, it is possible to investigate whether the edible packaging has a positive or negative influence on the sensory acceptance of the food.

For standardization purposes, the protocol was described for the evaluation of edible packaging only. However, the protocol can be applied to the other cases mentioned.

#### **3.1 Defining the Sensory Attributes to be Evaluated**

In acceptance tests, global acceptance (overall impression; i.e., the edible packaging as a whole) can be assessed or also the acceptance of specific sensory attributes of the edible packaging, such as color, appearance, thickness, aroma, texture, taste, and flavor. These attributes can be evaluated globally or by specifying a certain aroma, taste, and flavor (e.g., banana aroma, vinegar aroma, sweet taste, salty taste, acid taste, strawberry flavor, and chocolate flavor).

It is noteworthy that, when specifying a sensory attribute to be evaluated, the consumer will pay more attention to this attribute than he/she would do if he/she were evaluating global acceptance (without targeting a specific attribute). Therefore, researchers should analyze what is most interesting for the research, whether to draw the consumer's attention to specific attributes or to simulate the real consumption process, when no attribute is targeted.

The greater the number of attributes to be analyzed, the more complex the analysis will be for the evaluators (consumers). Therefore, researchers should limit the analysis to only those attributes that are central to the research.

#### **3.2 Defining the Scale**

There are several scales used to measure the sensory acceptance of food and packaging. Among the available scales, the Hedonic Scale stands out, which was described in detail by Jones et al. [11] and by Peryam and Pilgrim [12].

Among the existing Hedonic Scales, the nine-point scale, ranging from the terms 1 = "dislike extremely" to 9 = "like extremely" is the most used by the scientific community and industry (Fig. 1). Therefore, it will be the scale showcased in this protocol.

This scale is simple and easily understood by consumers. Through this scale, the consumer expresses sensory acceptance of the product, stating how much he/she liked or disliked the product.

Name: \_\_\_\_\_ Genre: \_\_\_\_\_ Age: \_\_\_\_\_

Please rinse your mouth with water before starting.

Please write the sample code, taste the sample and let us know how much you liked or disliked the appearance, aroma, texture, flavor and overall impression of the product. Write down the number for the answer that best reflects your judgment.

Code: \_\_\_\_\_

- 9 – Like extremely
- 8 – Like very much
- 7 – Like moderately
- 6 – Like slightly
- 5 – Neither like nor dislike
- 4 – Dislike slightly
- 3 – Dislike moderately
- 2 – Dislike very much
- 1 – Dislike extremely

**Answers**

Appearance: \_\_\_\_\_

Aroma: \_\_\_\_\_

Texture: \_\_\_\_\_

Flavor: \_\_\_\_\_

Overall impression: \_\_\_\_\_

Comments: \_\_\_\_\_

**Fig. 1** Model score sheet for acceptance test with a nine-point balanced Hedonic Scale

For more information on the other scales that can be used in acceptance tests, readers are recommended to refer to Lawless and Heymann [10], specifically Chaps. 7 and 14.

**3.3 Presentation of Edible Packaging**

The packaging samples can be served monadically (one at a time) and sequentially (one after the other), that is, a response required after each packaging. The samples may also be served all at once, but this requires the panelist to match the correct test sample to the correct three-digit code on the answer sheet. Therefore, for testing with untrained evaluators (consumers), it is safer to serve products one at a time and retrieve the sample after each response [10] (*see Note 1*).

**3.4 Defining the Number of Evaluators**

In affective tests, the team of evaluators should be composed of a group of people selected as a representative sample of a population. Usually, the population is the usual or potential consumer market for the product [8] (*see Note 2*).

Acceptance tests, performed in the laboratory, are used to preliminarily select samples for future tests and in the stages of new product development [8]. For laboratory tests, studies carried out recently and published in scientific journals have used teams composed of 80–150 consumers. Within this range, the greater the number of samples to be evaluated, the greater the number of consumers needed.

In addition to the laboratory, tests can also be carried out in central locations (e.g., supermarkets and restaurants) and households. In these places, there is less control of the environment and the analysis conditions (noise, inadequate lighting, absence of



individual cabin for analysis); therefore, a greater number of evaluators is necessary, when compared with laboratory tests. For more information, readers are recommended to refer to Meilgaard, Civille and Carr [13], Chap. 13 specifically.

### **3.5 Procedure for Analyzing Packaging Samples**

1. Code the samples with random three-digit numbers.
2. Prepare and print the evaluation answer sheet (Fig. 1) for all evaluators (one form per packaging sample).
3. Provide pens to fill in the answer sheet.
4. The analysis site must be quiet, with a pleasant temperature and white light (if the researchers are interested in the visual analysis of the packaging).
5. In another room, welcome the evaluators who will participate in the study.
6. Deliver, explain, and request a signature on the Free and Informed Consent Form (mandatory in research with human beings, consult the Ethics Committee for Research with Human Beings of the place where the research will be carried out).
7. Collect information about research participants. In the sensory evaluation, the evaluators are the instruments of analysis; therefore, characterizing the profile of the participants is necessary. The basic information needed is the age, gender, and frequency or intention of consumption of the product under study. Some information that can also be requested, according to the research interest, is the level of education, monthly family income, and occupation.
8. Deliver the evaluation form (Fig. 1) to the consumers.
9. Explain to the evaluators the number of samples to be analyzed, one at a time, and the analysis procedure: the evaluators (consumers) must taste the product and inform how much they liked or disliked the appearance, aroma, texture, flavor, and the overall impression of the product. Between evaluations, evaluators should rinse their mouths with water and wait for 3 min before testing another sample.
10. Clear the doubts of the evaluators.
11. Invite the evaluators to enter the packaging evaluation room.
12. Serve the edible packaging samples in a monadic and random manner.
13. As soon as the evaluator finishes analyzing the first packaging sample, collect the completed answer sheet and ask him/her to rinse the mouth with water.
14. After 3 min, serve the next sample to be analyzed (chosen randomly). Perform this procedure until all samples are analyzed.
15. Repeat **steps 5–14** for all evaluators, until the total number of evaluators is completed.

### 3.6 Data Analysis

The responses of each sensory attribute must be tabulated and analyzed separately. The data from the nine-point scales are assigned values one through nine, nine usually being the “like extremely” level.

The results can be analyzed by descriptive statistics, by means of frequency distribution graphs of the hedonic scores of each attribute. The frequency distribution graphs allow the researchers to visualize the segmentation of the hedonic scores of each sample within the scale. Thus, it is possible to compare the performance of two or more packaging samples, checking those that had the highest mean hedonic scores, that is, the most accepted one.

The results can also be analyzed using parametric statistics, t-tests on means for two packaging samples, or analysis of variance followed by comparisons of means for more than two packaging samples [10]. According to Lawless and Heymann [10], even though the scale may not achieve a true interval level of measurement, the parametric approach is usually justified based on the larger sample size in a consumer test.

For each sensory attribute, an analysis of variance (ANOVA) in completely randomized blocks (consumers) can be performed to determine whether there is a significant effect ( $p \leq 0.05$ ) of the packaging samples on the hedonic scores. The mathematical model that represents the analysis is shown in Eq. 1. The hypothesis of nullity of zero variability is tested between the packaging samples ( $H_0 : \sigma_R^2 = 0$ ).

$$Y_{ij} = m + P_i + C_j + e_{ij} \quad (1)$$

$Y_{ij}$ —hedonic scores of packaging  $i$  attributed by the consumer  $j$

$m$ —constant inherent to the model or the overall average value

$P_i$ —random effect of packaging  $i$

$C_j$ —random effect of consumer  $j$

$e_{ij}$ —normal random error, independent and equally distributed ( $0, \sigma^2$ ).

When necessary, comparisons of means should be performed.

The Preference mapping method can be used in order to evaluate the individual responses of each consumer and not just the average response of the group of consumers who analyzed the packaging. Through the Preference mapping, in a single graph, hedonic information for each consumer participating in the study is simultaneously presented in a multidimensional space representing and containing the evaluated packaging [10]. Preference mapping can give a clear idea of which changes must be made in product reformulation.

The Internal Preference mapping, sometimes called MDPREF, is usually a principal component analysis (PCA), in which the hedonic scores are arranged in a matrix of product (packaging)

(in  $p$  lines) for consumers (in  $n$  columns), which is reduced in a small number of independent components, minimizing the loss of original information (variation). The purpose of the internal Preference mapping is to find a small number of principal components (usually two or three) that explain a large percentage of the variation in the consumer hedonic responses [9, 10]. For internal Preference mapping, all consumers should evaluate all the products. According to Lawless and Heymann [10] and Lavine et al. [14], in order to have a reasonable perceptual map, the researcher should have the consumers evaluate at least six products that span the perceptual space.

**3.7 Presentation and Interpretation of the Results**

The results can be presented using tables and graphs. As an example, the results of a fictitious research on edible packaging will be presented.

**3.7.1 Frequency Distribution**

In Fig. 2, frequency distribution graphs of the hedonic scores are presented for the aroma and flavor attributes of three edible packaging samples (A, B, and C).

In Fig. 2, packaging sample A presented a higher frequency of higher hedonic scores (from 7 to 9), when compared with the other packaging, for the two attributes under study (aroma and flavor). In addition, packaging sample B presented the highest distribution of negative hedonic scores (from 1 to 4) for the aroma attribute, that is, sample B was the one that presented aromas with greater sensory rejection, while sample C presented the highest distribution of negative hedonic scores for the flavor attribute. The same analysis can be done for the other sensory attributes and the overall impression of the packaging samples.

**3.7.2 ANOVA**

Table 1 presents the results of the ANOVA and the comparison of means test of three edible packaging samples (A, B, and C). The samples did not differ in terms of acceptance as for the appearance and texture attributes ( $p > 0.05$ ). A significant effect of the packaging samples ( $p \leq 0.05$ ) in the ANOVA (Table 1) was verified in

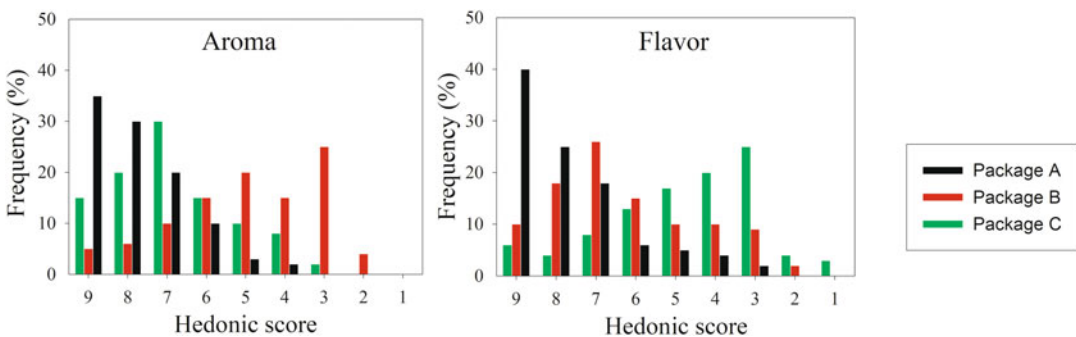


**Fig. 2** Examples of frequency distribution graphs of the hedonic scores for the aroma and flavor attributes of three packaging samples

**Table 1**  
**Summary of ANOVA, average hedonic scores, and Tukey's test for each packaging sample and sensory attribute**

| Attribute          | MSpac <sup>A</sup> | MSres <sup>B</sup> | p-value | Mean hedonic scores <sup>C</sup> |             |             |
|--------------------|--------------------|--------------------|---------|----------------------------------|-------------|-------------|
|                    |                    |                    |         | Packaging A                      | Packaging B | Packaging C |
| Appearance         | 0.36               | 1.34               | 0.7543  | 7.2 a                            | 7.1 a       | 7.1 a       |
| Aroma              | 4.52               | 1.44               | 0.0440  | 7.9 a                            | 4.9 b       | 7.0 a       |
| Texture            | 5.01               | 1.83               | 0.0649  | 6.4 a                            | 6.1 a       | 6.3 a       |
| Flavor             | 6.81               | 1.91               | 0.0228  | 8.2 a                            | 6.7 b       | 4.3 c       |
| Overall impression | 6.43               | 1.75               | 0.0238  | 7.8 a                            | 6.3 b       | 6.1 b       |

<sup>A</sup>Mean-square of the packaging sample

<sup>B</sup>Mean-square residue

<sup>C</sup>Means followed by at least one equal letter within the same row do not differ ( $p > 0.05$ ) by Tukey's test

the hedonic scores of the aroma and flavor attributes and overall impression. Packaging sample B presented the least accepted aroma. Sample C presented the least flavor acceptance. Packaging samples B and C showed the lowest overall impression, while sample A had the highest hedonic scores for flavor attribute and overall impression.

### 3.7.3 Internal Preference Mapping

The Internal Preference Map obtained from the overall impression analysis, of six edible packaging samples, is shown in Fig. 3.

The first principal component (PC1) accounted for 71.4% of the variation in the results, whereas the second principal component (PC2) accounted for 10.2% of the variation in the results, and the two together explained 81.6% of the variation in the results (Fig. 3) (*see Note 3*).

The data for each consumer are shown on the map as a black dot, which corresponds to the endpoint of the fitted vector. Most consumers are located to the right of the map, where packaging samples 1 and 4 are located. Therefore, the packages with the highest acceptance are 1 and 4, followed by 3. The sample 6 obtained the least sensory acceptance. The same graph can be generated for the results of acceptance of sensory attributes (e.g., appearance, aroma, texture, and flavor).

## 4 Final Considerations

In this protocol, the acceptance test was described using a nine-point Hedonic Scale and performed in the laboratory. However, there are many scales that can be used and different locations for running the test. A variety of useful methods are available to

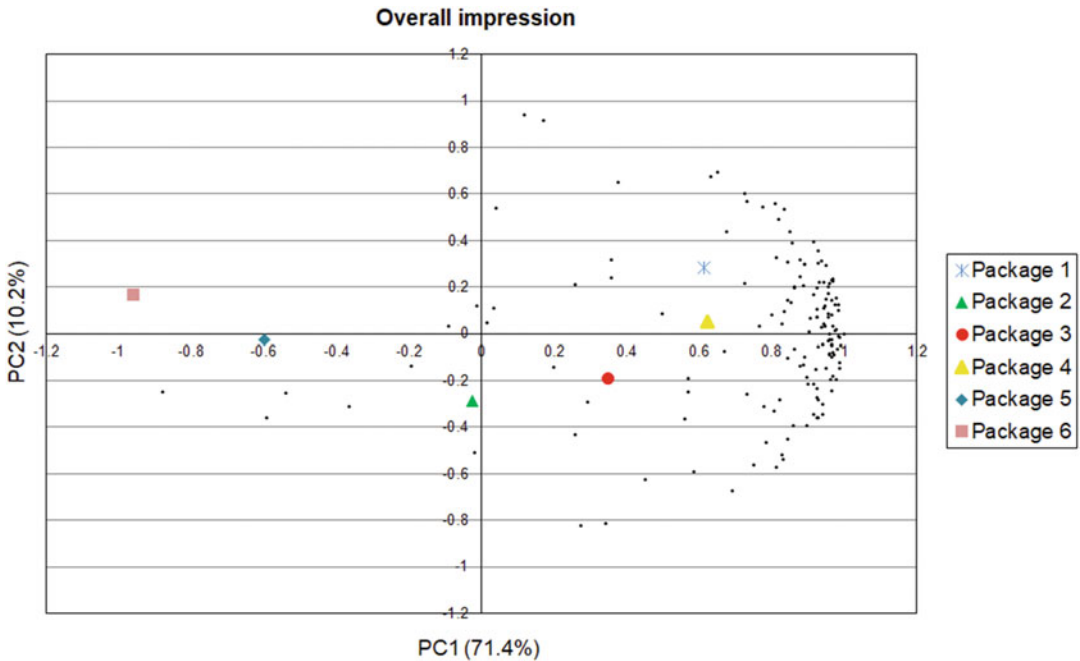


**Fig. 3** Internal preference map based on six edible packaging samples

researchers, providing vital information for edible packaging developers and marketers alike. As mentioned by Lawless and Heymann [10], high sensory acceptance does not guarantee that the product will be a market success. The likelihood of purchase (and most importantly, the repurchase) depends on the concept, price, brand, positioning, promotions, advertising, label information, consumer awareness, nutritional characteristics, and many other factors. However, sensory appeal is the essential “platform” without which the product is unlikely to succeed [10].

## 5 Notes

1. The packaging samples must be served randomly, so the effect of the order of presentation and the residual effect, characterized by the influence of a treatment in the evaluation of the subsequent one, is eliminated.
2. Potential consumers are individuals who do not have the habit to consume a product, but are consumers of the product in potential. The use of potential consumers is recommended when the product under evaluation is an unusual product and thus it does not have an established consumer Market.

3. Generally, an explanation of the variability of results by the first principal components (first and second principal components, for example) that is greater than 70% is considered satisfactory for the explanation of the results.

## References

1. Otoni CG, Avena-Bustillos RJ, Azeredo HMC, Lorevice MV, Moura MR, Mattoso LHC, McHugh TH (2017) Recent advances on edible films based on fruits and vegetables – a review. *Compr Rev Food Sci Food Saf* 16: 1151–1169. <https://doi.org/10.1111/1541-4337.12281>
2. Daniloski D, Petkoska AT, Lee NA, Bekhit AED, Carne A, Vaskoska R, Vasiljevic T (2021) Active edible packaging based on milk proteins: a route to carry and deliver nutraceuticals. *Trends Food Sci Technol* 111:688–705. <https://doi.org/10.1016/j.tifs.2021.03.024>
3. Petkoska AT, Daniloski D, D’Cunha NM, Naumovski N, Broach AT (2021) Edible packaging: sustainable solutions and novel trends in food packaging. *Food Res Int* 140:109981. <https://doi.org/10.1016/j.foodres.2020.109981>
4. Retratos da Economia (2015) Copo de café comestível é lançado para reduzir impacto ambiental. <https://economia.estadao.com.br/blogs/retratos-da-economia/copo-de-cafe-comestivel-reduz-impacto-ambiental/>. Accessed 22 apr 2021
5. Sociedade Nacional de Agricultura (2016) Embalagens comestíveis. <https://www.sna.agr.br/embalagens-comestiveis/>. Accessed 24 apr 2021
6. As melhores soluções sustentáveis (2017) Embalagem comestível é feita de algas. <https://catracalivre.com.br/as-melhores-solucoes-sustentaveis/embalagem-comestivel-e-feita-de-algas/>. Accessed 22apr 2021
7. Food Connection (2021) Empresa cria embalagem comestível a partir de fibras naturais. <https://www.foodconnection.com.br/empreendedorismo/empresa-cria-embalagem-comestivel-partir-de-fibras-naturais>. Accessed 23 apr 2021
8. Della Lucia SM, Minim VPR, Carneiro JDS (2018) Análise sensorial de alimentos. In: Minim VPR (ed) *Análise sensorial: estudos com consumidores*, 4th edn. Editora UFV, Viçosa, pp 13–49
9. Reis RC, Minim VPR (2018) Testes de aceitação. In: Minim VPR (ed) *Análise sensorial: estudos com consumidores*, 4th edn. Editora UFV, Viçosa, pp 69–85
10. Lawless HT, Heymann H (2010) *Sensory evaluation of food: principles and practices*, 2nd edn. Springer, New York. 596p
11. Jones LV, Peryam DR, Thurstone LL (1955) Development of a scale for measuring soldier’s food preferences. *J Food Sci* 20:512–520. <https://doi.org/10.1111/j.1365-2621.1955.tb16862.x>
12. Peryam DR, Pilgrim FJ (1957) Hedonic scale method of measuring food preferences. *Food Technol* 1957:9–14
13. Meilgaard MC, Civille GV, Carr BT (2016) *Sensory evaluation techniques*, 5th edn. CRC Press, Boca Raton. 588p
14. Lavine BK, Jurs PC, Henry DR (1988) Chance classifications by non-linear discriminant functions. *J Chemom* 2:1–10. <https://doi.org/10.1002/cem.1180020103>



# Chapter 21

## Consumer Choice Probabilities for Food Packaging

Tarcísio Lima Filho, Suzana Maria Della Lucia,  
and Valéria Paula Rodrigues Minim

### Abstract

Packaging is of extreme importance as it represents the very first contact among consumers and food or beverage. Packaging therefore plays a *silent seller* role and stimulates consumers to decide whether to buy the product or not. In this chapter, we discuss the modified choice-based conjoint analysis (MCBCA), a quantitative method that has been used to assist in the clarification of consumer behavior, especially when seeking to analyze the attributes of product packaging guiding consumer choice. The protocol for determining the consumer choice probabilities for food packaging based on MCBCA is presented. We intend to assist everyone involved in the process of designing new products, especially in the stages of developing the marketing strategy, production, and market testing, by studying the modification and choice of packaging and labels, contributing to increasing the product's competitiveness in the market.

**Key words** Modified choice-based conjoint analysis, Non-sensory characteristics, Likelihood of choice

---

## 1 Introduction

Most food and beverage products are sold packaged, with a label that has been designed, then printed or attached onto it [1]. In this context, studying the packaging itself is extremely important as it represents the consumer's first contact with the product, thus denoting the primary object for defining the choice and purchase of the packaged good [2]. Packaging therefore acts as a *silent seller* by providing information about the product, which is evaluated by the consumer to support the decision to whether buy the product or not.

Thus, it can be concluded that, the decision to purchase a certain product for the first time usually depends on the extrinsic information or characteristics, that is, the non-sensory characteristics related to this product, which are normally present on the packaging [3]. Packaging characteristics can lead the consumer to

purchase a product, while sensory characteristics confirm the acceptance and can determine recurring purchases [4, 5].

Among the information or characteristics presented in the packaging, the following can be highlighted: Label, brand, price, material, color, texture, design, format, illustrations, origin, preparation method, nutritional facts, expiry date, net weight, ingredient list, health-related label messages, and nutritional claims, among others. All these characteristics have specific influences on the consumer's intention to purchase or choose the product. This is because, from the consumer's perspective, a food is always associated with a packaging and is often selected through the information provided [2, 6, 7]. Therefore, packaging plays a vital role in decision making, as a specific combination of quality attributes therein presented determines the expected quality. An informed consumer aggregates knowledge about food from various available sources and compares it with the information on the product label [5]. Thus, it is expected that the presence of a well-designed packaging will have a powerful influence on the formation of the sensory expectations by the consumer, also influencing the choice and finally the purchase of the product. The expectation generated by the information contained in the packaging is particularly important because it can either improve or worsen the perception of the product even before its consumption [8].

While some of this information appearing on packaging is enforced by the law (e.g., in Brazil, the label must at least display the product's name, weight, and use by/best before date), further information—both textual and graphical—is often added to help inform the consumer, encourage favorable product expectations, and enhance the consumption process [1].

Studies have been developed with the aim of evaluating the role of packaging and/or factors contained in it on consumer behavior, because, as previously stated, it is of crucial importance to the choice of product during purchase [2, 6]. The Conjoint analysis technique has been widely and successfully used to carry out this type of study, in order to understand the attitudes and behaviors of consumers toward the packaging of food and beverages.

The Conjoint analysis was developed in the fields of psychometry and consumer research, being used as a support to understand how the consumer evaluates the quality of products. It allows one to understand how an individual develops a preference for products or services [9], based on their different characteristics. Its development dates from 1964 and its introduction in marketing research took place through Green and Rao, in 1971 [10]. This technique is one of the most important tools in assisting product development and decision making in marketing.

More specifically, the Conjoint analysis aims to investigate the joint effect of two or more independent variables on the evaluation of a dependent variable [2]. It is a quantitative method that has



been used to assist in the clarification of consumer behavior regarding a product, especially when seeking to analyze the attributes of product packaging on consumer choices and purchase [11]. In packaging studies, the application of the Conjoint analysis is based on data collection by combining specific levels of each factor or characteristic to be studied in the packaging to obtain a set of different treatments (possible packaging for the product); these investigated packaging systems are presented to consumers for the global assessment of preference, purchase intention, or choice [2]. The use of such a method enables the assessment of the packaging characteristics that are essential for increasing consumer intent to purchase or choose a product [11].

Researchers have developed over the years different types of data collection within the Conjoint analysis, as well as different data analysis techniques from this type of study. One of the types of analysis, the ratings-based conjoint analysis, uses data collection to mark the preference/purchase intention/acceptance of a packaging or product using scales. The rankings-based Conjoint analysis, in turn, relies on the ordering of treatments (such as packaging) according to preference/purchase intention/acceptance to obtain the data. In the third type, called choice-based, consumers choose a treatment (e.g., a packaging) from several options instead of assigning notes separately or ordering them [9].

In this chapter, the Modified choice-based conjoint analysis (MCBCA) is discussed, as presented by Della Lucia [6], Lima Filho et al. [11], and Carneiro et al. [12]. MCBCA outstands as the most realistic approach to collect data in the simulation of consumer purchasing behavior, which can lead to a greater validity of the results.

In this type of analysis, consumers must choose a packaging among several alternatives, assembled from a set of factors (the studied packaging characteristics) and their levels (different types that the characteristics can take), without having to assign notes of intention to purchase or rank the packaging treatments, which makes the data collection protocol closer to the reality of these consumers. The consumer's choice behavior is therefore investigated through the so-called "choice-based" Conjoint analysis [6, 13].

MCBCA allows one to estimate the probabilities of choice associated with the evaluated packaging, as well as compare the probabilities of choosing a specific packaging for any two levels of the same factor or characteristic of which they are constituted [6, 13]. MCBCA is particularly important when studying the consumer behavior. In this vein, the technique presented in this chapter is expected to assist those involved in the process of designing new products, especially in the stages of developing the marketing strategy, production, and market testing, supporting improvements,

modifications, and choices of packaging, therefore contributing to the product's commercial competitiveness.

---

## 2 Materials

- Packaging samples.
- Table for displaying all samples.
- White light.
- Stopwatch.
- Answer sheet and consent form (*see Note 1*).

---

## 3 Methods

### 3.1 Factors Related to Packaging and Their Respective Levels

First, it is necessary to determine which characteristics of the packaging (factors and their respective levels) are the most relevant to be evaluated. This is a very important step since the purpose of the method is to determine how these characteristics will influence the likelihood of consumer choices.

Therefore, the factors inherent to the packaging, which may interfere with the probability of choice, must be chosen (*see Note 2*).

The determination of these characteristics must be carried out considering the objectives and the experience of the researchers, considering information from the literature and, or, through Focus Group sessions (*see Note 3*).

Table 1 shows examples of factors and their levels, for studies with packaging, which can be investigated through the MCBCA.

#### 3.1.1 Case Study

**Table 1**  
**Examples of factors and levels of food or beverage packaging**

| Factors  | Levels  |
|----------|---|
| Material | Flanders, aluminum, glass, poly(ethylene terephthalate) (PET), or biaxially oriented polypropylene (BOPP) |
| Size     | Small, medium, or large (specifying dimensions)   |
| Volume   | 350, 600, or 1000 mL  |
| Format   | Rectangular, square, round, or triangular   |
| Color    | Red, black, gray, blue, or green  |

A case study is presented to exemplify the application of the method and allow a more didactic explanation of all stages of the MCBCA. In this fictitious study, the effect of beer packaging characteristics on the likelihood of Consumer choices is investigated. The packaging has three factors with two levels each, namely: material factor, with levels “glass” and “PET”; volume factor, with levels “350 mL” and “600 mL”; and color factor, with levels “amber” and “green.”

### 3.2 Data Collection

MCBCA encompasses an experiment with several factors, each with its own levels. The factors can be qualitative or quantitative variables. Each treatment (packaging) is obtained by combining the levels of the factors; therefore, the treatments are obtained by a factorial array.

The complete profile is the data collection method to be used in the MCBCA. In the complete profile, each package (treatment) is formed by the combination of all factors, that is, it is formed by the combination of a level of each factor.

### 3.3 Determining the Packaging Samples to Be Analyzed

After defining the factors, their levels, and the method of data collection, it is necessary to define which treatments will be analyzed by the evaluators. One can adopt the complete factorial or the fractional factorial.

In the *complete factorial*, all possible combinations of the levels of the factors will be analyzed. Therefore, the complete factorial should be adopted whenever the number of factors and levels to be evaluated is small. When there are a large number of factors and levels, *fractional factorials* should be adopted (*see Note 4*).

The MCBCA calculates the probability of choosing each package, seeking to investigate which package has the highest likelihood of choice. When using fractional factorial, leaving some packaging samples without evaluation, there is a risk of not analyzing the packaging that would have the greatest likelihood of consumer choices. Therefore, it is recommended, whenever possible, to give preference to the use of the complete factorial array.

#### 3.3.1 Case Study

The data will be collected using the complete profile method [15], and a complete factorial treatment array will be used [12]. Therefore, eight treatments will be applied, as outlined in Table 2.

### 3.4 Preparing Packaging Samples

The packaging samples to be studied must be prepared. Prototypes or photographs of the packaging can be used. The use of prototypes is recommended because it is a better representation of reality (in three dimensions) when compared with photographs (in two dimensions).

#### 3.4.1 Case Study

The eight packaging samples (treatments) of the case study are shown in Fig. 1.

**Table 2**  
**Treatments under study**

| Treatment | Material | Volume (mL) | Color |
|-----------|----------|-------------|-------|
| 1         | Glass    | 600         | Amber |
| 2         | Glass    | 600         | Green |
| 3         | Glass    | 350         | Amber |
| 4         | Glass    | 350         | Green |
| 5         | PET      | 600         | Amber |
| 6         | PET      | 600         | Green |
| 7         | PET      | 350         | Amber |
| 8         | PET      | 350         | Green |

**3.5 Defining the Order of Presentation of the Packaging Samples**

All packaging samples must be presented simultaneously to the evaluators. The order of disposal of the packages must follow a predefined experimental design (*see Note 5*).

**3.5.1 Case Study**

Annex 1 shows the design proposed by MacFie et al. [16] to present eight treatments, which would be the design used in the case study. There are 48 possible orders for the presentation of eight samples. All these orders must be considered during the evaluation of the packaging.

**3.6 Defining the Number of Evaluators**

In MCBCA, the evaluation of packaging must be carried out by traditional or potential consumers of the product. Assessors do not need to be previously trained. It is only necessary to explain, on the day of the analysis, how the evaluators should proceed to analyze the samples.

The number of evaluators that will carry out the analyses depends on the number of possible orders of the design and the number of repetitions defined. Equation 1 should be used to calculate the number of evaluators.

$$n_{\text{evaluators}} = n_{\text{order}} \cdot r \tag{1}$$

where  $n_{\text{evaluators}}$  is the number of evaluators;  $n_{\text{order}}$  is the number of possible orders of presentation of packaging in the design; and  $r$  is the number of repetitions (*see Note 6*).

**3.6.1 Case Study**

In the case study, for eight packages, there are 48 possible packaging presentation orders (Annex 1). If the researcher chooses to perform three repetitions, 144 evaluators (three repetitions × 48 orders) will be needed to complete the analysis. In this case, three evaluators will analyze the packaging samples in the same order of presentation. To facilitate and streamline the analysis



**Fig. 1** Example of treatments. (Image elements by vectorpocket on Freepik)

procedure, these three evaluators can carry out the analysis of the samples at the same time.

### 3.7 Procedure for Analyzing the Packaging Samples

1. Code the packages with random three-digit numbers.
2. Prepare and print the answer sheet in sufficient numbers for all evaluators (one sheet per evaluator) (Fig. 2).
3. Provide pens to fill in the answer sheet.
4. The place where the analysis will be taken must be quiet, with a pleasant temperature and white light. In the analysis room, arrange the packages on a table or gondola in the correct order of presentation. All packaging samples must be displayed simultaneously, and the order must follow the design of MacFie et al. [16].
5. In another room, welcome the evaluators who will participate in the study. The number of repetitions will be the number of evaluators who will carry out the analysis at the same time. Therefore, if it was decided to perform three repetitions, three evaluators should be invited at a time.
6. Deliver, explain, and request a signature on the Free and Informed Consent Form (*see Note 1*).
7. Collect information about research participants (*see Note 7*).

Consider that you want to buy (**product name**). Please write the product code you would buy.

Code: \_\_\_\_\_

Comments: \_\_\_\_\_

**Fig. 2** Answer sheet

8. Deliver the answer sheet to consumers (Fig. 2).
9. Explain the analysis procedure: the evaluators (consumers) must simulate the product purchase process at the supermarket. Evaluators will have 3 min to analyze all packages. At the end of this time, they must inform the product they would choose to buy.
10. Clear the doubts of the evaluators.
11. Invite the evaluators to enter the packaging evaluation room (the packaging must already be arranged in the correct presentation order).
12. Time 3 min.
13. Ask the evaluators to mark, on the answer sheet, the code of the package they would choose to buy.
14. Repeat **steps 4** through **13** until the packaging is arranged in all presentation orders [16].

**3.8 Tabulation of Data**

The evaluators choose only one package among those presented. In the tabulation of the results of the sheets, the value 1 is assigned to the chosen packaging, and the value 0 to the others. To perform the analysis of the results, the levels of the factors must also be coded.

**3.8.1 Case Study**

The coding of the levels of the case study is shown in Table 3.

**3.9 Data Analysis**

To carry out the MCBCA, the following considerations were made:

Let  $\gamma_k = (y_{1k}, y_{2k}, \dots, y_{Nk})'$  be the vector of answers for the  $k$ th consumer, with:

$y_{jk} = 0$  for not chosen packaging and  $y_{jk} = 1$  for the chosen package

As each appraiser chooses only one package, Eq. 2 applies:

$$\sum_{j=1}^N y_{jk} = 1 \tag{2}$$

For  $j = 1, 2, \dots, N$  treatments (packaging samples) analyzed by each of the  $k = 1, 2, \dots, E$  evaluators.

Equation 3 represents the matrix notation of the model

$$\gamma = X\beta \tag{3}$$

where

**Table 3**  
**Coding of the levels of factors (case study)**

| Factor     | Level    | Codification |
|------------|----------|--------------|
| 1—Material | 1—Glass  | 0            |
|            | 2—PET    | 1            |
| 2—Volume   | 1—600 mL | 0            |
|            | 2—350 mL | 1            |
| 3—Color    | 1—Amber  | 0            |
|            | 2—Green  | 1            |

$\Upsilon$  is the vector of the evaluators’ answers for the analyzed packages.  $X$  is the matrix with the coded values of the factor levels (Table 3).  $\beta$  is the vector of parameters to be estimated, with only one coefficient being estimated per factor.

The notation  $X_j\beta$  is used to indicate packaging  $j$ , where  $X_j\beta = (X_{1j}, X_{2j}, \dots, X_{sj})\beta$  (Eq. 4):

$$\beta = (\beta_1 \beta_2 \dots \beta_s)' \tag{4}$$

where

$X_{sj}$  represents the level of the  $s$ th factor present in the  $j$ th treatment. The coding  $X_{sj} = 0, 1, \dots, l - 1$  is adopted for  $l$  levels. For two levels, we have  $X_{sj} = 0, 1$ , as done in the coding presented in Table 3.

$P_j$  is the probability associated with  $j$ th packaging, satisfying Eq. 5:

$$\begin{aligned} 0 \leq P_j \leq 1 \\ \text{with} \\ \sum_{j=1}^N P_j = 1 \end{aligned} \tag{5}$$

The model proposed by McFadden [17], termed multinomial logit, is adopted to estimate the likelihood of the choice of a treatment (Eq. 6)

$$P_j = \frac{e^{X_j\beta}}{\sum_{j=1}^N e^{X_j\beta}} \tag{6}$$

where  $X$  is the matrix of encoded values of the factor levels and  $\beta$  is the vector of estimated parameters through iterative numerical methods to maximize the likelihood function ( $L$ ) of the sample or, similarly, the logarithms of the function  $L$ . For more details, we

recommend consulting Agresti [18], who presents an approach to estimation and inferences using this model.

When applying the MCBCA, the main objective is to estimate  $P_j$  for each package under study. In this way, it is possible to investigate which packaging is more likely to be chosen by the consumer.

The MCBCA also allows calculating the effect of choosing a treatment at one level of a factor over another level of the same factor (hazard ratio value), according to Eq. 7 [4, 11].

$$\text{Hazard ratio}_n = \frac{P(\text{level 2})}{P(\text{level 1})} = e^{\beta_s(X_{\text{level 2}} - X_{\text{level 1}})} \quad (7)$$

For the case study, with three factors and two levels each,  $s = 1, 2, 3$  factors,  $X_{\text{level 2}} = 1$  and  $X_{\text{level 1}} = 0$  (according to the encoding levels of each factor, Table 3).

**3.10 Presentation and Interpretation of Results (Case Study)**

The results can be presented using tables and graphs. As an example, the results of the case study will be presented. It is important to highlight that these data are fictitious, we use them only for didactic purposes.

The estimated coefficients ( $\beta'$ ) and the hazard ratio values are shown in Table 4.

The volume and color factors had a significant effect on the consumer choices according to the model used ( $p \leq 0.001$ ). The material factor showed no significant effect on the consumer evaluation ( $p > 0.001$ ) (Table 4).

The hazard ratio value for the material factor is

$$\text{Hazard ratio}_n = \frac{P(\text{level 2})}{P(\text{level 1})} = \frac{P(\text{PET material})}{P(\text{Glass material})} = 0.931$$

The hazard ratio value for the volume factor is

$$\text{Hazard ratio}_n = \frac{P(\text{level 2})}{P(\text{level 1})} = \frac{P(360 \text{ mL})}{P(600 \text{ mL})} = 2.436$$

**Table 4**  
**Summary of the analysis for estimating the model coefficients by maximum likelihood**

| Factor   | Estimated coefficient ( $\hat{\beta}$ ) | Hazard ratio value |
|----------|---|--------------------|
| Material | -0.12401 <sup>ns</sup>                  | 0.931              |
| Volume   | -1.05313*                               | 2.436              |
| Color    | -1.52820*                               | 3.449              |

\*Significant according to the chi-square test ( $p \leq 0.001$ )

<sup>ns</sup>Not significant according to the chi-square test ( $p > 0.001$ )



The hazard ratio value for the color factor is

$$\text{Hazard ratio}_n = \frac{P(\text{level 2})}{P(\text{level 1})} = \frac{P(\text{Green})}{P(\text{Amber})} = 3.449$$

The hazard ratio value is a ratio of estimated probabilities. The hazard ratio value of 0.931 for the material factor means that the probability of the consumers choosing a package with the material “glass” was 1.07 times greater than the probability of them choosing a package with the material “PET.” The value was quite close to 1.0, showing that the effect of the factor was weak (nonsignificant, as shown in Table 4).

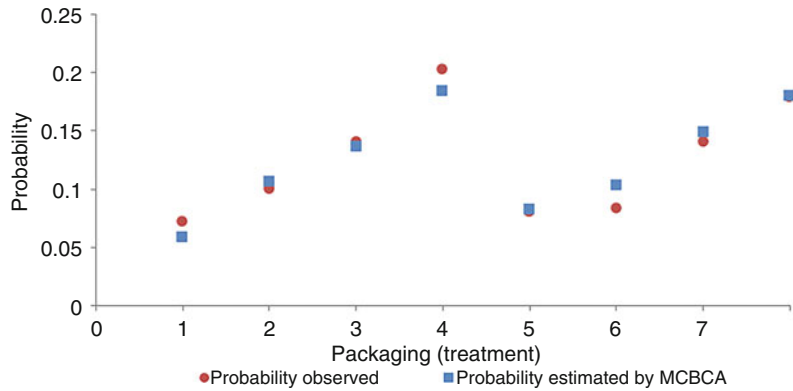
The probability of the consumers choosing a package with the volume “360 mL” was 2.436 times greater than the probability of them choosing a package with the volume “600 mL.” The probability of the consumers choosing a package with the color “green” was 3.449 times greater than the probability of them choosing a package with the color “amber.”

Table 5 and Fig. 3 show the congruence between the observed Choice Probabilities values and those estimated by the MCBCA for each study treatment.

The results recorded for the MCBCA show that treatment 4 (Fig. 3), referring to the packaging with the characteristics “glass,” “350 mL,” and “green,” possessed the highest estimated probability of Consumer choices ( $p = 0.1840$ ), followed by treatment 8 ( $p = 0.1803$ , Table 5). Both treatments generated estimated probabilities with rather close values and only differed regarding the material factor; that is, package 8 was made of PET material and package 4 was made of glass material. Therefore, these packages are likely to have a greater positive impact on consumers’ choice of beer.

**Table 5**  
**Observed and estimated probabilities by Modified choice-based conjoint analysis (MCBCA) for the treatments under study**

| Treatment | Observed probability | Estimated probability by MCBCA |
|-----------|----------------------|--------------------------------|
| 1         | 0.0724               | 0.0582                         |
| 2         | 0.1004               | 0.1065                         |
| 3         | 0.1406               | 0.1368                         |
| 4         | 0.2028               | 0.1840                         |
| 5         | 0.0806               | 0.0821                         |
| 6         | 0.0839               | 0.1031                         |
| 7         | 0.1405               | 0.1490                         |
| 8         | 0.1788               | 0.1803                         |



**Fig. 3** Observed and estimated probabilities for the study packaging

## 4 Notes

1. All research with human beings must be previously approved by an Ethics Committee. Typically, participants are required to sign a Consent Form. Consult the Ethics Committee for Research with Human Beings of the place where the research will be carried out.
2. Care should be taken to select only the relevant characteristics because a large number of factors and levels result in a large number of treatments (packaging samples) to be evaluated, which makes the analysis more complex for the evaluators and can affect the reliability of the results.
3. For more information on Focus Groups, read Chap. 16 by Lawless and Heymann [14].
4. The use of the complete factorial may become impracticable with the increase in the number of factors and levels due to the increase in the number of treatments to be analyzed by the evaluators. For example, in the case study presented, with three factors and each of them with two levels, we will have eight treatments. If we add one more factor with two levels, the number of treatments increases to 16. In this case, the evaluators would have to analyze 16 packaging samples and indicate which one would be chosen, and it is a more complex and laborious task than analyzing only eight samples. The increase in the number of treatments increases the complexity of the analysis to be made by the evaluators and, consequently, decreases the reliability of the results obtained.

As a suggestion, the use of three factors, each with two levels, as in the case study presented, has been quite satisfactory in packaging choice studies.

5. The experimental design proposed by MacFie et al. [16] is recommended because it ensures that each sample appears the same number of times in each position, in addition to being successive, and preceded, the same number of times by the other packages. In this way, the effect of the order of presentation of the packages and the residual effect, characterized by the influence of a treatment in the evaluation of the subsequent one, are eliminated.
6. Generally, three repetitions are sufficient to estimate the experimental error.
7. In the sensory evaluation, the evaluators are the instruments of analysis; therefore, characterizing the profile of the participants is necessary. The basic information needed is the age, gender, and frequency of consumption of the product under study. Some information that can also be requested, according to the research interest, is the level of education, monthly family income, occupation, and consumption habits of the product to be analyzed.

---

### Annex 1 – Presentation Design for 8 Treatments

| Session | Order of presentation |   |   |   |   |   |   |   |
|---------|-----------------------|---|---|---|---|---|---|---|
|         | 1                     | 2 | 3 | 4 | 5 | 6 | 7 | 8 |
| 1       | 5                     | 4 | 8 | 7 | 1 | 2 | 6 | 3 |
| 2       | 8                     | 5 | 1 | 4 | 6 | 7 | 3 | 2 |
| 3       | 4                     | 7 | 5 | 2 | 8 | 3 | 1 | 6 |
| 4       | 3                     | 6 | 2 | 1 | 7 | 8 | 4 | 5 |
| 5       | 7                     | 2 | 4 | 3 | 5 | 6 | 8 | 1 |
| 6       | 6                     | 1 | 3 | 8 | 2 | 5 | 7 | 4 |
| 7       | 2                     | 3 | 7 | 6 | 4 | 1 | 5 | 8 |
| 8       | 1                     | 8 | 6 | 5 | 3 | 4 | 2 | 7 |
| 9       | 1                     | 7 | 5 | 8 | 3 | 4 | 6 | 2 |
| 10      | 7                     | 8 | 1 | 4 | 5 | 2 | 3 | 6 |
| 11      | 6                     | 3 | 2 | 5 | 4 | 1 | 8 | 7 |
| 12      | 8                     | 4 | 7 | 2 | 1 | 6 | 5 | 3 |
| 13      | 5                     | 1 | 3 | 7 | 6 | 8 | 2 | 4 |
| 14      | 2                     | 6 | 4 | 3 | 8 | 5 | 7 | 1 |
| 15      | 4                     | 2 | 8 | 6 | 7 | 3 | 1 | 5 |
| 16      | 3                     | 5 | 6 | 1 | 2 | 7 | 4 | 8 |

(continued)

| Session | Order of presentation |   |   |   |   |   |   |   |
|---------|-----------------------|---|---|---|---|---|---|---|
|         | 1                     | 2 | 3 | 4 | 5 | 6 | 7 | 8 |
| 17      | 2                     | 6 | 5 | 1 | 7 | 3 | 4 | 8 |
| 18      | 7                     | 5 | 4 | 2 | 8 | 6 | 3 | 1 |
| 19      | 5                     | 2 | 7 | 6 | 4 | 1 | 8 | 3 |
| 20      | 1                     | 3 | 6 | 8 | 2 | 4 | 5 | 7 |
| 21      | 6                     | 1 | 2 | 3 | 5 | 8 | 7 | 4 |
| 22      | 4                     | 7 | 8 | 5 | 3 | 2 | 1 | 6 |
| 23      | 8                     | 4 | 3 | 7 | 1 | 5 | 6 | 2 |
| 24      | 3                     | 8 | 1 | 4 | 6 | 7 | 2 | 5 |
| 25      | 6                     | 1 | 3 | 4 | 8 | 5 | 7 | 2 |
| 26      | 8                     | 3 | 7 | 6 | 2 | 1 | 5 | 4 |
| 27      | 5                     | 2 | 4 | 7 | 1 | 8 | 6 | 3 |
| 28      | 2                     | 7 | 5 | 8 | 4 | 3 | 1 | 6 |
| 29      | 1                     | 4 | 6 | 5 | 3 | 2 | 8 | 7 |
| 30      | 3                     | 6 | 8 | 1 | 7 | 4 | 2 | 5 |
| 31      | 7                     | 8 | 2 | 3 | 5 | 6 | 4 | 1 |
| 32      | 4                     | 5 | 1 | 2 | 6 | 7 | 3 | 8 |
| 33      | 4                     | 1 | 2 | 7 | 5 | 6 | 8 | 3 |
| 34      | 7                     | 6 | 1 | 3 | 4 | 8 | 2 | 5 |
| 35      | 3                     | 8 | 6 | 5 | 7 | 2 | 1 | 4 |
| 36      | 1                     | 7 | 4 | 6 | 2 | 3 | 5 | 8 |
| 37      | 5                     | 2 | 8 | 4 | 3 | 1 | 6 | 7 |
| 38      | 6                     | 3 | 7 | 8 | 1 | 5 | 4 | 2 |
| 39      | 2                     | 4 | 5 | 1 | 8 | 7 | 3 | 6 |
| 40      | 8                     | 5 | 3 | 2 | 6 | 4 | 7 | 1 |
| 41      | 6                     | 1 | 5 | 8 | 3 | 4 | 2 | 7 |
| 42      | 3                     | 5 | 2 | 6 | 7 | 1 | 4 | 8 |
| 43      | 5                     | 6 | 3 | 1 | 2 | 8 | 7 | 4 |
| 44      | 1                     | 8 | 6 | 4 | 5 | 7 | 3 | 2 |
| 45      | 8                     | 4 | 1 | 7 | 6 | 2 | 5 | 3 |
| 46      | 7                     | 2 | 4 | 3 | 8 | 5 | 1 | 6 |
| 47      | 4                     | 7 | 8 | 2 | 1 | 3 | 6 | 5 |
| 48      | 2                     | 3 | 7 | 5 | 4 | 6 | 8 | 1 |

Source: MacFie et al. [16]

## References

1. Simmonds G, Woods AT, Spence C (2019) 'Shaping perceptions': exploring how the shape of transparent windows in packaging designs affects product evaluation. *Food Qual Prefer* 75:15–22. <https://doi.org/10.1016/j.foodqual.2019.02.003>
2. Della Lucia SM (2005) Conjoint analysis no estudo de mercado de café orgânico. Dissertation (Master in Food Science and Technology)—Brazil: Federal University of Viçosa, Viçosa—MG. 86 pp
3. Choi Y, Lee J (2019) The effect of extrinsic cues on consumer perception: a study using milk tea products. *Food Qual Prefer* 71:343–353. <https://doi.org/10.1016/j.foodqual.2018.08.004>
4. Della Lucia SM, Minim VPR, Silva CHO, Minim LA, Ceresino EB (2010) Expectativas geradas pela marca sobre a aceitabilidade de cerveja: Estudo da interação entre características não sensoriais e o comportamento do consumidor. *Bol Cent Pesqui Process Aliment* 28: 11–24. <https://doi.org/10.5380/cep.v28i1.17893>
5. Pinto VRA, Freitas TBO, Dantas MIS, Della Lucia SM, Melo LF, Minim VPR, Bressan J (2017) Influence of package and health-related claims on perception and sensory acceptability of snack bars. *Food Res Int* 101:103–113. <https://doi.org/10.1016/j.foodres.2017.08.062>
6. Della Lucia SM (2008) Métodos estatísticos para avaliação da influência de características não sensoriais na aceitação, intenção de compra e escolha do consumidor. Thesis (PhD in Food Science and Technology)—Brazil: Federal University of Viçosa, Viçosa—MG. 116 pp
7. Ballco P, De-Magistris T, Caputo V (2019) Consumer preferences for nutritional claims: an exploration of attention and choice based on an eye-tracking choice experiment. *Food Res Int* 116:37–48. <https://doi.org/10.1016/j.foodres.2018.12.031>
8. Della Lucia SM, Minim VPR (2018) Grupo de foco. In: Minim VPR (ed) *Análise sensorial: estudos com consumidores*, 4th edn. Editora UFV, Viçosa, pp 86–112
9. Hair Junior JF, Anderson RE, Tatham RL, Black WC (1995) *Conjoint Analysis*. In: Hair Junior JF, Anderson RE, Tatham RL, Black WC *Multivariate data analysis with readings*, 4th ed. Englewood Cliss: Prentice Hall, 556–615
10. Steenkamp JBEM (1987) Conjoint measurement in ham quality evaluation. *J Agric Econ* 38:473–480. <https://doi.org/10.1111/j.1477-9552.1987.tb01065.x>
11. Lima Filho T, Della Lucia SM, Lima RM, Minim VPR (2015) Conjoint analysis as a tool to identify improvements in the packaging for irradiated strawberries. *Food Res Int* 72:126–132. <https://doi.org/10.1016/j.foodres.2015.03.023>
12. Carneiro JDS, Silva CHO, Della Lucia SM, Minim VPR (2018) Análise conjunta de fatores. In: Minim VPR (ed) *Análise sensorial: estudos com consumidores*, 4th edn. Editora UFV, Viçosa, pp 191–242
13. Della Lucia SM, Minim VPR, Silva CHO, Minim LA (2018) Características não sensoriais e o comportamento do consumidor: Conceitos e métodos estatísticos de avaliação. In: Minim VPR (ed) *Análise sensorial: estudos com consumidores*, 4th edn. Editora UFV, Viçosa, pp 148–190
14. Lawless HT, Heymann H (2010) *Sensory evaluation of food: principles and practices*, 2nd edn. Springer, New York. 596p
15. Green PE, Srinivasan V (1978) Conjoint analysis in consumer research: issues and outlook. *J Consum Res* 5:103–123. <https://doi.org/10.1086/208721>
16. MacFie HJ, Bratchell N, Greenhoff K, Vallis LV (1989) Designs to balance the effect of order of presentation and first-order carry-over effects in hall tests. *J Sens Stud* 4(2): 129–148. <https://doi.org/10.1111/j.1745-459X.1989.tb00463.x>
17. McFadden D (1974) Conditional logit analysis of qualitative choice behaviour. In: Zarembka P (ed) *Frontiers in econometrics*. Academic, New York, pp 105–142
18. Agresti A (1990) *Categorical data analysis*. Wiley, New York. 558 p



## Thermal Performance of Food Packaging Containing Phase Change Materials

Bianca C. N. Fernandes and Ana S. Prata

### Abstract

The thermal performance of thermo-active food packaging is a key factor in ensuring its successful application. The enthalpy (latent heat) and temperature of fusion of the phase change materials (PCMs) must be certified to match the payload requirements. The PCM-functionalized material also must be characterized through kinetic experiments in a near-real application experimental setup. Reliable and comparable protocols for these characterizations are proposed in this chapter.

**Key words** Thermo-active packaging, Phase transitions, Temperature control, Thermal conductivity, Melting point, Thermal storage, Phase change packaging

---

### 1 Introduction

Phase change materials or PCMs are employed for developing temperature control packaging systems for the shipment or consumption of temperature-sensitive goods in various temperature ranges for food, pharmaceuticals, and life science industries [1–5]. They reliably keep the temperature inside the packaging stable, preventing it from falling below or exceeding a certain mark.

The PCM's state transition between liquid and solid states maintains a constant temperature equal to their melting/freezing points—mind that these are often temperature ranges instead of single temperatures. Several PCMs can be found as candidates to develop packaging systems, chosen to change phases at specific temperatures to match the payload requirements, but some commercial PCMs are unsuitable for food packaging or cold chain technologies due to the pungent odors, flammability, reduced cycling stability, and corrosive nature [6, 7].

Many organic compounds are suitable PCMs as they have good latent heat ( $160\text{--}190\text{ J g}^{-1}$ ), thermal and chemical stabilities, recyclability, noncorrosiveness, no subcooling properties, and

operating temperature within the major applications for human consumption. The melting point can be chosen for frozen ( $-18^{\circ}\text{C}$ ), refrigerated ( $2\text{--}8^{\circ}\text{C}$ ), room temperatures ( $25^{\circ}\text{C}$ ), or warm products for consumption ( $50^{\circ}\text{C}$ ). The PCM-based packaging systems developed nowadays are focused on the cold chain and large containers [8–13], but the absorption or encapsulation of the PCM into structured materials has been used to confine the PCMs, increasing their heat storage capacity. In the case of capsules, the reduction of particle dimensions allows achieving a high surface area-to-volume ratio, increasing the heat transfer [14–20], and hence thermal conductivity [21–24].

Normally, differential scanning calorimetry (DSC) measurements are employed to determine the main thermo-physical properties of PCM-loaded particles [16–18, 25–27]. Thermal conductivity, on the other hand, is of extremely difficult measurement due to the phase change and the limitations of available equipment for measurement, being many times determined (i) by numerical simulations, which are normally simplified due to the complexity [28], or (ii) indirectly by determining other thermo-physical properties, which also do not consider the differences from the solidification process driven by heat conduction and the melting process, dominated by the natural convection [29]. Some experimental alternatives for measuring the thermal conductivity in the liquid phase include the hot disk [23, 30] and hot wire [8, 12, 31–34] instruments.

The best way to experimentally determine the thermal performance of packaging systems is to reproduce the real systems and follow the temperature evolution at different points through a data acquisition system [8, 12, 31–34]. Then, the effective thermal management solutions will depend on (i) the thermal conductivity of both phases (i.e., liquid and solid), (ii) the optimum starting temperature condition determined by the melting point, (iii) the thermal stability, and (iv) the overall heat gained or lost by the packaging material, determined by the experimental setup that is depicted below.

---

## 2 Materials

### 2.1 Packaging Functionalization

1. PCM particles with a melting point of  $79^{\circ}\text{C}$  (we showcase packaging materials functionalized with 2-mm-diameter particles made up of commercial type-3 pale-yellow carnauba wax, extruded up to the softening point ( $60^{\circ}\text{C}$ ), and coated with an alginate solution in a fluidized bed [14], but this protocol can be extended to other encapsulated phase change packaging systems).

2. Two polymer (e.g., cellulose) cups with the same dimensions, one of which with the bottom removed.
3. Plastic adhesive.

### **2.2 Thermal Stability of the PCM Particles**

1. Thermogravimetric (TG), derivative TG (DTG), and DSC apparatuses.
2. Gases: oxygen and nitrogen.
3. Scale with precision of 10 mg.
4. Standard aluminum sample pans and lids.

### **2.3 Thermal Conductivity of the Packaging Material (Heat-Flow-Meter Method)**

1. Pencil, scissors, ruler, and caliper.
2. Heat-generating device.
3. Heavy marble plate with low thermal conductivity ( $k = 2.5 \text{ W m}^{-1} \text{ }^\circ\text{C}^{-1}$ ).
4. T-type thermocouples (precision of  $\pm 0.2 \text{ }^\circ\text{C}$ ).
5. Heat flux sensor ( $D = 0.06 \text{ m}$ ).
6. Insulator (e.g., ceramic fiber blanket).
7. Voltage variator (single phase, 20 A current, 2.5 kVA capacity).
8. Data Logger (AHLBORN model 2390-5).

### **2.4 Thermal Performance of the Packaging Material**

1. K-type thermocouples (precision  $\pm 0.5 \text{ }^\circ\text{C}$ ).
2. Thermal tape.
3. Thermostatic bath (DC-6515).
4. Data logger (Testo 177-T4, Brazil).
5. Commercial soybean oil (or other food according to the application).

---

## **3 Methods**

### **3.1 Packaging Functionalization**

1. Distribute uniformly a determined mass of particles (e.g., 10 g of particles) onto the external surface of the cup (e.g., diameter, 4 cm; height, 5 cm)—Fig. 1a.
2. Fix them with the adhesive.
3. Keep the system stand at least for 3 h at 25 °C, for drying.
4. Remove the bottom of the other cup and place the PCM-containing cup (serves as a shell) inside the bottomless cup (serves as outer shell)—the PCM particles will be enclosed within the annular space between the two concentric cups (Fig. 1b).





**Fig. 1** Packaging functionalization: (a) Particles distributed onto the external surface of the cup and the cup without bottom; (b) final packaging

### 3.2 Thermal Stability of the PCM Particles

1. Switch on the calorimeter and allow it to equilibrate for at least 30 min before the analysis; the calibration should be realized prior the measurements.
2. Adjust the pressure of the oxygen ( $50 \text{ mL min}^{-1}$ ) and nitrogen gas supplies according to the manufacturer's recommendations.
3. Set the run parameters: heating rate of  $10 \text{ }^\circ\text{C min}^{-1}$ , from 25 to  $600 \text{ }^\circ\text{C}$  (*see Note 1*);
4. Accurately weigh the sample pans and lids. An empty reference set of pan+lid must be employed (*see Note 2*).
5. Accurately weigh 10 mg of PCM particles in the pans, hermetically seal them, and record the final mass (pan + sample + lid) (*see Note 3*).
6. Enter the sample information (e.g., mass of particles, name) in the acquisition software.
7. Retrieve raw data from the experiment and treat as follows:
  - (a) Perform peak integration in order to obtain the values for enthalpy of fusion ( $\Delta H$ ) (*see Note 4*).
  - (b) From the endothermic peak, the minimum point (far from baseline) is taken as the melting temperature,  $T_m$ . For mixtures, this point defines the liquidus curve in the phase diagram (*see Note 5*).
  - (c) From the simultaneous TG and DSC apparatus, TG/DTG curves, it is taken the thermal stability and degradation temperature of the material, i.e., onset temperatures corresponding to the temperature to which 5% of the mass of the sample has evaporated or decomposed (*see Note 6*).

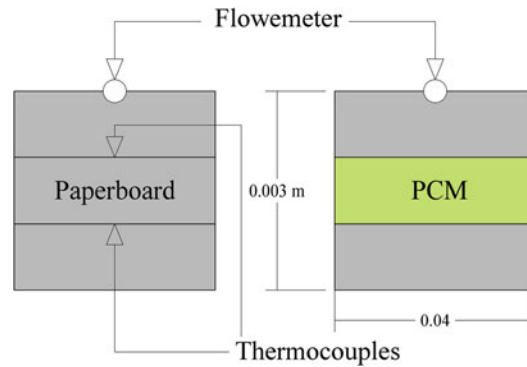
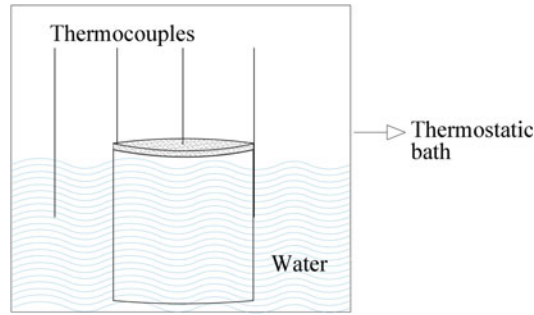


Fig. 2 Schematic experimental setup

### 3.3 Thermal Conductivity of the Packaging Material (Heat-Flow-Meter Method)

1. Shape the packaging material into 0.04-m-side squares with homogeneous thickness (*see Note 7*).
2. Measure sample thickness at least three different points and calculate the average value.
3. Calibrate the T-type thermocouples at five different temperatures (e.g., 0, +15, +25, +70, and +90 °C).
4. Place the samples between the heat-generating device on the bottom and the marble plate on top to compress the sample set and ensure contact (Fig. 2).
5. Install thermocouples at the interfaces (bottom and top) of the sample with the paper, and the flowmeter (on the top).
6. Enclose the system in a thermal insulator to eliminate lateral heat losses and guarantee the heat flow in the axial direction of the sample.
7. Turn on the heat-generating device using a voltage variator until a steady flow is reached (constant power supply of 700 W).
8. Record the data of temperature using the data logger coupled to the heat flux sensor and the thermocouples; the temperature is constant at temperatures around  $T_m$ .
9. Validate the measurement system using reference materials (*see Note 8*).
10. Calculate the thermal conductivity ( $k$ ) of the sample [ $\text{W m}^{-1} \text{ }^\circ\text{C}^{-1}$ ] that comes from unidimensional and steady-state Fourier equation (Eq. 1). From a known electric power supply ( $q$ ) and  $dT$ , the thermal conductivity ( $k$ ) is determined.

$$k = \frac{e \cdot q}{dT} \quad (1)$$



**Fig. 3** Schematic experimental setup

where  $dT$  is the temperature difference at the top and the bottom of the sample [ $^{\circ}\text{C}$ ];  $q$  is the heat flow [ $\text{W m}^{-2}$ ]; and  $e$  is the thickness [m]. Uncertainty of experiments was found to be in the range of  $\pm 2.5\%$ .

### 3.4 Thermal Performance

#### 3.4.1 Experimental Setup

1. Calibrate  $K$ -type thermocouples at five different temperatures (e.g., 0, +15, +25, +70, and +90  $^{\circ}\text{C}$ ).
2. Place them in different positions at the middle height of the package: inner surface, external surface, geometric center, and one in the external environment (*see Note 7*).
3. Attach them with a thermal tape to ensure the contact with the wall.

#### 3.4.2 Activation of PCM in Empty Cups

1. Place water in a thermostatic bath (DC-6515) and keep the temperature constant at 90  $^{\circ}\text{C}$ .
2. Put the empty cup in a way that the water reaches almost the border of the cup (Fig. 3).
3. Record the temperature evolution through a Datalogger by measuring the temperature every 3 s. When the thermocouple placed on the internal wall reaches 90  $^{\circ}\text{C}$ , keep the system in the water for an additional 20 min.
4. Remove the cup from the bath and place it at room temperature (ca. 25  $^{\circ}\text{C}$ ).
5. Record the temperature until it reaches 40  $^{\circ}\text{C}$ , i.e., far from the phase transition temperature of carnauba wax (79  $^{\circ}\text{C}$ ).
6. Repeat the steps above with the control (double cups without PCM particles).

#### 3.4.3 Activation of PCM in Filled Cups

1. Fill the volume of the cup with commercial soybean oil.
2. Employ an external resistance (127 V, titanium) into the oil for heating it to ca. 100  $^{\circ}\text{C}$  (Fig. 4).
3. Remove the external resistance from the cup.

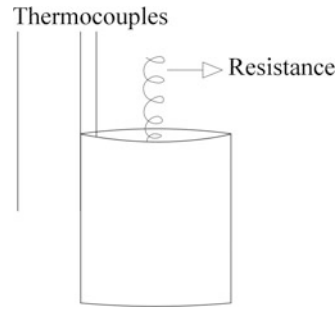


**Fig. 4** Schematic experimental setup

4. Record the temperature of cooling through a Datalogger (Testo 177-T4, Brazil) by measuring the temperature every 3 s.
5. Record the temperature until it reaches 25 °C, i.e., far from the phase transition temperature of carnauba wax (79 °C).
6. Repeat the steps above with the control (double cups without PCM particles).

---

## 4 Results

1. DSC is performed in a restricted temperature range to highlight the phase transition thermal event (the crystallization peak) of the PCM.
2. TG is useful for obtaining information on the physicochemical properties of different materials and its decomposition as a function of temperature.
3. The PCM application depends on the thermal conductivity. The greater the conductivity of the PCM, the greater the heat transfer from the particles to the packaging.
4. Comparing the behavior of the temperature in the empty cups and in the cups with oil, it is possible to verify the similarity in the cooling curves. Besides that, it is possible to observe that the packaging maintains the heat in the interior for a longer period when compared to the cups without PCM.

---

## 5 Notes

1. This rate was employed because of its good compromise between time and signal-to-noise ratio. Rates varying from 0.5 to 10 °C min<sup>-1</sup> were reported [35–38]. The operator may decrease it for more accurate signals. The temperature range may also be shifted depending on the PCM system and the target application.

2. Check the compatibility of the pan material with the PCM.
3. Both the mass of the empty pan and the poured sample have been measured using a scale with a maximum tolerance of  $\pm 0.001$  mg. This weight is suggested and should cover the bottom of the pan to ensure proper heat transfer. The heating rate is reported to be dependent on the mass and type of sample [39]. Larger amounts of particles improve the performance of measurement. If the sample is liquid, a syringe, or a disposable pipette (made of glass or plastic) can be used to measure the weight in the pan. Estimative value of 5  $\mu\text{L}$ . Thermal degradation may be higher under different exposition conditions. Open pan may be employed in nitrogen/oxygen mixture or inert atmosphere to evaluate the thermal behavior of samples [35].
4. Enthalpy of transition is obtained by integrating the area formed under the peak by placing a stable baseline in the endothermic event.
5. The melting point should also be taken from the interception of the extrapolated slope of the melting curve and the baseline of the peak (onset temperature— $T_{\text{onset}}$ ).  $T_{\text{onset}}$  is normally employed for pure substances. The same procedure can be used for the crystallization temperature in the exothermic peak for the evaluation of the subcooling effect.
6. The mass loss is determined by the difference in mass observed by the thermal event observed. The limit for this quantification is established by tracing two tangent horizontal lines over the TG curve, which defines the region of the thermal event. The first derivative of the mass loss curve, DTG curve, is used to locate the thermal event [36].
7. This dimension is suggested. Alternatively, place the PCM particles in a set of two external layers of paperboard or other packaging material. Transient hot wire (THW) method has been employed in the literature [37].
8. The Heat-Flow-Meter method is suitable for thermal conductivity determinations of packaging material, but it is always important that the experimental setup is validated. This can be done by repeating the procedure described in Subheading 3.3 using materials featuring the same thickness as the analyzed sample as well as known thermal conductivities. For example, polyurethane foam (low conductivity:  $0.035 \text{ W m}^{-1} \text{ K}^{-1}$ ) and rigid poly(vinyl chloride) films (intermediate conductivity:  $0.19 \text{ W m}^{-1} \text{ K}^{-1}$ ).
9. Thermocouples must be employed to measure the environment (ca.  $25 \text{ }^\circ\text{C}$ ) and the bulk temperature of the liquid as well. Attach them with a thermal tape to ensure the contact with the wall.

## References

1. Elliott MA, Halbert GW (2005) Maintaining the cold chain shipping environment for Phase I clinical trial distribution. *Int J Pharm* 299:49–54
2. Singh S, Gaikwad KK, Suk Y (2018) Phase change materials for advanced cooling packaging. *Environ Chem Lett* 16:845–859
3. Kahwaji S, Johnson MB, Kheirabadi AC et al (2017) Fatty acids and related phase change materials for reliable thermal energy storage at moderate temperatures. *Sol Energy Mater Sol* 167:109–120
4. Carson JK, East AR (2017) The cold chain in New Zealand—a review. *Int J Refrig* 87:185–192
5. Liu M, Saman W, Bruno F (2012) Review on storage materials and thermal performance enhancement techniques for high temperature phase change thermal storage systems. *Renew Sust Energ Rev* 16:2118–2132
6. Sharma A, Tyagi VV, Chen CR et al (2009) Review on thermal energy storage with phase change materials and applications. *Renew Sust Energ Rev* 13:318–345
7. Cabeza LF, Roca J, Nogués M et al (2002) Immersion corrosion tests on metal-salt hydrate pairs used for latent heat storage in the 48 to 58 °C temperature range. *Mater Corros* 53:902–907
8. Oró E, Cabeza LF, Farid MM (2013) Experimental and numerical analysis of a chilly bin incorporating phase change material. *Int J Refrig* 58:61–67
9. Lu YL, Zhang WH, Yuan P et al (2010) Experimental study of heat transfer intensification by using a novel combined shelf in food refrigerated display cabinets (Experimental study of a novel cabinets). *Appl Therm Eng* 30:85–91
10. Oró E, Miró L, Farid MM et al (2012) Improving thermal performance of freezers using phase change materials. *Int J Refrig* 35:984–991
11. Oro E, de Gracia A, Cabeza LF (2013) Active phase change material package for thermal protection of ice cream containers. *Int J Refrig* 36:102–109
12. Hoang HM, Leducq D, Pérez-Masia R et al (2015) Heat transfer study of submicro-encapsulated PCM plate for food packaging application. *Int J Refrig* 52:151–160
13. Alzuwaid F, Ge YT, Tassou SA et al (2015) The novel use of phase change materials in a refrigerated display cabinet: an experimental investigation. *Appl Therm Eng* 75:770–778
14. Hawlader MNA, Uddin MS, Khin MM (2003) Microencapsulated PCM thermal-energy storage system. *Appl Energy* 74:195–202
15. Paulo BB, Andreola K, Taranto O et al (2019) Coating approach for a Phase Change Material (PCM). *Powder Technol* 341:147–156
16. Chalco-Sandoval W, Fabra MJ, López-Rubio A et al (2015) Optimization of solvents for the encapsulation of a phase change material in polymeric matrices by electro-hydrodynamic processing of interest in temperature buffering food applications. *Eur Polym J* 72:23–33
17. Chalco-Sandoval W, Fabra MJ, Lopez-Rubio A et al (2017) Use of phase change materials to develop electrospun coatings of interest in food packaging applications. *J Food Eng* 192:122–128
18. Pérez-mMasía R, López-Rubio A, Lagarón JM (2013) Development of Zzein-based heat-management structures for smart food packaging. *Food Hydrocoll* 30:182–191
19. Mccann JT, Marquez M, Xia Y (2006) Melt coaxial electrospinning: a versatile method for the encapsulation of solid materials and fabrication of phase change nanofibers. *Nano Lett* 6:2868–2872
20. Johnston JH, Grindrod JE, Dodds M et al (2008) Composite nano-structured calcium silicate phase change materials for thermal buffering in food packaging. *Curr Appl Phys* 8:508–511
21. Wang Y, Zhang X, Ji J et al (2019) Thermal conductivity modification of n-octanoic acid-myristic acid composite phase change material. *J Mol Liq* 288:111092
22. Sheikholeslami M, Keshteli AN, Babazadeh H (2020) Nanoparticles favorable effects on performance of thermal storage units. *J Mol Liq* 300:112329
23. Wang J, Xie H, Xin Z et al (2010) Enhancing thermal conductivity of palmitic acid based phase change materials with carbon nanotubes as fillers. *Sol Energy* 84:339–344
24. Sahan N, Paksoy HO (2014) Thermal enhancement of paraffin as a phase change material with nanomagnetite. *Sol Energy Mater Sol* 126:56–61
25. Chalco-Sandoval W, Fabra MJ, López-Rubio A et al (2014) Electrospun heat management polymeric materials of interest in food refrigeration and packaging. *J Appl Polym Sci* 131:40661(1–11)
26. Chalco-Sandoval W, Fabra MJ, López-Rubio A et al (2015) Development of polystyrene-based

- films with temperature buffering capacity for smart food packaging. *J Food Eng* 164:55–62
27. Pérez-Masiá R, López-Rubio A, Fabra MJ et al (2014) Use of electrohydrodynamic processing to develop nanostructured materials for the preservation of the cold chain. *Innov Food Sci Emerg Technol* 26:415–423
  28. Wang G, Wei G, Xu C et al (2019) Numerical simulation of effective thermal conductivity and pore-scale melting process of PCMs in foam metals. *Appl Therm Eng* 147:464–472
  29. Karim Y el, Grosu Y, Faik A et al (2019) Investigation of magnesium-copper eutectic alloys with high thermal conductivity as a new PCM for latent heat thermal energy storage at intermediate-high temperature. *J Energy Storage* 26:100974
  30. Xie H, Gu H, Fujii M et al (2006) Short hot wire technique for measuring thermal conductivity and thermal diffusivity of various materials. In: *Measurement science and technology*. Institute of Physics Publishing, pp 208–214
  31. Lu W, Tassou SA (2013) Characterization and experimental investigation of phase change materials for chilled food refrigerated cabinet applications. *Appl Energy* 112:1376–1382
  32. Oró E, Miró L, Farid MM et al (2012) Thermal analysis of a low temperature storage unit using phase change materials without refrigeration system. *Int J Refrig* 1709–1714
  33. Vennapusa JR, Konala A, Dixit P et al (2020) Caprylic acid based PCM composite with potential for thermal buffering and packaging applications. *Mater Chem Phys* 253:123453
  34. Kozak Y, Farid M, Ziskind G (2017) Experimental and comprehensive theoretical study of cold storage packages containing PCM. *Appl Therm Eng* 115:899–912
  35. Haillot D, Bauer T, Kröner U et al (2011) Thermal analysis of phase change materials in the temperature range 120–150 °C. *Thermochim Acta* 513:49–59
  36. Müller L, Rubio-Pérez G, Bach A et al (2020) Consistent DSC and TGA methodology as basis for the measurement and comparison of thermo-physical properties of phase change materials. *Materials* 13:1–20
  37. Harish S, Orejon D, Takata Y et al (2015) Thermal conductivity enhancement of lauric acid phase change nanocomposite with graphene nanoplatelets. *Appl Energy* 80:205–211
  38. Pielichowski K, Flejtuch K (2002) Differential scanning calorimetry studies on poly(ethylene glycol) with different molecular weights for thermal energy storage materials. *Polym Adv Technol* 13:690–696
  39. Castellon C, Gunther E, Mehling H et al (2008) Determination of the enthalpy of PCM as a function of temperature using a heat-flux DSC—a study of different measurement procedures and their accuracy. *Int J Energy Res* 33:1258–1265

# INDEX

## A

- Absorbance
  - ORAC (*see* Oxygen Radical Absorbance Capacity (ORAC))
- Acceptance (sensory) ..... 337–346
- Acetyl tributyl citrate ..... 76
- Active (differs from bioactive)
  - agent ..... 311–323
  - packaging ..... 116, 280, 282, 303, 311, 312, 314–316
- Adhesive ..... 75, 79, 83, 88, 121, 122, 129, 186, 199, 367
- Affective method ..... 339
- Agglomeration ..... 172, 174, 175
- Alternating least square (ALS) ..... 107, 184
- Analysis of variance (ANOVA) ..... 343–345
- Antimicrobial activity
  - antibacterial assays
    - disk susceptibility test ..... 281
    - Kirby-Bauer disk diffusion test ..... 281, 282, 288
  - antifungal assays
    - Agar diffusion test ..... 261, 265–267
    - disk diameter test ..... 261, 265–267
    - film surface inoculation test ..... 262, 267
    - plate counting germination test ..... 262, 265, 268
- Antioxidant activity
  - ABTS assay/TEAC ..... 294, 295, 297–300, 303–305
  - DPPH assay ..... 295–298, 301–303
  - FRAP assay ..... 295–296, 304–306
  - ORAC assay ..... 296, 300–302, 306–307
- Arrhenius ..... 221
- Assimilation, *see* Bioassimilation
- Attribute (sensory)
  - appearance ..... 340, 344, 345
  - aroma ..... 340, 344, 345
  - color ..... 168, 340
  - flavor ..... 168, 340, 344, 345
  - overall impression ..... 340, 344, 345
  - taste ..... 168, 340
  - texture ..... 168, 340, 344, 345

## B

- Barrier properties
  - barrier to gases ..... 225
  - barrier to microorganism ..... 233
  - barrier to moisture ..... 109, 208
- Bioactive
  - compound ..... 326
  - packaging
    - prebiotic ..... 325–334
    - probiotic ..... 325–334
- Bioassimilation ..... 28
- Biobased packaging ..... 3, 4
- Biodegradable packaging/plastic
  - oxo-biodegradable packaging (*see* Oxo-biodegradable)
- Biodegradation
  - in compost ..... 29, 34, 57
  - in marine water ..... 5, 12–14, 29
  - in soil ..... 5, 11, 29, 30, 34
- Biodeterioration/bioerosion ..... 28, 29
- Biofilm ..... 28, 65, 69
- Biofragmentation ..... 28, 29
- Bisphenol ..... 91, 119, 121, 127

## C

- Calorimetry ..... 23
- Carbon dioxide (CO<sub>2</sub>)
  - headspace (*see* Modified atmosphere packaging)
  - permeability ..... 225–227, 230
  - respiration (*see* Respirometry)
  - transmission rate ..... 221
- Cellular structure ..... 28, 170
- Cellulose, *see* Natural polymer
- Chemometrics ..... 67, 184, 187, 190, 191
- Chitosan, *see* Natural polymer
- Choice probability/consumer choice ..... 349–359
- Chromatography
  - combustion ion chromatography (CIC) ..... 103, 104, 107–108
  - gas chromatography (GC) ..... 30, 67, 85, 88, 121, 323
  - liquid chromatography (LC) ..... 88, 102, 124
  - size-exclusion chromatography (SEC) ..... 29



|   |   |  |   |
|---|---|--|---|
| Clausius–Clapeyron equation .....                               | 211   | film .....   | 19, 205,<br>259–276, 325–334, 338   |
| Compostable packaging .....                                     | 101   | packaging .....  | 140, 280, 337–346   |
| Conjoint analysis .....   | 350, 351  | Emulsion .....   | 70, 109, 132, 261,<br>263–265, 271, 274, 275  |
| Consumer  |   |  |   |
| acceptance ( <i>see</i> Acceptance)                             |   |  |   |
| behavior .....  | 350, 351  |  |   |
| choice .....  | 349–359   |  |   |
| Contaminant .....   | 58, 68, 76, 77, 84,<br>100, 102, 115–132, 316, 327, 333   |  |   |
| Cramer’s rules .....  | 91  |  |   |
| Culture medium .....  | 30, 32, 34, 36, 39–45,<br>47, 48, 50, 51, 139, 141, 143, 144, 146, 154,<br>158, 159, 163, 236, 237, 239, 240, 263, 265,<br>282, 283, 285, 326, 327, 329, 330, 334 |  |   |
| Cumulative mass .....   | 319   |  |   |
| Curve resolution .....  | 184, 188, 189   |  |   |
| <b>D</b>  |   | <b>F</b>   |   |
| Damage .....  | 62, 63, 116, 127, 137,<br>150, 151, 161, 168, 170, 177, 337   | Ferric reducing antioxidant power (FRAP),<br><i>see</i> Antioxidant activity |   |
| Data  |   | Fiber .....  | 22, 60, 65, 66,<br>68, 70, 87, 88, 99, 101, 105, 106, 108, 171,<br>173, 174, 338, 367 |
| acquisition .....   | 177, 185, 199, 222, 366   | Fick’s law .....   | 207, 208, 220   |
| binning .....   | 190   | Flexible packaging .....   | 234, 235  |
| processing .....  | 170, 172  | Foam .....   | 22, 65, 102, 170, 372   |
| Defect/imperfection .....                                       | 167–178, 199  | Food simulant .....  | 85–90, 117–119,<br>121–126, 128–131, 314–319, 322                                     |
| Degradation .....   | 16, 17, 22, 23,<br>27–29, 58, 62, 65, 68, 76, 77, 100, 109, 120,<br>293, 314, 337, 368, 372   | Foodborne pathogen .....   | 246, 252,<br>257, 279, 280, 288   |
| Detector .....  | 67, 82, 88, 107, 127,<br>169, 170, 172, 173, 178, 185–187, 190, 199   | Food-contact material (FCM) .....  | 75–79, 81,<br>83, 90, 101, 115–131  |
| Dialkyl phosphate esters (diPAPs) .....                         | 102, 103  | Formaldehyde .....   | 60, 77  |
| Differential scanning calorimetry (DSC), <i>see</i> Calorimetry |   | Fruits and vegetables .....  | 219, 260, 261,<br>268, 270, 274, 279  |
| Diffusion   |   | Fungus/fungi .....   | 4, 27, 239,<br>259, 261, 265, 267–269, 272, 273, 275                                  |
| anomalous .....   | 315   |  |   |
| coefficient .....   | 77, 118, 121, 206,<br>209, 220, 222–224, 312  | <b>G</b>   |   |
| diffusional exponent .....                                      | 319, 320  | Gamma radiation, <i>see</i> Radiation  |   |
| diffusivity .....   | 76, 207, 221,<br>313–315, 320, 323  | Generally recognized as safe (GRAS) .....                                    | 116,<br>268, 269  |
| Digestion   |   | Grayscale .....  | 172, 175  |
| anaerobic .....   | 5, 6, 9, 10, 15   | Grease resistance .....  | 108, 109  |
| chemical .....  | 69, 132   |  |   |
| enzymatic .....   | 62, 159   | <b>H</b>   |   |
| <i>in vitro</i> .....   | 327, 331–333  | Headspace .....  | 12, 14, 23, 89,<br>219, 246, 247, 249, 253, 256, 280, 311, 313                        |
| model .....   | 331   | Heat transfer .....  | 366, 371, 372   |
| Disintegration .....  | 7, 8, 11–13,<br>29, 30, 303, 312  | Hedonic scale/score .....  | 337–346   |
| Distribution map .....  | 193, 194, 197, 198  | Henry’s law .....  | 206, 207  |
| DPPH assay, <i>see</i> Antioxidant activity                     |   | Homogeneity .....  | 194, 197, 198   |
| <b>E</b>  |   | Hydrophilic .....  | 106, 132, 205–217,<br>222, 227, 228, 230, 234, 303, 312                               |
| Edible  |   | Hydrophobic .....  | 99, 105, 106,<br>109, 208, 294, 301, 312  |
| coating .....   | 259–276, 282  | Hypercubes .....   | 185, 187, 188, 191  |
|   |   | Hyperspectral imaging (HSI) .....  | 84, 184–187, 190  |
|   |   | <b>I</b>   |   |
|   |   | Imperfection, <i>see</i> Defect  |   |
|   |   | Inhibition zone .....  | 265, 275,<br>281, 282, 288–290  |
|   |   | Intelligent packaging .....  | 116   |

Intentionally added substances (IAS) .....75–93,  
101, 120, 149  
Interactance ..... 186, 187  
Interface..... 170, 171, 199, 253, 313, 369

**K**

Kinetics  
microbial growth kinetics ..... 247–249  
mineralization/biodegradation kinetics/rate.... 16–17  
release kinetics .....280, 315, 319, 320, 322

**L**

Label ..... 77, 145, 168,  
214, 284, 346, 349, 350  
Lactic acid bacteria (LAB) .....247  
Lambert–Beer law .....169  
Layer  
monolayer.....86, 158, 159  
multilayer .....86, 109, 117,  
122, 129, 220, 245, 313  
Likelihood of choice ..... 353  
Line scanning ..... 187  
*Listeria* ..... 247, 255, 290

**M**

Macropixel..... 197, 198  
Mass transfer.....76, 83, 117, 207,  
211, 216, 247, 313, 314, 321  
McFarland standard .....283, 284, 286, 289, 327,  
330, 333  
Microbial growth kinetics, *see* Kinetics  
Micronucleus test..... 154, 158  
Microorganism-proof packaging.....240  
Microplastics  
primary..... 57, 58, 65  
secondary .....58, 65  
Microscopy  
confocal microscopy..... 84  
electron microscopy ..... 168  
fluorescence microscopy ..... 65  
infrared microscopy..... 30  
optical microscopy ..... 60, 65, 71, 168, 264  
Migration  
overall migration limit (OML)..... 90, 118  
specific migration limit (SML) ..... 76, 78, 90, 131  
Mineral oil hydrocarbons (MOH)  
mineral oil aromatic hydrocarbons  
(MOAH)..... 83, 125  
mineral oil saturated hydrocarbons (MOSH) ..... 83  
Mineralization ..... 16–17, 22, 28–30  
Misalignment..... 172  
Modified atmosphere packaging (MAP) ..... 116,  
219, 245–257

Modified choice-based conjoint analysis  
(MCBCA) ..... 351–354, 356, 358, 359  
Multivariate calibration ..... 189  
Multivariate curve resolution (MCR)..... 184

**N**

Nanotechnology  
nanoparticle ..... 83, 105, 121–132, 261  
nanotube..... 121, 290  
Natamycin.....314, 316–321, 323  
Natural polymer, *see* Polymers  
Near-infrared spectroscopy (NIR), *see* Spectroscopy  
Noise .....172, 174, 177, 192, 341  
Non-intentionally added substances (NIAS).....75–93,  
101, 116, 120, 128, 149  
Non-sensory characteristics ..... 349  
Nonylphenols (NPs) ..... 78  
Nutrient broth..... 153, 155, 156, 235,  
236, 239, 240

**O**

Oleophobic, *see* Hydrophilic  
Orthoslice ..... 171, 174, 176  
Overall migration, *see* Migration  
Oxo-biodegradable .....84, 85  
Oxygen  
oxygen permeability ..... 219, 230  
oxygen radical absorbance capacity  
(ORAC) ..... 294, 300–302, 306–307  
oxygen scavenger..... 311  
oxygen transmission rate ..... 229

**P**

Paperboard ..... 83, 108, 109,  
115, 125, 168, 170, 372  
Partial least squares (PLS) ..... 189, 193  
Partition coefficient..... 118, 313, 314, 321–323  
Pellet ..... 7, 10, 14, 30,  
60, 65, 84, 160, 200, 328  
Permeability  
carbon dioxide (CO<sub>2</sub>) (*see* Carbon dioxide  
permeability)  
oxygen (*see* Oxygen permeability)  
water vapor (*see* Water vapor permeability)  
Permeance ..... 208, 215, 228  
Permeation ..... 219–230, 233–240  
Phase change material (PCM)..... 365–372  
Phthalate.....38, 76, 120,  
121, 123, 128  
Pixel  
dead..... 190  
size ..... 188

Poly- and perfluorinated alkyl substances  
(PFAS)..... 99–109, 121, 149

Polymer

- natural polymer ..... 260, 338
  - cellulose ..... 7, 10, 14, 19,  
21, 23, 32, 43, 50, 66, 171, 185, 186, 189,  
196, 198, 220, 282, 338, 367
  - chitin ..... 338
  - polysaccharide..... 109, 110,  
230, 260, 326, 338
  - starch..... 50, 88, 89
  - zein..... 19, 109
- poly(2,6-diphenyl-p-phenylene oxide) ..... 132
- poly(ethylene terephthalate) (PET) ..... 63,  
69, 77, 83, 121, 123, 352, 353, 357, 359
- poly(lactic acid)/polylactide (PLA) ..... 3, 16,  
17, 31–33, 63, 109, 110
- poly(vinylidene fluoride) (PVDF) ..... 105
- polyamide ..... 60, 69, 90, 128, 222
- polybutylenesuccinate (PBS) ..... 17, 109
- polycaprolactone (PCL)..... 17, 18, 109
- polydimethylsiloxane (PDMS) ..... 109, 225, 226
- polyetheretherketone (PEEK)..... 108
- polyethylene
  - high-density (HDPE) ..... 36, 77, 265
  - low-density (LDPE)..... 17, 20, 36, 39,  
77, 121, 171, 290
- polyhydroxyalkanoate (PHA) ..... 109
- polyhydroxybutyrate (PHB) ..... 17, 18, 109
- polypropylene ..... 36, 37, 41,  
49, 77, 89, 121, 128
- polystyrene
  - expanded polystyrene (EPS)..... 77, 88, 89
- polytetrafluoroethylene (PTFE)..... 66, 70, 108, 186,  
187, 194, 197–199

Pore ..... 28, 70, 132, 142,  
169, 172, 173, 175, 234, 235

Porosity ..... 5, 66, 170

Positive list ..... 90, 91, 120, 123, 131

Postharvest disease control..... 260

Powder ..... 7, 10, 14,  
23, 32, 58, 124, 200, 264

Power law ..... 313, 319, 320

Prebiotic, *see* Bioactive packaging

Predictive microbiology ..... 246–248, 252, 255, 256

Preference mapping ..... 343–345

Pretreatment..... 63, 86, 87,  
103, 169, 187, 189–192, 195

Principal component analysis (PCA)..... 343

Probiotic, *see* Bioactive packaging

Produce..... 28, 50, 51,  
53, 58, 83, 84, 99, 150, 158, 160, 169, 259–  
276, 304, 307

Projection ..... 169, 170, 174, 177

**Q**

Quantitative segmentation data ..... 173

*Quasi*-isostatic method ..... 223, 224

**R**

Radiation

- gamma ..... 236
- ionizing..... 236
- optical ..... 186, 187
- ultraviolet (UV)..... 236
- X-ray..... 172

Raw data ..... 189, 368

Ready-to-eat (RTE) food ..... 252, 253, 255

Reconstruction ..... 169, 171, 172,  
174, 177, 178

Recycling ..... 77, 92

Reflectance..... 67, 186, 187, 189, 200

Region of interest (ROI) ..... 172, 175,  
178, 189, 190

Relative humidity (RH) ..... 11, 29, 125, 168,  
199, 206, 207, 211–213, 216, 221, 222, 227,  
228, 230, 265, 269

Release

- mechanism ..... 313
- profile ..... 319, 321–323
- rate ..... 312, 313

Rendering ..... 170, 172, 175, 178

Reshaping ..... 194, 197

Respirometry

- automated ..... 30
- Bartha ..... 34, 46–50
- nonautomated ..... 27–54

Risk assessment ..... 79, 82, 90–92,  
131, 246, 252, 256

**S**

*Salmonella*/*Escherichia coli* microsome assay  
(Ames test)..... 150, 153–159

Saturated saline solution ..... 227, 230

Seal/sealing ..... 34, 40, 46, 128,  
168, 205, 212, 213, 222, 233, 237, 248, 368

Segmentation ..... 170–172, 174, 176, 343

Sensor ..... 12, 103, 105–107,  
227–229, 367, 369

Sensory

- acceptance (*see* Acceptance)
- analysis/evaluation ..... 339, 342
- attribute (*see* Attribute)

Shelf-life ..... 86, 116,  
119, 167, 168, 177, 205, 219, 220, 233, 240,  
245–257, 311

Short times model..... 320, 321

Simulant, *see* Food simulant

Single-use packaging ..... 338  
 Sinogram ..... 169, 170  
 Smart label ..... 116  
 Smart packaging, *see* Intelligent packaging  
 Smoothing ..... 172, 191, 192  
 Solubility ..... 206, 207,  
     220–224, 230, 261, 313  
 Spatial dimension ..... 67, 184, 189, 190, 197  
 Specific migration ..... 118, 119, 132  
 Spectral dimension ..... 184, 190, 191, 193  
 Spectroscopy/spectrometry  
     infrared (vibrational) ..... 67  
     nuclear magnetic resonance (NMR) ..... 29, 121  
     Raman (vibrational) ..... 67  
     SERS ..... 82–84, 92, 105  
     X-ray ..... 59, 71  
 Spikes ..... 191  
 Spoilage microorganisms ..... 257, 260,  
     279, 280, 283, 288  
 Standard curve ..... 297, 303–305,  
     307, 314, 317, 319  
 Starch, *see* Natural polymer  
 Steam sterilization ..... 236  
 Storage temperature ..... 127, 246, 249,  
     252–254, 257, 269, 270  
 Surfactant ..... 79, 106  
 Swelling ..... 312, 313, 315, 320, 322

**T**

Tetrazolium salt  
     MTS assay ..... 141  
     MTT assay ..... 140  
     WST-1 assay ..... 141  
     XTT assay ..... 141  
 Thermal conductivity ..... 366, 367, 369–372  
 Thermogravimetry (TG) ..... 168, 367,  
     368, 371, 372  
 Three-dimensional (3D) mapped microstructure ..... 174  
 Three-dimensional (3D) reconstruction ..... 170  
 Three-dimensional (3D) structural characterization .. 169  
 Threshold of toxicological concern (TTC) ..... 90, 91,  
     122, 127, 236, 237, 239  
 Thresholding segmentation ..... 172, 175  
 Tomography ..... 169, 171  
 Toxicity  
     cytotoxicity ..... 78, 137–146, 157, 163  
     genotoxicity ..... 78, 149–163

immunotoxicity ..... 100  
 mutagenicity ..... 78, 149–163  
 phytotoxicity ..... 7, 11, 13  
 Transflectance ..... 186, 187  
 Transmission rate  
     carbon dioxide (*see* Carbon dioxide transmission rate)  
     oxygen (*see* Oxygen transmission rate)  
     water vapor (*see* Water vapor transmission rate)  
 Transmittance ..... 67, 186, 187  
 Trialkyl phosphate esters (triPAPs) ..... 102  
 Trolox equivalent antioxidant capacity (TEAC),  
     *see* Antioxidant activity  
 Turbidity ..... 235, 237,  
     240, 284, 286  
 Two-dimensional (2D) slice ..... 173

**V**

van't Hoff relationship ..... 221  
 Vegetable oil ..... 87, 119, 132  
 Vegetables, *see* Fruits and vegetables  
 Volatile organic compound (VOC) ..... 85  
 Volume of interest (VOI) ..... 172–176, 178

**W**

Water  
     activity ..... 227, 253, 274, 315  
     repellency ..... 109, 110  
     resistance ..... 109, 110  
     vapor permeability (WVP) ..... 109, 205–217  
     vapor pressure (WVP) ..... 208–211, 215–217  
     vapor transmission rate (WVTR) ..... 110, 208,  
         215, 216  
 Wickerham card ..... 283, 284

**X**

X-ray  
     attenuation ..... 170–173, 176  
     diffraction ..... 132  
     histogram ..... 172, 175  
     spectroscopy (*see* Spectroscopy)  
     tomography (*see* Tomography)  
     *See also* Radiation

**Z**

Zein, *see* Natural polymer